Multi-OMICS Approach Towards Understanding the Pathogenesis of Retinopathy of Prematurity

Thesis submitted for the degree of

DOCTOR OF PHILOSOPHY

To

THE DEPARTMENT OF ANIMAL BIOLOGY
SCHOOL OF LIFE SCIENCES
UNIVERSITY OF HYDERABAD
HYDERABAD – 500 046
INDIA

By

B. Satish Patnaik

Under the supervision of
Dr. Inderjeet Kaur
LVPEI

Co supervisor
Dr. Bindu Madhava Reddy
UOH

Kallam Anji Reddy Molecular Genetics Laboratory
Prof. Brien Holden Eye Research Centre
L V Prasad Eye Institute
Hyderabad- 500 034

November 2021

Enrolment No: **15LAPH12**

University of Hyderabad
Hyderabad-500 046, India

CERTIFICATE

This is to certify that this thesis entitled "**Multi-OMICS Approach Towards Understanding the Pathogenesis of Retinopathy of Prematurity"** submitted by **Mr B. Satish Patnaik** bearing registration number **15LAPH12** in partial fulfillment of the requirements for the award of Doctorof Philosophy in the Department of Animal Biology, School of Life Sciences, is a bonafide work carried out by him under my supervision and guidance. This thesis is free from plagiarism and has not been submitted previously in full or parts, have not been submitted to any other University or Institution for the award of any degree or diploma.

Parts of this thesis have been:

A. Published/Under review

1. **Patnaik S,** Rai M, Jalali S, Agarwal K, Badakere A, Puppala L, Vishwakarma S, Balakrishnan D, Rani PK, Kekunnaya R, Chhablani PP, Chakrabarti S and Kaur I. An interplay of microglia and matrix metalloproteinase MMP9 under hypoxic stress regulates the opticin expression in retina. Sci Rep. 2021 Apr 2;11(1):7444. doi: 10.1038/s41598-021- 86302-2.
2. Rathi S, Jalali S, **Patnaik S**, Shahulhameed S, Musada GR, Balakrishnan D, Rani PK, Kekunnaya R, Chhablani PP, Swain S, Giri L, Chakrabarti S, Kaur I. Abnormal Complement Activation and Inflammation in the Pathogenesis of Retinopathy of Prematurity. Front Immunol. 2017 Dec 22;8:1868. doi:10.3389/fimmu.2017.01868. PMID: 29312345
3. Rathi S, Jalali S, Musada GR, **Patnaik S**, Balakrishnan D, Hussain A, Kaur I. Mutation spectrum of *NDP*, *FZD4* and *TSPAN12* genes in Indian patients with retinopathy of prematurity. Br. J. Ophthalmol. 2018 Feb;102(2):276-281. doi: 10.1136/bjophthalmol-2017- 310958.

B. Presented in the following conferences

1. Poster presentation on "Matrix metalloproteases (MMPs) regulate Opticin expression in the Microglia Under Hypoxic Stress" in ARVO, 2019, Vancouver, Canada
2. Oral presentation on "MMPs regulates OPTICIN degradation in microglia under hypoxia" was given at IERG-ARVO Indian chapter meeting, 2018, L V Prasad Eye Institute, Hyderabad, India
3. Poster presentation on "Differential Gene Expression Profiling among Different Stages of Retinopathy of Prematurity" ARVO-India annual meeting (International chapter affiliation), 2017 held on at Aravind Eye Hospital, Madurai India

Further, the student has passed the following courses towards fulfillment of course work requirement for PhD

Name	Credits	Pass/Fail
Molecular Genetics	4	Pass
Research Ethics	2	Pass
Biostatistics	2	Pass
Cell Biology	4	Pass

Dr Inderjeet Kaur
Supervisor

Dr Bindu Madhava Reddy
Co-Supervisor
Dr. A. Bindu Madhava Reddy
Assistant Professor
Dept. of Animal Biology
School of Life Sciences
University of Hyderabad
Hyderabad-500 046.

K. Srinivasan
Head
Department of
Animal Biology
अध्यक्ष / HEAD
जंतु जैविकी विभाग
Department of Animal Biology

Dean
School of
Life Sciences
DEAN
School of Life Sciences
University of Hyderabad

University of Hyderabad
School of Life Sciences
Department of Animal Biology
Hyderabad-500 046, India

CERTIFICATE

This is to certify that this thesis entitled "***Multi-OMICS Approach Towards Understanding the Pathogenesis of Retinopathy of Prematurity***" submitted by **Mr B. Satish Patnaik** bearing registration number 15LAPH12 for the degree of Doctor of Philosophy to the University of Hyderabad is a bonafide record of research work carried out by him at the L V Prasad Eye Institute, Hyderabad under my supervision. The contents of this thesis, in full or parts have not been submitted to any other University or Institution for the award of any degree or diploma. I hereby, recommend his thesis for submission, for the award of the degree of Doctor of Philosophy from the University.

Dr Inderjeet Kaur
Supervisor

Dr Bindu Madhava Reddy
Co-Supervisor

Dr. A. Bindu Madhava Reddy
Assistant Professor
Dept. of Animal Biology
School of Life Sciences
University of Hyderabad
Hyderabad-500 046.

Head
Department of
Animal Biology

अध्यक्ष / HEAD
जंतु जैविकी विभाग
Department of Animal Biology

Dean
School of
Life Sciences

DEAN
School of Life Science
University of Hyderaba
Hyderabad-500 046.

University of Hyderabad
School of Life Sciences
Department of Animal Biology
Hyderabad-500 046, India

DECLARATION

I, B. **Satish Patnaik** hereby declare that this thesis entitled "***Multi-OMICS Approach Towards Understanding the Pathogenesis of Retinopathy of Prematurity***" submitted by me under the guidance and supervision of **Dr Inderjeet Kaur**, is an original and independent research work. I also declare that it has not been submitted to any other University or Institution for the award of any degree or diploma.

Date: 25th November 2021

B. Satish Patnaik
15LAPH12

DEDICATED

TO

DR. INDERJEET KAUR,

DR. SUBHABRATA CHAKRABARTI

MY LOVING FAMILY AND

ALL THE PRETERM INFANTS

This doctoral thesis work has been a unique and fulfilling learning process that helped me become a better version of myself academically and personally. Many people were involved directly or indirectly in successfully completing this doctoral research work. This would have been impossible without the help and continuous support of the fantastic people around. I could not possibly leave the institute without expressing my sincere gratitude.

First and foremost, I would like to express my deepest gratitude to my supervisor**, Dr. Inderjeet Kaur**, without whom this thesis would not have been possible. When I joined this institute, I hardly knew anything about retinal diseases. She was the one who introduced me to them, the conditions that lead to blindness in preterm infants. This motivated me and brought the enthusiasm to work efficiently in this field. I am fortunate to have such a dedicated supervisor with deep knowledge in the field of multi-omics. When I joined LVPEI, she introduced me to the importance of ROP research and trained me in scientific reasoning, experiment designing, scientific discussions and presentations. She has been highly motivating and supportive on a scientific and personal front and always receptive to my ideas. She helped me grow in every aspect of my life. I am short of words to describe her immense love and support towards her students. Whenever in need, she would try her best to help us in any way possible. Therefore, whatever I say for her here, it would be less.

Along with my supervisor, I would like to thank **Dr. Subhabrata Chakrabarti** for his kind help and guidance in my exome sequence experiments, data analysis and interpretation for good scientific temper and reasoning. His smart tips and tricks would always impact and bring out excellent quality data. Apart from research-related topics, he has been a very interactive and cheerful person and a fantastic host. We have had multiple memorable outings with **Inderjeet Ma'am** and **Subho Sir**, which I will cherish always.

Next, I would thank **Dr. Bindu Madhava Reddy** for being my co-guide. He has been always ready to help in all the administrative work and access the University infrastructures.

My sincere thanks also go to **Dr. GN Rao**, **Dr. Prashant Garg**, **Dr. Balasubramanian**, **Dr. G Chandrasekhar**, **Dr. Shivaji** and **Dr. Sayan Basu** for allowing and providing an excellent research facility at LVPEI and allowing me to carry out my research here.

Apart from this, without fail, I would like to express my gratitude to all the **preterm infants** and their **families** for participating in the study. Special thanks to **Dr. Subhadra Jalali** for being so passionate, enthusiastic and encouraging. She is the one who provided me with most of the clinical samples for my research. Also, I would like to thank **Dr. Padmaja Kumari Rani**, **Dr. Divya Balakrishnan**, **Dr. Komal Agarwal**, **Dr. Venkatesh**, **Dr. Laxmi** for providing precious clinical samples of ROP; without their help this research would not have proceeded. I would also thank all the clinicians for classifying the ROP phenotypes, which is very crucial for interpreting the data and understanding the disease pathogenesis. I am also thankful to **Dr. Ramesh Kekunnaya**, **Dr. Preeti Patil Chhablani**, and **Dr. Akshay Badakere** for providing control patient samples.

I would extend my thanks to all HoDs of the Department of Animal Biology, University of Hyderabad (UoH): **Dr. Sreenivasulu Kurukuti**; Dean, School of Life Sciences: **Prof. Dayananda Siddavattam;** The Vice-Chancellor, School of Life Sciences, University of Hyderabad, during my PhD. **Prof. Appa Rao Podile**, the Controller of Examinations and the School Board, for all the administrative help and access to the University infrastructure.

I would also thank **Dr. Manjunath Joshi**, Manipal University, for allowing me to use and perform experiments in their metabolomics facility. In addition, I extend my thanks to **Mr. Manoj Kumar** for his help and support in successfully carrying out my experiments.

I am grateful to other faculty members of LVPEI - **Dr. Chitra Kannabiran**, **Dr. Indumathi**, **Mariappan** and all the research faculties for providing their valuable comments and suggestions

for my research work. I would like to sincerely acknowledge **Dr. Dilip, Dr. Soumya Jakati, Mr. Sridhar** and **Mr. Naidu**, who helped me with IHC and its interpretation.

I am delighted to have a wonderful lab family-**Ms. Sushma Vishwakarama, Dr. Tarandeep Kaur, Ms. Prerna Kulshreshtha, Ms. Sharmeela Sharma, Mr. Saurabh Kumar, Ms. Suryadeepali Pahadsingh, Ms. Neha Sharma and Dr. Pallavi Goel**. I have learnt a great deal on determination from them. My heartfelt thanks to all of them for their contributions to my thesis work. I have also given pet-names to some of them. Thanks to **Sushma whom I usually call "Kondadanna".** She has always been around whenever I needed help and also, she is good at understanding people. **Tarandeep** joined as a post-doc in our lab 2 years back; she helped me in exome data analysis and thesis work. She was always patient to listen to what I want to say. Her pet-name is "Alien". **Prerna** was one of the persons who is always ready to help and talk around whenever required. I named her "**PreRNA"**. **Sharmeela** was a great help in my thesis work and also used to share her lunch box with me. After a long wait, I got a "male junior" **Saurabh** in my lab who also helped me in metabolomic analysis. Unfortunately, I didn't give any pet names to him. **Deepali** is our lab manager; I call her **Deep**. She is joyous and helpful in our lab. She always used to bring fruits for me. **Neha Sharma** and **Pallavi** are more new entries in our lab; they are always around and helped me whenever required with a smile on their faces. I will immensely miss them all when I will leave the institute. Thank you all so much!

I am indebted to my senior; **Dr. Sonika Rathi**, for providing me the platform for initiating my research project on ROP. My sincere thanks to my other senior's **Dr. Shahna Shahul Hameed** and **Dr. Ganesh Musada**, for being supportive. **Shahna** is also my good friend and has been helpful throughout my Ph.D. She is a strict senior to all except me. We used to fight but would come back to normal after a short time. I miss those fights. **Dr. Meha** is always helpful; she is an angry bird of our lab but with a good heart.

Continuing, I met one more soulmate during my PhD, **Syed Hameed**. I have learned so many good things from him. He is the one who taught me how to handle preterm babies to collect tear samples. **Dr. Praveen Joseph,** is like a brother to me, a loving and understanding friend and an awesome roommate and well-wisher for me. I always felt great happiness with him as a friend which I didn't see any other friends. **Mr. Vinay** is another great friend of mine and we had so many good memories. He is a calm and silent person for all except me. I have never seen him gossiping about others which is a great quality of his I adore. **Mr. Ranjit** is also my good friend; he would share his tiffin box with me. I learned so many good things from him. **Goutham** is a colleague of mine and a nice friend. He is an introvert, but I could trust him blindly.

I am grateful to **Savitri Ji** for her suggestions and help in cell culture lab and personal life. **Dr. Abhinav** is also a good friend of mine; he is a calm person and always ready to help. Also, I would like to thank **Trupti, Sudipta, Divya, Rishi, Sameer, Alice, Ashish** and **Jilu** for being a wonderful company throughout and for their help in non-scientific issues with a smile on their faces.

I am also thankful to my childhood friends **Dr. Venketesh**, **Ch. Siva, Hemanth, Mr. Suresh, Mr. Santhosh** and M.Sc. friends **Mr. Teja, Mr. Ramesh, Mr. Naresh**, **Mr. Vinod** and **Mr. Patan, and Ms.Sudha**

I am also pleased to thank **Ms. Elena Roopchandra** and **Mr. Poornachandra Rao** for providing me administrative support. The support and co-operation from the Institute's communications department, ISD (**Sunil**), purchase (**Mr. S. Jagadeesh**), accounts (**Mr. A. Srinivas**), stores, maintenance (**Mr. Ravi, Mr. Suneel Birusanti**), biomedical (**Giridhar**) and housekeeping departments were immense. I sincerely thank **Ms. Sabera Banu, Mr. Sudhakar Kothapalli** and **Mr. Quddus** from Library for helping me get all the books, journals and photocopies needed for my research work. I am fortunate to be a part of LVPEI and thankful to institute for providing

me with very good infrastructure, resources for laboratory work, informative lectures and seminars and a chance to meet eminent scholars from diverse fields.

Last but not the least, I am thankful to **my parents**, **sister** and my **brother**, without their support, blessings and encouragement, this work wouldn't have been possible.

Satish Patnaik B

ABSTRACT

Abstract

Retinopathy of prematurity (ROP) is a complex vaso-proliferative eye condition that affects prematurely born infants worldwide. It has a high prevalence of 24-47% in India. Despite timely interventions, a proportion of babies progress to severe stages of the disease. The overall molecular etiology leading to ROP pathogenesis is not well known.

Earlier research from our group revealed an interplay of microglia and MMPs in ROP pathogenesis. In the present study, we observed that tear MMP activation occurred prior to the development of severe ROP and thus could serve as a potential marker for early detection. Under hypoxic stress, activated microglial cells in the retina secreted MMP9, which led to the downregulation of Opticin. Further, the inhibition of the MMP activity by doxycycline and EDTA rescued Opticin degradation mediated by *NOTCH1*, *ERK1* and *WNT* signaling. These results confirmed that microglia-mediated inflammation degraded ECM proteins and led to angiogenesis in ROP eyes. Our whole-exome analysis on ROP exhibited novel mutations in genes involved in metalloendopeptidase, *WNT* pathways and metabolic pathways (fatty acid, arachidonic acid). Global gene expressions in these patients further confirmed the upregulation of angiogenic genes with concurrent downregulation of the *WNT* regulatory genes and anti-apoptotic NK cells regulatory genes in ROP. Likewise, metabolomic analysis of ROP vitreous samples indicated an increase in amino acid, lipids and bioenergetics derived metabolites leading to increased cell death, inflammation and abnormal angiogenesis in the retina. Our multi-OMICS approach demonstrated the potential involvement of several signaling pathways, including *WNT*, *MAPK*, *NOTCH1*, and the metabolism of amino acids and lipids in ROP pathogenesis.

List of Tables

List of Figures

List of Abbreviations

Abbreviations	Full forms
$CoCl_2$	Cobalt chloride
3PG	3-phosphoglycerate
3PHP	3-phosphohydroxypyruvate
A	Adenine
AA	Arachidonic acids
AMD	Age-related macular degeneration
AXIN2	Axis inhibition protein 2
BDT	Big dye terminator
bp	Base pair
BRB	Blood-retinal barrier
BW	Birth weight
C	Cytosine
C3	Complement component 3
C3DC	Malonyl carnitine
cDNA	Complementary DNA
CHME3	Immortalised human microglia cell line
COX	Cyclooxygenases
CRABP	Cellular Retinaldehyde-binding protein 1
CRBP	Cellular retinol-binding protein
CYP450	Cytochrome P450
DAB	3, 3' diamino benzidine
DGLA	dihomo-gamma-linolenic acid
DHA	Docosahexaenoic acid
DKK1	Dickkopf WNT Signaling Pathway Inhibitor 1
DMSO	Dimethylsulphoxide
dNTPs	Deoxy nucleotide triphosphates
dup	Duplication
EC	Endothelial cells
ECM	Extracellular matrix
EDTA	Ethylenediaminetetraacetic acid
EGR	Early growth response
ELBW	Extremely low birth weight
ELISA	Enzyme-linked immunosorbent assay
EPA	Eicosapentaenoic acid
EPHA1	EPH Receptor A1
EPHX2	Epoxide Hydrolase 2
ERK1	Extracellular signal-regulated kinases 1
ERK2	Extracellular signal-regulated kinases 2
FA	Fatty acid
FnII	Fibronectin type II

Abbreviations	Full forms
FOSB	FosB Proto-Oncogene
G	Guanine
GA	Gestational age
GC	Gas chromatography
GLA	Gamma-linolenic acid
Het	Heterozygous
HLA-DRB	human leukocyte antigen
Homo	Homozygous
HX	Hypoxanthine
IF	Immunofluorescence
IGF	Insulin growth factor
IgG	Immunoglobulin G
IHC	Immunohistochemistry
INL	Inner nuclear layer
IL	Interleukin
IPL	Inner plexiform layer
kb	Kilobase
kDa	Kilodalton
LC	Liquid chromatography
LMW	Low-molecular-weight
LN2	Liquid nitrogen
LOX	Lipoxygenases
M	Molar
MC	Mature control
MCP-1	Monocyte chemoattractant protein-1
MHC	Major histocompatibility complex
ml	Millilitre
mM	Millimolar
MMP2	Matrix metalloproteinase 2
MMP9	Matrix metalloproteinase 9
MS	Mass spectrometry
NFL	Nerve fiber layer
ng	Nano gram
NICU	Neonatal Intensive Care Unit
NMR	Nuclear magnetic resonance
NO	Nitric oxide
NOTCH	Notch Receptor 1
NPE	Non-pigmented epithelial
OIR	Oxygen induced retinopathy
OPTC	Opticin
OS	Outer segment

Abbreviations	Full forms
OXPHOS	Oxidative phosphorylation
PAGE	Polyacrylamide gel electrophoresis
PBS	Phosphate buffered saline
PC	Premature control
PCA	Principal component analysis
PCR	Polymerase chain reaction
PDB	Protein Data Bank
PDS	Pigment dispersion syndrome
PEDF	Pigment epithelium derived factor
PG	Pigmentary glaucoma
PKM2	Pyruvate kinase isoform M2
pM	Picomolar
POAG	Primary open angle glaucoma
PPARs	Peroxisome proliferator-activated receptors
PPP	Pentose phosphate pathway
PSAT1	Phosphoserine aminotransferase 1
PSPH	Phosphoserine phosphatase
PUFA	Polyunsaturated fatty acids
RA	Retinoic acid
RAR	Retinoic acid receptor
RARE	Retinoic acid response element
RBP4	Retinol-binding protein
RFLP	Restriction fragment length polymorphism
RGC	Retinal ganglion cells
RGH	Retinal growth hormone
ROP	Retinopathy of Prematurity
ROS	Reactive oxygen species
RPE	Retinal pigment epithelium
RPM	Revolutions per minute
RT	Retention time
RXR	Retinoid X receptor
S1P	Sphingosine-1-phosphate
SDS	Sodium dodecyl sulphate
SIFT	Sorting Intolerant from Tolerant
SLRPs	Small leucine rich proteins
SNP	Single nucleotide polymorphism
SOX	SRY-Box Transcription Factor 2
SREBP1	Sterol regulatory element-binding protein 1
T	Thymine
TAE	Tris acetate EDTA
TCA	Tricarboxylic acid cycle

Abbreviations	Full forms
TGF	Transforming Growth Factor Beta 1
TGFβ	Transforming growth factor-β
TGF-β	Transforming growth factor-β
TIC	Total ion chromatograms
TIMP 1	Tissue inhibitory metalloproteases 1
TIMP 2	Tissue inhibitory metalloproteases 2
TNF	Tumor Necrosis Factor
Tris	Tris (hydroxymethyl) aminomethane
UHPLC	Ultra-high-performance liquid chromatography
VEGF	Vascular endothelial growth facto
WES	Whole exome sequencing
WGS	Whole genome sequencing
X	Xanthine
µg	Microgram
µl	Microlitre
µM	Micromolar
Cu2+	Cupric ions
Cu1+	Cuprous ions
BCA	Bicinchoninic acid
BSA	Bovine serum albumin
MF	Mean fluorescence
OD	Optical densities
PVDF	Polyvinylidene Fluoride
IR	Near-Infrared
DMEM	Dulbecco's Modified Eagle Medium
FBS	Fetal Bovine Serum
M.Wt	Molecular weight
qRT	Quantitative Real Time PCR

GENERAL INTRODUCTION

0. GENERAL INTRODUCTION

Retinopathy of prematurity (ROP) is a serious potentially blinding disease. It is associated with aberrant blood vessels growth of the retina in prematurely born infants. ROP was initially reported as a retrolental fibroplasia (RLF) as defined in 1942 by Dr. Theodore Terry, an ophthalmologist in Boston hospital. He found fibrous tissue behind the lens covering the retinal blood vessels after birth. This fibrous membrane is termed retrolental fibroplasia (RLF) (Emsley *et al.*, 1998; Leaders, 1958). It was found that the pathogenesis of RLF mainly affects prematurely born infants (Owens & Owens, 1949) and later it was termed as ROP. It is a very complex retinal vascular disease affecting normal retinal blood vessel growth.

0.1. Embryonic development of the eye

Eye development in human embryo starts from the 3rd week of gestational age (GA). From 3-10 weeks, significant ocular growth takes place: optic nerve, iris, ciliary body epithelial and retina, derived from the neural tube ectoderm. The lens, conjunctival, corneal epithelia, eyelids and lacrimal system are derived from the surface ectoderm while Mesenchyme is responsible for the formation of remaining ocular structures. After 22 days of fertilization, the optic grooves will emerge from the developing forebrain and form the optic vesicle. The optic vesicles come and interact with the surface ectoderm and induce a pseudostratified thickening, which leads to creating the lens placode. The invagination of the lens placode forms the lens pit and lens vesicle. The optic vesicle invaginates to form the bilayered optic cup once the lens vesicle is formed. Retinal pigment epithelial (RPE) cells and neuronal retina develop from the outer and inner layers of the optic cup. Optic vesicles are formed as bilateral bulge from both sides of the developing forebrain (prosencephalon). They further grow and connect with the brain by optic stalks and further get attached to surface ectoderm. Along with the optic stalk, hyaloid vessels (blood vessels) also grow and pass into the optic cup, further developing the lens. The

developing optic cup and mesenchyme also form the retinal bilayers, iris, ciliary body and choroid.

0.1.1. Human eye and retina

The human eye functions as a camera; being an important sensory organ it facilitates light perception and empowers us to see the world. The cornea is the front part of the eye, a transparent membrane that allows light rays to penetrate the eye. It allows the light rays to meet, which further helps to focus the light rays onto the retina. These light rays are then perceived as an image by the visual cortex of the brain (eye structure and retinal cross-sections image given below Figure 1A). A clear gel-like fluid called vitreous base closely adheres to the peripheral retina's non-pigmented epithelium and internal limiting lamina between the lens and the retina. The retina is a sensory part at the posterior side of the eye, containing ten retinal layers (Figure 1B). The retina's photoreceptors capture the photons and subsequently activate the biochemical reactions, leading to action potentials or electrical signals across the retinal membrane. These potential signals are then transmitted via the optic stalk to the brain's visual cortex, where they have been interpreted as images. This cascade of reactions plays a significant role in constructing binocular vision, depth, color perception and visual response. In preterm infants, the retinal vasculature growth is incomplete at birth, later on these blood vessels grow abnormally leading to retinal detachment. The detachment of the retina affects the visual signaling pathways and thus leads to visual impairment. ROP develops when aberrant blood vessels sprout and spread throughout the retina. Therefore, understanding and preventing a preterm infant's vision loss has been a prime focus for several years. A focused overview of retinal anatomy and vitreous with emphasis on its development and function is as follow:

0.1.2. Anatomy of retina

The retina (Latin: rete = net) is a light-sensitive tissue, around 100-300μM thick and located at the eye's posterior part. The human retina consists of two component layers: one pigmented

layer and nine neural layers (F. Gonzalez-Fernandez, 2011). A brief overview of the retinal layers is described below:

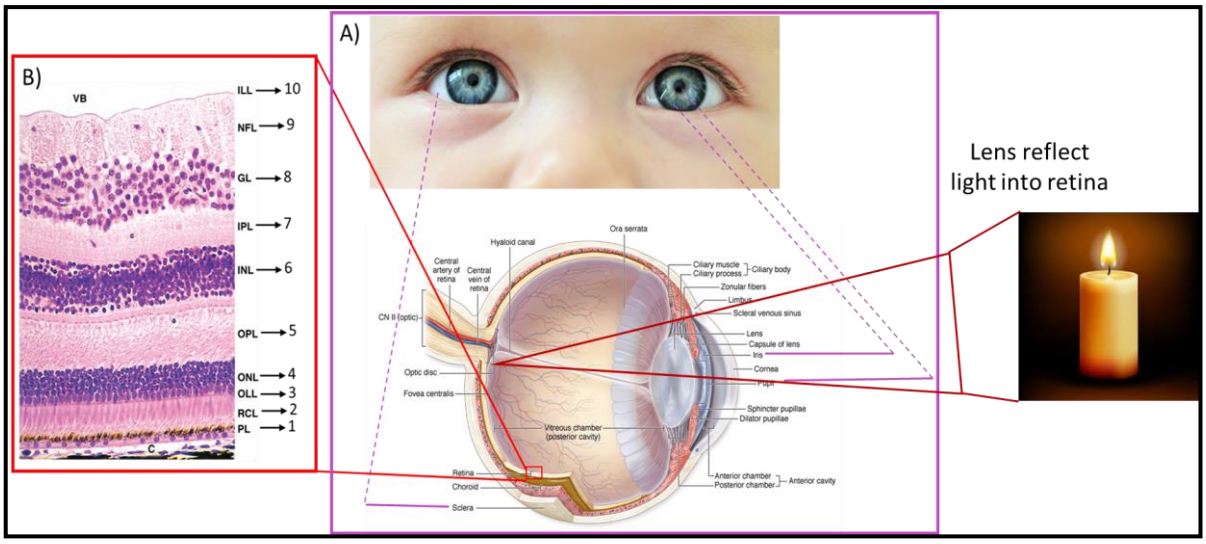

Figure 1. Cross sectional view of a human eye and retina; A. Cross sectional view of a human eye, showing the presence of a transparent cornea on the front, the crystalline lens in the middle and the light sensitive retina on the posterior side; B. Hematoxylin and eosin (H&E) stained section of the posterior segment of a human eye ball. Between the vitreous body (VB) and the choroid of an adult retina comprises of ten distinct layers namely: (1) retinal pigment epithelium (RPE); (2) rods and cones (photoreceptors-PL); (3) external limiting membrane (ELM or OLL); (4) outer nuclear layer (ONL); (5) outer plexiform layer (OPL); (6) inner nuclear layer (INL); (7) inner plexiform layer (IPL); (8) ganglion cell layer (GCL); (9) nerve fiber layer (NFL); (10) inner limiting membrane (ILM). Adapted and modified from (Mescher, 2018).

0.1.2.1. Retinal pigment epithelial cells (RPE) layer

RPE is the outermost retinal layer. It is sandwiched among the choroid and photoreceptor cells (Tamm & Ohlmann, 2012). Human eye contains approximately 3.5 million RPE cells (Panda-Jonas *et al.*, 1996). Structurally, RPE cells are hexagonal and tightly packed in the central retina, forming the unique cuboidal epithelium layer.

The tightly packed junctions of RPE contribute to the blood-retinal barrier (BRB) integrity, which mediates several essential functions in retinal physiology. These functions include transport of water, ions, nutrients, secretion of neurotrophic and vasculotrophic growth factors. RPE also regulate the metabolic transport between the choroid and neuroretina and the removal of the metabolic waste.

0.1.2.2. Photoreceptor layer

As the name suggests, it performs phototransduction and is comprised of the outer segments (OS) of photoreceptor cells (rod and cone) of retina. The photoreceptor layer converts light stimuli into nerve impulses and hence act as information barrier for visual system to form images.

0.1.2.3. Outer limiting membrane (OLM)

An outer or external limiting membrane is formed between the pigment epithelium and the outer nuclear layer. It contains tightly held rod and cone cells and form cellular junctions with Müller cells. The OLM helps to maintain the barrier for interphotoreceptor fluid and matrix so that these do not escape into the rest of the internal retina. The OLM is a part of the retinal barrier that gets interrupted in retinal pathological conditions.

0.1.2.4. Outer nuclear layer (ONL)

The photoreceptor cell bodies are located on the outer nuclear layer. It also includes synaptic terminals of rod and cone cells and contains neurons that extend towards the outer plexiform layer (OPL). ONL helps to retrieve oxygen and other nutrients by diffusion from the choroidal capillaries.

0.1.2.5. Outer/external plexiform layer (OPL)

OPL encompasses axonal processes of rods, cones, along with bipolar cells and horizontal cells and forms the synapses.

0.1.2.6. Inner nuclear layer (INL)

INL contains the connections between three types of cells i.e., amacrine, horizontal and bipolar neuronal cells.

0.1.2.7. Inner plexiform layer (IPL)

IPL is formed from the synaptic interactions with amacrine cells and inner nuclear layer. It also provides synaptic contact with the corresponding ganglion cell.

0.1.2.8. Ganglion cell layer (GCL)

This retinal layer consists of retinal ganglion cells and also interacts with amacrine cells, which plays an important role to receive visual information.

0.1.2.9. Nerve fiber layer (NFL)

The NFL is formed by the extensions of optic nerve fibres and this layer consists of the ganglion cells. The axons of these cells are towards ganglion cell layer and neurons towards the inner limiting membrane (vitreous).

0.1.2.10. Inner limiting membrane (ILM)

ILM contains müller cell terminal expansions towards the vitreous humor and form the retinal inner surface. It also contains astrocytes. The layer makes a boundary between the retina and the vitreous body.

0.2. ROP Epidemiology

Childhood blindness can be categorized as avoidable, preventable/treatable and irreversible. ROP classifies as avoidable childhood blindness condition that occurs worldwide except in undeveloped countries like Sub-Saharan Africa, where premature infants do not survive due to high infant mortality rates (IMRs). ROP leads to blindness in 50,000 preterm infants annually in developed countries such as the United States. In developing countries like India and China, far more number of premature infants are prone to develop the disease and go blind (Kong *et al.*, 2012; Gilbert, 2008). On the basis of incidence of ROP in different decades, the condition was classified in 3 different stages and termed as "ROP epidemics".

0.2.1. First epidemic of ROP

In 1940, when first epidemic of ROP was reported, oxygen therapy used to treat respiratory impairments in prematurely born infants was thought to be the major cause. The uncontrolled oxygen therapy to treat respiratory diseases led to developing the most common cause of childhood blindness, i.e., ROP. Further, randomized controlled trials were performed to monitor the dosage of oxygen to treat respiratory distress and compared premature infants with higher, lower and restricted oxygen treatment.

Oxygen was intensely controlled, but premature infants born with a birth weight (BW) of 1,000g rarely survived during the first epidemics of RLF/ROP and mature infants were blind. The first epidemic of RLF/ROP gave rise to consciousness and interest in understanding the disease mechanism for ophthalmologists and vision researchers. First in 1951, Campbell found the direct relationship of oxygen supplementation with increased incidence of ROP (Campbell, 1951). Later on, Kinsey *et al.* (1956), verified the O_2 involvement in RLF pathogenesis (Kinsey, 1956). These studies provided a hypothetical link of uncontrolled oxygen exposure with the development of RLF.

0.2.2. Second epidemic of ROP

The second epidemic of ROP began in the late 1970s. The introduction of monitoring of oxygen saturation levels and the advent of neonatal intensive care units (NICUs), cryotherapy and laser showed a positive impact on premature infant's survival and vision, particularly those born with weight less than 1000 grams (Lucey & Dangman, 1984). During 1950-1960, with the help of intensive care units, the rate of blindness was dramatically reduced from 7.9 per 100,000 premature infants to 1.2 per 100,000 premature infants in USA (Hatfield, 1972). Later in 1984-1994, by employing improved treatment options and NICUs there was significant rise in survival rate of low birth infants (27%-42%) that led to an exponential increase in vision disabilities like ROP, myopia and squint cases (Emsley *et al.*, 1998).

0.2.3. Third epidemic of ROP

The unrestricted oxygen usage and enhanced survival percentage of preterm infants during the first epidemics led to the development of the second epidemic in high-income countries. India and other developing countries have been dealing with the third epidemic of ROP from 1990-till now. Further, due to insufficient quality of neonatal care, inadequate screening protocols and lack of timely treatment interventions, ROP cases have increased. A few premature and mature babies progress to severe ROP in India and their phenotypical changes appeared similar to the first epidemics (Shah *et al.*, 2009) leading to irreversible blindness. Thus, strict neonatal care, oxygen administration care and its correlation with the pathogenesis of ROP is much required. In highly developed countries, the incidence of blindness due to ROP is relatively lower and restricted only to premature babies with BW<1000g (Gilbert *et al.*, 2005). This was due to an increase in technological sophistication and awareness of risk factors in neonatal care.

The three ROP epidemics are briefly mentioned in the Table 1.

Table 1. Epidemiology of ROP

Epidemics	Causes	Regions	Period
1st	Introduction of neonatal care & unmonitored oxygen	United States and western Europe	1940's and 1950's
2nd	Increased survival of extremely low birth weight babies combined with minimal screening and treatment	United States and western Europe	1980's
3rd	Increased access to medical technology that allows earlier viability age, yet without appropriate post-natal to counter pre-term diseases	Latin America, Eastern Europe, Africa, and Asia	1990's onwards

0.3. Global and National Burden of ROP

Blencowe *et al.* reported that approximately 184,700 preterm infants developed some grade of ROP in the year 2010. In India and other middle-income countries, the survival rate of preterm

infants increased due to oxygen supplementation. However, due to the lack of proper neonatal care and screening protocols, the incidence of ROP was still high (Blencowe, Lee, *et al.*, 2013) (Blencowe, Lee, *et al.*, 2013; Blencowe, Cousens, *et al.*, 2013). Worldwide 15 million-infants born prematurely in every year (Quinn, 2016; Blencowe, Cousens, *et al.*, 2013; Blencowe *et al.*, 2012), while around 3.5 million- premature births occur every year in India (Blencowe *et al.*, 2012). Among them, approximately 1 in 6 (about 600,000) children are born at GA <32 weeks and these are the infants who are more prone to develop ROP. Only 40% of these children receive neonatal care and among them, ~80% of children survive. Approximately 10% of these survived infants i.e., around 20,000 children are at risk of developing ROP every year (https://phfi.org/wp-content/uploads/2019/05/2018-ROP-operational-guidelines.pdf) (Figure 2).

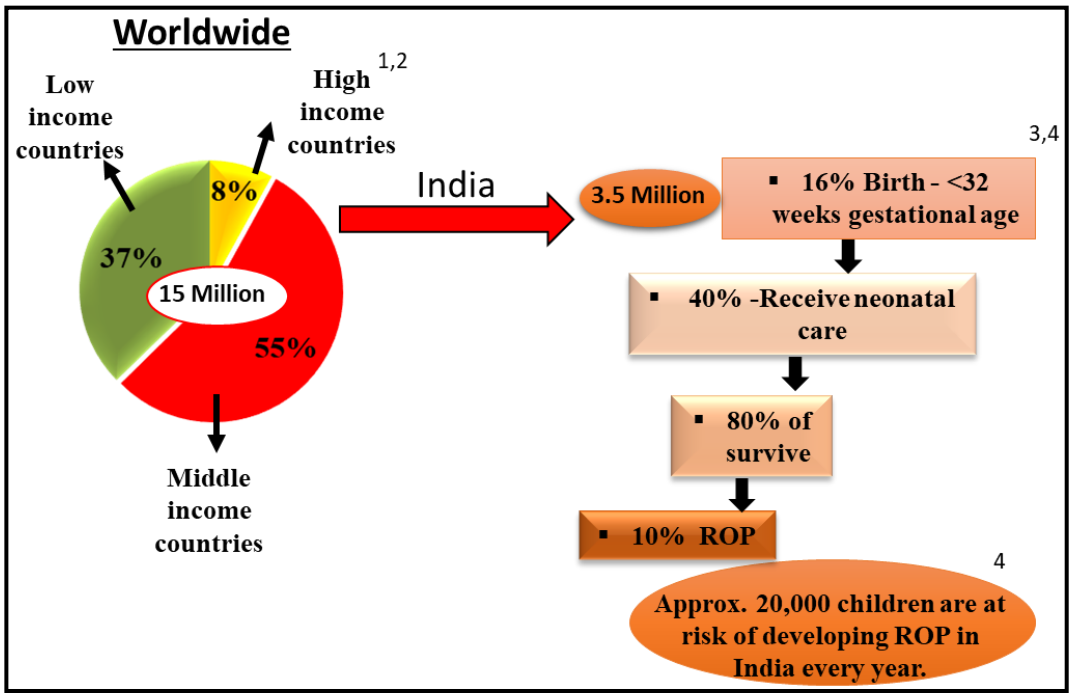

Figure 2. Incidence of premature births and ROP; Data source: adapted & modified from: (Quinn, 2016; Blencowe, Cousens, *et al.*, 2013; Blencowe *et al.*, 2012) and https://phfi.org/wp-content/uploads/2019/05/2018-ROP-operational-guidelines, 2019.

0.4. Ocular Complications of preterm birth other than ROP

Other than ROP, preterm infants are also prone to develop several ocular complications, including retinal fold, retinal tear, retinal detachment (rhegmatogenous and exudative), iris neovascularization, glaucoma, cataract myopia and many more (Smith & Tasman, 2005; Kaiser *et al.*, 2001).

0.5. Classification of ROP

According to the guidelines of the International Classification of ROP (ICROP), this disease is classified based on the location and extent of retinal involvement, degree of severity and vascular lesions in presence of dilated and tortuous vessels and vascularized and avascular retina. The different classification of ROP are described in the Table 2.

Table 2. Classification of ROP as per ICROP

International Classification of Acute Stages of Retinopathy of Prematurity
Location: • *Zone I*: (innermost zone) A circle centered around the optic disc, the radius of which is equal to twice the distance from the center of the optic disc to the macula • *Zone II*: Extends centrifugally from the edge of zone I to the nasal ora serrata • *Zone III*: The residual temporal crescent of retina anterior to zone II
Extent: Specified by the hours of the clock as the observer looks at the eye
Staging: • *Stage 0*: Immature vascularization, no ROP • *Stage 1*: Demarcation line separating avascular and avascular retina • *Stage 2*: Ridge which may have small isolated tufts of neovascular tissue on its surface known as "popcorn" • *Stage 3*: Ridge with extraretinal fibrovascular proliferation (neovascularization) extending into the vitreous • *Stage 4*: Partial retinal detachment ○ Stage 4a: extrafoveal retinal detachment ○ Stage 4b: foveal retinal detachment • *Stage 5*: Total retinal detachment
Plus disease: (+) Increased venous dilation and arteriolar tortuosity of the posterior pole vessels equal to or greater than the "standard" photograph v
Aggressive posterior (AP) ROP – Earlier know as rush disease Rapidly evolving pre-plus and plus disease Progress to stage IV & V in 2-3 weeks without passing characteristic stage II & III

0.6. Mechanism of ROP pathogenesis

Retinal vascularization and maturation is completed by 40 weeks of gestation, thus, in preterm infants, the vasculature formation is incomplete, leading to the avascularized peripheral retina. In this period, choroidal circulation provides oxygen to the avascularized retina. Besides that, premature infants do not have fully developed lungs as well. Therefore, to compensate for

impaired lung function, infants are usually kept in an oxygen chamber. The oxygen supplementation creates hyperoxia in the eye, leading to the cessation of retinal vessel development (vaso-obliteration/phase-I ROP/Stage 1 and 2). As the infants mature, they are returned to ambient air; due to increased metabolic rate, the oxygen demand in the retina increases for the development of retinal neurons/photoreceptors and other developmental processes. This increased demand for oxygen cannot be fulfilled by the choroidal vasculature alone (Weiter *et al.*, 1982) and hence, retina experiences hypoxia. Hypoxia thus generated results in the induction of various angiogenic growth factor including VEGF and alteration in other signaling pathways which leads to rapid growth of new vessels (Figure 3) (Neovascularization /Phase II ROP/stage 3, 4 and 5). These new vessels can either regress or progress to extraretinal neovascularization.

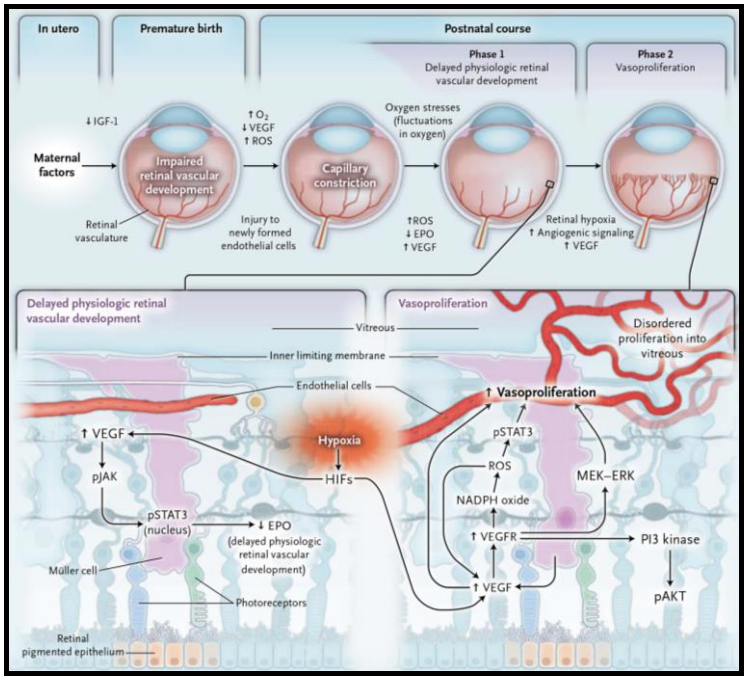

Figure 3. Mechanisms of ROP pathogenesis; in retinopathy of prematurity, physiologic retinal vascular development is delayed at first, resulting in a peripheral avascular region of the retina (phase 1). Later, at the junction of avascularized and vascularized retinas, vasoproliferation in the form of intravitreal angiogenesis can develop (phase 2). EPO: erythropoietin, O_2: oxygen, HIF: hypoxia-inducible factor, ROS: reactive oxygen species, ERK: extracellular signal-regulated kinase IGF1: insulin-like growth factor 1, MEK: mitogen-activated protein, pAKT: phosphorylated protein kinase B, PI3: phosphatidylinositol 3, pJAK: phosphorylated Janus kinase, pSTAT3: phosphorylated signal transducer and activator of transcription 3, VEGF: vascular endothelial growth factor and VEGFR: vascular endothelial growth factor receptor. Adapted from; (Hartnett & Penn, 2012)

Although several studies have been performed on oxygen-induced retinopathy (OIR) mouse model and ROP patients to understand the pathogenesis and management of ROP, the mechanism of ROP is still not entirely understood. Additionally, the incidence rate of ROP and other visual impairments are increasing. Though several environmental risk factors including prematurity, low birth weight, excessive light exposure, oxygen supplementation and hypoxia have been associated with ROP, "it's not clear why only some premature infants progress to the severe stage of ROP despite timely intervention whereas others show regression of ROP" is still unclear.

Gene expression and proteomic studies performed on OIR animal models have identified several genes/proteins involved in ROP pathogenesis. These identified genes/proteins are involved in various cellular pathways, e.g., development, metabolism, inflammation, apoptosis and visual processes. Global gene expression profiling of retinal tissue obtained from the OIR murine model revealed upregulation of inflammatory genes (*CCL2*, *TNFa*, and *MCP1*) in a hyperoxic phase of ROP (Ishikawa *et al.*, 2010). While in the hypoxic phase, there was marked upregulation of the angiogenic genes (*VEGF-A* and *Angiopoietin-2*) (Ishikawa *et al.*, 2010). In addition to this, in the same OIR murine model, Ishikawa and co-workers showed an increased expression of oxidative stress related genes (*SELENBP1* and *SELENBP2*), chemokines (*MCP*-1, *MIP*-1α and *1β*) and MHC by microarray analysis. Differential expression of VEGF and Ephrin pathway genes were identified in mice and rat OIR animal models (Recchia *et al.*, 2010). The metabolic pathways glycolysis, gluconeogenesis and cytoskeleton modeling related genes were identified by transcriptome profiling of OIR mice retina. It was also noted that these are the most critical pathways involved in ROP pathogenesis along with angiogenic and inflammatory pathways (Yang *et al.*, 2013). Till now, only one study has focused on global gene expression profiling of ROP patients and revealed a downregulation of genes related to

inflammatory pathways (Pietrzyk *et al.*, 2013). These genes are associated with maturity, implying further that immature or underdeveloped immune system in patients with premature birth.

Likewise, targeted protein profiling of serum and vitreous also identified several proteins like IGF-1, VEGF, etc., which could be act as potential biomarkers for disease progression. However, none of these proteins were replicated in other populations, thereby restricting their use as biomarkers. The above-mentioned studies on transcriptomic and proteomic analyses in OIR animal models have led to the identification of novel genes, proteins and associated signaling pathways.

Several mechanisms including HIF signaling, eNOS/iNOS, VEGF, complement, extracellular matrix metalloproteinases have been extensively studied for their role in retinal neovascularization. Hypoxia-induced HIFα stabilization transduces the expression of angiogenic genes, which further results in neovascularization (Krock *et al.*, 2011). Hypoxia also induces free radicals, superoxides, or peroxynitrite, that can cause oxidative stress, which further leads to apoptosis of vascular endothelial cells and vaso-obliteration via JAK/STAT (Hartnett, 2010) and PI3K/Akt, MAPK signaling pathway (Abdelsaid *et al.*, 2010). MMPs degrade the capillary basement membrane and vitreous collagen (Lambert *et al.*, 2002), thereby facilitating the migration and proliferation of EC to mediate neovascularization (Klagsbrun & Moses, 1999). Studies have also shown the role of complement components in the regulation of neovascularization through the activation of macrophages (Rathi *et al.*, 2017; Langer *et al.*, 2010) .

The clinical manifestations and phenotypic changes in ROP patients correlate with Familial exudative vitreoretinopathy (FEVR). This hints for the involvement of common genetic factors for these conditions that trigger the abnormal blood vessel proliferation as seen in severe ROP. The FEVR associated variants in functional genes such as *VEGF, LRP5, FZD4, NDP, ANGPT2, CFH, EPO, BDNF* and *CETP* were thus screened for their role in ROP by different

groups. In all the studies, polymorphic variants/SNPs were identified across all the targeted genes thereby providing insufficient evidences for the role of these gene in risk of ROP. Since ROP is a multifactorial disease, it is impossible to rule out the participation of many other potential genes beyond norrin-catenin signaling genes. Thus, besides analyzing the Wnt and norrin-catenin signaling pathway genes, there is a need to find other potential genes for ROP pathogenesis. Whole exome sequencing in ROP infants could be a better study design to help identify genetic risk factors that may predispose an infant to ROP development.

In addition, the global gene expression profiling for ROP is likely to provide further insights into the disease pathogenesis, which could eventually help better understand the disease. It would also help in identifying the relevant pathway(s) implicated in ROP progression. Another way of identifying the underline mechanisms is through metabolite profiling. The end products of these transcriptional and translational processes are different metabolites. These metabolites are also associated with interactions between genetic and environmental exposures; thus, are expected to closely correlate with distinct disease phenotypes, especially for multifactorial diseases like ROP. The metabolites and their associated pathways provide in-depth and phenotype changes in pathophysiology of ROP. Only one metabolite profiling study has been performed so far using ROP plasma samples, but there are no studies using ocular fluids.

ROP being a complex disorder, the major challenge lies in understanding the molecular mechanism or pathway involved in disease pathogenesis. Therefore, the current study was intended to understand the molecular mechanisms and pathways associated with ROP pathogenesis through targeted proteins, genes and metabolites expression profiling. This study would provide an in-depth understanding of critical proteins and genes and their mechanism of action in ROP progression. The detailed investigation of these pathways involved in ROP progression may help better understand the pathophysiology of the disease and its timely intervention. Further, the overall study approach and targeted analysis of crucial ROP pathways

might help to identify potential biological biomarker(s) for disease diagnosis and better therapeutic targets for arresting ROP progression. The present study is an attempt to address the lacunae in the existing knowledge about the underlying pathophysiology of ROP through 4 major independent chapters; those are:

- **Chapter 1**- Investigation of aberrant MMP activation under hypoxic stress and its role as potential marker for predictive testing.
- **Chapter 2**- Identification of rare and pathogenic gene variants in ROP conferring disease susceptibility.
- **Chapter 3**- Identification of putative biological pathways in ROP.
- **Chapter 4**- Identification of metabolic pathways involved in ROP pathogenesis.

The chapter wise adopted methodology, results and related discussion is given in proceeding chapters.

CHAPTER 1

INVESTIGATION OF ABERRANT MMP ACTIVATION UNDER HYPOXIC STRESS AND ITS ROLE AS POTENTIAL MARKER FOR PREDICTIVE TESTING

1.1. Introduction and review

ROP is a vitreoretinal disease that affects the retina and vitreous in the eyes of preterm infants by abnormal blood vessel proliferation under hypoxic stress and other development related factors. Vitreous is jelly like fluid present in the posterior chamber of the eye closely connected to the retina. The major protein components of the vitreous include collagens, albumins, IgG, cytokines, chemokines, proteoglycans, etc. Several cytokines, erythropoietin, VEGF, interleukins, G-CSF, GM-CSF, Eotaxin, FGF, RANTES, etc. are present in vitreous (Rathi *et al.*, 2017) with a balanced level of expression. When there is the breakdown of the BRB in retinal diseases, the circulatory proteins get leaked into the retina and gradually accumulates into the vitreous. Vitreous proteome using OIR mice models served to identify major proteins and essential pathways involved in ROP pathogenesis. The role of a specific protein signature to disease susceptibility and development in certain preterm infants was explained by earlier studies on protein profiling of ROP serum and vitreous humor samples. The composition of vitreous changes in response to any damage in the retina. Hence, studying the vitreous proteome could act as surrogate for studying retinal vascular events in ROP. Thus, to identify the mechanisms involved in ROP, we carried out genetic analysis on preterm infants with and without ROP using a targeted SNP array. We found a strong association of the complement genes such as *CFH*, *CFB*, ECM, *FBLN5*, *MMP2* and *TGFβ* with ROP. The strong association of complement genes found in our ROP patient cohort suggested for a major involvement of alternative complement pathway. Subsequent, systematic protein analysis of vitreous humor further confirmed an increased complement activation in the ROP eyes that causes microglial activation leading to disruption of retinal homeostasis via the release and activation of MMPs, other inflammatory cytokines and chemokines (Rathi *et al.*, 2017). Therefore, we next evaluated if MMP levels in the ROP eyes could be considered as markers of increased inflammation that can further contribute to neovascularization in ROP.

At first, we aimed to identify the inflammatory molecules as the disease biomarker in ocular fluids. We measured the MMP9 levels in the tear samples of a preterm infant with different stages of ROP and without ROP. Tears are the only non-invasive sample source near the retina, which can be collected from preterm infants at different stages of ROP development. While they are expected to display changes in the anterior chamber of the eye, several retinal diseases indicated that tear composition could reflect the retinal changes too (Torok *et al.*, 2013; Csosz *et al.*, 2012; Kim *et al.*, 2012) and thereby justify our choice of sample for biomarker development. Till now, no research has been done on assessing the tear fluid of ROP patients. We estimated the levels of inflammatory proteins, i.e. (cytokines and MMPs) as a possible biomarker in the tear samples of ROP patients. We further hypothesized that targeting MMPs could potentially attenuate the underlying inflammation, thereby preventing the abnormal proliferation of blood vessels in the ROP eyes.

1.1.1. Tears

We measured the MMPs levels in the tear samples of preterm infant's eyes, those without ROP and those who developed different stages of ROP. The composition and levels of tear secretion are controlled by lacrimal functional unit (LFU), that includes an integrated The lacrimal functional unit (LFU) includes the integrated unit of interconnecting sensory organs, motor nerves and lacrimal glands (Stern *et al.*, 1998). which further helps and maintains the surface hydration and homeostasis. The ocular tissue homeostasis is maintained by the blood-aqueous barrier (BAB) and BRB. Any damage to these barriers leads to the infiltration of several inflammatory cytokines into the anterior segment of the eye (Ramos *et al.*, 2021). The healthy ocular surface tear film is made up of three components (Figure 4).

a) Mucin layer- Contains the surface glycoproteins and maintains the hydration
b) Aqueous layer - Offers osmolarity nutrients and antimicrobial activity
c) Lipid layer- Prevents the aqueous layer

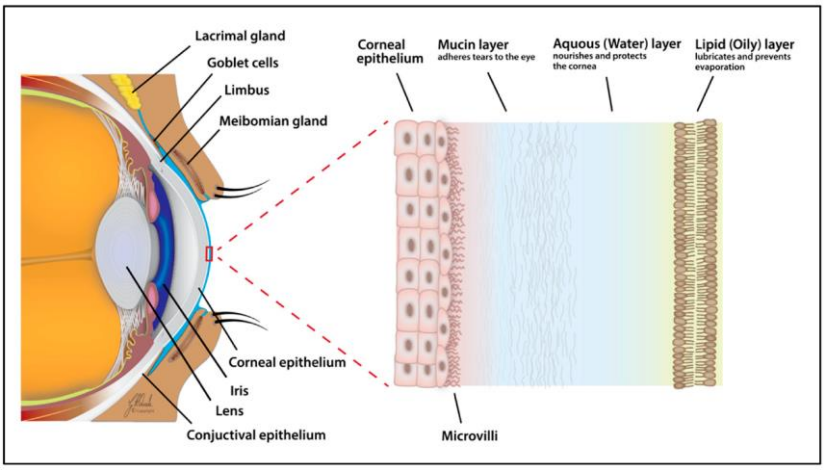

Figure 4. Structure of tear film adapted from (Yazdani *et al.*, 2019)

Based upon the mode of secretion, the composition of tears varies and tears are classified into following 3 types (Murube, 2009)

a) Basal tears- Continually covers the ocular surface, without any stimuli

b) Reflex tears- Produced with stimuli like a sneeze reflex, pinching etc.

c) Emotional tears- Secreted in emotions (sadness/happiness)

Studying human tears have several advantages as compared to the serum/plasma. Tears are non-invasive and proximal fluid to the ocular surface. Human tears contain more proteins, lipids, electrolytes, peptides, metabolites, water salts, etc. (Aass *et al.*, 2015) as compared to the secretions by ocular surface epithelial, nerve cells, goblet cells, meibomian glands and lacrimal glands (Zhou & Beuerman, 2012). There is an increased interest in exploring tear biomarkers in several ocular diseases like dry eye, diabetic retinopathy, glaucoma, keratopathy and type-2 diabetes mellitus (K. Patnaik *et al.*, 2017; Aass *et al.*, 2015; Leonardi *et al.*, 2014; Torok *et al.*, 2013; Aluru *et al.*, 2012). Several potential biomarkers for disease diagnosis have been identified from tear samples, in several ocular diseases described in below Table 3.

Table 3. Tear proteome in ocular diseases

Disease	Type of molecule	Molecules	References
Dry eye disease	Proteins	Lysozyme, Lactoferrin, LPRR4, Calgranulin A/S100 A8, LPRR3, nasopharyngeal carcinoma-associated PRP 4, α-1 antitrypsin α-enolase, α-1 acid glycoprotein 1, S100 A4, S100 A11 (calgizzarin), S100 A9/calgranulin B, LCN-1, Mammaglobin B, lipophilin A, β2M, S100A6, Annexin A1, Annexin A11, CST4, PLAA, Transferrin, LCN-1, Defensin-1, clusterin, lactotransferrin, Cathepsin S, Anti-SS-A, Anti-SS-B, Anti-α-fodrin antibodies, Malate dehydrogenase (MDH) 2, Palate lung nasal clone—PLUNC, (MUC)5AC	(Schicht *et al.*, 2015; Guo *et al.*, 2014; Li *et al.*, 2014; Hamm-Alvarez *et al.*, 2014; Versura *et al.*, 2013; Boehm *et al.*, 2013; Soria *et al.*, 2013; Aluru *et al.*, 2012; Tong *et al.*, 2011; Zhou *et al.*, 2009; Zandbelt *et al.*, 2009; Yavuz *et al.*, 2006; Grus *et al.*, 2005; Toker *et al.*, 2004; Argueso *et al.*, 2002; Goren & Goren, 1988; Boersma & van Bijsterveld, 1987; Mackie & Seal, 1986)
	Neuro-mediators	NGF, CGRP, NPY, Serotonin	(Chhadva *et al.*, 2015; Lambiase *et al.*, 2011)
	Cytokines/ chemokines	IL-1, IL-2, IL-5, IL-6, IL-8/CXCL8, IL-10, IL-12, IL-16, IL-33, GCSF, MCP1/CCL2, MIP1d (CCL15), ENA-78/CXCL5, sILR1, sIL-6R, SGP, sEGFR, sTNFR, IL-17A, IL-21, IL-22, IL-1RA, CXCL9/MIG, CXCL11/I-TAC, CXCL10/IP-10, MIP-1β/CCL4, RANTES/CCL5, EGF, TNF-α, INF-γ, MMP-9, MIP1-α/CCL3, VEGF, Fractalkine	(Lopez-Miguel *et al.*, 2016; Lim *et al.*, 2015; Aragona *et al.*, 2015; Tan *et al.*, 2014; Lee *et al.*, 2013; Teson *et al.*, 2013; Na *et al.*, 2012; J. F. Huang *et al.*, 2012; VanDerMeid *et al.*, 2012; Choi *et al.*, 2012; Boehm *et al.*, 2011; Enriquez-de-Salamanca *et al.*, 2010; Yoon *et al.*, 2010; Massingale *et al.*, 2009; Lam *et al.*, 2009; Yoon *et al.*, 2007; Ohashi *et al.*, 2003; Solomon *et al.*, 2001; Pflugfelder *et al.*, 1999; Tishler *et al.*, 1998)

Disease	Type of molecule	Molecules	References
Ocular graft versus host disease	Cytokines/ Chemokines	IL-6, INF-γ, Soluble TNF receptor 1 (sTNFR1), IL-2, IL-10, IL-17A, TNF-α, EGF, IL-1RA, IL-8/CXCL8, IP10/CXCL10	(Cocho *et al.*, 2016; Sakimoto *et al.*, 2014; Riemens *et al.*, 2012)
Ocular allergy	Cytokines/ Chemokines /Proteins	IL-1α, IL-1β, IL-2, IL-6, IL-12, IL-13, Eotaxin-1/CCL11, RANTES/CCL5, MCP-1/CCL2, IL-4,IL-5,IL-10,sIL-6R, Eotaxin-2/CCL24, TNF-α, IFN-γ, TNF-α/IFN-γ, IL-5/IFN-γ, IL-5/IL-10, Neutrophil myeloperoxidase, ECP, Eosinophil neurotoxin, sIL-2 receptor, Histamine, MMP-1,MMP-9, TIMP-2, Haemopexin, Substance P, CGRP, VIP, Transferrin, Mammaglobin B, Secretoglobin 1D, IgE	(Leonardi *et al.*, 2015; Leonardi *et al.*, 2014; Pong *et al.*, 2011; Sacchetti *et al.*, 2011; Pong *et al.*, 2010; Acera *et al.*, 2008; Sack *et al.*, 2007; Leonardi *et al.*, 2006; Shoji *et al.*, 2006; Nivenius *et al.*, 2004; Leonardi *et al.*, 2003; Montan & van Hage-Hamsten, 1996; Abelson *et al.*, 1995)
Keratoconus	Proteins	GCDFP-15/PIP, RANTES /CCL5, MMP-13, NGF, IL-6, MMP-9, IL-6, IL-6, IL-1β and IFN-γ, SFRP-1, Prolidase	(Goncu *et al.*, 2015; Shetty *et al.*, 2015; Sorkhabi *et al.*, 2015; Priyadarsini *et al.*, 2014; Kolozsvari *et al.*, 2014; You *et al.*, 2013)
Trachoma	Proteins	Immunoglobulins, IgG against cHSP60, CPAF and CT795, EGF, TGF-β1 and TNF-α	(Mowafy *et al.*, 2014; Skwor *et al.*, 2010; Satici *et al.*, 2003; Mahmoud *et al.*, 1994; Darougar *et al.*, 1978; Nema *et al.*, 1977; Sen *et al.*, 1977)
Thyroid-associated orbitopathy	Proteins	IL-1β, IL-6, IL-13, IL-17A, IL-18, TNF-α, RANTES/CCL5, IL-7	(D. Huang *et al.*, 2014; Cai & Wei, 2013; Ujhelyi *et al.*, 2012)
Aniridia	Proteins	Zinc-α2-glycoprotein, Lactoferrin, VEGF, Ap4A and Ap5A	(Peral *et al.*, 2015; Ihnatko *et al.*, 2013)

Disease	Type of molecule	Molecules	References
Glaucoma	Proteins	BDNF, Immunoglobulins, PIP, lysozyme C, LCN-1, protein S100, Lactotransferrin, PRP4, PIP, Zinc-alpha-2-glycoprotein, Polymeric immunoglobulin receptor, Cystatin S, Ig kappa chain C region, Ig alpha-2 chain C region, Immunoglobulin J chain, Ig alpha-1 chain, MUC5AC, Hcy	(Pieragostino *et al.*, 2013; Pieragostino *et al.*, 2012; Liu *et al.*, 2010; Ghaffariyeh *et al.*, 2009; Roedl *et al.*, 2008)
ROP	Proteins	C3, MMP2, and MMP9	(Rathi *et al.*, 2017)

1.1.2. Components involved in retinal neurovascular development

A focused overview of physiological function of retina and vitreous that plays an important role on visual functions is as follows:

The human retina is metabolically very active tissue and utilizes higher oxygen than the brain. The retina is comprised of a complex array of cells and highly organized vasculature to perform its functions. The retinal blood supply is from two sources, i.e., central artery and choroidal vessels and these both are originated from the ophthalmic artery. Until the 16th week of gestation age, the outer retina gets nourishment from choroidal blood vessels (Gonzalez-Fernandez, 2011). The normal retinal blood vessels reach the nasal side of the retina and further reaches the temporal region by the 36th week of GA, followed by regression of hyaloid vessels. At this time, the vessels from the central artery supply blood to the inner portion of the retina. This central artery is divided into two major trunks; each subdivides to form superior/inferior nasal and temporal arterial branches (Anand-Apte & Hollyfield, 2010). The branches from the central artery create two distinct networks: the GCL and the INL. Vessels grow 1–2mm from the optic disc during the 6th month and they continue to move outward towards the ora Serrata until around the 8th month (Anand-Apte & Hollyfield, 2010). These large arteries divide with small diameter until it reaches to ora Serrata, the retinal venous blood vessel branches are distributed in the same manner as arterial branches (Anand-Apte & Hollyfield, 2010). In the inner retina, these small arteries and venules form the dense capillary network.

Several studies have been performed to identify the potential disease prediction biomarkers for retinal diseases like ROP using biological fluids like plasma and serum. But they might not predict the localized molecular events of retinal pathogenesis. Several studies have also tried to evaluate retinal proteome using oxygen-induced retinopathy animal models to explore the potential molecular biomarker identification. However, the underlying molecular events in ROP

pathogenesis are still not completely understood. The localized molecular events can be better understood by analyzing the tissues present near the retina. The vitreous humor is preferred ocular tissue for such studies as it is present in close proximity to the retinal microenvironment. It can serve as an important starting material for the investigation of molecular mechanisms behind the pathogenesis of ROP.

1.1.3. Vitreous Humor

The human vitreous provides continuous support to the eye and is a reservoir for nutrients and metabolic factors. It maintains transparency to facilitate the entry of light into the retina. Due to its acellular, hydrated, viscous nature, it forms a transparent cavity behind the lens that enables light access into the retina on the posterior side.

1.1.3.1. Embryological development of vitreous

The human embryonic development of vitreous takes places in 3 stages (Figure 5), these stages are explained in the sections below:

1.1.3.1.1. Primary vitreous

The vitreous is formed between the lens and ILM of the retina. The lens vesicle occupies the majority of the optic cup at the embryonic stage. As the cup develops, a cavity called the vitreous cavity develops, which is filled with fibrillary material secreted primarily by the embryonic retina's neuroectoderm cells and partially by the developing len's ectodermal cells. The mesodermal cells infiltrate the cavity during the fourth week of pregnancy and differentiate into the hyaloid artery and its branches, known as the vasa hyaloidae propria (Pollard, 1997). As the hyaloid artery is formed at the 4th-5th week of gestation, more fibrillary material originates from the mesodermal cells of the artery and contributes to filling the space. This combined mass of the vitreous cavity is known as primary/primitive vitreous (Sang, 1987; Swann, 1980).

1.1.3.1.2. Secondary vitreous

It is produced from neuroectoderm of optic cup from 6 to 12 weeks of gestational age, the hyalocytes migrates along with increase in size of vitreous cavity (Newman & Reichenbach, 1996).

1.1.3.1.3. Tertiary vitreous

In the 4th month, tertiary vitreous is derived from the neural ectoderm (surface epithelium) of the ciliary body and shrinks into the individual zonules (Ishikawa *et al.*, 2010; Sang, 1987).

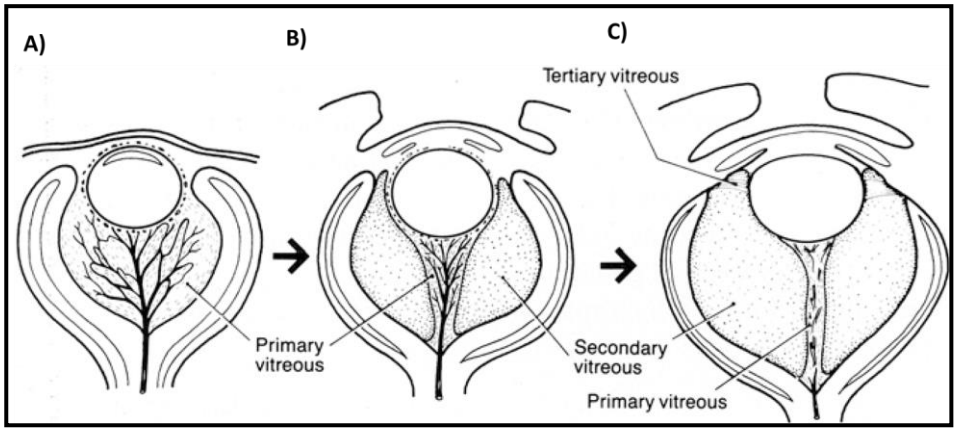

Figure 5. Stages of vitreous development. A, Primary vitreous and hyaloid vessels nourishing the embryonic lens. B, the secondary vitreous laid down around the primary vitreous, which condenses into Cloquet's canal. The secondary vitreous will become the adult vitreous. C, Tertiary vitreous (lens zonules or ligaments) at the lens periphery. Adapted from (Sang, 1987)

1.1.4. Anatomy, biochemistry and physiology of vitreous

Anteriorly vitreous is attached to the ciliary body, lens, zonules and posteriorly to the retina, macula and optic nerve. The human vitreous contains 98-99% water and the remaining is the mixture of proteins, hyaluronan (HA), proteoglycans, metabolites, lipids, salts, etc. Collagens are the most abundant protein in the vitreous. Among all collagens types, collagen II is the major one and is about ~75% of total collagen present in the vitreous (Seery & Davison, 1991), others collagens types being collagen V/XI and IX. These collagen fibrils are formed from a core of collagen V/XI, surrounded by type II collagen. The glycosaminoglycan's (GAGs) fill and connect the gap between the fibrils. (Bishop, 2000).

Along with hyaluronic acid, small leucine-rich repeat ECM proteins called Opticin also coats the collagen fibrils to maintain the short-range fibril spacing via binding to different GAGs (Figure 6). The GAG of chondroitin sulfate binds to collagens and Opticin to maintain enough space between the collagen fibrils. While the GAG keeps the spacing between collagen fibrils, the Opticin minimizes light scattering and supports transparency, thus providing an unhindered passage for light to enter into the retina.

In addition to these components, the vitreous also contains the hyalocytes and fibroblast cells. Hyalocytes are highest in number, oval/spindle-shaped cells located in the vitreous cortex, which form a unique 20-50μm single layer from the ILM of the retina to the vitreous base. Fibroblasts are the second-highest cells present in the vitreous, located cells are located in the vitreous base and optic disc; they synthesize glycosaminoglycans and collagen. A healthy vitreous total protein concentration is calculated as 0.5 mg/ml, and the major proteins in the vitreous other than collagen are albumins (60-70%), globulins, ECMs etc. (Ulrich *et al.*, 2008).

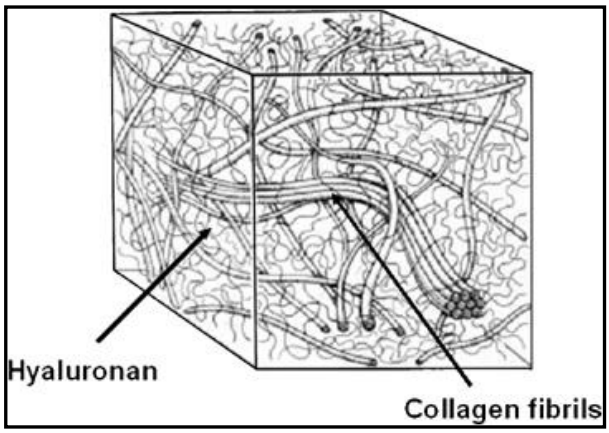

Figure 6. A schematic representation of collagen network responsible of vitreous for the gel structure, adapted from (Le Goff & Bishop, 2008)

1.1.5. Importance of vitreous for studying the retinopathy

The human vitreous is nourished by retinal vessels and the ciliary body. The pathological change in the retina is clearly reflected in the vitreous protein content (Wu *et al.*, 2004). The BRB restricts the entry of blood proteins, ions and metabolites into the retina and maintains

retinal integrity. The BRB breakage facilitates blood proteins and other inflammatory cytokines into the vitreous cavity and the retina. Most importantly, as vitreous is adherent to the retina therefore, any biochemical/molecular/metabolic alteration in the retina would affect vitreous composition While obtaining human retinal tissue to understand biochemical/molecular/metabolic alterations in ROP pathogenesis is impossible, the vitreous samples can be collected from ROP probands undergoing vitrectomy being done for the routine clinical management. Studying the vitreous proteome from these babies can definitely help in understanding the pathological events in retina in ROP infants.

1.1.6. Fibrovascular membrane formation and chemistry

The fibrovascular membranes are localized adjacent to the vitreous, and sandwiched between the vascular and avascular region of the retina. The fibrovascular membrane have increased thickness and width in the ridge formed in acute ROP cases (stage 2 plus to stage 3 ROP). The ridge membrane thickness and proliferation are gradually increased by numerous growth factors such as the HGF, VEGF and PDGF. These growth factors induce the cellular proliferation and migration of these cells from the ridge and into the vitreous, leading to the formation of the whitish vitreous membrane termed as a fibrovascular membrane. The molecular organization of the fibrovascular membrane is also associated with retinal detachment in severe ROP cases. This fibrovascular membrane binds to the anterior retina, lens and zonules and when it shrinks, it causes traction resulting in the detachment of retina from peripheral end.

1.1.6.1. Components of membrane

In stage 2 ROP, the demarcation line thickness increases and widen to form the ridge membrane, which acts as the barrier for the fibrovascular formation and followed by retinal detachment. This membrane led to the progression of the fibrovascular membrane from the ridge into the vitreous cavity. The fibrovascular membrane is composed of organized actin filaments and the

myofibroblast-like cells within it. These myofibroblast-like cells play a vital function in the vitreoretinal traction in ROP. During vitrectomy/membrane peeling surgery for ROP management, once the lens is removed, the whitish vitreoretinal membrane can be visualized clearly. The retinal surface membranes are further dissected starting from periphery then going towards the centre (Soong *et al.*, 1985).

The transmission electron microscopy has also been used in some studies to understand the key morphological features of retinal fibrovascular membranes. These studies confirmed the presence of myofibroblast-like cells such as fibroblast and smooth muscle cells (SMC) within it. The fibroblast cells were found to be enriched with rough endoplasmic reticulum. Few reports from the literature have also shown glia and microglia cells, pigment granules and lipid bodies in these membranes (Soong *et al.*, 1985). The retina consists of three major glial populations, such as astrocytes, Müller glia and retinal microglia.

Astrocytes and Müller glia are the retinal macroglial population and they share many common features due to homogeneity in their origin. But the role of macroglia and microglial cells in ROP is not clearly understood to date.

1.1.6.2. Glial cell and role of microglia in healthy retina

Human retina contains three major types of glial cell populations: muller cells, astrocytes and microglia. These cell types are explained below:

1.1.6.2.1. Möller glia

These cells are formed from multipotent retinal progenitor cells and neuroepithelium during the developmental process (Jadhav *et al.*, 2009). Müller glia is located from the OLM to ILM and provides functional connections, retinal neurons, vasculature and vitreous body. These cells play an indispensable role in homeostasis, metabolism, prevent neurons from amino acid and neuronal

survival (glutamate and γ-aminobutyric acid) (GABA) (Newman & Reichenbach, 1996) (Sorrentino *et al.*, 2016; Bringmann *et al.*, 2013; Sweetnam, 1976). The branched muller glia cells closely interact with blood capillaries and act as a barrier for the exchange of metabolites between the retinal vasculature and neurons (Vecino *et al.*, 2016).

1.1.6.2.2. Astrocytes

These are macroglia cells of CNS originating from neuroepithelium in the developmental process, and provides biochemical support to the endothelial cells besides forming the BRB. In the human retina, these cells reside in the innermost layer, i.e., the nerve fiber layer. The neuroretina acts as a scaffold for blood vessel development, synaptic transmission and neuronal function.

1.1.6.2.3. Microglia

These are primary resident immune cells present in the eye (Sierra *et al.*, 2016). These cells are of mesodermal origin and are derived from hematopoietic stem cells. They enter into the retina through blood circulation and distinguish into ramified parenchymal microglia at the time of development. Microglia have two forms; inactivated ramified shaped and activated amoeboid shaped microglia cells (Chen *et al.*, 2002). In the normal retinal layers, these microglia cells are located in GCL, IPL and OPL with ramified projection. These ramified-shaped microglia cells play a crucial function in surveillance of contact neuronal synapsis to monitor their functional status. Microglia cells also secrete several proteins, chemokines and cytokines to maintain retinal homeostasis.

Under stress conditions, these resting microglia cells become activated and acquire an amoeboid shape. They express several receptors for cellular activity on its surface and abundantly release chemokines and cytokines to restore homeostasis. Activated microglia cells have the migratory property to move at the site of injury (Hume *et al.*, 1983; Wake *et al.*, 2009). Their beneficial or

detrimental effects to the residual cells/tissues are correlate with the extent of microglial activation (Kettenmann *et al.*, 2011) (Figure 7).

Microglia cells perform a crucial function in neuronal growth and maturation (axon regulation by their role in synaptic pruning). Additionally, microglia are also required in the retinal blood vessel formation, during development and for neuronal survival. Activated microglia in the retina may affect synapse formation and pruning of neurons and the overall retinal homeostasis (Wang *et al.*, 2016). Activated microglia can adopt M1 phenotype or M2 phenotype. The pro-inflammatory cytokines, such as TNF-a, IL (1ß, 6, 12, 23) and MMPs, etc. are secreted by M1 type microglia cells. In contrast, M2 type microglia cells display anti-inflammatory properties by secreting the anti-inflammatory cytokines such as, arginase-1, IL (10, 4, 13) (Martinez *et al.*, 2009; Martinez & Gordon, 2014).

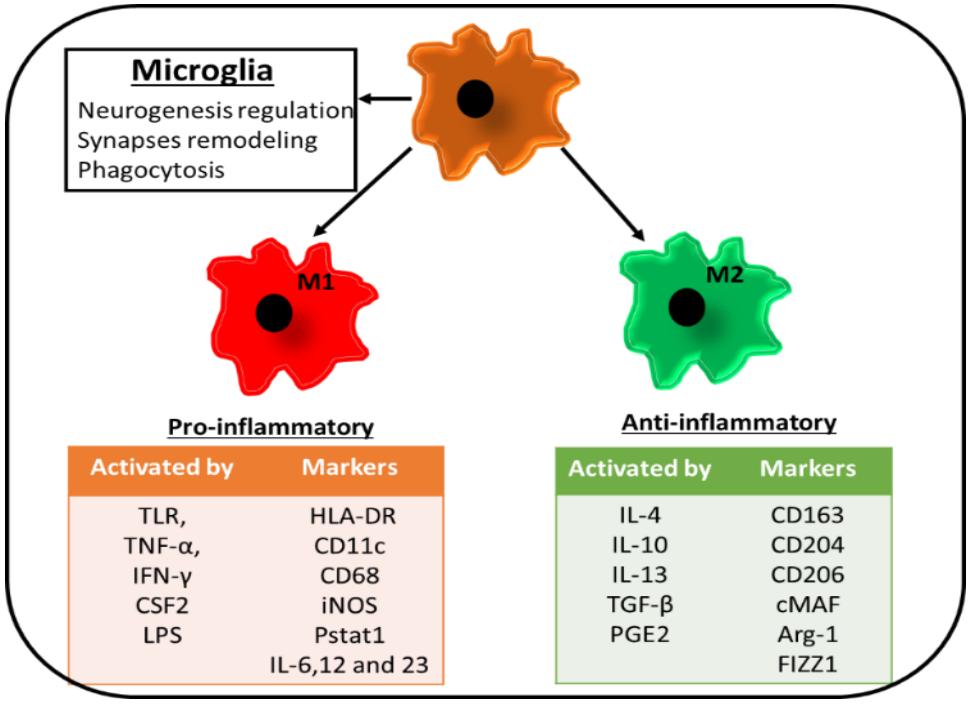

Figure 7. Polarizing agents, phenotypic markers and secreted cytokines and chemokines in M1 and M2 microglia based on microglial phenotypes

1.1.7. Microglia in retina

The microglia cells originate from the primitive yolk sac progenitors (Alliot *et al.*, 1999; Ashwell, 1990). These microglia enters from the circulatory system into CNS. Several transcription factors and cytokines regulate microglia cell survival.

1.1.8. Role of microglia in ROP

It is unclear why ROP regresses on its own in some preterm infants while developing to severe stages in others. To address this, we looked into the molecular mechanisms of ROP pathogenesis in previous work by a targeted genetic screening. This investigation found a significant link between ROP and complement genes like *C3*, *CFH* and *CFB* and ECM genes like *FBLN5*, *MMP2* and *TGF* genes. The strong associations of these genes in our ROP cohort suggested that the alternative complement pathway may be involved in ROP. Using ELISA, we assessed the target proteins to see whether complement proteins were involved in ROP. In the vitreous of ROP patients, VEGF, C3, C4 and CFH levels were substantially increased. Western blotting confirmed the complement activation in ROP. When comparing ROP patients to controls, intense bands of C3 fragments were observed. Because of immature immune systems, in preterm infants, complement factors are known to be downregulated. However, complement factors were shown to be elevated and activated in ROP infants. The results from this study has indicated a major role of complement pathway in ROP pathogenesis (Rathi *et al.*, 2017).

Moreover, H&E of ROP vitreous revealed the presence of activated macrophages/microglia, which was validated by immunostaining with CD68, a macrophage marker. Based on a literature search on the role of the activation of macrophages and microglia in inflammation. We hypothesized that higher expression of complement, VEGF and MMPs in the vitreous of ROP eyes is driven by activated macrophage/microglia. We also used multiplex ELISA to measure ECM proteins to see if they were involved. The levels of α2 macroglobulins, MMP9 and TIMP1 in the ROP vitreous were

found to be significantly higher. This indicates that microglia and MMP mediated inflammation causes neovascularization in ROP. Therefore, MMPs could be used as a biomarker for the progression of ROP (Rathi *et al.*, 2017).

The microglia cells are involved in both physiological and pathological events occurring in the retina. The activation of the retinal microglia, leads to aberrant retinal vascular development (Tremblay *et al.*, 2013). The microglia cells activated under hypoxic stress produce elevated levels of inflammatory cytokines, leading to the degeneration of the axonal, oligodendrocyte's death and BRB disruption (Kaur *et al.*, 2013). VEGF, MMPs and other inflammatory and angiogenic proteins secreted by microglia shows a significant function in expanding the retinal vasculature (Konnecke & Bechmann, 2013).

1.1.9. Hypoxia and other signaling pathways in ROP pathogenesis

Retinal ischemia/hypoxia is one of the major factors contributing to the disease causation however, the molecular and signaling mechanisms under hypoxia that are involved in the neovascularization of ROP are still not very well understood. Hypoxia refers to the low oxygen tension and the hypoxia signaling pathway gets activated by stabilization HIF1-α. Under normoxic condition, O_2 dependent prolyl-4-hydroxylases (PHDs) hydroxylate HIF-residues. E3 ubiquitin ligase, i.e., Von Hippel–Lindau protein (pVHL), adhere to OH-HIF1-α subunit. These E3 ubiquitin ligases and HIF-α substrate complex lead to HIF proteasomal degradation. The hydroxylation of HIF-ASP residues facilitates inhibition of HIF along with other co-activators (p300/CREB-binding protein) by factors inhibiting HIFs. In hypoxia, PHDs and FISHs activity gets suppressed, and HIF-1β translocates into the nucleus and forms HIF1-α: HIF-1β heterodimer complex. This complex then targets genes of hypoxia-responsive elements (HREs), which further leads to transcriptional upregulation of target genes (*VEGF, Glut-1, eNOS, EPO*, etc.) (Figure 8).

The angiogenic molecules such as the HIF1-α, ECM, and VEGF could act directly/indirectly to activate the retinal angiogenesis (Vadlapatla *et al.*, 2013; Krock *et al.*, 2011; Korpos *et al.*, 2009). ECM components are one of the most important targets in retinal angiogenesis and inflammation; the current study is aimed to understand the role of ECM proteins in ROP pathogenesis.

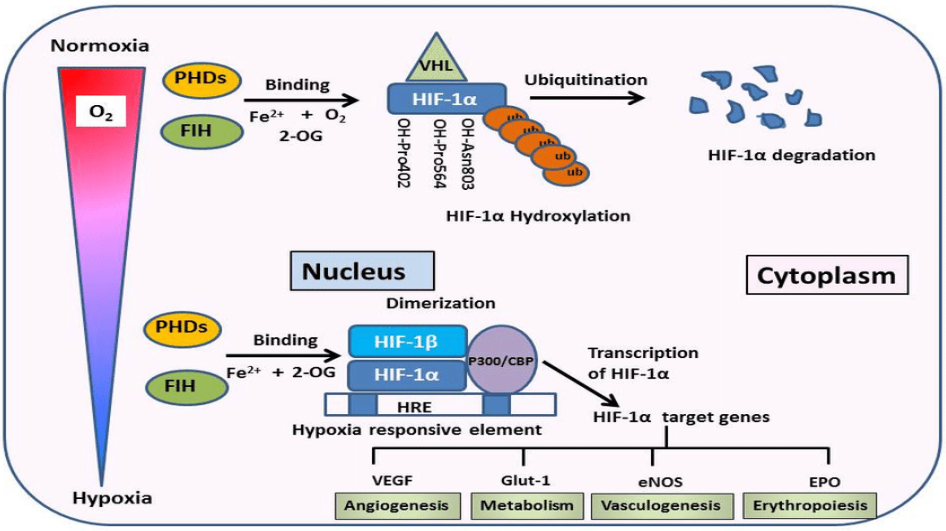

Figure 8. HIF-1α signalling pathway under normoxia and hypoxia, adapted from the (Devraj *et al.*, 2017)

1.1.10. Role of ECM proteins in angiogenesis

ECM act as a scaffold for cells to grow and thereby support cell proliferation and differentiation. It is one of the central reservoirs of the cells. It contains a network of macromolecules such as collagen, glycoproteins, etc., to support the cells. Studies have shown that ECM undergoes reorganization along with related structural changes under the disease conditions such as tissue fibrosis, inflammation and neovascularization (Arroyo & Iruela-Arispe, 2010; Korpos *et al.*, 2009; Wynn, 2008). There is loss/gain of function of homeostatic regulators of ECs, followed by activated migration and proliferation of endothelial by degradation of capillary basement membrane (Senger & Davis, 2011; Klagsbrun & Moses, 1999). These events of tissue remodeling and migration involve the proteolysis of ECM by matrix metalloproteases (MMPs).

1.1.11. Matrix metalloproteases (MMPs)

MMPs are Zn-dependent endoproteases enzymes responsible for ECM degradation, including collagens, elastins, gelatin, matrix-glycoproteins and proteoglycans. Several cytokines and cell surface molecules released by the cells come across the ECM, which are involved in physiological and pathological conditions like wound healing, angiogenesis, inflammation, tumor metastasis, etc. (Spinale, 2002; Nagase & Woessner, 1999; Werb, 1997) (Figure 9).

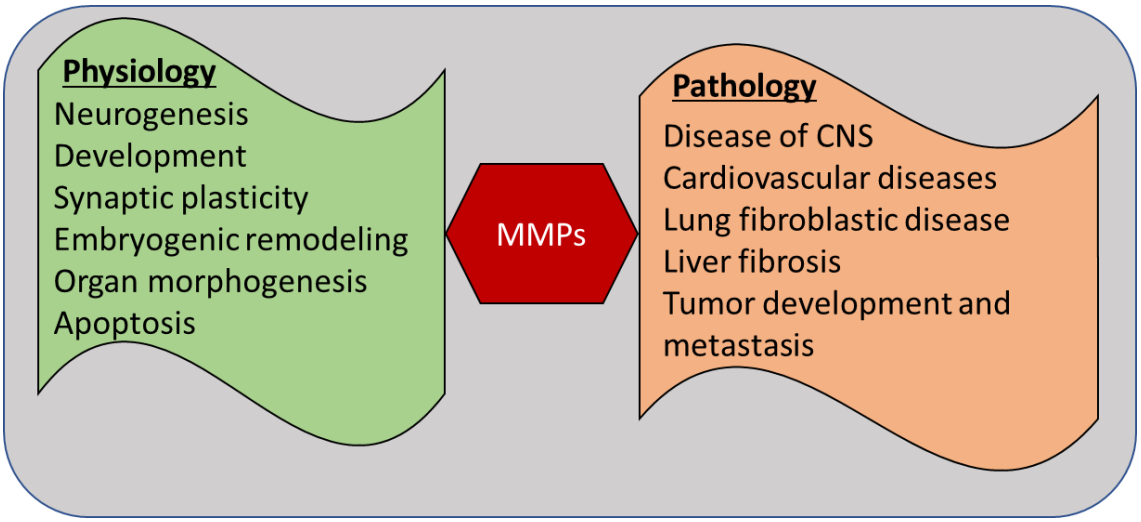

Figure 9. MMPs in physiological and pathological conditions

MMPs contain the three structural domains: (a) the propeptide domain, (b) the catalytic domain, and (c) the C-terminal (hemopexin-like) domain (Figure 10). MMPs are classified based upon their structure and/or their specific substrates (Table 4). MMP2 and MMP9 are associated with several retinal diseases like AMD and DR. (Chau *et al.*, 2008; Schulz *et al.*, 2004; Lambert *et al.*, 2003). The MMP2 and MMP9 act on type IV collagen leading to vitreous liquefaction (Coral *et al.*, 2008; Roach *et al.*, 2002). The activation of MMPs by plasminogen activator under stress conditions digest the ECM membrane and basement membranes. (Liekens *et al.*, 2001; Mignatti & Rifkin, 1996) . Plasmin cleaves pro-MMPs (pro-enzymes) and produces active MMPs regulated by tissue inhibitors of metalloproteinases (TIMPs).

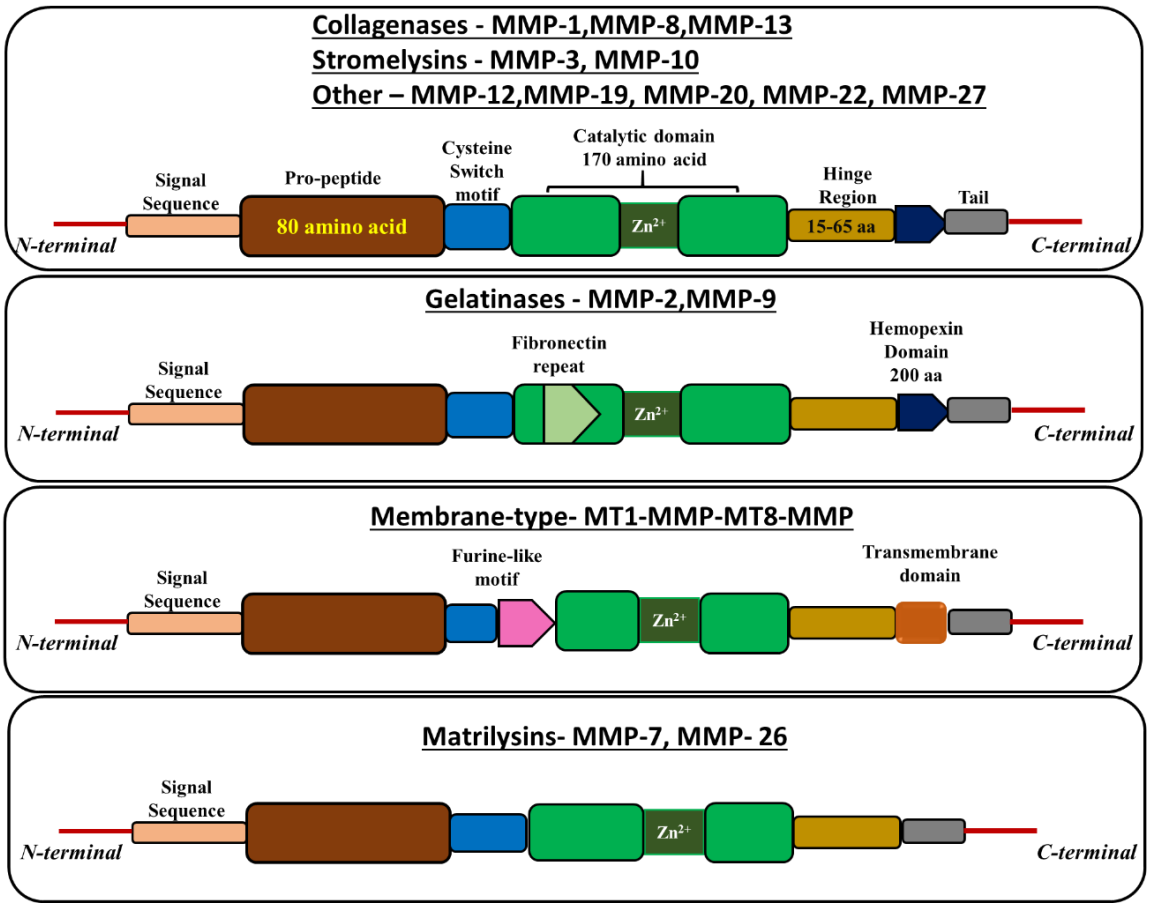

Figure 10. Domain Structure of different MMPs

MMPs are regulated at different levels like transcription, secretion and activation. Several factors, including the cytokines, hormones and growth factors, induce the MMPs expression under stress conditions. (Nagase & Woessner, 1999; Massova *et al.*, 1998; Nagase, 1997). Thus, regulation of MMP's activities might have therapeutic implication for checking retinal neovascularization in retinopathies. However, the precise roles of specific MMPs and their inhibitors in ocular pathologies needs to be explored further. A study by Barnett *et al.* (2007) showed a significant reduction of retinal neovascularization in an OIR model of pharmacologically altered rat with MMP inhibitors administration and MMP2 knockout mouse. This study described the potential function of MMP9 in angiogenesis in the retina. (Barnett *et al.*, 2007).

Table 4. Classification of MMPs and its substrates

Enzyme	Classification	Substrate
MMP-1	Collagenase	Collagens I, II, III, VII, VIII, X, and XI, gelatin, entactin, tenascin, aggrecan, fibronectin, vitronectin, myelin basic protein, ovostatin, casein, MMP-2, MMP-9, proMMP-2, proMMP-9
MMP-8	Collagenase	Collagen I, II, and III, fibronectin, PGs, aggrecan, ovostatin
MMP-13	Collagenase	Collagens I, II, III, IV, IX, X and XIV, gelatin, tenascin, plasminogen, osteonectin, fibronectin, aggrecan, casein
MMP-18	Collagenase	Collagen, gelatin
MMP-2	Gelatinase	Collagen I, III, IV, V, VII and X, gelatin, fibronectin, laminin, aggrecan, elastin, vitronectin, tenascin, myelin basic protein
MMP-3	Stromelysins	Collagen III, IV, V, IX, X and XI, gelatin, aggrecan, elastin, fibronectin, vitronectin, laminin, entactin, tenascin, decorin, myelin basic protein, ovostatin, casein, osteonectin, proMMP-1, proMMP-3, proMMP-8, proMMP-9
MMP-9	Gelatinase	Collagen IV, V, XI, elastin, aggrecan, decorin, laminin, entactin, myelin basic protein, casein
MMP-10	Stromelysins	Collagens III, IV and V, gelatin, elastin, fibronectin, aggrecan, casein
MMP-11	Stromelysins	Gelatin, fibronectin, collagen IV, laminin, elastin, casein, PGs
MMP-27	Stromelysins	Gelatin
MMP-7	Matrylisin	Collagens I and IV, gelatin, elastin fibronectin, vitronectin, laminin, entactin, tenascin, aggrecan, myelin, proMMP-1, proMMP-2, proMMP-9 transferrin, casein
MMP-26	Matrylisin	Collagen IV, gelatin, fibronectin, fibrinogen, pro-MMP9
MMP-14	MT-MMP (membrane type)	Collagen I, II and III, gelatin, fibronectin, tenascin, vitronectin, laminin, entactin, aggrecan, vibronectin, pro-MMP2
MMP-15	MT-MMP (membrane type)	Fibronectin, tenascin, entactin, laminin, aggrecan, gelatin, vibronectin, pro-MMP2
MMP-16	MT-MMP (membrane type)	Collagen III, gelatin, fibronectin, casein, laminin, pro MMP-2
MMP-17	MT-MMP (membrane type)	Gelatin, fibrinogen, pro MMP-2
MMP-24	MT-MMP (membrane type)	Fibronectin, gelatin, proteoglycans, pro-MMP2
MMP-25	MT-MMP (membrane type)	Collagen IV, gelatin, fibronectin, proteoglycans, pro-MMP2
MMP-12	Other Enzymes	Collagens I, V and IV, gelatin, elastin, fibronectin, vitronectin, laminin, entactin, osteonectin, aggrecan, myelin, vitronectin, fibrinogen
MMP-19	Other Enzymes	Collagen I and IV, gelatin, lamin, entactin, fibronectin, aggrecan.
MMP-20	Other Enzymes	Amelogenin, aggrecan.
MMP-21	Other Enzymes	N.D.
MMP-23	Other Enzymes	Gelatin
MMP-28	Other Enzymes	Casein

1.1.12. MMPs inhibitors

TIMPs are the key regulator of MMP's activity by inhibiting its activation. The maintenance of the MMPs/TIMPs ratio is an important aspect of the homeostatic balance of the tissues. Besides these, several synthetic MMPs inhibitors are available, such as Batimastat (BB94), Narimastat (BB-2516), Bryostatin 1, Doxycycline, EDTA, etc. Among these, doxycycline and EDTA have been widely used as inhibitor of the MMPs activity.

1.1.12.1. Doxycycline

It is FDA approved tetracycline derived antibiotic drug for inflammatory conditions. It shows anti-inflammatory properties by regulating MMPs activity either at transcriptional and translational levels (Jonat *et al.*, 1996) (Figure 11).

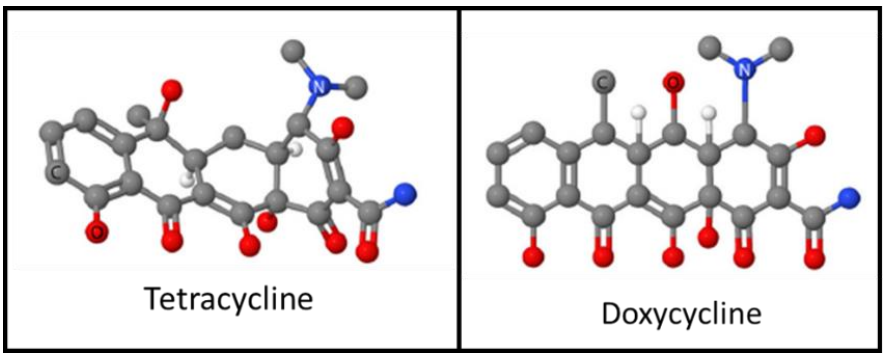

Figure 11. Chemical structure of tetracycline and doxycycline

The secretion of MMPs can be inhibited by doxycycline via inhibition of nitric oxide (NO) (Amin *et al.*, 1996). It shows anti-inflammatory property, by downregulating the transcription/synthesis of MMP9 (Jonat *et al.*, 1996).

1.1.12.2. EDTA

Ethylenediaminetetraacetic acid (EDTA) is an amino polycarboxylic acid. It inhibits MMP activity by chelating iron and calcium ions from MMP active site. Topical EDTA, which inhibits MMPs, has been used to treat corneal ulcers with promising results (Brooks & Ollivier, 2004) (Figure 12).

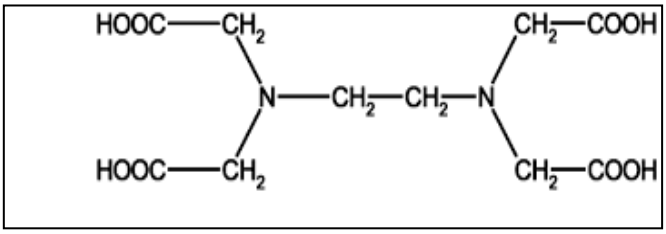

Figure 12. Chemical structure of EDTA

1.1.13. Opticin

Opticin is an ECM protein discovered in bovine vitreous by Reardon and co-workers (2000). It belongs to class III of small leucine-rich repeat proteins SLRPs (Reardon *et al.*, 2000; Iozzo, 1999). These SLRPs are classified into 5 different classes, as shown in Figure 13.

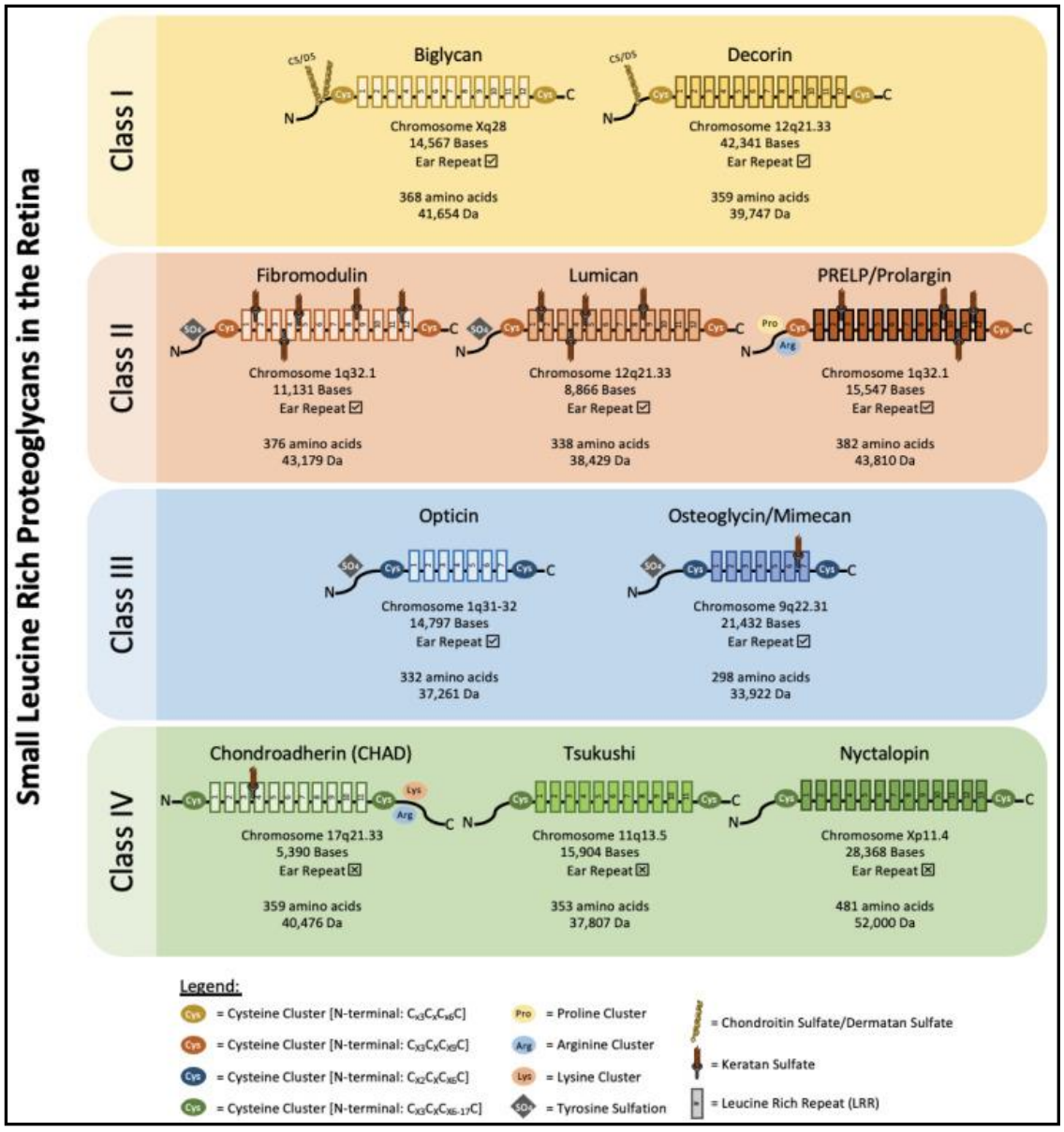

Figure 13. Classification of SLRPs adapted from the (Low *et al.*, 2021)

SLRPs have diverse functions in the ECM by regulating the assembly of collagens and maintenance of cellular proliferation and growth (Iozzo, 1999). Opticin has been immunolocalized to the

vitreous cavity, ILM and lens. The non-pigmented ciliary epithelium (NPE) is responsible for production of Opticin (Ramesh *et al.*, 2004; Bishop *et al.*, 2002) into the vitreous cavity. Further the Opticin protein has been shown to interacts with collagen and helps in the maintenance of the jelly-like state of the vitreous (Ramesh *et al.*, 2004; Bishop, 2000).

Opticin is expressed in the choroid, retina, vitreous, cornea, iris and ciliary body (Friedman *et al.*, 2002). It performs diverse functions in the retina. Growth hormones (GH), secreted by retinal ganglion cells (RGC) interacts with Opticin present in the vitreous cavity and has a paracrine effect on ocular development (Sanders *et al.*, 2003). Opticin interacts with heparin sulfate in the ILM of the retina (Ramesh *et al.*, 2004) and chondroitin sulfate in the vitreous cavity for stabilization of the vitreous jelly-like consistency (Hindson *et al.*, 2005). The few studies done on Opticin to characterize its functions are described in below Table 5.

Table 5. Role of Opticin

Disease model	Key findings on Opticin role	Reference
Embryonic day-8 chicks	Opticin binds retinal growth hormone in the embryonic vitreous	(Sanders *et al.*, 2003)
Human RPE cells	The effect of VEGF and hypoxia on the secretion of Opticin	(Ma *et al.*, 2011)
Solid-phase Opticin binding assay	Opticin binds to heparan and chondroitin sulfate proteoglycans	(Hindson *et al.*, 2005)
Ex-vivo chick chorioallantoic membrane assay	Antiangiogenic activity by regulating ECM matrix	(Le Goff, Sutton, *et al.*, 2012)
An Opticin knockout mouse	Opticin Inhibits Preretinal Neovascularization	(Le Goff, Sutton, *et al.*, 2012)
Human RPE Cells	Opticin production is reduced by hypoxia and VEGF in human retinal pigment epithelium via MMP-2 activation	(Le Goff, Lu, *et al.*, 2012)

1.1.14. Correlation of MMPs activity associated with Opticin expression

In the retina and vitreous, activated microglia produce activated pro-inflammatory signaling molecules and MMPs (Rathi *et al.*, 2017). The activated MMPs are responsible for the ECM degradation, which in turn promote angiogenesis. Goff and co-workers have shown that Opticin, a small leucine rich glycoprotein exhibits anti-angiogenic properties in a murine oxygen model (Le Goff, Sutton*, et al.*, 2012). The Opticin-knockout mice displayed an increased neovascularization in comparison to the wild-type mice (Le Goff, Sutton*, et al.*, 2012). In osteoarthritic (OA) cartilage, Opticin acts as a substrate for several MMPs that causes proteolytic degradation of intact Opticin (Tio *et al.*, 2014) (Figure 14).

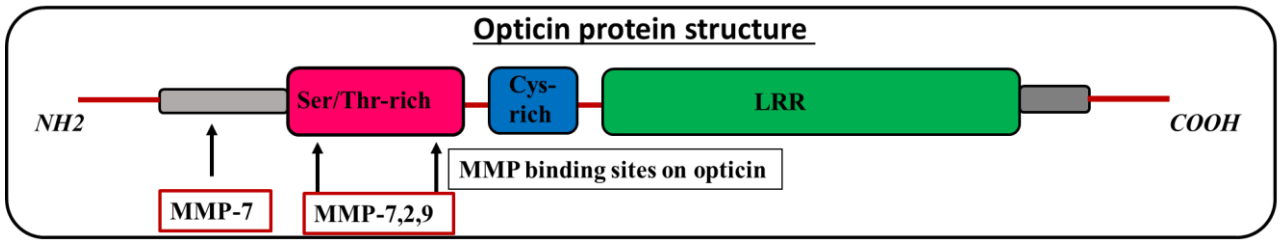

Figure 14. Schematic representation of the cleavage sites generated by the digestion of recombinant human Opticin with MMPs (adapted and modified from the (Tio *et al.*, 2014))

Our earlier study showed that increased expression of complement proteins and MMPs in ROP babies is due to infiltration of activated microglia/macrophages in the vitreous (Rathi *et al.*, 2017). ROP ridge membrane analysis found endothelial cells, proliferating cells, glia and microglia (Sun *et al.*, 2010). However, the precise function of these glial cells and microglia in ROP is still not clear. The activated MMPs, cytokines and other pro-inflammatory markers secreted by microglia into the vitreous and retina may promote angiogenesis by causing ECM breakdown. In an unpublished study on vitreous proteome profiling analysis of ROP patients, we have found a reduced expression of Opticin. Opticin protein is abundantly present in the human vitreous and it is also continually released into the vitreous by nonpigmented ciliary epithelium cells (Bishop *et al.*, 2002; Takanosu *et al.*, 2001). Opticin associates with collagen fibrils and retinal growth hormone (RGH) in vitreous humor (Sanders *et al.*, 2003). Opticin, an anti-angiogenic protein, was found in a murine OIR and a

cell culture model (Le Goff, Sutton*, et al.*, 2012), (Le Goff, Sutton*, et al.*, 2012). Based on this background, we hypothesized that increased activity of MMPs can explain the reduced expression of Opticin in ROP eyes and act as biomarker for ROP progression.

Specific objectives of the study are:

1) To assess if the inflammatory molecules in tear could be used as potential predictive marker for ROP.
2) To study if targeting inflammation can maintain the homeostatic balance in the retina and thereby prevent abnormal angiogenesis.

1.2. Methods

1.2.1. Vitreous humor and tear collection

50 to 100µL of vitreous humor was collected from infants at stage 4/5 ROP, during the vitrectomy surgery done as part of clinical management of ROP, in a sterile 1.5mL of cryovials and then immediately transported to the laboratory on ice. The detailed inclusion and exclusion criteria of the study participants are given in Table 6, and a copy of the ethics committee approved informed consent form executed in the study is attached (Annexure I). Vitreous samples were centrifuged at 12,000g for 10 minutes at 4°C to remove cellular debris. The supernatant was collected into a new vial and utilized for further experiments. The vitreous samples were lysed with an equal volume of RIPA lysis buffer. After that, four volumes of ice-cold acetone were added into the solution and incubated overnight at -80°C for precipitation. The samples were centrifuged at 14,000g for 30 minutes at 4 degrees Celsius after incubation. The supernatant was discarded without disturbing the pellet. The pellet was dissolved in 30µL of 1x PBS solution containing a protease inhibitor cocktail. Total protein was quantified by a BCA (Bicin Choninic acid Assay) assay.

Table 6. Inclusion and exclusion criteria for ROP sample collection

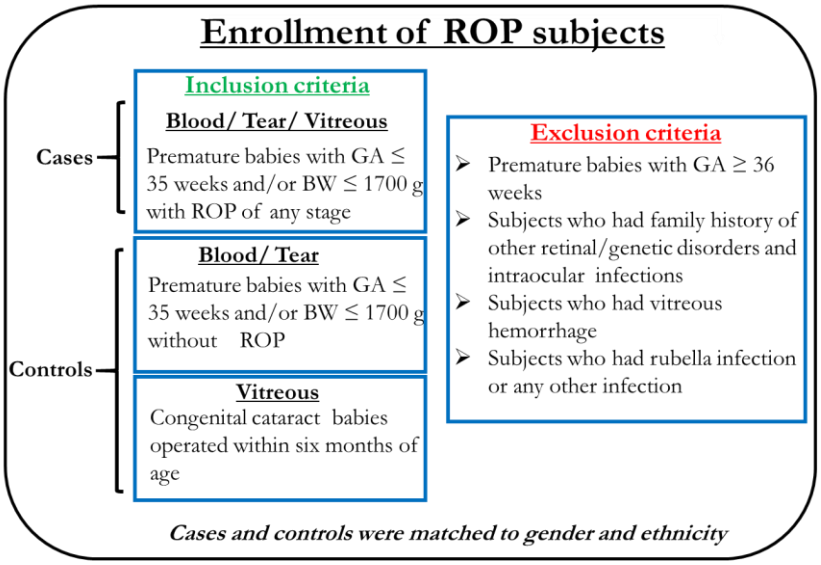

For tear protein analysis, 5-10µL of tear samples were collected from prematurely born babies with ROP (age < 1year, n=5) and without ROP in fresh 1.5 ml centrifuge tube using micro glass capillaries. These samples were transported to the laboratory immediately on ice. Further to eliminate cellular debris (if any), the samples were centrifuged at 12,000g for 10 minutes at 4°C. The supernatant was transferred to a new vial and stored till next use.

1.2.2. Protein estimation and normalization by BCA method

BCA is a biochemical assay used for the estimation of total protein. The basic principle behind protein concentration detection is based on Cupric ions (Cu^{2+}) are reduced to cuprous ions (Cu^{1+}) in an alkaline solution. The cysteine/cystine, tyrosine and tryptophan four major amino acids present in the proteins causes the reduction of copper and results into the formation of purple color which can be detected as absorbance at wavelength 595nm by using colorimetry.

1.2.3. Procedure for BCA assay

- 2 mg/mL BSA (bovine serum albumin) stock was prepared and 9 standards were made by serial dilution following the protocol provided in the kit.
- The test samples were diluted in 1:10 ratio with diluent (proteinase inhibitor cocktail containing water) and along with the blank pipetted into a 96 well plate in triplicate in their corresponding wells.
- Working reagents, A & B were mixed freshly by mixing in the ratio of 1:50 respectively (BCA working reagent)
- After adding 200µL of working reagent to all the wells, plate was covered with aluminum foil (light sensitive) and kept at 37˚C for 20 minutes.
- Protein concentration was calculated by taking the OD at absorbance maximum at 595nm using spectrophotometer.

1.2.4. Assessment of MMPs and inflammatory cytokines in tears of ROP patients for by multiplex ELISA and zymography

Tear samples diluted (1:10) to a final volume of 25μL were used for the assessment of Human Cytokine/Chemokine and MMPs by multiplex ELISA. The first magnetic bead panel included VEGF, EGF, IFN-γ, IL-10, TNF-α, MCP-1, PDGF-βB, IL-1α, IL1-b, IL-6, IL-8 while other MMP bead panel included MMP2, MMP8, MMP9 markers by multiplex ELISA.

1.2.5. Multiplex ELISA

MILLIPLEX® MAP High sensitivity human cytokine and MMP Panel is a magnetic bead-based antibody microarray working on the principle of sandwich immunoassay. The detailed protocol mentioned below Figure 15.

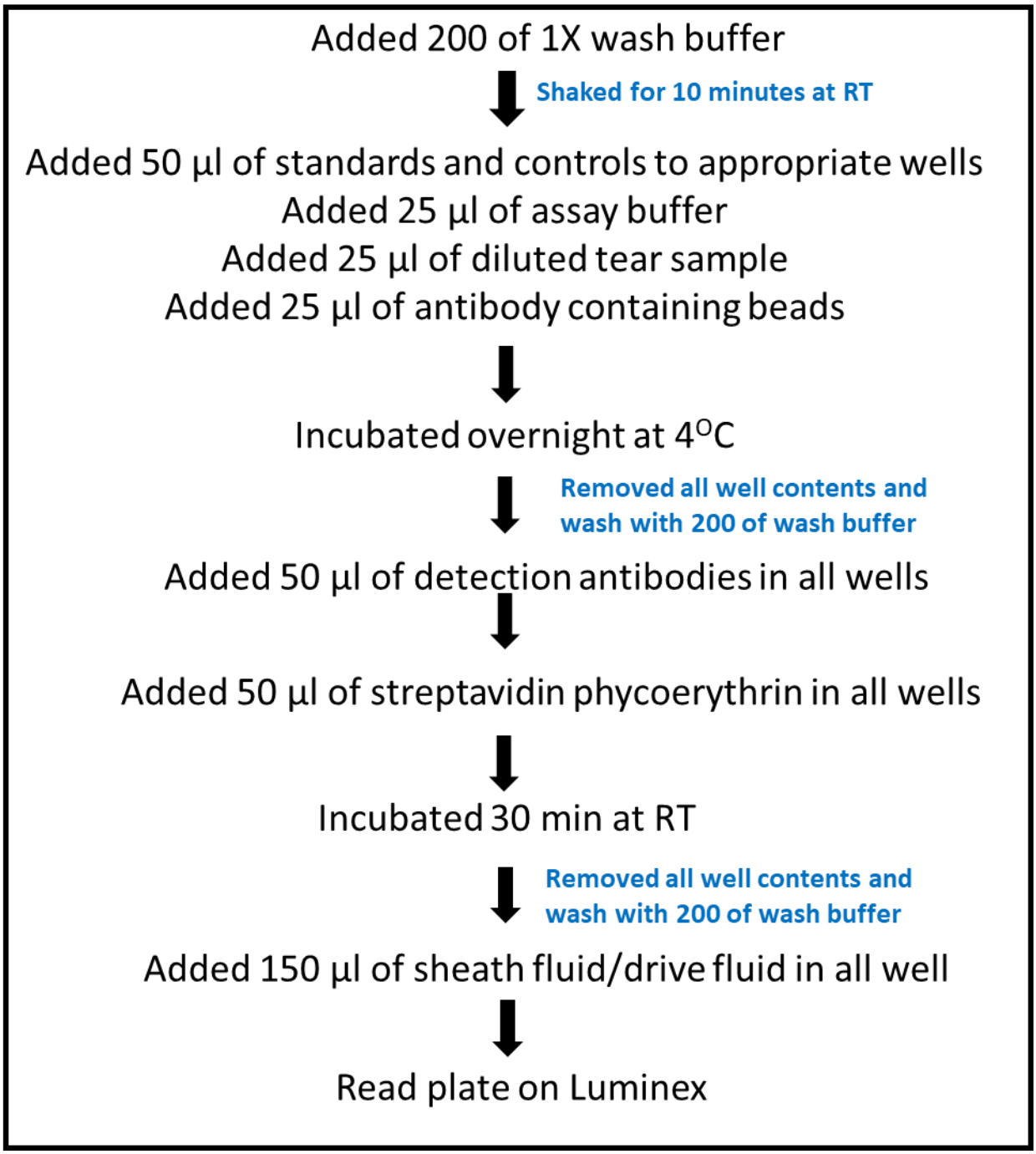

Figure 15. Workflow for multiplex ELISA

1.2.6. Tear multiplex ELISA data analysis

Raw data / mean fluorescence intensities (MFI) for each cytokines and protein markers was obtained and then exported to data analysis software after categorizing into the case and controls. Mean average signals were used to calculate the fold change and *p-value*. Fold change with 2 and *p-*

value ≥0.05 was considered to be statistically significant, and *p-value* ≥ 0.001 was considered to be statistically very significant.

1.2.7. Zymography

Zymography is a precise and sensitive method to evaluate proteinase activity in the targeted sample. Gelatin zymography is majorly used to detect metalloproteinases like MMP2 and MMP9; in this technique, gelatin served as a substrate that co-polymerizes with polyacrylamide gel and allows proteins to get separated in a matrix. Vitreous samples were run under the non-reducing conditions, SDS maintains the inactive forms of MMPs during the gel run. Following electrophoresis, the gel was washed with distilled water and then with Triton® X-100 for 30 minutes to remove SDS. After removal of SDS by triton X wash, the gel was then incubated in a calcium-containing buffer and was then stained with Commassie brilliant blue (CBB) solution. Depending upon the levels of MMP activation, gelatin gets degraded and lead to a clear zone and that can be identified as white band after staining the gel. The detailed protocol is given below.

Gel casting plates were cleaned with deionized water and after drying the plates were assembled vertically in the gel casting system.

- The gelatin resolving and stacking gels were prepared as described in annexure II (supplementary Table 1).
- Firstly, the resolving gel was poured between aligned glass plates, allowing enough space for the stacking gel.
- To avoid oxidation, a layer of water/saturated butanol was placed on upper side of the resolving gel, further left approximately for 45 minutes to polymerize the gel.
- Butanol was later removed and then the gel surface was cleaned with double distilled water (dd. H_2O) before the stacking gel was poured into the plate.

- After the polymerization of the polyacrylamide gel, 15µg of total vitreous protein samples were added into respective wells. In addition to this added 2µl of pre-stained protein marker and electrophoresis was carried out at 100V, until tracking reaches the bottom (run was performed in ice cold conditions).
- The gel was carefully separated from the gel cassette and was shifted to the gel box.
- The gel was then washed twice with autoclaved milli Q to remove SDS.
- 100ml of the 2.5% Triton X-100 (renaturing buffer) was added into the gelatin gel and incubated for 30 minutes at RT with gentle agitation.
- The gel was then washed with 300mL of deionized water by gentle agitation for 30 minutes.
- Further, 100mL of 1X developing buffer was added (0.05M Tris HCl, pH- 7.8, 0.2M NaCl, 5mM CaCl2, 0.02% Brij 35) and incubated for 30 min.
- After 30 minutes, the developing buffer was discarded and replaced with freshly made 1X developing buffer, which is now incubated for 16 hours at 37 degrees Celsius.
- After 16 hours of incubation, the developing buffer was decanted and 100mL of filtered CBB staining solution was added for 1 hour or until uniform blue staining appeared.
- After that the gel was washed with deionized water to remove excess blue dye
- The de-staining was carried out using the de-stain solution (5% methanol and 10% acetic acid in dH_2O), based on the gelatinolytic activity of sample the intensity of clear sharp bands appears over the blue background.
- The matrix metalloprotease activity in ROP and control vitreous samples was estimated based on band intensity by using Image J software.

1.2.7.1. Estimation of MMP activity in ROP tear samples

To validate the MMP levels in tears, further zymography was performed using the similar protocol as mentioned above. Band intensity was measured by image J and calculated *p-values* for the same. The demographic details of the study participants are given in the Table 7.

Table 7. Demographics details of study subjects used for tear samples for zymography

Tear	Mean ± SD				
	Age (Months)	GA (weeks)	Weight at birth (grams)	O_2 supplementation (days)	Gender and number
Controls	3.27 ± 2.94	25.2+ 10.3	1.43± 0.23	5.92 ± 2.60	M =8, F =10
Mild ROP-regressed	3.3 ± 2.50	21.3+ 11.6	1.39± 0.22	6.28 ± 0.92	M =8, F =5
Mild ROP-progressed	3.58 ± 2.64	29.3+ 1.2	1.26± 0.18	5.25 ± 2.05	M =5, F =7
Severe ROP	8.4 ± 1.68	24.5+ 9.2	1.21± 0.25	5.57 ± 1.3	M =10, F =6

1.2.8. Estimation of Protein concentration

- Samples average optical densities (OD) were calculated by subtracting the blank OD value from each standard. By plotting the test OD in the standard graph and corresponding concentrations in the Y-axis, a linear regression plot with r2>0.09 was used to calculate the test sample concentration. An equal concentration of protein from the controls and patients were used for further experiments.
- Protein samples were normalized to final concentration of 15µg and used for proteomic studies i.e., western blotting and zymography.

1.2.9. Western blotting

In this technique, the vitreous protein samples were run in the SDS-PAGE followed by washing of the gel with distilled water and transfer of proteins to the PVDF membrane. This membrane is used for the detection of the protein of interest. For the estimation of Opticin (ab170886, Abcam) levels, a total of 30 vitreous samples of severe ROP (stage 4a, b and 5) and 30 vitreous samples from the control individuals diagnosed with congenital cataract were analysed by western blot analysis under non-reducing conditions. Demographic details of these individuals are given in the

Table 8. The detection was done using a secondary antibody, Anti-Rabbit. The detailed protocol for western blot analysis is as follows:

A. Cleaned glass plates were assembled vertically in the gel casting system.

B. 10% resolving gel was prepared for SDS-PAGE by adding all the components as mentioned in Annexure II (Supplementary Table 2).

C. All the components were uniformly mixed and placed between the glass plates, allowing sufficient space for stacking gel and comb. Around 500µl of water/methanol were poured on top of the gel to avoid oxygen diffusion and gel polymerization inhibition.

D. As shown in the Table 6, 5% stacking gel was prepared and gently poured on top of the polymerized resolving gel.

Table 8. Demographics details of study subjects used for vitreous western blotting analysis

Vitreous	Age (Months)	Gender	GA (weeks)	Weight at birth (Grams)
Control (n=30)	4.137 ± 1.917	F,n=15,M,n=15	38.258 ± 1.683	2.38 ± 0.71
ROP (n=30)	3.566 ± 1.951	F,n=13,M,n=17	29.7 ± 2.119	1.467 ± 0.273

1.2.9.1. Vitreous sample preparation

All the samples were quantified using the standard BCA method as mentioned above and normalized to 15µg/mL. Samples were diluted to 1X in 4X sample loading buffer (LI-COR) and heated at 90˚C for 10 minutes to denature the proteins before loading on the gel and snap chilled the samples in ice. The composition of resolving and stacking gels were given in Annexure II (Supplementary Table 2)

1.2.9.2. Loading of samples

Once the gel was polymerized entirely, the comb was removed carefully without disturbing the wells. To remove the unpolymerized acrylamide gel the polymerized gel was then washed with double distilled water. The gel was placed in the electrophoresis apparatus. Freshly prepared 1X

running buffer (Tris-Glycine-SDS) was added from the bottom reservoirs. Snap chilled samples were centrifuged and loaded into the appropriated wells, along with the 2μL of LICOR color stained protein marker.

75V voltage was used for electrophoresis of protein samples while in stacking gel, and the current was increased to 100V once the dye front migrated into the resolving gel. The electrophoretic run was continued until the tracking dye (bromophenol blue bands) touched the bottom of the resolving gel.

1.2.9.3. Transfer of proteins to low Polyvinylidene Difluoride (PVDF) membrane

- The gel was carefully taken from the glass plate and rinsed in 100mL of distilled water, and equilibrated in transfer buffer containing 1.92M glycine, 25mM Tris and 20% methanol for 15 min.
- PVDF (Immobilon®-FL transfer membrane, Millipore) membrane which was of same size as that of gel was soaked in methanol for 3 minutes followed by washing with autoclaved Milli. Q and finally the membrane was shifted to the transfer buffer. Two filter paper sheets (3mm thick Whatman Grade 3) and blotting pads of similar sizes were also equilibrated in transfer buffer approximately for 5 minutes.
- For transferring the proteins to PVDF membrane, a sandwich of gel membrane was prepared from cathode to anode direction (pre-wet sponge pad-pre-wet filter paper-gel-PVDF membrane-prewet filter paper-prewet sponge pad without any air bubbles) in the transfer blot module (XCell IITM Blot Module, Thermo Fisher scientific) and placed the cassette in the transfer system (XCell SureLock Mini-Cell, Thermo fisher Scientific) horizontally.
- The blot module was permeated with 1X transfer buffer until the gel sandwich was covered entirely. The outer chamber was filled with ice-cold deionized water to avoid heat generation during transfer.

- Semi-wet transfer done for 1 hour at 21V. Further, Confirmed the protein transfer by simple Ponceau S staining

1.2.9.4. Ponceau S staining

Ponceau S is red colored stain, with a negative charge that binds both with non-polar regions of proteins and positively charged amino groups and can detect even upto 250 nanogram proteins in a PVDF membrane. Due to the lack of suitable housekeeping genes in vitreous samples, Ponceau stain was used for normalization and equal loading control for the western blotting experiments. After 1-hour of transfer, the PVDF membrane was shifted to a clean tray, washed once with 50ml of deionized water and then submerged in 100mL of Ponceau S solution for 5-10 minutes with constant agitation. The extra stain was washed with deionized water, and images were recorded for confirmation and comparison with the expression of western blot bands. De-staining of Ponceau S was done with deionized water until the stain was completely washed away from the PVDF membrane.

1.2.9.5. Blocking

To avoid non-specific signals, the membrane was blocked with 1mL of LICOR- Odyssey Blocking buffer for at least 1 hour at RT with gentle shaking in a sealed sterile plastic bag.

1.2.9.6. Primary and secondary antibody incubation

After an hour of blocking treatment, the membrane was incubated with Opticin primary antibody (Cat.log number ab170886, Abcam), overnight at 4˚C with continuous agitation.

1.2.9.7. Secondary antibody incubation

After overnight incubation with primary antibody, the membrane was washed thrice with 1X PBST (0.1% of Tween20) prior to secondary antibody addition. IRDye® secondary antibody (cat.log

number-926-32211, Anti-Rabbit 800CW) was diluted (1:7500) in Odyssey blocking solution along with 0.2% of Tween20 and incubated the blot for 1 hour.

1.2.9.8. Detection

After 1 hour, the PVDF membrane was carefully removed and washed thrice (3X) with 1X PBST for 5 minutes with continuous agitation at RT for 5 min each time. The PVDF membrane's protein transfer side was placed on the fluorescent scanner. Air bubbles were removed slowly by using the roller and fluorescence detection was done using the Odyssey imaging system.

1.2.10. *In-vitro* analysis

To check whether the increased activity of MMPs in the ROP eyes regulates the decreased expression of Opticin, the effect of MMP's activity on Opticin levels was assessed in human microglial cell line (CHME3) under hypoxic conditions.

1.2.10.1. Cell culture

To understand how MMPs act on Opticin levels, *in-vitro* analysis was conducted using cultured human microglial cell line (CHME3). These cells were grown in a DMEM medium comprised of 10% FBS along with penicillin and streptomycin antibiotics. Approximately 10,000 cells per well were used for this experiment. Detailed work flow given in the Figure 16.

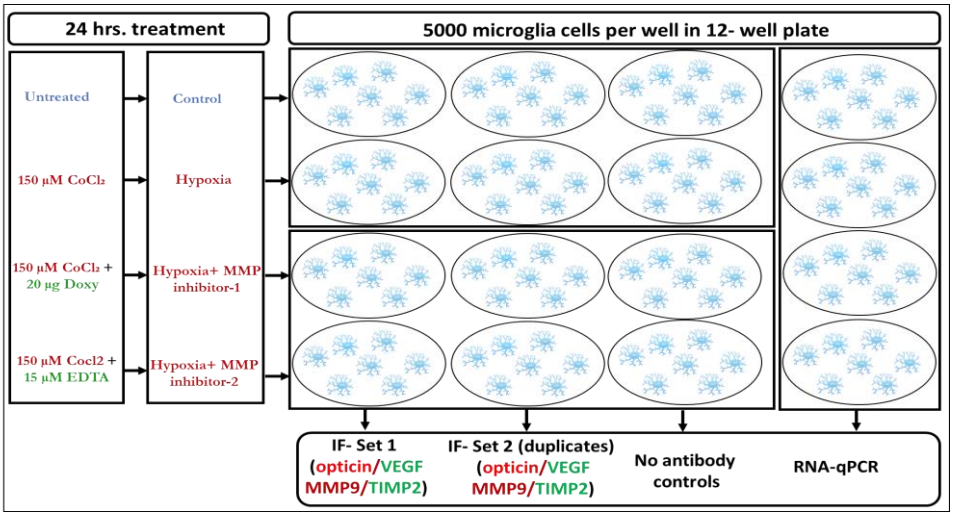

Figure 16. Schematic presentation for *in vitro* analysis

1.2.10.1.1. Hypoxia induction by chemical method (Cobalt Chloride)

- After sterilization by flaming the cover slips were placed immediately in 6 well plates and UV treatment was given for 1 hour.
- 5000 microglial cells/well were seeded on sterile glass coverslip and further allowed the cells to attain 70% confluency.
- 25mM $CoCl_2$ (Sigma, cat. No. C8661, $CoCl_2 \cdot 6H_2O$, M.Wt =237.9) stock solution was freshly prepared by dissolving it in DMEM and filtered through 0.2µm syringe filter. The $CoCl_2$ at the final concentration of 150µM in DMEM media was used to induce hypoxia.
- For 6 hours, microglia cells were pre-treated with serum-free medium. Later, hypoxia was induced by 150µM of $CoCl_2$.
- In addition to this, in different sets of coverslips, the MMP activity in hypoxia induced cells was also inhibited by 10µg EDTA, 20µg of Doxycycline-20µg for 24 hours, as a control, cells which had not been treated were used.

1.2.10.1.2. Cell viability by Alamar blue method

Alamar blue cell viability reagent resazurin-based solution was used to identify the healthy/dead cells in the dish. The reagent works based on the metabolic reduction ability of the cells and acts as an oxidation-reduction indicator that produce a change in fluorescence-based on the cell's metabolic activity. Metabolically active cells reduce resazurin to resorufin continuously and fluorescent changes from pink to red color, which can be measured calorimetrically and directly proportional to the cell's viability. The detailed protocol is explained below

- In 96 well plate, 1000 microglia cells/well were seeded and permitted to reach 70-80% confluency.
- $CoCl_2$ and doxycycline/EDTA treated cells were taken after 24 hours, 10µL of Alamar blue dye (Life Technologies, Cat.no. DAL1025) was added and kept at 37°C in CO_2 incubator. Incomplete DMEM media along with Alamar blue was taken as blank.

- After 3 hours of incubation, the absorbance was determined, and the blank readings were deducted from the OD of the cells. The viability percentage was calculated as

$$Percentage\ of\ cell\ viability = \frac{\text{Absorbance of treated cells}}{\text{Absorbance of untreated cells}} \times 100$$

1.2.10.1.3. Immunofluorescence (IF)

IF is a very sensitive method to detect the targeted antibody with either nuclear or cytoplasmic antigens present in the cells. Targeted secondary fluorescent labelled antibody attaches to FC portion of the primary antibody, the detailed protocol given below:

- After 24 hours $CoCl_2$ and doxycycline/EDTA treatment, microglia cells were fixed with 4 percent formaldehyde for 10 minutes at RT, then washed three times with 1X PBS.
- For permeabilization, the cells were treated with 0.3 percentage of triton X 100 at RT for 15 minutes, followed by three washings of 1XPBS.
- The blocking was performed by incubating with 2% BSA for an hour (HIGH MEDIA, Cat.no TC194).
- After blocking, the coverslips were incubated with the targeted primary antibodies for overnight at 4°C. After incubation is completed, three washing were given with 1XPBS to remove any unbound excess primary antibody. The details regarding primary antibody dilution are given in the Table 9.
- After washes cells were incubated with fluorescent labelled secondary antibody at RT for 1 hour and removed unbound excess antibody with three washing with 1xPBS.
- The detection was done with fluorescent labelled secondary antibodies and the mount was done with slow fade gold antifade including DAPI (Life tech, ref.ID-S36939) and measured targeted proteins expression by using an EVOS fluorescence microscope.

Table 9. Primary and secondary antibodies list

S.No	Antibody	Dilutions (µL)	Company	Catalogue No.
1	Rabbit monoclonal to Opticin	1.5	Abcam	ab170886
2	Rabbit polyclonal to MMP9	1.5	Abcam	ab38898
3	Mouse monoclonal to TIMP2	1.3	Santacruz	sc-365671
4	Mouse monoclonal to VEGF	1.2	R&D	MAB 293
5	Goat anti Rb 488	0.25	Life Tech.	A-11008
6	Goat anti Ms 48 8	0.25	Life Tech.	A-10680
7	Goat anti Ms 594	0.25	Life Tech.	A-11005
8	Goat anti Rb594	0.25	Life Tech.	A-11012

1.2.10.1.4. RNA isolation from the microglial cells

1. RNA was extracted by trizol method from another similar set of the microglial cells (treated vs untreated). 1mL of trizol (Thermo Fisher Scientific) was added to the microglial cells
2. The cells (pellet) were homogenized in trizol using pipette without any mechanical stress and then incubated on ice for 10 min.
3. Transferred the trizol containing microglial cells in 1.5mL autoclaved tubes, added 200µL of chloroform and vortexed for 10s followed by incubation for two minutes in ice.
4. Centrifuged the mixture at 12,000g for 15 minutes at 4°C and the aqueous phase was collected in a fresh sterile vial.
5. To precipitate the RNA, add 500µL of isopropyl alcohol to the aqueous phase and incubate for 10 minutes on ice and later centrifuge for 10 minutes for 12,000g at 4°C.
6. After centrifugation the supernatant was removed and white RNA containing pellet was washed with 70% ethanol followed by centrifugation at 7500rpm for 5 min at 4°C.
7. After washing with 70% ethanol, the pellet was air dried, once the ethanol droplets are removed, the pellet was suspended in RNAase free water.

8. RNA quantity and quality were assessed by nanodrop and agarose gel electrophoresis respectively. The preparation of stock solutions is given in Annexure-II.

1.2.10.1.5. cDNA preparation

1. cDNA was converted from 500ng of total microglia RNA. (Thermo Fisher Scientific, cat no. AB1453A).
2. The master mix was prepared in ice cold conditions as per the composition in below Table 10.

Table 10. cDNA master mix details

S.No	Reagent	Volume (µL)
1	5X cDNA synthesis buffer	4
2	dNTP mix	2
3	Oligo dT	1
4	RT enhancer	1
5	RT enzyme	1
6	RNA template	X (500ng)
7	Nuclease free H_2O	**Makeup to 20µL**

3. After preparing the master mix, cDNA was synthesized by reverse transcription PCR underneath the following conditions:

   - 25°C-10 minutes,
   - 42°C- 30 minutes for cDNA synthesis for 1 cycle,
   - 72°C for 5 minutes.

1.2.10.1.6. Quantitative Real Time PCR (qRT - PCR)

To confirm the cDNA conversion, PCR was performed for gene specific internal control (beta actin) primers. The composition of master mix and thermal cycler steps are given in Tables 11 and 12 respectively.

Table 11. Preparation of PCR master mix

S.No	Reagents (Stock concentrations)	Working concentration	Volume(µL)
1	Taq Buffer containing $MgCl_2$ (10X)	1 X	2.5
2	dNTPS (100mM)	2 mM	2.5
3	Forward primer	5 pm/µL	1
4	Reverse primer	5 pm/µL	1
5	Taq polymerase (2U/µL) (Bangalore Genei Cat. No. 105919)	2U/µL	0.5
6	Template	X	X
7	Autoclaved MilliQ	--	**Made up to final reaction volume of 25µL**

Table 12. Thermal cycler program for amplification of selected regions in the house keeping gene (β actin)

S.No	Step	Temperature (°C)	Time	Cycles
1	Initial denaturation	95	5 minutes	1
2	Denaturation	95	30 sec	35
3	Annealing	55	30 sec	
4	Elongation	72	30 sec	
5	Final elongation	72	5 minutes	1
6	Hold	4	5 minutes	1

The confirmation of the amplification of PCR products is done by using internal control (β-actin) and the samples were run on 1.5% agarose gel electrophoresis. Further to check the relative expression of targeted genes (Table 13) in microglia cells, performed qPCR by using SYBR green chemistry that works based on its capability to bind the minor groove of the double-stranded (ds) DNA and measures the number of DNA copies by producing a fluorescent signal. The amount of signal is directly proportional to the amount of RNA copies generated.

Table 13. Primer sequences and annealing temprature used for semi-quantitative real time PCR

S.No.	Gene	Forward primer (5'-3')	Reverse primer (5'-3')
1	*OPTC*	AACCGCATCAGCCGTATC	CGGAAGGCATCAATTATCG
2	*MMP2*	KiCqStart™ SYBR primer from sigma code -FH1_MMP2	
3	*MMP9*	KiCqStart™ SYBR primer from sigma code -FH3_MMP9	
4	*TIMP2*	CTTCCACAGGTCCCACAACC	CAGCCCTGGCTCCCGAGGC
5	*VEGF*	ATCTTCAAGCCATCCTGTGTGC	CAAGGCCCACAGGGATTTTC
6	*MAPK1/ ERK2*	CAGGGAAGATGGGCCGGTTA GAGA	TGAAGCGCAGTAAGATTTTT
7	*MAPK3/ ERK1*	CCTGCGACCTTAAGATTTGTGATT	CAGGGAAGATGGGCCGGTTAGAGA
8	*NOTCH1*	TTGGGAGGAGCAGATTTTTG	CACTGGCATGACACACAACA
9	*DKK1*	GATCATAGCACCTTGGATGGG	GGCACAGTCTGATGACCGG
10	*β Actin*	TCTACAATGAGCTGCGTGTG	GGTGAGGATCTTCATGAGGT

9µL of master mix (Table 14) was loaded into MicroAmp™ optical 96 well reaction plate (Table 15) respectively as per the plate map without any bubbles.

Table 14. Preparation of qPCR reaction master mix

S.No	Reagents	Volume(µL)
1	iTaq™ Universal SYBR® Green Supermix (BIO-RAD, Cat no. 38220090)	5
2	Forward primer (200nm)	0.5 (5p.mol)
3	Reverse primer (200nm)	0.5 (5p.mol)
4	cDNA (Before preparing master mix added individual 50ng of samples into respective wells as per plate map)	1
5	Milli.Q	3
	Total volume	**10**

The MicroAmp™ optical plate was tightly sealed with an optical adhesive sheet (Thermo Fisher Scientific. Cat. No. 4311971). The plate sample sheet was prepared as per the plate map and reaction was run on Applied Biosystems 7900 HT system. The SDS 2.4 software (Applied Biosystems) was used to measure the target gene expression (CT) and normalized the gene expression by using housekeeping gene (β actin), further the fold change, SEM and *p-values* for three technical replicates was calculated.

Table 15. Thermal cycler program

S.No	Step	Temperature (°C)	Time	Cycles
1	Stage 1	50	2 min	1
2	Stage 2	95	10 min	1
		95	15 sec	
3	Stage 3	60	1 minute	40
4	Stage 3	95	15 sec	1
5	Dissociation curve	60	15 sec	1
		95	15 sec	

1.2.11. Immunohistochemistry (IHC)

Immunohistochemistry is a method to detect the protein expression in tissues using an antibody specific to the antigen. The visualization of the antigen can be either by chromogenic method or by fluorescent labelling. The detailed protocol followed for IHC is given below.

1.2.11.1. Fibrovascular membranes collection from ROP probands

Membrane peeling (n=3) was performed by surgeon after obtained parental informed consent. Using liquid nitrogen (N_2), the membrane tissue was immediately frozen in OCT tissue freezing medium in the tissue mould.

1.2.11.2. Retinal tissue collection from the healthy individuals

The retinal tissue was collected from "Ramayamma International Eye Bank, LV Prasad Eye Institute, Hyderabad". A normal retinal tissue was used as a positive control for immunohistochemistry. Detailed protocol followed for IHC is given below.

1.2.11.3. Tissue embedding and sectioning

Retinal tissue was fixed with 4% formalin and placed in tissue mould along with liquid paraffin and permitted to cool to get an immobilized tissue embedded blocks. 5m thick slices of embedded tissue were taken on charged slides.

1.2.11.4. Haematoxylin and Eosin (H&E) staining:

- H&E staining was used to inspect the orientation and quality of membranes
- Fibrovascular membranes and whole retina sections were stained with Harris haematoxylin stain. For that the slides were incubated in a jar containing haematoxylin-eosin stain for 2-3 minutes with the help of a slide holder.
- After incubation with the stain, these slides were gently washed with water for 5 minutes followed by incubated with 1% acidic alcohol.
- The dehydration of sections was then performed by washing with 3 different grades of alcohol (80, 90 and 100%) for 3 minutes each.
- The dehydration was then followed by three washings with xylene.
- Stained section was mounted with cover slip by using DPX mountant. Finally, the sections were observed at 10X, 20X and 40X magnification under light microscope to visualize the nuclei in blue (haematoxylin stained) and cytoplasm in light to dark red (eosin stained) in EVOS fluorescent microscope.

1.2.11.5. Retinal sections deparaffinization and rehydration

- Deparaffinization was done by placing the tissue sections at 70˚C for 30 minutes in a hot air oven and followed by washing with xylene.
- Rehydrated the sections by treating with 100% and 95% ethanol respectively, followed by washing in running tap water, distilled water and 1X PBS.

1.2.11.5.1. Antigen retrieval

- Antigenic sites for antibody binding will be hampered by protein-cross links formed during formalin fixation. To unmask the antigen epitopes, antigen retrieval done using sodium citrate buffer. For antigen retrieval, slides were placed in jar containing retrieval buffer and heated in

microwave thrice at full power (5 min each). Washed the slides with a 1X PBS thrice (3X) after coming to room temperature.

- Fibrovascular membranes and retinal tissues are processed together from this step. To permeabilize the cells, tissue section was treated with 0.3 percent triton X-100 at room temperature for 10 minutes and further rinsed and washed 3 times with 1x PBS. Followed by blocking done using 2% BSA (HIGH MEDIA, Cat.no TC194) for 1-hour.
- Tissue sections were incubated with primary antibodies (targeted antibodies and dilution details given in the Table 9) overnight at 4°C, to washed the unbound primary antibody slides were again washed with 1X PBS three times.
- Secondary antibodies (fluorescently labelled) have been used for identification for 1 hour at room temperature, followed by three washes given with 1X PBS.
- A slow fade gold antifade containing DAPI (Life Tech, ref. S36939) was used to mount the slides and later the expression of targeted proteins was assessed using an EVOS fluorescence microscope.

1.3. Results

Objective 1: To identify the inflammatory molecules as the disease biomarker in ocular fluids for the early detection of ROP.

The expression of MMPs was studied in the tear fluid of prematurely born infants to establish as a biological tool for risk prediction of the ROP.

1.3.1.1. Multiplex ELISA

MMPs levels in tear samples were estimated by using multiplex ELISA for different categories of ROP which involves severe ROP, mild ROP and premature controls. We have found significantly elevated levels of MMP2 and MMP9 while there was no change in MMP8 levels (Figure 17).

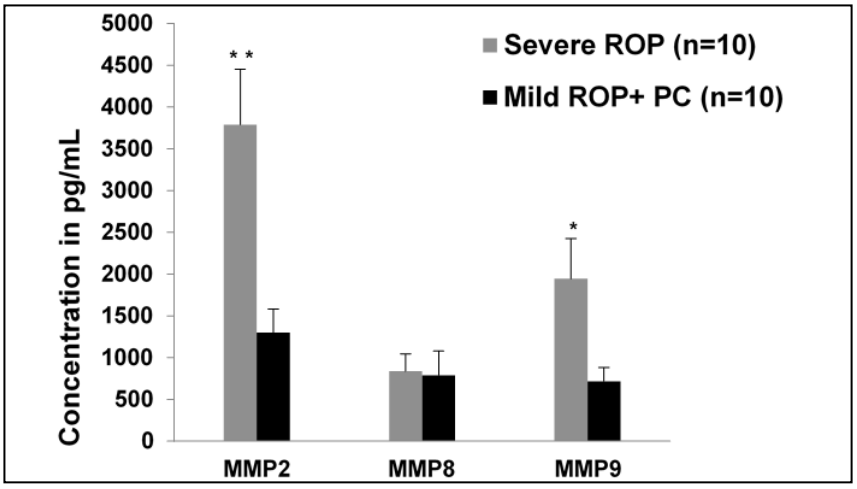

Figure 17. MMPs in ROP in tear samples (5 µL each), differential levels of MMPs in ROP and control tear [*p < 0.05, **p < 0.005, ***p < 0.0005]

1.3.1.2. Zymography

Zymography confirmed activated MMPs in tears of cases with severe stages of ROP. Interestingly, a mild ROP patient also showed almost similar levels of the activated MMPs as in the severe ROP patients. Further investigation of the clinical data showed that this patient who had mild ROP (ROP T18) at the time of sample collection, later, progressed to severe ROP (within two weeks after sample collection) and had a poor prognosis even after the laser treatment (Table 16).

This was further confirmed by analyzing the MMP activity in an extended cohort of premature infants, who were sub-categorized into mild to regress, mild to progressive ROP, no ROP and severe ROP (Figure 18).

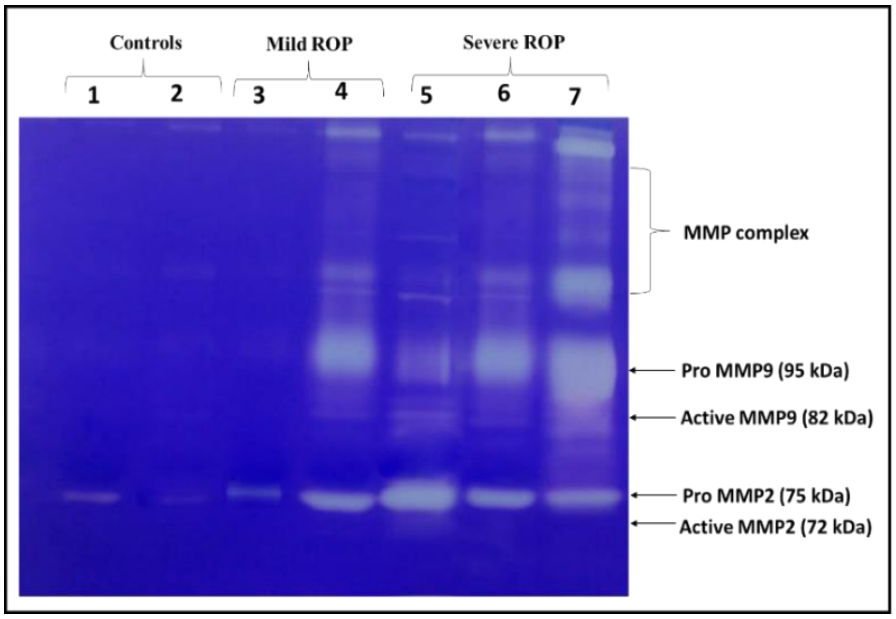

Figure 18. Tear MMPs levels estimation by zymography in control, mild and severe ROP

Table 16. Demographical and clinical details of patients

Study number	Collection method	Gender	Age (Months)	GA (Weeks)	Diagnosis at time of collection	Date of collection	Samples loading order	Final outcome
ROP.T25	Capillary	Female	2	32	Mature retina-OU	09-06-2016	1	Mature retina-OU
ROP.T21	Capillary	Male	4	30	Mature retina-OU	08-06-2016	2	Mature retina-OU
ROP.T20	Capillary	Male	3	28	Stage II-OU	16-06-2016	3	Regressed ROP-OU
ROP.T18	Capillary	Male	4	31	Stage II-OD , stage II plus-OS	21-07-2016	4	Progressed ROP so laser done on 28-07-2016 and shown regression on next follow-up (04-08-2016)
ROP.T42	Capillary	Female	9	30	Stage V ROP-OU	21-06-2016	5	Poor visual outcome-OU
ROP.T37	Capillary	Male	10	30	Stage V ROP-OU	26-04-2016	6	Moderate vision improvement so suggested to continue the vision therapy at home
ROP.T35	Capillary	Male	10	28	Stage IV ROP-OU	03-04-2016	7	Reattached retina

Our results demonstrated a severity-dependent increase in MMP activation in ROP cases. Those who have mild and later regressed have lesser MMP activation compared to mild progressive. Similarly, severe ROP cases showed increased activation of MMPs as compared to mild progressive ROP. (Figure 19 and 20).

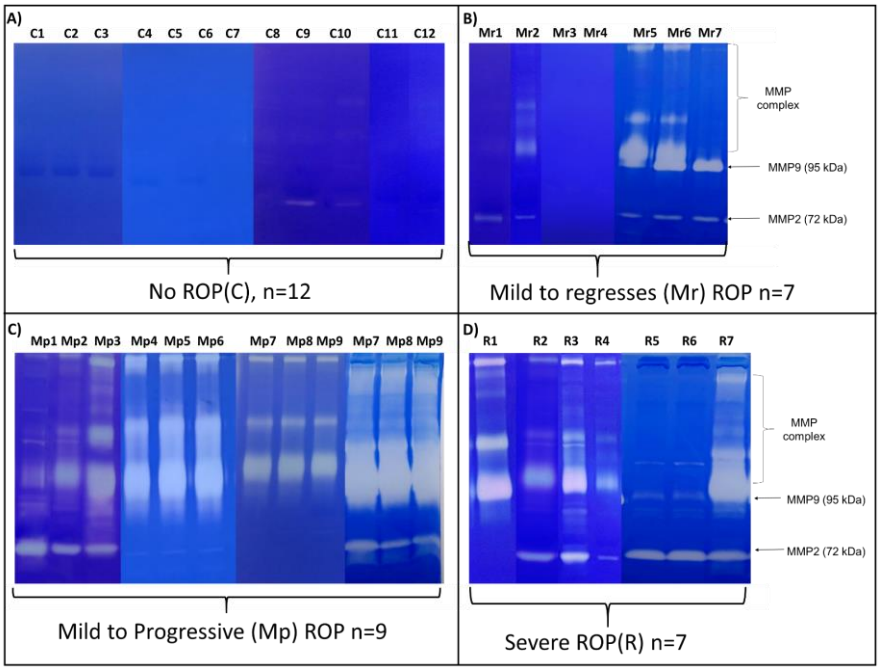

Figure 19. Zymogram showing a stage dependent MMPs increase in the MMP activity among ROP tears samples

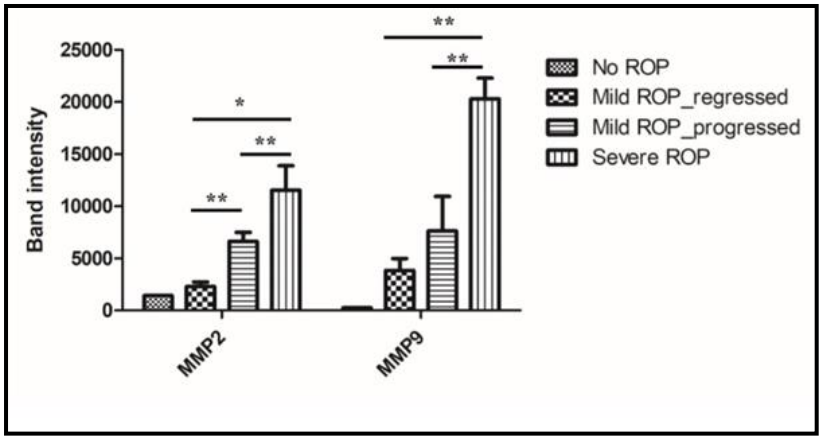

Figure 20. Validation of MMPs levels in ROP tears samples by zymography in an extended cohort. Band intensities of MMP9 and MMP2 were quantified and compared for severe ROP (n = 16), mild-progressed ROP (n = 12), mild ROP-regressed ROP (n = 12), and no ROP premature controls (n = 18), **p = 0.001, *p = 0.05; data represented as mean ± SEM

To confirm the results obtained from vitreous, we assessed the expression of other inflammatory markers and MMPs in tear samples (Rathi *et al.*, 2017). Multiplex ELISA was performed for the tear samples for targeted inflammatory markers, including the IFN-Ÿ, MCP-1IL-10, IL-1ra, IL-6, IL-8,

and TNF-α. In severe ROP cases, we noticed significantly higher expressions of IL-1ra and IL-8 compared to mild ROP and no-ROP tear samples (Figure 21).

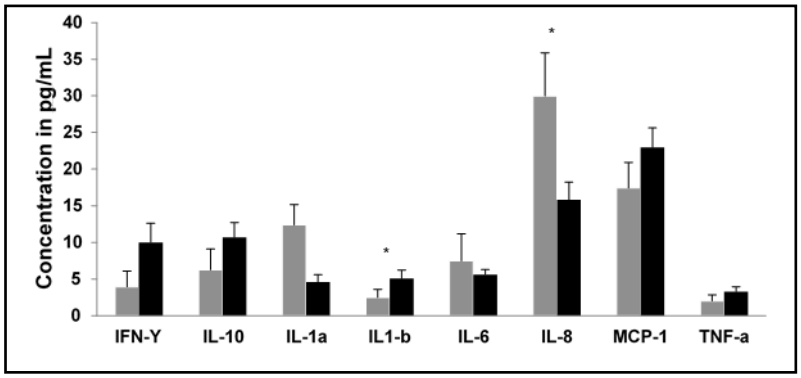

Figure 21. Inflammatory markers in ROP tears samples (5 µL each) by ELISA, differential levels of cytokines in ROP and control tears [*p < 0.05, **p < 0.005, ***p < 0.0005]

Thus, the levels of inflammation based on MMPs in tear samples might be utilized as a biomarker for establishing a ROP progression prediction test. The next step was to assess if increased inflammation could be targeted with the appropriate inhibitors to reduce the severity of ROP.

1.3.2. Objective 2

To target inflammation using suitable inhibitors so that ROP severity can be prevented

1.3.2.1. ECM proteins in vitreous of ROP

Zymography analysis and western blotting of ECM proteins showed the down-regulation of 45kda Opticin protein expression (Figure 22), with significantly increased MMPs activation (MMP2 and MMP9) respectively in the vitreous samples belonging to similar subjects (ROP and controls) (Figure 23). The increase in activation of MMP2, MMP9 and downregulation of Opticin in ROP vitreous was statistically significant (Figure 24).

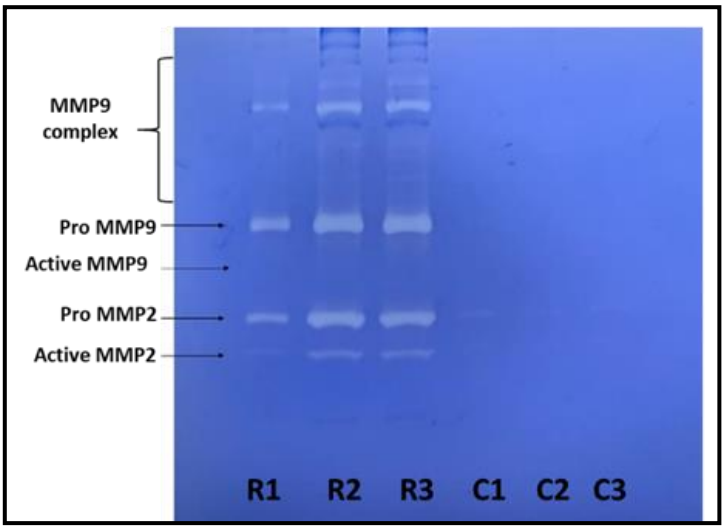

Figure 22. Represntative image of a zymogram showing differential activity of MMP2 & MMP9 in vitreous from ROP (n=10) and congenital cataract [controls, n=10]

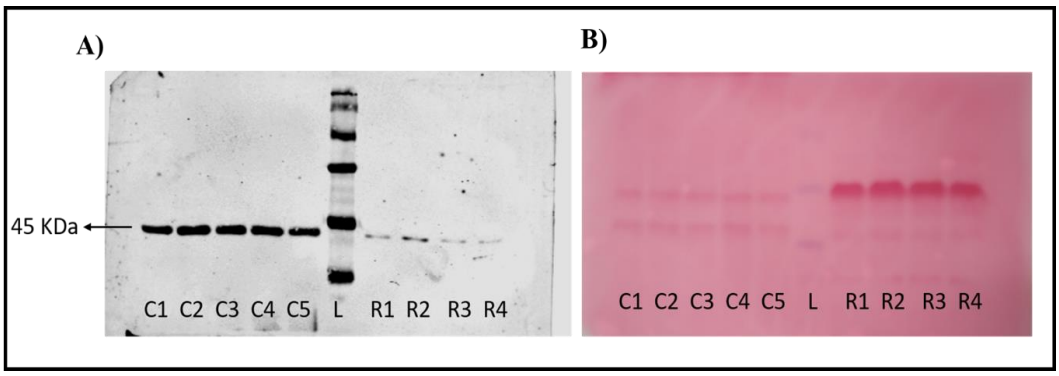

Figure 23. Representative image of (A) western blot of Opticin levels in vitreous from ROP (n=30) and congenital cataract [controls, n=30] (B) Ponceau staining of the same blot for normalization of protein concentration

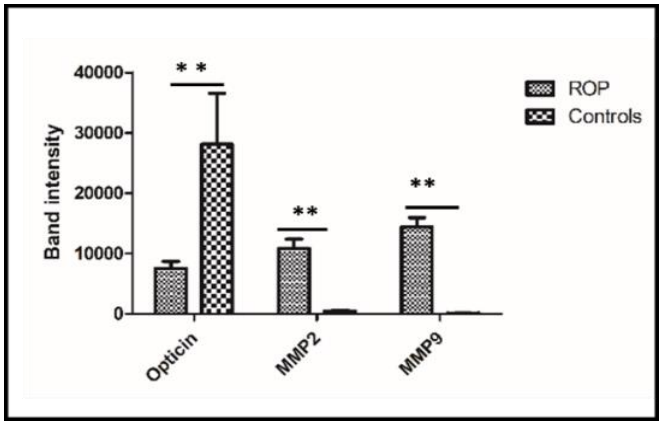

Figure 24. Bar graph showing differential expression of Opticin (45KDa) in ROP (n=30) and control vitreous (n=30). **p = 0.001, *p = 0.05; data represented as mean ± SEM, C, control vitreous; R, ROP vitreous; L, protein ladder

1.3.3. *In-vitro* analysis

1.3.3.1. Targeted genes expression profiling of *MMP9*, *OPTC*, and others in the microglia under hypoxic stress, with and without treatment with selective MMP inhibitors

Human microglial (human CHME3) cells under hypoxia ($CoCl_2$) treated with MMP inhibitors were tested using a quantitative real-time PCR. Under hypoxic stress induced by $CoCl_2$, *MMP9* expression substantially increased in human microglial cells, while *OPTC* expression was reduced. However, these cells after treatment of doxycycline and EDTA did not show the upregulation of MMPs expression and downregulation of *OPTC* under hypoxia. However, *TIMP2* and *VEGF* expression were not altered significantly after the inhibition of MMP activity under hypoxia (Figure 25).

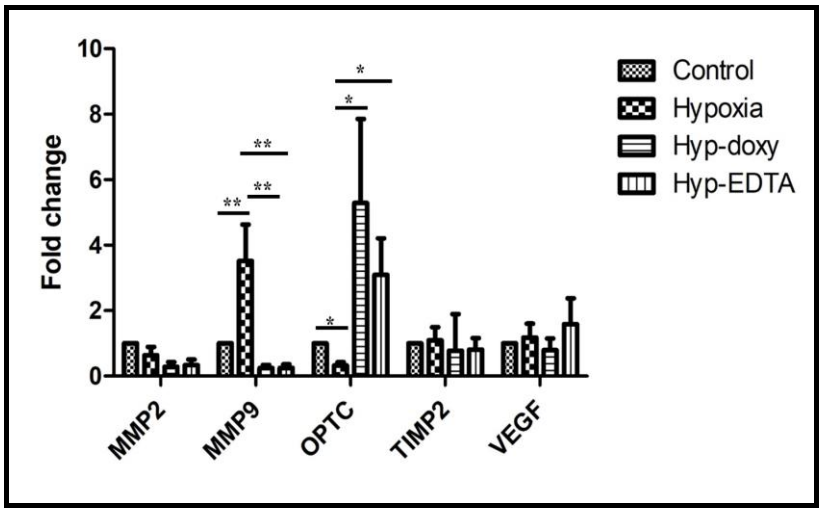

Figure 25. Differential gene expression based on quantitative PCR in microglial cells (n=3), **p = 0.001, *p = 0.05; data represented as mean ± SEM, FC=Fold change.

1.3.3.2. Investigation of targeted signaling pathways genes

We next wanted to assess how the inhibition of MMP activity by using doxycycline and EDTA was regulating the expression of ECM genes under hypoxia. To do so, we performed qPCR of key genes involved in various signaling mechanisms that are known to alter under hypoxia. Induction of hypoxia ($CoCl_2$) in human CHME3 cells showed a significant downregulation of several signaling

genes including *ERK2, DKK1* and *NOTCH1,* but there was no change in the expression of *ERK1* as compared to controls. After doxycycline mediated inhibition of MMPs activity in hypoxia induced cells; *ERK2*, *DKK1*, and *NOTCH1* were not down-regulated, however *ERK1* levels remained unchanged. In the presence of EDTA, the hypoxia treated cells exhibited increased levels of *ERK2* and *DKK1* expression, but *NOTCH1*, and *ERK1*, levels were not changed (Figure 26).

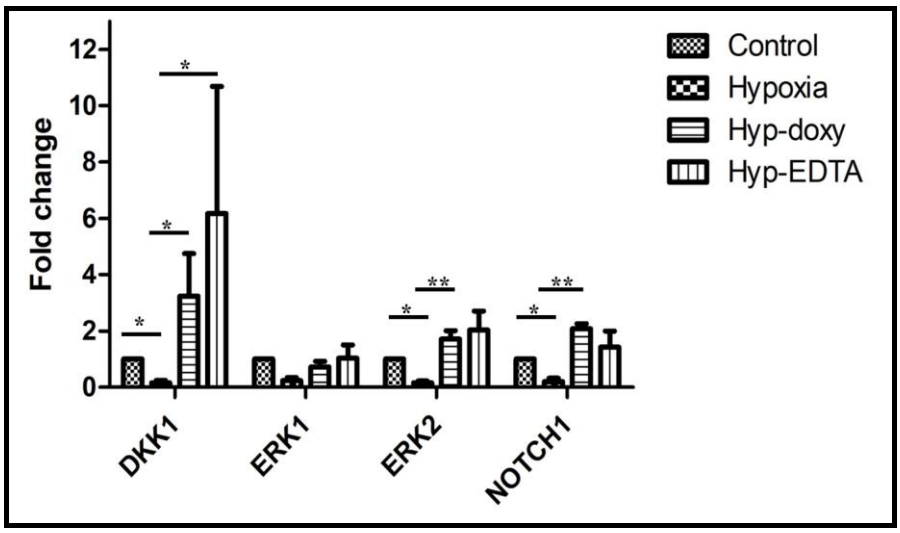

Figure 26. Differential expression of potential signaling pathway genes in microglial cells, **$p = 0.001$, *$p = 0.05$; data represented as mean ± SEM

1.3.3.4. Role of MMP's on Opticin expression under hypoxic conditions

Furthermore, to see if the enhanced activity/secretion of MMPs in the retina and vitreous regulated the downregulation of Opticin in ROP, we tested the levels of these two proteins in microglial cells by immunofluorescence. The expression of Opticin and MMPs were as expected at the baseline level in untreated (control) cells. Hypoxia ($CoCl_2$), on the other hand, increased MMP9 expression with a concurrent reduction in the Opticin expression possible suggesting its degradation by increased MMP9 activity. Inhibition of MMP9 activity by doxycycline and EDTA seemed to rescue the Opticin expression (Figure 27 and 28). Further there was no change in the levels of TIMP2 that regulates MMP9 and VEGF upon the inhibition of MMP9 activity by doxycycline and EDTA under hypoxia.

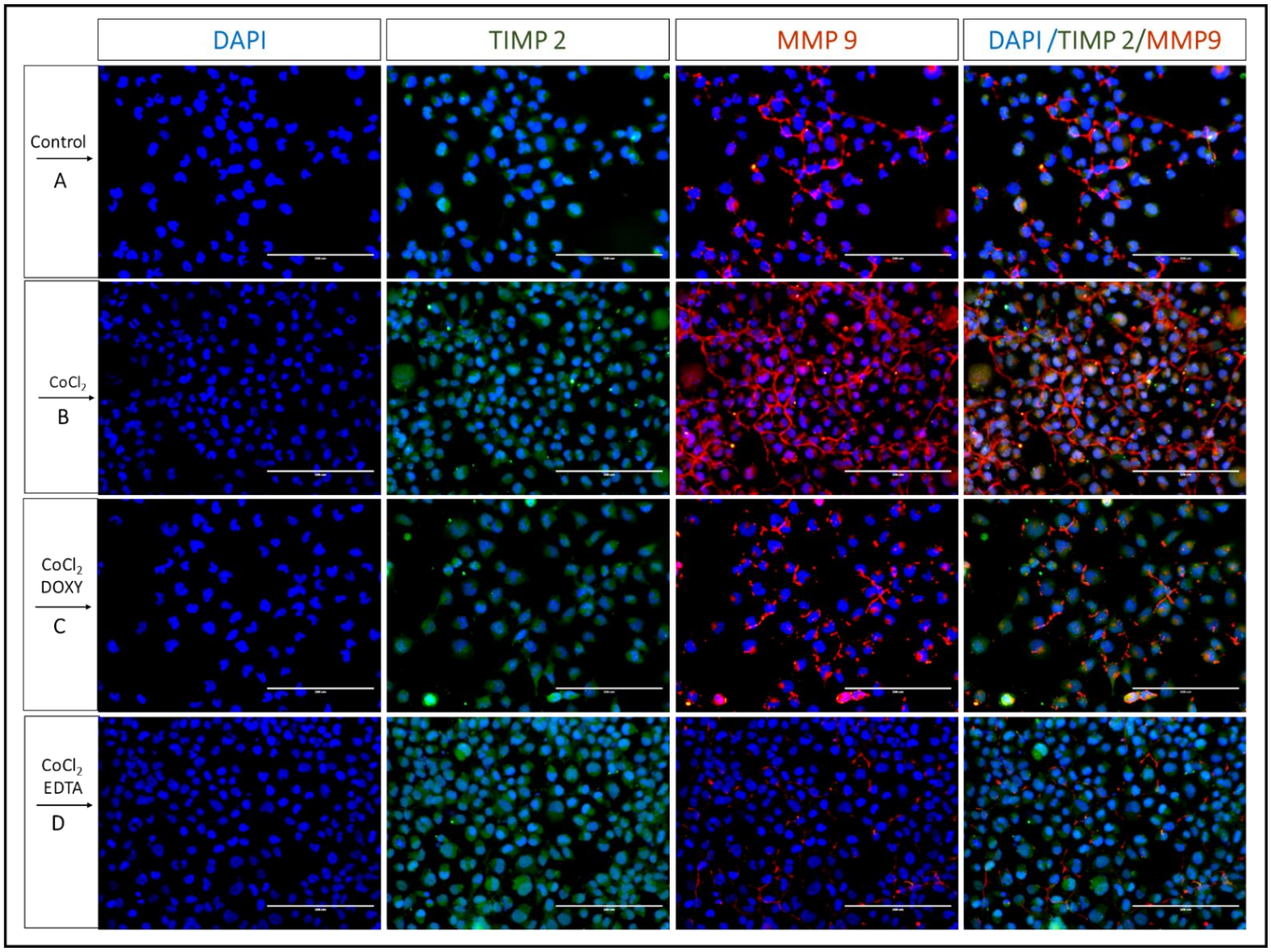

Figure 27. Representative images of the 20X magnified immunofluorescence showing the hypoxia mediated TIMP2 and MMP9 activity in human microglial cells from (A) Control and (B) $CoCl_2$ (C) $CoCl_2$ and doxycycline (D) $CoCl_2$ and EDTA

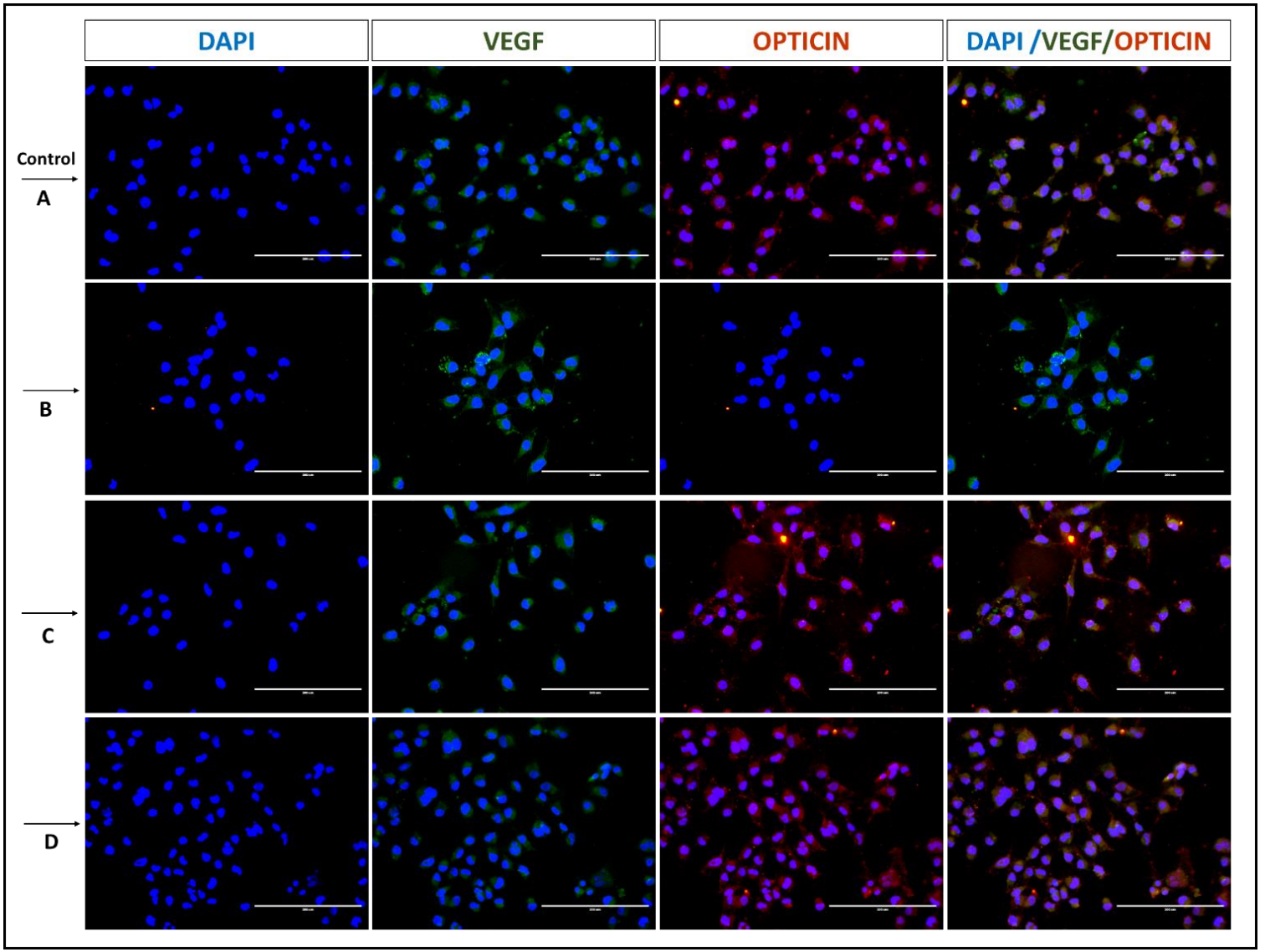

Figure 28. Representative images of the 20X magnified immunofluorescence showing the hypoxia mediated Opticin and VEGF activity in human microglial cells from (A) Control and (B) $CoCl_2$ (C) $CoCl_2$ and doxycycline (D) $CoCl_2$ and EDTA

1.3.4. Immuno-histochemical examination of ROP fibrovascular membranes

We next evaluated human tissue samples from ROP subjects for the expression of MMP9 and Opticin. Since the FVM are the only tissue that can be obtained from ROP eyes and is known to harbor macroglia, Microglia and ECM proteins, the normal expression and distribution of targeted protein was assessed in the healthy retina (n=1) and fibrovascular membrane (n=3) by IHC. Activated microglia, were confirmed by staining with CD11b, TIMP2 and Opticin expression was detected in the retinal layers of OS, IL, IPL and in the NFL, MMP9 expression was noted in all retinal layers except photoreceptor layers (Figure 29.I). Thus, ROP fibrovascular membrane showed an increased MMP9 and CD11b expression corresponding to microglial cells but no Opticin expression (Figure 29.II).

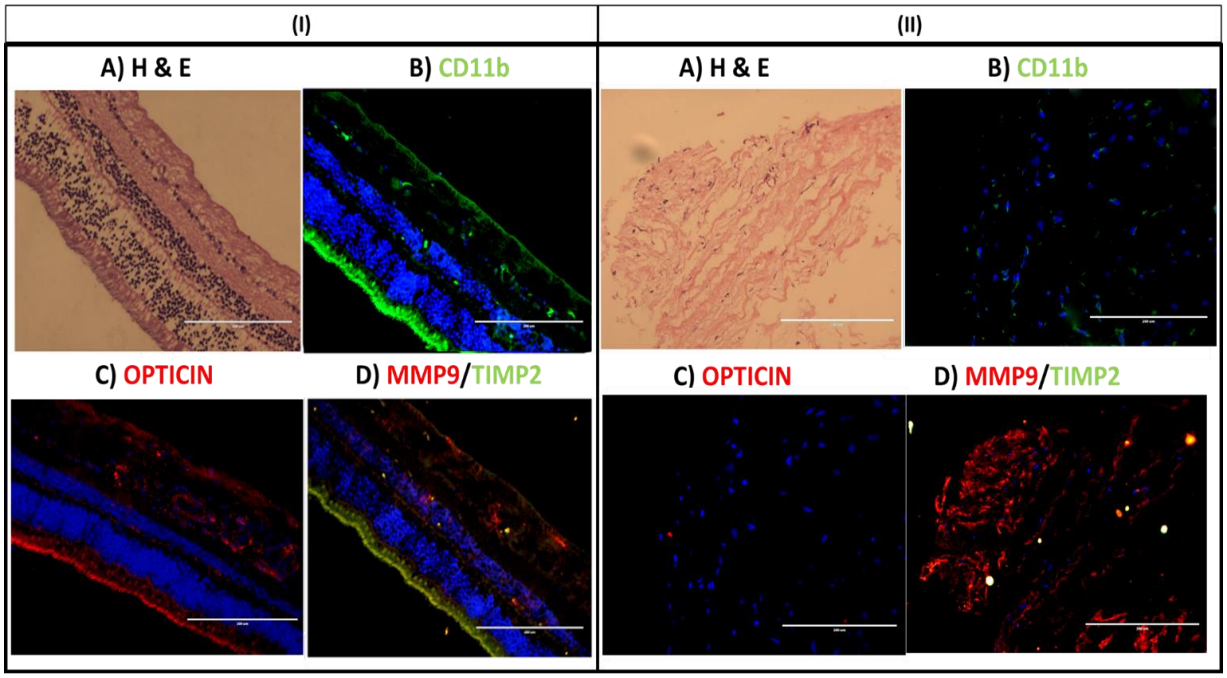

Figure 29. Representative image of (A) H & E, immunofluorescence of (B) CD11b, (C) Opticin (D) MMP9 and TIMP2 in (I) normal retinal tissue and (II) fibrovascular membrane collected from stage V.

1.4. Discussion

ROP is a vaso-proliferative eye condition that affects prematurely born infants, especially those who have lesser BW and a low GA. It is a self-limiting disease, but it also switches to progressive ROP in some of prematurely born infants. However, it is not clear why only a subset of preterm infant with the same GA develops ROP when exposed to similar environmental risk factors (Pietrzyk *et al.*, 2013).

Macrophage/microglial activation has been shown to promote inflammation in ROP eyes. Both activated macrophage/microglia and increased levels of complement, VEGF, and ECM components (MMP9) were noted in ROP vitreous. An imbalance of TIMP/MMP ratio in the ROP vitreous could lead to the degradation of the basement membrane in the blood vessel that further allows other blood components to leak into the vitreous, leading to vitreous hemorrhage and liquefaction. MMP9 may potentially have a role in VEGF secretion and endothelial cell invasion, both of which contribute to neovascularization in ROP (Rathi *et al.*, 2017).

Many ocular disease pathologies have been linked to an imbalance in MMP and TIMP expression levels. MMPs upregulation has been seen in many major ocular disorders, such as AMD, PVR, and secondary cataract (Federici, 2011). An elevated level of MMPs in the Bruch's membrane were observed in AMD. Notably, higher levels were also seen in region of choroidal neovascularization (Hussain *et al.*, 2011). Changes in MMPs are thought to contribute to higher outflow resistance in glaucomatous eyes (Ghanem *et al.*, 2011), and enhanced MMP-9 activity is linked to corneal stromal pathology in the dysfunctional tear state (Sambursky & O'Brien, 2011). Furthermore, increased MMP-9 activity has been detected in the eyes of patients with cortical cataracts, and activity rises with age in epithelial cells of lens of patients with age-related cataracts (Alapure *et al.*, 2008). These reports suggest that MMPs are involved in various eye related pathologies. Inflammatory markers (MMP9, TIMP1 and alpha 2-microglobulin) seen in the vitreous of young preterm infants may

indicate an inflammatory stimulus contributing to ROP. Based on these findings, the present study investigated if higher MMP levels in tear samples from ROP eyes may signal higher inflammation in the retina, and its role as a predictive marker for ROP progression. While tear collection from preterm eyes is not so easy and limited by volume, tear were chosen as they are relatively non-invasive, safe, and unlike vitreous are accessible even from preterm infants with no ROP and different stages of ROP. The study results indicated significantly higher MMP levels in tears of severe ROP compared to no-ROP and mild ROP, indicating that it could be adopted as a predictive marker for an early detection of the disease. Interestingly, in the initial experiments for the assessment of tear MMP levels, activated MMPs very similar to the concentration as in the severe ROP was noted in a mild ROP case. The case history and follow up details revealed that this baby, who presented with mild ROP progressed to severe ROP type within two weeks of sample collection and did not respond to laser therapy. This observation suggested that MMP activation may occur well before the development of severe ROP and could potentially be utilized as a marker for ROP detection. Further analysis of MMP9 levels in tears of an extended cohort of premature infants with different grades of disease revealed a severity-dependent increase in MMP9 levels and activity (Figure 1.4.1) and thus, tear MMP9 could reliably act as a surrogate marker for underlying inflammation in retina and be utilized as a predictive marker for ROP progression.

The invasion of blood vessels during neovascularization requires the proteolytic degradation of ECM. Increased MMP-2 and MMP-9 in proliferative diabetic retinopathy PDR have been demonstrated to promote ECM remodeling, resulting in the breakdown of collagen and followed by vitreous liquefaction (Coral *et al.*, 2008). Activated MMP-9 and elevated TIMP1, TIMP2, and α2-macroglobulins found in ROP eyes. The activated macrophages are responsible for the secretion of activated MMP9 levels in the ROP vitreous suggesting that it could be responsible for further induction of MMPs expression by interacting with LDL-Receptor protein 1. (Sanchez *et al.*, 2006), (Caceres *et al.*, 2010). MMPs can degrade ECM proteins and hence play a crucial function in various

physiological and pathological processes. TIMPs, on the other hand, tend to counteract MMP activity and therefore aid in the maintenance of ECM stability (Palosaari *et al.*, 2003).

Opticin belongs to small leucine rich proteins (SLRP) family of ECM protein and is a known antiangiogenic protein that binds to collagen I and II, causing poor endothelial cell adhesions, and thus blocking collagen binding to integrins (Le Goff, Sutton*, et al.*, 2012). Opticin is known to be expressed in ocular tissue like iris, optic nerve, RPE and retina (Ramesh *et al.*, 2004), while there are no reports of Opticin expression in microglia cells. This is the first study to show its expression in microglial cells. Based on a strong inverse correlation that exist between MMP9 and the Opticin in the ROP vitreous, we hypothesized that increased MMP levels in ROP probands would degrade the Opticin. To test this, we performed *in-vitro* analysis; by subjecting human microglia cells to hypoxia and then measured MMP activity and Opticin expression. Under hypoxic stress, the microglia cells got activated, and secreted and activated MMPs. These activated MMPs may degrade the ECM proteins like Opticin. MMP activity was inhibited by targeted inhibitors like doxycycline and EDTA. Doxycycline, a chemically altered tetracycline-derived molecule, binds directly to the Zinc ion domain of MMPs at the active site. Increased expression of MMPs can be inhibited by doxycycline either via inhibition of nitric oxide (NO) (Amin *et al.*, 1996) or by downregulating the transcription/synthesis of MMP9 (Jonat *et al.*, 1996). Doxycycline binds and irreversibly inhibits MMP activity by chelating the metal ions (Ca^{++} and Zn^{++}) at the catalytic site, which leads to changes in the structural conformation in MMPs.

There are numerous types of pharmacological MMP inhibitors, most of these inhibitors work by binding to the MMP's zinc site and inhibiting its action. Doxycycline inhibits MMP 1, 2, 7, 8, 9, 12, and 13 and is considered as the most powerful MMP inhibitor with a broad spectrum (Wang *et al.*, 2011). Bisphosphonates, another synthetic MMP inhibitor, have strong MMP inhibitory effects, most likely due to cation-chelation of zinc (Hidalgo & Eckhardt, 2001)]. Pharmacological

suppression of MMPs has been demonstrated to prevent retinal and choroidal neovascularization (Samtani *et al.*, 2009) and block MMP-9-mediated retinal vascular permeability and inflammation (Reddy *et al.*, 2009). In addition, a synthetic MMP inhibitor was also shown to inhibits the development of proliferative vitreoretinopathy (Bhatt & Addepalli, 2010; Ozerdem *et al.*, 2000) . EDTA is also an MMP inhibitor, which chelates metal ions at active sites in most receptor-mediated signaling processes.

MMP9 induces the expression of several signaling pathways associated genes like *TNF, TGF, MAPK/ERK*. Further, pathway analysis for MMPs activation under hypoxia, revealed downregulation of *MAPK, DKK1, NOTCH1* signaling pathway genes while *MAPK3* expression remains unchanged. MAPK is an important signaling molecule for diverse cell metabolism, differentiation, and proliferation. The cross talk between DKK1, a Wnt signaling inhibitor and membrane-type-MMP (MT-MMP) is essential for the activation of Wnt signaling. MMP inhibitors like a doxycycline and EDTA disturb of the cross-talk of DKK1 and MT-MMP, which further activated the Wnt signaling pathway. The future studies, may further explore the role of MMP inhibitors in regulating of Wnt signaling genes to prevent abnormal angiogenesis.

Hypoxia induction also resulted in transcriptional level regulation of genes, causing higher expression of *MMP9*, and downregulation of *OPTICIN, ERK2*, *DKK1* and *NOTCH1* signaling genes in microglia. On the other hand, Doxycycline and EDTA restored the expression of crucial signaling pathway genes while decreasing inflammation by inhibiting MMP activity. We confirmed the same phenomena in ROP eyes by examining the fibrovascular membranes produced in severe ROP phases. Glial cells, including microglia and extracellular matrix protein, make up these fibrovascular membranes. Previously, Sun *et al.* (2010) characterized the stage II ridge membrane by IHC and found the presence of few microglial cells (CD68), positive proliferative cells (Ki67),

endothelial cells (CD31 and CD34), astrocytes (GFAP) and astrocyte precursor cells (PAX2) in the ROP ridge membrane (Sun *et al.*, 2010) (Figure 30).

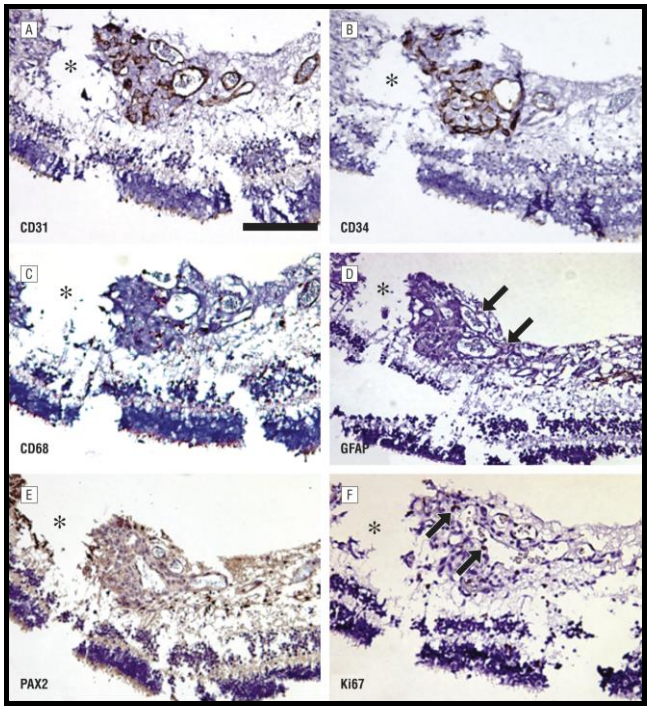

Figure 30. Characterization of ROP ridge membrane Adapted from: (Sun *et al.*, 2010)

The present study also demonstrated that MMPs are the key regulators of Opticin expression in microglia cells besides retinal pigment epithelial cells as shown in the previous studies (Le Goff, Lu, *et al.*, 2012). A further validation of the same phenomenon was shown by immunohistochemistry of ROP patient's fibrovascular membrane and the normal cadaveric retina as a positive control. The expressions of microglial specific marker (CD11b), TIMP2, and Opticin were found in the outer segment (OS), inner layer (IL), inner plexiform layer (IPL) and nerve fiber layer (NFL) in normal retina while MMP9 showed expression in all retinal layers except photoreceptor layer. The fibrovascular membrane from ROP patient showed the expression of CD11b with a very high expression of MMP9 and no expression of Opticin. The major limitation for this study was that due to the lack of age-matched retinal membranes, the relative expression of targeted proteins could not be assessed. Based on the above findings, we confirmed that MMPs and other signaling

mechanisms are dysregulated in hypoxic stress, which plays a vital role in ROP pathogenesis. Inhibition of inflammation by MMP targeted inhibitors can rescue the Opticin and other key signaling molecules involved in angiogenesis at both transcript and protein levels (Figure 31).

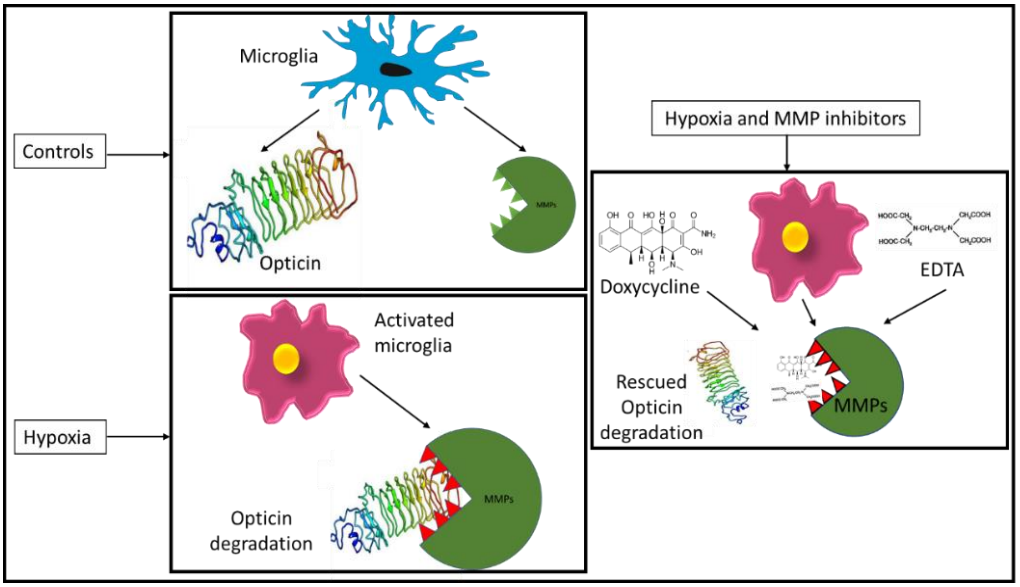

Figure 31. Graphical demonstration of MMPs role in presence of hypoxia and MMP inhibitors (S. Patnaik *et al.*, 2021)

In summary, the present study found the inflammatory proteins in the tear samples could be used as a predictive marker for ROP progression. Further, targeting inflammation by inhibiting MMP activity may help in delaying the progression and obtaining the best visual outcome in severe stages of ROP.

CHAPTER-2

CONTRIBUTIONS OF HERITABILITY IN ROP SUSCEPTIBILITY

2.1. General introduction and review of literature

The current chapter aims to study the genetic contributions towards ROP susceptibility. Several studies have been conducted on the OIR-mouse model and ROP patients to explore the genetic factors associated with ROP. However, the pathogenesis and management of ROP are yet unclear. It is not understood why some preterm infants with low birth weight (LBWT) and gestational age (GA) do not develop ROP, while, others progress to severe ROP. Furthermore, maternal and post-gestational risk factors don't explain the risk of ROP progression completely. This indicates that besides the known risk factors, others such as genetics may play a crucial role in the development of ROP.

We have also performed gene expression, metabolome and targeted protein profiling in ROP infants to understand disease pathogenesis and progression that are provided in the subsequent chapters. Genetic components are fundamental building blocks of human life and studying the genotype and phenotype correlation can help identify essential components in ROP progression. Over these years, many high throughput screening technologies and advances in genome sequencing technologies have facilitated the identification of underlying genetic mechanisms different complex diseases. It has also led to the identification of disease-associated pathogenic rare variants, which is clinically relevant and can be used in DNA-based diagnosis.

The massive and accurate genetic information generated by whole-genome (WGS) and whole-exome sequencing (WES), have provided additional information pertaining to and precise genome sequence variations across organisms. WES that analyses only the coding regions (exons), is a cost-effective and efficient method of sequencing that is widely used in rare diseases. Unlike traditional Sanger sequencings (chain-termination), NGS produces an immense amount of sequencing data at a lesser time and cost. The defined workflows from sample processing to data interpretation, exome sequencing is an effective tool for identifying

disease-causing variants in rare and complex diseases. Earlier, WES was performed to identify pathogenic variants in ocular disorders like FEVR, retinitis pigmentosa and multifactorial diseases like glaucoma and age-related macular degeneration (Micheal *et al.*, 2018; Huang *et al.*, 2018; Zhou *et al.*, 2017; Ferre-Fernandez *et al.*, 2017; Sardell *et al.*, 2016) . In order to understand the genetic contribution in ROP, we have employed a combination of candidate gene screening and WES to identify the potential rare and pathogenic variants associated with ROP and assess their biological significance.

2.1.1. Candidate genes

Earlier studies have identified few candidate genes in ROP based on their involvement in the disease pathogenesis (Rathi *et al.*, 2018; Ells *et al.*, 2010; Mohamed *et al.*, 2009; Hiraoka *et al.*, 2001). Mutation screening was undertaken in these studies, which was not replicated across multiple patient cohorts. The Wnt-norrin-catenin signaling is essential for retinal vasculature development (Figure 32). Genes identified in this pathway are involved in numerous retinal vascular disorders such as a Coat's disease, Norrie disease and FEVR. For instance, genes involved in the Norrin signaling pathway during retinal development are also suggested to be responsible for ROP development as the phenotypes of ROP and FEVR are very similar. Likewise, *FZD4, LRP5, NDP* and *TSPAN12,* which are the candidate genes involved in the Wnt-β catenin signaling pathways in FEVR are also involved in ROP. Their roles are described below:

2.1.1.1. *LRP5*

LRP5 is a low-density lipoprotein receptor that transmits signals from Wnt proteins in combination with other members of the frizzled protein family. The *LRP5* gene consists of 23-exons, that accounts for a 1615-amino-acid containing protein. LRP5 assists in maintaining bone mass and early development of the retina (Gong *et al.*, 2001) and also maintains balanced cholesterol and glucose metabolism (Fujino *et al.*, 2003). The cytoplasmic domain of the

LRP5/6 protein comprises five closely conserved PPPSPxS signature motifs that bind to AXIN (Wnt regulator) and causes GSK-3 and CK1 kinases to phosphorylate (B. T. MacDonald & He, 2012). The β-catenin molecules stabilize and aggregate in the cytoplasm. After accumulating in the cytoplasm, they might translocate into the nucleus, displacing transcription factors from TCF/LEF (T-cell factor/lymphoid enhancer factor) (Tam & Watts, 2010). Further, TCF/LEF transcription factors activate the expression of Wnt β-catenin signaling target genes.

LRP5 gene expression has already been detected in a wide range of human tissues, including the bone, heart, eye, skin and pancreas, with the liver showing the highest expression level. Across different populations, *LRP5* mutations account for 10 to 25% of FEVR cases (Yang *et al.*, 2012; Nikopoulos *et al.*, 2010; Boonstra *et al.*, 2009; Qin *et al.*, 2005; Toomes *et al.*, 2004). Further details are provided in Table 17. These findings indicate the role of genetic alterations in the Wnt signaling pathway in ROP development.

2.1.1.2. *FZD4*

FZD4 belongs to the G protein-coupled receptor and norrin is explicitly bound to FZD4. Kirikoshi and co-workers first mapped the *FZD4* gene on chromosome 11q14-q21 (Kirikoshi *et al.*, 1999). The gene comprises of two exons that encodes for a 537-amino-acid protein (Kirikoshi *et al.*, 1999). The *FZD4* transcript (7.7 kb) is expressed in almost every human tissue, with relatively higher expressions in the fetal kidney, adult heart, skeletal muscle and ovary (Kirikoshi *et al.*, 1999).

Fzd4$^{-/-}$ knockout in mice revealed that it is essential for retinal vascular growth and blood-brain barrier (BBB) differentiation (Paes *et al.*, 2011). The role of *FZD4* was also demonstrated in retinal angiogenesis and wild-type *FZD4* was found to activate a portion of the Wnt/Ca^{2+} signaling pathway, unlike the mutant (Robitaille *et al.*, 2002). Furthermore, *FZD4* signaling in

endothelial cells resulted in defective vascular growth in conditional knockout mice and cell culture models, contributing to retinal neuron loss and disruption the BBB's integrity (Ye *et al.*, 2009). *FZD4* mutations have been linked to ROP in various populations. Advanced stages of ROP have been associated with *FZD4* variants (Table 17).

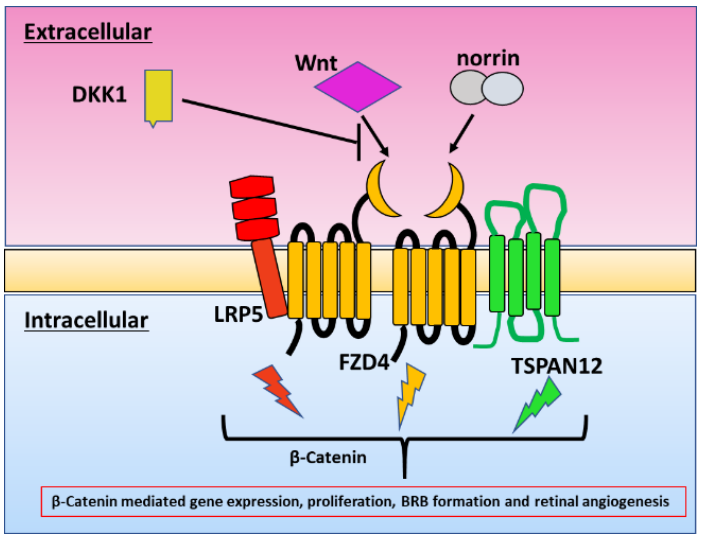

Figure 32. Schematic representation of *Wnt* β-catenin signaling in retinal development and maturation

2.1.1.3. *TSPAN12*

TSPAN12 gene encodes the 305 amino-acid protein, implicated in Norrin signaling and retinal neovascularization. This gene is located on chromosome 7q31.31, has 8-exons and codes for a protein with four transmembrane domains and two extracellular loops (Nikopoulos *et al.*, 2010). Its gene expression was detected in retinal endothelial cells and is a vital component of the norrin-β catenin signaling pathway (Junge *et al.*, 2009). It has been documented that mutations in this gene cause 3 to 10% of FEVR cases (Hemler, 2005). Very few studies have looked into the connection between the *TSPAN12* gene and ROP. We have earlier reported the involvement of this gene in ROP (Rathi *et al.*, 2018). Several studies have reported variations in the *TSPAN12* gene-mediated Wnt β-catenin signaling, which might be contributing to ROP pathogenesis (Table 17).

2.1.1.4. *NDP*

The *NDP* locus was first mapped on chromosome Xp11.3 in a 150-kb region (Sims *et al.*, 1992) that encodes for a 133-amino acid containing norrin protein. Norrin can affect cells, tissue's function and lead to Norrie disorder. Due to the abundance of essential amino acid residues, Norrin can bind with the extracellular matrix through ionic interactions. Norrie is an FZD4 receptor-specific ligand that inhibits the Wnt β-catenin signaling directly. The former is also found in müller glial cells in the retina. This signaling pathway is critical for the retina's vascularization during development. Genetic variants in the 5' and 3' UTRs of exon 1 of the *NDP* gene have been identified in a few ROP cases (Talks *et al.*, 2001; Hiraoka *et al.*, 2001). These variants indicate that *NDP* gene-mediated Wnt signaling may be involved with ROP (Table 17).

2.1.2. Other candidate genes in ROP pathogenesis

The biochemical, cellular and genetic factors regulate various signaling molecules and pathways implicated in ROP pathogenesis. VEGF is a crucial regulator of angiogenesis and linked to ROP development in prematurely born infants (Smith, 2002; Aiello, 1997). In progressive and severe ROP infants, significantly elevated expressions of VEGF were observed in the subretinal fluid of eyes in severe ROP cases (Lashkari *et al.*, 2000).

Two variants in the human *VEGF* have been widely studied in previous studies. The *VEGF*-634 G>C genotypes was associated with progressive ROP (Cooke *et al.*, 2004). In contrast to the -634 C allele, the G allele exhibited increased basal promoter activity (Stevens *et al.*, 2003). It was also discovered that this -634 C allele was significantly more prevalent in preterm infants with threshold ROP than those without ROP (Vannay *et al.*, 2005). In progressive (threshold) ROP, homozygous variation of the G allele led to higher VEGF expression (Cooke *et al.*, 2004). In addition to this, VEGF expression was controlled by HIF-1α response to low oxygen levels that are essential for tissue maintenance and homeostasis (Semenza, 2011). HIF-1α is an

essential gene involved in ROP pathogenesis and regulates *VEGF, VEGFR1, PDGF, SDF-1* and *ANG2* under hypoxic stress (Campochiaro, 2015).

Thus, ROP is a complex disorder that might be associated with multiple alleles and other gestational risk factors with varying degrees of effect. The cumulative impact of these variants across different population groups, explains only a small contribution to ROP susceptibility. Since ROP is a multifactorial disease, it is impossible to rule out the participation of other potential genes beyond those in the norrin-catenin signaling pathway. Therefore, there is a need to find other genes involved in ROP pathogenesis.

Table 17. List of variants associated with ROP across different ethnic groups

List	Gene	Study country	Clinical characteristic / Stages of ROP	Location	Base change	Amino acid change	Reference
Candidate genes	*LRP5*	Japan	ROP, Stage 4A (OU)	Exon 17	c.3656G>A	p.R1219H	(Kondo *et al.*, 2013)
			Stage5 (OD), Stage 4B (OS)	Exon 20	c.4148A>C	p.H1383P	
			Stage 4B (OS) / 5(OD)	Exon 23	c.4619C>T	p.T1540M	
			Advanced ROP	5'UTR	c.237 A>G	-	(Hiraoka *et al.*, 2010)
		China	Stage 1	Exon 11	c.2447A >C*	p.Q816P	(Li *et al.*, 2020)
			Stage 4A	Exon 11	c.2431A >G	p.I811V	
				Exon 7	c.1434G >A	p.W478X	
	FZD4	United States	ROP	Exon 1 and 2	c.502 C>T, c.97 C>T;	p.P33S; p.P168S	(Dailey *et al.*, 2015)
			ROP	Exon 2	c.1271 G>A	p.G424E	
		India	Stage 4/5	Exon 1	c.97C>T	p.P33S	(Rathi *et al.*, 2018)
				Exon 2	c.502 C>T	p.P168S	
					c.576 C>T	p.I192I	
					c.1078 A>G	p.I360V	
				3'UTR	c.*2G>T	NA	
		Japan	APROP/stage 4A (OU)	Exon 1	c.205C>T	p.H69Y	(Kondo *et al.*, 2013)
			APROP/stage 5 (OU)	Exon 2	c.380G>A	p.R127H	

List	Gene	Study country	Clinical characteristic / Stages of ROP	Location	Base change	Amino acid change	Reference
			ROP		c.502C>T	p.P168S	(Drenser *et al.*, 2009), (Ells *et al.*, 2010)
			Stage 3 (OU)		c.609G>T	p.K203N	(Ells *et al.*, 2010)
			APROP/stage 4A (OU)		c.631T>C	p.Y211H	(Kondo *et al.*, 2013)
			not described		c.766A>G	p.I256V	(M. L. MacDonald *et al.*, 2005)
			Stage 3 (OU)		c.1109C>G	p.A370G	(Ells *et al.*, 2010)
			Stage 3 (OU)		c.1396C>T	p.R466W	
		Unspecified	Advanced ROP	Exon 2	c.766A>G	p.I256V	(M. L. MacDonald *et al.*, 2005)
		Canada	Advanced ROP	Exon 2	c.1109C>G	p.A370G	(Ells *et al.*, 2010)
				-	c.609G>T	p.K203N	
		China	Stage 1 OD /Stage 4 OS	Exon 2	c.313A >G	p.M105V	(Li *et al.*, 2020)
			Stage 4B OD /Stage 1 OS		c.40_49del	p.P14fs	
	TSPAN12	India	Stage 4/5	Exon 5	c.356T>G	p. L119R	(Rathi *et al.*, 2018)
				Exon 8	c.765 G>T	p. P255P	
				3'UTR	c.*39C>T	-	

List	Gene	Study country	Clinical characteristic / Stages of ROP	Location	Base change	Amino acid change	Reference
					c.*334A>T	-	
					c.*1243A>T	-	
		China	Stage 4 OU	Exon 4	c.194C > T	p.P65L	(Li *et al.*, 2020)
	NDP	United States	Stage 3 (threshold)	3'UTR	c.1572G>A	-	(Hutcheson *et al.*, 2005)
					c.1253:1 bp insertion	-	
					c.*824G>A	-	
		Japan	4A/3/AP ROP		c.*237A>G	-	(Hiraoka *et al.*, 2010)
		Australia	Severe ROP	Exon 1	14 bp deletion	-	(Dickinson *et al.*, 2006)
		Kuwait	Advanced stages of ROP	Exon 3	c.597C>A	-	(Haider *et al.*, 2002b)
					c.110C>G	-	
		United States	Stage 4B		c.121C>T	R121W	(Shastry *et al.*, 1997)
					-	L108P	
		India	Stage 4B	3’ and 5' UTR	-	-	(Rathi *et al.*, 2018)
			Stage 4	Intron 1	(c.*522T>C)	-	
		China	Stage 5/4b	Exon 3	c.181C >A*	-	(Li *et al.*, 2020)
				Exon 2	c.134T >G*	p.V45G	
					c.134T >A*	p.V45E	

List	Gene	Study country	Clinical characteristic / Stages of ROP	Location	Base change	Amino acid change	Reference
Other associated genes	*ACE*	Italy	Stage 5/4b	Intron 16	Alu I/D (287 bp)	NA	(Poggi *et al.*, 2015)
				5' near gene (promotor)	-240A>T	NA	
		Kuwait	Stage 5/4b	Absence of 287-bp insertion in intron 16	-	-	(Haider *et al.*, 2002a)
	AGT	Italy	-	Exon 2	c.803T>C	p.M235T	(Poggi *et al.*, 2015)
	AGTR1		ROP	3'-UTR	c.1166 A>C	-	
	CETP	United States	ROP	Intergenic	-	-	(Mohamed *et al.*, 2009)
					-	-	
	CFH				-	-	
					-	-	
	EPAS1	United States			-	-	
	GP1BA				-	-	
	NOS3	Italy	ROP	Intron 4	c.298G>T	-	(Poggi *et al.*, 2015)
				5' near gene	-786 T>C	-	
		Hungary	Severe ROP	Promotor	(−786T>C)	-	(Rusai *et al.*, 2008)
		United States	ROP	Intron	(894G>T)	-	(Yanamandra *et al.*, 2010)

List	Gene	Study country	Clinical characteristic / Stages of ROP	Location	Base change	Amino acid change	Reference
	HMOX1	Italy	ROP	5' near gene	GT repeat	-	(Poggi *et al.*, 2015)
	IHH	United States	ROP	Intergenic	-	-	(Mohamed *et al.*, 2009)
	TBX5				-	-	
	TGFB1	United Kingdom	ROP	-	−509C>T	-	(Cooke *et al.*, 2004)

2.1.3. Whole exome sequencing

Earlier studies on ROP that looked at specific gene variant were largely inconclusive as these accounted for few cases (Swan *et al.*, 2018; Hartnett & Cotten, 2015; Hartnett *et al.*, 2014; Nikopoulos *et al.*, 2010; Poulter *et al.*, 2010). The candidate genes in ROP account for ~3-11% of cases (Shastry, 2010). In order to find other genes contributing to ROP pathogenesis, whole-exome sequencing (WES) is warranted. So far, there is only one study on WES that observed two significantly enriched pathways associated with ROP. But this could not identify specific variants underlying ocular defects in ROP. Therefore, the present study was designed to identify rare pathogenic variants in different sets of ROP twins for performing WES.

2.1.4. WES in ROP twins

The twin study model works under the assumption that monozygotic (MZ) twins share their genes and their early environmental factors. MZ twins are born from a single fertilized egg (zygote) and have similar genetic code. On the other hand, dizygotic (DZ) twins share an average of 50% of their genome (Figure 33). Due to this, MZ twins are referred to as "identical twins." Thus, discrepancies between MZ twins (discordance) would be assumed to be due to environmental factors.

In contrast, DZ twins (with two independently fertilized eggs would be expected to differ due to both genetic and environmental factors. Twins also share many aspects of their environment (e.g., *In-utero* environment, parenting style). Twin studies are an excellent way to learn more about the genetics of complex characteristics and trait variability in complex diseases (Figure 33) (van Dongen *et al.*, 2012).

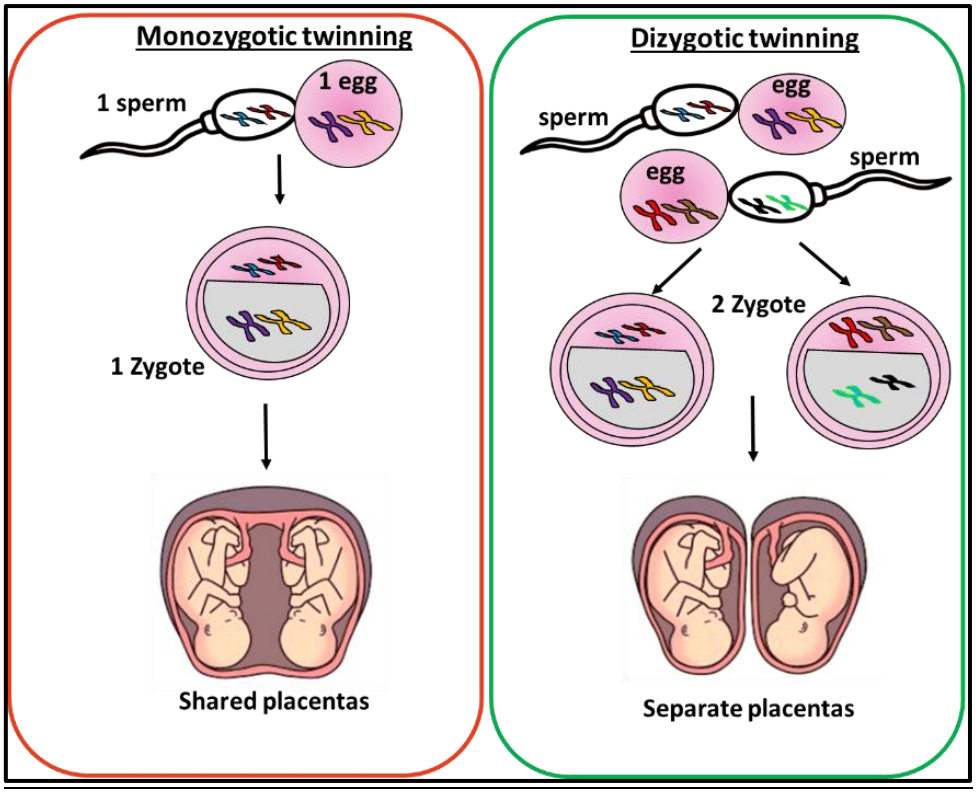

Figure 33. Mechanism of twinning in monozygotic and dizygotic twins

In order to determine heritability, we generally do not get a positive family history in ROP cases due to the nature of its etiology. So, we have selected twins to study heritability based on the concordance of ROP among the twin pairs. Concordance indicates that both pairs have a common clinical trait. So, if specific gene variant(s) are responsible for a particular clinical trait in one sibling, then it is likely to be present in the other sib within the same twin pair.

Moreover, the same should not be present in discordant twins. Discordant indicates if only one member of the pair has a trait and does not share genetic makeup. Both twins mild/AP/severe ROP/and no ROP, were classified as concordance twins. Discordant twins were the ones with only one twin with ROP and another without ROP.

2.1.5. Genetic variability in ROP twins

There is evidence of genetic susceptibility in ROP as seen in studies on humans and animal models, but no definite genetic component has yet been established.

The inter sibling variability in twins was explored as a possible risk factor based on a retrospective examination on twins with ROP at a tertiary institution (January 2004 to December 2008). The incidence and risk factors at different stages of ROP among siblings of multiple gestations revealed that 16% of babies with multiple gestations had discordant ROP (Sanghi *et al.*, 2012). In both multiple and singleton deliveries, the incidence of ROP has been observed to be the same (Blumenfeld *et al.*, 1998; Friling *et al.*, 1997; Schaffer *et al.*, 1993). Inter sibling differences in the prevalence and severity of ROP occur despite being exposed to a comparable prenatal environment (Blumenfeld *et al.*, 1998; Holmstrom *et al.*, 1998; Friling *et al.*, 1997; Fellows *et al.*, 1995; Hall *et al.*, 1995). A probable reason for this variance might be post-gestational and genetic risk factors.

In twin siblings, a lower birth weight may not indicate a higher risk of severe ROP (Blumenfeld *et al.*, 1998). A similar study identified that birth weight discordance was a unique risk factor for severe ROP in both the twins (Fellows *et al.*, 1995). Another study reported that in discordant ROP group, there was no increased risk of ROP associated with LBWT (Blumenfeld *et al.*, 1998). In a study of twin pairs with discordant birth weights, it was found that the twin with higher birth weight may be at an increased risk of developing ROP (Fellows *et al.*, 1995). GA, BWT and postnatal variables were found to be ineffective in predicting ROP severity in twins (Sanghi *et al.*, 2012). It may be indicative of genetic predisposition in some ROP infants.

The WES study performed by Kim *et al.* (2021), was conducted on 100 non-Hispanic Caucasians (58 severe ROP, control group-42 mild/no-ROP), wherein, the authors identified pathogenic variations and performed gene set enrichment analysis (GSEA) in severe ROP cases after adjusting for gestational age and birth weight. Authors used GSEA to determine ROP-related pathways from various data sources, (KEGG, Reactome, and Wikipathways). The identified pathways included the β 2 adrenergic receptor signaling system, dopamine

receptor-mediated signaling pathway, T cell activation, nicotinate/nicotinamide metabolism and platelet-derived growth factor (PDGF) signaling. The GSEA enrichment analysis exhibited two substantially related pathways (smooth endoplasmic reticulum and vitamin C metabolism). However, their GWAS analysis on 100 preterm infants could not find any genome-wide significance by enriching the implicated genes in ROP that were observed through GSEA. While the authors incorporated different phenotypic categories to compensate for the small sample size, they did not have adequate severe ROP cases. Thus, the implicated pathways in this study needs validation in additional cohorts with a robust research design.

To summarize, there are evidences of substantial genetic contributions to ROP pathogenesis in the literature. So far, few studies have explored candidate genes in ROP using a targeted screening approach. However, their contributions to ROP development and progression are yet unclear. In order to address this, WES under a robust study design may reveal novel genes in ROP pathogenesis. Therefore, the current study was planned with following aims:

1. To identify novel rare pathological variations by WES in different twin pairs with ROP, who were categorised based on their clinical severity.

2. Understanding the gene enrichment pathways that may be implicated in ROP pathogenesis.

2.2. Methodology

2.2.1. Enrolment of ROP cases and control subjects

The study was approved by the Institutional Review Board (IRB) of L V Prasad Eye Institute, Hyderabad, India, (Ref no LEC06104) and adhered to the tenets of the Declaration of Helsinki. Written informed consent was obtained from the parents/guardians of the minors before sample collection. The study subjects were enrolled from the Smt. Kannuri Santhamma Centre for Vitreo Retinal Diseases at the L. V. Prasad Eye Institute and Niloufer Hospital located in Hyderabad, India.

2.2.2. Sample collection

The ROP cases were categorized into five phenotypic conditions of disease severity that included twin pairs from each category (n=3). Blood samples (0.3-1mL) were collected from twin pairs (similar gender) in EDTA-coated vacutainers by venipuncture and stored in -20^{0}C deep freezer for further use. The overall distributions of twin pairs are indicated in Figure 34.

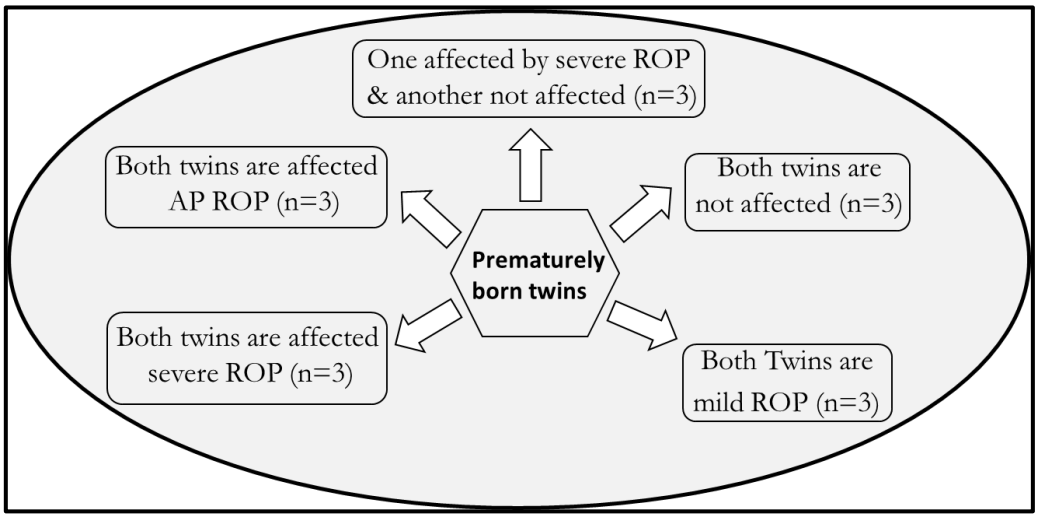

Figure 34. Different ROP twin pairs used in WES

Subsequently, the twin's maternal and clinical history was documented (gestational age, birth weight, age, geographic location, consanguinity and family history of the disease) in a

predesigned proforma. The pedigrees of the patients were drawn with the Cyrillic 2.1 software (Figure 35).

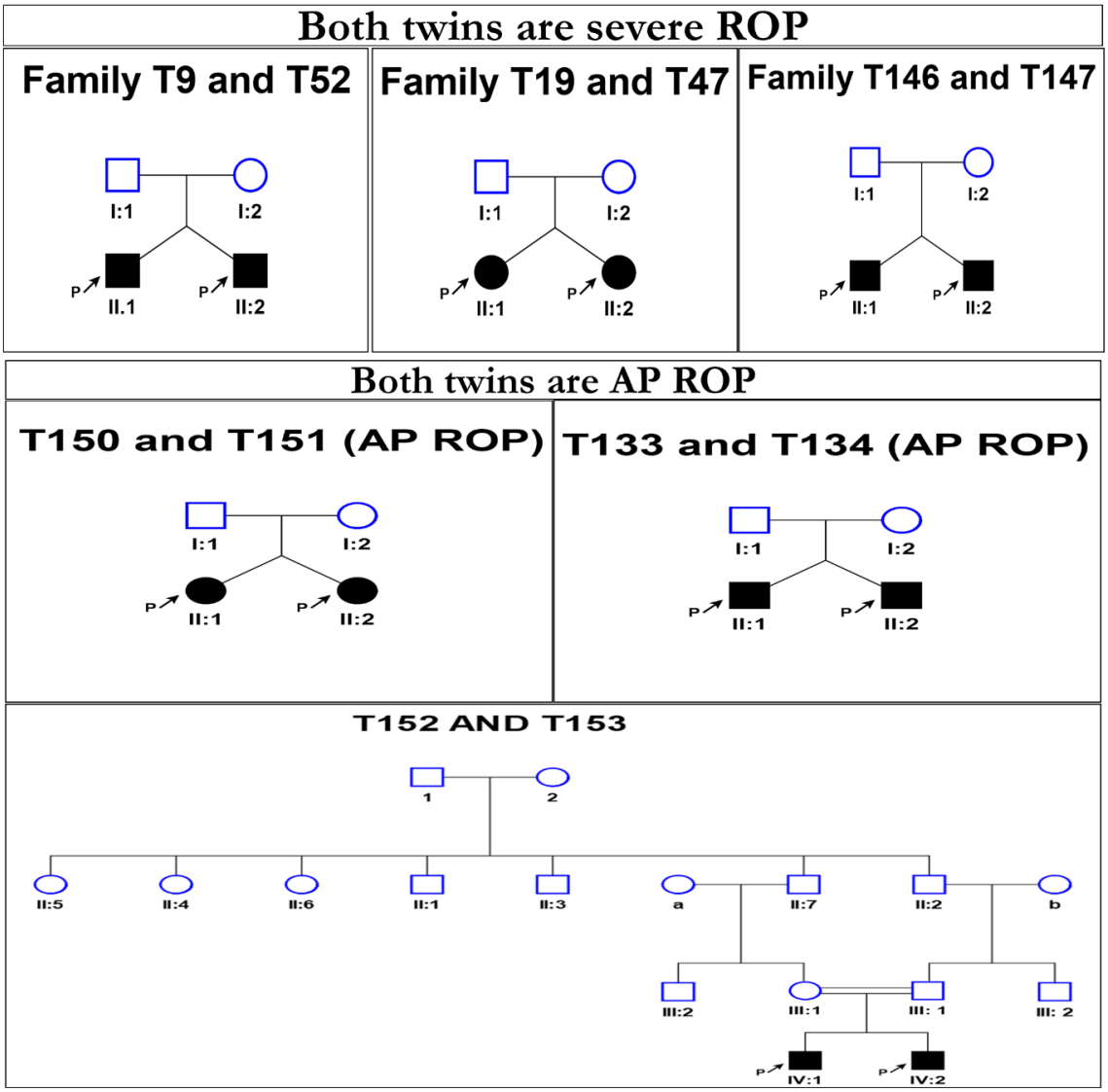

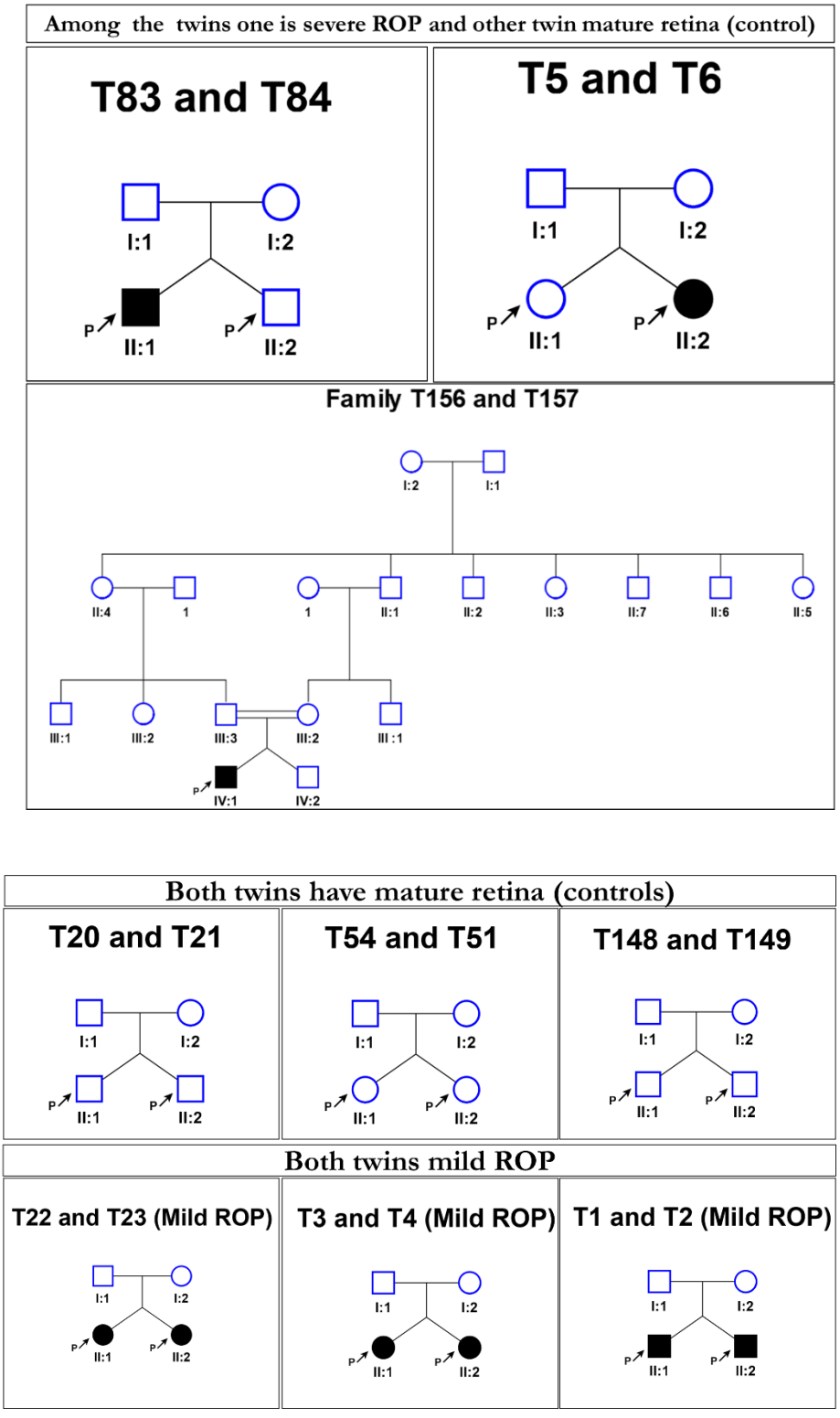

Figure 35. Pedigree of concordant and discordant ROP twins with different stages of ROP

The inclusion and exclusion criteria of the patients and controls have been detailed in chapter 1 (Table 6). The probands were recruited through the ROP screening program conducted by L V Prasad Eye Institute. All premature infants underwent detailed retinal examination by a retina specialist, which was further confirmed independently by another clinician. The second clinician was also responsible for grading the various stages of ROP.

2.2.3. Molecular genetic analysis

The genomic DNA was isolated from the peripheral blood of the ROP twins using an automated DNA extraction machine (MagNa Pure LC 2.0 Roche USA).

2.2.3.1. **Extraction of genomic DNA**

MagNA Pure LC 2.0 System is based on magnetic bead technology (Roche Applied Science) and was used to extract genomic DNA from the blood samples of the subjects. This technology is based on DNA's affinity to bind to the silica surface of chromatographic microcolumns or paramagnetic DNA binding microparticles, forming a DNA-bead complex, which is separated from cellular debris by magnetic separation and eluted at high temperature during the removal of magnetic glass particles (MGPs). 300µL-1000µL of frozen blood samples were thawed on ice before the extraction procedure and transferred into Roche sample cartridges as per the designed plate map. Extraction was done as per the manufacturer's protocol. Around 100µL of eluted DNA was transferred to a 0.5mL tube.

2.2.3.2. DNA quality check by agarose gel electrophoresis

DNA samples were run on a 1% agarose gel for qualitative assessment. The electrophoresis was carried out at 100 V for 30 minutes and the DNA bands were visualized under a UV transilluminator (Biorad, USA). Note: The preparation of stock solutions in detail is given in Appendix II.

2.2.3.3. Quantification of the genomic DNA by UV Spectrophotometer (NanoVue™ Plus) and Qubit™ assay

The quality and concentration of genomic DNA were measured by using Nanodrop NanoVue™ Plus. The purity of the DNA was assessed by calculating the Optical Density (OD) ratio at two different wavelengths, 260 and 280 (OD 260/OD 280). An OD of ~1.8 at 260/280nm was considered "pure DNA" for further experiments. Before WES, double-stranded DNA (dsDNA) quality was assessed by Qubit™ dsDNA HS assay (Thermo Fisher Scientific, catalogue no#Q32851). Qubit assay explicitly measured the double standard DNA and detection limit range from 10pg/μL to 100ng/μL.

2.2.4. Whole Exome Sequencing (WES)

WES for ROP twins was performed on an Ion Proton platform (Thermofisher, USA) using the Ion AmpliSeq Exome RDY chemistry (Cat no # 4489061) and following the manufacturer's guidelines. A detailed protocol of WES is mentioned below. (Figure 36)

2.2.4.1. Library preparation

Whole exome library was prepared by using Exome RDY plate (Cat no #4489061) precoated with 12 primer pools in two defined rows of a 96 well plate. Detailed protocol of library preparation is as follows.

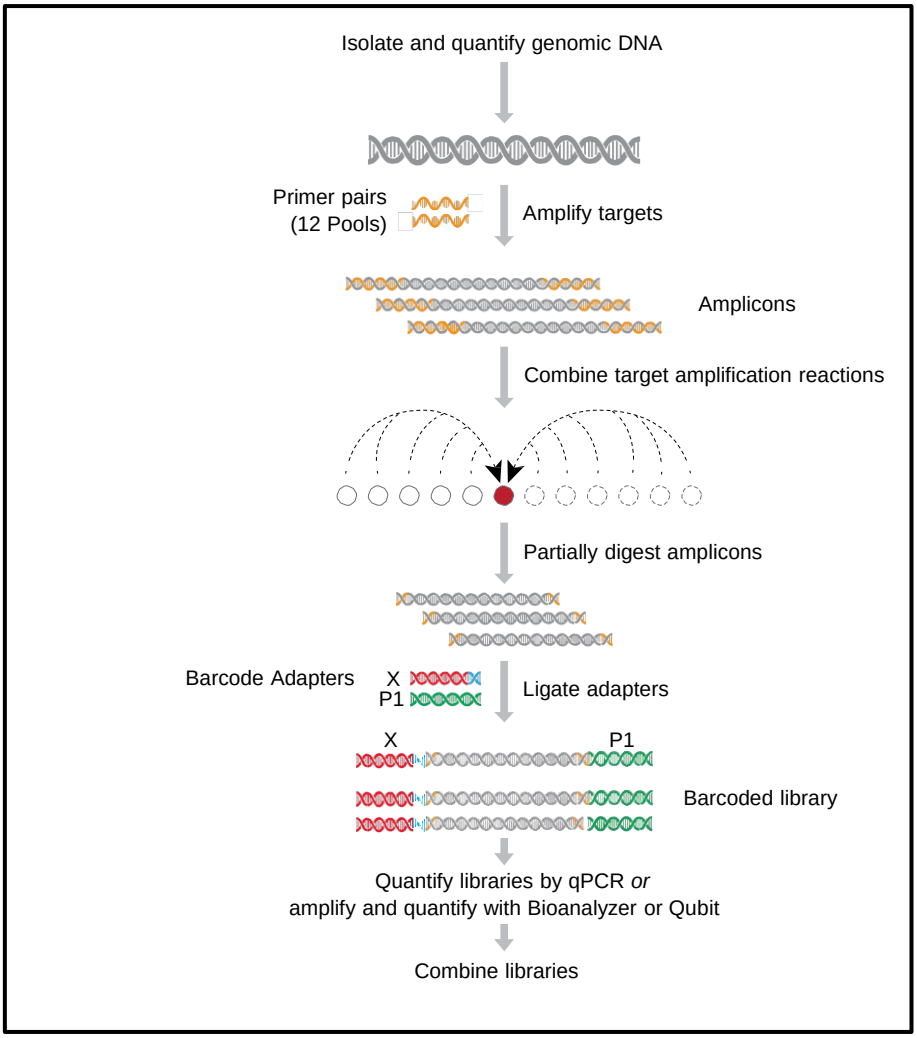

Figure 36. RDY whole exome sequencing work flow

2.2.4.2. Amplifications of targets

DNA samples were amplified together for WES. Two separate master mixes were prepared for each sample (Table 20), 20.5µL of master mixes were added on to rows with the primer pools, respectively. Prior to amplification, the RDY plate was sealed with a MicroAmp™ clear adhesive seal and was briefly centrifuged for proper mixing. The components of the master mix used for amplification is shown in Table 18 and conditions are described in Figure 37.

Table 18. Composition of the master mix to amplify the target

Components	Master mix (volume)
5X Ion Ampliseq HiFi mix	14µL
100ng of gDNA	X
Nuclease free water	56-X µL
Total volume	70µL

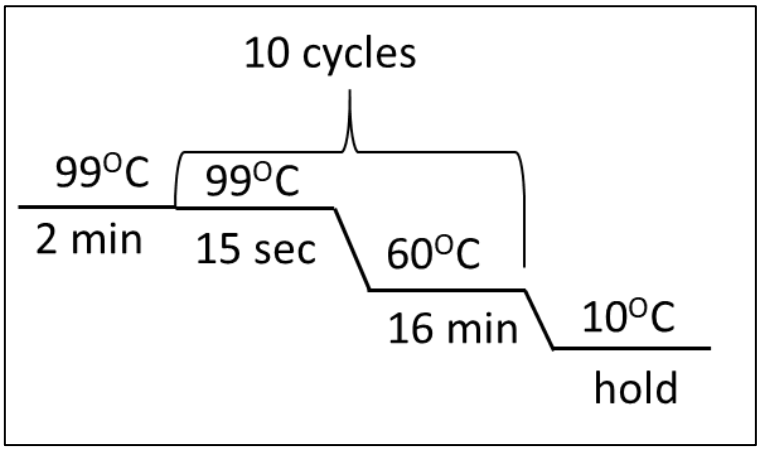

Figure 37. PCR conditions used for target amplification

2.2.4.3. Combine target amplificons and partial digestion

Post amplification, the amplicons coating plate was centrifuged shortly and the amplicons were combined. For partial digestion of the samples, 6µL of FUPA reagent was added in the combined amplification mix (60µL). The reaction mixture was thoroughly mixed and the plate was sealed and placed on a thermal cycler. The conditions for partial digestion of the samples are described in Figure 38.

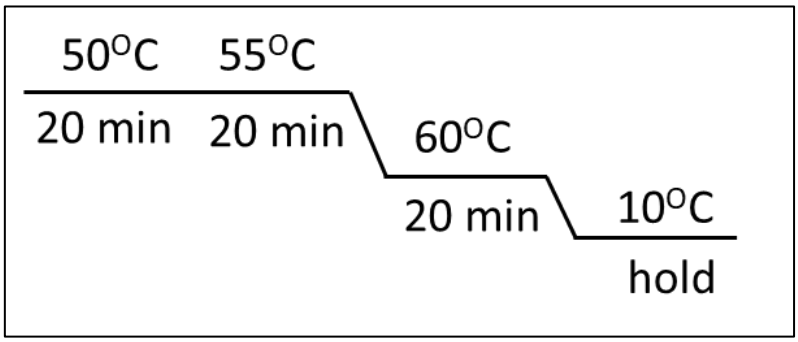

Figure 38. PCR conditions used for partial digestion

2.2.4.4. Ligate adapters to the amplicons and purify

Two exome amplicons were pooled together and sequenced in a single run to ligate adapters. The amplicons were ligated to IonCode™ Barcode Adapters to give them a unique identity. The components and concentrations of the ligation mixture are represented in Table 19. The total reaction volume was 80µL. Barcode adapter ligation conditions are represented in Figure 39.

Table 19. Composition of ligation mixture

Components	Master mix 1 (volume)	Master mix 2 (volume)
Switch Solution (yellow cap)	12µL	12µL
IonCode™ Barcode Adapters	X1-6µL	X2-6µL
DNA Ligase (blue cap)	6µL	6µL
Total volume	**~84µL**	**~84µL**

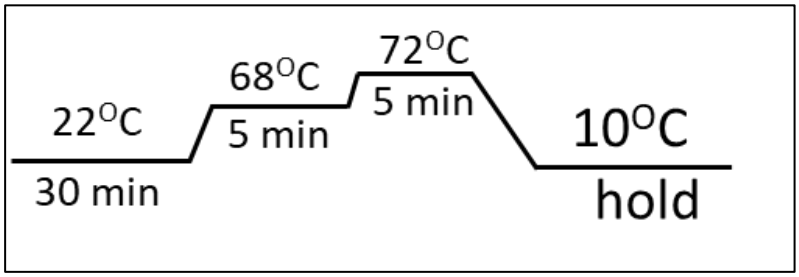

Figure 39. Amplification conditions used to ligate adapters to the amplicons

To purify the unamplified library, the plate seal was carefully removed without disturbing the reaction mixture. The library was then transferred to 1.5mL sterile tubes followed by the addition of 80µL (1X of sample volume) Agencourt™ reagent to each library. The Agencourt™ AMPure™ XP reagent was brought to room temperature (RT) before use and bead suspension was vortexed to make it homogeneous. The beads were slowly mixed with the library using a pipette and incubated for 5 minutes at RT. The 1.5mL tube was placed

onto a magnetic stand for 5 min. The pellets were carefully discarded without touching the beads. The beads were washed repeatedly with freshly prepared 70% ethanol (150µL) and air-dried at RT for 5 minutes.

2.2.4.5. Amplification of the beads in the library and purification

Once air dried, the 1.5mL tubes were removed from the magnetic stand. 50µL of 1X library amp Mix and 2µL of 25X library amp primers were added into each bead containing pellet (library amplifications receipts presence of AMPure™ XP beads) and were mixed thoroughly using a micropipette. Further, the complete reaction mix was transferred into a sterile PCR tube and loaded onto a thermal cycler. The conditions for PCR amplification are described below Figure 40.

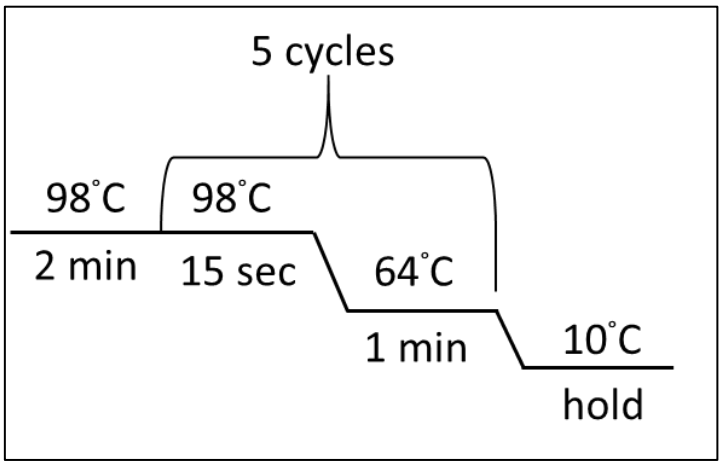

Figure 40. Conditions used for amplify the amplicons

After the amplification, two exome libraries were purified with two rounds of purification procedure using AMpure beads. The reaction mixture was prepared using 25µL (0.5X sample volume) of AMPure™ XP beads to each library (~50µL) and mixed thoroughly with the purified library using a pipette. The library mix was then incubated at RT for 5 minutes, the pellets were discarded and the supernatant containing the final libraries were carefully collected into fresh sterile tubes.

For second round of purification, 1.2X concentration of Agencourt™ AMPure™ XP beads (60µL) were mixed to the final library (i.e., the supernatant collected after the first round of purification) and were incubated at RT for 5 minutes. After incubation, the tube was then placed on the magnetic stand for 5 minutes. Amplicons were bound to the pellet, so supernatant was discarded without disturbing the pellet. Further, the beads were washed twice thoroughly by adding freshly prepared 70% ethanol (150µL) to each library. The tubes were placed at RT in a magnetic strand to ensure that no ethanol droplets remain. 50µL of Low TE was added to the pellet. The mixture was thoroughly mixed and incubated at RT for 2 minutes, followed by the magnetic stand for 2 minutes. The final purified library amplicons (49µL) were collected into the sterile Eppendorf labelled tubes.

2.2.4.6. Quantification of library by Bioanalyzer

The amplified and purified final libraries were quantified before sequencing using Agilent-Bioanalyzer 2100; this system facilitates the automated sizing and quantification in a digital format with high sensitivity. The Agilent DNA Nanochip contains 16 wells and each well is interconnected through a microchannel. Once fluorescent dye (light-sensitive) and polymer are injected, the chip acts as an integrated electrical circuit.

All high sensitivity reagents were thawed 20 min before chip loading. Once the reagents were at RT, DNA, dye concentrate and gel matrix were equilibrated at RT for 30 min. Gel dye mix was prepared by adding 15µL of dye to gel matrix and centrifuged at 2240g for 10 minutes at room temperature. The libraries containing DNA chip was carefully placed in chip prime station and vortexed for 1 minute. Immediately loaded on the Bioanalyzer chip prime station and started run. Library quality and quantity was assessed based on marker and ladder (Figure 41).

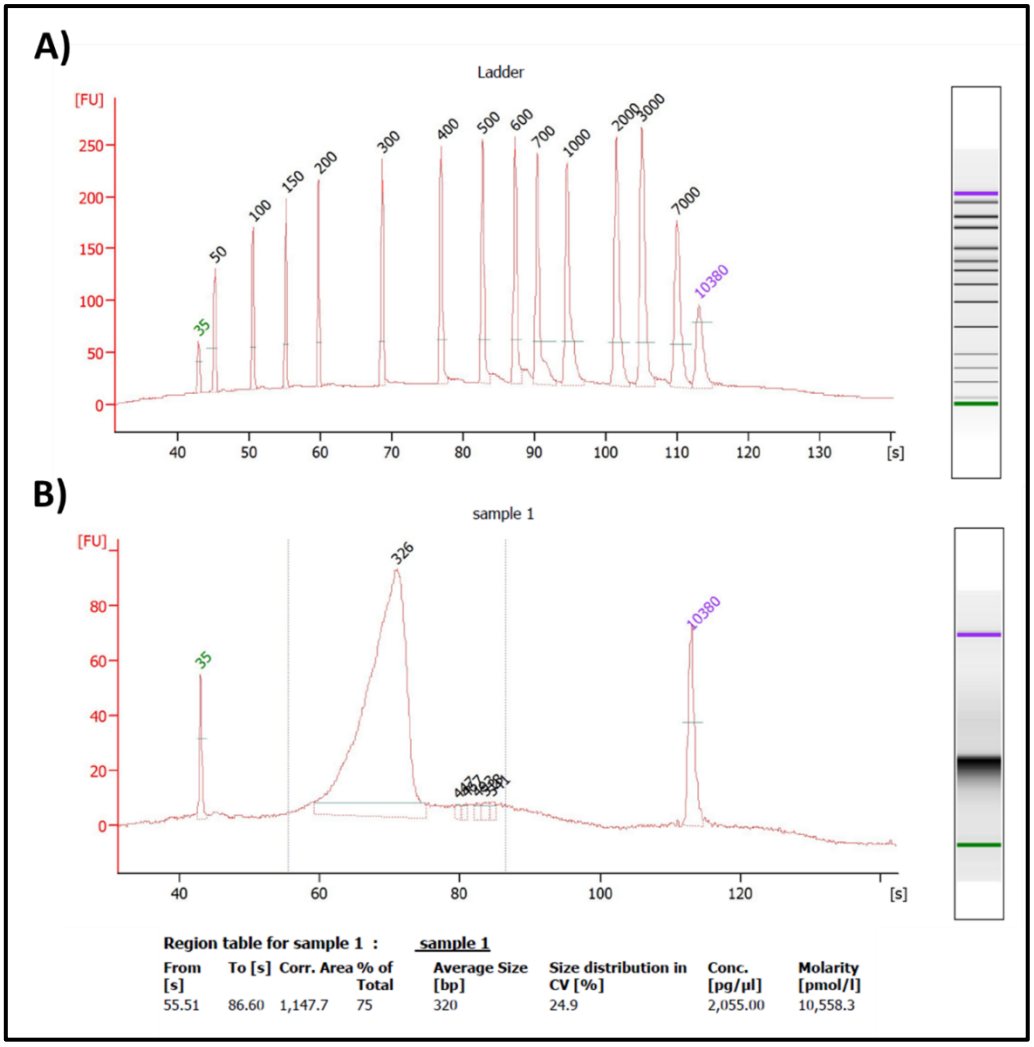

Figure 41. Profile of DNA ladder by Bioanalyzer electropherograms (left panel) and gel like image (right panel) A; Bioanalyzer Profile of DNA library with the concentration (molarity) details of average size fragments (320bp)

2.2.4.7. Template preparation, enrichment and chip loading

Post library enrichment and chip loading was performed on a robotic platform (Ion Chef, Thermofisher, USA). These libraries were subsequently diluted to a concentration of 150pM and two libraries were pooled. Before using the Ion P1 HiQ Chef, reagents were kept at room temperature for 45 minutes. The equipment was first sterilized using UV light on the deck. Chef Solutions and Chef Reagents provided with the kit were loaded on the Ion Chef for template preparation. Prior to initiating the run, the sample cartridges, tips and chips were aligned. The total run time was for 17 hours. Following enrichment, both the chips were loaded

simultaneously on the Ion Proton platform (Thermofisher, USA). While the first chip was loaded, the second one was stored in a 4^0C refrigerator.

2.2.4.8. Cleaning and initialization the Ion Proton System

The Ion PGM™ Sequencer was cleaned with 18MΩ water and Chlorite before initialisation. The instrument was cleaned and initialized approximately for 1.5 hours as per the manufacturer's protocol.

A P1 HiQ chip was used for initialization. Wash 2 (W2) and wash 3 (W3) solutions from the Ion P1 Hi-Q Sequencing 200 solutions kit (cat # A26430) were used for this purpose. 45ml of W3 solution and 32µL of 1M NaOH (W1) (Sigma, cat no # 72068) were added. Diluted 1920ml deionized water along with W2 solution and 6µL of 1M NaOH were added. New sippers and reagent bottles were installed and the Ion Proton was initialized. The sequencing nucleotides (catalogue number A26432) were thawed on ice and 70µL of each nucleotide (dGTP, dCTP, dATP, and dTTP) were put in the tubes for setting up the pH. Towards the end of initialization, the sequencer measured the pH of the reagents (Figure 42). Later, one chip was placed in the chip clamp of the Ion Proton sequencer with the planned run for this chip being selected for sequencing. The Sequencer's chip had been calibrated before the run (1 minute). Once the initial chip run was finished, the fluid lines were cleaned with the same chip. The second chip was kept at RT for 20 minutes prior to loading. Sequencing of each P1 chip was accomplished in 2.5 hours followed by data capture.

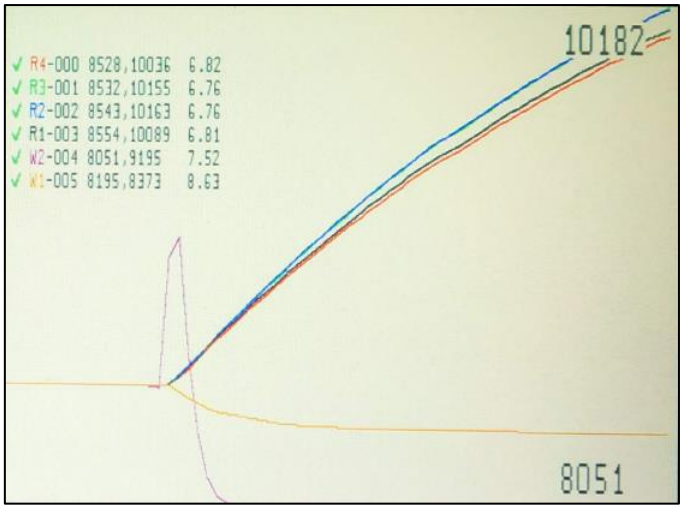

Figure 42. A snapshot of the pH of dNTPs and reagents (W1 and W2) used in initialization

2.2.5. Quality control and raw data analysis

Standard quality control (Aligned reads, polyclonality, ISP loading, mean length, and mass coverage) measures were taken care of and the filtered reads were aligned to reference genome (GRCh37, UCSC hg19). Based on the raw flow data, the Torrent Suite software captured the nucleotides. These were then aligned to a reference sequence (hg19). Further, Variant Call Format (VCF) files were generated from the Binary Alignment Map (BAM) files and uploaded in the Ion reporter Software (version 5.2). Sequencing was performed at an average depth of 100X. Finally, rare alleles were investigated using non-synonymous pathogenic variations evaluated by SIFT, PolyPhen-2 and Grantham. At points of variance among various samples, the depth of coverage was also assessed. A detailed workflow is shown in Figure 43.

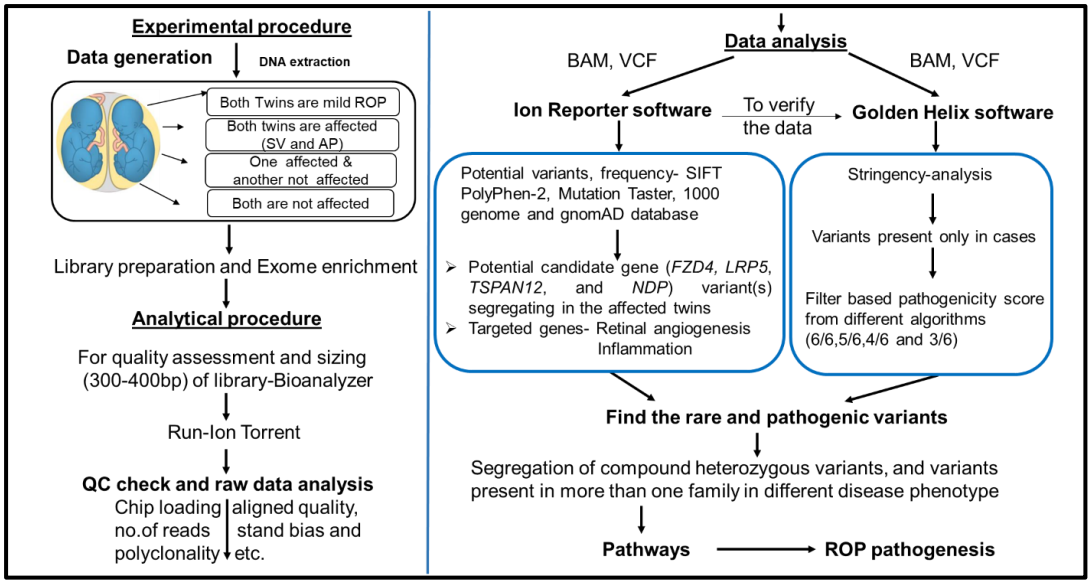

Figure 43. A detailed workflow in understanding the genetics of ROP

2.2.6. Variant analysis using Ion Reporter software

Ion Reporter software was initially used to conduct variant analysis. Multiple bioinformatic tools were integrated with Ion Reporter software to simplify and automate data processing and annotation. SNPs, multi-nucleotide variants and insertion/deletions (indels) in the genomic area were detected using this software.

2.2.7. *In-silico* analysis

Variants with Minor allele frequency (MAFs) lesser or equal to 0.05 in any of these general population databases [1000 Genomes Project (1000G) and Genome Aggregation Database (gnomAD)] were included from the WES results from ROP twins. Bioinformatic tools were used to assess pathogenicity for all identified variations. SIFT, PolyPhen-2 and Mutation Taster 2were used to predict pathogenicity.

Initially, we focused on variations in four potential candidate genes (*FZD4*, *LRP5*, *TSPAN12* and *NDP*) in ROP twins. Next, we selected genes associated with upstream and downstream of angiogenic, inflammatory and oxygen sensing pathways. These genes are also known to be

associated with other proliferative retinopathies. We focused on new variations found in ROP twins in the third phase of the investigation. We segregated the compound heterozygous variations found in more than one family in different phenotypes after finding the rare and pathogenic variations in ROP twins.

2.2.8. Variant analysis using Golden helix software

The whole exome data was further analyzed using Golden Helix SVS software. Various *in silico* prediction methods were used to understand the impact on protein function. Further details are provided in Table 20.

Table 20. Bioinformatic analysis to predict the effect of variations in genes

S.No	Name	Category	Deleterious threshold	Information used
1	SIFT	Function prediction	≤0.05	Protein sequence conservation among homologs
2	PolyPhen-2	Function prediction	≤0.05	Eight protein sequence features, three protein structure features
3	Mutation Taster 2	Function prediction	≤0.05	DNA sequence conservation, splice site prediction, mRNA stability prediction and protein feature annotations
4	Mutation Assessor	Function prediction	0-1	Sequence homology of protein families and sub-families within and between species
5	FATHMM	Function prediction	≥0.45	Sequence homology
6	FATHMM MKL Coding Pred	Function prediction	≥0.45	Integrates functional annotations from encode with nucleotide-based sequence conservation measures.

Further, variants were filtered out based on pathogenicity score and pathogenicity score of 6 was considered. The variants present in both twins affected by ROP were considered for further analysis and variations in the control group were excluded.

2.3. Results

ROP is a complex disease involving multifactorial etiology. The present study was designed to understand the genetic basis of ROP. This study was accomplished by whole-exome sequencing in ROP twins.

2.3.1. Whole Exome Sequencing

WES in 15 twin pairs (n=30) indicated ~40000 variations that includes the missense, nonsense, indels (frameshifts), splice site and synonymous variations. From these variations we have filtered rare pathogenic variants responsible for ROP.

2.3.1.1. Quality controls

Prior to data analysis, we checked for quality of loading, aligned reads and final library to be more than 90%. Further details are provided in Annexure III (Supplementary Table 1).

2.3.2. Genes identified by Ion reporter software

Once a rare pathogenic variant was observed, further analysis was performed as -

a) Identification of genes that had single variation present in multiple families

b) Identification of a gene that exhibited multiple variations across families

As a result, a total of 8 variants were identified in more than one severe form of ROP (Table 21) and 6 genes had single variations in multiple families (Table 22).

Table 21. **Single variants identified in more than one form of ROP phenotypes**

Gene	Chromosomal Position	Twin ID's	Phenotype	Reference sequence/Allele	Variant sequence	cDNA mutation	Zygosity	Protein Change	SIFT score	Global Allele frequency (1000 Genomes)
C7	chr5:40936541	T152, T153	Both twins with APROP	T	C	c.382T>C	Hetero	p.C128R	0 (deleterious)	0.0262
		T3, T4	Both twins with Mild ROP							
CYP1A2	chr15:75047337	T133, T134	Both twins with APROP	G	A	c.1459G>A	Hetero	p.V487M	0.09 (tolerated)	0.0048
		T3, T4	Both twins with Mild ROP							
CYP4F2	chr19:15989554	R1008	Infant with severe ROP	T	C	c.*27A>G	Hetero	p.?	-	0.0048
		T152,	Both twins with APROP							
		T153								
EPHX2	chr8:27361148	T150,	Twins both with APROP	A	G	c.214A>G	Hetero	p.R72G	0.03 (deleterious)	0.0002
		T151								
		T2	Infant with mild ROP							
FOXG1	chr14:29236386	T19, T47	Both twins with severe ROP	G	T	c.-100G>T	Homo	p.?	-	-
		T22	Infant with mild ROP							
GP1BA	chr17:4837260	T47	Infant with severe ROP	CAAT	ACTA	c.1363_1364delATinsCA	Hetero	p.P454H;Ile455Y	-	-
		T146	Infant with severe ROP							
		T83	Infant with severe ROP							

Gene	Chromosomal Position	Twin ID's	Phenotype	Reference sequence/Allele	Variant sequence	cDNA mutation	Zygosity	Protein Change	SIFT score	Global Allele frequency (1000 Genomes)
KIF17	chr1:20991214	T19	Infant with severe ROP	T	G	c.2953A>C	Hetero	p.N985H	0.12 (tolerated)	-
		T157	Infant with severe ROP							
KIF17	chr1:20991256	T83	Infant with severe ROP	C	T	c.2912-1G>A	Hetero	p.?	-	0.0018
		T152,	Both twins with APROP							
		T153								
LRP4	chr11:46917556	T6	Infant with severe ROP	AC	A	c.1061delG	Hetero	p.G354Vfs	-	-
		T133	Infant with APROP							
LRP4	chr11:46917501	T146, T147	Both twins with severe ROP	G	A	c.1117C>T	Hetero	p.R373W	0.02 (deleterious)	0.0106
		T133,	Both twins with APROP							
		T134								
RERE	chr1:8716108	T47	Infant with severe ROP	CT	C	c.248delA	Hetero	p.L83Sfs	-	-
		T157	Infant with severe ROP					Ter12		
		T133	Infant with APROP							

Table 22. Single gene with multiple variations across different ROP phenotypes

Gene	Chromosomal Position	Twin ID's	Phenotype	Reference sequence/ Allele	Variant sequence	cDNA mutation	Zygosity	Protein Change	SIFT score	Global Allele frequency (1000 Genomes)
ALMS1	chr2:73784447	T133, T134	Both twins with APROP	TAAAGAAAAA	TAAGAAAAA	c.10185A>G|c.10179delA	Hetero	p.L3395=|p.E3394LfsTer24	-	-
	chr2:73612952	T150, T151	Both twins with APROP	C	G	c.-45C>G	Hetero	p.?	-	-
CYP4F2	chr19:15996828	T146, T147	Both twins with severe ROP	G	C	c.1021C>G	Hetero	p.L341V	-	0.0042
	chr19:15989554	R1008	Infant with severe ROP	T	C	c.*27A>G	Hetero	p.?	-	0.0048
		T152, T153	Both twins with APROP							
EPHX2	chr8:27364410	T133, T134	Both twins with APROP	G	A	c.559G>A	Hetero	p.G187R	0.04 (deleterious)	-
	chr8:27398993	T133, T134	Both twins with APROP	TC	T	c.1385delC	Hetero	p.P462LfsTer2	-	-
	chr8:27361148	T150, T151	Both twins with APROP	A	G	c.214A>G	Hetero	p.R72G		0.0002

Gene	Chromosomal Position	Twin ID's	Phenotype	Reference sequence/ Allele	Variant sequence	cDNA mutation	Zygosity	Protein Change	SIFT score	Global Allele frequency (1000 Genomes)
		T2	Infant with mild ROP						0.03 (deleterious)	
KIF17	chr1:20991214	T19	Infant with severe ROP	T	G	c.2953A>C	Hetero	p.N985H	0.12 tolerated)	-
		T157	Infant with severe ROP							
	chr1:20991256	T83	Infant with severe ROP	C	T	c.2912-1G>A	Hetero	p.?		0.0018
		T152	Both twins with APROP						-	
		T153								
	chr1:20991002	T133	Both twins with APROP	C	T	c.*75G>A	Hetero	p.?	-	0.0058
		T134								
LRP4	chr11:46917556	T6	Infant with severe ROP	AC	A	c.1061delG	Hetero	p.G354VfsTer43	-	-
		T133	Infant with APROP							
	chr11:46917501	T146	Both twins with severe ROP	G	A	c.1117C>T	Hetero	p.R373W		0.0106
		T147								

Gene	Chromosomal Position	Twin ID's	Phenotype	Reference sequence/ Allele	Variant sequence	cDNA mutation	Zygosity	Protein Change	SIFT score	Global Allele frequency (1000 Genomes)
		T133 T134	Both twins with APROP						0.02 (deleterious)	
RERE	chr1:8419847	T19 T47	Both twins with severe ROP	C	CGCGCTC	c.3594_3595insGAGCGC	Hetero	p.R1200_E1201dup	-	-
	chr1:8716108	T47	Infant with severe ROP	CT	C	c.248delA	Hetero	p.L83SfsTer12	-	-

2.3.2.1. Genetic interactions and pathway enrichment analysis

2.3.2.1.1. Common variants detected in both concordant and discordant affected twin

Total 220 targeted genes were chosen from Ion Reporter software of which, 3 novel pathogenic gene (*LRP4, GP1BA* and *KIF17*) variants were common to both concordant and discordant affected twins. Genes or pathogenic variants were chosen to predict the possible interactions using Cytoscape-Genemania analysis. The network is automatically laid out and visualized with Cytoscape showing interaction strength (edge thickness) and interaction type (color). The black circle denotes targeted input genes provided. This analysis shows that most of these genes were co-expressed, co-localized and showed predictive interactions (Figure 44A).

The gene ontology (GO) analysis was performed for the common genes (*LRP4, GP1BA, KIF17*) by the DAVID software (Database for Annotation, Visualization and Integrated Discovery; version 6.8). Several pathways like cellular developmental processes, neurogenesis, nervous system development, protein localization, cell morphogenesis and neuron differentiation were found to be associated with ROP (Figure 44B).

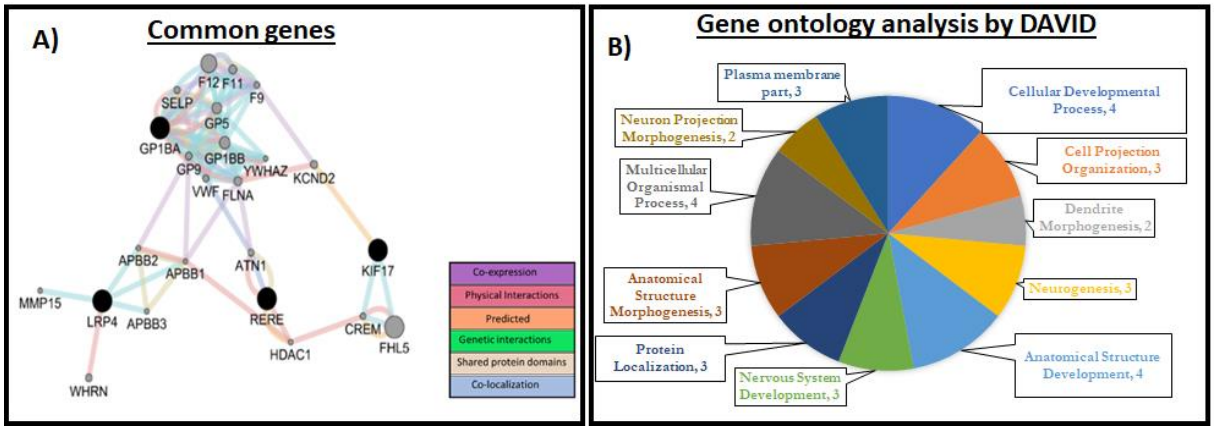

Figure 44. Common variants are detected in both concordant and discordant affected twins; Interactions of genes using the GeneMANIA interaction network. A: Gene ontology analysis for common genes; B: Number of genes identified in the enriched pathway

2.3.2.1.1.1. Single variants present in multiple twin pairs

The single variant which was present in multiple families were chosen to predict the possible interactions using Cytoscape-Genemania analysis. Most of them had shared protein domains, genetic interactions and shows co-expression (Figure 45A). DAVID analysis indicated epoxygenase, arachidonic, long chain fatty acid metabolic process, nervous system development, cellular, lipid metabolic process, regulation of stress, protein activation cascade and developmental process (Figure 45B) to be associated with ROP.

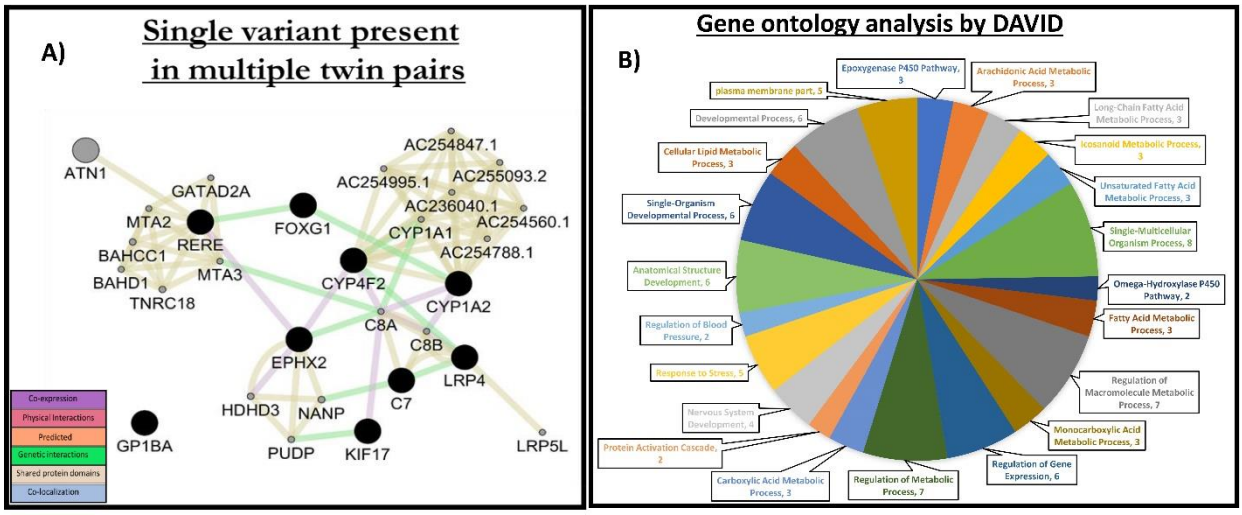

Figure 45. Single variants present in multiple twin pairs: Interactions of genes using the GeneMANIA interaction network. A; Gene ontology analysis for common genes; B: Number of genes identified in the enriched pathway

2.3.2.1.1.2. Single genes with multiple variants

Genes with multiple variants were used to predict the possible gene interaction by Cytoscape-Genemania and pathway enrichment analysis by DAVID. The interaction analysis by Cytoscape-Genemania showed that most of the genes are co-expressed and have genetic interactions (Figure 46A). The gene ontology (GO) analysis by the DAVID found similar pathways viz. epoxygenease, arachidonic, long chain fatty acid metabolic process, nervous system development, cellular lipid metabolic process, homeostatic process, dendrite

development & morphogenesis and neuron developmentprocesses associated with ROP as was mentioned above (Figure 46B).

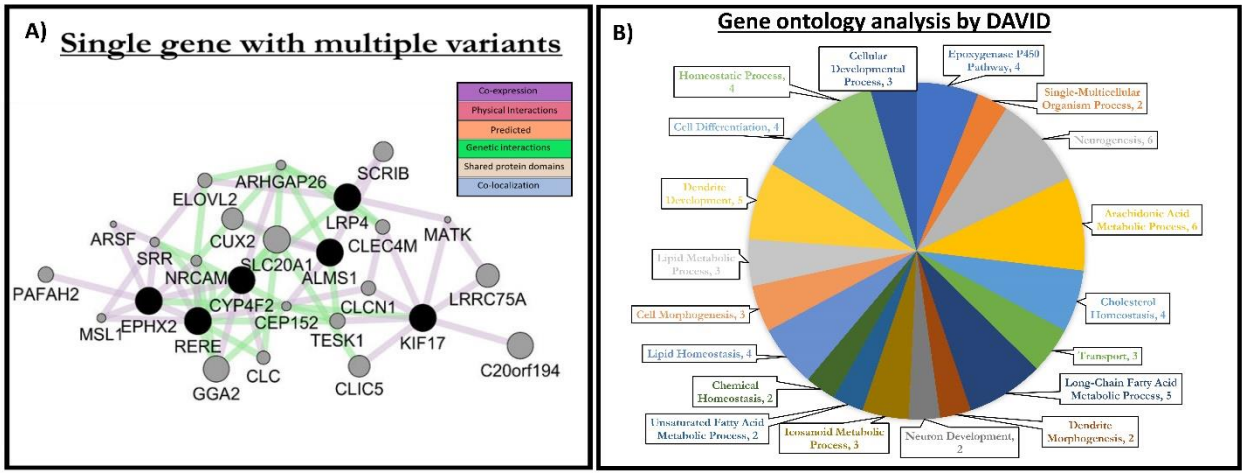

Figure 46. Single genes with multiple variants: Interactions of genes using the GeneMANIA interaction network. A; Gene ontology analysis for common genes; B: Number of genes identified in the enriched pathway

2.3.3. Variants identified by Golden Helix

We further validated and explored all the rare-pathogenic variants using the Golden Helix SVS software. This software uses six *in-silico* predictive tools to integrate information with predictions about the impact of variant on protein function. Of the 6 tools used for prediction, pathogenicity was indicated by at least 4/6 tools. We observed 673 gene variants in severe ROP and 109 in AP ROP to be pathogenic. Based on increased stringency, variants identified in 11 genes from AP ROP (Table 23) and 84 genes from severe ROP (Table 24) were considered pathogenic by all the six tools. The Venn diagram shows (Figure 47) the predictive damage based on the 6 tools and its distribution in severe, AP and mild ROP. These variants were unique among the groups.

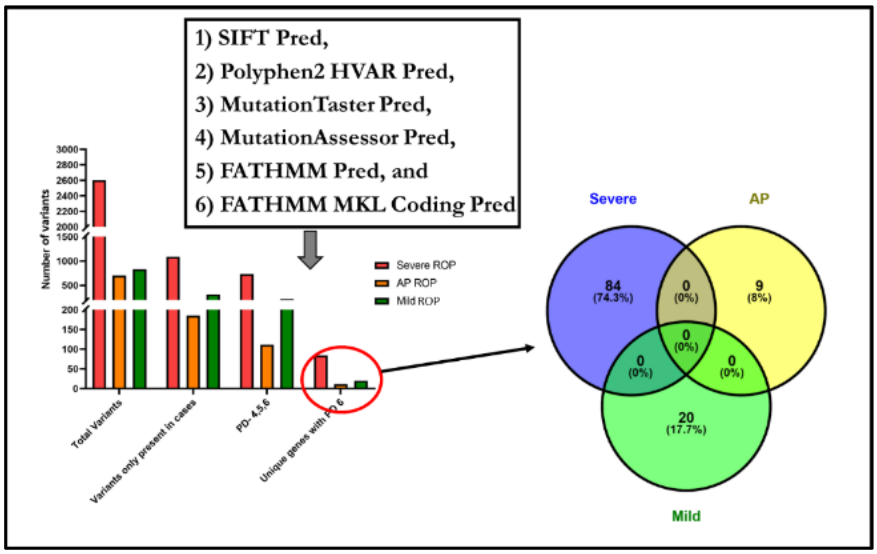

Figure 47. Distribution of potentially implicated genes across different phenotypes of ROP based on 6 prediction tools

Table 23. List of potentially implicated genes in AP ROP

S.No	Gene	Chromosome position	rs ID	cDNA position	Ref/Alt	Allele frequency in cases (n=21)	Allele frequency in controls (n=9)	GnomAD	1000 genome
1	*ATP2C2*	16:84473044	rs202026876	c.2614G>T	G/A	0.0476	0	0.001986	-
2	*CBS*	21:44479029	rs138211175	c.1390G>A	C/T	0.0476	0	0.0001839	0.0004
3	*DNASE 1*	16:3707257	rs148373909	c.1592T>C	C/T	0.0476	0	0.001526	0.003594
4	*FUT2*	19:49206524	rs149356814	c.616A>G	C/T	0.0476	0	0.000699	0.001203
5	*ITPR3*	6:33658862	rs370516286	c.84G>T	C/T	0.0476	0	9.90E-05	-
6	*KLC3*	19:45852819	rs201196936	c.37G>A	G/A	0.0476	0	0.0001179	0.0002
7	*LRP2*	2:170103277	rs201299366	c.3170G>A	T/C	0.0476	0	0.000214	0.00122
8	*LTBP2*	14:74978010	rs76172717	c.712C>T	G/C	0.0476	0	0.004807	0.005591
9	*MX1*	21:42811638	rs142294097	c.1777A>G	G/A	0.0476	0	0.0000389	0.0002
10	*MYH7B*	20:33575434	rs45522831	c.337G>A	C/T	0.0476	0	0.005566	0.002596
11	*STOX1*	10:70644705	rs200117499	c.311C>T	G/A	0.0476	0	0.004619	0.009984

Table 24. List of potentially implicated genes in severe ROP

S.No	Gene	Chromosome position	rs ID	cDNA position	Ref/Alt	Allele frequency in cases (n=21)	Allele frequency in controls (n=9)	GnomAD	1000 genome
1	*ABCA3*	16:2349458	rs570927625	c.339C>G	C/T	0.0238	0	0.0004245	0.000399
2	*ACSL3*	2:223773680	rs547612841	c.2353G>A	C/T	0.0238	0	0.0001435	0.000399
3	*ACTBL2*	5:56777892	rs534551351	c.3331G>A	C/G	0.0476	0	0.0005496	0.001398
4	*ADAMTSL4*	1:150530536	rs139296719	c.926G>A	C/T	0.0476	0	0.0001746	0.0001746
5	*APBB3*	5:139938322	rs150554513	c.188G>A	G/A	0.0476	0	0.0004218	0.000599
6	*ATN1*	12:7048185	rs1253028361	c.2635T>C	G/A	0.0238	0	-	-
7	*ATP2B1*	12:90028584	rs765489529	c.1381C>A	G/C	0.0238	0	4.16E-05	-
8	*ATRIP*	3:48493151	rs762807851	c.1367G>A	A/G	0.0476	0	9.97E-05	-
9	*B3GNTL1*	17:80915351	rs368158155	c.1166C>T	G/A	0.0476	0	0.0000304	-
10	*BEND6*	6:56879992	rs551551087	c.434C>T	G/T	0.0238	0	0.001359	0.002796
11	*BRINP1*	9:121971061	rs146310694	c.285C>G	G/C	0.0476	0	0.0008383	0.001
12	*BYSL*	6:41899165	rs41273804	c.263C>T	G/A	0.0238	0	0.0002	0.0002
13	*CARS1*	11:3069156	rs779162754	c.784T>G	G/A	0.0238	0	0.0000178	-
14	*CCDC27*	1:3683159	rs144089943	c.7420G>A	A/C	0.0238	0	0.007791	0.009585
15	*CDC14A*	1:100964774	rs61752469	c.554G>A	G/A	0.0238	0	0.002526	-
16	*CLCA2*	1:86907173	rs201243498	c.193C>T	G/T	0.0238	0	0.0009798	0.001398
17	*CYB561*	17:61513499	rs543874201	c.394C>T	G/A	0.0238	0	0.00002391	0.0002
18	*DAZL*	3:16639612	rs572265820	c.5056G>C	C/T	0.0238	0	0.00004404	0.0002
19	*DCHS2*	4:155298458	rs376441129	c.2067C>A	C/T	0.0238	0	0.001856	0.002796
20	*DGKD*	2:234343524	rs140466615	c.824T>C	C/T	0.0238	0	7.97E-06	
21	*DGKZ*	11:46393109	rs375795823	c.166C>T	G/A	0.0238	0	7.97E-06	0.0002
22	*DOCK2*	5:169412872	rs148694888	c.2327A>T	T/C	0.0238	0	0.000873	0.000799
23	*DOCK7*	1:63119694	rs570514826	c.1418T>G	C/T	0.0476	0	0.001617	0.003195
24	*ECHDC3*	10:11791500	rs552383167	c.235T>C	G/A	0.0238	0	0.0001791	0.0002
25	*EIF2AK4*	15:40326590	rs762015746	c.1105G>C	C/G	0.0238	0	-	-
26	*EMC4*	15:34517374	rs752656560	c.2103T>G	A/G	0.0476	0	-	-
27	*ESR2*	14:64727231	rs559087939	c.463C>T	C/T	0.0238	0	-	0.000799
28	*ETV5*	3:185798898	rs773508609	c.1066G>A	G/A	0.0238	0	0.0001394	
29	*FAF2*	5:175921085	rs529401341	c.958C>T	G/A	0.0238	0	0.00007074	0.0002
30	*HECTD4*	12:112717110	rs368477197	c.111C>G	C/T	0.0476	0	8.05E-06	-
31	*HEXB*	5:74011499	rs181898554	c.757G>A	G/A	0.0476	0	0.00005319	0.0002
32	*HLA-DOA*	6:32975286	rs34987694	c.52A>G	A/G	0.0476	0	0.004204	0.005192
33	*HLA-DQB2*	6:32726657	rs202167169	c.403T>C	T/C	0.0476	0	0.0006164	-
34	*HSPA9*	5:137897387	rs572429102	c.238G>A	A/G	0.0238	0	0.0001432	0.0002
35	*INPP5J*	22:31529613	rs557118372	c.9245C>T	A/T	0.0238	0	0.0001665	0.000599
36	*ITPR1*	3:4726798	rs547074301	c.59T>C	G/A	0.0238	0	0.0006394	0.001198
37	*KIAA1549*	7:138591719	rs543944276	c.274T>G	T/C	0.0238	0	0.0001573	0.000399
38	*KIF1B*	1:10381802	rs551543997	c.1517G>A	T/C	0.0238	0	0.002556	0.005391

S.No	Gene	Chromosome position	rs ID	cDNA position	Ref/Alt	Allele frequency in cases (n=21)	Allele frequency in controls (n=9)	GnomAD	1000 genome
39	*KIRREL1*	1:158064864	rs141015499	c.4306G>A	C/T	0.0238	0	0.002254	0.0002
40	*KLHDC7B*	22:50987296	rs372048048	c.11462T>C	G/A	0.0714	0	0.002254	0.004393
41	*LAMA2*	6:129762081	rs117884199	c.1123G>A	A/G	0.0238	0	0.0003791	0.001597
42	*LDLRAD4*	18:13645186	rs377513129	c.1438C>G	C/A	0.0238	0	0.0002158	0.0006
43	*LNX1*	4:54344768	rs376500430	c.3826C>T	C/T	0.0238	0	0.001859	0.002796
44	*LRFN3*	19:36430484	rs755450034	c.907C>G	G/A	0.0238	0	0.00001266	-
45	*MCCC2*	5:70898412	rs141030969	c.638A>G	C/T	0.0238	0	0.00004242	-
46	*MMP14*	14:23313980	rs3751489	c.5015G>T	G/A	0.0476	0	0.00175	-
47	*MYH6*	14:23874868	rs750029272	c.1289G>A	G/T	0.0238	0	0.00001988	-
48	*MYL10*	7:101267529	rs146674429	c.535G>A	G/A	0.0476	0	0.001017	0.002796
49	*NAT2*	8:18257770	rs771145519	c.1086G>A	C/A	0.0238	0	0.00004799	-
50	*NFATC1*	18:77170463	rs769824411	c.569G>A	C/G	0.0238	0	0.0001405	-
51	*NMUR2*	5:151784592	rs150054462	c.2073C>A	C/A	0.0476	0	0.0023	0.001997
52	*NOL11*	17:65714092	rs539405439	c.2695C>T	T/C	0.0238	0	0.002269	0.003794
53	*NPC1L1*	7:44579335	rs114376659	c.760C>T	G/A	0.0476	0	0.0085	0.002995
54	*OR13A1*	10:45799078	rs372706541	c.860A>T	C/T	0.0238	0	0.001044	0.001398
55	*OR52W1*	11:6220691	rs566661987	c.724C>T	A/C	0.0238	0	0.00017	0.000799
56	*OR5H1*	3:97851543	rs150362159	c.664C>T	T/C	0.0476	0	0.000694	0.000998
57	*PDCD2*	6:170889175	rs138337157	c.1022C>A	T/C	0.0476	0	0.002826	0.004393
58	*PDHX*	11:35016479	rs533512853	c.541G>T	G/A	0.0238	0	0.0005568	0.002196
59	*PDLIM3*	4:186446267	rs755994888	c.664C>T	G/A	0.0238	0	0.00003183	
60	*PLA2G4F*	15:42434312	rs530535423	c.4421C>T	T/C	0.0238	0	0.0007556	0.000599
61	*PLEC*	8:144998480	rs367715409	c.3011G>C	C/T	0.0238	0	0.00004069	-
62	*POGK*	1:166818316	rs573690726	c.713C>T	G/C	0.0238	0	0.0001768	-
63	*PPL*	16:4943273	rs779503542	c.313C>A	G/C	0.0476	0	0.00003127	-
64	*PPP1R9A*	7:94917894	rs149869201	c.1411C>T	G/A	0.0238	0	0.002131	0.002796
65	*PRCP*	11:82564317	rs202003232	c.1270G>A	A/T	0.0238	0	0.002627	0.005591
66	*RBM19*	12:114395805	rs150685892	c.1883A>G	T/C	0.0238	0	0.001857	0.001597
67	*RPS6KL1*	14:75375560	rs201985029	c.2165A>C	G/A	0.0238	0	0.0008753	0.001398
68	*SBF2*	11:9853807	rs1307459430	c.614T>C	C/T	0.0238	0	3.98E-06	-
69	*SCN5A*	3:38595989	rs199473618	c.670G>A	C/T	0.0238	0	0.0002709	0.000599
70	*SLC12A7*	5:1089239	rs778796256	c.343C>T	G/A	0.0238	0	0.00002409	
71	*SLC30A9*	4:42051452	rs138544445	c.526C>T	A/G	0.0238	0	0.0007422	0.001597
72	*SMPDL3B*	1:28275641	rs548367412	c.1205A>G	G/A	0.0238	0	0.0004613	0.000399
73	*SPTA1*	1:158609433	rs369714529	c.4886A>G	G/C	0.0476	0	0.001537	0.002196
74	*SRPK3*	X:153049823	rs1557068204	c.5065C>T	G/A	0.0952	0	-	-
75	*SUPT20H*	13:37596152	rs74906774	c.2998G>A	C/G	0.0476	0	0.002581	0.003395
76	*TBC1D1*	4:38104628	rs199992726	c.1021C>G	C/T	0.0238	0	0.00001417	0.000399
77	*TFAP2E*	1:36056256	rs114404250	c.227C>T	G/A	0.0238	0	0.002152	0.00619
78	*THY1*	11:119290869	rs551289954	c.10648C>T	G/A	0.0238	0	0.0001074	0.0002
79	*TMCC3*	12:94976125	rs141857063	c.127C>T	C/T	0.0238	0	0.001867	0.00599
80	*TMEM255B*	13:114498154	rs150323609	c.1324G>C	G/C	0.0476	0	0.007773	0.008986
81	*TRIO*	5:14492908	rs575988358	c.311C>T	C/T	0.0476	0	0.00016	0.0002
82	*TRPM1*	15:31354784	rs755943745	c.1292G>T	G/A	0.0238	0	0.00001203	-
83	*VWA8*	13:42189142	rs73464952	c.2632C>T	C/T	0.0238	0	0.004556	0.002196
84	*ZNF99*	19:22940459	rs374487196	c.1903C>G	T/C	0.0476	0	0.0002995	0.000599

2.3.3.1. Gene interaction and pathway analysis

2.3.3.1.1. Single variant present in multiple twin families of AP ROP

Genes harbouring single rare pathogenic variants present in multiple twin pairs of AP-ROP were chosen to predict possible genetic interactions using Cytoscape-Genemania. Most genes were found to take part in physical interactions, had shared protein domains and showed co-localization (Figure 48A). The gene ontology (GO) by DAVID showed associations of calcium binding, calcium dependent phosphor lipid binding, lipid binding and phospholipid pathways with ROP (Figure 48B).

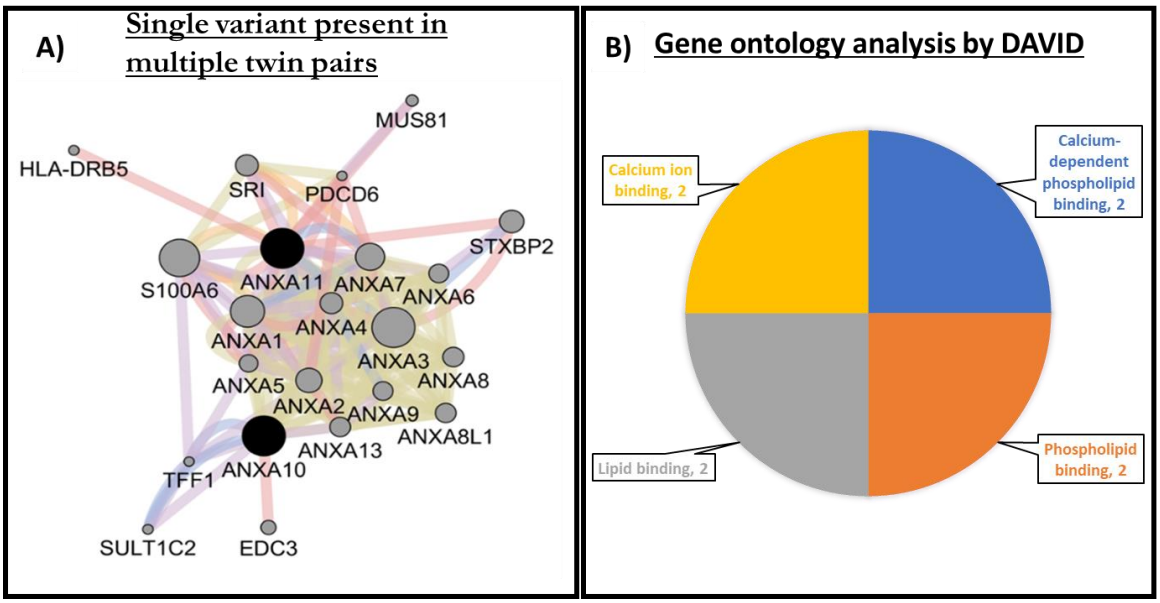

Figure 48. Single variant present in multiple twin families of AP ROP: Interactions of genes using the GeneMANIA interaction network. A: Gene ontology analysis for common genes; B: Number of genes identified in the enriched pathway.

2.3.3.1.2. Single gene with multiple variants in AP ROP infants

Individual genes with multiple variants in twin pairs of AP-ROP were chosen to predict the possible genetic interactions using Cytoscape-Genemania. They were involved in physical interactions, had shared protein domains and shows co-localization (Figure 49). GO analysis using DAVID exhibited association of G-protein coupled receptor signaling with ROP.

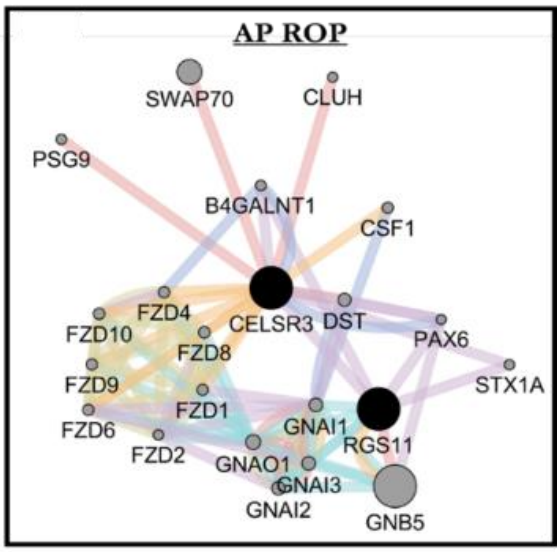

Figure 49. Single gene with multiple variants in AP ROP infants: Interactions of genes using the GeneMANIA interaction network; A: Gene ontology analysis for common genes; B: Number of genes identified in the enriched pathway

2.3.3.1.3. Single variant present in multiple twin families of severe ROP

Genes harbouring single rare pathogenic variants present in multiple twin family of severe ROP were analyzed for possible interactions using Cytoscape-Genemania. Most of these genes showed co-expression (Figure 50A). GO analysis by DAVID revealed co-enzyme, fatty acid oxidation, NAD binding, lipid oxidation and protein secretion to be associated with ROP (Figure 50B).

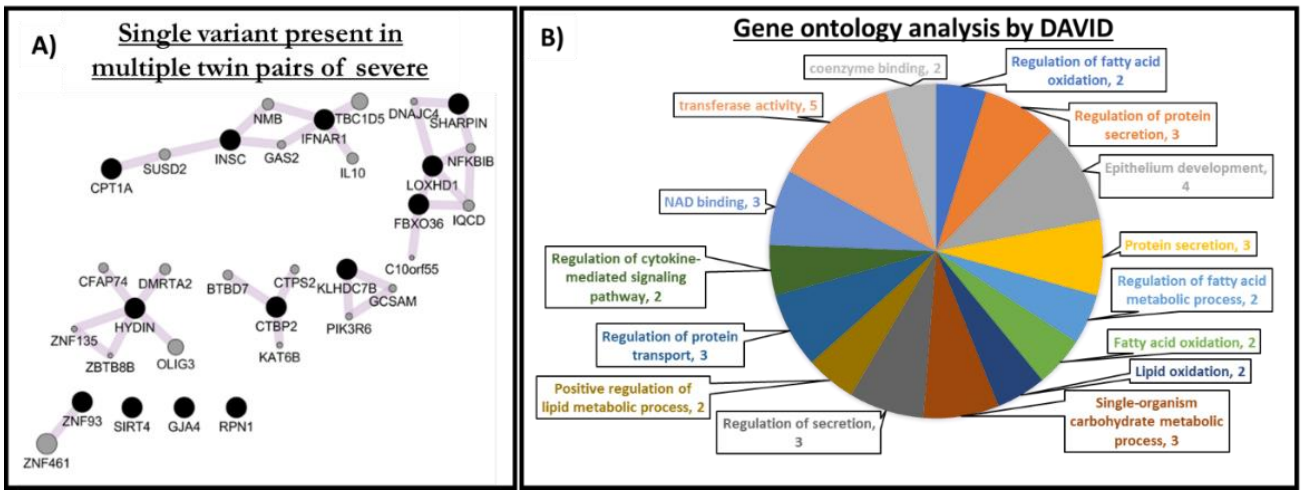

Figure 50. Single variant present in multiple twin families of severe ROP: Interactions of genes using the GeneMANIA interaction network; A: Gene ontology analysis for common genes; B: Number of genes identified in the enriched pathway

2.3.3.1.4. Single gene with multiple variants in severe ROP infants

Individual genes with multiple variants in twin pairs of severe-ROP were analyzed with Cytoscape-Genemania that indicated genetic interactions, shared protein domains, co-expressions and co-localizations (Figure 51A). GO analysis by DAVID identified metal ion binding, nucleotide binding, ECM, inflammation, complement, nervous system development and biological adhesion pathways in ROP (Figure 51B).

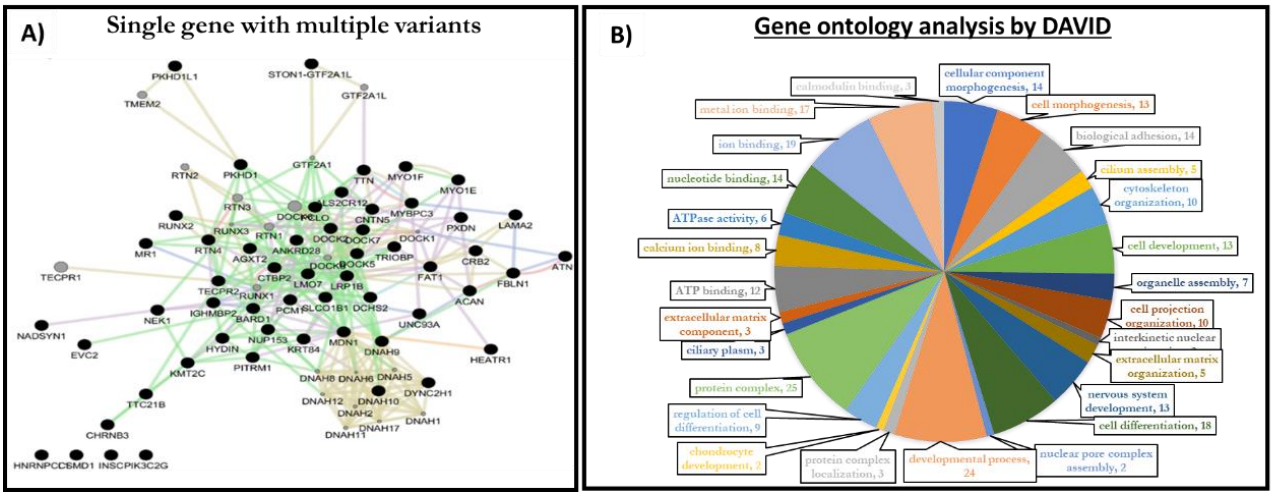

Figure 51. Single gene with multiple variants in severe ROP infants: Interactions of genes using the GeneMANIA interaction network; A: Gene ontology analysis for common genes; B: Number of genes identified in the enriched pathway

2.4. Discussion

ROP is a multifactorial vaso-proliferative eye disease of premature infants (Kondo *et al.*, 2013). It is a progressive and self-limiting disease; some premature infants despite getting proper antenatal and prenatal care develop severe ROP. A subgroup of infants with similar conditions develops mild ROP, regresses spontaneously, whereas others do not develop ROP (Pietrzyk *et al.*, 2013). However, it is unclear why only a subgroup of infant's progress to ROP among premature infants. This suggests for an underlying genetic etiology in ROP.

In order to understand genetic susceptibility in ROP, we collected 100 twin samples who were born prematurely. Other than the gestational age and birth weight, there were no other known risk factors associated with ROP. Only a few preterm infants developed severe ROP in this cohort with lower GA and birth weights (Table 25). The heterogeneity of demographic and clinical risk factors suggested that other risk factors such as genetics may play a crucial role in ROP pathogenesis. Based on this, our study attempted to address the contributions of heritability in ROP susceptibility by WES.

Table 25. Clinical parameters associated with ROP

50 twin pairs (n=100)	**Controls (n=46)**		**ROP (n=54)**		***McNemar's P value***
Gender (0-male, 1-female)	Male, (43.4%)	Female, (56.5%)	Male, (59.2%)	Female, -40.70%	Male- 0.1375 Female- 0.1258,
Gestational age	25-30, (63.1 %)	30-36 (36.9 %)	25-30, (40.7 %)	30-36 (59.2 %)	25 to 30, p= 0.0302 and > 30, p= 0.0321
Weight at birth	<1.2, n=26 (56.5 %)	>1.2 (43.4 %)	<1.2, n=13 (24.1 %)	>1.2 (74.4 %)	< 1.2- 0.0005, > 1.2 -0.0055
Oxygen (no-0, yes-1)	1=45/46 (97 %)		1=8/54 (85 %)		0.4149
Types of delivery (vaginal-0, cesarean-1)	1=24/46 (52.1 %)		1=32/54 (59.2 %)		0.569
Blood transfusion (no-0, yes-1)	1=27/46 (58.6 %)		1=27/54 (50 %)		0.5006

50 twin pairs (n=100)	Controls (n=46)	ROP (n=54)	*McNemar's P value*
Phototherapy (no-0, yes-1)	1=44/46 (95.6 %)	1=46/54 (85.1 %)	0.5023
Parental consanguinity (no-0, yes-1)	1=1/46 (2.1 %)	1=1/54 (1.8.1 %)	0.7488
Preeclampsia (no-0, yes-1)	1=12.9%	1=5.5 %	0.1687
Sepsis (no-0, yes-1)	1=1.8%	1=6.5 %	0.1824

Previous studies suggested that Wnt-Norrin signaling genes (*FZD4, LRP5, TSPAN12* and *NDP*) were involved in ROP pathogenesis, but the results were inconsistent among populations (Hiraoka *et al.*, 2010; Kim *et al.*, 2002). In Caucasian, Korean and Japanese ROP patients, the roles of *NDP* and *FZD4* genes in disease progression have been explored. There is only one study on *TSPAN12* screening albeit negative, in ROP in the Japanese population (Kondo *et al.*, 2013). Our earlier studies indicated a minimal involvement of candidate genes in ROP (Rathi *et al.*, 2018). Our results confirmed the earlier *FZD4* variants [p.P33S, p.P168S, p.P33S, p.P168S] along with a novel variant p.I360V to be associated with all stages of ROP. We also observed a patient with threshold ROP harboring a heterozygous variant p.L119R in the *TSPAN12* gene and two novel intronic variants (IVS1+16A>G, c.522 T>C in 3'UTR) in the *NDP* gene. Unfortunately, our targeted screening could not explain the entire genetic basis of ROP. Out of which, we have validated the T cell activation pathway from the previously reported study in the current study.

Generally, ROP is not associated with a positive family history to determine heritability. As a result, we designed our study including twins to understand the genetic basis of ROP. We used the twin pairs with AP ROP and severe stages (4 and 5) of ROP to find the shared genetic components. In addition, mild ROP cases were included to determine the genes with moderate effects on ROP progression. As mild ROP infants usually do not progress to severe stages of

ROP, the twins with mild and no ROP were used as controls. Discordant twins with "severe" and "no ROP" were used to find shared pathogenic variants in ROP (Figure 52).

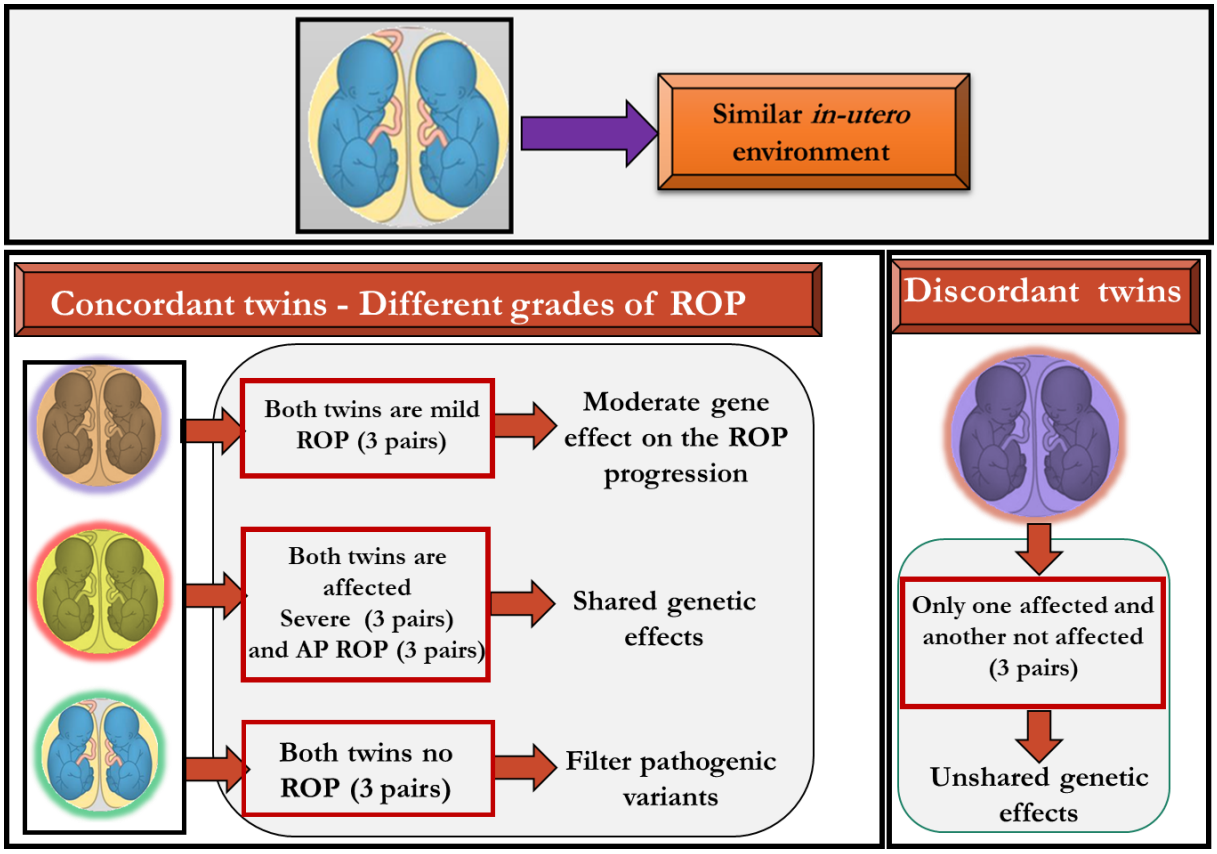

Figure 52. Strategy used for whole exome sequencing

2.4.1. Rare pathogenic single gene variants segregation and multiple variants in individual genes among ROP twins

Overall, WES revealed 673 gene variants in severe ROP and 109 in AP ROP. Following data filtration, the final rare pathogenic variants were 84 and 11 in severe ROP and AP ROP, respectively. All these gene variants were unique with varied distributions across different stages of ROP. The results indicated different genetic signatures for different stages of ROP and suggested the involvement of multiple genes in ROP with varying effects across these phenotype categories.

3 novel pathogenic gene (*LRP4, GP1BA* and *KIF17*) variants were common to both concordant and discordant affected twins. The interactions among the observed genes

indicated that they were co-expressed (Figure 44). The interactions of common variants present in both concordant and discordant twins were involved in inflammation, developmental and neuroprotection pathways. Our recent study observed that microglial activation led to the disruption of retinal homeostasis via the release of activated MMPs and other inflammatory cytokines and chemokines in ROP eyes (Rathi *et al.*, 2018). The increased inflammation (MMPs) under hypoxia can regulate Opticin (antiangiogenic) protein expression (Patnaik S *et al* 2021). The present study also validated the involvement of inflammation in ROP infants as was observed in (Rathi *et al.*, 2017; Dammann, 2010) .

Pathway enrichment analysis of individual variants in multiple twin pairs and individual genes with multiple variants found epoxy-P450 and arachidonic acid (*CYP4F2, EPHX*2 and *CYP1A2*), multicellular organism process (*RERE, CYP4F2, CYPA2, FOXG1, LRP4, EPHX2, GP1BA* and *KIF12*), response to stress (*C7, CYP4FA2, EPHX2, CYPA2, GPABA*) and metabolic pathways (*CYPF2, EPHX2, CYPA2*) to be involved in ROP. These enriched pathways are already known to be involved in the inflammatory and developmental process(Rathi *et al.*, 2017; Rivera *et al.*, 2017), but most of them have not been explored in ROP pathogenesis. The arachidonic acid (AA) pathway is involved in many inflammatory conditions, including asthma and arthritis (Wang *et al.*, 2021; Insuela *et al.*, 2020; Vane & Botting, 1987).

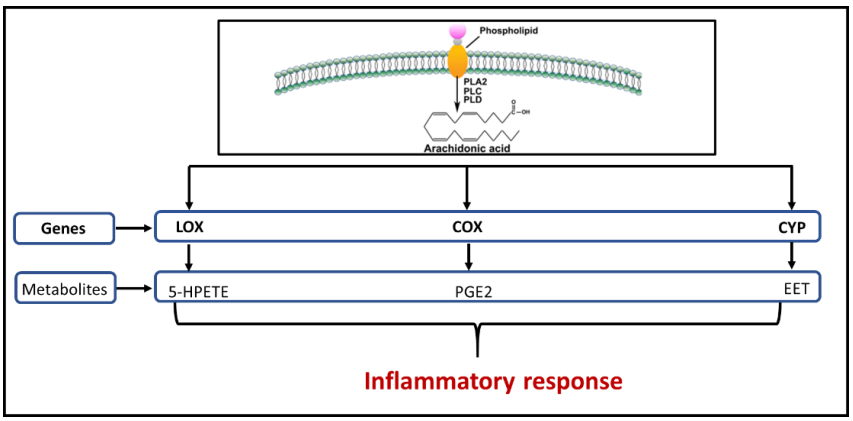

Figure 53. Metabolizing genes in inflammatory response

We also found rare pathogenic variants (*CYP*s and *EPHX2*) in ROP that are involved in several metabolic pathways. Our data revealed variations in *KIF* in severe forms of ROP. This indicates that *KIF17* may have a potential role in ROP progression. KIF17 is a kinesin superfamily protein, facilitating the ATP-dependent molecular motors that can carry cargos along with microtubules. The KIF17 binds to the MAPKs, colocalizes with JNK along with microtubules and are required for the formation of the OS of photoreceptor's cells. Additionally, we found variations in *RERE* gene among the severe forms of ROP, indicating its potential role in ROP progression. The *RERE* gene encodes the arginine-glutamic acid dipeptide repeats and is a widely-expressed nuclear receptor coregulator that positively regulates retinoic acid signaling. Data from zebrafish and mouse models suggest that haploinsufficiency of *rere* might contribute to intellectual disability, developmental delay, structural brain anomalies, vision problems, hearing loss, congenital heart defects, cardiomyopathy and renal anomalies (Plaster *et al.*, 2007).

Overall, our results on network analysis of genes harbouring pathogenic variations in ROP indicated developmental processes, cell differentiation, cellular developmental process, biological adhesion, cell-cell signaling, metal ion transport, regulation of neurogenesis, calcium-mediated signaling, neuron projection morphogenesis, astrocyte cell migration, lipid metabolism, purine nucleoside binding, neuron projection, ATP binding, MHC class II receptor activity and metalloendopeptidase activity to be associated with ROP.

We found the Ca^{2+} signaling pathways in both AP ROP and severe ROP cases. Calcium is the secondary messenger and a central intrinsic signaling system present in the retinal cells. It plays a vital role in various biological functions, such as glial Ca^{2+} modulating neuronal activity. Hence, the intracellular Ca^{2+} signaling pathway might play a crucial role in glial activity in the retina and its effect on neuronal cells under stress conditions. Other unique pathway present in the ROP twins was found to be axon guidance. This pathway is needed for retinal neuronal

function and thus provide good visual acuity (Prieur & Rebsam, 2017). GO-annotation for cellular components, biological process and molecular function identified increased ECM proteins in ROP infants (severe and AP ROP), including proteins of an extracellular region, extracellular region part and extracellular space. The ECM matrix provides mechanical support and acts as a scaffold for the cells to grow. Vitreous is an ECM matrix, but under an altered tissue microenvironment, the retinal cells or inflammatory cells can secrete extracellular proteins, further accelerating ECM reorganization and its breakdown (Neve *et al.*, 2014). One of the major pathways identified in severe and AP ROP includes lipid and fatty acid metabolism. The macular layer in the retina is rich in long-chain polyunsaturated fatty acids (PUFAs) such as arachidonic acids (AA), Linoleic Acid (LA), which is prone to frequent lipid peroxidation and structural modification (Liu *et al.*, 2013). Fatty acids serve as structural and signals to mediate molecules in the endothelial layer, immune cells, maintain optimal retinal physiology and anatomy (Eelen *et al.*, 2018) and inflammatory response (Alhouayek *et al.*, 2021; Chiurchiu *et al.*, 2018).

To the best of our knowledge, this is perhaps the first extensive study to delineate the genetic basis of ROP. Novel genes and pathways observed here may be considered as potential targets for undertaking future studies. Understanding the biological basis of pathogenesis and identification of biomarkers would be critical in complex retinal diseases like ROP.

CHAPTER 3

IDENTIFICATION OF PUTATIVE BIOLOGICAL PATHWAYS IN ROP

3. Introduction and review of literature

ROP is a major complication of premature birth that results in vision loss worldwide. Unfortunately, the response to current treatment therapies is highly variable because disease etiology is very poorly understood. The available treatments of ROP including photocoagulation, laser, anti-VEGF and vitrectomy aim to halt the abnormal blood vessel growth in the eyes and prevents retinal detachment. However, there are no treatment options till date to predict and prevent ROP development at the first place. The earlier two objectives from this study attempted to fill this lacuna by performing a genetic screening for identifying genetic predisposition and targeted protein analysis among premature infants with and without ROP to assess their role in predicting disease progression. The findings suggested an extensive array of genes and associated pathways that could have potential role in disease development or progression. However, detecting significant genetic associations (mutations/polymorphisms) with ROP may not be enough to assess disease risk and needs to be complemented with further functional validation of the key variants/genes using suitable approaches. Gene expression is one such method that allows to study cellular response under different conditions with an underlying genetic signature. Thus, studying differentially expressed genes during different stages of ROP development would help to understand the molecular mechanisms and genetic mediators involved in disease progression.

The present chapter, aimed to identify key pathways involved in ROP development and progression by performing extensive data analysis for global transcription profiles among different stages of ROP generated in our lab and validation of some of the key pathways identified by quantitative PCR based approaches.

3.1. Microarray

Microarray enables evaluation of the expression of thousands of genes all at once within a given mRNA sample. Microarray chip contains oligonucleotide probes and each probe denotes the gene of interest. When hybridized with labelled cDNA (from the patient's sample), it emits fluorescence, indicating the expression level for the respective probe/gene. The microarray chips are then scanned to obtain the fluorescent intensity of the probe sets. The data is received in the image format, which is processed for background correction. Each gene's signal intensity is used to find the differentially expressed genes between the groups (e.g. disease vs control). Unfortunately, there are no studies done to identify the differentially regulated genes in different stages of ROP. Therefore, in the present study, we compared gene expression and its associated pathways for different stages of ROP along with premature and mature controls used as model systems to investigate the molecular basis of ROP. The approach was to monitor global gene expression in preterm infants by microarrays to identify genes involved in disease progression in ROP infants. However, numerous genes and molecular pathway networks require programmed data mining approaches to retrieve information and biological interpretation.

3.1.1. Global Gene expression analysis using different data mining approaches

Data mining for big gene expression data sets is done to determine the unknown and implicit in-depth knowledge from studying large amounts of data. Acquiring a data set of differentially expressed genes is just the first step. Integrating differential expression profiles in a biological context is required to interpret the results from experimental data. To begin with, the data set were normalized and evaluated based on the clustering (discrimination of gene expression of one dataset with respective other groups), classification (differentially expressed genes between the groups) and pathway/network interaction (genes enrichment for their involvement in various cellular pathways) and also to identify its interacting partners (DNA, RNA and protein).

The available software and tools for clustering pathway analysis are listed below Table 26 and 27 (Selvaraj & Natarajan, 2011; Tan *et al.*, 2008).

Table 26. List of programs available for clustering analysis

S.No.	Software	Algorithm/Method
1	Cluster and Tree view	Hierarchical clustering, K-means clustering self-organizing maps etc.
2	dChip	Hierarchical clustering, K-means clustering self-organizing maps etc.
3	MeV	Hierarchical clustering, K-means clustering, Tree EASE, self-organizing maps, & QT-clustering etc.
4	MAGIC Tools	Hierarchical clustering, K-means clustering, and QT-clustering
5	CAGED	Bayesian clustering program on a-temporal expression data.
6	R studio	Hierarchical clustering, K-means clustering

Table 27. List of software's available for pathway and network analysis (Selvaraj & Natarajan, 2011; Tan *et al.*, 2008)

S.No.	Software	Application
1	Pathway Studio	Pathway network analysis, data mining, and visualization etc.
2	Ingenuity Pathway Analysis	Pathway network analysis.
3	Cytoscape	PPI network analysis, gene annotation and pathway integration, etc
4	Partek	Analysis and visualization of large networks, etc
5	GenMAPP2	Gene expression, Pathway analysis, and GO analysis
6	ArrayXPath	Mapping, visualizing expression data, and pathway analysis
7	PathExpress	Pathway analysis and visualization
8	GO-cluster	GO based pathway analysis
9	GO-view	GO based pathway analysis
10	Onto-Express	GO based pathway analysis
11	Pathway Miner	Cellular and regulatory pathway analysis
12	GoMiner	GO based pathway analysis

3.1.2. Gene Expression studies done for ROP

Transcriptomics based approaches provide global profiles of various disease-related genes expression, which may aid in a greater understanding of disease pathogenesis. It is also helpful in recognizing genes that display significant differences in disease conditions and can have potential role in early disease diagnosis and development. Since ROP progresses from mild to progressive, i.e., from stage 2 to 5 and changes in gene expression profiles could alter and depict the severity of the disease. Therefore, it is important to check the gene expression at mild, severe form of ROP and AP ROP cases, especially when the disease is active. Unfortunately, there have been relatively few reports on ROP transcriptomics to date and none of them studied the expression profile of different stages of ROP.

3.1.3. Genes and its associated pathways analysis in ROP pathogenesis

Only a few studies have been performed to study global gene expression profiles in human ROP and OIR-animal models. The number of differentially expressed genes and key biological pathways identified by this approach in these studies are listed in the table (Table 30).

Sato and co-workers, in 2009 quantified gene expression of 94 selected genes in the retina of the OIR-mice model using TaqMan low-density arrays (TLDA). The resultant gene expression values for 94 genes were converted into log2 values to assess differential gene expression profiles. Further, a hierarchical cluster analysis of differentially expressed genes showed the association of inflammation and angiogenesis-related pathways (Sato *et al.*, 2009).

However, a major limitation of this study is that it targeted only genes involved in inflammation and angiogenesis. Another study compared global gene expression profiles from retina of OIR rat model in response to 3 days hyperoxia and normoxia using two different rat strains, i.e., F344 (resistant to OIR) and SD (susceptible to OIR). The Partek Genomics Suite software was used for data analysis followed by GO analysis using DAVID (Database for Annotation,

Visualization and Integrated Discovery) tool that revealed several genes involved in key pathways for hypoxia (Table 30). These pathways were confirmed by real-time PCR for significant differentially expressed genes (Tea *et al.*, 2009).

Table 28. Lists the genes/biological pathways identified in ROP/OIR model by transcriptomic (microarray) studies

S.No.	Study models	No. of differently expressed genes	Approach	Biological process/pathways	References
1	Murine-OIR	P7-75% O_2 given for 5 days vs room air: 38 genes	TaqMan low-density array (TLDA)	Angiogenesis and inflammatory response	(Sato *et al.*, 2009)
2	Rat-OIR	F344 vs. SD: 269 genes under exposure to O_2 F344 vs. SD: 168 genes (F344-Resistant to OIR; SD-Susceptible to OIR,)	Affymetrix GeneChip Gene 1.0 ST Rat Arrays	Peptide transport, cell localization, immune response, and nervous system development	(Tea *et al.*, 2009)
3	Murine - OIR	Among hyperoxic and normoxic retinas: 83 genes Among hypoxic and hyperoxic retinas: 95 genes	Sentrix Bead Chip Array Mouse-6; Illumina	Inflammation, neovascularization	(Ishikawa *et al.*, 2010)
4	Rat and mouse-OIR	Early phase (in both models) :43 genes, Late phase:26 for rat and 22 genes for mouse	Rat Genome 230 2.0 or Mouse Genome 430 2.0; Affymetrix, In	Ephrin receptor signalling, VEGF signalling, amyotrophic lateral sclerosis, axonal guidance signalling, hepatic fibrosis/hepatic stellate cell activation	(Recchia *et al.*, 2010)
5	Murine-OIR and normal	P8: 45 genes, P12 : 62 genes, P 13- 135 genes	Phalanx Mouse Whole Genome One Array microarray	Cytoskeleton organization, glycolysis, nitric oxide mediated signal transduction, angiogenesis, response to oxygen levels.	(Yang *et al.*, 2013)
6	111-(ROP vs no ROP)	5th DOL: 794, 14th DOL: 1077 28th DOL:3223 – (Day of life -DOL)	GeneChip Human Gene 1.0 ST arrays	Cytokine–cytokine receptor interaction, T-cell receptor signaling pathway, cell adhesion molecules, pyrimidine and purine metabolism, aminoacyl-tRNA biosynthesis	(Pietrzyk *et al.*, 2013)
7	Mouse-OIR	1519 genes	SurePrint G3 Mouse Gene Expression 8x60K Microarray	Immune system process, cell adhesion, angiogenesis, positive regulation of cell migration, extracellular matrix organization	(Zasada *et al.*, 2020)

Ishikawa and co-workers also conducted a similar microarray based global gene expression profiling using murine model of OIR. C57BL/6N mice were exposed to 75% O_2 for 5 days to induce hypoxia. The retina isolated from hypoxic and normoxic mice were used for microarray and further validation of significant genes was done by qPCR. The gene expression was calculated by Gene spring version 7.3 software (Agilent Technologies, Santa Clara, CA). Gene ontology analysis was performed by the DAVID tool (Ishikawa *et al.*, 2010). Enriched pathways are described in the Table 28. In 2010, Reccia *et al.* compared retinal gene expression using rodent models of OIR (rat & mouse) to identify critical genes and pathways in ROP. The gene expression data was analyzed by Genomics Suite ver. 6.4 software (Partek Inc., St. Louis, MO) and a set of significant genes were subjected to pathway analysis by IPA software. The associated pathways are mentioned in the above Table 28 (Recchia *et al.*, 2010).

Yang *et al.* also conducted a similar transcriptomic profiling of OIR mice retinas at P8 to P12 however, here the mice were subjected to OIR induction as per the standard protocol and then returned to ambient air. Differential expression of the genes was calculated by the SAM 3.11 software (Stanford University, Stanford, CA) and significant genes were validated by qPCR. Genes of interest were further subjected to cluster analysis by using the cluster 3 program (Yang *et al.*, 2013).

All these studies in murine models performed whole-genome expression and were only different with respect to the duration of oxygen therapy and strain of animals used. Since, these studies were performed at neovascularization stage of ROP, changes in gene expression at the early ROP (mild ROP) was not taken into account. Recently, Zasada M *et al.* assessed the impact of hyperoxia on the gene expression of PBMCs and retina of the OIR model (Zasada *et al.*, 2020). A total of 120 mice were categorized into P12, P17 and P28. RNA was isolated from the PBMCs and retinal cells, followed by microarray analysis. Validation of gene expression was performed for randomly selected genes. This study could identify about 1500 differentially

expressed genes in the pathways that have been already reported. One of the major limitations of all these studies is the use of mice model of oxygen induced retinopathy for identifying gene expression. However, these may not provide accurate information to understand the disease pathogenesis. Since, the mice/rats were subjected only to varying oxygen saturation conditions during foetal stage, the changes due to low gestational age, birth weight and maternal factors could not be captured by these models.

Till now, there is only a single study on gene expression profiling of human premature infants that compared global gene expression profiles of infants with gestational age less than 32 weeks with and without ROP in the 5^{th}, 14^{th} and 28^{th} days of development after the delivery date (DOL) using microarrays. The significant differential gene expression was calculated by ANOVA, significance was computed by T-test and Benjamini–Hochberg method was employed to check or control the false discovery rate (FDR) (Pietrzyk *et al.*, 2013). Significantly expressed genes were functionally annotated using Gene Ontology and further classified into three categories (biological process, molecular function and cellular component) using DAVID (Pietrzyk *et al.*, 2013; Ishikawa *et al.*, 2010). However, the significantly dysregulated genes were not validated with qPCR and gene expression was not quantified for different stages of ROP. While all these studies performed gene expression and pathway analysis, they could not provide much functional insight on their role in ROP pathogenesis and particularly its progression among at risk preterm infants. Thus, the present study tried to address some of the lacunae in ROP research using a more stringent and comprehensive analysis strategy.

We compared and analysed differential gene expression among different stages of ROP to get a clear understanding on the genetic pathways involved in ROP pathogenesis. The aim was to identify molecular pathways contributing to ROP based on quantitative gene expression profiling with two major objectives:

1. Global gene expression data analysis to identify the genes and pathways responsible for the development and progression of ROP by comparing their expression among different categories/stages of ROP with premature controls.

2. Validation of the significant differentially expressed genes by real-time PCR.

3.2. Material and Methods

At first, differential gene expression analysis was performed for the global gene expression profiles already generated in the lab for different categories of ROP among preterm infants to identify key genes/signalling pathways contributing to ROP development and progression. In the next step, the identified genes/pathways were validated by real-time PCR for their role in disease pathogenesis.

3.2.1. Sample demographic details

ROP cases were categorized into mild, severe and AP ROP. A detailed sample category is given in Table 29.

Table 29. Categorization of ROP according to the severity of disease

S. No	Category	No. of samples (n=80)	Description
1	Severe ROP	20	Stage 3, 4 and 5 ROP
2	Mild ROP	20	Stage 1 and 2 ROP (which usually regresses by itself)
3	Aggressive Posterior (AP) ROP	20	AP ROP is rapidly progressive
4	Controls	20	Prematureinfants (PC) with no ROP

3.2.2. RNA isolation by using QIamp RNA kit and quality check

Total RNA was isolated from 0.3-1mL of whole blood samples from different stages of ROP and no ROP preterm infants (controls) using RNeasy mini kit from Qiagen, detailed protocol given below:

- Collected 0.3-1mL of fresh whole blood from different stages of ROP patients.
- Added 5 volumes of erythrocyte lysis (EL) buffer into the 1 volume of blood in a 15mL tube and incubated on ice for 15 minutes.

- After incubation centrifuged the samples at 400 x g for 10min at 4°C and discarded the supernatant.
- Above step repeated until we got a clear white pellet (WBCs).
- Added RLT (lysis buffer) solution (2/3rd volume of RLT along with 1/100th β-ME to the total volume blood).
- Homogenized the pellet, transferred it into the QIAshredder spin column and centrifuged for 2 minutes at maximum speed (RT).
- Added 70% ethanol (1x volume) and carefully mixed with a pipette, transferred the total sample along with precipitate into the new QIAamp spin column (preactivated with 100% ethanol) and centrifuged sample for 8000 x g for 15sec.
- Added 350µL Buffer RW1 to spin column and centrifuged for 15 second at 8000 x g to wash and remove remaining salts.
- To avoid DNA contamination, DNase treatment was given to each sample prior to washing and elution. DNase prepared by 10µL DNase-I stock solution along with 70µL RDD buffer was transferred to 80µL of DNase directly into the column membrane without touching any edges and incubated for 15 minutes at RT.
- After incubation, 350µL Buffer RW1 added to the spin column and centrifuged for 15 second at 8000 x g.
- Next washed with 500µL of RPE buffer (wash buffer 2) to the membrane and centrifuged for 15 second at 8000 x g.
- Repeat washing of the membrane with 500µL of RPE solution at 14,000 rpm for 3 minutes.
- After making sure that there are no ethanol droplets, added 30-50µL of elution buffer and centrifuge for 15 second at 8000x g.
- RNA quality and quantity were assessed by Nanodrop and 1.2% agarose gel electrophoresis (mentioned in chapter 1).

3.2.3. Microarray Data analysis

The raw data for Global gene expression for different stages of ROP vs premature controls was analysed using the genome studio software. The software assessed the data quality and normalised the bead signal intensities. Further, online bioinformatics tools were used for differential gene expression and pathways analysis and their interactions.

3.2.3.1. Quality control and Data analysis

Prior to differential gene expression analysis, the data was obtained from the microbead array and subjected to a series of quality control (QC) checks to assess data quality and detect outliers using the genome studio software. A list of probes, genes and their signal intensities were generated that were then used for next analysis as described below.

3.2.3.2. Cluster analysis

Principal component analysis (PCA) and heat map help in visualizing the variable and similar pattern of expression in a given target group. Hierarchical clustering generates a tree-like dendrogram with branches of individual objects (samples or variables). The algorithm pairs object with the highest degree of similarity in a particular sequence. First, the hierarchical clustering dendrogram is frequently displayed alongside a heatmap that depicts the whole data matrix, with elements colour-coded by their value. Following that, the columns of the given dataset are reshuffled based on the hierarchical clustering result, grouping similar observation matrices around each other. This representation of the data matrix can help identify factors that appear to have unique expressions to each sample cluster. We have used R studio to look at the two most popular approaches: PCA and heatmaps, along with hierarchical clustering analysis of the microarray data generated using mRNA expression profiles for different categories of ROP.

3.2.3.3. Identification of Differentially Expressed Genes

This study included the two types of controls: premature control (PC), who do not develop ROP and mature control (MC) who are born after completing 40 weeks of gestation and have no signs of any genetic and retinal diseases. Since prematurity is considered as an altered development related condition it may be associated with a different gene expression profile as compared to those who are born with normal gestation. Hence to identify the ROP associated genes, significant genes those strongly associated with prematurity should be assessed by comparing the expression between the PC vs MC. This would further allow to differentiate between the prematurity-associated genes from those involved in ROP. Further, to find the genes that are involved in ROP progression in prematurely born infants, comparisons were made across different categories/stages of ROP and premature controls with no ROP (PC). Following different categories were used for comparison of gene expression:

a) PC vs MC
b) All ROP (Mild+ AP+ Severe) vs all controls (PC + MC)
c) All ROP (Mild+ Severe+ AP) vs premature controls with no ROP (PC)
d) Aggressive ROP (AP) vs Mild + Severe ROP
e) Plus ROP (AP + Severe) vs Mild ROP
f) Plus ROP (AP + Severe) vs No Plus controls (Mild + PC)
g) Severe vs PC
h) Mild vs PC
i) AP vs PC

Genes that exhibited ≥ 1.3-fold up and down regulation in cases versus controls with a *P-value* ≤ 0.05 were considered to be significantly dysregulated genes.

3.2.3.4. Biological knowledge extraction

Interpreting the meaningful knowledge from genome-wide expression data is a challenging task. The earlier work emphasized accurately identifying differentially expressed genes and their functional significance. Thus, for the present study, the focus was on studying the gene-gene interactions in different biological pathways to have a comprehensive understanding of the disease mechanisms involved in ROP.

3.2.3.5. Enrichment analysis of biological functional groups and pathways

A) Annotation of the genes by DAVID

We have taken the differentially expressed genes (both upregulated and down-regulated) among the different stages of ROP with ≥ 1.3-fold and $p \leq 0.05$. DAVID version 6.7 (online tool (https://david.ncifcrf.gov/summary.jsp) was used for the functional classification of significantly dysregulated genes. DAVID provides the complete functional annotation of the genes to understand and interpret their biological roles.

B) Network analysis by GeneMANIA-cytoscape

The same sets of differentially expressed genes based on their functionality were analysed for possible interactions using GeneMANIA-Cytoscape network analysis (Montojo *et al.*, 2010). Using GeneMANIA, all the possible network interactions were predicted, such as co-expression, genetic, protein and other interactions.

3.2.4. Validation of microarray data by real time PCR (qRT)

Semi-quantitative real time PCR (RT-PCR) was used for validation of the expression of targeted genes as determined by microarray. Genes *HLA DRB1, HLA DRB5, EGR2, FOSB, NOS3* and *AXIN 2* were validated as per the standard protocol. RT-PCR reactions were performed in biological duplicates between different stages of ROP [severe (n=20), mild (n=20), AP ROP

(n=20)] and premature control (n=20). 10µL of SYBR® Green (BIO-RAD, Cat no. 38220090) containing master mix was prepared as described in chapter 1 (Table 16). The primer sequence used for qRT PCR is given in Table 30. The plate was tightly sealed with an optical adhesive sheet (Thermo Fisher Scientific. Cat. No. 4311971) and loaded on the Applied Biosystems 7900 HT system as conditions mentioned in chapter 1 (Table 17). The relative measure of the concentration of the target gene (CT) was calculated using software SDS 2.4 (Applied Biosystems). Gene expression was calculated from the CT values using the formula 2-ΔΔCT. β actin was used as a housekeeping gene for normalization. Statistical analyses were performed using 2-ΔΔCT± SEM, and student t-test was used to calculate the significance.

Table 30. Primer sequences or code used for semi-quantitative real time PCR

S.No.	Gene name	Forward primer	Reverse primer
1	*HLA DRB1*	CGGGGTTGGTGAGAGCTTC	AACCACCTGACTTCAATGCTG
2	*HLA DRB5*	ACTTCACCCAACAGGACTCG	ATAACGTAGTGCATTTGTGGC
3	*EGR2*	TCTTCCCAATGATCCCAGACT	TTACGGATTGTAGAGAGTGGAGT
4	*FOSB*	GCTGCAAGATCCCCTACGAAG	ACGAAGAAGTGTACGAAGGGTT
5	*NOS3*	TGATGGCGAAGCGAGTGAAG	ACTCATCCATACACAGGACC
6	*AXIN 2*	TACACTCCTTATTGGGCGATCA	TTGGCTACTCGTAAAGTTTTGGT

3.3. Results

3.3.1. Objective 1

Global gene expression analysis to identify the genes and pathways responsible for the development and progression of ROP by comparing their expression among different categories/stages of ROP with premature controls.

3.3.1.1. Global Gene expression profiling of ROP

This current chapter assessed differently expressed genes involved in crucial pathways among different stages of ROP patients and premature controls to understand the disease mechanism responsible for disease progression.

3.3.1.2. Microarray data quality assessment

The hybridization controls worked in the high/medium/low-intensity gradient in all the samples. Stringency controls measured the assay's stringency/specificity by comparing the perfect fit (PM) signals to the mismatch (MM2) signal and PM>MM2 in all samples suggested a perfect stringency (Figure 54).

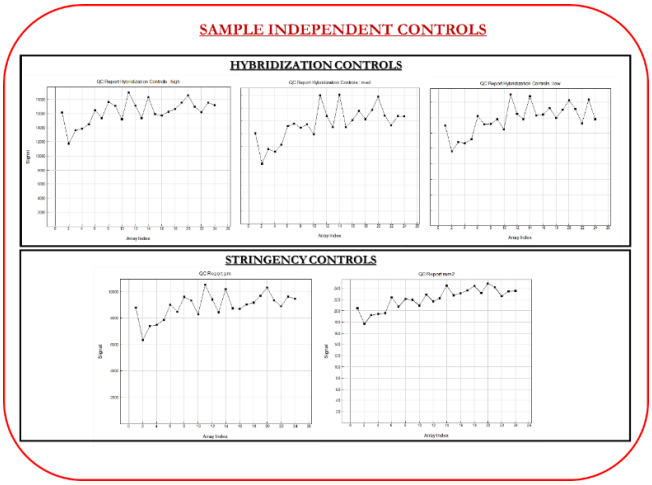

Figure 54. Quality parameters for sample independent controls

Sample-based controls were also checked for any sample related issues. The housekeeping control probe intensities were in the 8000-12000 range, suggesting good sample efficiency. In

addition, negative controls that are made up of random sequences with no associated targets in the genome, were tested to ensure that the samples were free of contamination. Negative probe intensities were found to be poor in this sample, suggesting undetectable contamination. All the samples displayed good quality control and were then further analysed for differential gene expression (Figure 55).

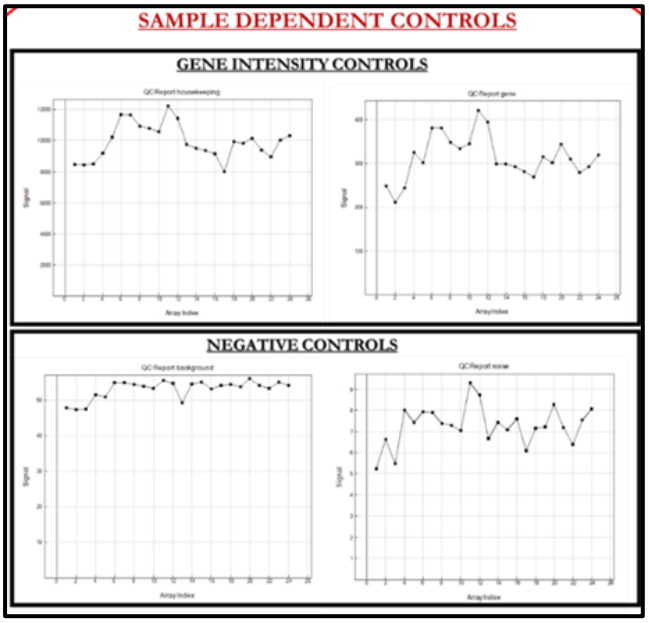

Figure 55. Quality parameters for sample dependent controls

3.3.1.3. Differential gene expression profile among various stages of ROP and controls

The p-value <0.05 and fold change >1.3 were considered to be significantly dysregulated between the two groups. The heat map and cluster analysis showed the differential gene expression among the different stages of ROP vs premature and mature controls (Figure 56).

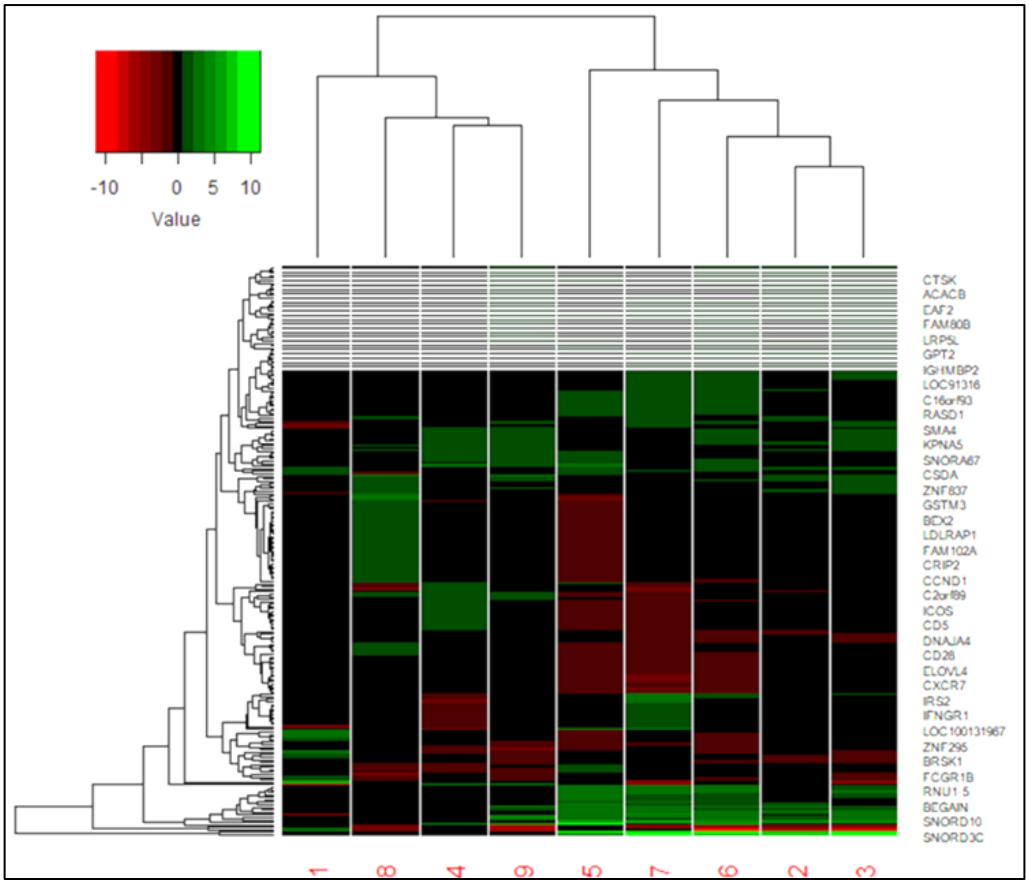

Figure 56. Heat map showing differential gene expression among different stages of ROP as compared to controls; 1- PC vs MC, 2. Mild+ AP+ Severe vs PC + MC, 3. Mild+ Severe + AP vs PC, 4. AP vs Mild + Severe, 5. AP + Severe vs mild, 6. AP + Severe vs Mild + PC, 7. Severe vs PC, 8. Mild vs PC, 9. AP vs PC

A. Differential gene expression profile among premature and mature controls

Microarray data analysis of premature and mature controls indicated that 98 genes were differentially expressed between PC and MC (Table 31). The PCA plot showed two clearly distinct and separate cluster for PC and MC indicating different gene expression profiles for these two groups (Figure 57).

Table 31. Top 25 up-regulated and down-regulated genes (≥ 1.3-fold change and p <0.05) in premature controls/mature controls

PC vs MC					
S.No	Up-regulated genes		S.No	Down-regulated genes	
	Symbol	Fold change		Symbol	Fold Change
1	*CCL8*	5.542011997	1	*EGR2*	-6.592874996
2	*DSC2*	5.323185027	2	*HRASLS2*	-2.493379646
3	*CLEC4C*	3.817384031	3	*GCAT*	-2.482479758
4	*MAP1A*	3.645413504	4	*SAP30*	-2.477779244
5	*HLA-DRB5*	3.453316275	5	*LOC728741*	-2.440380917
6	*FLJ10357*	3.01180992	6	*LOC100131727*	-2.320386572
7	*USMG5*	2.844962198	7	*AMDHD1*	-2.30995772
8	*HBA2*	2.685539049	8	*OXCT2*	-2.227245897
9	*HBB*	2.657517036	9	*LOC652694*	-2.117252982
10	*FBN2*	2.553700238	10	*LOC653080*	-2.116900508
11	*LOC646753*	2.386996545	11	*NT5DC2*	-2.050632743
12	*BAMBI*	2.371298054	12	*GLDC*	-2.047708475
13	*DAB2*	2.291436323	13	*LOC647450*	-1.90432847
14	*EMR1*	2.217433083	14	*IGJ*	-1.862747865
15	*PALLD*	2.206250754	15	*CCR9*	-1.842850615
16	*GNB4*	2.204028429	16	*ELL2*	-1.821285177
17	*TNFRSF21*	2.194188253	17	*LOC652493*	-1.816172396
18	*LOC644928*	2.170791139	18	*MYL6B*	-1.730494385
19	*C1orf198*	2.12260727	19	*LOC100133923*	-1.720547147
20	*CA13*	2.070662814	20	*LOC642113*	-1.696662217
21	*ZDHHC1*	2.064135089	21	*C10orf119*	-1.582350083
22	*BMP6*	2.037018268	22	*SMA4*	-1.499950462
23	*RHOBTB3*	1.985403157			
24	*PAPSS2*	1.971402839			
25	*ITPRIPL2*	1.964895883			

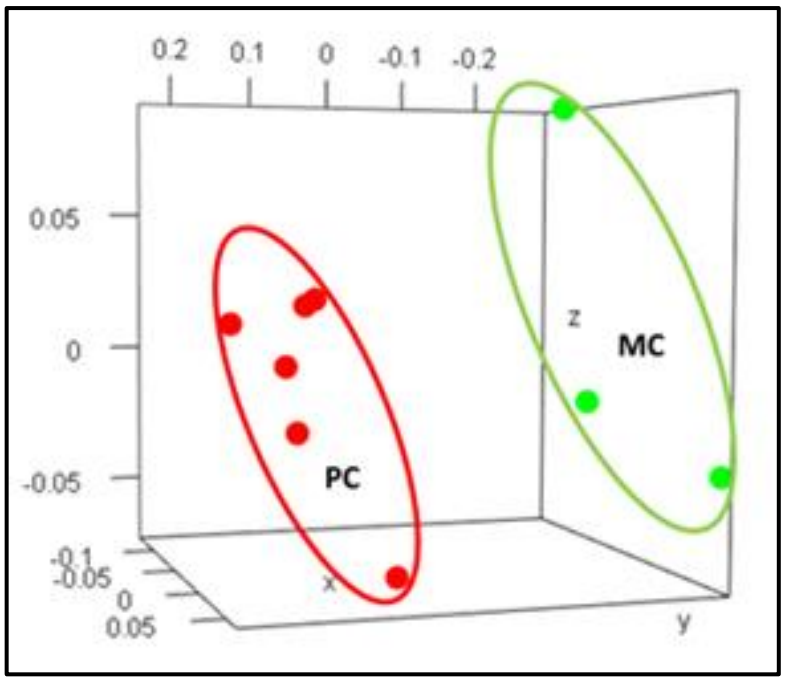

Figure 57. Differential gene expression among PC vs MC

The possible interactions among the differentially expressed genes were predicted using Cytoscape-Genemania analysis, that showed, most of these genes to be co-expressed and shared predicted genetic interactions however they did not show much physical interaction, co-localization and shared protein domains (Figure 58A)

Further, gene ontology (GO) analysis was performed for the same set of genes using the DAVID tool that showed several cell communication pathways, golgi membrane, oxygen binding, intracellular vesicles and ATP binding pathways to be associated with prematurity (Figure 58 B, C, D).

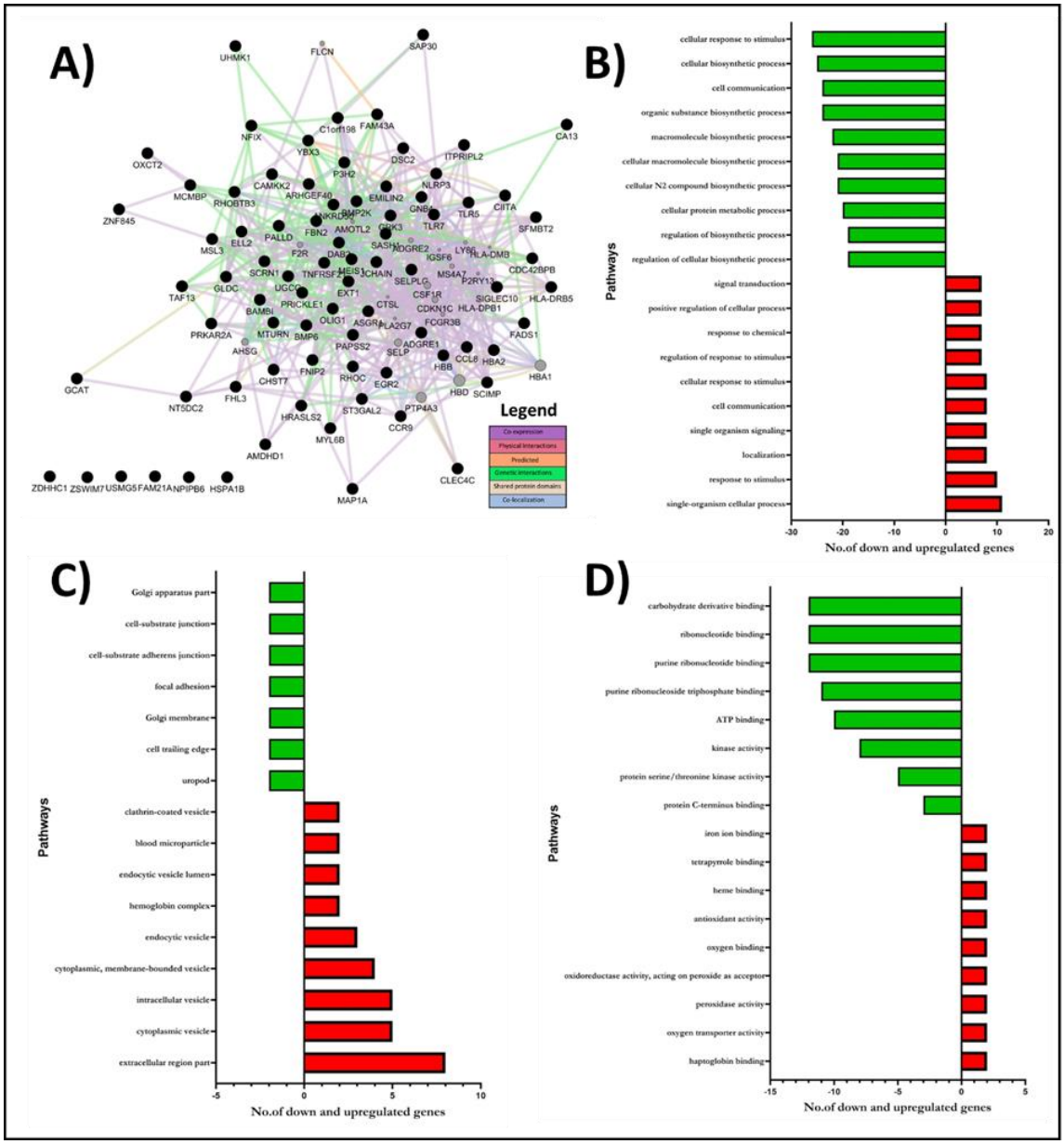

Figure 58. Dysregulated genes/ pathways among PC vs MC, A: Interactions of genes using the GeneMANIA interaction network, B: Gene ontology analysis-Biological process, C: cellular components and D: molecular function

B. All ROP (Mild+ AP+ Severe) vs controls (PC + MC)

First, we looked at the differential expression among all ROP cases vs controls to identify significant genes involved in disease pathogenesis that showed 98 genes were significantly differentially expressed. Of these, 84 genes were up-regulated and 14 genes were down-regulated (Table 32).

Further PCA analysis for significant genes showed two separate cluster for all ROP and controls with a few samples sharing some overlapping features (genes) (Figure 59).

Table 32. Top 25 up-regulated and down-regulated genes (≥ 1.3-fold change and p <0.05) in all ROP (Mild+ AP+ Severe) vs controls (PC + MC)

All ROP (Mild+ AP+ Severe) vs Controls (PC + MC)					
S.No	Up-regulated genes		S.No	Down-regulated genes	
	Symbol	Fold_Change		Symbol	Fold_Change
1	*SNORD3C*	7.834657462	1	*HLA-DRB5*	-6.06449
2	*SNORD3D*	7.203449329	2	*HLA-DRB1*	-3.73085
3	*SNORD3A*	4.721265215	3	*APOL6*	-1.60623
4	*CNTNAP2*	2.483075907	4	*LOC642161*	-1.56356
5	*RNU11*	2.289895701	5	*HSPA1B*	-1.51896
6	*MIR1974*	2.173879466	6	*PLA2G7*	-1.4974
7	*SNORD10*	2.139760382	7	*H1F0*	-1.4777
8	*LOC652479*	2.106714775	8	*LOC442535*	-1.45512
9	*LOC728070*	1.939475411	9	*ATF5*	-1.43157
10	*BEGAIN*	1.914286169	10	*LOC153684*	-1.35783
11	*LOC645381*	1.803147855	11	*RSRC1*	-1.34077
12	*KRT73*	1.776146678	12	*ADH5*	-1.3308
13	*CABP5*	1.731623497	13	*BYSL*	-1.31501
14	*HIST1H2BN*	1.652623043	14	*BRSK1*	-1.30032
15	*TBC1D17*	1.647189255			
16	*HRK*	1.634301163			
17	*KIAA1407*	1.624347143			
18	*CD1C*	1.599744204			
19	*KIAA0125*	1.570202824			
20	*TLE1*	1.558662641			
21	*SNORD68*	1.556447388			
22	*C16orf74*	1.540086935			
23	*PNPLA7*	1.51695988			
24	*KPNA5*	1.515426037			
25	*FAM30A*	1.514145453			

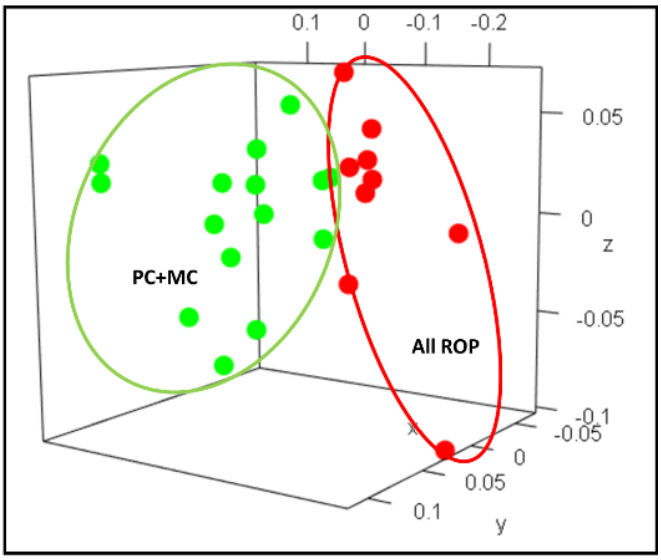

Figure 59. Differential gene expression among all ROP vs PC+ MC

All the significant genes were shown to be interacting with each other by genetic interactions, and were co-expressed however not many share protein domains, co-localization and physical interactions (Figure 60A). Next, the gene ontology analysis was performed using DAVID to find out the biological processes, cellular components and molecular function affected by these genes. These genes are involved in lipid binding, transport activities, peptide antigen binding and are also part of T-cell activation, lipid transport, antigen processing and B-cell receptor signalling pathway (Figure 60 B, C, D).

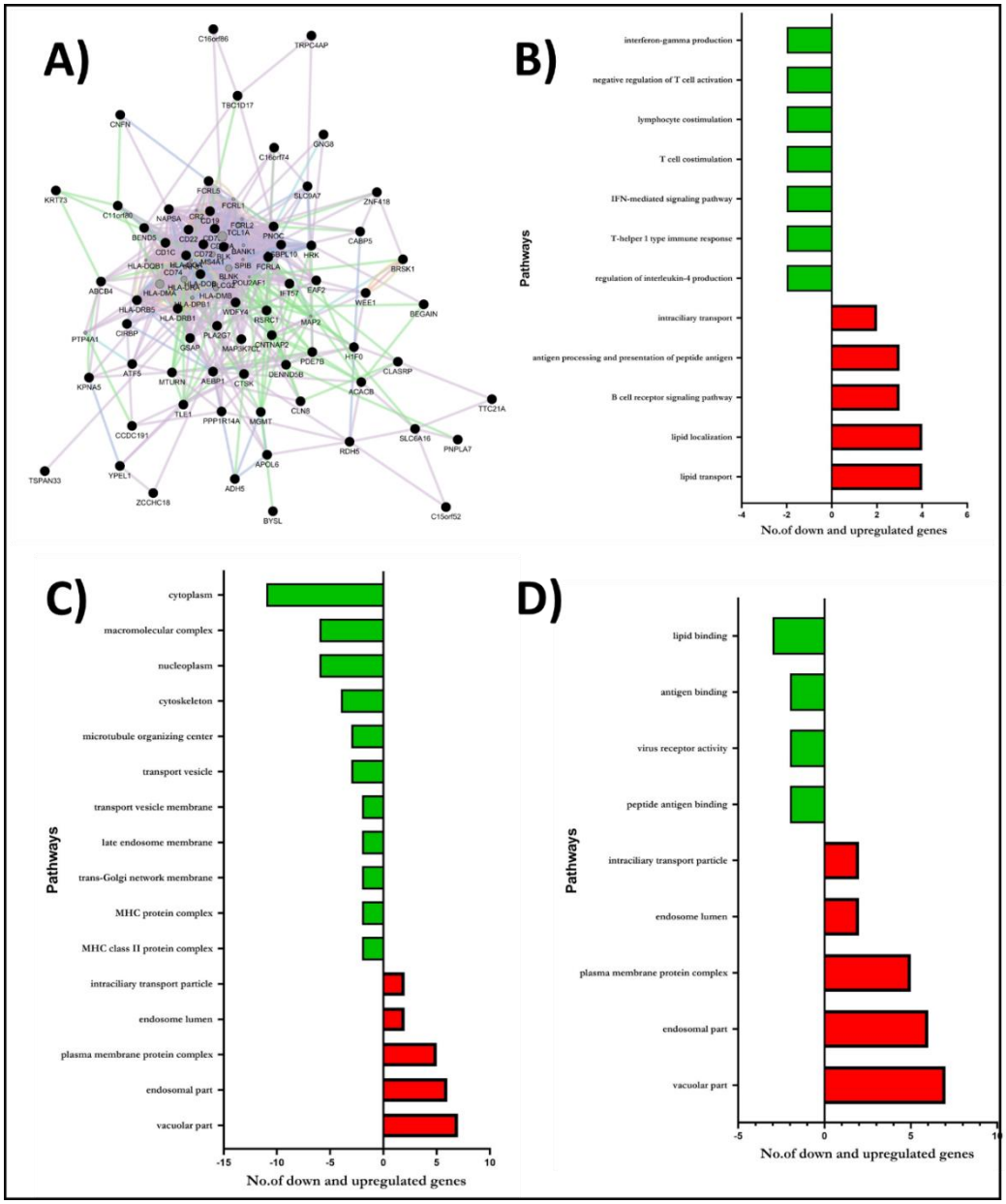

Figure 60. Dysregulated genes/ pathways among all ROP (Mild+ AP+ Severe) vs PC + MC, A: Interactions of genes using the GeneMANIA interaction network, B: Gene ontology analysis-Biological process, C: cellular components and D: molecular function

C. All ROP (Mild+ Severe + AP) Vs premature controls with no-ROP (PC)

Next, the differential expression analysis was performed among all stages of ROP with no ROP premature infants that served as controls to identify genes that are exclusively dysregulated during ROP only. 118 genes were significantly differentially expressed among Mild+ AP+ Severe ROP vs PC of these, 95 were up-regulated and 23 were down-regulated (Table 33).

The PCA results shows the differential gene expression all forms of ROP vs PC (Figure 61).

Table 33. Top 25 up-regulated and down-regulated genes (≥ 1.3-fold change and p <0.05) in all ROP (Mild+ Severe + AP) Vs PC

All ROP (Mild+ Severe + AP) Vs PC					
S.No	Up-regulated genes		S.No	Down-regulated genes	
	Symbol	Fold Change		Symbol	Fold Change
1	*SNORD3D*	8.745150525	1	*HLA-DRB5*	-7.96860368
2	*SNORD3C*	8.376691542	2	*HLA-DRB1*	-4.82647009
3	*SNORD3A*	4.006779789	3	*CCL8*	-3.86300937
4	*FOSB*	3.58421094	4	*LOC162073*	-2.19736185
5	*LOC652479*	3.543045188	5	*FCGR1B*	-1.96289215
6	*RNU1G2*	2.410284313	6	*HSPA1B*	-1.77167887
7	*SAP30*	2.360811514	7	*SASH1*	-1.70464078
8	*SNORD10*	2.327710441	8	*PLA2G7*	-1.60475096
9	*PTGS2*	2.280262567	9	*ITPRIPL2*	-1.56607761
10	*RNU11*	2.258220887	10	*LOC442535*	-1.54437
11	*CNTNAP2*	2.238380061	11	*RAB20*	-1.51163068
12	*RNU1-5*	2.155962545	12	*B3GALNT2*	-1.47230718
13	*RNU1-3*	2.155478536	13	*FBN2*	-1.46326479
14	*LOC728070*	2.101262395	14	*PRKAR2A*	-1.40486991
15	*MIR1974*	1.85000457	15	*FBXO42*	-1.39683335
16	*LOC645381*	1.849527258	16	*GALNT4*	-1.36230403
17	*KRT73*	1.815618633	17	*BRSK1*	-1.36083346
18	*DDIT4*	1.763792861	18	*RBAK*	-1.35580756
19	*SNORD68*	1.688920512	19	*CALHM2*	-1.34981313
20	*LOC100134654*	1.675603631	20	*TPM4*	-1.33260326
21	*FAM30A*	1.670128023	21	*DNAJA4*	-1.32884151
22	*KIAA0125*	1.640501302	22	*ITGAV*	-1.31663947
23	*AMDHD1*	1.626248556	23	*RHOU*	-1.31338263
24	*KPNA5*	1.605230402			
25	*CXCR4*	1.600748909			

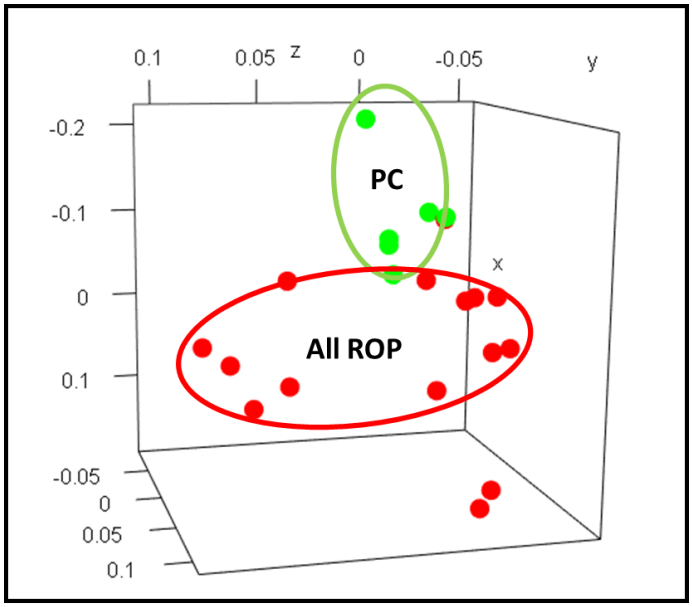

Figure 61. Differential gene expression among all ROP vs PC

All the identified genes were shown to be interacting with each other by physical interactions, co-expression, shared protein domains, co-localization and predicted curated databases using Cytoscape-Genemania (Figure 62A). Next, gene ontology analysis was performed by DAVID to find out the biological processes, cellular components and molecular function affected by these genes. The significant genes identified are known to be involved in antigen binding, ligase activity, ribonucleotide binding, part of phagocytic vesicle endosome membrane, cell junctions and are largely involved in protein modifications, ion transport, cell migration and proliferation pathways (Figure 62 B, C D).

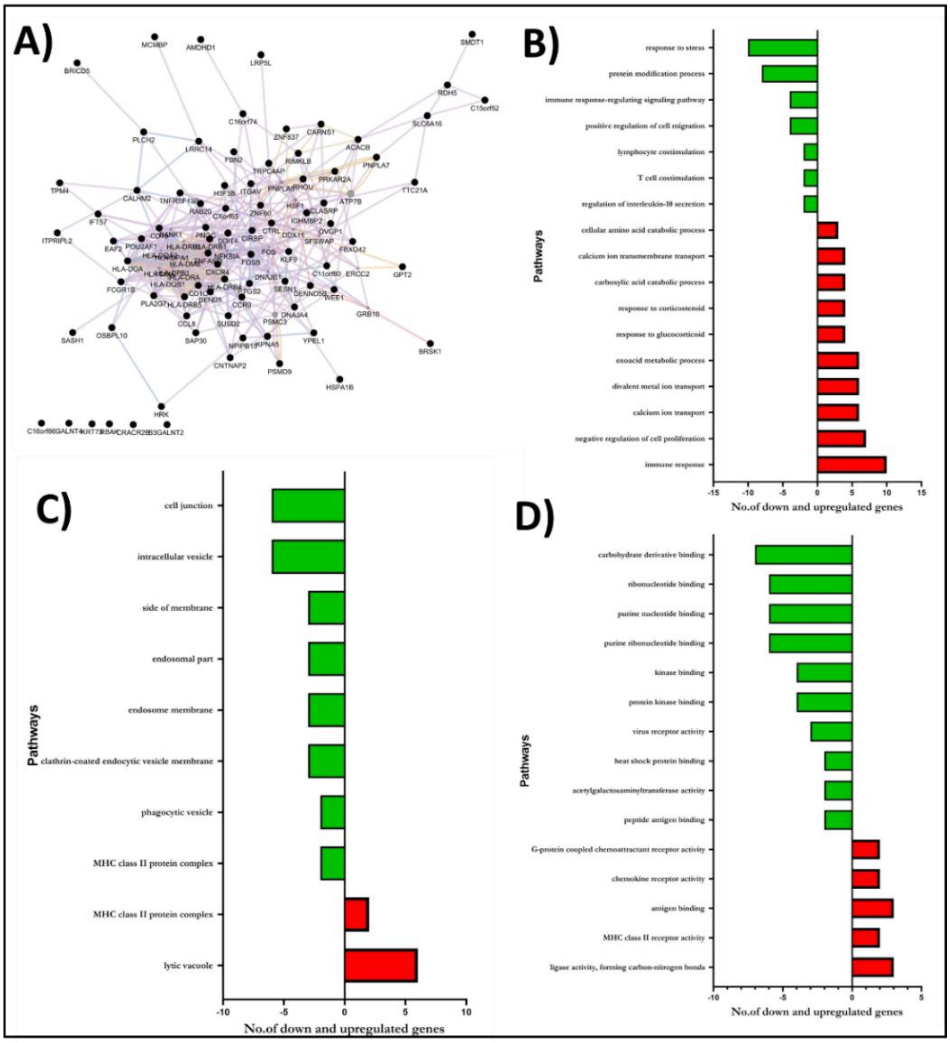

Figure 62. Dysregulated genes/ pathways among All ROP (Mild+ AP+ Severe) vs PC, A: Interactions of genes using the GeneMANIA interaction network, B: Gene ontology analysis-Biological process, C: cellular components and D: molecular function.

D. Aggressive Posterior (AP) vs Severe+ mild ROP

Since AP ROP shows a different disease course (rapid and severe presentation of neovascularization) as compared to mild and severe ROP these were compared to identify genes responsible for this aggressive form of ROP. 418 genes were differentially expressed, of these, 232 were up-regulated and 186 were down-regulated (Table 34). The PCA results showed two clearly distinct and separate cluster for AP and other ROP patients indicating different etiologies for these conditions (Figure 63).

Table 34. Top 25 up-regulated and down-regulated genes (≥ 1.3-fold change and p <0.05) in Aggressive Posterior (AP) vs Severe+ mild ROP

AP vs Severe+ mild					
S.No.	Up-regulated genes		S.No.	Down-regulated genes	
	Symbol	Fold Change		Symbol	Fold Change
1	*CDC42SE1*	3.4622049	1	*LOC649923*	-3.69901
2	*EGR2*	3.1240002	2	*ORM1*	-3.21145
3	*TSGA10*	2.6149383	3	*VNN1*	-3.05884
4	*MYOM2*	2.3688761	4	*PGLYRP1*	-2.78724
5	*LOC100134551*	2.2765864	5	*LOC100131967*	-2.68959
6	*LOC440993*	2.2626134	6	*NRBF2*	-2.65714
7	*ZNF215*	2.245027	7	*MOSC1*	-2.50903
8	*FLJ22536*	2.1515492	8	*CLEC4E*	-2.39156
9	*HBEGF*	2.115633	9	*HECW2*	-2.39131
10	*PVALB*	2.1032283	10	*CYP1B1*	-2.34381
11	*LOC100233209*	2.0729063	11	*THBS1*	-2.30662
12	*DZIP3*	2.0554609	12	*NLRP2*	-2.1813
13	*EMP1*	2.0494936	13	*ERLIN1*	-2.17365
14	*NPCDR1*	2.0416533	14	*DAPK2*	-2.15778
15	*C1orf150*	2.0356831	15	*IRS2*	-2.14189
16	*HUS1B*	2.0284466	16	*RBP7*	-2.12172
17	*TNF*	2.0013434	17	*TLR2*	-2.1155
18	*TAGLN*	1.9929611	18	*CD163*	-2.098
19	*SNORD38A*	1.9484841	19	*LOC100131727*	-2.09044
20	*ZNF507*	1.9476479	20	*CEACAM4*	-2.06914
21	*C20orf100*	1.9466537	21	*MOXD1*	-2.06546
22	*TOX2*	1.941657	22	*LOC152195*	-2.06523
23	*SNORD100*	1.8912574	23	*ALDH1A1*	-2.05693
24	*SCARNA17*	1.8826839	24	*NDST1*	-2.05381
25	*IPW*	1.8628849	25	*TRPM4*	-2.03671

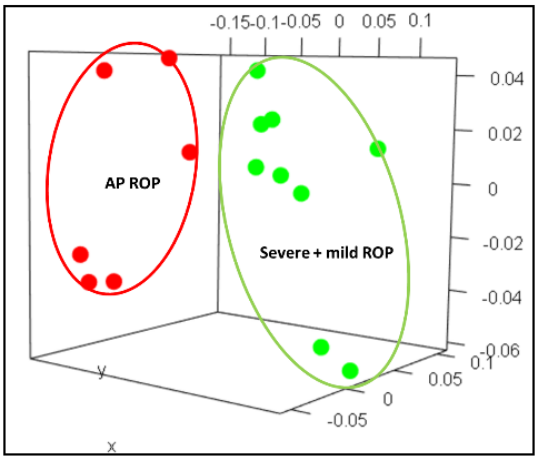

Figure 63. Differential gene expression among AP ROP vs severe + mild ROP

Cytoscape-Genemania analysis showed all the significantly dysregulated genes were interacting with each other by physical interactions, co-expression, shared protein domains, co-localization and predicted curated databases (Figure 64A). Further DAVID analysis revealed that these genes are a part of plasma membranes, cytoplasmic and intracellular vesicles, involved in kinase activity, collagen, lipid and cholesterol binding and are a part of important biological processes such as lipid metabolism, autophagy regulation, ROS metabolism and immune response (Figure 64 B, C, D).

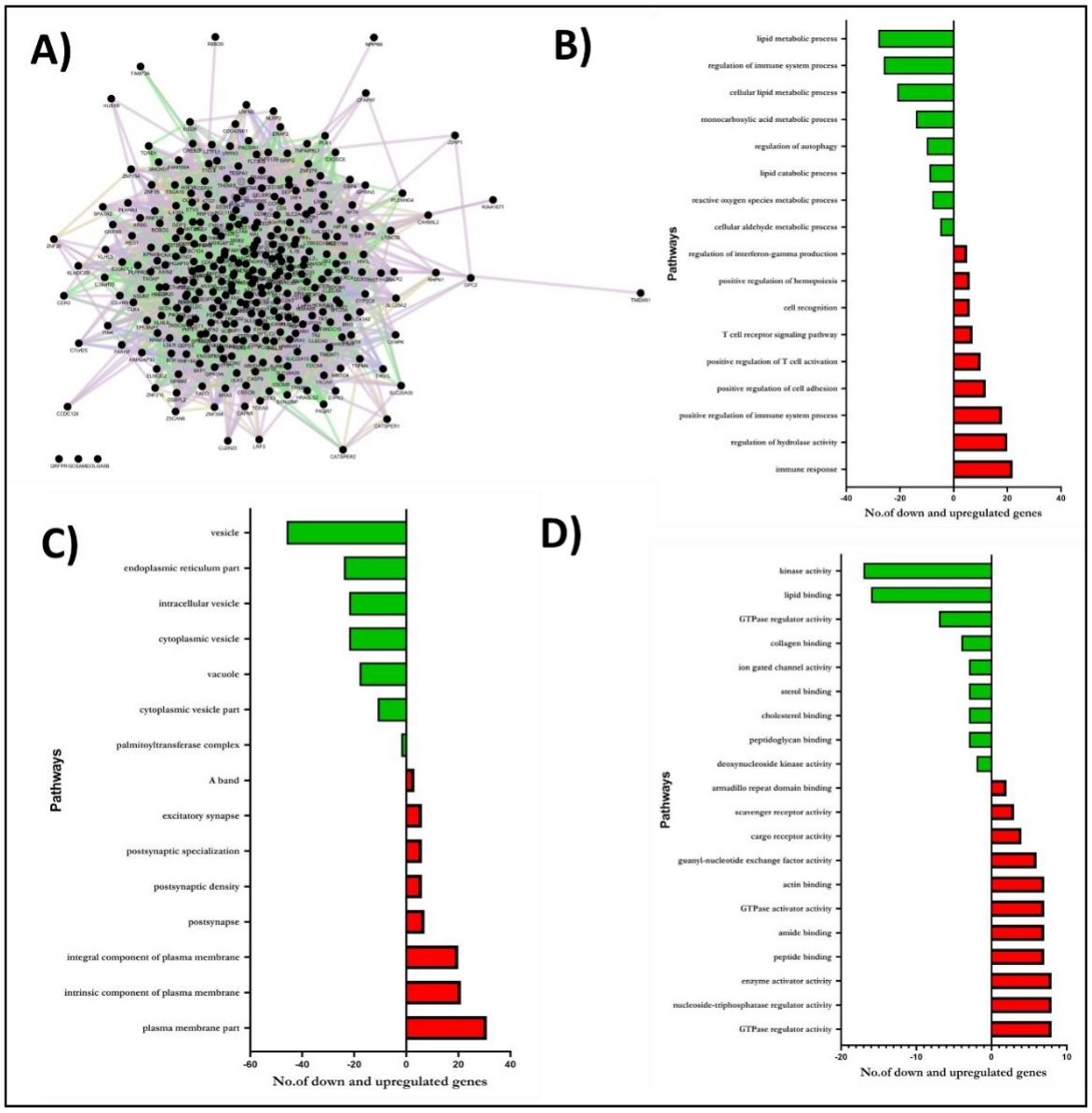

Figure 64. Dysregulated genes/ pathways among AP vs Severe+ Mild ROP, A: Interactions of genes using the GeneMANIA interaction network, B: Gene ontology analysis-Biological process, C: cellular components and D: molecular function.

E. Plus disease (AP + Severe) vs no plus (MILD)

Neovascularization in the retina of patients marks the onset of plus ROP as seen in severe and AP ROP while Mild ROP does not show the same. Thus, to identify genes/pathways involved in neovascularization in the retina, gene expression profiles were compared for AP + Severe vs mild that indicated 505 genes to be significantly dysregulated. Of these, 283 genes were up-regulated and 222 genes were down-regulated (Table 35). Further PCA plots confirmed that

these significant genes could distinguish plus ROP from no plus/mild ROP by forming two distinct and independent clusters (Figure 65).

Table 35. Top 25 up-regulated and down-regulated genes (≥ 1.3-fold change and p <0.05) in plus disease (AP + Severe) vs no plus (MILD)

AP + Severe vs Mild					
S.No.	Up-regulated genes		S.No.	Down-regulated genes	
	Symbol	Fold Change		Symbol	Fold Change
1	*SNORD3D*	11.20554138	1	*CCDC58*	-2.58780056
2	*CDC42SE1*	10.74515107	2	*TRIM47*	-2.52446875
3	*ARG1*	7.476040241	3	*DSC1*	-2.22636596
4	*RGS1*	5.986299107	4	*PI16*	-2.14970549
5	*HBG1*	5.350159364	5	*SOX8*	-2.14501999
6	*SNORD3A*	5.280166008	6	*SDK2*	-2.11786998
7	*SNORD3C*	5.205295556	7	*LOC100131971*	-2.02851333
8	*HBG2*	5.082957176	8	*ZNF286A*	-2.02499109
9	*MYOM2*	3.959133013	9	*CD248*	-1.98922087
10	*LAIR2*	3.071868832	10	*C10orf35*	-1.9770733
11	*RNU11*	3.035699864	11	*UBE2K*	-1.97632924
12	*HIST1H4E*	2.973445951	12	*CD40LG*	-1.94540819
13	*IDO1*	2.961092156	13	*CD28*	-1.94356608
14	*DUSP2*	2.846494794	14	*RPS26P10*	-1.92820485
15	*SCARNA2*	2.83891968	15	*LOC100131662*	-1.92308015
16	*RSAD2*	2.82768274	16	*LOC100133823*	-1.9101471
17	*RNU1-3*	2.767677413	17	*WDR86*	-1.90397182
18	*RNU1-5*	2.755782275	18	*CXCR7*	-1.89939935
19	*CNTNAP2*	2.736970356	19	*NLRP2*	-1.89396381
20	*LIPN*	2.706048072	20	*KLHL34*	-1.88612997
21	*SAP30*	2.700634767	21	*LOC100129552*	-1.88384933
22	*SERPING1*	2.689062198	22	*NOS3*	-1.88209046
23	*DDIT4*	2.617381379	23	*LOC646753*	-1.87715506
24	*RNU1G2*	2.591548984	24	*ID3*	-1.86438803
25	*S100A12*	2.588847617	25	*LOC645979*	-1.86154855

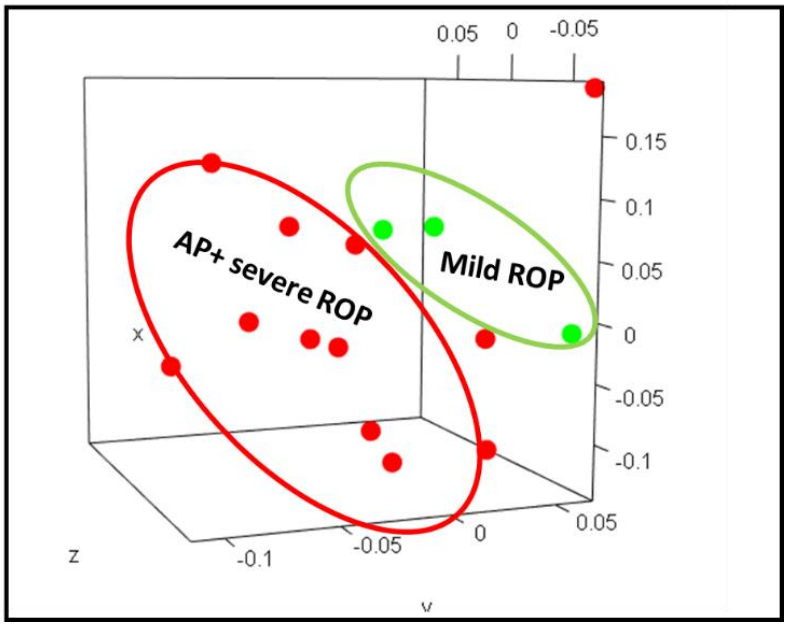

Figure 65. Differential gene expression among AP + severe ROP Vs mild ROP

Cytoscape-Genemania based gene interaction analysis also found all the identified genes to be interacting with each other by physical interactions, co-expression, shared protein domains, co-localization and predicted curated databases (Figure 66A). Gene ontology analysis using DAVID tool revealed that these genes are a part of mitochondrion, cell junctions, plasma membranes, ribosomal subunits and are involved in crucial pathways such as developmental processes, cell proliferation, apoptosis, inflammation, cell activation and immune response (Figure 66 B, C, D).

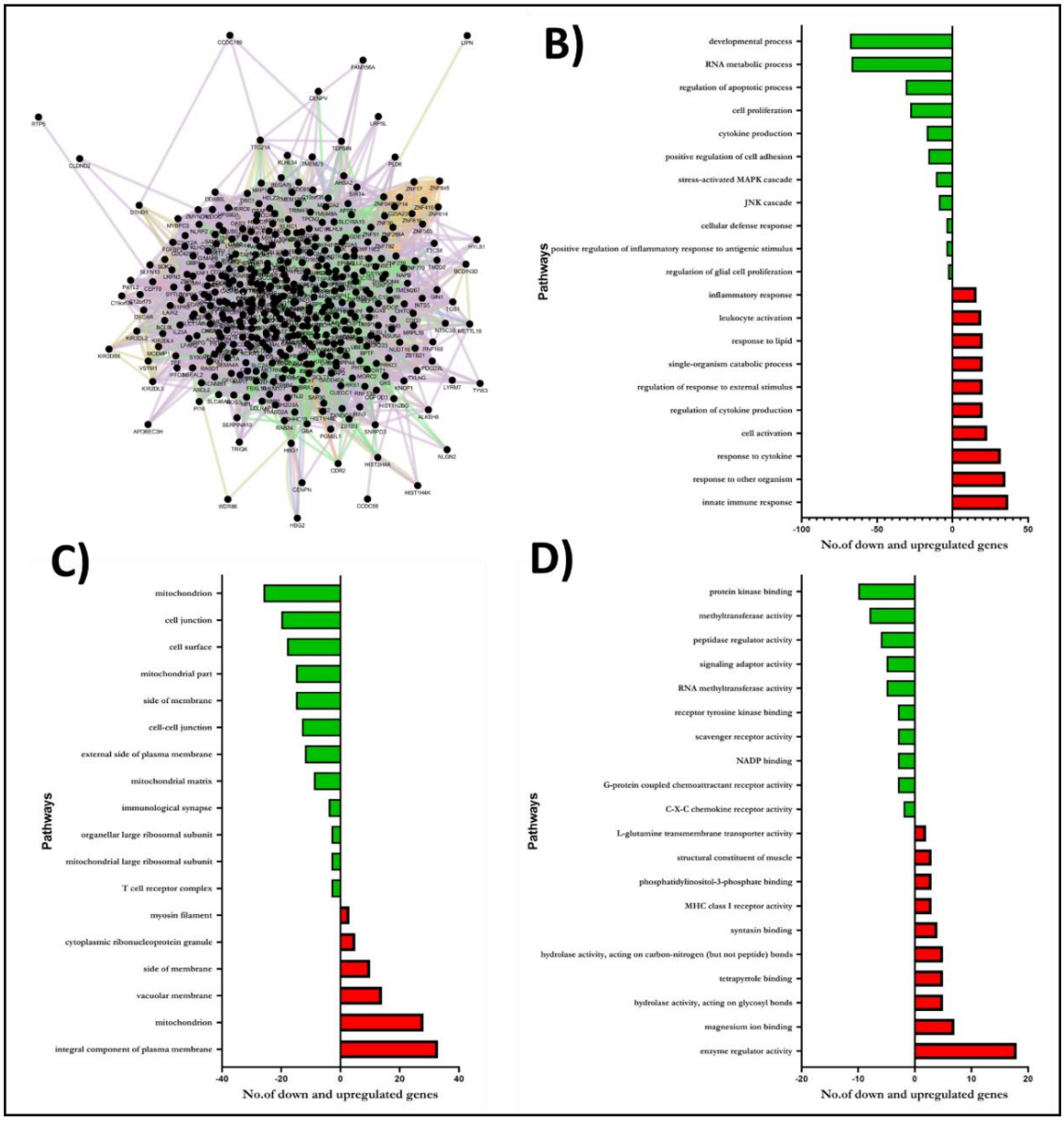

Figure 66. Dysregulated genes/ pathways among AP +severe vs Mild, A: Interactions of genes using the GeneMANIA interaction network, B: Gene ontology analysis-Biological process, C: cellular components and D: molecular function

F. Plus ROP (AP + Severe) vs No Plus controls Mild + PC

Further to confirm the gene involved in retinal neovascularization, gene expression profiles were compared among plus ROP (AP + Severe) vs mild + PC that indicated 187 genes to be significantly dysregulated. Of these, 113 genes were up-regulated and 74 genes were down-regulated (Table 36). The PCA plot showed two different cluster for the two categories however

some of the subject from no plus ROP and controls seemed to have overlapping features with plus ROP cases. (Figure 67).

Table 36. Top 25 up-regulated and down-regulated genes (≥ 1.3-fold change and p <0.05) in plus ROP (AP + Severe) vs Mild + PC

AP + Severe vs Mild + PC					
S.No.	Up-regulated genes		S.No.	Down-regulated genes	
	Symbol	Fold Change		Symbol	Fold Change
1	*SNORD3D*	10.86261	1	*HLA-DRB5*	-8.48399
2	*SNORD3C*	7.632344	2	*HLA-DRB1*	-3.97621
3	*SNORD3A*	4.92585	3	*CCR4*	-1.94639
4	*CDC42SE1*	4.27564	4	*NLRP2*	-1.84723
5	*LOC652479*	3.322712	5	*LOC650298*	-1.76646
6	*RNU11*	2.735138	6	*SOX8*	-1.75205
7	*SAP30*	2.704296	7	*LOC646753*	-1.74831
8	*RNU1G2*	2.693736	8	*RPS26L*	-1.73367
9	*SCARNA2*	2.664167	9	*LOC644928*	-1.70584
10	*CNTNAP2*	2.618757	10	*LOC650646*	-1.66853
11	*SNORD10*	2.585214	11	*ZNF286A*	-1.6654
12	*RNU1-3*	2.561947	12	*KLHL34*	-1.64597
13	*RNU1-5*	2.557128	13	*CD40LG*	-1.6421
14	*LAIR2*	2.336623	14	*CXCR7*	-1.63601
15	*DUSP2*	2.308863	15	*SIGLEC14*	-1.60771
16	*DDIT4*	2.179649	16	*LOC100129650*	-1.60733
17	*LOC645381*	2.149112	17	*GOLGA7B*	-1.60168
18	*MIR1974*	2.030852	18	*EPHA1*	-1.59467
19	*FLJ16686*	1.968794	19	*NOS3*	-1.59124
20	*BEGAIN*	1.962061	20	*CD28*	-1.57629
21	*HIST1H4E*	1.950902	21	*INSL3*	-1.55311
22	*RNU1A3*	1.913976	22	*LOC644934*	-1.55307
23	*NUDT16P*	1.880046	23	*ID3*	-1.54976
24	*LOC440993*	1.828336	24	*CD248*	-1.54958
25	*RN5S9*	1.770212	25	*LOC653598*	-1.47299

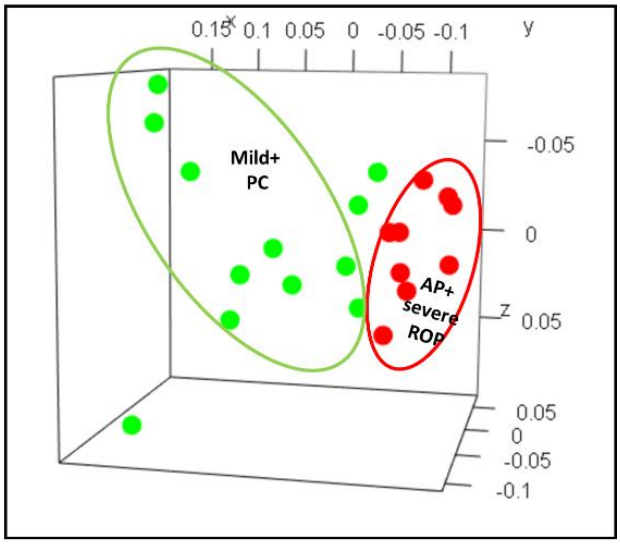

Figure 67. Differential gene expression among AP + severe ROP vs mild ROP + PC

Possible interactions among those genes were predicted using Cytoscape-Genemania analysis that found most of these genes to be co-expressed, co-localized, had shared protein domains and showed predictive interactions (Figure 68A). Next, gene ontology analysis revealed these genes to be involved in crucial pathways such as immune response, T-cell and B-cell activation, inflammation, cell proliferation and activation (Figure 68B, C, D).

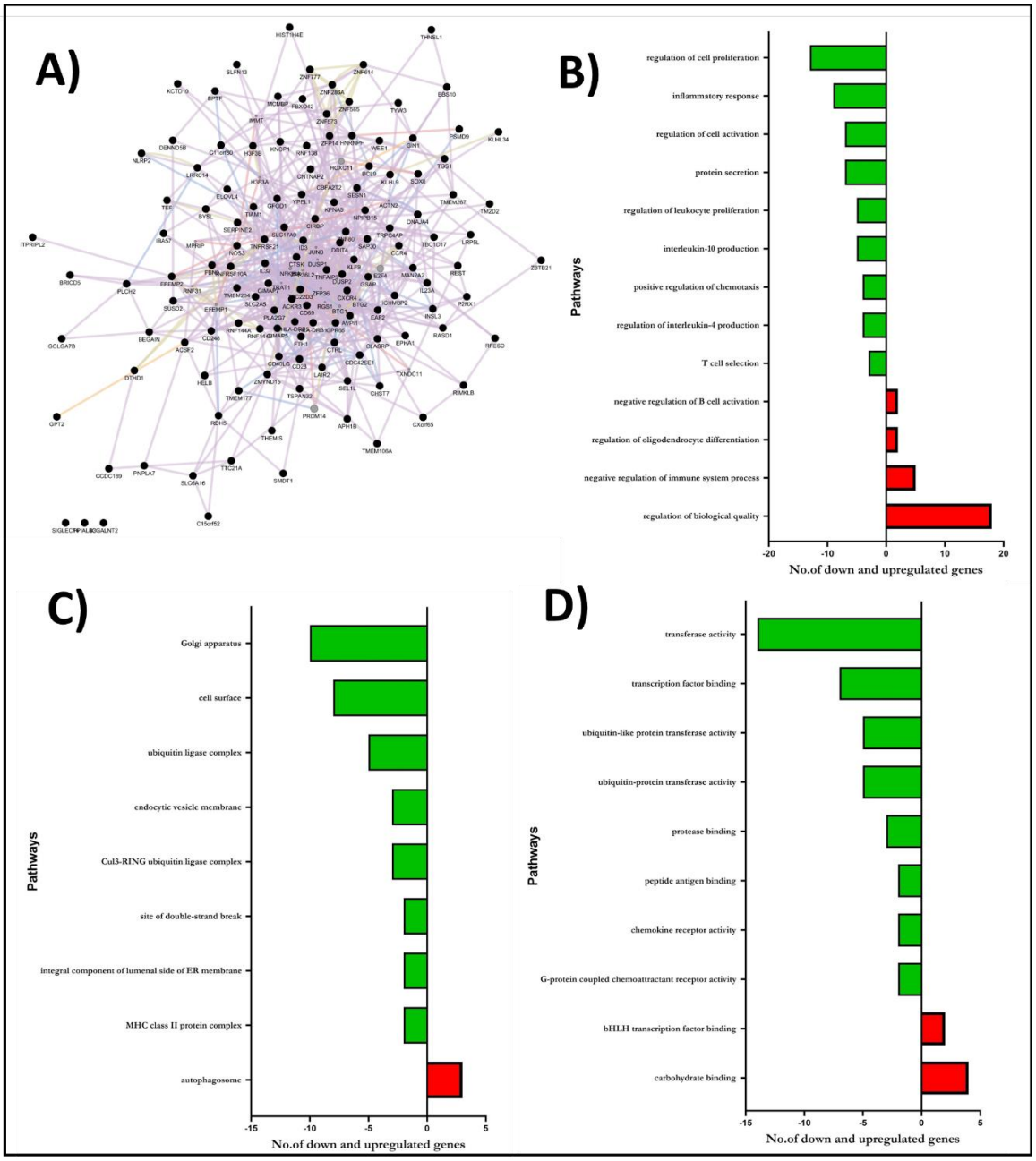

Figure 68. Dysregulated genes/ pathways among AP +severe vs Mild + PC, A: Interactions of genes using the GeneMANIA interaction network, B: Gene ontology analysis-Biological process, C: cellular components and D: molecular function

G. Severe vs PC

Differential analysis of gene expression for severe vs PC indicated that 280 genes were significantly dysregulated. Of these, 114 genes were up-regulated and 166 genes were down-regulated (Table 37). PCA plot for significant genes showed clearly distinct clusters for the two groups (Figure 69).

Table 37. **Top 25 up-regulated and down-regulated genes (≥ 1.3-fold change and p <0.05) in Severe vs PC**

Severe vs PC					
S.No.	Up-regulated genes		S.No.	Down-regulated genes	
	Symbol	Fold Change		Symbol	Fold Change
1	*SNORD3D*	10.58911553	1	*HLA-DRB1*	-4.61386174
2	*SNORD3C*	10.46894303	2	*CCL8*	-4.32164533
3	*SNORD3A*	5.246396891	3	*DSC1*	-3.49666884
4	*HIST1H4B*	4.202567101	4	*PVALB*	-2.93753595
5	*SAP30*	4.159763448	5	*LOC100233209*	-2.82843799
6	*ADORA3*	4.020625282	6	*NOG*	-2.69798121
7	*ORM2*	3.760509062	7	*GOLGA7B*	-2.60469516
8	*LOC652479*	3.341728604	8	*KLHL34*	-2.52272369
9	*LOC654053*	3.16996153	9	*SOX8*	-2.49163602
10	*RNU1G2*	2.942406736	10	*NOS3*	-2.46981608
11	*RNU11*	2.921504923	11	*LOC642178*	-2.44367935
12	*LOC100131967*	2.81433255	12	*EGR2*	-2.34906673
13	*IRS2*	2.704720635	13	*LOC642161*	-2.32140867
14	*RNU1-3*	2.688759434	14	*EPHA1*	-2.2861089
15	*DDIT4*	2.679033385	15	*CD40LG*	-2.19702438
16	*RNU1-5*	2.615741185	16	*AXIN2*	-2.11557463
17	*CNTNAP2*	2.516918159	17	*C6orf190*	-2.07919955
18	*NUDT16P*	2.408958233	18	*LOC442535*	-2.01803239
19	*LOC645381*	2.352691062	19	*IGSF9B*	-2.01078184
20	*SESN1*	2.350054183	20	*CD28*	-1.98278558
21	*LOC152195*	2.323536401	21	*ICOS*	-1.98221379
22	*PGLYRP1*	2.246897191	22	*MAL*	-1.97792577
23	*SYTL3*	2.245416425	23	*SIGLEC14*	-1.97093505
24	*BEGAIN*	2.239985145	24	*TRAT1*	-1.96518024
25	*CLEC4E*	2.234156282	25	*SLFN5*	-1.94822194

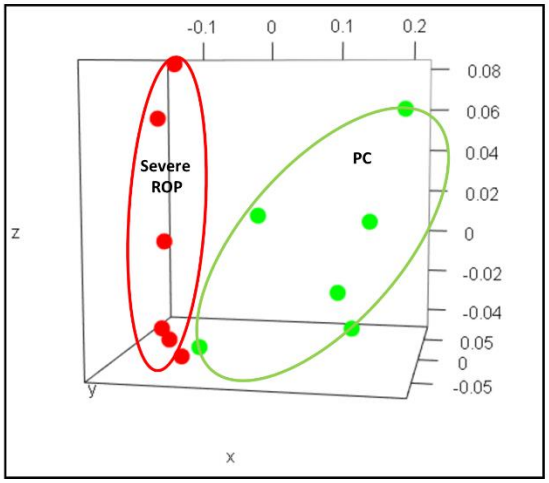

Figure 69. Differential gene expression among Severe ROP vs PC

Significantly dysregulated genes for severe ROP were checked for possible interactions by Cytoscape-Genemania analysis and as expected all of them were found to be co-expressed, co-localized, had shared protein domains and showed predictive interactions (Figure 70A). Gene ontology analysis showed that these genes constitute important functions in golgi bodies, cell membranes, ECM, cell junctions and play important roles in apoptosis, cell-cell adhesion, Wnt signalling pathway, MAPK cascade, cell proliferation, NK T cell activation, autophagy, lipid metabolism and inflammatory response (Figure 70B, C D).

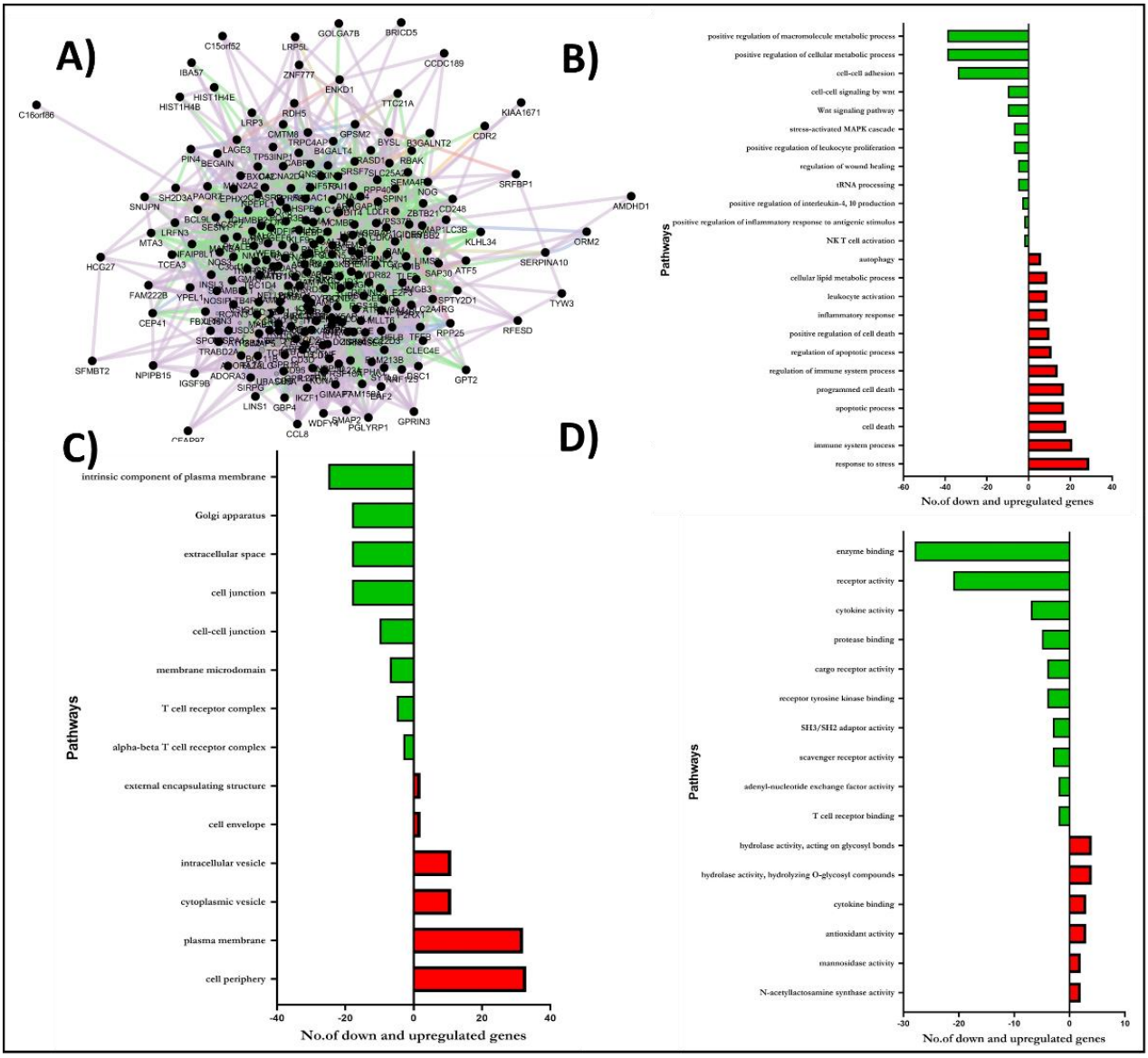

Figure 70. Dysregulated genes/ pathways among Severe vs PC, A: Interactions of genes using the GeneMANIA interaction network, B: Gene ontology analysis-Biological process, C: cellular components and D: molecular function

H. Mild vs PC

Microarray data analysis of severe vs PC indicated that 163 genes were differentially expressed. Of these, 81 genes were up-regulated and 82 genes were down-regulated (Table 38). The PCA plot showed two distinct clusters for each group (Figure 71).

Table 38. Top 25 up-regulated and down-regulated genes (≥ 1.3-fold change and p <0.05) in mild vs PC

Mild Vs PC					
S.No.	Up-regulated genes		S.No.	Down-regulated genes	
	Symbol	Fold Change		Symbol	Fold Change
1	*CCDC58*	2.713146701	1	*CASP5*	-3.9340926
2	*LOC728070*	2.68664905	2	*LOC728744*	-3.78053936
3	*PI16*	2.681353461	3	*HLA-DRB5*	-3.69561195
4	*SDK2*	2.089618886	4	*HLA-DRB1*	-3.65556592
5	*GSTM3*	1.947263521	5	*ANXA3*	-3.13115417
6	*KRT72*	1.940494474	6	*PLSCR1*	-2.83912916
7	*LOC401676*	1.935580233	7	*FCGR1B*	-2.81795834
8	*ZNF785*	1.889188795	8	*PVALB*	-2.49924964
9	*KRT73*	1.888660391	9	*VSTM1*	-2.3296939
10	*C10orf35*	1.8841437	10	*SASH1*	-2.19731905
11	*KIAA1324*	1.816048904	11	*LOC100170939*	-2.16251357
12	*TEAD2*	1.763917302	12	*SOCS3*	-2.16068083
13	*CRIP2*	1.726976475	13	*DCBLD1*	-2.11746726
14	*FAM167A*	1.708503088	14	*SLAMF8*	-2.10343994
15	*CABP5*	1.705691142	15	*RNASE2*	-2.09482828
16	*NELL2*	1.64697274	16	*C6orf150*	-2.09444302
17	*CBR3*	1.637441135	17	*HK3*	-2.06629282
18	*EFCAB4A*	1.632299632	18	*PFKFB3*	-2.03911695
19	*LOC642934*	1.61137995	19	*FLJ46906*	-2.02118685
20	*C8orf13*	1.590096953	20	*TNFSF13B*	-1.98234631
21	*LOC100131662*	1.586436932	21	*IL18RAP*	-1.97919335
22	*ZNF837*	1.554764674	22	*CCR1*	-1.89363153
23	*LOC442270*	1.552707311	23	*PID1*	-1.88546862
24	*RPS23*	1.552600452	24	*GYG1*	-1.8419154
25	*DENND5B*	1.546439188	25	*BAMBI*	-1.82012324

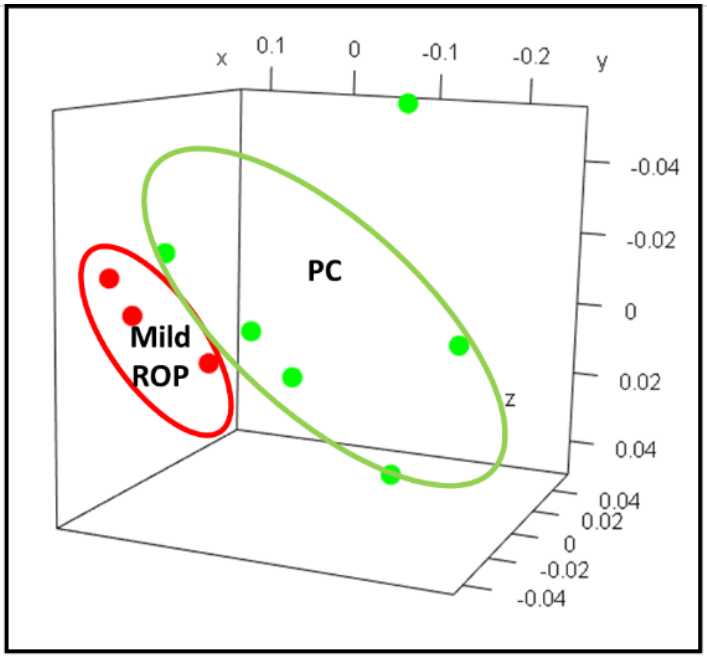

Figure 71. Differential gene expression among mild ROP vs PC

Cytoscape-Genemania analysis was employed to identify the possible interactions among the significantly dysregulated genes. Most of the genes were found to be co-expressed, co-localized, had shared protein domains, and showed predictive interactions (Figure 72A). GO analysis showed that these genes are involved in crucial pathways such as MAP kinase activity, inflammation, immune response, protein transport and cell activation (Figure 72B, C D).

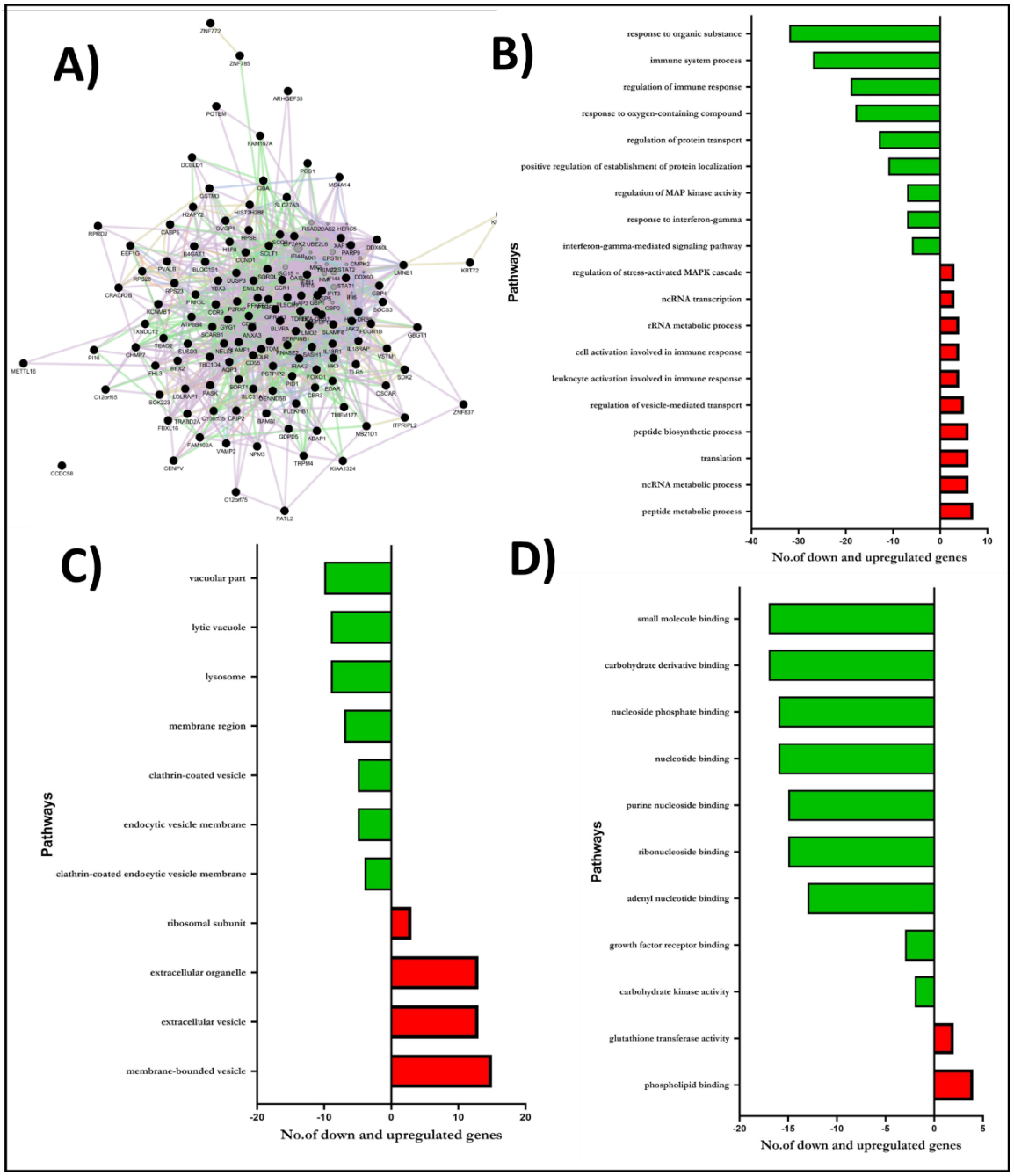

Figure 72. Dysregulated genes/ pathways among Mild vs PC, A: Interactions of genes using the GeneMANIA interaction network, B: Gene ontology analysis-Biological process, C: cellular components and D: molecular function

I. AP vs PC

Differential gene expression analysis among AP vs PC indicated that 261 genes were differentially expressed. Of these, 175 genes were up-regulated and 86 genes were down-regulated (Table 39). The PCA results shows the differential gene expression (Figure 73).

Table 39. **Top 25 up-regulated and down-regulated genes (≥ 1.3-fold change and p <0.05) in AP vs PC**

AP vs PC					
S.No.	Up-regulated genes		S.No.	Down-regulated genes	
	Symbol	Fold Change		Symbol	Fold Change
1	*FOSB*	5.882606518	1	*HLA-DRB1*	-6.0670481
2	*LOC652479*	4.716043231	2	*HLA-DRB5*	-5.68707817
3	*CDC42SE1*	4.681501281	3	*BPI*	-4.52838524
4	*SNORD10*	3.405517632	4	*LOC649923*	-2.63931776
5	*PTGS2*	3.135087483	5	*NLRP2*	-2.63877964
6	*TSGA10*	2.957107891	6	*CLEC4D*	-2.34728642
7	*CNTNAP2*	2.608940983	7	*NRBF2*	-2.31304754
8	*FLYWCH1*	2.52958822	8	*TRPM4*	-2.20633933
9	*EGR2*	2.346930675	9	*FCGR1B*	-2.14432973
10	*LOC728070*	2.290191666	10	*CLDN23*	-2.12646878
11	*SNORD68*	2.259385749	11	*HSPA1B*	-1.98007393
12	*KPNA5*	2.210946771	12	*NDN*	-1.96957075
13	*SNORD38A*	2.150312145	13	*PLA2G7*	-1.94012283
14	*LOC440993*	2.130430349	14	*SDSL*	-1.92566766
15	*HUS1B*	2.065218518	15	*FBN2*	-1.91535765
16	*ZNF215*	2.038791643	16	*BST1*	-1.908474
17	*KIAA0125*	2.005263752	17	*LOC728519*	-1.88487321
18	*KRTCAP3*	1.995736632	18	*LPAR1*	-1.86620753
19	*KLHL35*	1.970220421	19	*RAB20*	-1.81993888
20	*SNORD35B*	1.965854539	20	*SASH1*	-1.80024712
21	*C1orf150*	1.940822826	21	*PEX11A*	-1.76532894
22	*FAM30A*	1.92660252	22	*CD163*	-1.7141858
23	*LOC143666*	1.912340111	23	*LPCAT2*	-1.67283166
24	*SUSD2*	1.900450756	24	*ITPRIPL2*	-1.65889346
25	*SNORA45*	1.88143938	25	*C10orf11*	-1.65836093

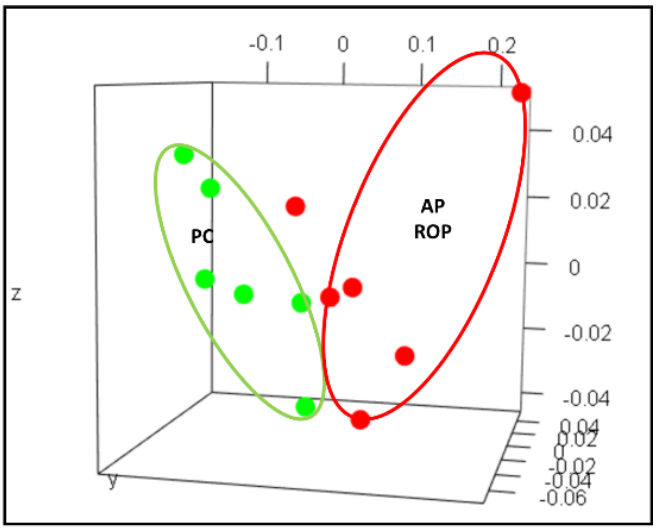

Figure 73. Differential gene expression among AP ROP vs PC

Similarly, genes found dysregulated in AP vs PC were also shown to be interacting among each other based on co-expression, co-localization, shared protein domains and predictive interactions by Cytoscape-Genemania analysis (Figure 74A). Gene ontology analysis for the same revealed the involvement of these genes in cellular pathways involved in defence, inflammation, lipid metabolism and immune response (Figure 74B, C, D).

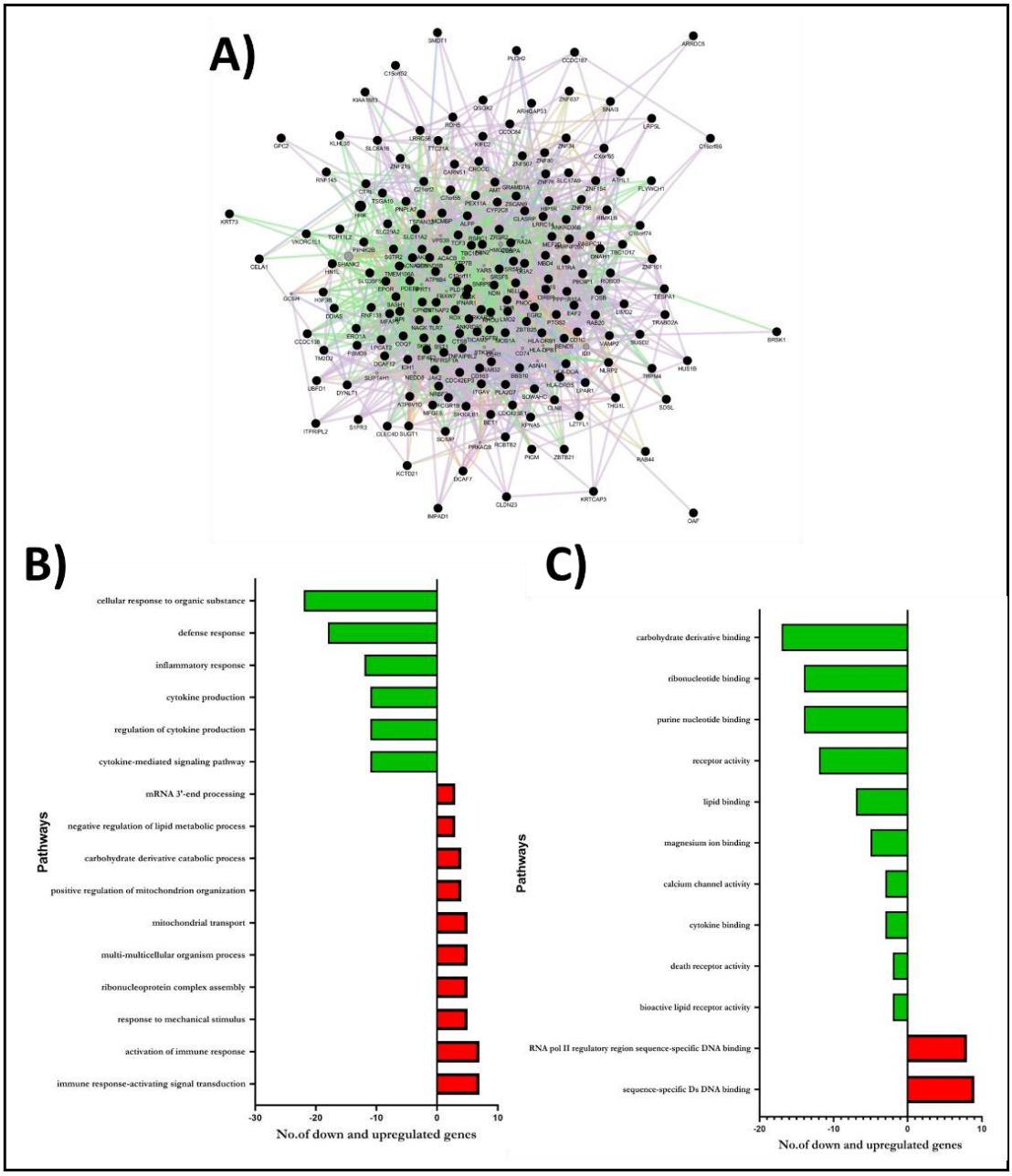

Figure 74. Dysregulated genes/pathways among AP vs PC, A: Interactions of genes using the GeneMANIA interaction network, B: Gene ontology analysis-Biological process, C: molecular function

3.2.3. Validation of significantly dysregulated genes

The next aim was to validate the expression of genes involved in key pathways in different categories of ROP by semi-quantitative PCR.

A. Significantly dysregulated genes in AP ROP

The expression *FOSB* and *EGR2* (transcription factor) genes were found to be significantly upregulated in only AP ROP phenotypes by microarray-based approach (fold change: 5.9 and *p*-value= 0.05; fold change: 2.34 and *p*-value= 0.022 respectively). The real time PCR based validation for *FOSB* in different categories of ROP confirmed it upregulation (fold change: 1.7 and *p*-value= 0.1) in cases vs controls in AP ROP and also in mild and severe ROP (Figure 75 & 76). Semi quantitative PCR confirmed significant upregulation of *EGR2* (fold change: 2.34; p-value: 0.042) too in APROP, while for severe ROP it showed a reverse trend though not statistically significant.

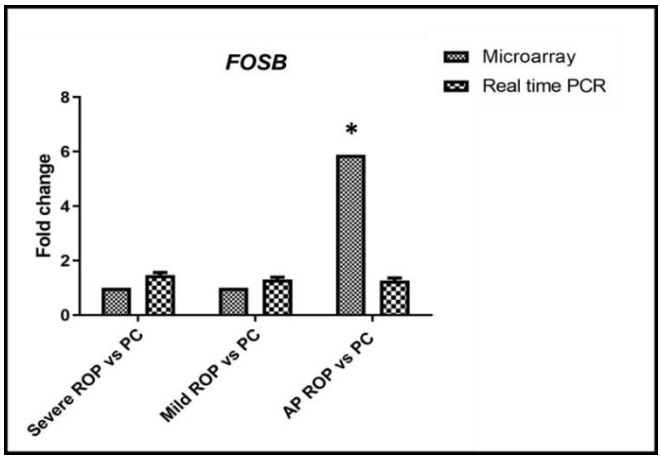

Figure 75. Gene Expression profile of *FOSB*. The data are represented as fold change ± SEM (n=20 in each), *p<0.05. *p<0.01.

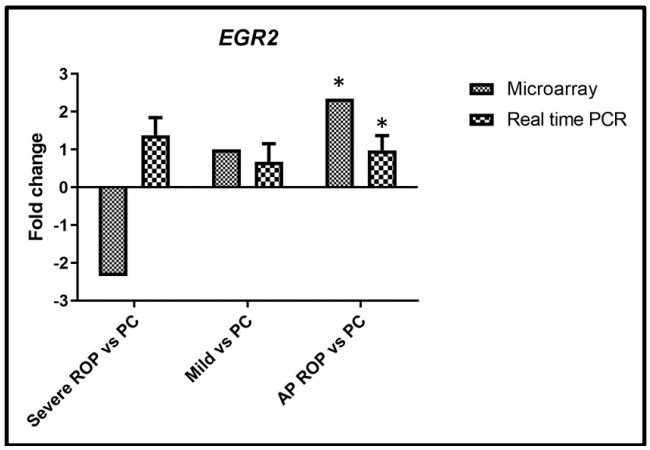

Figure 76. Gene Expression profile of *EGR2*. The data are represented as fold change ± SEM (n=20 in each), *p<0.05. *p<0.01

B. Significantly dysregulated genes in Severe ROP:

AXIN2, a regulatory gene of Wnt signalling pathway and *NOS3* a known vasodilator gene were found significantly downregulated in severe ROP phenotypes by microarray (fold change: -2.34 and *p*-value= 0.012; fold change: -2.46 and *p*-value= 0.029) respectively and same was confirmed by qPCR (fold change: 1.6 and *p*-value= 0.041; fold change: 1.34 and *p-value*= 0.051) (Figure 77 & 78).

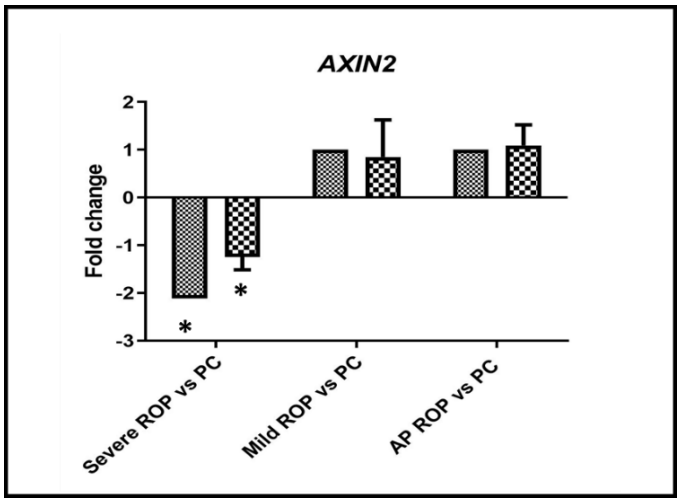

Figure 77. Gene Expression profile of *AXIN 2*. The data are represented as fold change ± SEM (n=20 in each), *p<0.05. *p<0.01

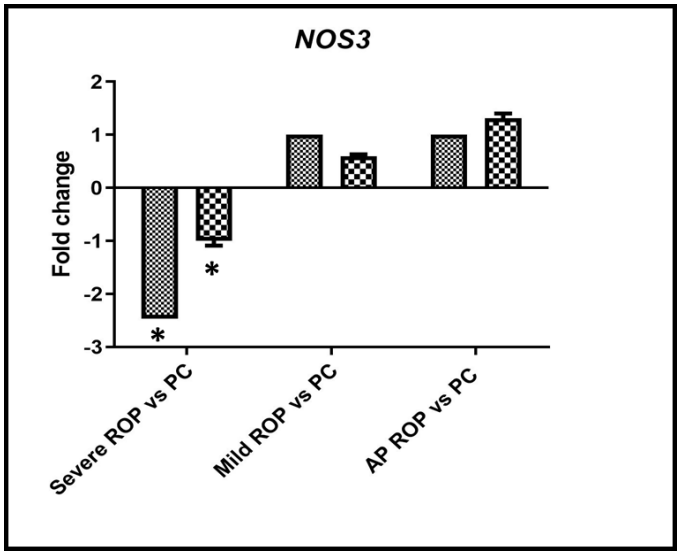

Figure 78. Gene Expression profile of *NOS3*. The data are represented as fold change ± SEM (n=20 in each), *p<0.05. *p<0.01

C. Significantly dysregulated genes in all forms of ROP

Selected significantly downregulated genes with potential implication in all stages of ROP including NK cell regulatory genes i.e. *HLA-DRB1* (severe ROP fold change: -4.63, *p-value*= 0.025; AP ROP fold change: -6.0728, *p-value*= 0.013; mild ROP fold change: -3.65, *p-value*= 0.059) and *DRB5* (AP ROP fold change: -5.67, *p-value*= 0.015563035; mild ROP fold change: -3.68; *p-value*= 0.094) were validated by qPCR and confirmed downregulation of *DRB5* (severe ROP fold change: -4.3, *p-value*= -0.045; AP ROP fold change: -2.728; *p-value*= 0.012) (Figure 79 A &B).

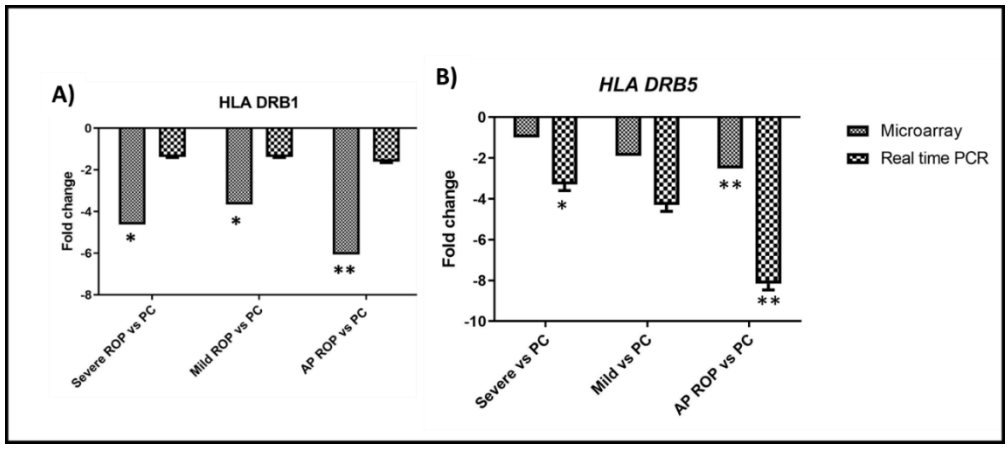

Figure 79. Gene Expression profile of inflammatory genes, *HLA DRB1 (A), HLA DRB5 (B).* The data are represented as fold change ± SEM (n=20 in each), *p<0.05. *p<0.01

The metabolizing enzyme *CYP2C8* expression found significantly upregulated in severe + AP ROP phenotypes by microarray (fold change: 1.63 and *p-value*= 0.017) and this was confirmed in Severe +AP ROP by qPCR (fold change: 3.9 and *p-value*= 0.05) (Figure 80).

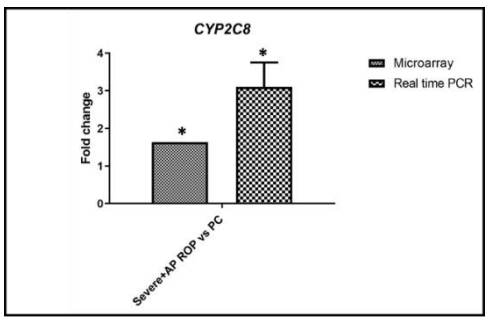

Figure 80. Gene Expression profile of inflammatory genes, *CYP2C8.* The data are represented as fold change ± SEM (n=20 in each), *p<0.05. *p<0.01

3.4. Discussion

3.4.1. Global gene expression profiling in ROP

The most challenging aspect of ROP is identifying which subgroup of prematurely born infants would progress to severe stages of ROP. Gene expression is a strictly controlled cell fate that can change its expression under pathological conditions and alter the protein product. Thus, unravelling differentially expressed genes during ROP would help understand the molecular mechanism of disease progression (Yang *et al.*, 2013; Ishikawa *et al.*, 2010; Recchia *et al.*, 2010). Only a single study analyzed differential gene expression among preterm infants with ROP and no-ROP, however it could not provide much information regarding the genes involved in disease mechanisms/pathways (Pietrzyk *et al.*, 2013). Therefore, our study performed microarray data mining approaches to identify the disease-associated pathways in different stages of ROP. Global transcriptomics of ROP patients and the OIR mice models showed the association of immune, inflammation, angiogenesis-related genes with ROP (Pietrzyk *et al.*, 2013; Sato *et al.*, 2009). The involvement of inflammatory and immune pathways in ROP infants was confirmed in the present study too (Figure 81). A systematic analysis of genes/pathways that could contribute to ROP progression is quite challenging primarily due to difficulties in obtaining samples for a long term/longitudinal study. The present study is first one that attempted to understand the differential gene expression profiles among different stages of ROP (Table 40) and their potential role in disease pathogenesis.

Except for single human study, most earlier studies on genes expression analysis were conducted on an oxygen-induced retinopathy animal model (Yang *et al.*, 2013; Ishikawa *et al.*, 2010; Recchia *et al.*, 2010; Sato *et al.*, 2009) that found multiple pathways, some of which are also shown to be involved in human ROP patients. Besides confirming the significant dysregulation of immune response, inflammation and angiogenesis-related genes among different stages of ROP, several novel signaling pathways are also found (lipid metabolism, Wnt

and MAPK signalling etc) to be dysregulated. These are subsequently functionally validated by metabolite profiling in the vitreous of ROP patients.

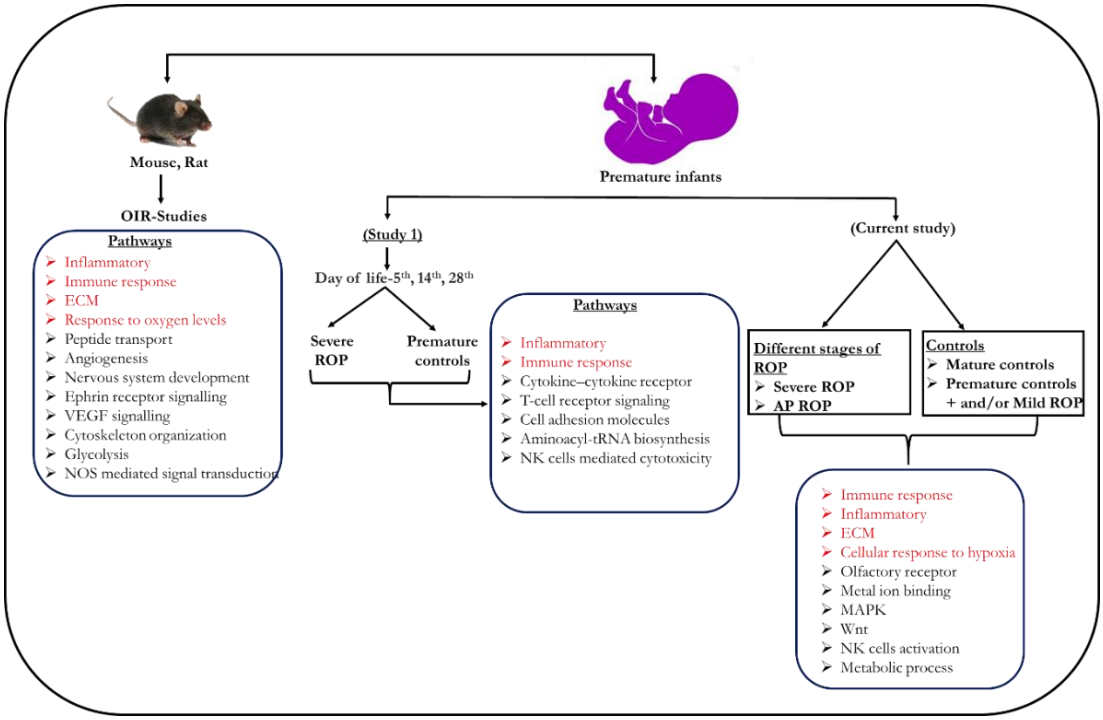

Figure 81. Schematic diagram of identified pathways in ROP research

Table 40. Comparison of pathways among ROP sub groups

S.No	Pathways	1. MC vs PC	2. Mild + AP + Severe vs PC + MC	3. Mild + AP + Severe Vs PC	4. AP Vs Mild + T1	5.AP + Severe Vs Mild	6.AP + Severe Vs Mild + PC	7.Severe Vs PC	8.Mild Vs PC	9. AP vs PC
1	Interferon-gamma production	No	Yes	No	Yes	Yes	Yes	Yes	Yes	Yes
2	Immune response	No	No	Yes	Yes	Yes	Yes	Yes	Yes	Yes
3	Golgi apparatus	No	No	Yes	No	No	Yes	Yes	Yes	Yes
4	Adaptive immune response	No	No	Yes	Yes	Yes	Yes	Yes	Yes	Yes
5	Positive regulation of inflammatory	No	No	No	Yes	Yes	Yes	Yes	No	Yes
6	Regulation of interleukin-4 and 10 production	No	Yes	Yes	No	Yes	Yes	Yes	No	No
7	Primary metabolic process	No	No	No	No	Yes	Yes	Yes	No	No
8	Nucleic acid metabolic process	No	No	No	No	Yes	Yes	Yes	No	No
9	Regulation of phosphorylation	No	No	No	No	Yes	No	Yes	Yes	Yes
10	Cell communication	Yes	No	Yes	No	Yes	No	Yes	Yes	Yes
11	Positive regulation of phosphate metabolic process	No	No	No	No	Yes	No	Yes	Yes	No
12	Apoptotic signaling pathway	No	No	No	Yes	Yes	No	Yes	No	Yes
13	Endothelial cell apoptotic process	No	No	No	No	Yes	No	Yes	No	No
14	Wnt signaling pathway	No	No	No	No	Yes	No	Yes	No	No
15	NF-κβ import into nucleus	No	No	No	No	Yes	No	Yes	No	No
16	tRNA processing	No	No	No	No	No	No	Yes	No	No
17	NK T cell activation	No	No	No	No	No	No	Yes	No	No
18	Metal ion transport	No	No	Yes	No	No	No	Yes	Yes	No
19	Phospholipid metabolic process	No	No	No	Yes	No	No	No	No	Yes
20	Leukotriene metabolic process	No	No	No	Yes	No	No	No	No	No

Among the significantly dysregulated genes, the genes involved in early developmental processes, such as *EGR2, EPHA1, SOX-8* and *IGSF9b* were found down-regulated in plus /severe ROP (stage 4/5 ROP and AP-ROP). Transcription factors genes involved in nervous system development were upregulated in AP ROP such as FOSB and *EGR2*. Later is a zinc finger transcription factor that binds to target genes and activates cellular activities such as cell proliferation, division and apoptosis during the developmental process (Chandra *et al.*, 2013; Yokota *et al.*, 2010). EGR2 regulates the expression of interleukin-6 (IL6), indoleamine dioxygenase-1 (IDO1) and cyclooxygenase-2/prostaglandin-endoperoxide synthase 2 (COX2/PTGS2) by binding to their promoter regions (Barbeau *et al.*, 2014). *EGR2* silencing has been shown to reduce the synthesis of prostaglandin E2 (an anti-inflammatory mediator) and downregulate *COX2* genes (Barbeau *et al.*, 2014). This gene is also involved in early hindbrain growth, primarily myelination and mature neuronal activity, as well as B-cell and T-cell maturation and proliferation (Li *et al.*, 2012; Swanberg *et al.*, 2009). Several early developmental genes, including *EGR2, FOSB, CYP2C8* and *CNTNAP2* were found to be substantially upregulated in AP ROP patients. Other genes implicated in inflammatory pathways including the toll receptor signaling pathway, NK cells mediated cytotoxicity and metabolic enzymes required for inflammatory responses, were found downregulated in severe ROP cases. AXIN 2 (also known as conductin or axil inhibitor 2) is a negative regulator of the Wnt signaling pathway. It is required for assembling a multiprotein complex that facilitates the degradation of catenin, thus inhibiting the Wnt signaling pathway. This study found downregulation of *AXIN 2* gene expression in severe ROP thereby suggesting that a loss of *AXIN 2* expression could promote Wnt signalling leading to increased angiogenesis as seen in severe ROP cases.

The early growth response (*EGR2*), is known to be induced in activated T-cells under hypoxic stress and regulates *FOS* expression. Increased FOS further triggers the angiogenic process via

STAT3 and *VEGF*. In addition to this, upregulation of *VEGF* activates the P13K-AKT pathway leading to *NOS3* mediated oxidative stress. The *NOS3* regulates NO production and SOD2, which in turn, prevents oxidative stress. NOS3 is one of the vasodilators that keeps the endothelium functioning. Vasodilators and vasoconstrictors maintain endothelium stability and homeostasis. NOS3, also known as endothelial NOS (eNOS) or constitutive NOS (cNOS) is a vascular endothelial enzyme that creates nitric oxide (NO). NO is mainly involved in blood flow dilation by counteracting the effects of vasoconstrictors such as angiotensin II and endothelin (Davignon & Ganz, 2004). It also regulates cell proliferation, leukocyte adhesion, platelet aggregation, vasoconstriction, smooth muscle proliferation, LDL oxidation and MMP activation (Forstermann & Munzel, 2006).

EGR2 promotes angiogenesis via cFOS and NOS3 (Figure 82). Their differential expression in different stages of ROP was further validated in an extended cohort by qPCR. Wnt pathway genes were found to be associated with all severe forms of ROP. Our data found that the expression of Wnt receptors and ligands such as LRP5 and NDP were also upregulated in the patient samples. At the same time, Wnt regulators *DKK* and *AXIN 2* were downregulated. The same was also validated by qPCR. Dysregulation of Wnt signaling in ROP may lead to abnormal angiogenesis. Also, the expression of Wnt inhibitors such as DKK1 was downregulated under hypoxic stress as demonstrated in the aim 1 of the present study.

HLA-DRB1 and HLA-DRB5 are MHC class II molecules found on antigen-presenting cells (APC) such as macrophages, lymphocytes and dendritic cells and play a significant role in the immune system by recruiting CD4 T-cells to immune recognition sites. Neutrophils and macrophages are innate immune cells that play a crucial role in defence mechanisms. Neutrophil-mediated apoptosis could be induced by interactions with death receptors present on the neutrophil surface. Under normal physiological conditions, this activity of NK cells is inhibited by their interactions with HLAs (Figure 83).

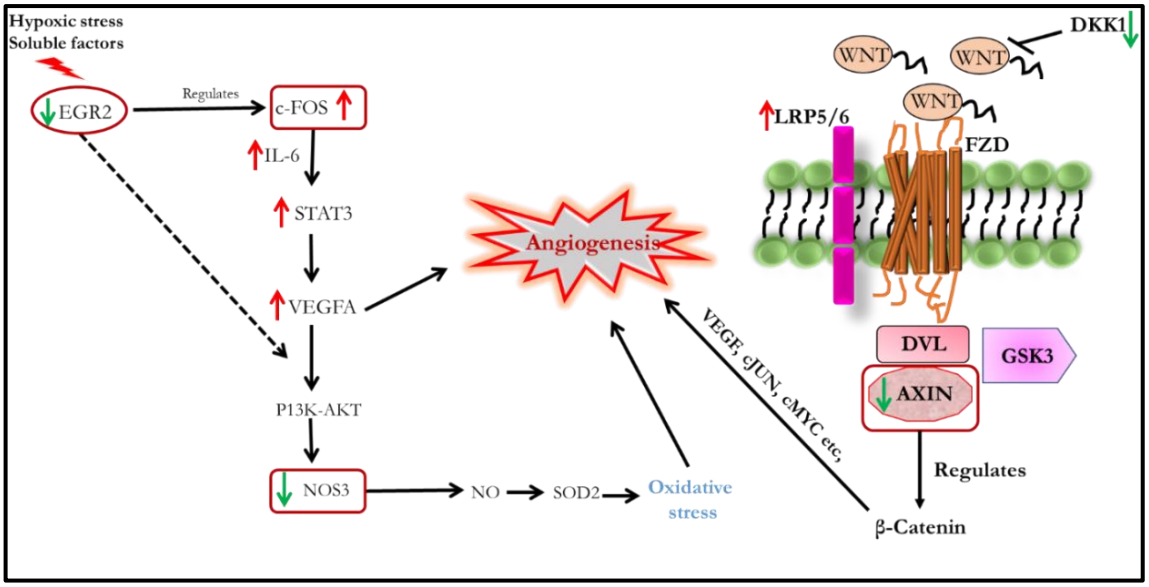

Figure 82. Key genes involved in angiogenesis in retina of ROP patients

Interestingly, our analysis demonstrated downregulation of *HLA DRB1* & *HLA DRB5* in ROP infants. Thus, lack of HLA regulation of NK cells, could aberrantly induce apoptosis and release of inflammatory cytokines in ROP infants. It may be noted that *HLA-DRB1* and *HLA-DRB5* were under-expressed in all the stages of ROP. Further, in addition to HLA, many other immune-related molecules (*VSTM1, PLSCR1, SLAMF8, CD40LG, CCL8*, and *TNF*) were also downregulated in ROP.

Arachidonic acid is metabolized via cyclooxygenase, lipoxygenase and cytochrome P-450 (CYP) enzymes. Arachidonic acid is released and oxygenated by enzyme systems, leading to inflammatory mediators, i.e. eicosanoids. In our data, *CYP1B1* and *CYP2C8* were significantly upregulated in severe ROP.

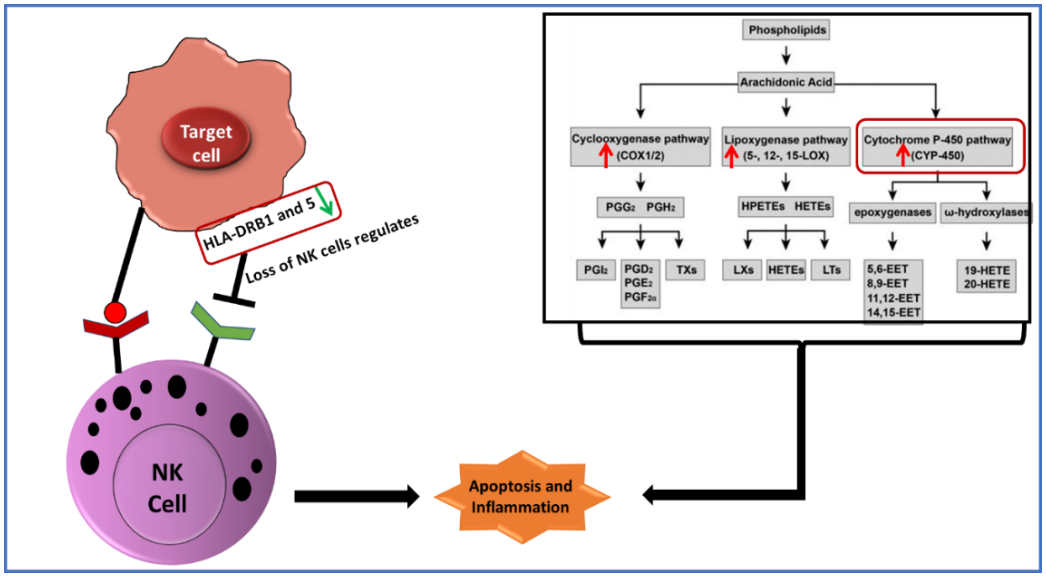

Figure 83. Validation of important gene expression involved in inflammatory process

In summary, data from global gene expression suggests that genes involved in metalloendopeptidase, Inflammation, MAPK, Wnt, ECM modelling angiogenesis and metabolism of fatty acids particularly arachidonic acid metabolism showed association with severe stages of ROP suggesting for their strong involvement in ROP pathogenesis. The study for the first time could clearly demonstrate different signalling/pathways being involved in different categories of ROP. Performing studies in premature infants is a time consuming and arduous task owing to the complex disease etiology and lack of appropriate and enough samples required for such studies, however not withstanding these major limitations, the present study has tried to expand the knowledge on underlying mechanisms that could potentially contribute to ROP progression. An in-depth functional characterization of these identified significant pathways in ROP is being pursued in our lab by using appropriate *in vitro* and *in vivo* assays.

CHAPTER-4

IDENTIFICATION OF METABOLIC PATHWAYS INVOLVED IN ROP PATHOGENESIS

4. Introduction and review of literature

Metabolomics is an emerging field that encompasses comprehensive analysis of all the metabolites and low molecular weight (LMW; <1kDa) compounds in a biological sample (Table 41). To better understand the underlying mechanism of ROP, it is essential to assess the metabolomic changes in addition to the genome and proteome (Figure 84). Metabolomics is a rapidly developing tool to detect and quantify all endogenous and exogenous LMW molecules/metabolites in a biological system using high-throughput mass spectroscopy-based methods. These LMW metabolites are involved in biological events and act as a substrate for several biochemical reactions in the human body. Retina is a metabolically highly active tissue of human body. Metabolites are considered to have a close relationship with phenotypes, particularly in complex diseases. The type of metabolites derived from various metabolic reactions suggests the underlying biochemical changes in response to any stress or change in normal physiology which could be detected from a variety of biological fluids such as urine, blood and vitreous. The metabolic flux is highly dynamic and not stable as genetic profile, therefore, these could give a snapshot of disease related alterations (Suhre & Gieger, 2012). Thus, studying metabolites are better suited to understand the underlying mechanisms of physiological and pathological conditions. It is widely applied for addressing different biological questions and clinical applications particularly for identification and development of newer drug targets. The number of metabolites and their abundance varies across different pathological conditions. The human metabolome database (HMDB) currently maintains approximately 1,41,100 metabolites (Wishart *et al.*, 2018). These metabolites can have concentrations ranging from sub-nanomolar to millimolar depending on the biological matrix, and their physical characteristics vary significantly.

Table 41. Basic terms and their definitions used in the metabolomics

Term	Definition
Metabolite	A low-molecular-weight chemical compound that is related to metabolism but not directly derived from the genome and nor structurally bound in the cell
Metabolome	The complete set of metabolites associated with a cell/organism at any given time. The metabolome is subdivided into the endo- and exo-metabolome that cover the intra- and extra-cellular metabolites, respectively
Metabolite profiling	Chemical analysis of numerous metabolites
Metabolic fingerprinting	A chemical signature or snapshot of (intracellular) metabolites in crude extracts. The fingerprints are mainly used for classification and biomarker discovery
Metabolomics	The research field focussing on comprehensive chemical analysis of the metabolome and integration of data through data mining and biochemistry

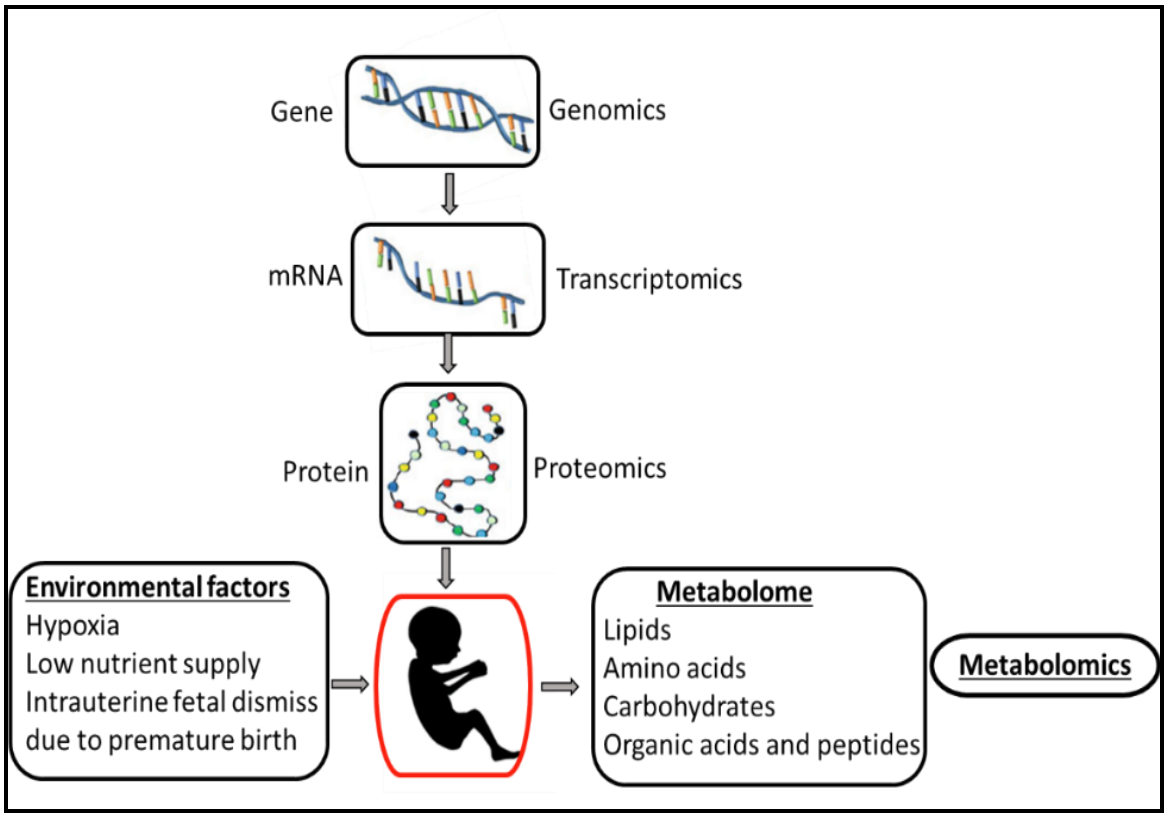

Figure 84. Genome (DNA), transcriptome (RNA), proteome (proteins) and metabolome (metabolite) are the building block of life. Metabolome is the final event in the biological process and can provide the information of disease phenotype and can be influenced by several environmental factors

4.1.1. Analytical platforms for metabolomics

The ideal methodology for measuring all metabolites should be sensitive, selective and repeatable with a broad dynamic range and unbiased detection. Mass spectrometry (MS) is frequently used in conjunction with other separation techniques, such as gas chromatography (GC) or liquid chromatography (LC) for studying metabolites. MS based techniques have the advantage of detecting compounds in much lower concentrations with an extensive dynamic range to detect the metabolites. This technique is particularly useful for a very low quantity of biological samples such as those available for ocular diseases.

The basic principle of MS is based on the ionization of compounds/low molecular weight molecules which exist in a given biological sample, separation of ions based on their mass to charge ratio (m/z) and measuring their abundance. Metabolite profiling can be done either by a targeted or untargeted method (Gertsman & Barshop, 2018). Targeted metabolite profiling is used for studying the predefined chemically annotated metabolites. Although it only applies to a small proportion of metabolites, this method allows for their absolute measurement. Untargeted or global metabolite profiling, on the other hand is applied to study all metabolites in a cell, tissue or system. A clear comparison of the two approaches in metabolomics is provided in the Figure 85.

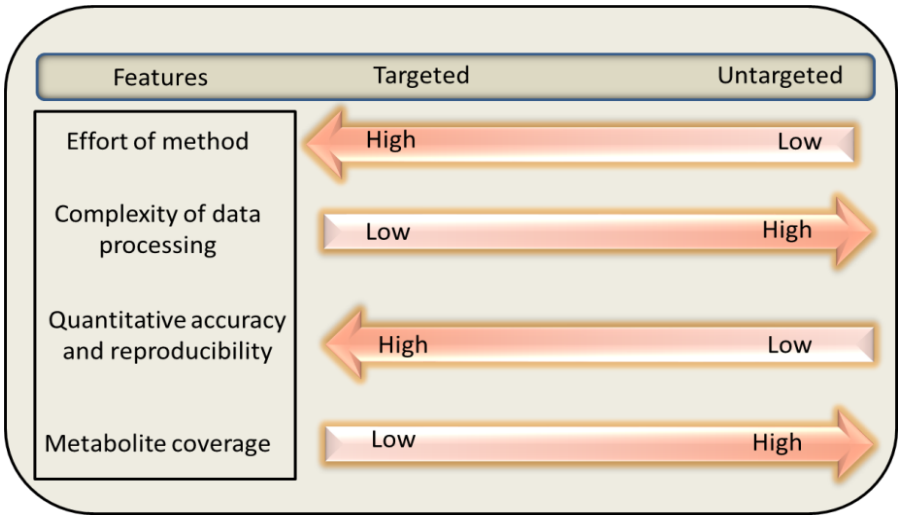

Figure 85. Comparison of targeted vs. untargeted metabolite profiling

4.1.2. Key metabolic pathways for retinal functions and diseases

Study of metabolites in retina, a highly metabolically active tissue may provide clear information on pathways involved under both physiological and pathological conditions. This also offers in-depth understanding of their regulation by different genes/enzymes. The known metabolic pathways in the retina are described below:

4.1.2.1. Retinoic acid metabolism in early retinal development and maturation

Vitamin A interacts with retinoic acid (RA) and plays a crucial role in the visual cycle and its regulation. (Mark *et al.*, 2006). RA is a by-product of vitamin-A metabolism. It passes into the nucleus by binding to the nuclear receptor and directly regulates the targeted genes. Besides, it is essential for cell to cell communication during early developmental phase of retina including the posterior neuroectoderm, foregut endoderm and mesoderm. It remains crucial for even retinal maturation.

Retinoic acid is converted initially to retinol and transported to cells by retinol-binding protein (RBP4) via STRA6 receptor. Inside the cells, cellular retinol binding proteins (CRBP) converts retinol to retinyl esters. Retinol is also oxidized and converted into retinaldehyde by retinal dehydrogenase (RDH) and then to retinoic acid (RA). RA is oxidized and degraded by cytochrome P450 (CYP2C6) in a non-RA target tissue. While in a RA target tissue, the cellular RA binding protein (CRABP) facilitates RA binding and transport into the nucleus via the RA receptor leading to the formation of the ternary complex [retinoic acid receptor (RAR), retinoid X receptor (RXR), and a retinoic acid response element (RARE)] (Figure 86).

4.1.2.2. Warburg effect on retinal metabolism

The cancer cells continuously reprogram and use glucose for several anabolic processes, i.e., RNA and protein synthesis. Cancer cells express the pyruvate kinase M2 (PKM2) isoform for its reprogramming, which is further used for glycolytic machinery. In human retina, energy can

be generated similar to cancer cells even in the presence of oxygen by glycolysis. This type of aerobic glycolysis is called the Warburg effect. According to Warburg, hypoxia stimulates glycolysis in retinal cells. Palsson-McDermott EM *et al.* in 2013 described the Warburg effect in detail in multiple cell types such as embryonic stem cells, T lymphocytes, neutrophils, macrophages and dendritic cells (Palsson-McDermott & O'Neill, 2013).

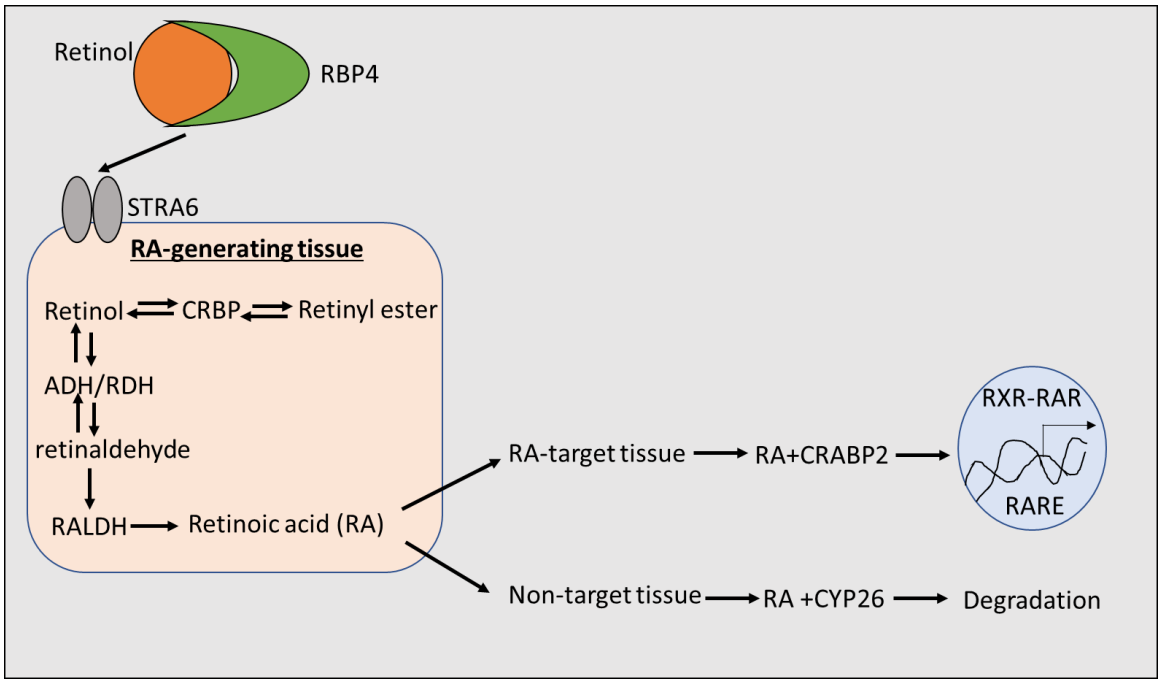

Figure 86. Mechanism of retinoic acid (RA) signalling, adapted and modified from the (Duester, 2008)

ATP is a cellular energy source for all living organisms and is generated by 2 metabolic pathways; glycolysis and oxidative phosphorylation (OXPHOS) (Romano & Conway, 1996). A glucose molecule is converted into 2 pyruvate and 2 ATP molecules (Romano & Conway, 1996) in an anaerobic condition. When oxygen levels drop, pyruvate shifts from OXPHOS and is transformed to lactate by the enzyme lactate dehydrogenase (LDH). This results in the formation of nicotinamide adenine dinucleotide (NAD+) (Xie *et al.*, 2020; Solaini *et al.*, 2010). These enzymatic reactions play an important role in cell mobility, regulation of transcription and apoptosis (Zheng *et al.*, 2003; Winkler *et al.*, 2003; Racker, 1974).

4.1.2.3. Endothelial cell metabolism in retina

Endothelial cell (EC) proliferation is associated with and triggered by angiogenic stimuli. Any imbalance between inflammatory/anti-inflammatory and angiogenic/antiangiogenic molecule ratios under differential stress conditions may lead to abnormal ocular angiogenesis. EC cells rapidly shift to the angiogenic or proliferative state under ischaemia (Carmeliet, 2003). EC requires glycolytic activity for normal physiological activities and under stress/angiogenic conditions, there is higher demand for glycolytic activity at the migratory tip cells of EC. This requires remodelling of actin cytoskeleton in its filopodia and lamellipodia (Figure 87) (De Bock *et al.*, 2013).

Under hypoxic stress conditions, EC does not depend on the O_2 dependent energy production metabolisms and the glycolytic activity is regulated by the enzyme fructose-2, 6-bisphosphatase 3 (PFKFB3) (Xu *et al.*, 2014). VEGF and MMPs are known to be elevated in the angiogenic state by increase in the glycolytic flux (De Bock *et al.*, 2013; Parra-Bonilla *et al.*, 2010; Peters *et al.*, 2009). Delta-like ligand 4 (DII4) is a negative regulator of angiogenesis. Upon stimulation of Dll4, glycolytic flux reduces via downregulation of PFKFB3 protein levels (De Bock *et al.*, 2013). Along with PFKFB3, other glycolytic enzymes also co-localize at the F-actin binding sites (lamellipodia and filopodia) of EC (De Bock *et al.*, 2013). The localization of enzymes for glycolytic activity facilitates the production of ATP molecules via glycolysis. This in turn provides enough energy to promote cell migration and angiogenesis (De Bock *et al.*, 2013). The EC involves the Crabtree effects which means higher levels of glucose leads to suppression of mitochondrial respiration via carbohydrate or glutamine-driven pathways and oxidation of fatty acids (Koziel *et al.*, 2012; Dagher *et al.*, 2001; Krutzfeldt *et al.*, 1990).

Glycolytic pathways shift to the pentose phosphate pathway (PPP) and hexosamine biosynthesis pathway (HBP). The HBP-pathway has been shown to utilize excessive glucose and glutamine in case of diabetes and cancer (Slawson *et al.*, 2010). PPP pathways facilitate

ROS scavenging by offering ribose units required for nucleotide synthesis and NADPH production (Riganti *et al.*, 2012). Leopold et al. explored the decreased PPP pathway involvement using the anti-sense oligonucleotide enzyme for a specific target of glucose-6-phosphate dehydrogenase (G6PD). The result showed lowered VEGF-stimulated proliferation, migration and tube formation in ECs (Leopold *et al.*, 2003).

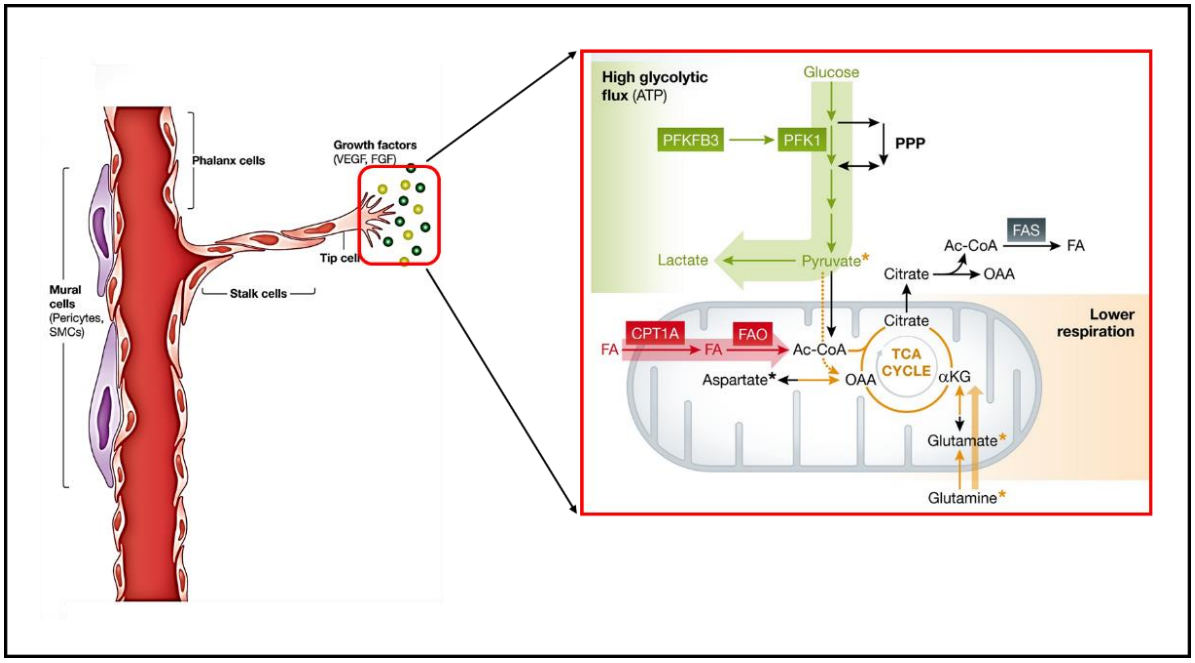

Figure 87. Endothelial cell metabolism and glycolytic flux

4.1.2.4. Nucleotide metabolism in angiogenesis

Degradation of the purines (ATP, GTP) and pyrimidine nucleotides (NAD+, NADH) has been reported in ischemic conditions (Seifart *et al.*, 1980). Catabolic by-products of purine nucleotides such as adenosine, hypoxanthine, xanthine, inosine, guanine, uric acid and pyrimidine nucleotide such as nicotinamide are released from myocardium and accumulated in the coronary venous blood (Fox *et al.*, 1979). Under hypoxic and ischemic conditions, these metabolites serve as potential candidates for angiogenesis (Morris *et al.*, 1989). Pyrimidine derivatives are released from ischemic tissue and promotes vascular growth in response to ischemia. Nucleotide degradation derived metabolites have not been explored in retinal diseases like ROP.

4.1.2.5. Amino acid metabolism in angiogenesis

Amino acid metabolism plays a crucial role in several biological functions such as coagulation, cell growth, differentiation, vascular tone, immune system, inflammatory and redox homeostasis. On the basis of their *de novo* synthesis, amino acids are further categorized as essential or non-essential ones. An exogenous supply of amino acids provides nutrient support for the highly proliferative cells. D*e novo* synthesis of amino acids is not able to fulfil the demand for the rapidly growing cells. Further, oxidative stress can lead to changes in the amino acid metabolic flux thereby affecting the production of energy and antioxidant mechanisms in the eye. Glutamine, a free α-amino acid, inhibits nitric oxide (NO) production through endothelial-derived nitric oxide (eNOS).

The glutamine homeostasis is maintained by continuous sequential events of absorption, reabsorption and followed by delivery to the targeted tissues with the help of membrane transporters (Mann *et al.*, 2003). Glutamine produces energy (ATP) for biosynthesis via Na-K ATPase pump in corneal cells (Zhang *et al.*, 2017). Glutamine is converted into the glutamate-ammonia in the presence of the phosphate-dependent glutaminase (GLS2) enzyme. Defects in glutamine and asparagine catabolism are correlated with aberrant angiogenesis (Oberkersch & Santoro, 2019). GLS2 depletion in ECs leads to ROS generation by loss of balanced ratio between glutathione oxidized glutathione (Suzuki *et al.*, 2010).

Arginine, an essential amino acid, plays a vital function in several cellular metabolic signalling pathways. It acts as a substrate for eNOS and produces NO that regulate sensitive oxidative pathways, neurotransmission, vascular functions, blood pressure and immune response (Tousoulis *et al.*, 2012). Serine is one of the non-essential amino acids that plays an essential role in glycolysis and heme synthesis needed for maintaining mitochondrial homeostasis (Vandekeere *et al.*, 2018). Serine hydroxymethyl transferase generates glycine from the serine. Glycine being a non-essential amino acid shows differential functions in antioxidant activity

and nucleotide synthesis. It also promotes VEGF-mediated angiogenesis (Guo *et al.*, 2017). Proline is required for the formation of ECM and collagen production and its elevated levels may lead to vascular remodelling (H. Li *et al.*, 2001).

4.1.2.6. Lipid derived metabolites in angiogenesis and inflammation

Arachidonic acids (AA), eicosapentaenoic acid (EPA) and docosahexaenoic acid (DHA) are long chain polyunsaturated fatty acids (PUFAs) and abundantly present in the macular region of retina. These produce key intracellular messengers such as cis-epoxyeicosatrienoic and mid-chain cis-trans-conjugated dienols via the activity of cytochrome P450 enzymes which are required for angiogenesis and maintenance of blood flow. While lipids play a vital role in cellular and metabolic pathways, these are prone to oxidation under oxidative stress generating free radicals. These further interact with cell membranes causing cell damage. The polyunsaturated fatty acids (PUFA) contain the double bonds between methylene bridges (-CH2-) that form reactive hydrogen species. The altered lipid metabolism and signaling has been explored in various diseases (Fliesler & Anderson, 1983).

Many chronic inflammatory disorders, including DR, Macular Disease and Peripheral Neuropathy ROP and others have been associated with altered lipid metabolism (Forrester *et al.*, 2020; Gantner *et al.*, 2019; Malamas *et al.*, 2017). Omega-3 and omega-6 PUFAs are required for cell membrane function and signalling. Eicosanoids are formed in the enzymatic cascades from these PUFAs. Eicosanoids are bioactive signalling molecules with pro-inflammatory and anti-inflammatory properties. These are generated by cyclooxygenases (COX-1/2), lipoxygenases (5 and 15 LOX) and epoxygenases (cytochrome P450 or CYP). Omega-6 PUFA AA and its derivatives are implicated in modulating inflammation (for example, T-cell and monocyte activation and chemotaxis), platelet aggregation and endothelial cell adhesions. The omega-3 fatty acids EPA and DHA and their derivatives are essential for retina and brain growth, cognitive function and production of minimal inflammatory eicosanoids such as

resolvins and various tissue protectants (Rose & Connolly, 1999; van 't Veer *et al.*, 1996). Leukotrienes are LOX enzyme derivatives of AA and have role in chemotaxis and inflammation (Figure 88). In response to an inflammatory signal, phospholipase A2 releases AA from monocyte phospholipid membranes, resulting in a predominantly pro-inflammatory response. AA-derived prostaglandin E2 and other series-two prostaglandins and thromboxanes are produced by COX-1 and COX-2 enzymes (Yates *et al.*, 2014; Russo, 2009). Lipids act as second messengers and play a vital role in the human retina. These lipid derivatives act as a second messenger in various signalling pathways. Oxidative stress, apoptosis and inflammation are vital hallmarks in ROP progression, but altered lipid metabolites have not explored in ROP patients.

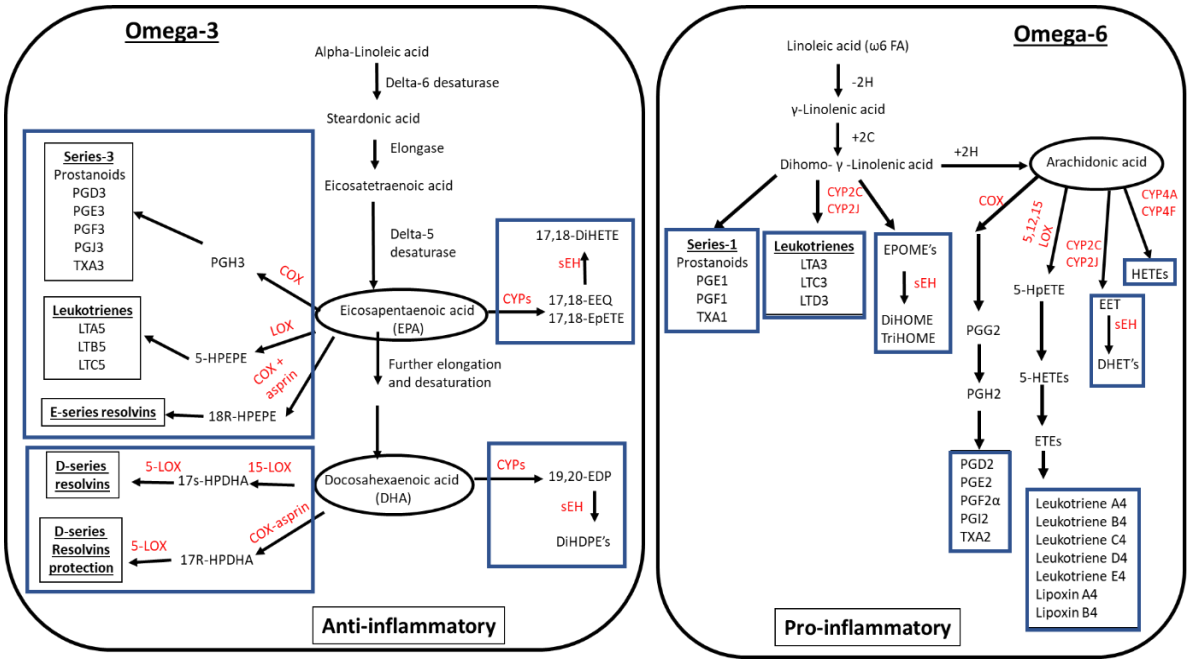

Figure 88. Metabolic pathways for omega-3 and omega-6 fatty acids leading to a variety of inflammation mediators and cell function effectors

So far, metabolic profiling was undertaken in several ocular diseases employing both ocular and non-ocular biological specimens such as retina, tear, vitreous, plasma and serum. A list of metabolites identified from these studies is provided in the Table 42.

Table 42. List of the metabolites identified and type of platforms used in different ocular diseases.

Disease	Biochemical Group	Metabolite	Sample	Analytical Platform	References
AMD	Amino acids and derivatives	**Glutathione, Cysteine**	Human plasma	LC-MS	(Osborn *et al.*, 2013; Brantley *et al.*, 2012)
		Decanoylcarnitine, Octanoylcarnitine, Arginine, Citrulline, Ornithine, Proline	Human vitreous humor	LC-MS and LCMS/MS (MRM)	(Paris *et al.*, 2016)
	Fatty acyls, Imidazoles	**11(12)-EET, 12-HETE, 15-HETE, 5-HETE, Allantoin, Xanthine, 14(15)-EET, Arachidonic acid, Linoleic acid**	Human vitreous humor	LC-MS and LCMS/MS (MRM)	(Paris *et al.*, 2016; J. Xia *et al.*, 2014; Schwartzman *et al.*, 2010)
	Furanone	**Ascorbic acid**	Human vitreous humor	1H-NMR	(Barba *et al.*, 2010)
	Hydroxy acid, Methionine derivatives	**2-Deoxyribonic acid, 3,4-Dihydroxybutyric acid, 3-Hydroxybutyric acid, Ribose, Adenosine, Methionine, Galactitol**	Human plasma	GC-MS, LC-MS and LCMS/MS (MRM)	(L. Chen *et al.*, 2016; Paris *et al.*, 2016; X. Li *et al.*, 2011)
	Purines and Pyrimidine derivatives	**Inosine, Hypoxanthine, Cytosine, Cytidine, Thymidine**	Human plasma	LC-MS and LCMS/MS (MRM)	(J. Xia *et al.*, 2014; J. F. Xia *et al.*, 2011)
	Sugar acids and derivatives	**Gluconic acid, Erythritol**	Human plasma	GC-MS	(L. Chen *et al.*, 2016)
Dry eye	Amino acid	**Butyrylcarnitine/isobutyrylcarnitine, Glutamic acid, Glutamine, Leucine, N-acetylglutamine, Phenylalanine, Isovalerylcarnitine, Phenylalanine, Tryptophan, Tyrosine, Valine, Methionine**	Human conjunctival epithelial cells	LC-MS/MS (DDA)	(Barba *et al.*, 2010)
	Energy	**Pantothenic acid, Glutamic acid,**	Human conjunctival epithelial cells	1H-NMR	(Barba *et al.*, 2010)
		N-acetylglucosamine, Cis-aconitic acid	Human reflex tears	LC-MS/MS (DDA)	(Karamichos *et al.*, 2015; Galbis-Estrada *et al.*, 2014)

Disease	Biochemical Group	Metabolite	Sample	Analytical Platform	References
		Carnitine, Phosphocholine, Glutaminyl-leucine, Glycerophosphocholine	Human conjunctival epithelial cells	LC-MS/MS (DDA)	(Barba *et al.*, 2010)
	Cholines	**Cholines**	Human reflex tears	1H-NMR	(Galbis-Estrada *et al.*, 2014)
	Imidazoles	**Xanthine**	Human conjunctival cell line	LC-MS/MS (DDA)	(Barba *et al.*, 2010)
	Pyridines and derivatives	**Niacinamide (nicotinamide), UDP-N-acetylglucosamine**	Human conjunctival epithelial cells	LC-MS/MS (DDA)	(Barba *et al.*, 2010)
	Acyl carnitines	**Palmitoylcarnitine**	Human Plasma/MOUSE	LC-MS	(Edwards *et al.*, 2014)
	Amino acids and derivatives	**Alanine**	Rat aqueous humor	1H-NMR	(Mayordomo-Febrer *et al.*, 2015)
		Asymmetric dimethylarginine (ADMA), Symmetric dimethylarginine (SDMA)	Human Serum	LC-MS/MS	(Javadiyan *et al.*, 2012)
	Sphingolipid	**Sphinganine (C17), Sphingosine-1-phosphate (C19**	Human plasma	LC-MS	(Burgess *et al.*, 2015)
Keratoconus	Amino acids and derivatives	**Ornithine**	Human tear fluid	LC-MS/MS (MRM)	(Karamichos *et al.*, 2015)
	Fatty acyls	**Malonyl-coA**	Human tear fluid	LC-MS/MS (MRM)	(Karamichos *et al.*, 2015)
	Sugar acids and derivatives	**1,3-Bisphosphoglyceric acid**	Human tear fluid	LC-MS/MS (MRM)	(Karamichos *et al.*, 2015)
Non-Arteritic Anterior Ischemic	Acyl carnitines	**Palmitoylcarnitine**	Human plasma	LC-MS and LCMS/MS	(Andrade *et al.*, 2015)
	Fatty acyls	**Octadecanoic acid, Sphinganine (C17)**	Human plasma	LC-MS and LCMS/MS	(Andrade *et al.*, 2015)

Disease	Biochemical Group	Metabolite	Sample	Analytical Platform	References
Optic Neuropathy	Indoles	**Indoleacrylic acid**	Human plasma	LC-MS and LCMS/MS	(Andrade *et al.*, 2015)
PVR	Amino acid and Alkyl-phenylketones	**5-Hydroxykynurenamine, Isoglutamine, Tryptophan, Allantoic acid, Creatine, Phenylalanine, Threonic acid Creatinine**	Human vitreous humor	LC-MS	(M. Li *et al.*, 2014)
	Carboxylic acids and Derivatives	**Glucoronolactone, Homoisocitric acid, Succinic acid**	Human vitreous humor	LC-MS	
	Fatty acid	**3-Ethylmalic acid, Linelaidic acid**	Human vitreous humor	LC-MS	
	Energy	**Ascorbic acid, Phenylpyruvic acid**	Human vitreous humor	LC-MS	
	Purines and derivatives	**Hypoxanthine, Uric acid, Inosine**	Human vitreous humor	LC-MS	
RRD	Alkyl-phenylketones	**5-Hydroxykynurenamine**	Human vitreous humor	LC-MS	
	Amino acids and derivatives	**3-Methylhistidine, Allantoic acid, Creatine, Isoglutamine, Tryptophan, Valine, Phenylalanine**	Human vitreous humor	LC-MS	(M. Li *et al.*, 2014)
	Carboxylic acids and derivatives	**Citric acid, Glucoronolactone, Homoisocitric acid, Succinic acid, Citric acid**	Human vitreous humor	LC-MS	
	Carnitines	**Carnitine**	Human vitreous humor	LC-MS	
	Fatty acyls	**3-Ethylmalic acid, Linelaidic acid**	Human vitreous humor	LC-MS	
	Keto acids and derivatives	**2-Oxoglutaric acid, Ascorbic acid**	Human vitreous humor	LC-MS	
	Purines and derivatives	**Hypoxanthine, Uric acid, Inosine**	Human vitreous humor	LC-MS	
	Sugar acids and	**Glyceric acid, Threonic acid**	Human vitreous humor	LC-MS	
RRDCD*	Acyl carnitines	**Acetylcarnitine**	Human vitreous	LC-MS	(Yu *et al.*, 2015)

Disease	Biochemical Group	Metabolite	Sample	Analytical Platform	References
			humor		
	Amino acids and derivatives	**Alanine, Creatine, Glutamine**	Human vitreous humor	LC-MS	
	Benzenoid and Carnitines	**2-Phenylacetamide, Hippuric acid, Phenylpyruvic acid, Carnitine, Choline**	Human vitreous humor	LC-MS	
	Fatty acyls	**Arachidonic acid, Linoleic acid, Glycerophosphocholine, Sphinganine (C18), Phytosphingosine**	Human vitreous humor	LC-MS	
	Hydroxy acid and	**2-Hydroxyglutaric acid**	Human vitreous humor	LC-MS	
	Imidazoles	**Allantoin**	Human vitreous humor	LC-MS	
	Purines and derivatives	**Uric acid, Urea**	Human vitreous humor	LC-MS	
	Sugar acids and Ureas derivatives	**Threonic acid,**	Human vitreous humor	LC-MS	
ROP	Amino acids and derivatives	**Glycine, malonyl carnitine**	Blood	LC-MS	(Yang *et al.*, 2020)
ROP	Carbohydrates and carbohydrate conjugates	**Trehalose**	Plasma	LC-MS	(Zhou *et al.*, 2020)
	Bile acids, alcohols and derivatives	**Glycochenodeoxycholate, Pantothenate**		LC-MS	
	Purine nucleosides	**Adenosine**		LC-MS	
	Amino acids, peptides, and analogues	**Betaine, L-Glutamate, N6, N6, N6-Trimethyl-L-lysine, L-Glutamine, D-Proline, 1-Aminocyclopropanecarboxylic acid, L-Indole-3-lactic acid, L-Tryptophan, L-Methionine, L-Pyroglutamic acid, 4-**		LC-MS	

Disease	Biochemical Group	Metabolite	Sample	Analytical Platform	References
		Guanidinobutyric acid, L-Lysine, L-Citrulline, Cysteine-S-sulfate, Hypoxanthine, L-Tyrosine, L-Tryptophan,			
	Lipids and lipid-like molecules	**Taurocholate, Glycochenodeoxycholate, trans-Vaccenic acid, Linoleic acid, cis-9-Palmitoleic acid, Citramalic acid, D-Mannitol, all cis-(6,9,12)-Linolenic acid, Dodecanoic acid, Sphingomyelin, PC (16:0/16:0), Myristic acid, Cortisone acetate, Palmitic acid, Linoleic acid, Glycocholic acid**		LC-MS	

Note: Red color-Unregulated; Green color-Down regulated

4.1.2.7. Metabolome studies in human ROP cases

Till date, three studies have been performed on metabolomic profiling for ROP: one in OIR-rat and two in ROP probands using systemic fluids (blood and plasma). The functional evaluation of the key metabolites identified from blood samples in ROP has not been performed yet. Zhou *et al* studied altered metabolism in ROP and identified several important pathways such as central carbon metabolism protein, digestion, absorption, aminoacyl-tRNA synthesis and ABC transporters (Zhou *et al.*, 2020). Recently, Yang *et al.* performed a targeted screening of metabolite changes in blood samples using the LC-MS and found higher levels of glycine, glutamate, serine, leucine, piperidine, tryptophan, valine, citruline, malonyl carnitine (C3DC) and homocysteine malonyl carnitine (C3DC) in ROP infants as compared to no ROP preterm infants(Yang *et al.*, 2020). Most of these metabolites generated by glycolytic flux, leads to lower nitric oxide production and vascular endothelial growth factor (VEGF) that eventually affects choroidal neovascularization. These studies have a major limitation of using non-ocular fluids and a targeted screening for the metabolites that might have ignored other significant interacting processes and pathways in ROP. Therefore, to address these limitations, the present study aimed to carry out a global metabolomics profiling (untargeted approach) in vitreous humor specimens from ROP patients.

Specific objectives of the study are;

- Global metabolomic profiling of vitreous from ROP and no-ROP subjects with maximum number of metabolites identification by LC-MS and MS/MS
- To identify the key metabolic pathways involved in ROP progression

Methods

4.2.1: Metabolomics

4.2.1.1. Enrolment of study participants

Vitreous samples were collected from preterm infants (gestational age less than 35 weeks and birth weight less than 1700 grams) with stage 4 and 5 ROP at the time of vitrectomy and immediately transferred to fresh sterile cryovials. Since many metabolites are labile, the samples were very carefully collected in cold and sterile conditions and processed immediately for metabolite extractions after removing any cellular debris by a short spin (maximum speed for five minutes). The metabolites in methanol were promptly snap-frozen in LN2 and stored till next use. All the clinical parameters of patients and controls were recorded in a predesigned proforma. All the babies enrolled in this study had a mean fasting time for 5 hrs before vitrectomy procedure. The samples were normalized for age and gender and their time of collection (Table 43)

Table 43. Demographical details of participants

Clinical features	(Mean±SD)	
	Cases	Controls
Number of samples	15	15
Age (months)	3.83 + 1.090	3.41 + 1.66
Gestational age (weeks)	33.7 + 2.99	37.53 + 2.09
Gender (Male=M, Female=F)	M=7, F=8	M=9, F=6
Weight at birth (grams)	1.28 + 0.23	2.44 + 0.53
Country/State/City	South India	

4.2.2: Sample collection for methanol extracts

The vitreous samples were collected in sterile cryovials and quickly transferred to the laboratory on ice. Centrifugation was done at 14,000g speed for 5 minutes at 4°C to eliminate all cellular debris. 800µl of ice-cold methanol was mixed with 200µl of vitreous sample. The

vitreous-methanol extracts were vortexed and centrifuged for 10 minutes at 4° C at a speed of 9,838g. The methanol extract (upper layer) was lyophilized and then immediately stored appropriately at -80°degree freezer.

4.2.3. Global liquid chromatography–mass spectrometry (LC-MS)

The vitreous specimen was reconstituted in 20µl of the solvent mixture water: acetonitrile (95:5) with 0.1 percent formic acid (FA) (Patnaik *et al.*, 2019). Furthermore, 8µl of methanol extracts were injected into the Zorbax C18 column. (Phenomenex- Kinetex, C18, 250 x 4.6mm, 5 µm). LC1200 system coupled to Q-TOF, mass spectrophotometer (Agilent 6520 LC; ESI-QTOF, USA) was used for separating ions. All samples were run in a positive (basic and neutral metabolites) ESI mode with a mass scan range of 40–1700 M/Z and a scan rate of 1.4 spectra/sec at a 0.4mL/min flow rate. (Ion source parameters are provided in Annexure IV). The overall workflow of LC-MS/MS is given in the flow chart (Figure 89)

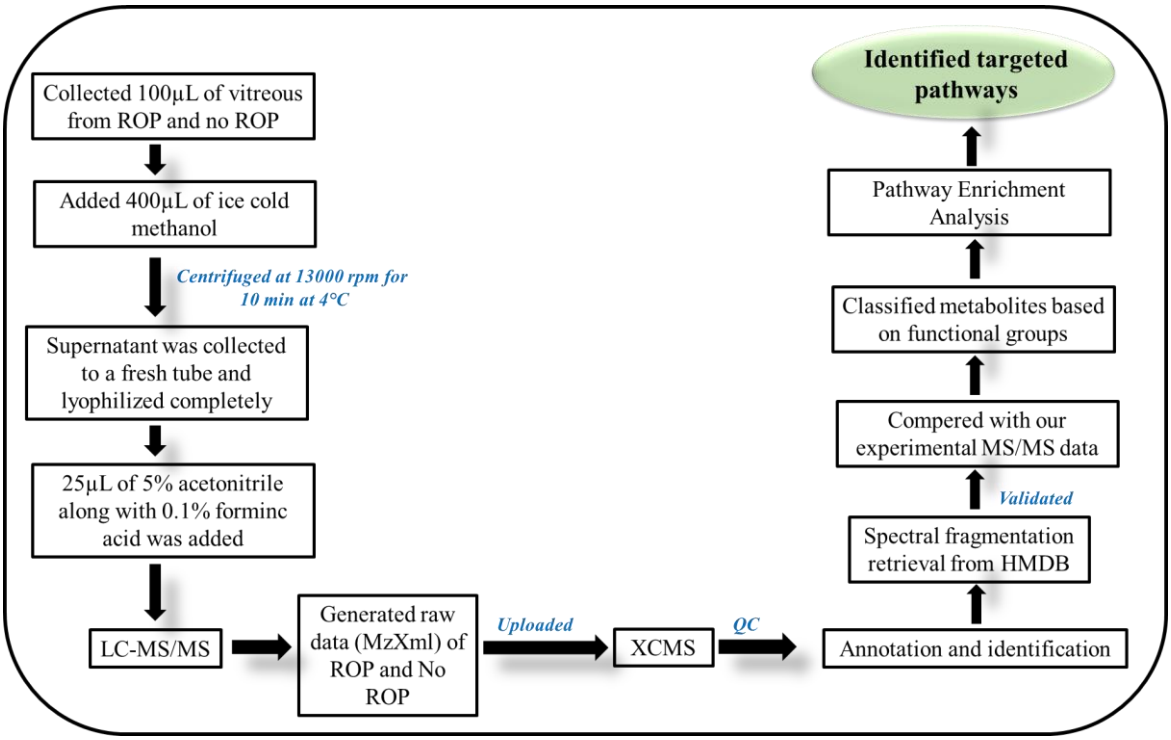

Figure 89. Overall work flow for LC-MS/MS and data analysis

4.2.4. Data analysis

The global metabolite data output was checked for the quality and its correlation with disease phenotype was assessed using different approaches using freely available online softwares. First step in the analysis was to export the data based on M/Z ratio for individual samples into mzXML and CSV format. A step-by-step analysis flow is explained below:

4.2.4.1. Metlin-XCMS

XCMS is freely available cloud-based platform for metabolomics data analysis (https://xcmsonline.scripps.edu) and was used in the present study for untargeted metabolomics profiling. It contains the web-based R package for data processing, which integrates the metabolite feature annotation and metabolite identification with graphical data representation. First step in the data analysis was to import the data (cases and controls files) in the mzXML format into the server. Once analysis was completed, the data in the form of retention time, heat map and enriched pathways was generated.

The Metlin database is used to identify both known and undiscovered metabolites. This database has a collection of over 1 million features including the lipids, amino acids, small peptides, carbohydrates and other classes of small molecules. Targets were searched by the feature of M/Z that allowed to search small molecules with a defined mass tolerance of 15.

4.2.4.2. Upload preparation and analysis

Before starting analysis, the data files were exported into the MzXML format. These were then uploaded in separate data sets for cases and controls groups for a pairwise alignment. Further, the data corresponding annotated metabolites, classes and subclasses was exported in separate spreadsheet. Quality checks were performed for the data obtained prior to further analysis. All the metabolites that could not be annotated and those derived from plant or drug

sources were excluded from subsequent analysis. Only metabolites that showed good consistency were included for the next differential expression analysis.

4.2.5. Pathway analysis

Metlin-XCMS tool was used to analyse differential expression among the ROP cases and control and for identifying the affected pathways. XCMS also generated all possible endogenous metabolites and list of important pathways and cloud plot of differentially expressed metabolites. The data was further subjected to principal component analysis and heat maps was generated for cases and control to identify unique metabolite signature for ROP.

4.2.6. MS/MS spectrum match

Further validation of significant and novel metabolites identified for ROP was done by performing the MS/MS spectral daughter ion fragmentation. Top 100 significantly dysregulated metabolites were validated by this approach. Metabolite daughter ion fragmentation pattern (M/Z values) (LC-MS/MS Spectrum - 40V, Positive mode) were retrieved from the HMDB based on their parent M/Z values and then matched with our experimental LC-MS/MS spectrum fragments to confirm the annotation of metabolites. Abundance values for each of the significant metabolites ($\geq$1.3 fold change) in the major pathways were then used to generate box plot and PCA plots to assess if these can clearly differentiate cases from controls.

4.3. Results

The present study, aimed to understand if dysfunctional metabolic flux in retina play a crucial role in the ROP pathogenesis. The overall strategy included performing global metabolites profiling from the vitreous humor samples and identifying key metabolic pathways involved in ROP pathogenesis and further validation of significant pathways and their metabolites by MS/MS fragmentation analysis.

4.3.1. Global metabolomic profiling

4.3.2. Quality assessment

The raw data obtained from MS analysis was analysed by using XCMS online tool to study the global metabolomic profiles for ROP. Before performing data analysis, the data quality was assessed by reviewing each sample's total ion chromatograms (TIC). TIC obtained for all the subjects were subjected to pairwise alignment after retention time correction. All the samples showed a good quality peak without any significant deviation; hence, all were included for subsequent analysis (Figure 90).

The total LC-MS chromatogram peak quality and consistency was compared across all the samples and triplicates. The LC curve plots for both cases and controls indicated notably different signatures of low molecular weight molecules in ROP.

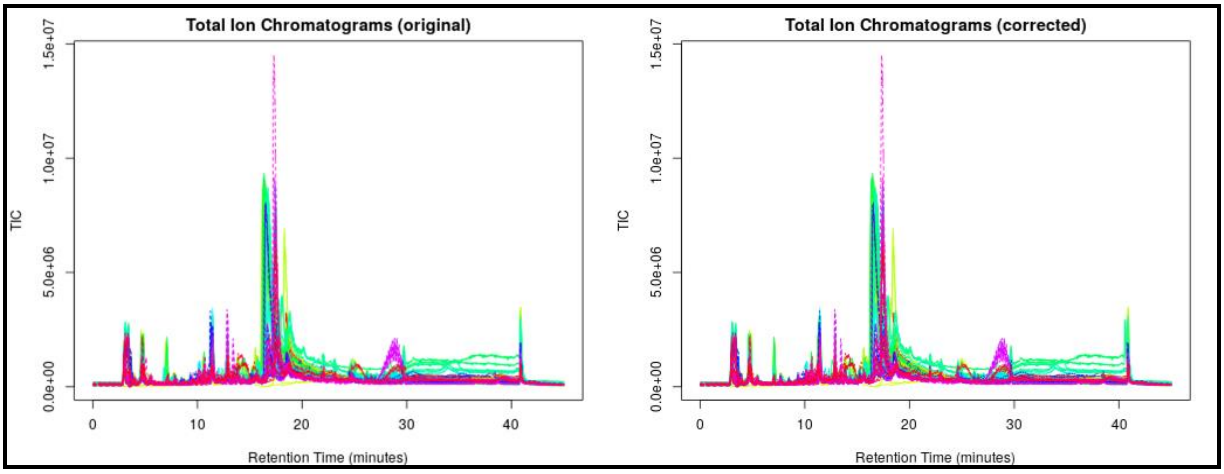

Figure 90. An overlay of total ion chromatograms acquired (TIC) for all samples is shown before (A) and after retention time correction (B)

Once the data for each of the samples passed the quality check, the M/Z values for metabolites/features were measured for assessing their consistency across cases and controls. Most of the features/compounds showed more than 80% consistency (shown in Figure 91). Thus, all features/compounds passed the quality check.

$$\frac{\text{Presence of metabolite in no. of samples}}{\text{Total no. of samples}} \times 100$$

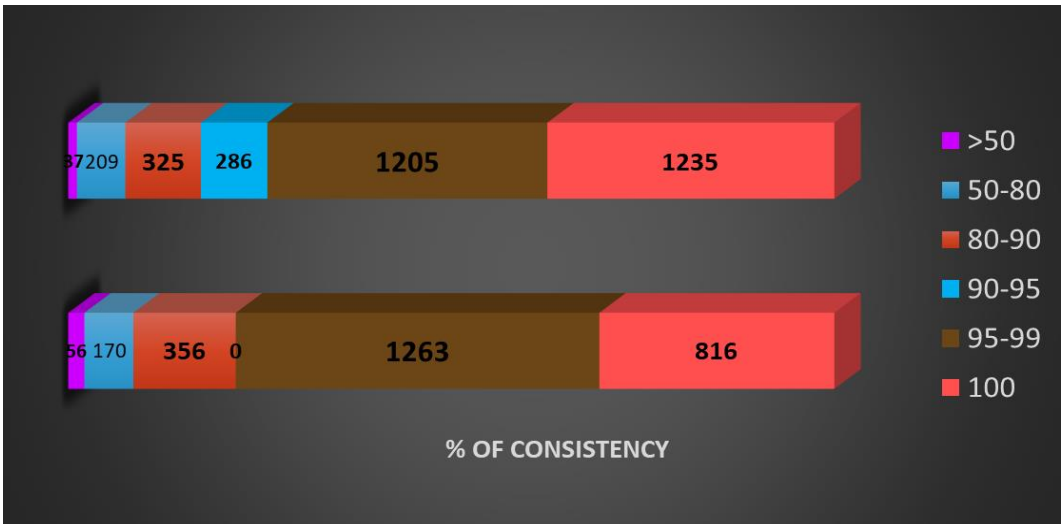

Figure 91. Percentage consistency of features in triplicates across cases and controls

4.3.3. ROP and no ROP group comparison by Interactive cloud plot

1549 (both annotated and unannotated) out of 3297 features were found to be significantly differential expressed with fold change of greater than 1.3 and *p*-value of 0.05 or less. Applying the error rate of less than 15PPM (parts per million) and excluding all drugs and plant derived metabolites, a total of 1445 features were annotated. An interactive cloud plot, also termed as a "mirror plot" showed features/metabolites with differential expression across cases and controls based on statistical parameters given input (*p-value* 0.01, fold change: 1.3). Down-regulated features are shown by red circles. Up-regulated features are depicted in green circles. Size of each circle corresponds to the (log) fold change of the relative intensity. Size of circles depicts increased fold change peaks; large circles represent greater fold changes. The colour shade represents the *p-value*, with brighter circles representing lower *p-values*. (Figure 92).

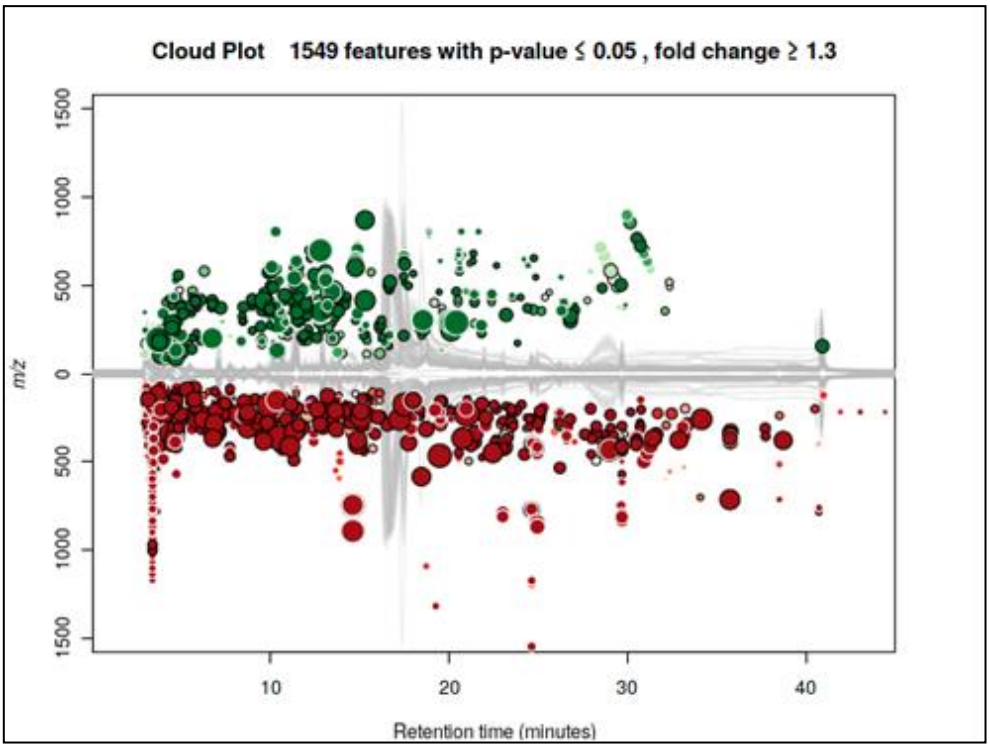

Figure 92. The cloud plot represents metabolites that are significantly down-regulated on the down side (dark red) of the volcano-axis and those that are up-regulated (green) on the up side of the axis, p-value of < 0.05 was for the analysis

4.3.4. Classification of metabolites

As a next step, the significantly differentially expressed metabolites among cases and controls were further classified based on chemical class and functional groups to study their possible involvement in disease pathogenesis. Maximum number of differentially expressed metabolites belonged to lipids and lipid-like molecules, followed by organ heterocyclic compounds, organic acids derivatives (Amino acids, peptides and analogues), benzenoids, organic oxygen compounds and others. The number of metabolites seen in each class has been shown in the Figure 93.

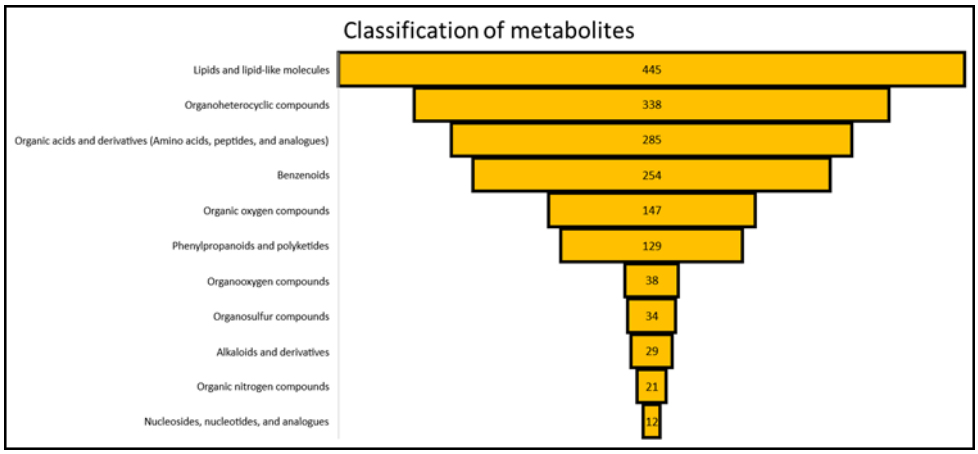

Figure 93. Categorization of differentially expressed metabolites according to chemical class and functional types along with the number of metabolites per class

4.3.5. Annotation of metabolites

Of the 3297 features observed, only 1445 Metlin IDs could be annotated by the XCMS METLIN tool. 1013 IDs belonging to the plant, drug and other non-human peptides sources were excluded from the data set. Further, the fold change and p-value of differentially expressed metabolites based on the abundance of features was calculated after excluding the inconsistent metabolites across triplicates. Heatmap generated using 520 significantly (fold change >1.3, p-value-0.05) dysregulated metabolites showed a distinct signature for ROP cases and controls and unique separate cluster on a PCA plot (Figure 94). These metabolites were further enriched for pathway analysis by MetaboAnalyst 5

(https://www.metaboanalyst.ca/MetaboAnalyst/ModuleView.xhtml). The detailed workflow for annotation of features and further analysis is shown in Figure 95.

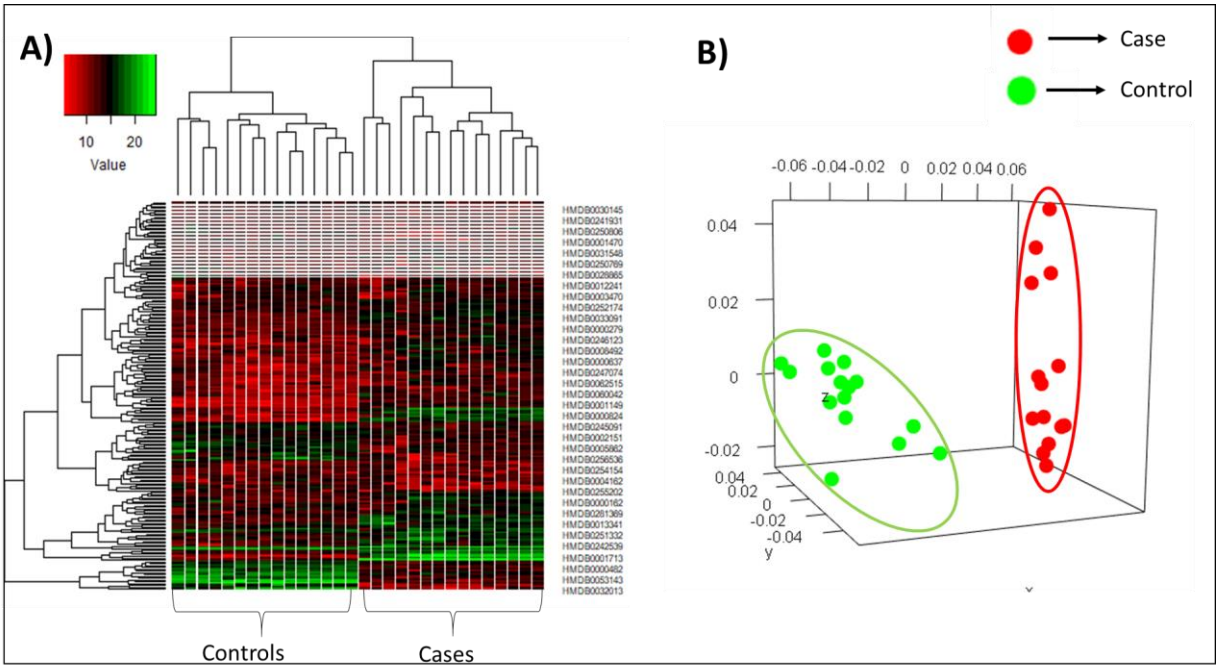

Figure 94. Heatmap A and PCA cluster plot B showed distinct signature and clusters for ROP and controls based on the abundance of significantly dysregulated metabolites

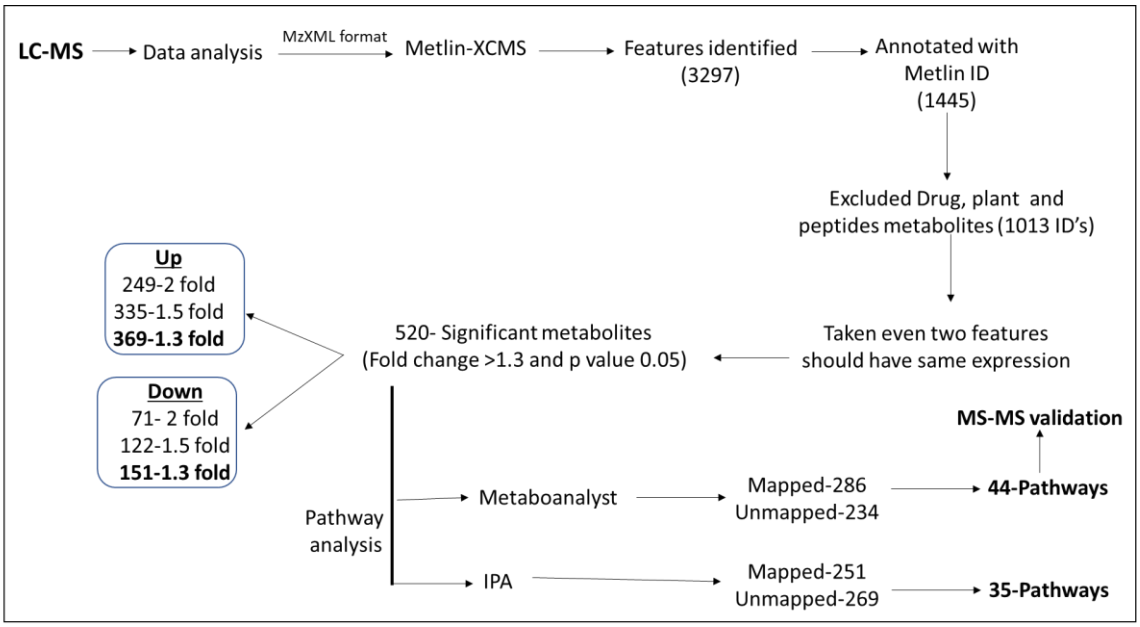

Figure 95. Detailed work flow for metabolites annotation and pathways-based enrichment analysis

4.3.6. Pathway enrichment analysis

Global metabolomic profiling of vitreous can provide the snapshot information of downstream effects of biological and metabolic processes in ROP infants. Pathway enrichment analysis was performed for 520 significantly dysregulated metabolites by using MetaboAnalyst. The significantly dysregulated metabolites identified in ROP vitreous were found to be associated with multiple pathways and their functional impact in disease pathogenesis is shown in the Figure 96. A detailed list of the pathways associated with ROP and number of significant metabolites from the present data set is provided in Table 44.

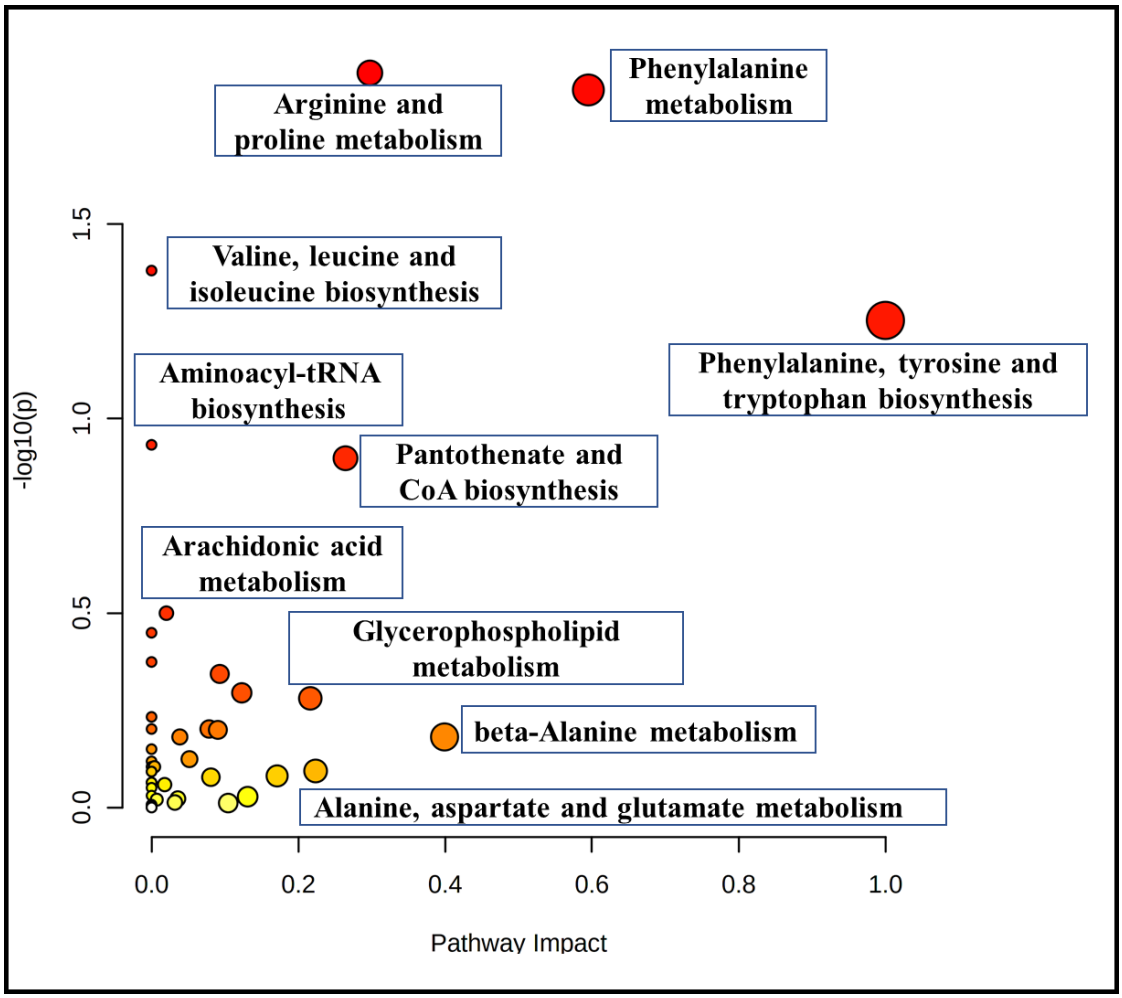

Figure 96. A summary of identified metabolic pathways and their potential impact with respect to disease pathogenesis; the node color is based on its p value and the node radius is determined based on their pathway impact values

Table 44. Pathways identified in ROP

S.No	Metabolisms	Total	Expected	Hits	Raw p	Minus LOG10(p)	Holm adjust	FDR	Impact
1	Arginine and proline metabolism	38	3.9471	9	0.012909	1.8891	1	0.59967	0.29751
2	Phenylalanine metabolism	10	1.0387	4	0.014278	1.8453	1	0.59967	0.59524
3	Valine, leucine and isoleucine biosynthesis	8	0.83097	3	0.041608	1.3808	1	1	0
4	Phenylalanine, tyrosine and tryptophan biosynthesis	4	0.41548	2	0.055896	1.2526	1	1	1
5	Aminoacyl-tRNA biosynthesis	48	4.9858	8	0.11678	0.93265	1	1	0
6	Pantothenate and CoA biosynthesis	19	1.9735	4	0.12643	0.89814	1	1	0.26428
7	Arachidonic acid metabolism	36	3.7394	5	0.31645	0.49969	1	1	0.02023
8	D-Arginine and D-ornithine metabolism	4	0.41548	1	0.3554	0.44928	1	1	0
9	Linoleic acid metabolism	5	0.51935	1	0.42253	0.37414	1	1	0
10	Glycine, serine and threonine metabolism	33	3.4277	4	0.45355	0.34337	1	1	0.09293
11	Histidine metabolism	16	1.6619	2	0.50726	0.29477	1	1	0.12295
12	Glycerophospholipid metabolism	36	3.7394	4	0.52409	0.2806	1	1	0.21631
13	Taurine and hypotaurine metabolism	8	0.83097	1	0.585	0.23285	1	1	0
14	Ubiquinone and other terpenoid-quinone biosynthesis	9	0.93484	1	0.62833	0.20181	1	1	0
15	Vitamin B6 metabolism	9	0.93484	1	0.62833	0.20181	1	1	0.07843
16	Citrate cycle (TCA cycle)	20	2.0774	2	0.63164	0.19953	1	1	0.09038
17	Sphingolipid metabolism	21	2.1813	2	0.65866	0.18134	1	1	0.03854
18	beta-Alanine metabolism	21	2.1813	2	0.65866	0.18134	1	1	0.39925

S.No	Metabolisms	Total	Expected	Hits	Raw p	Minus LOG10(p)	Holm adjust	FDR	Impact
19	Propanoate metabolism	23	2.389	2	0.70795	0.15	1	1	0
20	Lysine degradation	25	2.5968	2	0.75119	0.12425	1	1	0.05164
21	alpha-Linolenic acid metabolism	13	1.3503	1	0.76107	0.11857	1	1	0
22	Arginine biosynthesis	14	1.4542	1	0.7861	0.10452	1	1	0
23	Glycosylphosphatidylinositol (GPI)-anchor biosynthesis	14	1.4542	1	0.7861	0.10452	1	1	0.00399
24	Alanine, aspartate and glutamate metabolism	28	2.9084	2	0.80573	0.09381	1	1	0.22356
25	Butanoate metabolism	15	1.5581	1	0.80852	0.09231	1	1	0
26	Nicotinate and nicotinamide metabolism	15	1.5581	1	0.80852	0.09231	1	1	0
27	Tyrosine metabolism	42	4.3626	3	0.82961	0.081126	1	1	0.17109
28	Porphyrin and chlorophyll metabolism	30	3.1161	2	0.83596	0.077814	1	1	0.08087
29	Pentose and glucuronate interconversions	18	1.8697	1	0.8627	0.064139	1	1	0
30	Terpenoid backbone biosynthesis	18	1.8697	1	0.8627	0.064139	1	1	0
31	Primary bile acid biosynthesis	46	4.7781	3	0.87345	0.058763	1	1	0.01782
32	Fructose and mannose metabolism	20	2.0774	1	0.89005	0.050584	1	1	0
33	Valine, leucine and isoleucine degradation	40	4.1548	2	0.93236	0.030418	1	1	0
34	Tryptophan metabolism	41	4.2587	2	0.93828	0.027667	1	1	0.13094
35	Galactose metabolism	27	2.8045	1	0.9496	0.022461	1	1	0.03577
36	Glutathione metabolism	28	2.9084	1	0.95492	0.020031	1	1	0.00709
37	Glyoxylate and dicarboxylate metabolism	32	3.3239	1	0.97119	0.012695	1	1	0.03175

S.No	Metabolisms	Total	Expected	Hits	Raw p	Minus LOG10(p)	Holm adjust	FDR	Impact
38	Cysteine and methionine metabolism	33	3.4277	1	0.97425	0.011331	1	1	0.10446
39	Amino sugar and nucleotide sugar metabolism	37	3.8432	1	0.98357	0.007196	1	1	0
40	Pyrimidine metabolism	39	4.051	1	0.98688	0.0057359	1	1	0
41	Fatty acid biosynthesis	47	4.8819	1	0.99468	0.0023147	1	1	0
42	Drug metabolism - Cytochrome P450	55	5.7129	1	0.99786	0.00093148	1	1	0
43	Purine metabolism	65	6.7516	1	0.99932	0.00029677	1	1	0
44	Steroid hormone biosynthesis	85	8.829	1	0.99993	2.94E-05	1	1	6.00E-05

4.3.7. Validation of metabolites involved in enriched pathways

The vitreous metabolomic enrichment analysis for ROP showed approximately over 45 pathways to be involved in the disease pathogenesis. The significantly dysregulated metabolic pathways were categorized into amino acid, lipid and energy metabolisms (Figure 97). These 3 pathways are known to have a direct/indirect role in retinal inflammation and angiogenesis in the ROP eye.

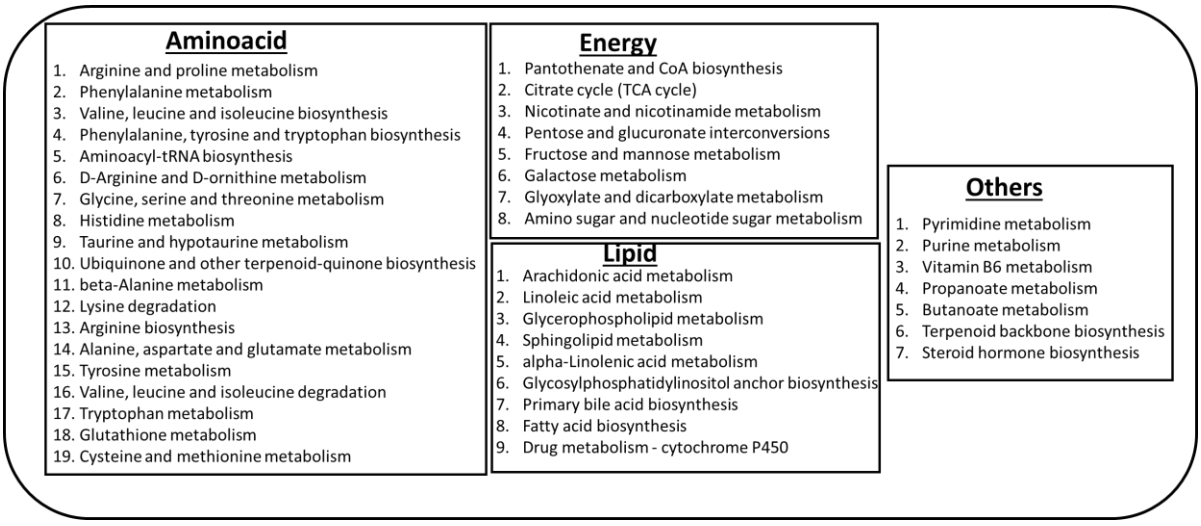

Figure 97. Categorization of identified metabolic pathways: Amino acid metabolism; Lipid metabolism; Bioenergetics metabolism

Next, the pathway enriched metabolites were used for MS-MS fragmentation analysis. The daughter ion fragmentation pattern (M/Z values) (LC-MS/MS 40V, Positive mode) for significant metabolites were retrieved from the HMDB based on their parent M/Z values as a reference. The fragmentation pattern for each of the test metabolite was obtained from HMDB MS/MS spectral fragmentation library and then matched with our experimental LC-MS/MS spectrum fragments to confirm the annotation of metabolites.

4.3.7.1. Amino acid metabolism

Amino acid metabolism plays a vital role in the neuronal retina. In vitreous humor of ROP patients, all pathways involved in amino acid metabolism were upregulated. Differential expression of amino acid metabolites showed clearly distinct pattern for patients and controls

as shown in heatmap (below Figure 98) while PCA plot showed that the significant metabolites in these pathways could clearly differentiate patients from controls as seen by two separate clusters for patients and controls.

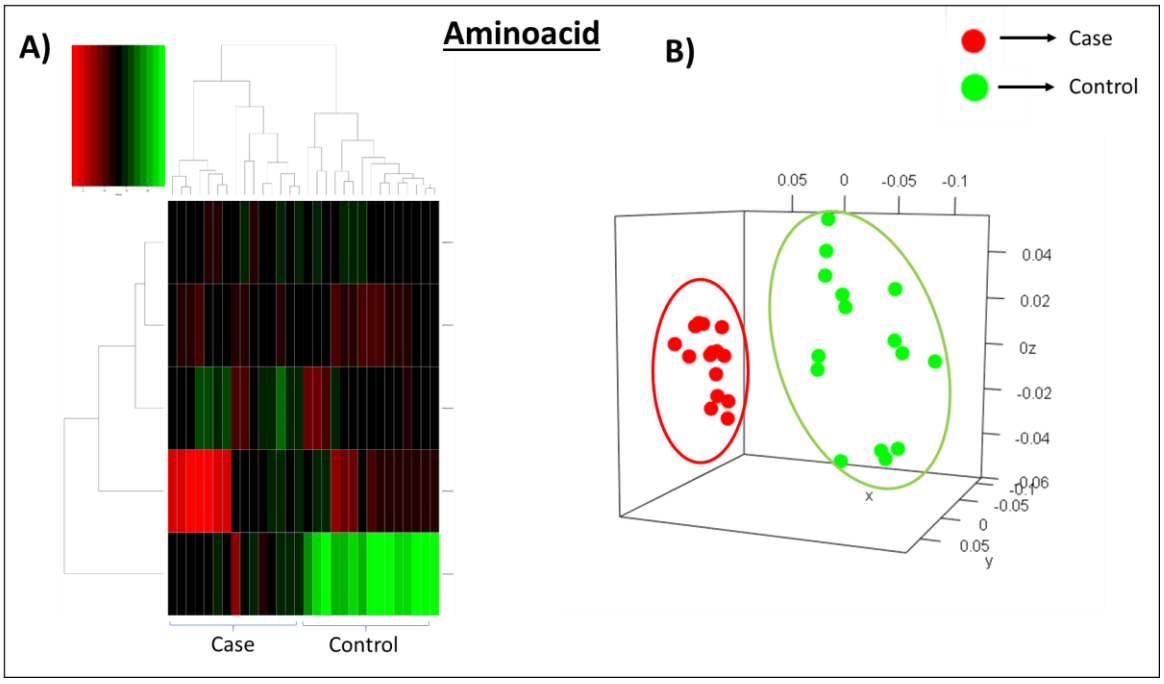

Figure 98. Amino acid metabolism: Heatmap (A) and PCA analysis plot (B) generated for significantly dysregulated metabolites based on their abundance in ROP as compared to control vitreous

4.3.7.1.1. Validation of the metabolic pathway:

The significantly deregulated metabolites and their respective amino acid pathways as shown in the Figure below (Figure 99) confirmed their role in the altered metabolic activity and ROP pathogenesis. Further, these metabolites expression was validated and quantified by comparing the abundance of each metabolite. The box plot for each of the differentially expressed metabolites showed their upregulation in ROP in Figure 100. Some of these metabolites selected randomly were further validated by checking their MS/MS fragmentation pattern (Table 45).

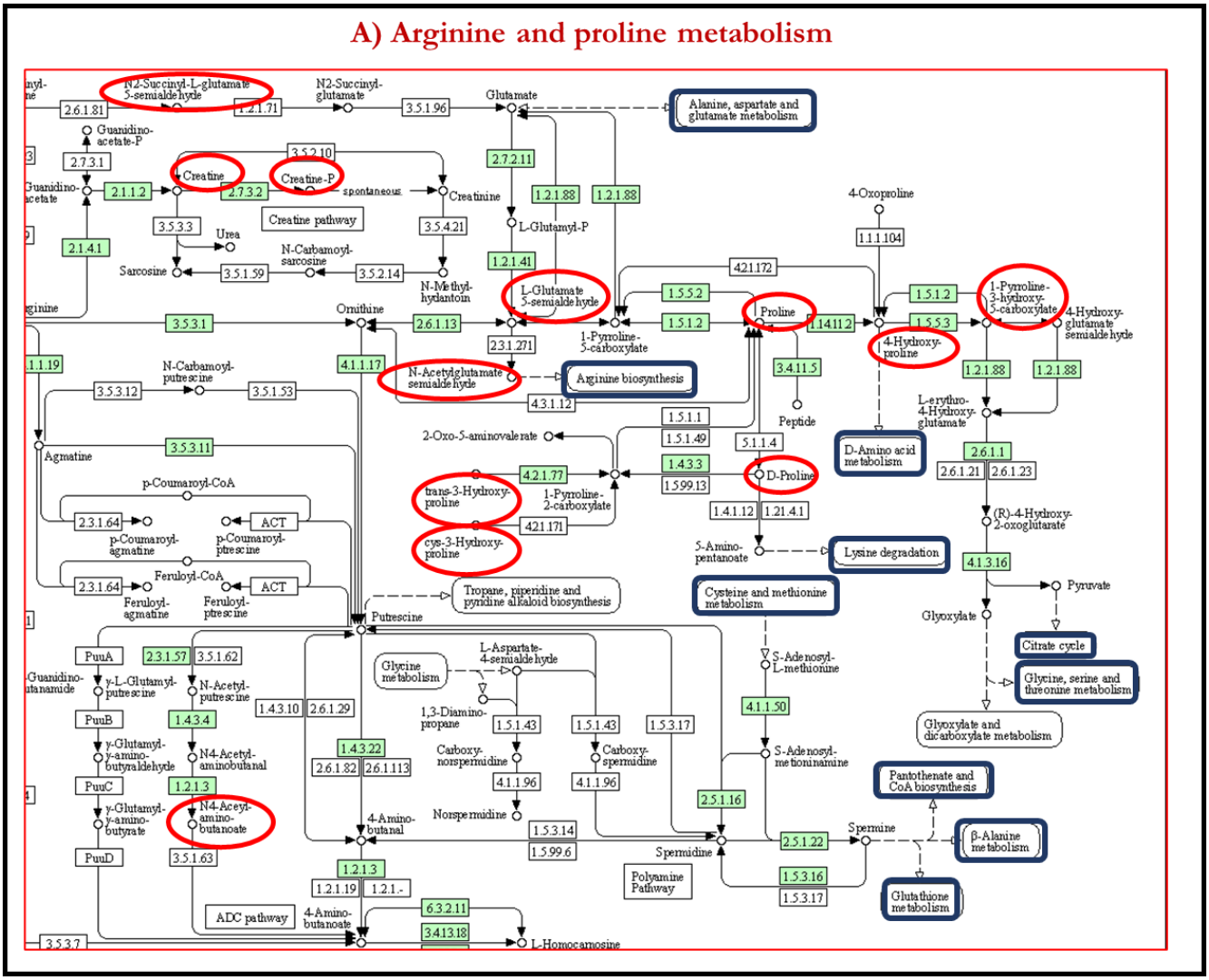
A) Arginine and proline metabolism
N2-Succinyl-L-glutamate 5-semialdehyde
N2-Succinyl-glutamate
Glutamate
Alanine, aspartate and glutamate metabolism
Guanidino-acetate-P
Creatine
Creatine-P
spontaneous
Creatinine
Creatine pathway
Urea
Sarcosine
N-Carbamoyl-sarcosine
N-Methyl-hydantoin
L-Glutamyl-P
L-Glutamate 5-semialdehyde
4-Oxoproline
Ornithine
Proline
1-Pyrroline-5-carboxylate
4-Hydroxy-proline
1-Pyrroline-3-hydroxy-5-carboxylate
4-Hydroxy-glutamate semialdehyde
N-Carbamoyl-putrescine
N-Acetylglutamate semialdehyde
Arginine biosynthesis
Peptide
D-Amino acid metabolism
L-erythro-4-Hydroxy-glutamate
Agmatine
2-Oxo-5-aminovalerate
D-Proline
trans-3-Hydroxy-proline
cys-3-Hydroxy-proline
1-Pyrroline-2-carboxylate
(R)-4-Hydroxy-2-oxoglutarate
p-Coumaroyl-CoA
p-Coumaroyl-agmatine
p-Coumaroyl-ptrescine
ACT
Feruloyl-CoA
Feruloyl-agmatine
Feruloyl-ptrescine
5-Amino-pentanoate
Lysine degradation
Tropane, piperidine and pyridine alkaloid biosynthesis
Cysteine and methionine metabolism
Pyruvate
Glyoxylate
Citrate cycle
Glycine, serine and threonine metabolism
Putrescine
PuuA
PuuB
PuuC
PuuD
γ-L-Glutamyl-putrescine
N-Acetyl-putrescine
γ-Glutamyl-γ-amino-butyraldehyde
N4-Acetyl-aminobutanal
γ-Glutamyl-γ-amino-butyrate
N4-Acetyl-amino-butanoate
Guanidino-butanamide
Glycine metabolism
L-Aspartate-4-semialdehyde
1,3-Diamino-propane
Carboxy-norspermidine
Carboxy-spermidine
Norspermidine
4-Amino-butanal
S-Adenosyl-L-methionine
S-Adenosyl-methioninamine
Glyoxylate and dicarboxylate metabolism
Pantothenate and CoA biosynthesis
Spermine
Spermidine
β-Alanine metabolism
Polyamine Pathway
Glutathione metabolism
ADC pathway
4-Amino-butanoate
L-Homocarnosine

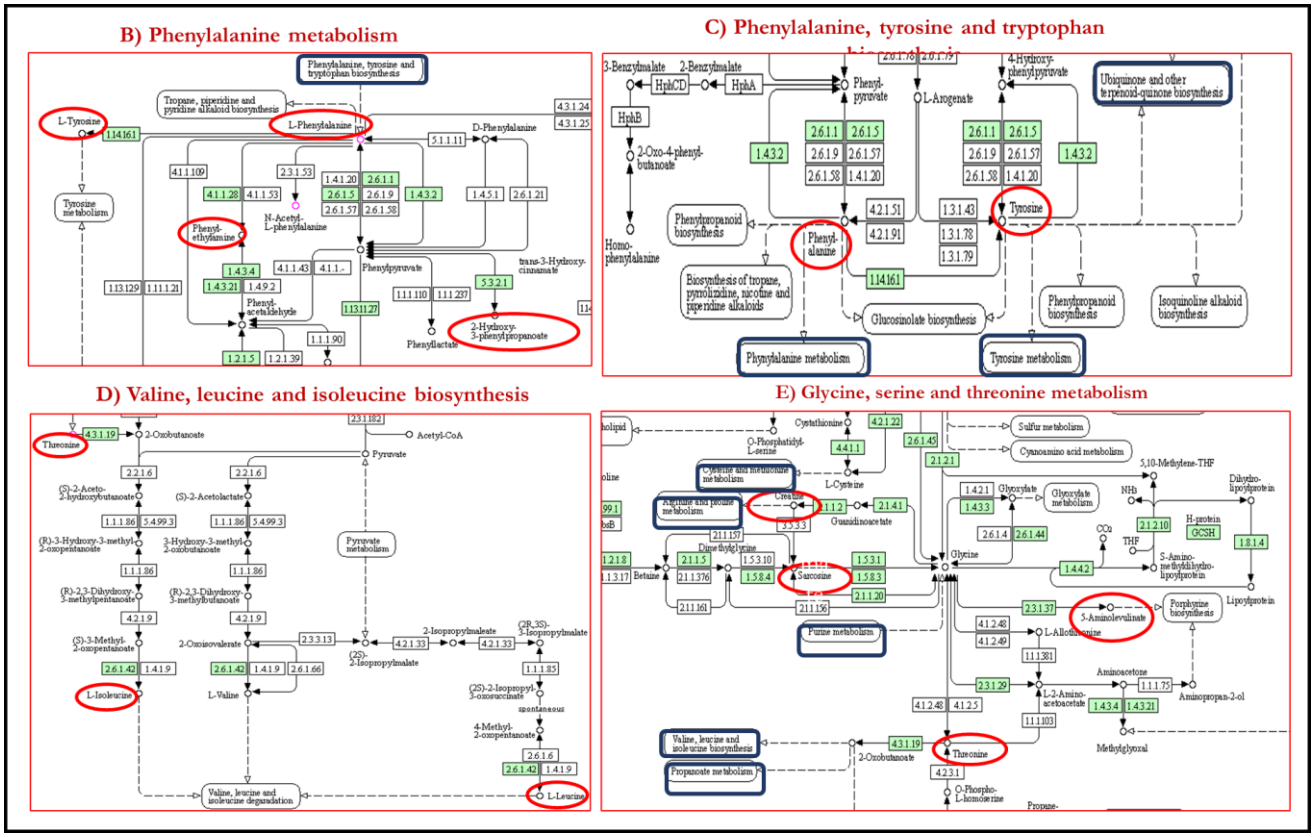
B) Phenylalanine metabolism
C) Phenylalanine, tyrosine and tryptophan
D) Valine, leucine and isoleucine biosynthesis
E) Glycine, serine and threonine metabolism

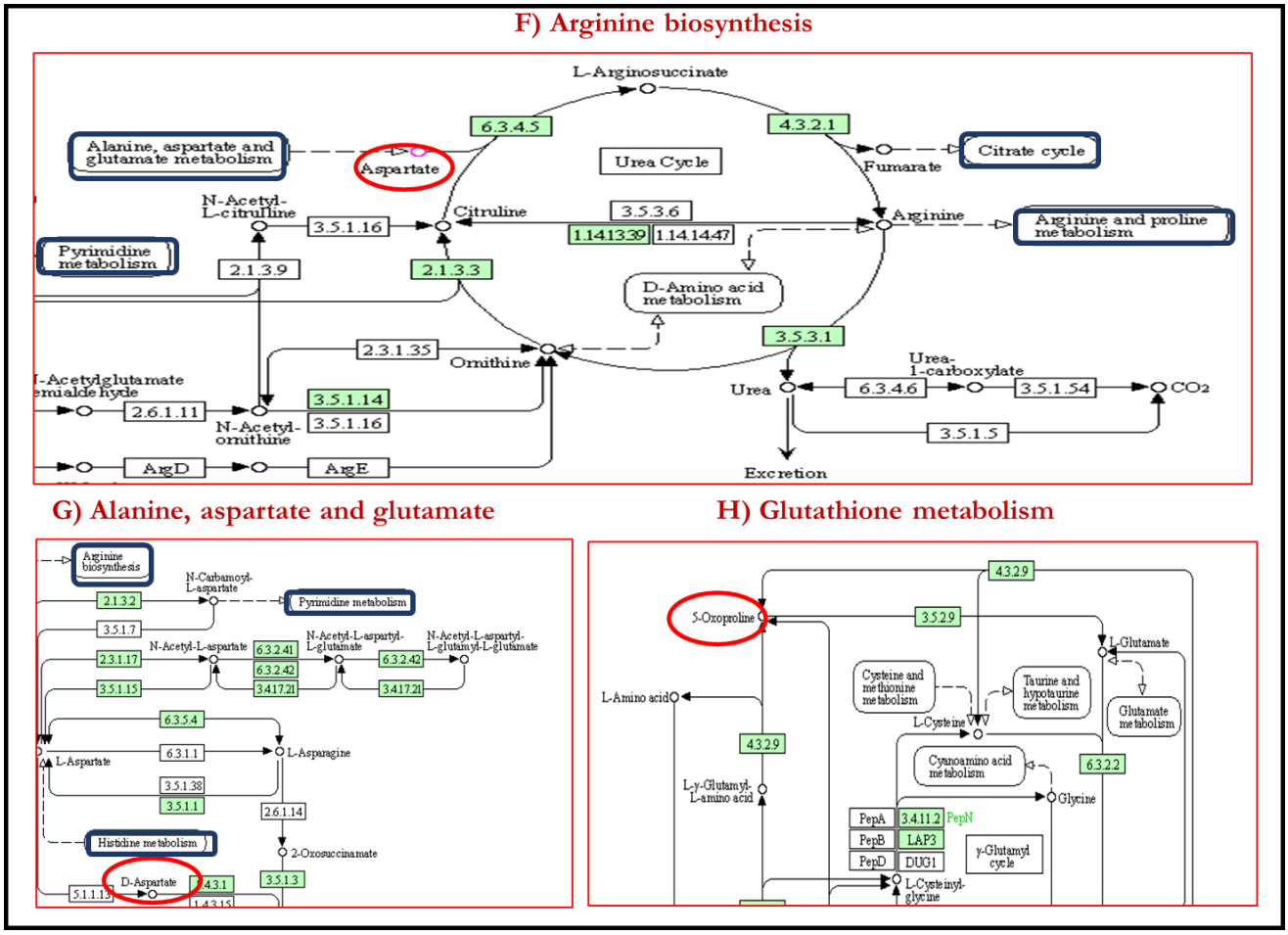
F) Arginine biosynthesis
G) Alanine, aspartate and glutamate
H) Glutathione metabolism

I) Tyrosine metabolism

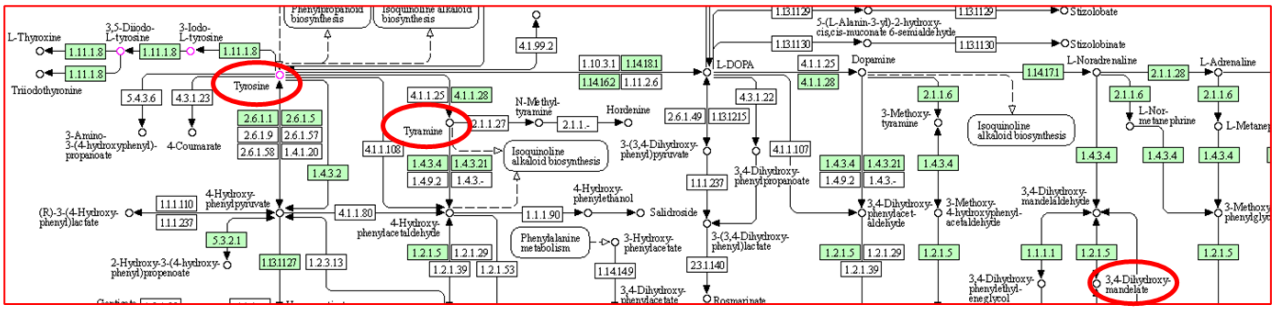

J) Valine, leucine and isoleucine degradation

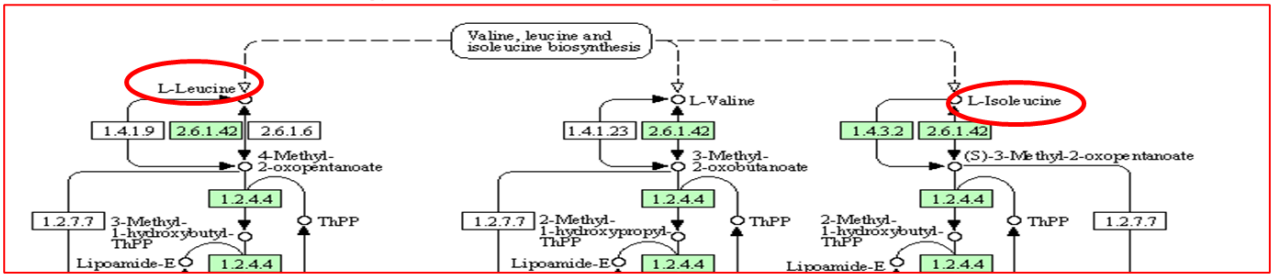

K) Tryptophan metabolism

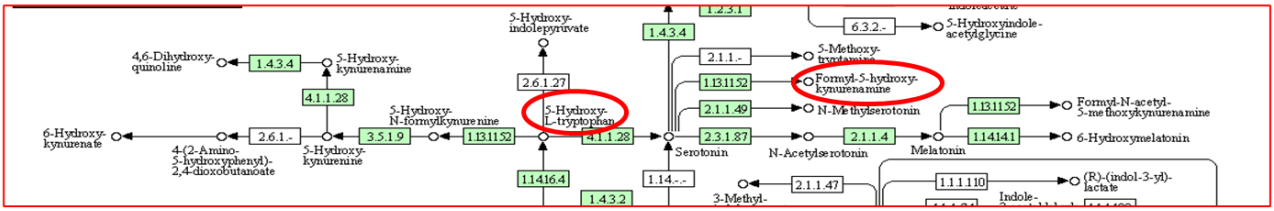

L) Cysteine and methionine metabolism

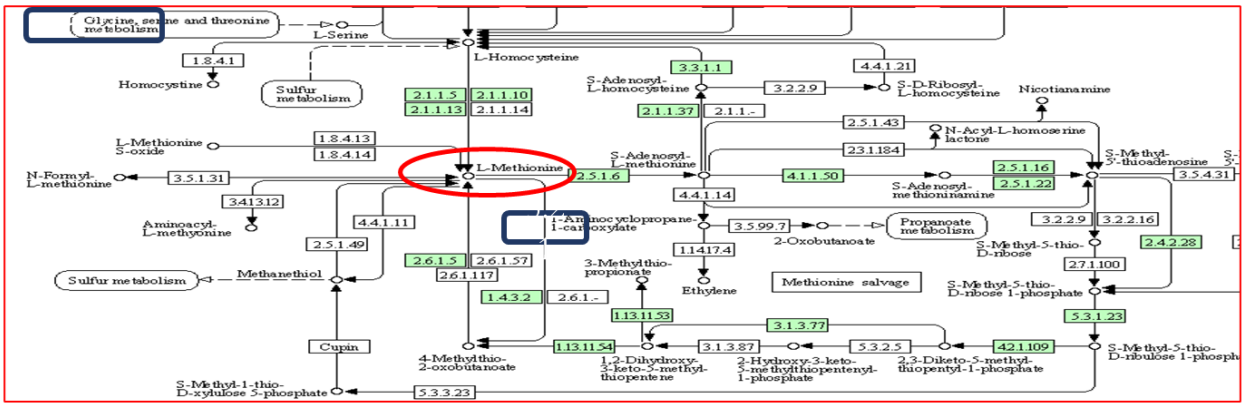

M) Pantothenate and CoA biosynthesis

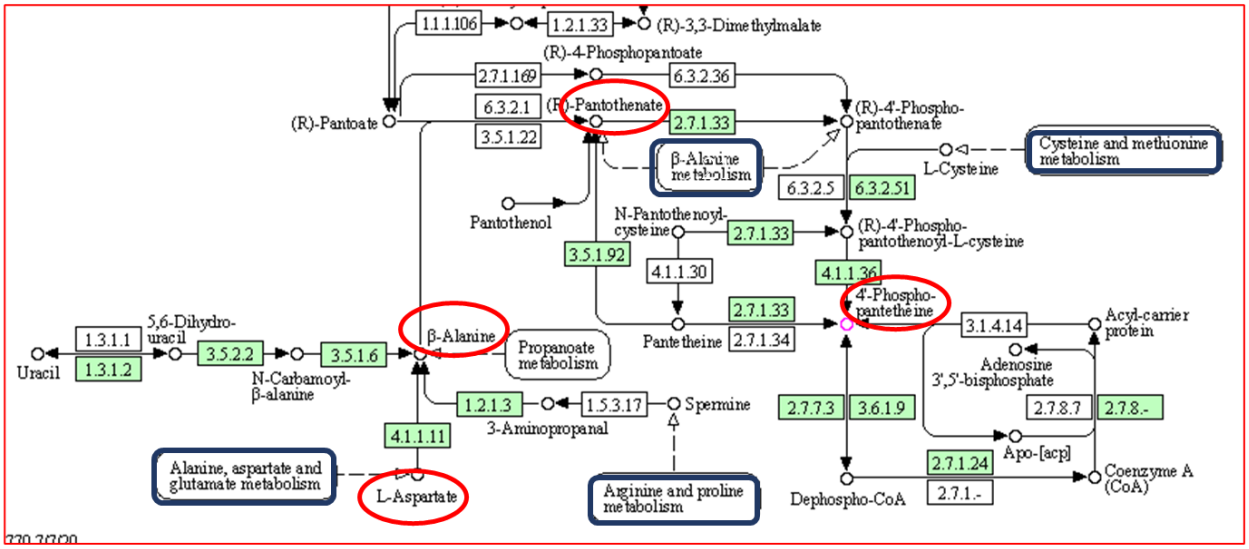

N) Aminoacyl-tRNA biosynthesis

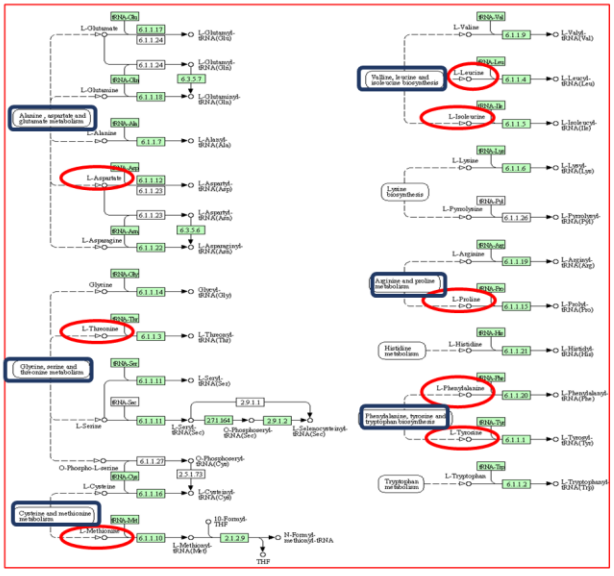

O) Lysine degradation

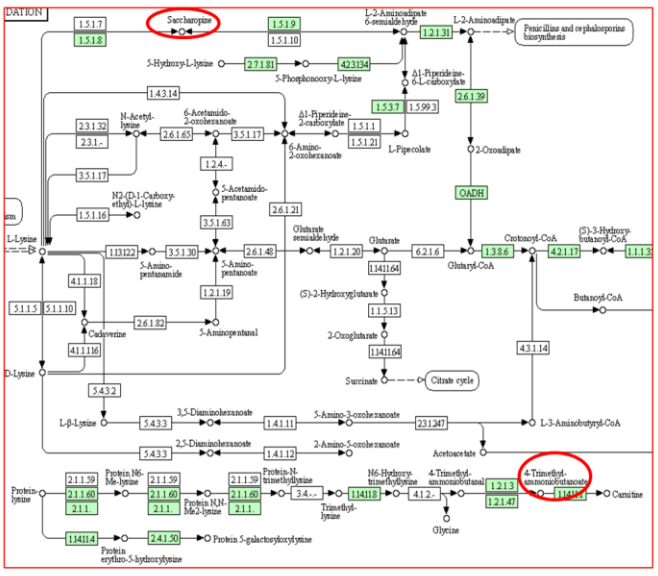

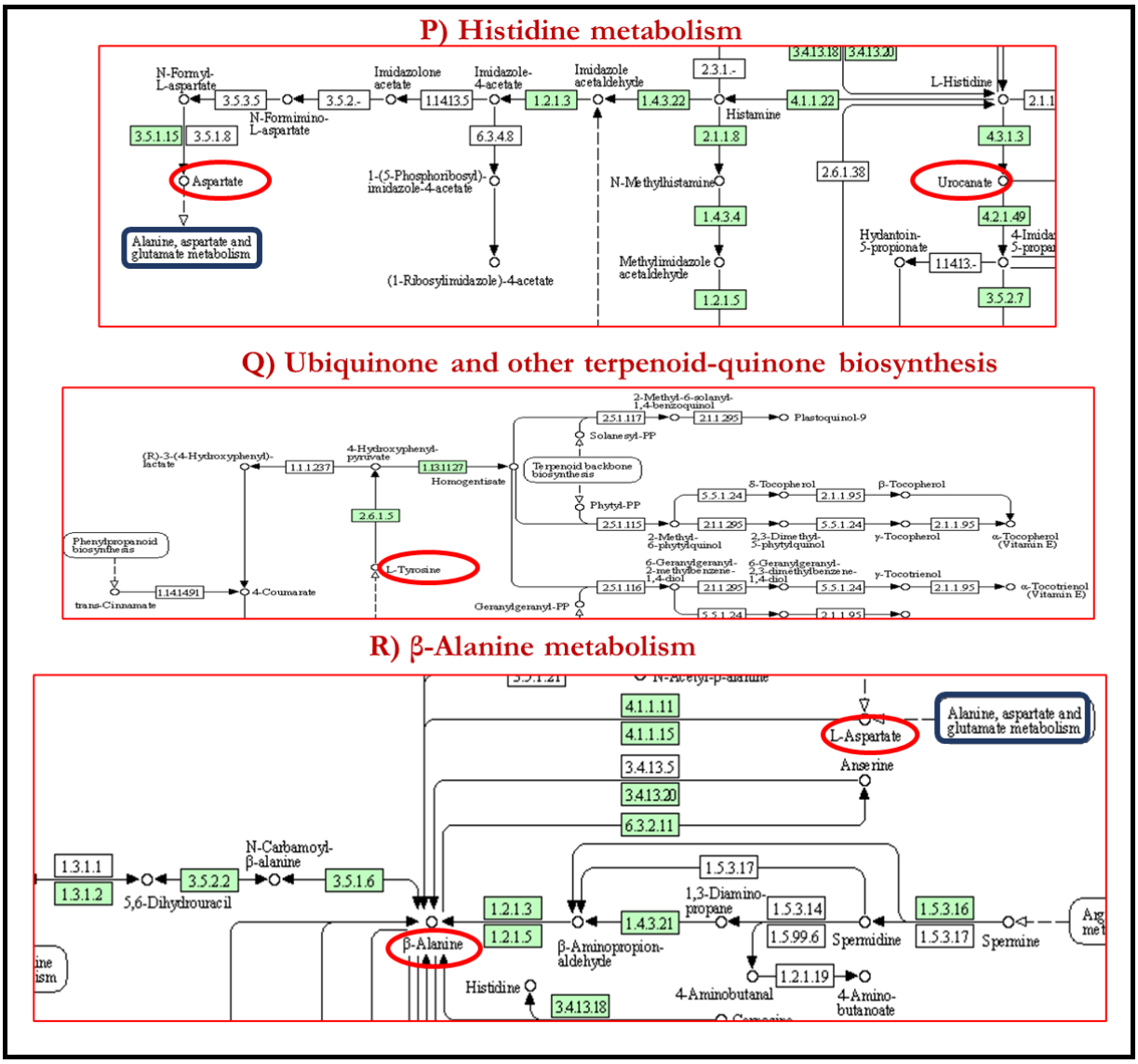

Figure 99. Schematic representation of amino acid metabolic pathways and significant metabolites identified from the present study. The red color circle represents the significantly upregulated metabolite, and the blue colored box denotes associated metabolism.

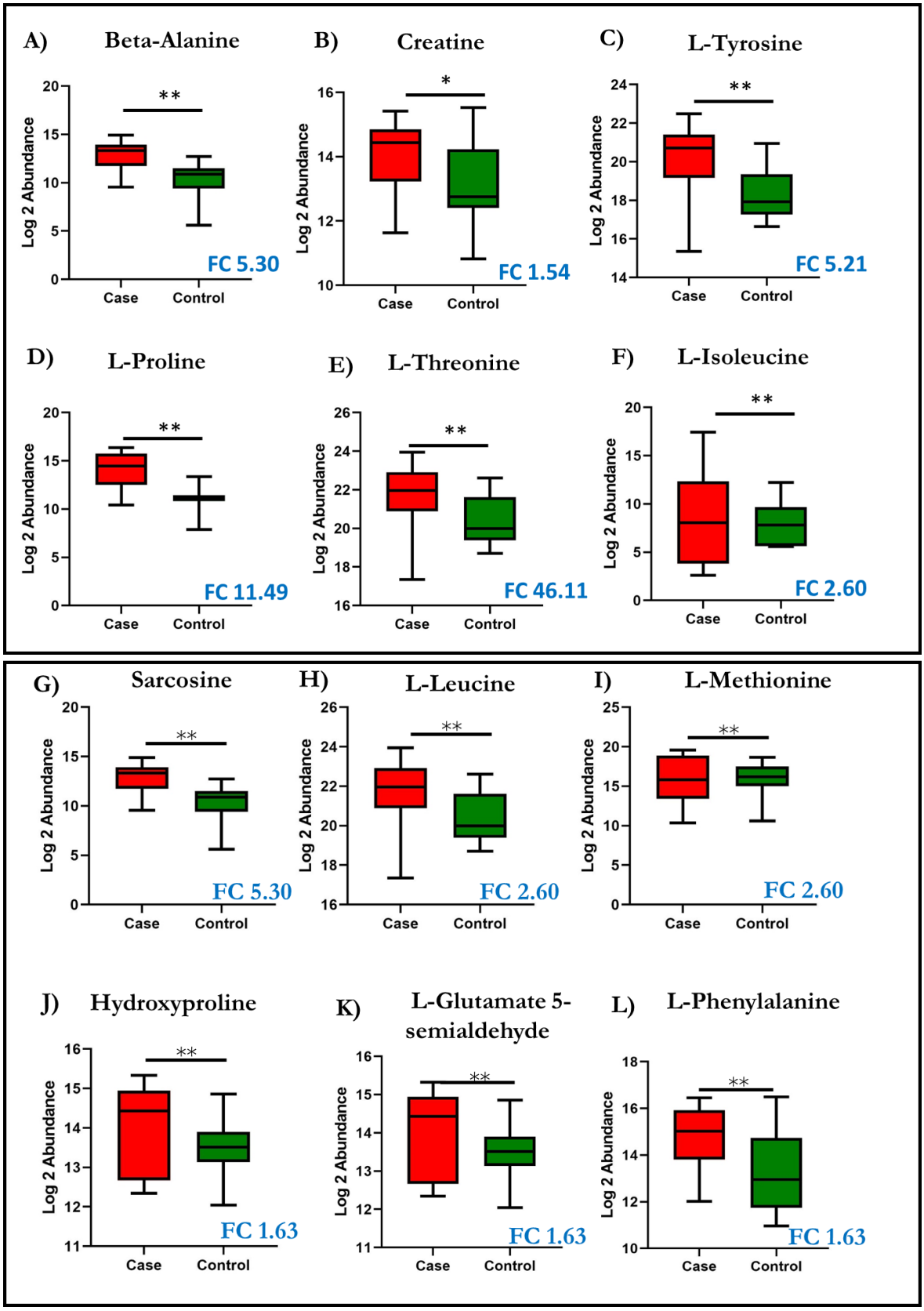
A) Beta-Alanine
B) Creatine
C) L-Tyrosine
D) L-Proline
E) L-Threonine
F) L-Isoleucine
G) Sarcosine
H) L-Leucine
I) L-Methionine
J) Hydroxyproline
K) L-Glutamate 5-semialdehyde
L) L-Phenylalanine
Log 2 Abundance
Case
Control
FC 5.30
FC 1.54
FC 5.21
FC 11.49
FC 46.11
FC 2.60
FC 2.60
FC 5.30
FC 2.60
FC 1.63
FC 1.63
FC 1.63

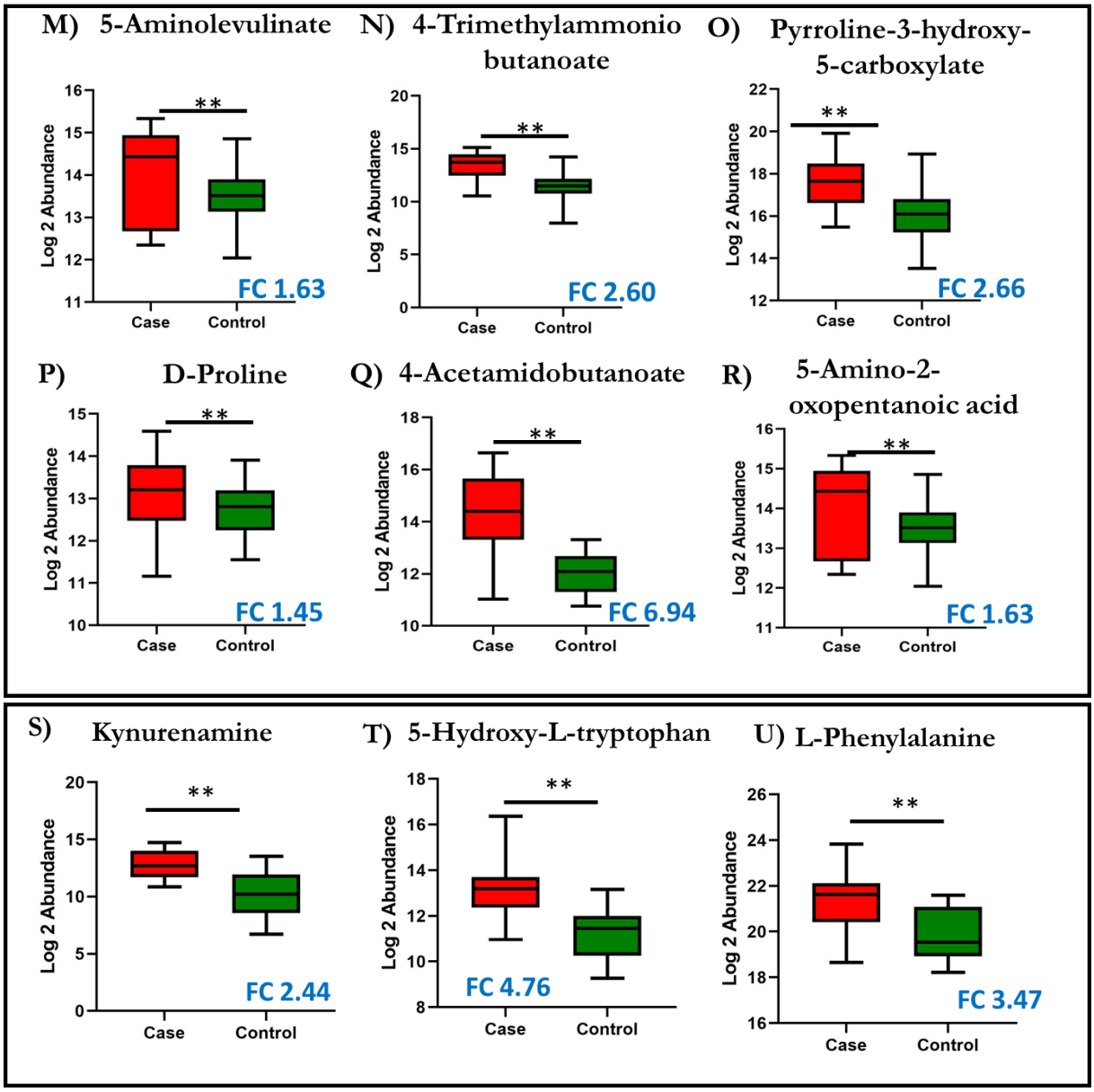

Figure 100. Box plots showing abundance (log 2) of the metabolites among ROP cases and control, FC-fold change, p*=<0.05, p=<0.01.**

Table 45. MS/MS fragmentation pattern validation

Amino acid				
S. No	**HMDB ID**	**Name**	**Controls MS/MS fragmentation**	**Cases MS/MS fragmentation**
1	HMDB0000056	beta-Alanine	NF	NF
2	HMDB0000687	L-Leucine	NF	101.97,103.05,103.51,120.07
3	HMDB0000696	L-Methionine	100.07,102.01,117.54	100.11,102.05432975,118.08,
4	HMDB0002234	1-Pyrroline-4-hydroxy-2-	NF	NF

		carboxylate		
5	HMDB0000064	Creatine	113.5225206	NF
6	HMDB0000162	D& L-Proline	NF	115.9660715
7	HMDB0060460	L-1-Pyrroline-3-hydroxy-5-carboxylate	113.5225206	113.73
8	HMDB0006488	L-Glutamate 5-semialdehyde	111.5009845	NF
9	HMDB0000167	L-Threonine	NF	NF
10	HMDB0000159	L-Phenylalanine	101.50,101.50,103.51, 103.51,105.50,113.50, 114.50,131.51,132.51, 133.50,149.52	104.35,104.355,105.95,150.08

4.3.7.2. Lipid Metabolism

Differential expression of these significant lipids and fatty acid metabolites showed a clearly distinct pattern for patients and controls as shown in heatmap (below Figure 101) while PCA plot showed that the significant metabolites in these pathways could clearly differentiate patients from controls as seen by forming two separate clusters.

The lipid metabolic pathways and their associated metabolites are shown below (Table 46 and Figure 102). The pathways enrichment analysis showed several significantly deregulated metabolites and pathways involved in lipids and fatty acid metabolism in the ROP vitreous humor.

Table 46. List of upregulated and downregulated metabolites among ROP patients and controls in various lipid metabolism pathways

Lipid Metabolism		
Pathways	**Upregulated Metabolites**	**Downregulated Metabolites**
Arachidonic acid metabolism	**11,12-EET, Prostaglandin E2**	-
Glycerophospholipid metabolism	**Phosphatidylcholine, Acteylcholine**	**Phosphatidylethanolamine**
Sphingolipid metabolism	-	**Digalactosylceramide, Digalactosylceramide**

Alpha-Linolenic acid metabolism	Phosphatidylcholine	-
Linoleic acid metabolism	Phosphatidylcholine	-
Glycerophospholipid metabolism	-	Phosphatidylethanolamine
Glycosylphosphatidylinositol (GPI)-anchor biosynthesis	-	Phosphatidylethanolamine
Primary bile acid biosynthesis	7alpha-Hydroxy-3-oxo-4-cholestenoate	Glycochenodeoxycholate
Fatty acid biosynthesis	Octanoic acid	-
Drug metabolism - cytochrome P450	5-Phenyl-1,3-oxazinane-2,4-dione	-

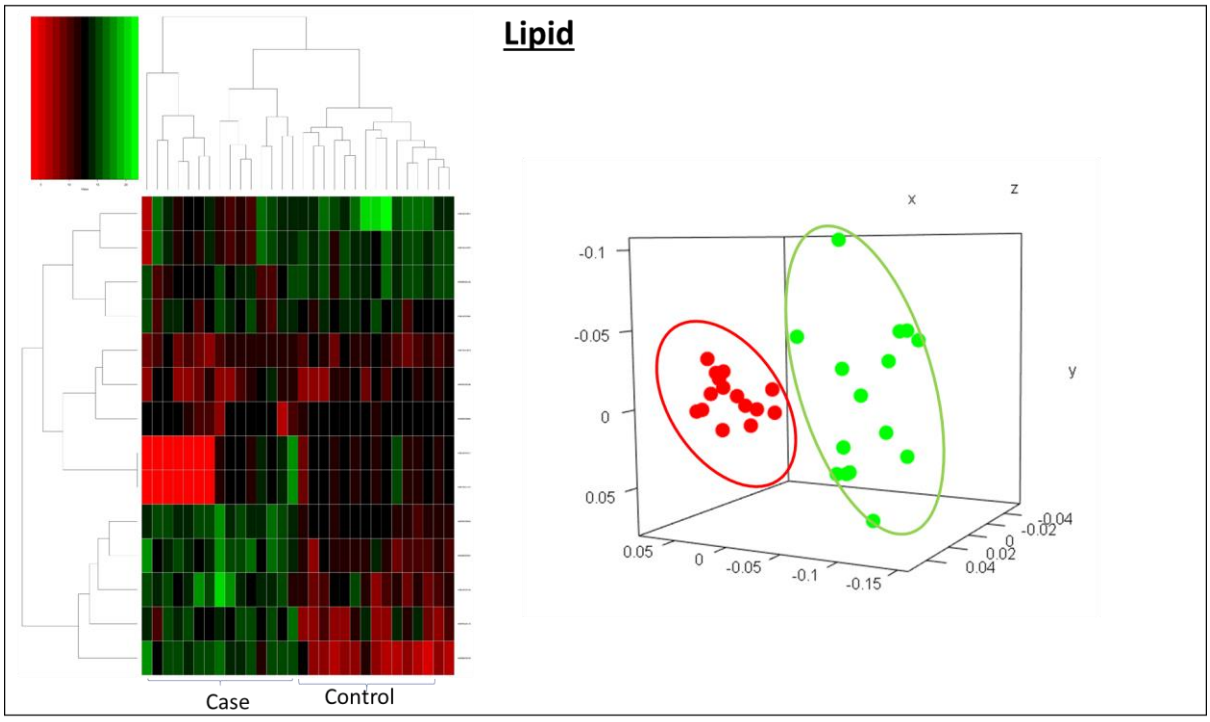

Figure 101. Lipid metabolism: Heatmap (A) and PCA cluster analysis (B) generated for significantly dysregulated metabolites based on their abundance in ROP cases as compared to controls.

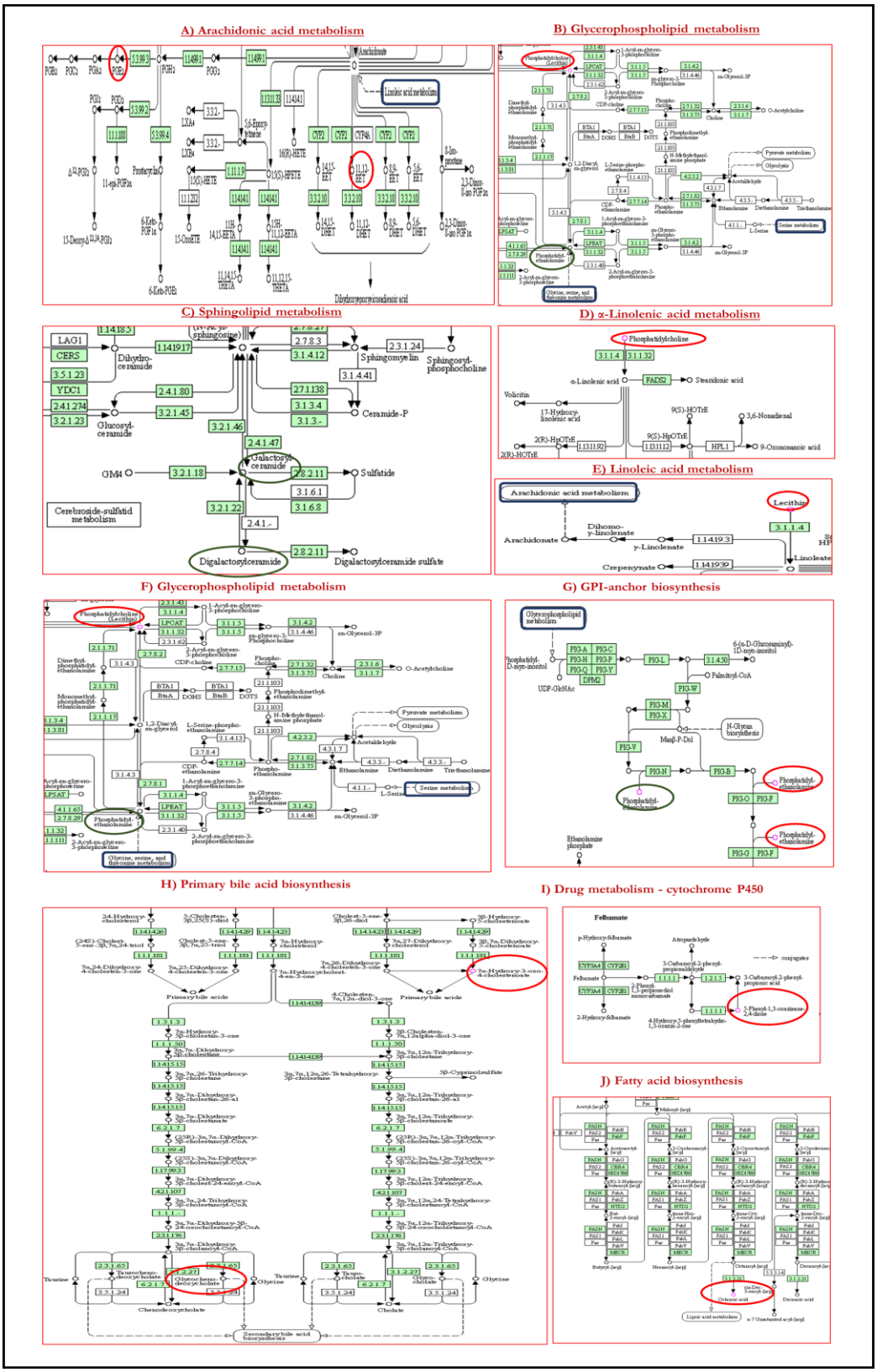

Figure 102. Schematic representation of lipids and fatty acid metabolic pathways and significant metabolites in theses pathways. The red color circle represents the significantly upregulated metabolite, and the blue colored box denotes associated metabolism

4.3.7.2.1 Validation of the metabolic pathway

Further, the differential expression of metabolites was quantified and validated by comparing the abundance of each metabolite. Significant differentially expressed pathways and metabolites are shown in Figure 103. Among the significant metabolites identified in lipid pathways, 3 were randomly selected and validated for their annotation by matching their MS/MS fragmentation pattern (Table 47).

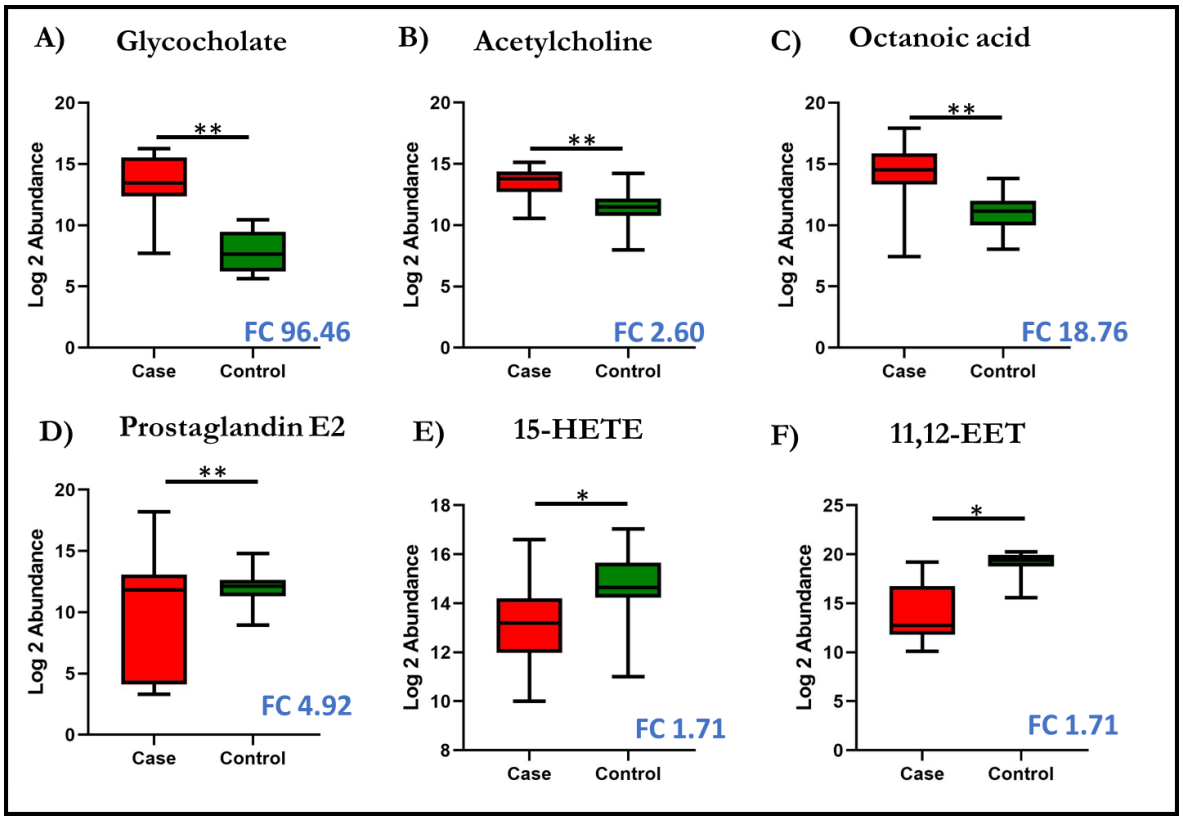

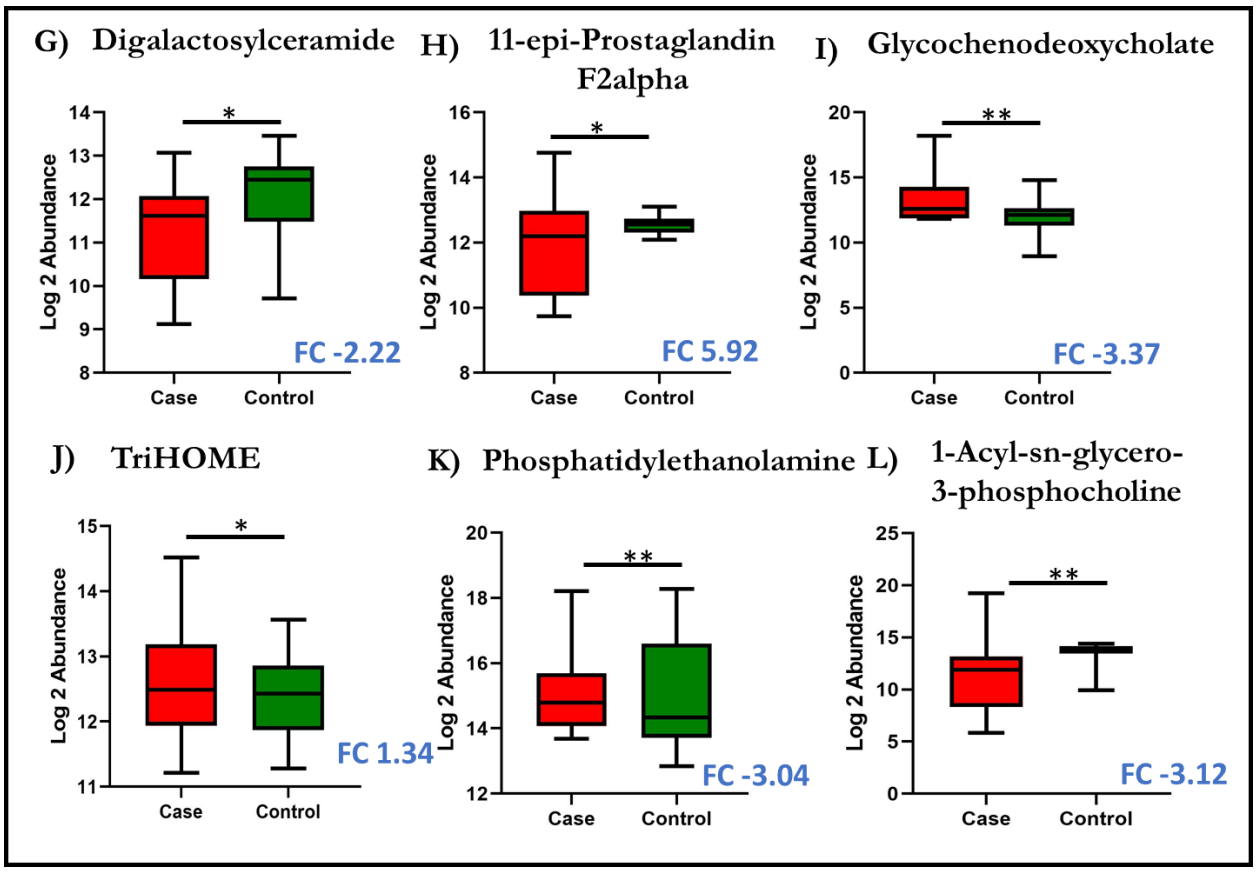

Figure 103. Box plots showing abundance (log 2) of the metabolites among ROP cases and control, FC-fold change, p*=<0.05, p=<0.01.**

Table 47. MS/MS fragmentation pattern validation

Lipid				
S.No.	HMDB ID	Name	Controls MS/MS fragmentation	Cases MS/MS fragmentation
1	HMDB0060041	PGE2	119,129.1,137.1,139.1,141.1,221.2,259.2,261.2,273.2,275.2,289.2	119,129.1,137.1,139.1,141.1,221.2,259.2,261.2,273.2,275.2
2	HMDB0003876	5,6-Ep-15S-HETE	107.1,147.1,175.1	161.1,229.2,241.2,
3	HMDB0001139	11-deoxy PGF2	123.1,137.1,195.1,223.1,277.2	123.1,137.1,179.1,195.1,207.1,209.1,221.1,221.2,223.1,223.2,235.1,237.1,263.2,275.2,277.2,291.2,293.2,

4.3.7.3. Metabolites involved in Bioenergetics metabolism

The demand for neuronal energy is met and fulfilled by a vascular organization of the eye that necessities supplements and O_2. The human retina is one of the most energy-demanding organs that requires and sources energy for its physiological and cellular functions through several metabolic pathways (H. Liu & Prokosch, 2021; Viegas & Neuhauss, 2021). Some of these including the TCA cycle, glycogenolysis and nicotinamide pathways were significantly dysregulated suggesting for their possible role in ROP pathogenesis shown below in Table 48.

Table 48. Pathways in bioenergetics metabolism and identified metabolites in ROP vitreous

Energy Metabolism		
Pathways	**Upregulated Metabolites**	**Downregulated Metabolites**
TCA cycle	**Citric acid, Oxalosuccinic acid**	-
Pantothenate and CoA biosynthesis	**Pantothenate**	-
Nicotine degradation	**L-Aspartate, beta-Alanine**	-
Fructose and Mannose metabolism	**6-Deoxy-L-galactose**	-

The TCA cycle pathway metabolites including citric acid and oxalosuccinic acid were up regulated in ROP cases than controls. Other than these Pantothenate and CoA biosynthesis, nicotine degradation, fructose and mannose metabolism pathway metabolites were also up regulated in ROP cases than controls. Differential expression of these significant energy pathway metabolites showed a clearly distinct pattern for patients and controls as shown in heatmap (below Figure 104) while PCA plot showed that the significant metabolites in these pathways could clearly differentiate patients from controls as seen by forming two separate clusters. The deregulated energy metabolic pathways and their associated metabolites are shown in the below Figure 105.

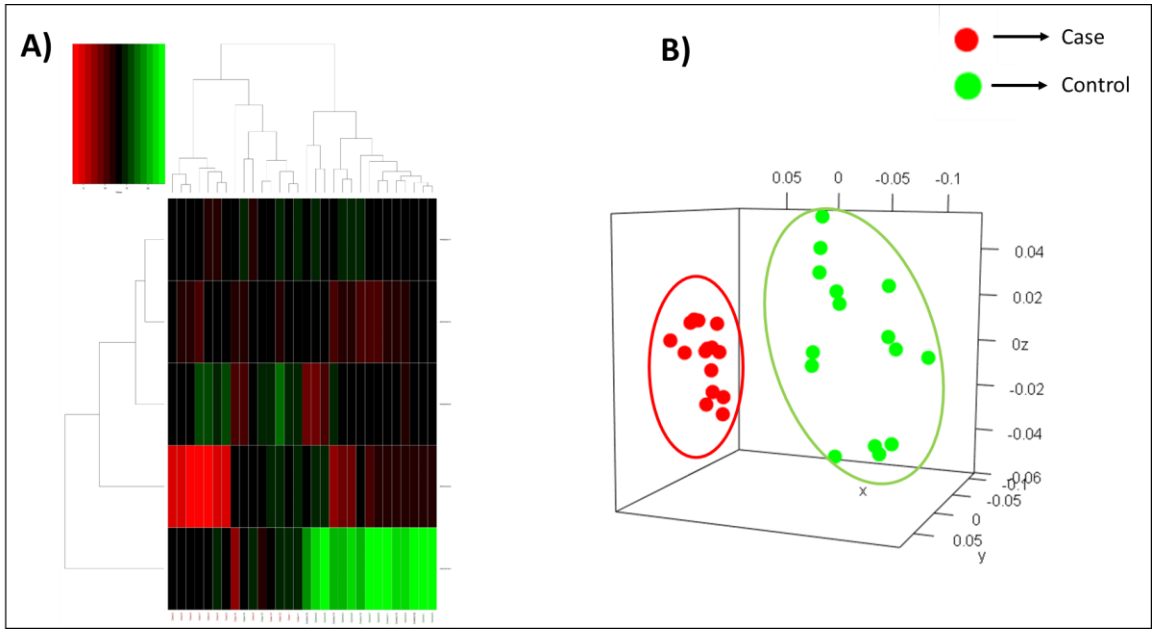

Figure 104. Bioenergetics metabolism; A: Heatmap generated for significantly dysregulated metabolites based on abundance in ROP as compared to control vitreous; B: PCA cluster analysis.

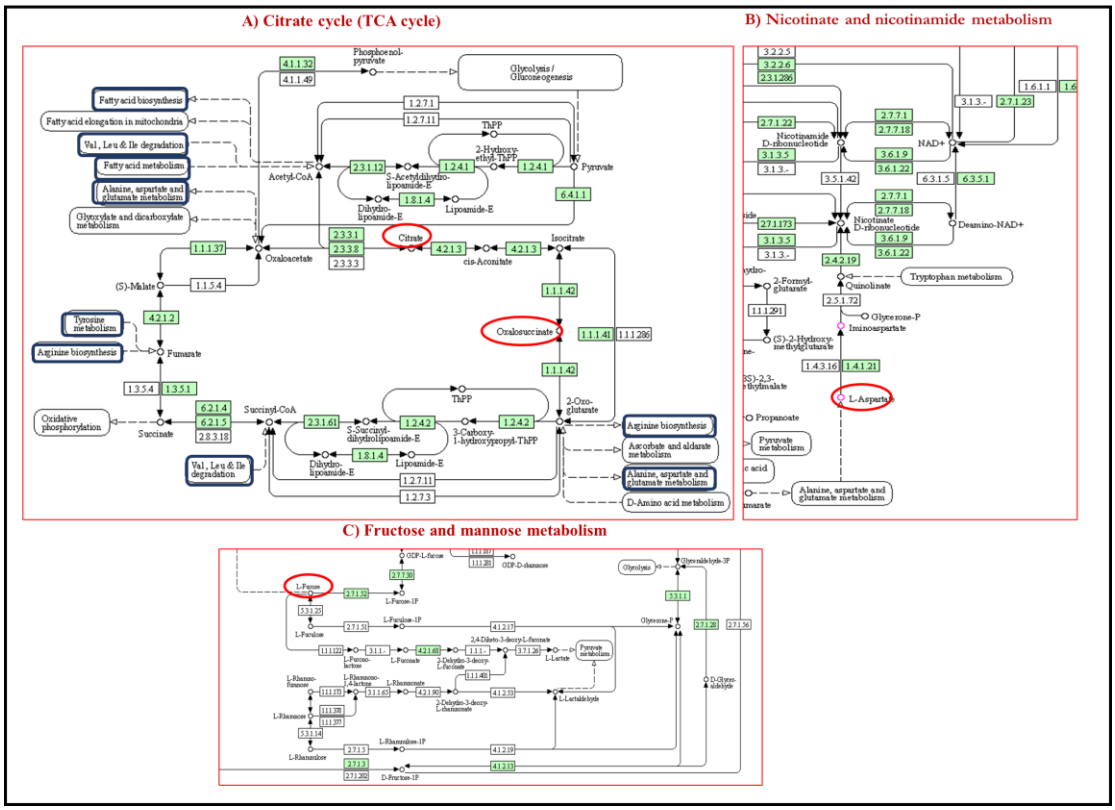

Figure 105. Schematic representation of pathways involved in bioenergetics metabolism and identified metabolites. The red color circle represents the significantly upregulated metabolite and the blue colored box denotes associated metabolism.

4.3.7.3.1. Validation of the energy metabolic pathway

Further, these metabolites expression was quantified and validated by comparing the abundance of each metabolite. Significant differentially expressed pathways and metabolites in energy production/cycle are shown in Figure 106. Among the significant metabolites identified in energy cycle, 2 succinic acid and oxalosuccinate were randomly selected and validated for their annotation by matching their MS/MS fragmentation pattern (Table 49).

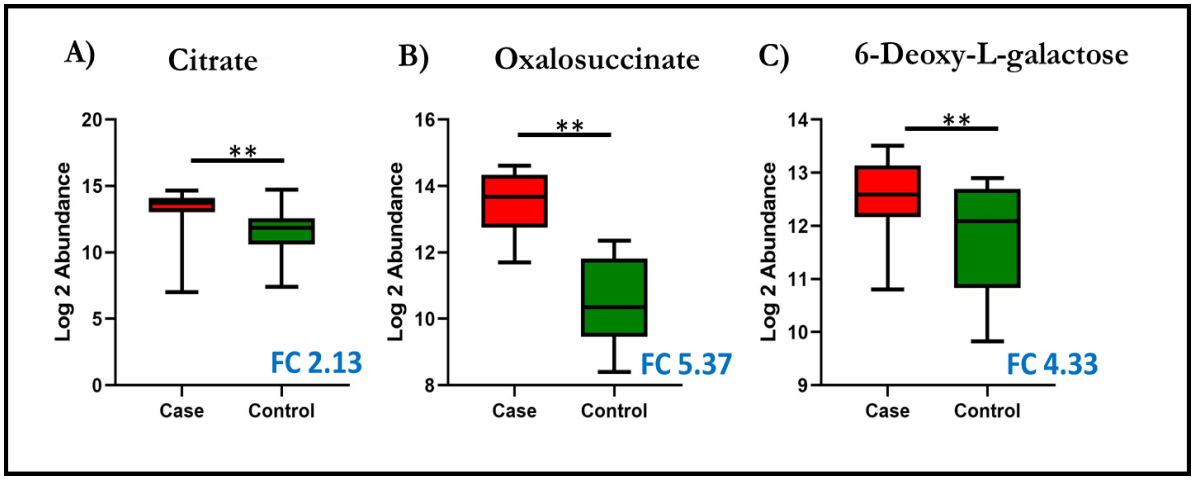

Figure 106. Box plots showing abundance (log 2) of the metabolites among ROP cases and control, FC-fold change, p*=<0.05, p=<0.01**

Table 49. Validation of metabolities by MS/MS fragmentation

Energy				
S.No	HMDB ID	Name	Controls MS/MS fragmentation	Cases MS/MS fragemention
1	HMDB0000254	Succinic acid	100.62,119.24	119.1040015
2	HMDB0003974	Oxalosuccinate	101.38, 143.11, 145.05, 191.14	NF

4.4. DISCUSSION

Metabolomic profiling gives a snapshot of all the compounds present in a given sample at a specific time point. Our earlier studies on ROP found a strong association of gene variants involved in cholesterol metabolism (Rathi *et al.*, 2017) and this was further confirmed by the exome sequencing and gene expression performed in ROP infants as part of aim 2 and 3 in the present study. Thus, besides genetic factors, protein and metabolic alterations could be strongly involved in the retinal vasculature formation and underlying inflammation as seen in ROP. However, there is not enough evidence to implicate metabolic alterations in the pathophysiology or progression of ROP. The present study attempted to fill this lacuna for the first time by investigating metabolomic alteration and its associated pathways in the vitreous of ROP infants.

4.4.1. Role of metabolomics in ROP

Understanding the metabolic alterations in ROP was quite challenging owing to the complexity of disease and unavailability of ocular samples from preterm infants with different stages of disease, required ideally for a better assessment of disease progression. Till date, only 3 studies have performed metabolomics for ROP, however, these were either done using plasma samples of OIR model of ROP (Zhou, Tan*, et al.*, 2021; Paris *et al.*, 2016) and/or human patients (Zhou, Xu*, et al.*, 2021; Yang *et al.*, 2020; Zhou *et al.*, 2020) by performing targeted/untargeted metabolomic profiling. However, vitreous humor can only serve as a reliable and accessible human ocular tissue to explore the metabolic changes in retinal diseases. Being most proximally attached to the retina, it can provide a snapshot of all the pathological metabolic changes occurring within retina. A major function of vitreous is to maintain proper O_2 metabolism. According to Shui et al. (2009), the lens and trabecular meshwork are protected from oxidative stress due to O_2 metabolism in the retina/vitreous.(Shui *et al.*, 2009). Therefore, study of the vitreous metabolome can help in elucidating the pathogenesis of retinal diseases like ROP. So far, no studies are reported that targeted vitreous metabolome for understanding ROP

pathogenesis. The present study compared the vitreous metabolome of ROP with controls and measured the abundance of altered metabolites by using mass spectrometry. Since vitreous cannot be taken from individuals unless advised for the management of an ocular condition, control vitreous was obtained from infants undergoing vitrectomy during cataract surgery with one year of birth.

4.4.2. MS-based vitreous metabolome characterization

MS is a sensitive technique that provides a broad spectrum and high resolution of molecules in body fluid like vitreous humor. Since the available metabolomic data of ROP is highly variable and limited, it suggests for the need to identify and establish standard and composite protocol/method to detect and extract the all-possible retinal metabolites. Further, this should be sensitive enough to identify novel vitreous metabolites those even with low abundance and comparable to circulating metabolites in the systemic fluids.

4.4.3. Identification of novel vitreous metabolites and pathways

We compared the data on metabolic pathways and metabolites from the present study with previously published data for ocular metabolites. The present study found 580 significantly dysregulated metabolites in the vitreous of ROP patients. Annotated metabolites were classified into lipids, organic acid derivatives, benzenoids, vitamins, nucleotide derivatives, etc. A further comparison of the identified pathways with the published metabolome data showed that majority of the identified metabolites in the current study were significantly dysregulated among ROP patients. In addition, 43 metabolites in the blood/plasma samples that were reported earlier for ROP (Yang *et al.*, 2020; Zhou *et al.*, 2020), were also confirmed in the present study. A further comparison of pathways identified and methods used in different metabolome studies revealed that the approaches and protocols established and employed for studying metabolic alterations in the present study were quite robust and sensitive demonstrated great resolution at par with the published reports (Table 50). Further, 45 significant pathways for ROP identified in the present

study were listed for other ocular diseases as well however with varying extent and impact. Most of the identified metabolites in present study belong to the lipid (leukotriene, lipoxin biosynthesis, Ketogenesis), amino acid (RNA charging) and energy (mitochondria, Coenzyme A Biosynthesis) derived metabolism.

Table 50. Comparison of metabolic pathways and methods used in different vitreous metabolome studies

S.No	Diseases	Platform used	Pathway analysis	Pathways Identified	Top 20 pathways	Referene
1	AMD	LC-FTMS	KEGG	5	Nucleotides, Sugars,lipids, and Steroid metabolites	(Osborn *et al.*, 2013)
2	DR	GC-MS	MetaboAnalyst	2	Pentose phosphate pathway, Galactose metabolism	(L. Chen *et al.*, 2016)
3	AMD	LC-MS/MS	MetaboAnalyst4.0	66	Methionine, Cysteine, SAM and Taurine Metabolism, Alanine and Aspartate Metabolism, Glutathione Metabolism, Leucine, Isoleucine and Valine Metabolism, Tryptophan Metabolism, Histidine Metabolism, Tocopherol Metabolism, Nicotinate and Nicotinamide Metabolism,Hemoglobin and Porphyrin Metabolism, Lysoplasmalogen, Plasmalogen, Phosphatidylcholine (PC), Fatty Acid Metabolism(Acyl Carnitine), Diacylglycerol, Phosphatidylinositol (PI), Phospholipid Metabolism,Fatty Acid Metabolism (Acyl Choline), Phosphatidylethanolamine (PE), Purine Metabolism, Adenine containing, Pyrimidine Metabolism, Cytidine	(Lains *et al.*, 2019)
4	PDR	GC-MS	MetaboAnalyst4.0	62	Pyrimidine metabolism, Alanine, Aspartate and glutamate metabolism, Caffeine metabolism,beta-Alanine metabolism, Purine metabolism, Cysteine and methionine metabolism, Sulfur metabolism,Sphingolipid metabolism, Arginine and proline metabolism, Linoleic acid metabolism, Nitrogen metabolism,D-Glutamine and D-glutamate metabolism, Glycine, Serine and threonine metabolism, Steroid hormone biosynthesis, Pantothenate and CoA biosynthesis, Taurine and hypotaurine metabolism, D-Arginine and D-ornithine metabolism, Cyanoamino acid metabolism, Histidine metabolism, Phenylalanine metabolism	(X. R. Zhu *et al.*, 2019)
5	ROP	LC-MS/MS	KEGG	4	Protein digestion, absorption, Aminoacyl-tRNA biosynthesis, Central carbon metabolism in cancer, ABC transporters	(Zhou *et al.*, 2020)
6	macular neovascular	GC-MS	MetaboAnalyst4.0	251 (10 provided)	Pentose phosphate pathway, Mitochondrial electron transport chain (ETC), Pentose and glucuronate interconversion, Ascorbate and aldarate metabolism, Purine, Gycolysis, Glycogenesis, Thaimine metabolism, Arginine and proline metabolism	(K. Liu *et al.*, 2020)
7	PVR	LC-MS	KEGG	30	Arginine and proline metabolism, Glyoxylate and dicarboxylate metabolism, Lysine degradation, Arginine and proline metabolism, Pyrimidine metabolism, Ascorbate and aldarate metabolism, Valine, leucine and isoleucine degradation, Tyrosine metabolism, Tyrosine metabolism, Histidine metabolism, Metabolism ,Purine metabolism, Ascorbate and aldarate metabolism, Lysine biosynthesis, Valine, Leucine and isoleucine degradation, Citrate cycle, Atrazine degradation, Histidine metabolis, Histidine metabolism, Citrate cycle, Glycolysis, Glycine, Serine and threonine metabolism, Purine metabolis	(M. Li *et al.*, 2014)
8	RRD	LC-Q-TOF-MS	KEGG	31	Arginine and proline metabolism, Glyoxylate and dicarboxylate metabolism, Lysine degradation, Pyrimidine metabolism, Ascorbate and aldarate metabolism,Valine, Leucine and isoleucine degradation, Tyrosine metabolism, Tyrosine metabolism, Histidine metabolism, Tryptophan metabolism, Purine metabolism, Lysine biosynthesis, Valine, leucine and isoleucine degradation, citrate cycle,Atrazine degradation,Histidine metabolism, Citrate cycle, Glycolysis, Glycine, Serine and threonine metabolism, Ascorbate and aldarate metabolism, Citrate cycle,Citrate cycle, Ascorbate and aldarate metabolism, Glycolysis, Tyrosine metabolism, Phenylalanine, Tyrosine metabolism	(M. Li *et al.*, 2014)
9	RRD	LC-Q-TOF-MS	KEGG	9	Alanine and asparate metabolism, Citrate cycle, Fatty acid metabolism, Tyrosine metabolism, Glutamate metabolism, Purine metabolism, Phenylalanine metabolism, Tryptophan metabolism, Glycine, Serine and threonine metabolism, Butaoate metabolism, D-Glutamine and D-Glutamate, Pyramidine metabolism, Arginine and proline metabolism, Pyruvate metabolism, Glycolysis, Gluconogenesis, Ascorbate and aldarate metabolism, Arachidonic acid metabolism, Propanoate metabolism, Sphinolipid metabolism	(Yu *et al.*, 2015)

10	Ischemic retinopathy	LC-MS	MetaboAnalyst program	5	Protein synthesis, arginine and proline metabolism, ammonia detoxification,purine metabolism and fatty acid oxidation	(Paris *et al.*, 2016)
11	Cataract	LC-MS	MetaboAnalyst	47	Nitrogen metabolism,Aminoacyl-tRNA biosynthesis,Phenylalanine, tyrosine, and tryptophan biosynthesis,Valine, leucine, and isoleucine biosynthesis,Phenylalanine metabolism,Taurine hypotaurine metabolism,Biotin metabolism,Arginine and proline metabolism,Pantothenate and CoA biosynthesis,Beta-alanine metabolism, Glycine, serine, threonine metabolism,Glyoxylate and dicarboxylate metabolism,Tryptophan metabolism,Pyrimidine metabolism,Alanine, aspartate, and glutamate	(Pietrowska *et al.*, 2017)
12	DR and RRD	LC-MS Thermo Q Exactive mass spectrometer	MetaboAnalyst 3.0	3	Glucose metabolism, Pentose phosphate pathway, Purine metabolism	(Haines *et al.*, 2018)
13	RRD	UHPLC-HRMS	MetScape,KEGG	22	Aminoacid, peptides and analogues, Phospholipidspinolipids, Fatty acid and conjugates, Fatty acid esters, Benzoic acid and dervatives, Phenylpropylamines, Tricarboxylic acid and ervitatives, Pyrimidines and pyrimine dervatives, Bile acid, Sugar alcohol, Glycerolphosphocholines, Hydroxycinnamic acid and derivatives, Steroidal glycosides, Sulfones, Quinone and hydroxyquinone lipids, Glycerolphosphoglycerols, Pyridinecarboxy acid ,Fucoric acid derivatives, Phenysulfates, Phenylacetic acid derivatives	(Kowalczuk *et al.*, 2018)
14	Gluacoma	GC-TOF-MS	Metaboanalyst	1 (targeted- AA Metabolism)	Aminoacyl-tRNA biosynthesis,valine, Leucine, and isoleucine biosynthesis, Arginine and proline metabolism, aspartate, and glutamate metabolism	(X. Chen *et al.*, 2019)
15	AMD	LC-MS/MS	KEGG, Metaboanalyst	10	Protein digestion and absorption, Mineral absorption, Lysine degradation, Glycine, Serine, Threnoine metabolism, Ciitric acid (TCA cycle), Biosynthesis of aminoacids, Arginine and proline metabolism, Aminoacyl-t RNA biosynthesis, ABC transporters, 2-Oxocarboxyl acid metabolism	(Han *et al.*, 2020)
16	DR	NMR	MetaboAnalyst4.0	2	Glucose levels, Glucolytic products (lactate), β-oxidation (ketone body-derived metabolite/acetate) aldose reductase or polyol pathway (galactitol), and AA defense against oxidative stress, polyol pathway	(Barba *et al.*, 2010)
17	ROP	LC MS	XCMS, MetaboAnalyst4.10	44	Arginine and proline metabolism, Phenylalanine metabolism, Valine, Leucine and isoleucine biosynthesis, Phenylalanine, tyrosine and tryptophan biosynthesis, Aminoacyl-tRNA biosynthesis, Pantothenate and CoA biosynthesis, Arachidonic acid metabolism, D-Arginine and D-ornithine metabolism, Linoleic acid metabolism, Glycine, Serine and threonine metabolism, Histidine metabolism, Glycerophospholipid metabolism, Taurine and hypotaurine metabolism, Ubiquinone and other terpenoid-quinone biosynthesis, Vitamin B6 metabolism, Citrate cycle (TCA cycle, Sphingolipid metabolism, beta-Alanine metabolism, Propanoate metabolismn	Present study

4.4.4. Amino acid metabolism

Amino acid (AA) metabolism plays a crucial role in controlling vascular activity, cell growth, vascular tone, coagulation, fibrinolysis, differentiation and immune response that are crucial for angiogenesis (Rohlenova *et al.*, 2018; Treps *et al.*, 2016).

Tryptophan is an essential AA required for the biosynthesis of proteins. L-tryptophan plays an important role in both prokaryotes and eukaryotes. The indole pathway is majorly involved in bacteria while the kynurenine and serotonin pathways are involved in tryptophan metabolism in human cells. Dietary tryptophan is converted to kynurenine via kynurenine pathway (KP). Imbalance or disruption in KP has been associated with several neurodegenerative disorders such as Parkinson's (Marti-Masso *et al.*, 2013). The present study found metabolites specific to human kynurenine and serotonin pathways in ROP cases. Kynurenine pathways is initiated by tryptophan degradation, ultimately leading to the formation of NAD^+ particularly to meet high energy demands during immune activation. Kynurenine is also a known endogenous ligand for aryl hydrocarbon receptor required for regulating the Aryl Hydrocarbon Receptor Nuclear Translocator (ARNT) complex. This complex is essential for HIF1α activation under hypoxic stress (Nguyen *et al.*, 2014). Major metabolites generated in the cascade of KP includes Kynurenine and 3-hydorxylkynurenine that are known to be involved in neuroinflammation, vaso-dilation and oxidative stress (Hajsl *et al.*, 2020). 3-hydorxylkynuremine has been shown to be involved in microglial cell proliferation (Garrison *et al.*, 2018; O'Farrell *et al.*, 2017). Thus, an upregulation of Kynurenine and 3-hydorxylkynuremine in ROP, explains its potential role in microglial mediated immune activation and inflammation (Rathi *et al.* 2017). Previously, accumulation of 3-hydroxykynurenine was also linked with cataract formation (Chiarugi *et al.*, 1999) and an increased expression of kynurenine, kynurenic acid and 3-hydroxykynurenine was seen in diabetic retinopathy patients (Munipally *et al.*, 2011) suggesting for their possible role in disease progression.

Besides these, Indoleamine 2,3-dioxygenase1 (IDO-1), a crucial enzyme involved in KP is expressed by human eye corneal cells and provides immune privilege to the organ by maintaining blood retinal barrier and secreting immunosuppressive cytokines which in turn induces regulatory T cells (treg cells) (Niederkorn, 2012; Ryu & Kim, 2007). Thus, tryptophan metabolism is a major metabolic pathway in the eye that contributes to different ocular diseases, including ROP.

Other than the tryptophan, non-essential amino acids such as L-Arginine was also found upregulated in ROP cases. The role of arginine has been widely investigated in regulating M1 and M2 macrophage polarisation (Rath *et al.*, 2014). Macrophages metabolises arginine via 2 pathways. When metabolised via Nitric oxide synthase (NOS) to NO and citrulline, it adopts M1 phenotype (pro-inflammatory). On the other hand, upon metabolised by arginase into ornithine and urea, it switches to M2 phenotype which is anti-inflammatory (Mills, 2012). Therefore, the fate of macrophages (pro or anti-inflammatory) depends on the route of L-arginine metabolism (Wang *et al.*, 2011; Hnia *et al.*, 2008). An upregulation of L arginine in ROP needs to be investigated further to understand its role in causing or alleviating the inflammation in the retina. Several Aminoacyl-tRNA synthetase (ARS) metabolites (L-Phenylalanine, L-Tyrosine, L-Isoleucine, L-Leucine, L-Proline, L-Threonine, L-Threonine and L-Aspartate) were also found upregulated in ROP cases. The primary function of these metabolites is to catalyze the binding of the amino acids to its cognate tRNA with help of ATP for initiating protein synthesis. ARSs are primarily involved in the maturation, transcription, activation and recruitment of immune cells, thus playing a crucial role in the development of immune cells (Nie *et al.*, 2019). Thus, an increased activity of ARS could regulate inflammation and angiogenesis via activation of the CXC-receptor (CXCR) family leading to maturation and recruitment of immune cells particularly microglia and macrophages as observed in ROP vitreous (Rathi *et al.*, 2017). These aminoacyl

tRNA metabolites can also affect the proliferation and survival of endothelial cells and further promotes the angiogenesis (Mirando *et al.*, 2017; Mirando *et al.*, 2014; Romagnani *et al.*, 2004).

All together an increased expression of Kynurenine, IDO-1, ARS and several other amino acid metabolites found in the present study explains a major possible role of amino acid metabolism in activation of immune pathways, inflammation leading to abnormal angiogenesis seen in ROP eyes.

4.4.5. Fatty acid and derived metabolites in ROP

Human retina is rich in many classes of lipids and its derivatives that are involved in controlling several molecular functions, including cell growth and proliferation (Anderson *et al.*, 2020; Rotstein *et al.*, 2010). Fatty acids are a major class of lipids, in mitochondria these fatty acids are broken down into the acetyl-CoA by beta oxidation. Acetyl CoA is required for the initiation of Krebs cycle to produce energy. (Wanders *et al.*, 2010). Fatty acids including triglycerides (TG), and phospholipids (PL) are processed by Cyclooxygenase (COX2), Lipoxygenase (LOX) and CYPs to produce several metabolites including the leukotrienes (LTs), prostaglandins (PG), eicosanoids and epoxyeicosatrienoic acids (EETs). These metabolites bind to the receptors like the peroxisome proliferator-activated receptors (PPARs), G protein-coupled receptors, TLR4 and sterol regulatory element-binding protein 1 (SREBP1). The receptor-metabolite binding facilitates the macrophages functions including cellular energy metabolism, survival, proliferation, differentiation, cell migration and inflammation processes (Figure 107).

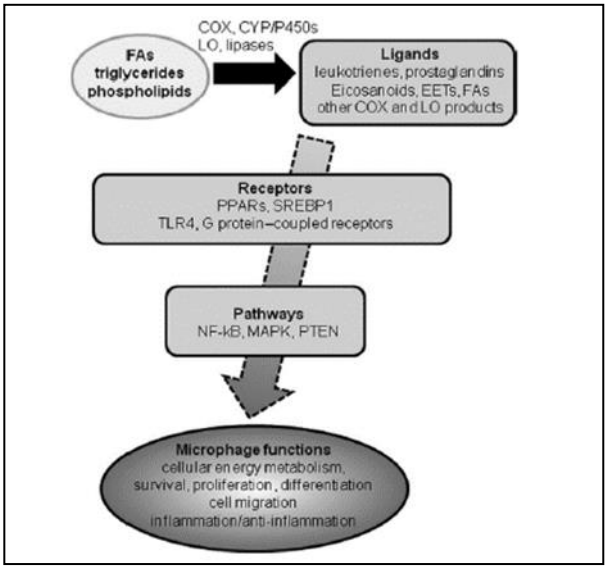

Figure 107. Effect of fatty acids on macrophage functions adapted from (L. Zhu *et al.*, 2015)

Lipid metabolites derived from different PUFAs participates in a wide range of biological activities. Epoxy-octadecenoic acids [EpOMEs] and leukotoxins synthesized from linoleic acid by CYP family enzymes are converted to the equivalent 1, 2-diols (dihydroxy-octadecenoic acids) DiHOMEs, with the help of soluble epoxy hydrolase (EPHX2). Likewise, trihydroxyoctadecenoic acids (TriHOMEs) are linoleic acid-derived formed by 15-LOX. In the present study, an upregulation of 11,12,13-TriHOME was seen in ROP vitreous. These TriHOMEs have earlier been reported to be dysregulated in chronic inflammatory diseases such as asthma and chronic obstructive pulmonary disease (COPD) (Fuchs *et al.*, 2020; Lemiere *et al.*, 2006). TriHOMEs have ability to aggregate neutrophils (Nording *et al.*, 2010) and act as important mediators of inflammation. The neutrophils in turn contributes to the production and secretion of inflammatory molecules including cytokines, chemokines and prostaglandins (Wright *et al.*, 2010). Prostaglandins also act as the secondary messengers produced by COX enzymes in arachidonic acid induced inflammatory responses inside the retina that can further lead to neuroinflammation and neurodegeneration (Bar-Ilan *et al.*, 1991). Significant increased synthesis and expression of PGE2, PGD2, PGI2, prostaglandins and leukotriene D4 metabolites

in ROP vitreous suggests that increased COX2 activity might have a role in exacerbating or alleviating the excessive inflammation in this disease.

On the other hand, we found the Phosphatidylethanolamine (PE) and Galactosylceramide downregulated in ROP infants. PE is the most abundantly present phospholipid in animals (Vance, 2015) and facilitates numerous functions, including protein folding and stimulating oxidative phosphorylation (OXPHOS) (Tasseva *et al.*, 2013). Any deficiency of PE in mitochondria leads to alteration in its morphology and impairs the OXPHOS. The Galactosylceramide is formed by ceramide and galactose. It is one of the major glycolipids presents in humans. These alpha-galactoceramides molecules binds to the NK cell surface receptors via OH group and under stress conditions thereby guiding NK cells to recognize and kill target cells that have lost their MHC-I expression (Wagner *et al.*, 2021) and can also lead to cytolytic activity. (Franck, 2012; Hayakawa *et al.*, 2002). Interesting, the gene expression data from this study (chapter 3), also showed a significant lower expression of NK cell regulatory genes (*HLA DRB1* and *DRB5*). This dysregulation of NK cells regulatory genes and increased expression of galactosylceramide metabolites in ROP might explain the inflammation in ROP eyes. Thus, the lipid metabolism in the retina has an important role in ROP pathogenesis and its role as a therapeutic target needs to be investigated further.

4.4.5.1. Bioenergetics metabolism in the ROP retina/vitreous

The human retina is a highly organized layer in the eye and can be influenced by multiple factors, including O_2 supplementation, blood and nutrient supply to the retinal layers (Rabin, 2013). The retinal layers at each step are composed of different types of cells with varying energy demands. First, Endothelial cells which are the prime cells responsible in maintaining the BRB. They are the hub of oxygen and nutrient supply to the highly metabolic tissue i.e retina. Under stress condition or injury, they double their glycolytic flux for migration or proliferation. These cells rely on glycolysis for ATP and can control angiogenesis. Glucose is transported through blood to

cells via glucose transporters. Under hypoxic conditions, endothelial cells were shown to increase the expression of their primary glucose receptor to meet the surge in energy metabolism (GLUT/SLC2A1) (Yeh *et al.*, 2008).

Along with endothelial cells, glucose is also the primary fuel for photoreceptor cells (rods and cones) present inside the retina, facilitated via "ATP and Na^+" dependent glucose transporter (GLUT1) at blood-retinal barriers and by passive diffusion transversely across the Bruch's membrane (Ban & Rizzolo, 2000; Kumagai *et al.*, 1996). Retinal layers also contain a population of different type of glial cells. These glial cells contain fewer mitochondria thereby any disruption in energy metabolism makes them vulnerable to disruptions and functional failure. The metabolic reprogramming of microglia further plays a vital role in microglial polarization. The macrophages/microglial polarization demands more energy which is met by the anaerobic glycolytic pathway (Odegaard & Chawla, 2011; Rodriguez-Prados *et al.*, 2010). However, anaerobic glycolysis is less efficient and produces only 2 ATP per glucose molecule as compared to 32 in complete oxidation of glucose (Granchi *et al.*, 2010).

In the present study, bioenergetics metabolites were significantly upregulated in ROP probands eye as compared to controls. Importantly, the energy metabolites of TCA cycle [succinic acid, citric acid and oxallosuccinate] fructose and mannose metabolism [6-deoxy, l-galactose] were all upregulated. None of the metabolome studies explored energy metabolism for ROP so far, thus this increased expression of bioenergetics metabolites in ROP vitreous needs to be explored further for understanding their role in ROP pathogenesis.

TCA cycle plays a crucial role in retinal cell [astrocytes, glia cells (macrophages/microglia)] activation. Succinate from TCA cycle inhibits the prolyl hydroxylases. Proryl hydroxylases hydroxylates HIF1, resulting in its stability (Tannahill *et al.*, 2013). Under hypoxic environment, HIF-1α is phosphorylated by MAPK, which further translocates to the nucleus to form HIF-

1α/HIF-1β complex. This complex can secure the target promotor sequence (5′TAGCGTGH3′) of the hypoxia response genes (HRE) which includes *VEGF* (angiogenesis), *NOS* (vasodilation), *MMPs* (matrix remodeling), *NQO1* (antioxidant), *EPO* (erythropoiesis), *ET-1* (mitogen) and *GLUT-1* (glucose transporter) (X. Li *et al.*, 2012; Krock *et al.*, 2011) (Figure 108). All these hypoxia responsive genes and succinate were also found to be upregulated in ROP cases and that possibly explains abnormal angiogenesis and increased inflammation as seen in ROP eyes.

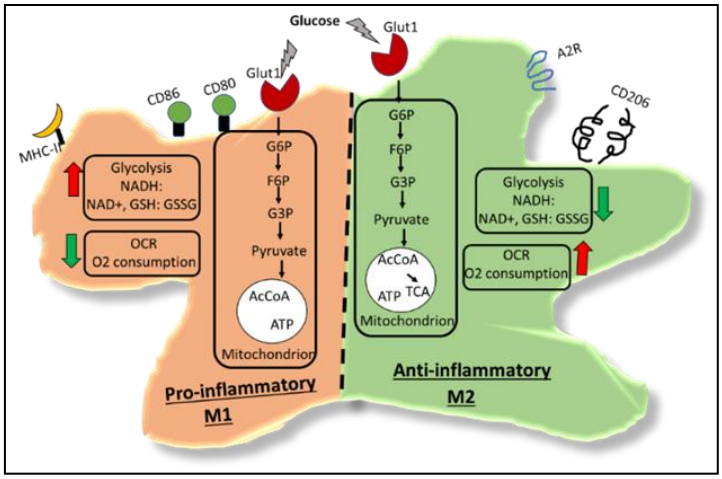

Figure 108. Energy metabolism involved in microglial (M1 & M2) polarization.

In summary, the global metabolomics profile of ROP shows involvement of several vital pathways such as amino acid, fatty acid energy and bioenergetics metabolism. The present study, is a first report on vitreous metabolome profiling for ROP patients and is an important addition to the existing databases on ocular metabolome. However, further, investigation and validation of identified metabolites and pathways in extended cohorts and different ethnic populations is highly warranted. Future work: our laboratory is focussing on performing the functional validation of the important metabolic pathways in ROP using suitable biochemical and cellular assays. Such studies definitely have a long way for developing better diagnostic and therapeutics for the prevention of childhood blindness contributed by ROP.

CONCLUSIONS

5. CONCLUSIONS

Aim 1: Investigation of aberrant MMP activation under hypoxic stress and its role as a predictive marker for ROP testing

1. Severity-dependent MMP activation was observed in ROP infants.
2. Elevation of MMP levels prior to the onset of ROP in preterm infants suggested its potential role as a disease marker.
3. A strong inverse correlation existed between MMP9 and Opticin protein levels in the vitreous humor of ROP patients.
4. *In-vitro* assays confirmed that reduced Opticin in ROP vitreous was secreted by the activated microglia and regulated by MMP9. In hypoxic stress, microglial cells exhibited upregulated inflammatory (MMP9) response, while Opticin levels were low.
5. Inhibiting MMP activity by doxycycline and EDTA *in-vitro*, rescued the expression of key signaling molecules and Opticin even under hypoxic stress.

Aim 2: Identification of rare and pathogenic gene variants in ROP conferring disease susceptibility

1. Whole exome sequencing led to the identification of several rare-pathogenic variations. Among them, 660 gene variants were found in severe ROP and 108 in AP ROP.
2. Further filtration indicated three novel pathogenic variants in *LRP4*, *GP1BA*, and *KIF17* genes that were common among the concordant and discordant twin pairs.
3. Overall, these gene variants were involved in *Wnt* signaling, inflammation, developmental processes, cell differentiation, cell-cell signaling, metal ion transport, regulation of neurogenesis, calcium-mediated signaling, neuron projection morphogenesis, astrocyte cell migration, purine nucleotide binding, neuron projection, ATP binding, MHC class II receptor activity and lipid metabolism.

Aim 3: Identifications of putative biological pathways in ROP

1. Hierarchical clustering analysis of significantly expressed (fold change >1.3, p-value 0.05) genes revealed differential gene expression across different stages of ROP (mild, severe, and APROP).
2. Significant upregulations were observed in *EGR2* gene of APROP patients along with other early developmental genes, including *FOSB* and *CYP2C8*.
3. The inflammatory pathways included toll-like receptor signaling pathway and NK cell regulatory genes (*HLA-DRB1* and *DRB5*), which were downregulated across all ROP stages.
4. *AXIN2*, a negative regulator of the *Wnt* signaling pathway, was downregulated in severe ROP cases.
5. Gene expression profiling supported the observations from genetic and proteomic studies pertaining to the involvement of inflammation, MAPK, *Wnt*, angiogenesis, metabolism of fatty acid, ECM, and arachidonic acid. It also provided a better understanding of the different pathways involved in ROP development and progression.

Aim 4: Identification of metabolic pathways involved in ROP pathogenesis

1. In ROP infants, 520 metabolites were identified to be significantly dysregulated (fold change >1.3 and p-value< 0.05).
2. The ROP vitreous metabolomic enrichment analysis revealed 45 pathways to be associated with disease pathogenesis. The metabolic pathways that were significantly dysregulated could be grouped into three categories, namely, amino acid, lipid, and bioenergetic metabolism.
3. The amino acid, lipid and bioenergetic metabolism also highlighted the potential role of macrophage/microglia polarization and their subsequent activation in ROP pathogenesis.

4. The upregulation of TCA cycle metabolite (succinate) activated the HIF-1 complex through a series of downstream signaling events, that further highlighted the prime role of hypoxia and retinal ischemia mediated pathogenesis in ROP.

CONTRIBUTIONS

6. Specific contributions of the study

1. The present study highlights the potential involvement of MMPs and its importance as a predictive marker for early detection of disease and progression.
2. The results further emphasizes the genetic susceptibility and pathways involved in the pathogenesis of proliferative ROP.
3. This study also demonstrated the role of several key metabolites in the vitreous of ROP babies and its potential implications in disease pathogenesis.

LIMITATIONS

7. Limitations

1. The Opticin and MMP expression levels as seen in fibrovascular membranes of ROP cases could not be quantitatively compared with age matched controls due to unavailability of retinal tissues.
2. Whole-exome sequencing could be performed only in a limited number of twin pairs based on their availability and requires validations in extended cohorts.
3. Due to unavailability of retinal tissue from the eyes of preterm infants with ROP and controls, the gene expression study was conducted using blood samples, which may not directly correlate with disease pathogenesis.
4. A further validation of the key metabolites and pathways in an extended cohort via targeted approaches could not be done due to unavailability of vitroeus humor from cases and controls.
5. The significant genetic pathways associated with ROP based on genomics, proteomics and metabolomics data could not be functionally validated due to lack of time and resources

FUTURE SCOPES

8. Future scopes

1. Establishing the potential implications of novel genes identified by WES in ROP pathogenesis
2. Determining the functional roles of genes in the significantly dysregulated pathways in ROP pathogenesis
3. Evaluation of the novel molecular targets as susceptible markers for ROP pathogenesis and progression.

REFERENCES

9. References

Aass, C., Norheim, I., Eriksen, E. F., Thorsby, P. M., & Pepaj, M. (2015). Single unit filter-aided method for fast proteomic analysis of tear fluid. *Anal Biochem, 480*, 1-5. doi:10.1016/j.ab.2015.04.002

Abdelsaid, M. A., Pillai, B. A., Matragoon, S., Prakash, R., Al-Shabrawey, M., & El-Remessy, A. B. (2010). Early intervention of tyrosine nitration prevents vaso-obliteration and neovascularization in ischemic retinopathy. *J Pharmacol Exp Ther, 332*(1), 125-134. doi:10.1124/jpet.109.157941

Abelson, M. B., Leonardi, A. A., Smith, L. M., Fregona, I. A., George, M. A., & Secchi, A. G. (1995). Histaminase activity in patients with vernal keratoconjunctivitis. *Ophthalmology, 102*(12), 1958-1963. doi:10.1016/s0161-6420(95)30768-3

Acera, A., Rocha, G., Vecino, E., Lema, I., & Duran, J. A. (2008). Inflammatory markers in the tears of patients with ocular surface disease. *Ophthalmic Res, 40*(6), 315-321. doi:10.1159/000150445

Aiello, L. P. (1997). Vascular endothelial growth factor. 20th-century mechanisms, 21st-century therapies. *Invest Ophthalmol Vis Sci, 38*(9), 1647-1652.

Alapure, B. V., Praveen, M. R., Gajjar, D., Vasavada, A. R., Rajkumar, S., & Johar, K. (2008). Matrix metalloproteinase-9 activity in human lens epithelial cells of cortical, posterior subcapsular, and nuclear cataracts. *J Cataract Refract Surg, 34*(12), 2063-2067. doi:10.1016/j.jcrs.2008.08.016

Alhouayek, M., Ameraoui, H., & Muccioli, G. G. (2021). Bioactive lipids in inflammatory bowel diseases - From pathophysiological alterations to therapeutic opportunities. *Biochim Biophys Acta Mol Cell Biol Lipids, 1866*(2), 158854. doi:10.1016/j.bbalip.2020.158854

Alliot, F., Godin, I., & Pessac, B. (1999). Microglia derive from progenitors, originating from the yolk sac, and which proliferate in the brain. *Brain Res Dev Brain Res, 117*(2), 145-152. doi:10.1016/s0165-3806(99)00113-3

Aluru, S. V., Agarwal, S., Srinivasan, B., Iyer, G. K., Rajappa, S. M., Tatu, U., . . . Narayanasamy, A. (2012). Lacrimal proline rich 4 (LPRR4) protein in the tear fluid is a potential biomarker of dry eye syndrome. *PLoS One, 7*(12), e51979. doi:10.1371/journal.pone.0051979

Amin, A. R., Attur, M. G., Thakker, G. D., Patel, P. D., Vyas, P. R., Patel, R. N., . . . Abramson, S. B. (1996). A novel mechanism of action of tetracyclines: effects on nitric oxide synthases. *Proc Natl Acad Sci U S A, 93*(24), 14014-14019. doi:10.1073/pnas.93.24.14014

Anand-Apte, B., & Hollyfield, J. G. (2010). *Developmental Anatomy of the Retinal and Choroidal Vasculature.*

Anderson, D. M. G., Messinger, J. D., Patterson, N. H., Rivera, E. S., Kotnala, A., Spraggins, J. M., . . . Schey, K. L. (2020). Lipid Landscape of the Human Retina and Supporting Tissues Revealed by High-Resolution Imaging Mass Spectrometry. *J Am Soc Mass Spectrom, 31*(12), 2426-2436. doi:10.1021/jasms.0c00119

Andrade, F., Sánchez-Ortega, A., Llarena, M., Pinar-Sueiro, S., Galdós, M., Goicolea, M. A., . . . Aldámiz-Echevarría, L. (2015). Metabolomics in non-arteritic anterior ischemic optic neuropathy patients by liquid chromatography–quadrupole time-of-flight mass spectrometry. *Metabolomics, 11*(2), 468-476. doi:10.1007/s11306-014-0710-6

Aragona, P., Aguennouz, M., Rania, L., Postorino, E., Sommario, M. S., Roszkowska, A. M., . . . Puzzolo, D. (2015). Matrix metalloproteinase 9 and transglutaminase 2 expression at the ocular surface in patients with different forms of dry eye disease. *Ophthalmology, 122*(1), 62-71. doi:10.1016/j.ophtha.2014.07.048

Argueso, P., Balaram, M., Spurr-Michaud, S., Keutmann, H. T., Dana, M. R., & Gipson, I. K. (2002). Decreased levels of the goblet cell mucin MUC5AC in tears of patients with Sjogren syndrome. *Invest Ophthalmol Vis Sci, 43*(4), 1004-1011.

Arroyo, A. G., & Iruela-Arispe, M. L. (2010). Extracellular matrix, inflammation, and the angiogenic response. *Cardiovasc Res, 86*(2), 226-235. doi:10.1093/cvr/cvq049

Ashwell, K. (1990). Microglia and cell death in the developing mouse cerebellum. *Brain Res Dev Brain Res, 55*(2), 219-230. doi:10.1016/0165-3806(90)90203-b

Ban, Y., & Rizzolo, L. J. (2000). Regulation of glucose transporters during development of the retinal pigment epithelium. *Brain Res Dev Brain Res, 121*(1), 89-95. doi:10.1016/s0165-3806(00)00028-6

Bar-Ilan, A., Naveh, N., Weissman, C., Belkin, M., & Schwartz, M. (1991). Prostaglandin E2 changes in the retina and optic nerve of an eye with injured optic nerve. *Neuroscience, 45*(1), 221-225. doi:10.1016/0306-4522(91)90118-8

Barba, I., Garcia-Ramirez, M., Hernandez, C., Alonso, M. A., Masmiquel, L., Garcia-Dorado, D., & Simo, R. (2010). Metabolic fingerprints of proliferative diabetic retinopathy: an 1H-NMR-based metabonomic approach using vitreous humor. *Invest Ophthalmol Vis Sci, 51*(9), 4416-4421. doi:10.1167/iovs.10-5348

Barbeau, D. J., La, K. T., Kim, D. S., Kerpedjieva, S. S., Shurin, G. V., & Tamama, K. (2014). Early growth response-2 signaling mediates immunomodulatory effects of human multipotential stromal cells. *Stem Cells Dev, 23*(2), 155-166. doi:10.1089/scd.2013.0194

Osborn, M. P., Park, Y., Parks, M. B., Burgess, L. G., Uppal, K., Lee, K., . . . Brantley, M. A., Jr. (2013). Metabolome-wide association study of neovascular age-related macular degeneration. *PLoS One, 8*(8), e72737. doi:10.1371/journal.pone.0072737

Barnett, J. M., McCollum, G. W., Fowler, J. A., Duan, J. J., Kay, J. D., Liu, R. Q., . . . Penn, J. S. (2007). Pharmacologic and genetic manipulation of MMP-2 and -9 affects retinal neovascularization in rodent models of OIR. *Invest Ophthalmol Vis Sci, 48*(2), 907-915. doi:10.1167/iovs.06-0082

Bhatt, L. K., & Addepalli, V. (2010). Attenuation of diabetic retinopathy by enhanced inhibition of MMP-2 and MMP-9 using aspirin and minocycline in streptozotocin-diabetic rats. *Am J Transl Res, 2*(2), 181-189.

Bishop, P. N. (2000). Structural macromolecules and supramolecular organisation of the vitreous gel. *Prog Retin Eye Res, 19*(3), 323-344. doi:10.1016/s1350-9462(99)00016-6

Bishop, P. N., Takanosu, M., Le Goff, M., & Mayne, R. (2002). The role of the posterior ciliary body in the biosynthesis of vitreous humour. *Eye (Lond), 16*(4), 454-460. doi:10.1038/sj.eye.6700199

Blencowe, H., Cousens, S., Chou, D., Oestergaard, M., Say, L., Moller, A. B., . . . Born Too Soon Preterm Birth Action, G. (2013). Born too soon: the global epidemiology of 15 million preterm births. *Reprod Health, 10 Suppl 1*, S2. doi:10.1186/1742-4755-10-S1-S2

Blencowe, H., Cousens, S., Oestergaard, M. Z., Chou, D., Moller, A. B., Narwal, R., . . . Lawn, J. E. (2012). National, regional, and worldwide estimates of preterm birth rates in the year 2010 with time trends since 1990 for selected countries: a systematic analysis and implications. *Lancet, 379*(9832), 2162-2172. doi:10.1016/S0140-6736(12)60820-4

Blencowe, H., Lee, A. C., Cousens, S., Bahalim, A., Narwal, R., Zhong, N., . . . Lawn, J. E. (2013). Preterm birth-associated neurodevelopmental impairment estimates at regional and global levels for 2010. *Pediatr Res, 74 Suppl 1*, 17-34. doi:10.1038/pr.2013.204

Blumenfeld, L. C., Siatkowski, R. M., Johnson, R. A., Feuer, W. J., & Flynn, J. T. (1998). Retinopathy of prematurity in multiple-gestation pregnancies. *Am J Ophthalmol, 125*(2), 197-203. doi:10.1016/s0002-9394(99)80092-0

Boehm, N., Funke, S., Wiegand, M., Wehrwein, N., Pfeiffer, N., & Grus, F. H. (2013). Alterations in the tear proteome of dry eye patients--a matter of the clinical phenotype. *Invest Ophthalmol Vis Sci, 54*(3), 2385-2392. doi:10.1167/iovs.11-8751

Boehm, N., Riechardt, A. I., Wiegand, M., Pfeiffer, N., & Grus, F. H. (2011). Proinflammatory cytokine profiling of tears from dry eye patients by means of antibody microarrays. *Invest Ophthalmol Vis Sci, 52*(10), 7725-7730. doi:10.1167/iovs.11-7266

Boersma, H. G., & van Bijsterveld, O. P. (1987). The lactoferrin test for the diagnosis of keratoconjunctivitis sicca in clinical practice. *Ann Ophthalmol, 19*(4), 152-154.

Boonstra, F. N., van Nouhuys, C. E., Schuil, J., de Wijs, I. J., van der Donk, K. P., Nikopoulos, K., . . . Hoefsloot, L. H. (2009). Clinical and molecular evaluation of probands and family members with familial exudative vitreoretinopathy. *Invest Ophthalmol Vis Sci, 50*(9), 4379-4385. doi:10.1167/iovs.08-3320

Brantley, M. A., Jr., Osborn, M. P., Sanders, B. J., Rezaei, K. A., Lu, P., Li, C., . . . Sternberg, P., Jr. (2012). Plasma biomarkers of oxidative stress and genetic variants in age-related macular degeneration. *Am J Ophthalmol, 153*(3), 460-467 e461. doi:10.1016/j.ajo.2011.08.033

Bringmann, A., Grosche, A., Pannicke, T., & Reichenbach, A. (2013). GABA and Glutamate Uptake and Metabolism in Retinal Glial (Muller) Cells. *Front Endocrinol (Lausanne), 4*, 48. doi:10.3389/fendo.2013.00048

Brooks, D. E., & Ollivier, F. J. (2004). Matrix metalloproteinase inhibition in corneal ulceration. *Vet Clin North Am Small Anim Pract, 34*(3), 611-622. doi:10.1016/j.cvsm.2003.12.005

Burgess, L. G., Uppal, K., Walker, D. I., Roberson, R. M., Tran, V., Parks, M. B., . . . Brantley, M. A., Jr. (2015). Metabolome-Wide Association Study of Primary Open Angle Glaucoma. *Invest Ophthalmol Vis Sci, 56*(8), 5020-5028. doi:10.1167/iovs.15-16702

Caceres, L. C., Bonacci, G. R., Sanchez, M. C., & Chiabrando, G. A. (2010). Activated alpha(2) macroglobulin induces matrix metalloproteinase 9 expression by low-density lipoprotein receptor-related protein 1 through MAPK-ERK1/2 and NF-kappaB activation in macrophage-derived cell lines. *J Cell Biochem, 111*(3), 607-617. doi:10.1002/jcb.22737

Cai, K., & Wei, R. (2013). Interleukin-7 expression in tears and orbital tissues of patients with Graves' ophthalmopathy. *Endocrine, 44*(1), 140-144. doi:10.1007/s12020-012-9840-7

Campbell, K. (1951). Intensive oxygen therapy as a possible cause of retrolental fibroplasia; a clinical approach. *Med J Aust, 2*(2), 48-50.

Campochiaro, P. A. (2015). Molecular pathogenesis of retinal and choroidal vascular diseases. *Prog Retin Eye Res, 49*, 67-81. doi:10.1016/j.preteyeres.2015.06.002

Carmeliet, P. (2003). Angiogenesis in health and disease. *Nat Med, 9*(6), 653-660. doi:10.1038/nm0603-653

Chandra, A., Lan, S., Zhu, J., Siclari, V. A., & Qin, L. (2013). Epidermal growth factor receptor (EGFR) signaling promotes proliferation and survival in osteoprogenitors by increasing early growth response 2 (EGR2) expression. *J Biol Chem, 288*(28), 20488-20498. doi:10.1074/jbc.M112.447250

Chau, K. Y., Sivaprasad, S., Patel, N., Donaldson, T. A., Luthert, P. J., & Chong, N. V. (2008). Plasma levels of matrix metalloproteinase-2 and -9 (MMP-2 and MMP-9) in age-related macular degeneration. *Eye (Lond), 22*(6), 855-859.

Chen, L., Cheng, C. Y., Choi, H., Ikram, M. K., Sabanayagam, C., Tan, G. S., . . . Wong, T. Y. (2016). Plasma Metabonomic Profiling of Diabetic Retinopathy. *Diabetes, 65*(4), 1099-1108. doi:10.2337/db15-0661

Chen, L., Yang, P., & Kijlstra, A. (2002). Distribution, markers, and functions of retinal microglia. *Ocul Immunol Inflamm, 10*(1), 27-39. doi:10.1076/ocii.10.1.27.10328

Chhadva, P., Lee, T., Sarantopoulos, C. D., Hackam, A. S., McClellan, A. L., Felix, E. R., . . . Galor, A. (2015). Human Tear Serotonin Levels Correlate with Symptoms and Signs of Dry Eye. *Ophthalmology, 122*(8), 1675-1680. doi:10.1016/j.ophtha.2015.04.010

Chiarugi, A., Rapizzi, E., Moroni, F., & Moroni, F. (1999). The kynurenine metabolic pathway in the eye: studies on 3-hydroxykynurenine, a putative cataractogenic compound. *FEBS Lett, 453*(1-2), 197-200. doi:10.1016/s0014-5793(99)00724-3

Chiurchiu, V., Leuti, A., & Maccarrone, M. (2018). Bioactive Lipids and Chronic Inflammation: Managing the Fire Within. *Front Immunol, 9*, 38. doi:10.3389/fimmu.2018.00038

Choi, W., Li, Z., Oh, H. J., Im, S. K., Lee, S. H., Park, S. H., . . . Yoon, K. C. (2012). Expression of CCR5 and its ligands CCL3, -4, and -5 in the tear film and ocular surface of patients with dry eye disease. *Curr Eye Res, 37*(1), 12-17. doi:10.3109/02713683.2011.622852

Cocho, L., Fernandez, I., Calonge, M., Martinez, V., Gonzalez-Garcia, M. J., Caballero, D., . . . Enriquez-de-Salamanca, A. (2016). Biomarkers in Ocular Chronic Graft Versus Host Disease: Tear Cytokine- and Chemokine-Based Predictive Model. *Invest Ophthalmol Vis Sci, 57*(2), 746-758. doi:10.1167/iovs.15-18615

Paris, L. P., Johnson, C. H., Aguilar, E., Usui, Y., Cho, K., Hoang, L. T., . . . Friedlander, M. (2016). Global metabolomics reveals metabolic dysregulation in ischemic retinopathy. *Metabolomics, 12*, 15. doi:10.1007/s11306-015-0877-5

Cooke, R. W., Drury, J. A., Mountford, R., & Clark, D. (2004). Genetic polymorphisms and retinopathy of prematurity. *Invest Ophthalmol Vis Sci, 45*(6), 1712-1715. doi:10.1167/iovs.03-1303

Coral, K., Angayarkanni, N., Madhavan, J., Bharathselvi, M., Ramakrishnan, S., Nandi, K., . . . Krishnakumar, S. (2008). Lysyl oxidase activity in the ocular tissues and the role of LOX in proliferative diabetic retinopathy and rhegmatogenous retinal detachment. *Invest Ophthalmol Vis Sci, 49*(11), 4746-4752. doi:10.1167/iovs.07-1550

Csosz, E., Boross, P., Csutak, A., Berta, A., Toth, F., Poliska, S., . . . Tozser, J. (2012). Quantitative analysis of proteins in the tear fluid of patients with diabetic retinopathy. *J Proteomics, 75*(7), 2196-2204. doi:10.1016/j.jprot.2012.01.019

Dagher, Z., Ruderman, N., Tornheim, K., & Ido, Y. (2001). Acute regulation of fatty acid oxidation and amp-activated protein kinase in human umbilical vein endothelial cells. *Circ Res, 88*(12), 1276-1282. doi:10.1161/hh1201.092998

Dailey, W. A., Gryc, W., Garg, P. G., & Drenser, K. A. (2015). Frizzled-4 Variations Associated with Retinopathy and Intrauterine Growth Retardation: A Potential Marker for Prematurity and Retinopathy. *Ophthalmology, 122*(9), 1917-1923. doi:10.1016/j.ophtha.2015.05.036

Dammann, O. (2010). Inflammation and retinopathy of prematurity. *Acta Paediatr, 99*(7), 975-977. doi:10.1111/j.1651-2227.2010.01836.x

Darougar, S., Treharne, J. D., Minassian, D., El-Sheikh, H., Dines, R. J., & Jones, B. R. (1978). Rapid serological test for diagnosis of chlamydial ocular infections. *Br J Ophthalmol, 62*(8), 503-508. doi:10.1136/bjo.62.8.503

Davignon, J., & Ganz, P. (2004). Role of endothelial dysfunction in atherosclerosis. *Circulation, 109*(23 Suppl 1), III27-32. doi:10.1161/01.CIR.0000131515.03336.f8

De Bock, K., Georgiadou, M., Schoors, S., Kuchnio, A., Wong, B. W., Cantelmo, A. R., . . . Carmeliet, P. (2013). Role of PFKFB3-driven glycolysis in vessel sprouting. *Cell, 154*(3), 651-663. doi:10.1016/j.cell.2013.06.037

Devraj, G., Beerlage, C., Brune, B., & Kempf, V. A. (2017). Hypoxia and HIF-1 activation in bacterial infections. *Microbes Infect, 19*(3), 144-156. doi:10.1016/j.micinf.2016.11.003

Dickinson, J. L., Sale, M. M., Passmore, A., FitzGerald, L. M., Wheatley, C. M., Burdon, K. P., . . . Mackey, D. A. (2006). Mutations in the NDP gene: contribution to Norrie disease, familial exudative vitreoretinopathy and retinopathy of prematurity. *Clin Exp Ophthalmol, 34*(7), 682-688. doi:10.1111/j.1442-9071.2006.01314.x

Drenser, K. A., Dailey, W., Vinekar, A., Dalal, K., Capone, A., Jr., & Trese, M. T. (2009). Clinical presentation and genetic correlation of patients with mutations affecting the FZD4 gene. *Arch Ophthalmol, 127*(12), 1649-1654. doi:10.1001/archophthalmol.2009.322

Duester, G. (2008). Retinoic acid synthesis and signaling during early organogenesis. *Cell, 134*(6), 921-931. doi:10.1016/j.cell.2008.09.002

Edwards, G., Aribindi, K., Guerra, Y., & Bhattacharya, S. K. (2014). Sphingolipids and ceramides of mouse aqueous humor: Comparative profiles from normotensive and hypertensive DBA/2J mice. *Biochimie, 105*, 99-109. doi:10.1016/j.biochi.2014.06.019

Eelen, G., de Zeeuw, P., Treps, L., Harjes, U., Wong, B. W., & Carmeliet, P. (2018). Endothelial Cell Metabolism. *Physiol Rev, 98*(1), 3-58. doi:10.1152/physrev.00001.2017

Pietrowska, K., Dmuchowska, D. A., Samczuk, P., Kowalczyk, T., Krasnicki, P., Wojnar, M., . . . Ciborowski, M. (2017). LC-MS-Based Metabolic Fingerprinting of Aqueous Humor. *J Anal Methods Chem, 2017*, 6745932. doi:10.1155/2017/6745932

Ells, A., Guernsey, D. L., Wallace, K., Zheng, B., Vincer, M., Allen, A., . . . Robitaille, J. M. (2010). Severe retinopathy of prematurity associated with FZD4 mutations. *Ophthalmic Genet, 31*(1), 37-43. doi:10.3109/13816810903479834

Emsley, H. C., Wardle, S. P., Sims, D. G., Chiswick, M. L., & D'Souza, S. W. (1998). Increased survival and deteriorating developmental outcome in 23 to 25 week old gestation infants, 1990-4 compared with 1984-9. *Arch Dis Child Fetal Neonatal Ed, 78*(2), F99-104. doi:10.1136/fn.78.2.f99

Enriquez-de-Salamanca, A., Castellanos, E., Stern, M. E., Fernandez, I., Carreno, E., Garcia-Vazquez, C., . . . Calonge, M. (2010). Tear cytokine and chemokine analysis and clinical correlations in evaporative-type dry eye disease. *Mol Vis, 16*, 862-873.

Federici, T. J. (2011). The non-antibiotic properties of tetracyclines: clinical potential in ophthalmic disease. *Pharmacol Res, 64*(6), 614-623. doi:10.1016/j.phrs.2011.06.013

Fellows, R. R., McGregor, M. L., Bremer, D. L., Rogers, G. L., & Miller, D. (1995). Retinopathy of prematurity in discordant twins. *J Pediatr Ophthalmol Strabismus, 32*(2), 86-88.

Ferre-Fernandez, J. J., Aroca-Aguilar, J. D., Medina-Trillo, C., Bonet-Fernandez, J. M., Mendez-Hernandez, C. D., Morales-Fernandez, L., . . . Escribano, J. (2017). Whole-Exome Sequencing of Congenital Glaucoma Patients Reveals Hypermorphic Variants in GPATCH3, a New Gene Involved in Ocular and Craniofacial Development. *Sci Rep, 7*, 46175. doi:10.1038/srep46175

Fliesler, S. J., & Anderson, R. E. (1983). Chemistry and metabolism of lipids in the vertebrate retina. *Prog Lipid Res, 22*(2), 79-131. doi:10.1016/0163-7827(83)90004-8

Forrester, J. V., Kuffova, L., & Delibegovic, M. (2020). The Role of Inflammation in Diabetic Retinopathy. *Front Immunol, 11*, 583687. doi:10.3389/fimmu.2020.583687

Forstermann, U., & Munzel, T. (2006). Endothelial nitric oxide synthase in vascular disease: from marvel to menace. *Circulation, 113*(13), 1708-1714. doi:10.1161/CIRCULATIONAHA.105.602532

Fox, A. C., Reed, G. E., Meilman, H., & Silk, B. B. (1979). Release of nucleosides from canine and human hearts as an index of prior ischemia. *Am J Cardiol, 43*(1), 52-58. doi:10.1016/0002-9149(79)90044-4

Franck, R. W. (2012). C-Galactosylceramide: Synthesis and Immunology. *C R Chim, 15*(1), 46-56. doi:10.1016/j.crci.2011.05.006

Friedman, J. S., Faucher, M., Hiscott, P., Biron, V. L., Malenfant, M., Turcotte, P., . . . Walter, M. A. (2002). Protein localization in the human eye and genetic screen of opticin. *Hum Mol Genet, 11*(11), 1333-1342. doi:10.1093/hmg/11.11.1333

Friling, R., Rosen, S. D., Monos, T., Karplus, M., & Yassur, Y. (1997). Retinopathy of prematurity in multiple-gestation, very low birth weight infants. *J Pediatr Ophthalmol Strabismus, 34*(2), 96-100.

Fuchs, D., Tang, X., Johnsson, A. K., Dahlen, S. E., Hamberg, M., & Wheelock, C. E. (2020). Eosinophils synthesize trihydroxyoctadecenoic acids (TriHOMEs) via a 15-lipoxygenase dependent process. *Biochim Biophys Acta Mol Cell Biol Lipids, 1865*(4), 158611. doi:10.1016/j.bbalip.2020.158611

Fujino, T., Asaba, H., Kang, M. J., Ikeda, Y., Sone, H., Takada, S., . . . Yamamoto, T. T. (2003). Low-density lipoprotein receptor-related protein 5 (LRP5) is essential for normal cholesterol metabolism and glucose-induced insulin secretion. *Proc Natl Acad Sci U S A, 100*(1), 229-234. doi:10.1073/pnas.0133792100

Galbis-Estrada, C., Martinez-Castillo, S., Morales, J. M., Vivar-Llopis, B., Monleon, D., Diaz-Llopis, M., & Pinazo-Duran, M. D. (2014). Differential effects of dry eye disorders on metabolomic profile by 1H nuclear magnetic resonance spectroscopy. *Biomed Res Int, 2014*, 542549. doi:10.1155/2014/542549

Gantner, M. L., Eade, K., Wallace, M., Handzlik, M. K., Fallon, R., Trombley, J., . . . Friedlander, M. (2019). Serine and Lipid Metabolism in Macular Disease and Peripheral Neuropathy. *N Engl J Med, 381*(15), 1422-1433. doi:10.1056/NEJMoa1815111

Garrison, A. M., Parrott, J. M., Tunon, A., Delgado, J., Redus, L., & O'Connor, J. C. (2018). Kynurenine pathway metabolic balance influences microglia activity: Targeting kynurenine monooxygenase to dampen neuroinflammation. *Psychoneuroendocrinology, 94*, 1-10. doi:10.1016/j.psyneuen.2018.04.019

Gertsman, I., & Barshop, B. A. (2018). Promises and pitfalls of untargeted metabolomics. *J Inherit Metab Dis, 41*(3), 355-366. doi:10.1007/s10545-017-0130-7

Haines, N. R., Manoharan, N., Olson, J. L., D'Alessandro, A., & Reisz, J. A. (2018). Metabolomics Analysis of Human Vitreous in Diabetic Retinopathy and Rhegmatogenous Retinal Detachment. *J Proteome Res, 17*(7), 2421-2427. doi:10.1021/acs.jproteome.8b00169

Ghaffariyeh, A., Honarpisheh, N., Shakiba, Y., Puyan, S., Chamacham, T., Zahedi, F., & Zarrineghbal, M. (2009). Brain-derived neurotrophic factor in patients with normal-tension glaucoma. *Optometry, 80*(11), 635-638. doi:10.1016/j.optm.2008.09.014

Ghanem, A. A., Arafa, L. F., & El-Baz, A. (2011). Connective tissue growth factor and tissue inhibitor of matrix metalloproteinase-2 in patients with exfoliative glaucoma. *Curr Eye Res, 36*(6), 540-545. doi:10.3109/02713683.2011.565541

Gilbert, C. (2008). Retinopathy of prematurity: a global perspective of the epidemics, population of babies at risk and implications for control. *Early Hum Dev, 84*(2), 77-82. doi:10.1016/j.earlhumdev.2007.11.009

Gilbert, C., Fielder, A., Gordillo, L., Quinn, G., Semiglia, R., Visintin, P., . . . International, N. O. R. O. P. G. (2005). Characteristics of infants with severe retinopathy of prematurity in countries with low, moderate, and high levels of development: implications for screening programs. *Pediatrics, 115*(5), e518-525. doi:10.1542/peds.2004-1180

Goncu, T., Akal, A., Adibelli, F. M., Cakmak, S., Sezen, H., & Yilmaz, O. F. (2015). Tear Film and Serum Prolidase Activity and Oxidative Stress in Patients With Keratoconus. *Cornea, 34*(9), 1019-1023. doi:10.1097/ICO.0000000000000510

Gong, Y., Slee, R. B., Fukai, N., Rawadi, G., Roman-Roman, S., Reginato, A. M., . . . Osteoporosis-Pseudoglioma Syndrome Collaborative, G. (2001). LDL receptor-related protein 5 (LRP5) affects bone accrual and eye development. *Cell, 107*(4), 513-523. doi:10.1016/s0092-8674(01)00571-2

Gonzalez-Fernandez. (2011). *Pediatric Retina* (J. Reynolds & S. E. Olitsky Eds.). Heidelberg: Springer, Berlin.

Gonzalez-Fernandez, F. (2011). Development of the Retina. In J. Reynolds & S. Olitsky (Eds.), *Pediatric Retina* (pp. 1-37). Berlin, Heidelberg: Springer Berlin Heidelberg.

Goren, M. B., & Goren, S. B. (1988). Diagnostic tests in patients with symptoms of keratoconjunctivitis sicca. *Am J Ophthalmol, 106*(5), 570-574. doi:10.1016/0002-9394(88)90587-9

Granchi, C., Bertini, S., Macchia, M., & Minutolo, F. (2010). Inhibitors of lactate dehydrogenase isoforms and their therapeutic potentials. *Curr Med Chem, 17*(7), 672-697. doi:10.2174/092986710790416263

Grus, F. H., Podust, V. N., Bruns, K., Lackner, K., Fu, S., Dalmasso, E. A., . . . Pfeiffer, N. (2005). SELDI-TOF-MS ProteinChip array profiling of tears from patients with dry eye. *Invest Ophthalmol Vis Sci, 46*(3), 863-876. doi:10.1167/iovs.04-0448

Guo, D., Murdoch, C. E., Xu, H., Shi, H., Duan, D. D., Ahmed, A., & Gu, Y. (2017). Vascular endothelial growth factor signaling requires glycine to promote angiogenesis. *Sci Rep, 7*(1), 14749. doi:10.1038/s41598-017-15246-3

Guo, Q., Huang, H., Pi, Y., & Zhang, H. (2014). Evaluation of tear malate dehydrogenase 2 in mild dry eye disease. *Eye Sci, 29*(4), 204-208.

Haider, M. Z., Devarajan, L. V., Al-Essa, M., & Kumar, H. (2002a). Angiotensin-converting enzyme gene insertion/deletion polymorphism in Kuwaiti children with retinopathy of prematurity. *Biol Neonate, 82*(2), 84-88. doi:10.1159/000063092

Haider, M. Z., Devarajan, L. V., Al-Essa, M., & Kumar, H. (2002b). A C597-->A polymorphism in the Norrie disease gene is associated with advanced retinopathy of prematurity in premature Kuwaiti infants. *J Biomed Sci, 9*(4), 365-370. doi:10.1007/BF02256593

Hajsl, M., Hlavackova, A., Broulikova, K., Sramek, M., Maly, M., Dyr, J. E., & Suttnar, J. (2020). Tryptophan Metabolism, Inflammation, and Oxidative Stress in Patients with Neurovascular Disease. *Metabolites, 10*(5). doi:10.3390/metabo10050208

Hall, J. G., Freedman, S. F., & Kylstra, J. A. (1995). Clinical course and systemic correlates of retinopathy of prematurity in quintuplets. *Am J Ophthalmol, 119*(5), 658-660. doi:10.1016/s0002-9394(14)70233-8

Hamm-Alvarez, S. F., Janga, S. R., Edman, M. C., Madrigal, S., Shah, M., Frousiakis, S. E., . . . Stohl, W. (2014). Tear cathepsin S as a candidate biomarker for Sjogren's syndrome. *Arthritis Rheumatol, 66*(7), 1872-1881. doi:10.1002/art.38633

Hartnett, M. E. (2010). The effects of oxygen stresses on the development of features of severe retinopathy of prematurity: knowledge from the 50/10 OIR model. *Doc Ophthalmol, 120*(1), 25-39. doi:10.1007/s10633-009-9181-x

Hartnett, M. E., & Cotten, C. M. (2015). Genomics in the neonatal nursery: Focus on ROP. *Semin Perinatol, 39*(8), 604-610. doi:10.1053/j.semperi.2015.09.007

Hartnett, M. E., Morrison, M. A., Smith, S., Yanovitch, T. L., Young, T. L., Colaizy, T., . . . Genomics, S. (2014). Genetic variants associated with severe retinopathy of prematurity in extremely low birth weight infants. *Invest Ophthalmol Vis Sci, 55*(10), 6194-6203. doi:10.1167/iovs.14-14841

Hartnett, M. E., & Penn, J. S. (2012). Mechanisms and management of retinopathy of prematurity. *N Engl J Med, 367*(26), 2515-2526. doi:10.1056/NEJMra1208129

Hatfield, E. M. (1972). Blindness in infants and young children. *Sight Sav Rev, 42*(2), 69-89.

Hayakawa, Y., Takeda, K., Yagita, H., Smyth, M. J., Van Kaer, L., Okumura, K., & Saiki, I. (2002). IFN-gamma-mediated inhibition of tumor angiogenesis by natural killer T-cell ligand, alpha-galactosylceramide. *Blood, 100*(5), 1728-1733.

Hemler, M. E. (2005). Tetraspanin functions and associated microdomains. *Nat Rev Mol Cell Biol, 6*(10), 801-811. doi:10.1038/nrm1736

Hidalgo, M., & Eckhardt, S. G. (2001). Development of matrix metalloproteinase inhibitors in cancer therapy. *J Natl Cancer Inst, 93*(3), 178-193. doi:10.1093/jnci/93.3.178

Hindson, V. J., Gallagher, J. T., Halfter, W., & Bishop, P. N. (2005). Opticin binds to heparan and chondroitin sulfate proteoglycans. *Invest Ophthalmol Vis Sci, 46*(12), 4417-4423. doi:10.1167/iovs.05-0883

Hiraoka, M., Berinstein, D. M., Trese, M. T., & Shastry, B. S. (2001). Insertion and deletion mutations in the dinucleotide repeat region of the Norrie disease gene in patients with advanced retinopathy of prematurity. *J Hum Genet, 46*(4), 178-181. doi:10.1007/s100380170085

Hiraoka, M., Takahashi, H., Orimo, H., Hiraoka, M., Ogata, T., & Azuma, N. (2010). Genetic screening of Wnt signaling factors in advanced retinopathy of prematurity. *Mol Vis, 16*, 2572-2577.

Hnia, K., Gayraud, J., Hugon, G., Ramonatxo, M., De La Porte, S., Matecki, S., & Mornet, D. (2008). L-arginine decreases inflammation and modulates the nuclear factor-kappaB/matrix metalloproteinase cascade in mdx muscle fibers. *Am J Pathol, 172*(6), 1509-1519. doi:10.2353/ajpath.2008.071009

Holmstrom, G., Broberger, U., & Thomassen, P. (1998). Neonatal risk factors for retinopathy of prematurity--a population-based study. *Acta Ophthalmol Scand, 76*(2), 204-207. doi:10.1034/j.1600-0420.1998.760216.x

Huang, C., Xie, L., Wu, Z., Cao, Y., Zheng, Y., Pang, C. P., & Zhang, M. (2018). Detection of mutations in MYOC, OPTN, NTF4, WDR36 and CYP1B1 in Chinese juvenile onset open-angle glaucoma using exome sequencing. *Sci Rep, 8*(1), 4498. doi:10.1038/s41598-018-22337-2

Kowalczuk, L., Matet, A., Dor, M., Bararpour, N., Daruich, A., Dirani, A., . . . Turck, N. (2018). Proteome and Metabolome of Subretinal Fluid in Central Serous Chorioretinopathy and Rhegmatogenous Retinal Detachment: A Pilot Case Study. *Transl Vis Sci Technol, 7*(1), 3. doi:10.1167/tvst.7.1.3

Huang, D., Luo, Q., Yang, H., & Mao, Y. (2014). Changes of lacrimal gland and tear inflammatory cytokines in thyroid-associated ophthalmopathy. *Invest Ophthalmol Vis Sci, 55*(8), 4935-4943. doi:10.1167/iovs.13-13704

Huang, J. F., Zhang, Y., Rittenhouse, K. D., Pickering, E. H., & McDowell, M. T. (2012). Evaluations of tear protein markers in dry eye disease: repeatability of measurement and correlation with disease. *Invest Ophthalmol Vis Sci, 53*(8), 4556-4564. doi:10.1167/iovs.11-9054

Hume, D. A., Perry, V. H., & Gordon, S. (1983). Immunohistochemical localization of a macrophage-specific antigen in developing mouse retina: phagocytosis of dying neurons and differentiation of microglial cells to form a regular array in the plexiform layers. *J Cell Biol, 97*(1), 253-257. doi:10.1083/jcb.97.1.253

Hussain, A. A., Lee, Y., Zhang, J. J., & Marshall, J. (2011). Disturbed matrix metalloproteinase activity of Bruch's membrane in age-related macular degeneration. *Invest Ophthalmol Vis Sci, 52*(7), 4459-4466. doi:10.1167/iovs.10-6678

Hutcheson, K. A., Paluru, P. C., Bernstein, S. L., Koh, J., Rappaport, E. F., Leach, R. A., & Young, T. L. (2005). Norrie disease gene sequence variants in an ethnically diverse population with retinopathy of prematurity. *Mol Vis, 11*, 501-508.

Ihnatko, R., Eden, U., Lagali, N., Dellby, A., & Fagerholm, P. (2013). Analysis of protein composition and protein expression in the tear fluid of patients with congenital aniridia. *J Proteomics, 94*, 78-88. doi:10.1016/j.jprot.2013.09.003

Insuela, D. B. R., Ferrero, M. R., Coutinho, D. S., Martins, M. A., & Carvalho, V. F. (2020). Could Arachidonic Acid-Derived Pro-Resolving Mediators Be a New Therapeutic Strategy for Asthma Therapy? *Front Immunol, 11*, 580598. doi:10.3389/fimmu.2020.580598

Iozzo, R. V. (1999). The biology of the small leucine-rich proteoglycans. Functional network of interactive proteins. *J Biol Chem, 274*(27), 18843-18846. doi:10.1074/jbc.274.27.18843

Ishikawa, K., Yoshida, S., Kadota, K., Nakamura, T., Niiro, H., Arakawa, S., . . . Ishibashi, T. (2010). Gene expression profile of hyperoxic and hypoxic retinas in a mouse model of oxygen-induced retinopathy. *Invest Ophthalmol Vis Sci, 51*(8), 4307-4319. doi:10.1167/iovs.09-4605

Jadhav, A. P., Roesch, K., & Cepko, C. L. (2009). Development and neurogenic potential of Muller glial cells in the vertebrate retina. *Prog Retin Eye Res, 28*(4), 249-262. doi:10.1016/j.preteyeres.2009.05.002

Javadiyan, S., Burdon, K. P., Whiting, M. J., Abhary, S., Straga, T., Hewitt, A. W., . . . Craig, J. E. (2012). Elevation of serum asymmetrical and symmetrical dimethylarginine in patients with advanced glaucoma. *Invest Ophthalmol Vis Sci, 53*(4), 1923-1927. doi:10.1167/iovs.11-8420

Jonat, C., Chung, F. Z., & Baragi, V. M. (1996). Transcriptional downregulation of stromelysin by tetracycline. *J Cell Biochem, 60*(3), 341-347. doi:10.1002/(sici)1097-4644(19960301)60:3<341::aid-jcb6>3.0.co;2-w

Junge, H. J., Yang, S., Burton, J. B., Paes, K., Shu, X., French, D. M., . . . Ye, W. (2009). TSPAN12 regulates retinal vascular development by promoting Norrin- but not Wnt-induced FZD4/beta-catenin signaling. *Cell, 139*(2), 299-311. doi:10.1016/j.cell.2009.07.048

Kaiser, R. S., Trese, M. T., Williams, G. A., & Cox, M. S., Jr. (2001). Adult retinopathy of prematurity: outcomes of rhegmatogenous retinal detachments and retinal tears. *Ophthalmology, 108*(9), 1647-1653. doi:10.1016/s0161-6420(01)00660-1

Karamichos, D., Zieske, J. D., Sejersen, H., Sarker-Nag, A., Asara, J. M., & Hjortdal, J. (2015). Tear metabolite changes in keratoconus. *Exp Eye Res, 132*, 1-8. doi:10.1016/j.exer.2015.01.007

Kaur, C., Rathnasamy, G., & Ling, E. A. (2013). Roles of activated microglia in hypoxia induced neuroinflammation in the developing brain and the retina. *J Neuroimmune Pharmacol, 8*(1), 66-78. doi:10.1007/s11481-012-9347-2

Kettenmann, H., Hanisch, U. K., Noda, M., & Verkhratsky, A. (2011). Physiology of microglia. *Physiol Rev, 91*(2), 461-553. doi:10.1152/physrev.00011.2010

Kim, H. J., Kim, P. K., Yoo, H. S., & Kim, C. W. (2012). Comparison of tear proteins between healthy and early diabetic retinopathy patients. *Clin Biochem, 45*(1-2), 60-67. doi:10.1016/j.clinbiochem.2011.10.006

Kim, J. H., Yu, Y. S., Kim, J., & Park, S. S. (2002). Mutations of the Norrie gene in Korean ROP infants. *Korean J Ophthalmol, 16*(2), 93-96. doi:10.3341/kjo.2002.16.2.93

Kinsey, V. E. (1956). Retrolental fibroplasia; cooperative study of retrolental fibroplasia and the use of oxygen. *AMA Arch Ophthalmol, 56*(4), 481-543.

Kirikoshi, H., Sagara, N., Koike, J., Tanaka, K., Sekihara, H., Hirai, M., & Katoh, M. (1999). Molecular cloning and characterization of human Frizzled-4 on chromosome 11q14-q21. *Biochem Biophys Res Commun, 264*(3), 955-961. doi:10.1006/bbrc.1999.1612

Klagsbrun, M., & Moses, M. A. (1999). Molecular angiogenesis. *Chem Biol, 6*(8), R217-224. doi:10.1016/S1074-5521(99)80081-7

Kolozsvari, B. L., Petrovski, G., Gogolak, P., Rajnavolgyi, E., Toth, F., Berta, A., & Fodor, M. (2014). Association between mediators in the tear fluid and the severity of keratoconus. *Ophthalmic Res, 51*(1), 46-51. doi:10.1159/000351626

Kondo, H., Kusaka, S., Yoshinaga, A., Uchio, E., Tawara, A., & Tahira, T. (2013). Genetic variants of FZD4 and LRP5 genes in patients with advanced retinopathy of prematurity. *Mol Vis, 19*, 476-485.

Kong, L., Fry, M., Al-Samarraie, M., Gilbert, C., & Steinkuller, P. G. (2012). An update on progress and the changing epidemiology of causes of childhood blindness worldwide. *J AAPOS, 16*(6), 501-507. doi:10.1016/j.jaapos.2012.09.004

Konnecke, H., & Bechmann, I. (2013). The role of microglia and matrix metalloproteinases involvement in neuroinflammation and gliomas. *Clin Dev Immunol, 2013*, 914104. doi:10.1155/2013/914104

Korpos, E., Wu, C., & Sorokin, L. (2009). Multiple roles of the extracellular matrix in inflammation. *Curr Pharm Des, 15*(12), 1349-1357. doi:10.2174/138161209787846685

Koziel, A., Woyda-Ploszczyca, A., Kicinska, A., & Jarmuszkiewicz, W. (2012). The influence of high glucose on the aerobic metabolism of endothelial EA.hy926 cells. *Pflugers Arch, 464*(6), 657-669. doi:10.1007/s00424-012-1156-1

Krock, B. L., Skuli, N., & Simon, M. C. (2011). Hypoxia-induced angiogenesis: good and evil. *Genes Cancer, 2*(12), 1117-1133. doi:10.1177/1947601911423654

Krutzfeldt, A., Spahr, R., Mertens, S., Siegmund, B., & Piper, H. M. (1990). Metabolism of exogenous substrates by coronary endothelial cells in culture. *J Mol Cell Cardiol, 22*(12), 1393-1404. doi:10.1016/0022-2828(90)90984-a

Kumagai, A. K., Vinores, S. A., & Pardridge, W. M. (1996). Pathological upregulation of inner blood-retinal barrier Glut1 glucose transporter expression in diabetes mellitus. *Brain Res, 706*(2), 313-317. doi:10.1016/0006-8993(95)01335-0

Lam, H., Bleiden, L., de Paiva, C. S., Farley, W., Stern, M. E., & Pflugfelder, S. C. (2009). Tear cytokine profiles in dysfunctional tear syndrome. *Am J Ophthalmol, 147*(2), 198-205 e191. doi:10.1016/j.ajo.2008.08.032

Lambert, V., Munaut, C., Jost, M., Noel, A., Werb, Z., Foidart, J. M., & Rakic, J. M. (2002). Matrix metalloproteinase-9 contributes to choroidal neovascularization. *Am J Pathol, 161*(4), 1247-1253. doi:10.1016/S0002-9440(10)64401-X

Lambert, V., Wielockx, B., Munaut, C., Galopin, C., Jost, M., Itoh, T., . . . Rakic, J. M. (2003). MMP-2 and MMP-9 synergize in promoting choroidal neovascularization. *FASEB J, 17*(15), 2290-2292. doi:10.1096/fj.03-0113fje

Lambiase, A., Micera, A., Sacchetti, M., Cortes, M., Mantelli, F., & Bonini, S. (2011). Alterations of tear neuromediators in dry eye disease. *Arch Ophthalmol, 129*(8), 981-986. doi:10.1001/archophthalmol.2011.200

Langer, H. F., Chung, K. J., Orlova, V. V., Choi, E. Y., Kaul, S., Kruhlak, M. J., . . . Chavakis, T. (2010). Complement-mediated inhibition of neovascularization reveals a point of convergence between innate immunity and angiogenesis. *Blood, 116*(22), 4395-4403. doi:10.1182/blood-2010-01-261503

Lashkari, K., Hirose, T., Yazdany, J., McMeel, J. W., Kazlauskas, A., & Rahimi, N. (2000). Vascular endothelial growth factor and hepatocyte growth factor levels are differentially elevated in patients with advanced retinopathy of prematurity. *Am J Pathol, 156*(4), 1337-1344. doi:10.1016/S0002-9440(10)65004-3

Le Goff, M. M., & Bishop, P. N. (2008). Adult vitreous structure and postnatal changes. *Eye (Lond), 22*(10), 1214-1222. doi:10.1038/eye.2008.21

Le Goff, M. M., Lu, H., Ugarte, M., Henry, S., Takanosu, M., Mayne, R., & Bishop, P. N. (2012). The vitreous glycoprotein opticin inhibits preretinal neovascularization. *Invest Ophthalmol Vis Sci, 53*(1), 228-234. doi:10.1167/iovs.11-8514

Le Goff, M. M., Sutton, M. J., Slevin, M., Latif, A., Humphries, M. J., & Bishop, P. N. (2012). Opticin exerts its anti-angiogenic activity by regulating extracellular matrix adhesiveness. *J Biol Chem, 287*(33), 28027-28036. doi:10.1074/jbc.M111.331157

Leaders. (1958). Leaders in Research. *The Lancet, 271*(7026), 893. doi:10.1016/s0140-6736(58)91638-6

Lee, S. Y., Han, S. J., Nam, S. M., Yoon, S. C., Ahn, J. M., Kim, T. I., . . . Seo, K. Y. (2013). Analysis of tear cytokines and clinical correlations in Sjogren syndrome dry eye patients and non-Sjogren syndrome dry eye patients. *Am J Ophthalmol, 156*(2), 247-253 e241. doi:10.1016/j.ajo.2013.04.003

Lemiere, C., Ernst, P., Olivenstein, R., Yamauchi, Y., Govindaraju, K., Ludwig, M. S., . . . Hamid, Q. (2006). Airway inflammation assessed by invasive and noninvasive means in severe asthma: eosinophilic and noneosinophilic phenotypes. *J Allergy Clin Immunol, 118*(5), 1033-1039. doi:10.1016/j.jaci.2006.08.003

Leonardi, A., Borghesan, F., Faggian, D., & Plebani, M. (2015). Microarray-based IgE detection in tears of patients with vernal keratoconjunctivitis. *Pediatr Allergy Immunol, 26*(7), 641-645. doi:10.1111/pai.12450

Leonardi, A., Curnow, S. J., Zhan, H., & Calder, V. L. (2006). Multiple cytokines in human tear specimens in seasonal and chronic allergic eye disease and in conjunctival fibroblast cultures. *Clin Exp Allergy, 36*(6), 777-784. doi:10.1111/j.1365-2222.2006.02499.x

Leonardi, A., Jose, P. J., Zhan, H., & Calder, V. L. (2003). Tear and mucus eotaxin-1 and eotaxin-2 in allergic keratoconjunctivitis. *Ophthalmology, 110*(3), 487-492. doi:10.1016/S0161-6420(02)01767-0

Leonardi, A., Palmigiano, A., Mazzola, E. A., Messina, A., Milazzo, E. M., Bortolotti, M., & Garozzo, D. (2014). Identification of human tear fluid biomarkers in vernal keratoconjunctivitis using iTRAQ quantitative proteomics. *Allergy, 69*(2), 254-260. doi:10.1111/all.12331

Leopold, J. A., Walker, J., Scribner, A. W., Voetsch, B., Zhang, Y. Y., Loscalzo, A. J., . . . Loscalzo, J. (2003). Glucose-6-phosphate dehydrogenase modulates vascular endothelial growth factor-mediated angiogenesis. *J Biol Chem, 278*(34), 32100-32106. doi:10.1074/jbc.M301293200

Li, B., Sheng, M., Li, J., Yan, G., Lin, A., Li, M., . . . Chen, Y. (2014). Tear proteomic analysis of Sjogren syndrome patients with dry eye syndrome by two-dimensional-nano-liquid chromatography coupled with tandem mass spectrometry. *Sci Rep, 4*, 5772. doi:10.1038/srep05772

Li, H., Meininger, C. J., Hawker, J. R., Jr., Haynes, T. E., Kepka-Lenhart, D., Mistry, S. K., . . . Wu, G. (2001). Regulatory role of arginase I and II in nitric oxide, polyamine, and proline syntheses in endothelial cells. *Am J Physiol Endocrinol Metab, 280*(1), E75-82. doi:10.1152/ajpendo.2001.280.1.E75

Li, M., Li, H., Jiang, P., Liu, X., Xu, D., & Wang, F. (2014). Investigating the pathological processes of rhegmatogenous retinal detachment and proliferative vitreoretinopathy with metabolomics analysis. *Mol Biosyst, 10*(5), 1055-1062. doi:10.1039/c3mb70386j

Li, S., Miao, T., Sebastian, M., Bhullar, P., Ghaffari, E., Liu, M., . . . Wang, P. (2012). The transcription factors Egr2 and Egr3 are essential for the control of inflammation and antigen-induced proliferation of B and T cells. *Immunity, 37*(4), 685-696. doi:10.1016/j.immuni.2012.08.001

Li, X., Ji, Z., Ma, Y., Qiu, X., Fan, Q., & Ma, B. (2012). Expression of hypoxia-inducible factor-1alpha, vascular endothelial growth factor and matrix metalloproteinase-2 in sacral chordomas. *Oncol Lett, 3*(6), 1268-1274. doi:10.3892/ol.2012.645

Li, X., Luo, X., Lu, X., Duan, J., & Xu, G. (2011). Metabolomics study of diabetic retinopathy using gas chromatography-mass spectrometry: a comparison of stages and subtypes

diagnosed by Western and Chinese medicine. *Mol Biosyst, 7*(7), 2228-2237. doi:10.1039/c0mb00341g

Li, Y., Li, J., Zhang, X., Peng, J., Li, J., & Zhao, P. (2020). Identification of Gene Mutations in Atypical Retinopathy of Prematurity Cases. *J Ophthalmol, 2020*, 4212158. doi:10.1155/2020/4212158

Liekens, S., De Clercq, E., & Neyts, J. (2001). Angiogenesis: regulators and clinical applications. *Biochem Pharmacol, 61*(3), 253-270. doi:10.1016/s0006-2952(00)00529-3

Lim, S. A., Nam, D. H., Lee, J. H., Kwok, S. K., Park, S. H., & Chung, S. H. (2015). Association of IL-21 cytokine with severity of primary Sjogren syndrome dry eye. *Cornea, 34*(3), 248-252. doi:10.1097/ICO.0000000000000363

Liu, A., Terry, R., Lin, Y., Nelson, K., & Bernstein, P. S. (2013). Comprehensive and sensitive quantification of long-chain and very long-chain polyunsaturated fatty acids in small samples of human and mouse retina. *J Chromatogr A, 1307*, 191-200. doi:10.1016/j.chroma.2013.07.103

Liu, H., & Prokosch, V. (2021). Energy Metabolism in the Inner Retina in Health and Glaucoma. *Int J Mol Sci, 22*(7). doi:10.3390/ijms22073689

Liu, W., Li, H., Lu, D., Liang, J., Xing, X., Liu, A., . . . Ji, J. (2010). The tear fluid mucin 5AC change of primary angle-closure glaucoma patients after short-term medications and phacotrabeculectomy. *Mol Vis, 16*, 2342-2346.

Lopez-Miguel, A., Teson, M., Martin-Montanez, V., Enriquez-de-Salamanca, A., Stern, M. E., Gonzalez-Garcia, M. J., & Calonge, M. (2016). Clinical and Molecular Inflammatory Response in Sjogren Syndrome-Associated Dry Eye Patients Under Desiccating Stress. *Am J Ophthalmol, 161*, 133-141 e131-132. doi:10.1016/j.ajo.2015.09.039

Low, S. W. Y., Connor, T. B., Kassem, I. S., Costakos, D. M., & Chaurasia, S. S. (2021). Small Leucine-Rich Proteoglycans (SLRPs) in the Retina. *Int J Mol Sci, 22*(14). doi:10.3390/ijms22147293

Lucey, J. F., & Dangman, B. (1984). A reexamination of the role of oxygen in retrolental fibroplasia. *Pediatrics, 73*(1), 82-96.

Ma, J., Zhu, T. P., Zhang, Q. R., & Ou, H. L. (2011). [The effect of vascular endothelial growth factor and hypoxia on the secretion of opticin in retinal pigment epithelium cells]. *Zhonghua Yan Ke Za Zhi, 47*(11), 1012-1018.

MacDonald, B. T., & He, X. (2012). Frizzled and LRP5/6 receptors for Wnt/beta-catenin signaling. *Cold Spring Harb Perspect Biol, 4*(12). doi:10.1101/cshperspect.a007880

MacDonald, M. L., Goldberg, Y. P., Macfarlane, J., Samuels, M. E., Trese, M. T., & Shastry, B. S. (2005). Genetic variants of frizzled-4 gene in familial exudative vitreoretinopathy and advanced retinopathy of prematurity. *Clin Genet, 67*(4), 363-366. doi:10.1111/j.1399-0004.2005.00408.x

Mackie, I. A., & Seal, D. V. (1986). Confirmatory tests for the dry eye of Sjogren's syndrome. *Scand J Rheumatol Suppl, 61*, 220-223.

Mahmoud, E. A., Sheikh, A. H., Domeika, M. A., & Mardh, P. A. (1994). Prevalence of trachoma among displaced persons in the Sudan: a clinical and sero-epidemiological study. *Eye (Lond), 8 (Pt 1)*, 130-133. doi:10.1038/eye.1994.26

Malamas, A., Chranioti, A., Tsakalidis, C., Dimitrakos, S. A., & Mataftsi, A. (2017). The omega-3 and retinopathy of prematurity relationship. *Int J Ophthalmol, 10*(2), 300-305. doi:10.18240/ijo.2017.02.19

Mann, G. E., Yudilevich, D. L., & Sobrevia, L. (2003). Regulation of amino acid and glucose transporters in endothelial and smooth muscle cells. *Physiol Rev, 83*(1), 183-252. doi:10.1152/physrev.00022.2002

Mark, M., Ghyselinck, N. B., & Chambon, P. (2006). Function of retinoid nuclear receptors: lessons from genetic and pharmacological dissections of the retinoic acid signaling pathway during mouse embryogenesis. *Annu Rev Pharmacol Toxicol, 46*, 451-480. doi:10.1146/annurev.pharmtox.46.120604.141156

Marti-Masso, J. F., Bergareche, A., Makarov, V., Ruiz-Martinez, J., Gorostidi, A., Lopez de Munain, A., . . . Paisan-Ruiz, C. (2013). The ACMSD gene, involved in tryptophan metabolism, is mutated in a family with cortical myoclonus, epilepsy, and parkinsonism. *J Mol Med (Berl), 91*(12), 1399-1406. doi:10.1007/s00109-013-1075-4

Martinez, F. O., & Gordon, S. (2014). The M1 and M2 paradigm of macrophage activation: time for reassessment. *F1000Prime Rep, 6*, 13. doi:10.12703/P6-13

Martinez, F. O., Helming, L., & Gordon, S. (2009). Alternative activation of macrophages: an immunologic functional perspective. *Annu Rev Immunol, 27*, 451-483. doi:10.1146/annurev.immunol.021908.132532

Massingale, M. L., Li, X., Vallabhajosyula, M., Chen, D., Wei, Y., & Asbell, P. A. (2009). Analysis of inflammatory cytokines in the tears of dry eye patients. *Cornea, 28*(9), 1023-1027. doi:10.1097/ICO.0b013e3181a16578

Massova, I., Kotra, L. P., Fridman, R., & Mobashery, S. (1998). Matrix metalloproteinases: structures, evolution, and diversification. *FASEB J, 12*(12), 1075-1095.

Mayordomo-Febrer, A., Lopez-Murcia, M., Morales-Tatay, J. M., Monleon-Salvado, D., & Pinazo-Duran, M. D. (2015). Metabolomics of the aqueous humor in the rat glaucoma model induced by a series of intracamerular sodium hyaluronate injection. *Exp Eye Res, 131*, 84-92. doi:10.1016/j.exer.2014.11.012

Mescher, A. L. (2018). Author. In *Junqueira's Basic Histology: Text and Atlas, 15e*. New York, NY: McGraw-Hill Education.

Micheal, S., Saksens, N. T. M., Hogewind, B. F., Khan, M. I., Hoyng, C. B., & den Hollander, A. I. (2018). Identification of TP53BP2 as a Novel Candidate Gene for Primary Open Angle Glaucoma by Whole Exome Sequencing in a Large Multiplex Family. *Mol Neurobiol, 55*(2), 1387-1395. doi:10.1007/s12035-017-0403-z

Mignatti, P., & Rifkin, D. B. (1996). Plasminogen activators and matrix metalloproteinases in angiogenesis. *Enzyme Protein, 49*(1-3), 117-137. doi:10.1159/000468621

Mills, C. D. (2012). M1 and M2 Macrophages: Oracles of Health and Disease. *Crit Rev Immunol, 32*(6), 463-488. doi:10.1615/critrevimmunol.v32.i6.10

Mirando, A. C., Abdi, K., Wo, P., & Lounsbury, K. M. (2017). Assessing the effects of threonyl-tRNA synthetase on angiogenesis-related responses. *Methods, 113*, 132-138. doi:10.1016/j.ymeth.2016.11.007

Mirando, A. C., Francklyn, C. S., & Lounsbury, K. M. (2014). Regulation of angiogenesis by aminoacyl-tRNA synthetases. *Int J Mol Sci, 15*(12), 23725-23748. doi:10.3390/ijms151223725

Mohamed, S., Schaa, K., Cooper, M. E., Ahrens, E., Alvarado, A., Colaizy, T., . . . Dagle, J. M. (2009). Genetic contributions to the development of retinopathy of prematurity. *Pediatr Res, 65*(2), 193-197. doi:10.1203/PDR.0b013e31818d1dbd

Montan, P. G., & van Hage-Hamsten, M. (1996). Eosinophil cationic protein in tears in allergic conjunctivitis. *Br J Ophthalmol, 80*(6), 556-560. doi:10.1136/bjo.80.6.556

Montojo, J., Zuberi, K., Rodriguez, H., Kazi, F., Wright, G., Donaldson, S. L., . . . Bader, G. D. (2010). GeneMANIA Cytoscape plugin: fast gene function predictions on the desktop. *Bioinformatics, 26*(22), 2927-2928. doi:10.1093/bioinformatics/btq562

Morris, P. B., Ellis, M. N., & Swain, J. L. (1989). Angiogenic potency of nucleotide metabolites: potential role in ischemia-induced vascular growth. *J Mol Cell Cardiol, 21*(4), 351-358. doi:10.1016/0022-2828(89)90645-7

Mowafy, M. A., Saad, N. E., El-Mofty, H. M., ElAnany, M. G., & Mohamed, M. S. (2014). The prevalence of chlamydia trachomatis among patients with acute conjunctivitis in Kasr

Alainy ophthalmology clinic. *Pan Afr Med J, 17*, 151. doi:10.11604/pamj.2014.17.151.3818

Munipally, P. K., Agraharm, S. G., Valavala, V. K., Gundae, S., & Turlapati, N. R. (2011). Evaluation of indoleamine 2,3-dioxygenase expression and kynurenine pathway metabolites levels in serum samples of diabetic retinopathy patients. *Arch Physiol Biochem, 117*(5), 254-258. doi:10.3109/13813455.2011.623705

Murube, J. (2009). Basal, reflex, and psycho-emotional tears. *Ocul Surf, 7*(2), 60-66. doi:10.1016/s1542-0124(12)70296-3

Na, K. S., Mok, J. W., Kim, J. Y., Rho, C. R., & Joo, C. K. (2012). Correlations between tear cytokines, chemokines, and soluble receptors and clinical severity of dry eye disease. *Invest Ophthalmol Vis Sci, 53*(9), 5443-5450. doi:10.1167/iovs.11-9417

Nagase, H. (1997). Activation mechanisms of matrix metalloproteinases. *Biol Chem, 378*(3-4), 151-160.

Nagase, H., & Woessner, J. F., Jr. (1999). Matrix metalloproteinases. *J Biol Chem, 274*(31), 21491-21494. doi:10.1074/jbc.274.31.21491

Nema, H. V., Gupta, R., & Shenoy, U. (1977). Immunoglobulins in trachoma. *Indian J Ophthalmol, 25*(3), 1-4.

Neve, A., Cantatore, F. P., Maruotti, N., Corrado, A., & Ribatti, D. (2014). Extracellular matrix modulates angiogenesis in physiological and pathological conditions. *Biomed Res Int, 2014*, 756078. doi:10.1155/2014/756078

Newman, E., & Reichenbach, A. (1996). The Muller cell: a functional element of the retina. *Trends Neurosci, 19*(8), 307-312. doi:10.1016/0166-2236(96)10040-0

Nguyen, N. T., Nakahama, T., Le, D. H., Van Son, L., Chu, H. H., & Kishimoto, T. (2014). Aryl hydrocarbon receptor and kynurenine: recent advances in autoimmune disease research. *Front Immunol, 5*, 551. doi:10.3389/fimmu.2014.00551

Chen, X., Chen, Y., Wang, L., & Sun, X. (2019). Metabolomics of the aqueous humor in patients with primary congenital glaucoma. *Mol Vis, 25*, 489-501.

Nie, A., Sun, B., Fu, Z., & Yu, D. (2019). Roles of aminoacyl-tRNA synthetases in immune regulation and immune diseases. *Cell Death Dis, 10*(12), 901. doi:10.1038/s41419-019-2145-5

Niederkorn, J. Y. (2012). Ocular immune privilege and ocular melanoma: parallel universes or immunological plagiarism? *Front Immunol, 3*, 148. doi:10.3389/fimmu.2012.00148

Nikopoulos, K., Gilissen, C., Hoischen, A., van Nouhuys, C. E., Boonstra, F. N., Blokland, E. A., . . . Collin, R. W. (2010). Next-generation sequencing of a 40 Mb linkage interval

reveals TSPAN12 mutations in patients with familial exudative vitreoretinopathy. *Am J Hum Genet, 86*(2), 240-247. doi:10.1016/j.ajhg.2009.12.016

Nivenius, E., Montan, P. G., Chryssanthou, E., Jung, K., van Hage-Hamsten, M., & van der Ploeg, I. (2004). No apparent association between periocular and ocular microcolonization and the degree of inflammation in patients with atopic keratoconjunctivitis. *Clin Exp Allergy, 34*(5), 725-730. doi:10.1111/j.1365-2222.2004.1950.x

Nording, M. L., Yang, J., Hegedus, C. M., Bhushan, A., Kenyon, N. J., Davis, C. E., & Hammock, B. D. (2010). Endogenous Levels of Five Fatty Acid Metabolites in Exhaled Breath Condensate to Monitor Asthma by High-Performance Liquid Chromatography: Electrospray Tandem Mass Spectrometry. *IEEE Sens J, 10*(1), 123-130. doi:10.1109/JSEN.2009.2035736

O'Farrell, K., Fagan, E., Connor, T. J., & Harkin, A. (2017). Inhibition of the kynurenine pathway protects against reactive microglial-associated reductions in the complexity of primary cortical neurons. *Eur J Pharmacol, 810*, 163-173. doi:10.1016/j.ejphar.2017.07.008

Oberkersch, R. E., & Santoro, M. M. (2019). Role of amino acid metabolism in angiogenesis. *Vascul Pharmacol, 112*, 17-23. doi:10.1016/j.vph.2018.11.001

Odegaard, J. I., & Chawla, A. (2011). Alternative macrophage activation and metabolism. *Annu Rev Pathol, 6*, 275-297. doi:10.1146/annurev-pathol-011110-130138

Ohashi, Y., Ishida, R., Kojima, T., Goto, E., Matsumoto, Y., Watanabe, K., . . . Tsubota, K. (2003). Abnormal protein profiles in tears with dry eye syndrome. *Am J Ophthalmol, 136*(2), 291-299. doi:10.1016/s0002-9394(03)00203-4

Osborn, M. P., Park, Y., Parks, M. B., Burgess, L. G., Uppal, K., Lee, K., . . . Brantley, M. A., Jr. (2013). Metabolome-wide association study of neovascular age-related macular degeneration. *PLoS One, 8*(8), e72737. doi:10.1371/journal.pone.0072737

Owens, W. C., & Owens, E. U. (1949). Retrolental fibroplasia in premature infants. *Am J Ophthalmol, 32*(1), 1-21. doi:10.1016/0002-9394(49)91102-2

Ozerdem, U., Mach-Hofacre, B., Cheng, L., Chaidhawangul, S., Keefe, K., McDermott, C. D., . . . Freeman, W. R. (2000). The effect of prinomastat (AG3340), a potent inhibitor of matrix metalloproteinases, on a subacute model of proliferative vitreoretinopathy. *Curr Eye Res, 20*(6), 447-453.

Paes, K. T., Wang, E., Henze, K., Vogel, P., Read, R., Suwanichkul, A., . . . Rice, D. S. (2011). Frizzled 4 is required for retinal angiogenesis and maintenance of the blood-retina barrier. *Invest Ophthalmol Vis Sci, 52*(9), 6452-6461. doi:10.1167/iovs.10-7146

Palosaari, H., Pennington, C. J., Larmas, M., Edwards, D. R., Tjaderhane, L., & Salo, T. (2003). Expression profile of matrix metalloproteinases (MMPs) and tissue inhibitors of MMPs in mature human odontoblasts and pulp tissue. *Eur J Oral Sci, 111*(2), 117-127. doi:10.1034/j.1600-0722.2003.00026.x

Palsson-McDermott, E. M., & O'Neill, L. A. (2013). The Warburg effect then and now: from cancer to inflammatory diseases. *Bioessays, 35*(11), 965-973. doi:10.1002/bies.201300084

Panda-Jonas, S., Jonas, J. B., & Jakobczyk-Zmija, M. (1996). Retinal pigment epithelial cell count, distribution, and correlations in normal human eyes. *Am J Ophthalmol, 121*(2), 181-189. doi:10.1016/s0002-9394(14)70583-5

Paris, L. P., Johnson, C. H., Aguilar, E., Usui, Y., Cho, K., Hoang, L. T., . . . Friedlander, M. (2016). Global metabolomics reveals metabolic dysregulation in ischemic retinopathy. *Metabolomics, 12*, 15. doi:10.1007/s11306-015-0877-5

Parra-Bonilla, G., Alvarez, D. F., Al-Mehdi, A. B., Alexeyev, M., & Stevens, T. (2010). Critical role for lactate dehydrogenase A in aerobic glycolysis that sustains pulmonary microvascular endothelial cell proliferation. *Am J Physiol Lung Cell Mol Physiol, 299*(4), L513-522. doi:10.1152/ajplung.00274.2009

Patnaik, K., Pradeep, A. R., Nagpal, K., Karvekar, S., Singh, P., & Raju, A. (2017). Human chemerin correlation in gingival crevicular fluid and tear fluid as markers of inflammation in chronic periodontitis and type-2 diabetes mellitus. *J Investig Clin Dent, 8*(1). doi:10.1111/jicd.12181

Patnaik, S., Jalali, S., Joshi, M. B., Satyamoorthy, K., & Kaur, I. (2019). Metabolomics Applicable to Retinal Vascular Diseases. *Methods Mol Biol, 1996*, 325-331. doi:10.1007/978-1-4939-9488-5_24

Patnaik, S., Rai, M., Jalali, S., Agarwal, K., Badakere, A., Puppala, L., . . . Kaur, I. (2021). An interplay of microglia and matrix metalloproteinase MMP9 under hypoxic stress regulates the opticin expression in retina. *Sci Rep, 11*(1), 7444. doi:10.1038/s41598-021-86302-2

Peral, A., Carracedo, G., & Pintor, J. (2015). Diadenosine polyphosphates in the tears of aniridia patients. *Acta Ophthalmol, 93*(5), e337-342. doi:10.1111/aos.12626

Peters, K., Kamp, G., Berz, A., Unger, R. E., Barth, S., Salamon, A., . . . Kirkpatrick, C. J. (2009). Changes in human endothelial cell energy metabolic capacities during in vitro cultivation. The role of "aerobic glycolysis" and proliferation. *Cell Physiol Biochem, 24*(5-6), 483-492. doi:10.1159/000257490

Pflugfelder, S. C., Jones, D., Ji, Z., Afonso, A., & Monroy, D. (1999). Altered cytokine balance in the tear fluid and conjunctiva of patients with Sjogren's syndrome keratoconjunctivitis sicca. *Curr Eye Res, 19*(3), 201-211. doi:10.1076/ceyr.19.3.201.5309

Pieragostino, D., Agnifili, L., Fasanella, V., D'Aguanno, S., Mastropasqua, R., Di Ilio, C., . . . Del Boccio, P. (2013). Shotgun proteomics reveals specific modulated protein patterns in tears of patients with primary open angle glaucoma naive to therapy. *Mol Biosyst, 9*(6), 1108-1116. doi:10.1039/c3mb25463a

Pieragostino, D., Bucci, S., Agnifili, L., Fasanella, V., D'Aguanno, S., Mastropasqua, A., . . . Del Boccio, P. (2012). Differential protein expression in tears of patients with primary open angle and pseudoexfoliative glaucoma. *Mol Biosyst, 8*(4), 1017-1028. doi:10.1039/c1mb05357d

Pietrzyk, J. J., Kwinta, P., Bik-Multanowski, M., Madetko-Talowska, A., Jagla, M., Tomasik, T., . . . Saugstad, O. D. (2013). New insight into the pathogenesis of retinopathy of prematurity: assessment of whole-genome expression. *Pediatr Res, 73*(4 Pt 1), 476-483. doi:10.1038/pr.2012.195

Plaster, N., Sonntag, C., Schilling, T. F., & Hammerschmidt, M. (2007). REREa/Atrophin-2 interacts with histone deacetylase and Fgf8 signaling to regulate multiple processes of zebrafish development. *Dev Dyn, 236*(7), 1891-1904. doi:10.1002/dvdy.21196

Poggi, C., Giusti, B., Gozzini, E., Sereni, A., Romagnuolo, I., Kura, A., . . . Dani, C. (2015). Genetic Contributions to the Development of Complications in Preterm Newborns. *PLoS One, 10*(7), e0131741. doi:10.1371/journal.pone.0131741

Pollard, Z. F. (1997). Persistent hyperplastic primary vitreous: diagnosis, treatment and results. *Trans Am Ophthalmol Soc, 95*, 487-549.

Pong, J. C., Chu, C. Y., Chu, K. O., Poon, T. C., Ngai, S. M., Pang, C. P., & Wang, C. C. (2010). Identification of hemopexin in tear film. *Anal Biochem, 404*(1), 82-85. doi:10.1016/j.ab.2010.04.036

Pong, J. C., Chu, C. Y., Li, W. Y., Tang, L. Y., Li, L., Lui, W. T., . . . Pang, C. P. (2011). Association of hemopexin in tear film and conjunctival macrophages with vernal keratoconjunctivitis. *Arch Ophthalmol, 129*(4), 453-461. doi:10.1001/archophthalmol.2011.41

Poulter, J. A., Ali, M., Gilmour, D. F., Rice, A., Kondo, H., Hayashi, K., . . . Toomes, C. (2010). Mutations in TSPAN12 cause autosomal-dominant familial exudative vitreoretinopathy. *Am J Hum Genet, 86*(2), 248-253. doi:10.1016/j.ajhg.2010.01.012

Prieur, D. S., & Rebsam, A. (2017). Retinal axon guidance at the midline: Chiasmatic misrouting and consequences. *Dev Neurobiol, 77*(7), 844-860. doi:10.1002/dneu.22473

Priyadarsini, S., Hjortdal, J., Sarker-Nag, A., Sejersen, H., Asara, J. M., & Karamichos, D. (2014). Gross cystic disease fluid protein-15/prolactin-inducible protein as a biomarker for keratoconus disease. *PLoS One, 9*(11), e113310. doi:10.1371/journal.pone.0113310

Qin, M., Hayashi, H., Oshima, K., Tahira, T., Hayashi, K., & Kondo, H. (2005). Complexity of the genotype-phenotype correlation in familial exudative vitreoretinopathy with mutations in the LRP5 and/or FZD4 genes. *Hum Mutat, 26*(2), 104-112. doi:10.1002/humu.20191

Quinn, G. E. (2016). Retinopathy of prematurity blindness worldwide: phenotypes in the third epidemic. *Eye Brain, 8*, 31-36. doi:10.2147/EB.S94436

Rabin, J. C. (2013). The Retina: An Approachable Part of the Brain. *90*(1), e36. doi:10.1097/OPX.0b013e3182805b2b

Racker, E. (1974). History of the Pasteur effect and its pathobiology. *Mol Cell Biochem, 5*(1-2), 17-23. doi:10.1007/BF01874168

Ramesh, S., Bonshek, R. E., & Bishop, P. N. (2004). Immunolocalisation of opticin in the human eye. *Br J Ophthalmol, 88*(5), 697-702. doi:10.1136/bjo.2003.031989

Ramos, M. F., Brassard, J., & Masli, S. (2021). Immunology and Pathology in Ocular Drug Development. *Toxicologic Pathology, 49*(3), 483-504. doi:10.1177/0192623320978396

Rath, M., Muller, I., Kropf, P., Closs, E. I., & Munder, M. (2014). Metabolism via Arginase or Nitric Oxide Synthase: Two Competing Arginine Pathways in Macrophages. *Front Immunol, 5*, 532. doi:10.3389/fimmu.2014.00532

Rathi, S., Jalali, S., Musada, G. R., Patnaik, S., Balakrishnan, D., Hussain, A., & Kaur, I. (2018). Mutation spectrum of NDP, FZD4 and TSPAN12 genes in Indian patients with retinopathy of prematurity. *Br J Ophthalmol, 102*(2), 276-281. doi:10.1136/bjophthalmol-2017-310958

Rathi, S., Jalali, S., Patnaik, S., Shahulhameed, S., Musada, G. R., Balakrishnan, D., . . . Kaur, I. (2017). Abnormal Complement Activation and Inflammation in the Pathogenesis of Retinopathy of Prematurity. *Front Immunol, 8*, 1868. doi:10.3389/fimmu.2017.01868

Reardon, A. J., Le Goff, M., Briggs, M. D., McLeod, D., Sheehan, J. K., Thornton, D. J., & Bishop, P. N. (2000). Identification in vitreous and molecular cloning of opticin, a novel member of the family of leucine-rich repeat proteins of the extracellular matrix. *J Biol Chem, 275*(3), 2123-2129. doi:10.1074/jbc.275.3.2123

Recchia, F. M., Xu, L., Penn, J. S., Boone, B., & Dexheimer, P. J. (2010). Identification of genes and pathways involved in retinal neovascularization by microarray analysis of two animal models of retinal angiogenesis. *Invest Ophthalmol Vis Sci, 51*(2), 1098-1105. doi:10.1167/iovs.09-4006

Reddy, A. B., Ramana, K. V., Srivastava, S., Bhatnagar, A., & Srivastava, S. K. (2009). Aldose reductase regulates high glucose-induced ectodomain shedding of tumor necrosis factor (TNF)-alpha via protein kinase C-delta and TNF-alpha converting enzyme in vascular smooth muscle cells. *Endocrinology, 150*(1), 63-74. doi:10.1210/en.2008-0677

Riemens, A., Stoyanova, E., Rothova, A., & Kuiper, J. (2012). Cytokines in tear fluid of patients with ocular graft-versus-host disease after allogeneic stem cell transplantation. *Mol Vis, 18*, 797-802.

Riganti, C., Gazzano, E., Polimeni, M., Aldieri, E., & Ghigo, D. (2012). The pentose phosphate pathway: an antioxidant defense and a crossroad in tumor cell fate. *Free Radic Biol Med, 53*(3), 421-436. doi:10.1016/j.freeradbiomed.2012.05.006

Rivera, J. C., Holm, M., Austeng, D., Morken, T. S., Zhou, T. E., Beaudry-Richard, A., . . . Chemtob, S. (2017). Retinopathy of prematurity: inflammation, choroidal degeneration, and novel promising therapeutic strategies. *J Neuroinflammation, 14*(1), 165. doi:10.1186/s12974-017-0943-1

Roach, D. M., Fitridge, R. A., Laws, P. E., Millard, S. H., Varelias, A., & Cowled, P. A. (2002). Up-regulation of MMP-2 and MMP-9 leads to degradation of type IV collagen during skeletal muscle reperfusion injury; protection by the MMP inhibitor, doxycycline. *Eur J Vasc Endovasc Surg, 23*(3), 260-269. doi:10.1053/ejvs.2002.1598

Robitaille, J., MacDonald, M. L., Kaykas, A., Sheldahl, L. C., Zeisler, J., Dube, M. P., . . . Samuels, M. E. (2002). Mutant frizzled-4 disrupts retinal angiogenesis in familial exudative vitreoretinopathy. *Nat Genet, 32*(2), 326-330. doi:10.1038/ng957

Rodriguez-Prados, J. C., Traves, P. G., Cuenca, J., Rico, D., Aragones, J., Martin-Sanz, P., . . . Bosca, L. (2010). Substrate fate in activated macrophages: a comparison between innate, classic, and alternative activation. *J Immunol, 185*(1), 605-614. doi:10.4049/jimmunol.0901698

Roedl, J. B., Bleich, S., Schlotzer-Schrehardt, U., von Ahsen, N., Kornhuber, J., Naumann, G. O., . . . Junemann, A. G. (2008). Increased homocysteine levels in tear fluid of patients with primary open-angle glaucoma. *Ophthalmic Res, 40*(5), 249-256. doi:10.1159/000127832

Rohlenova, K., Veys, K., Miranda-Santos, I., De Bock, K., & Carmeliet, P. (2018). Endothelial Cell Metabolism in Health and Disease. *Trends Cell Biol, 28*(3), 224-236. doi:10.1016/j.tcb.2017.10.010

Romagnani, P., Lasagni, L., Annunziato, F., Serio, M., & Romagnani, S. (2004). CXC chemokines: the regulatory link between inflammation and angiogenesis. *Trends Immunol, 25*(4), 201-209. doi:10.1016/j.it.2004.02.006

Romano, A. H., & Conway, T. (1996). Evolution of carbohydrate metabolic pathways. *Res Microbiol, 147*(6-7), 448-455. doi:10.1016/0923-2508(96)83998-2

Rose, D. P., & Connolly, J. M. (1999). Omega-3 fatty acids as cancer chemopreventive agents. *Pharmacol Ther, 83*(3), 217-244. doi:10.1016/s0163-7258(99)00026-1

Rotstein, N. P., Miranda, G. E., Abrahan, C. E., & German, O. L. (2010). Regulating survival and development in the retina: key roles for simple sphingolipids. *J Lipid Res, 51*(6), 1247-1262. doi:10.1194/jlr.R003442

Rusai, K., Vannay, A., Szebeni, B., Borgulya, G., Fekete, A., Vasarhelyi, B., . . . Szabo, A. J. (2008). Endothelial nitric oxide synthase gene T-786C and 27-bp repeat gene polymorphisms in retinopathy of prematurity. *Mol Vis, 14*, 286-290.

Russo, G. L. (2009). Dietary n-6 and n-3 polyunsaturated fatty acids: from biochemistry to clinical implications in cardiovascular prevention. *Biochem Pharmacol, 77*(6), 937-946. doi:10.1016/j.bcp.2008.10.020

Ryu, Y. H., & Kim, J. C. (2007). Expression of indoleamine 2,3-dioxygenase in human corneal cells as a local immunosuppressive factor. *Invest Ophthalmol Vis Sci, 48*(9), 4148-4152. doi:10.1167/iovs.05-1336

Sacchetti, M., Micera, A., Lambiase, A., Speranza, S., Mantelli, F., Petrachi, G., . . . Bonini, S. (2011). Tear levels of neuropeptides increase after specific allergen challenge in allergic conjunctivitis. *Mol Vis, 17*, 47-52.

Sack, R., Conradi, L., Beaton, A., Sathe, S., McNamara, N., & Leonardi, A. (2007). Antibody array characterization of inflammatory mediators in allergic and normal tears in the open and closed eye environments. *Exp Eye Res, 85*(4), 528-538. doi:10.1016/j.exer.2007.07.004

Sakimoto, T., Ohnishi, T., & Ishimori, A. (2014). Significance of ectodomain shedding of TNF receptor 1 in ocular surface. *Invest Ophthalmol Vis Sci, 55*(4), 2419-2423. doi:10.1167/iovs.13-13265

Sambursky, R., & O'Brien, T. P. (2011). MMP-9 and the perioperative management of LASIK surgery. *Curr Opin Ophthalmol, 22*(4), 294-303. doi:10.1097/ICU.0b013e32834787bb

Samtani, S., Amaral, J., Campos, M. M., Fariss, R. N., & Becerra, S. P. (2009). Doxycycline-mediated inhibition of choroidal neovascularization. *Invest Ophthalmol Vis Sci, 50*(11), 5098-5106. doi:10.1167/iovs.08-3174

Sanchez, M. C., Barcelona, P. F., Luna, J. D., Ortiz, S. G., Juarez, P. C., Riera, C. M., & Chiabrando, G. A. (2006). Low-density lipoprotein receptor-related protein-1 (LRP-1) expression in a rat model of oxygen-induced retinal neovascularization. *Exp Eye Res, 83*(6), 1378-1385. doi:10.1016/j.exer.2006.07.016

Sanders, E. J., Walter, M. A., Parker, E., Aramburo, C., & Harvey, S. (2003). Opticin binds retinal growth hormone in the embryonic vitreous. *Invest Ophthalmol Vis Sci, 44*(12), 5404-5409. doi:10.1167/iovs.03-0500

Sang, D. N. (1987). Embryology of the vitreous. Congenital and developmental abnormalities. *Bull Soc Belge Ophtalmol, 223 Pt 1*, 11-35. doi:10.1007/978-1-4757-1901-7_2

Sanghi, G., Dogra, M. R., Dutta, S., Katoch, D., & Gupta, A. (2012). Intersibling variability of retinopathy of prematurity in twins and its risk factors. *Int Ophthalmol, 32*(2), 113-117. doi:10.1007/s10792-012-9533-5

Sardell, R. J., Bailey, J. N., Courtenay, M. D., Whitehead, P., Laux, R. A., Adams, L. D., . . . Pericak-Vance, M. A. (2016). Whole exome sequencing of extreme age-related macular degeneration phenotypes. *Mol Vis, 22*, 1062-1076.

Satici, A., Guzey, M., Dogan, Z., & Kilic, A. (2003). Relationship between Tear TNF-alpha, TGF-beta1, and EGF levels and severity of conjunctival cicatrization in patients with inactive trachoma. *Ophthalmic Res, 35*(6), 301-305. doi:10.1159/000074067

Sato, T., Kusaka, S., Hashida, N., Saishin, Y., Fujikado, T., & Tano, Y. (2009). Comprehensive gene-expression profile in murine oxygen-induced retinopathy. *Br J Ophthalmol, 93*(1), 96-103. doi:10.1136/bjo.2008.142646

Schaffer, D. B., Palmer, E. A., Plotsky, D. F., Metz, H. S., Flynn, J. T., Tung, B., & Hardy, R. J. (1993). Prognostic factors in the natural course of retinopathy of prematurity. The Cryotherapy for Retinopathy of Prematurity Cooperative Group. *Ophthalmology, 100*(2), 230-237. doi:10.1016/s0161-6420(93)31665-9

Schicht, M., Rausch, F., Beron, M., Jacobi, C., Garreis, F., Hartjen, N., . . . Paulsen, F. (2015). Palate Lung Nasal Clone (PLUNC), a Novel Protein of the Tear Film: Three-Dimensional Structure, Immune Activation, and Involvement in Dry Eye Disease (DED). *Invest Ophthalmol Vis Sci, 56*(12), 7312-7323. doi:10.1167/iovs.15-17560

Schulz, C. G., Sawicki, G., Lemke, R. P., Roeten, B. M., Schulz, R., & Cheung, P. Y. (2004). MMP-2 and MMP-9 and their tissue inhibitors in the plasma of preterm and term neonates. *Pediatr Res, 55*(5), 794-801. doi:10.1203/01.PDR.0000120683.68630.FB

Schwartzman, M. L., Iserovich, P., Gotlinger, K., Bellner, L., Dunn, M. W., Sartore, M., . . . Sack, R. (2010). Profile of lipid and protein autacoids in diabetic vitreous correlates with the progression of diabetic retinopathy. *Diabetes, 59*(7), 1780-1788. doi:10.2337/db10-0110

Seery, C. M., & Davison, P. F. (1991). Collagens of the bovine vitreous. *Invest Ophthalmol Vis Sci, 32*(5), 1540-1550.

Seifart, H. I., Delabar, U., & Siess, M. (1980). The influence of various precursors on the concentration of energy-rich phosphates and pyridine nucleotides in cardiac tissue and its possible meaning for anoxic survival. *Basic Res Cardiol, 75*(1), 57-61. doi:10.1007/BF02001394

Selvaraj, S., & Natarajan, J. (2011). Microarray data analysis and mining tools. *Bioinformation, 6*(3), 95-99. doi:10.6026/97320630006095

Semenza, G. L. (2011). Oxygen sensing, homeostasis, and disease. *N Engl J Med, 365*(6), 537-547. doi:10.1056/NEJMra1011165

Sen, D. K., Sarin, G. S., & Saha, K. (1977). Immunoglobulins in tear in trachoma patients. *Br J Ophthalmol, 61*(3), 218-220. doi:10.1136/bjo.61.3.218

Senger, D. R., & Davis, G. E. (2011). Angiogenesis. *Cold Spring Harb Perspect Biol, 3*(8), a005090. doi:10.1101/cshperspect.a005090

Shah, P. K., Narendran, V., Kalpana, N., & Gilbert, C. (2009). Severe retinopathy of prematurity in big babies in India: history repeating itself? *Indian J Pediatr, 76*(8), 801-804. doi:10.1007/s12098-009-0175-1

Shastry, B. S. (2010). Genetic susceptibility to advanced retinopathy of prematurity (ROP). *J Biomed Sci, 17*, 69. doi:10.1186/1423-0127-17-69

Shastry, B. S., Pendergast, S. D., Hartzer, M. K., Liu, X., & Trese, M. T. (1997). Identification of missense mutations in the Norrie disease gene associated with advanced retinopathy of prematurity. *Arch Ophthalmol, 115*(5), 651-655. doi:10.1001/archopht.1997.01100150653015

Shetty, R., Ghosh, A., Lim, R. R., Subramani, M., Mihir, K., Reshma, A. R., . . . Ghosh, A. (2015). Elevated expression of matrix metalloproteinase-9 and inflammatory cytokines in keratoconus patients is inhibited by cyclosporine A. *Invest Ophthalmol Vis Sci, 56*(2), 738-750. doi:10.1167/iovs.14-14831

Shoji, J., Inada, N., & Sawa, M. (2006). Antibody array-generated cytokine profiles of tears of patients with vernal keratoconjunctivitis or giant papillary conjunctivitis. *Jpn J Ophthalmol, 50*(3), 195-204. doi:10.1007/s10384-005-0319-4

Shui, Y. B., Holekamp, N. M., Kramer, B. C., Crowley, J. R., Wilkins, M. A., Chu, F., . . . Beebe, D. C. (2009). The gel state of the vitreous and ascorbate-dependent oxygen consumption: relationship to the etiology of nuclear cataracts. *Arch Ophthalmol, 127*(4), 475-482. doi:10.1001/archophthalmol.2008.621

Sierra, A., de Castro, F., Del Rio-Hortega, J., Rafael Iglesias-Rozas, J., Garrosa, M., & Kettenmann, H. (2016). The "Big-Bang" for modern glial biology: Translation and comments on Pio del Rio-Hortega 1919 series of papers on microglia. *Glia, 64*(11), 1801-1840. doi:10.1002/glia.23046

Sims, K. B., Lebo, R. V., Benson, G., Shalish, C., Schuback, D., Chen, Z. Y., . . . Breakefield, X. O. (1992). The Norrie disease gene maps to a 150 kb region on chromosome Xp11.3. *Hum Mol Genet, 1*(2), 83-89. doi:10.1093/hmg/1.2.83

Skwor, T., Kandel, R. P., Basravi, S., Khan, A., Sharma, B., & Dean, D. (2010). Characterization of humoral immune responses to chlamydial HSP60, CPAF, and CT795 in inflammatory and severe trachoma. *Invest Ophthalmol Vis Sci, 51*(10), 5128-5136. doi:10.1167/iovs.09-5113

Slawson, C., Copeland, R. J., & Hart, G. W. (2010). O-GlcNAc signaling: a metabolic link between diabetes and cancer? *Trends Biochem Sci, 35*(10), 547-555. doi:10.1016/j.tibs.2010.04.005

Smith, B. T., & Tasman, W. S. (2005). Retinopathy of prematurity: late complications in the baby boomer generation (1946-1964). *Trans Am Ophthalmol Soc, 103*, 225-234; discussion 234-226.

Smith, L. E. (2002). Pathogenesis of retinopathy of prematurity. *Acta Paediatr Suppl, 91*(437), 26-28. doi:10.1111/j.1651-2227.2002.tb00157.x

Solaini, G., Baracca, A., Lenaz, G., & Sgarbi, G. (2010). Hypoxia and mitochondrial oxidative metabolism. *Biochimica et Biophysica Acta (BBA) - Bioenergetics, 1797*(6), 1171-1177. doi:https://doi.org/10.1016/j.bbabio.2010.02.011

Solomon, A., Dursun, D., Liu, Z., Xie, Y., Macri, A., & Pflugfelder, S. C. (2001). Pro- and anti-inflammatory forms of interleukin-1 in the tear fluid and conjunctiva of patients with dry-eye disease. *Invest Ophthalmol Vis Sci, 42*(10), 2283-2292.

Soong, H. K., Eller, A. W., Hirose, T., Hanninen, L., & Kenyon, K. R. (1985). In situ actin distribution in excised retrolental membranes in retinopathy of prematurity. *Arch Ophthalmol, 103*(10), 1553-1556. doi:10.1001/archopht.1985.01050100129033

Soria, J., Duran, J. A., Etxebarria, J., Merayo, J., Gonzalez, N., Reigada, R., . . . Suarez, T. (2013). Tear proteome and protein network analyses reveal a novel pentamarker panel for tear film characterization in dry eye and meibomian gland dysfunction. *J Proteomics, 78*, 94-112. doi:10.1016/j.jprot.2012.11.017

Sorkhabi, R., Ghorbanihaghjo, A., Taheri, N., & Ahoor, M. H. (2015). Tear film inflammatory mediators in patients with keratoconus. *Int Ophthalmol, 35*(4), 467-472. doi:10.1007/s10792-014-9971-3

Sorrentino, F. S., Allkabes, M., Salsini, G., Bonifazzi, C., & Perri, P. (2016). The importance of glial cells in the homeostasis of the retinal microenvironment and their pivotal role in the course of diabetic retinopathy. *Life Sci, 162*, 54-59. doi:10.1016/j.lfs.2016.08.001

Spinale, F. G. (2002). Matrix metalloproteinases: regulation and dysregulation in the failing heart. *Circ Res, 90*(5), 520-530. doi:10.1161/01.res.0000013290.12884.a3

Stern, M. E., Beuerman, R. W., Fox, R. I., Gao, J., Mircheff, A. K., & Pflugfelder, S. C. (1998). The pathology of dry eye: the interaction between the ocular surface and lacrimal glands. *Cornea, 17*(6), 584-589. doi:10.1097/00003226-199811000-00002

Stevens, A., Soden, J., Brenchley, P. E., Ralph, S., & Ray, D. W. (2003). Haplotype analysis of the polymorphic human vascular endothelial growth factor gene promoter. *Cancer Res, 63*(4), 812-816.

Suhre, K., & Gieger, C. (2012). Genetic variation in metabolic phenotypes: study designs and applications. *Nat Rev Genet, 13*(11), 759-769. doi:10.1038/nrg3314

Sun, Y., Dalal, R., & Gariano, R. F. (2010). Cellular composition of the ridge in retinopathy of prematurity. *Arch Ophthalmol, 128*(5), 638-641. doi:10.1001/archophthalmol.2010.59

Suzuki, S., Tanaka, T., Poyurovsky, M. V., Nagano, H., Mayama, T., Ohkubo, S., . . . Prives, C. (2010). Phosphate-activated glutaminase (GLS2), a p53-inducible regulator of glutamine metabolism and reactive oxygen species. *Proc Natl Acad Sci U S A, 107*(16), 7461-7466. doi:10.1073/pnas.1002459107

Swan, R., Kim, S. J., Campbell, J. P., Paul Chan, R. V., Sonmez, K., Taylor, K. D., . . . Informatics in, R. O. P. R. C. (2018). The genetics of retinopathy of prematurity: a model for neovascular retinal disease. *Ophthalmol Retina, 2*(9), 949-962. doi:10.1016/j.oret.2018.01.016

Swanberg, S. E., Nagarajan, R. P., Peddada, S., Yasui, D. H., & LaSalle, J. M. (2009). Reciprocal co-regulation of EGR2 and MECP2 is disrupted in Rett syndrome and autism. *Hum Mol Genet, 18*(3), 525-534. doi:10.1093/hmg/ddn380

Swann, D. A. (1980). Chemistry and biology of the vitreous body. *Int Rev Exp Pathol, 22*, 1-64.

Sweetnam, R. (1976). Surgical treatment of osteogenic sarcoma. *Proc R Soc Med, 69*(8), 547-549.

Takanosu, M., Boyd, T. C., Le Goff, M., Henry, S. P., Zhang, Y., Bishop, P. N., & Mayne, R. (2001). Structure, chromosomal location, and tissue-specific expression of the mouse opticin gene. *Invest Ophthalmol Vis Sci, 42*(10), 2202-2210.

Talks, S. J., Ebenezer, N., Hykin, P., Adams, G., Yang, F., Schulenberg, E., . . . Gregory-Evans, C. Y. (2001). De novo mutations in the 5' regulatory region of the Norrie disease gene in retinopathy of prematurity. *J Med Genet, 38*(12), E46. doi:10.1136/jmg.38.12.e46

Tam, S. J., & Watts, R. J. (2010). Connecting vascular and nervous system development: angiogenesis and the blood-brain barrier. *Annu Rev Neurosci, 33*, 379-408. doi:10.1146/annurev-neuro-060909-152829

Tamm, E. R., & Ohlmann, A. (2012). [Development of the human eye]. *Ophthalmologe, 109*(9), 911-928. doi:10.1007/s00347-012-2644-6

Tan, M. P., Smith, E. N., Broach, J. R., & Floudas, C. A. (2008). Microarray data mining: a novel optimization-based approach to uncover biologically coherent structures. *BMC Bioinformatics, 9*, 268. doi:10.1186/1471-2105-9-268

Tan, X., Sun, S., Liu, Y., Zhu, T., Wang, K., Ren, T., . . . Zhu, L. (2014). Analysis of Th17-associated cytokines in tears of patients with dry eye syndrome. *Eye (Lond), 28*(5), 608-613. doi:10.1038/eye.2014.38

Tannahill, G. M., Curtis, A. M., Adamik, J., Palsson-McDermott, E. M., McGettrick, A. F., Goel, G., . . . O'Neill, L. A. (2013). Succinate is an inflammatory signal that induces IL-1beta through HIF-1alpha. *Nature, 496*(7444), 238-242. doi:10.1038/nature11986

Tasseva, G., Bai, H. D., Davidescu, M., Haromy, A., Michelakis, E., & Vance, J. E. (2013). Phosphatidylethanolamine deficiency in Mammalian mitochondria impairs oxidative phosphorylation and alters mitochondrial morphology. *J Biol Chem, 288*(6), 4158-4173. doi:10.1074/jbc.M112.434183

Tea, M., Fogarty, R., Brereton, H. M., Michael, M. Z., Van der Hoek, M. B., Tsykin, A., . . . Williams, K. A. (2009). Gene expression microarray analysis of early oxygen-induced retinopathy in the rat. *J Ocul Biol Dis Infor, 2*(4), 190-201. doi:10.1007/s12177-009-9041-7

Teson, M., Gonzalez-Garcia, M. J., Lopez-Miguel, A., Enriquez-de-Salamanca, A., Martin-Montanez, V., Benito, M. J., . . . Calonge, M. (2013). Influence of a controlled

environment simulating an in-flight airplane cabin on dry eye disease. *Invest Ophthalmol Vis Sci, 54*(3), 2093-2099. doi:10.1167/iovs.12-11361

Tio, L., Martel-Pelletier, J., Pelletier, J. P., Bishop, P. N., Roughley, P., Farran, A., . . . Monfort, J. (2014). Characterization of opticin digestion by proteases involved in osteoarthritis development. *Joint Bone Spine, 81*(2), 137-141. doi:10.1016/j.jbspin.2013.05.007

Tishler, M., Yaron, I., Geyer, O., Shirazi, I., Naftaliev, E., & Yaron, M. (1998). Elevated tear interleukin-6 levels in patients with Sjogren syndrome. *Ophthalmology, 105*(12), 2327-2329. doi:10.1016/S0161-6420(98)91236-2

Toker, E., Yavuz, S., & Direskeneli, H. (2004). Anti-Ro/SSA and anti-La/SSB autoantibodies in the tear fluid of patients with Sjogren's syndrome. *Br J Ophthalmol, 88*(3), 384-387. doi:10.1136/bjo.2003.028340

Tong, L., Zhou, L., Beuerman, R. W., Zhao, S. Z., & Li, X. R. (2011). Association of tear proteins with Meibomian gland disease and dry eye symptoms. *Br J Ophthalmol, 95*(6), 848-852. doi:10.1136/bjo.2010.185256

Toomes, C., Bottomley, H. M., Jackson, R. M., Towns, K. V., Scott, S., Mackey, D. A., . . . Inglehearn, C. F. (2004). Mutations in LRP5 or FZD4 underlie the common familial exudative vitreoretinopathy locus on chromosome 11q. *Am J Hum Genet, 74*(4), 721-730. doi:10.1086/383202

Torok, Z., Peto, T., Csosz, E., Tukacs, E., Molnar, A., Maros-Szabo, Z., . . . Csutak, A. (2013). Tear fluid proteomics multimarkers for diabetic retinopathy screening. *BMC Ophthalmol, 13*(1), 40. doi:10.1186/1471-2415-13-40

Tousoulis, D., Kampoli, A. M., Tentolouris, C., Papageorgiou, N., & Stefanadis, C. (2012). The role of nitric oxide on endothelial function. *Curr Vasc Pharmacol, 10*(1), 4-18. doi:10.2174/157016112798829760

Tremblay, S., Miloudi, K., Chaychi, S., Favret, S., Binet, F., Polosa, A., . . . Sapieha, P. (2013). Systemic inflammation perturbs developmental retinal angiogenesis and neuroretinal function. *Invest Ophthalmol Vis Sci, 54*(13), 8125-8139. doi:10.1167/iovs.13-12496

Treps, L., Conradi, L. C., Harjes, U., & Carmeliet, P. (2016). Manipulating Angiogenesis by Targeting Endothelial Metabolism: Hitting the Engine Rather than the Drivers-A New Perspective? *Pharmacol Rev, 68*(3), 872-887. doi:10.1124/pr.116.012492

Ujhelyi, B., Gogolak, P., Erdei, A., Nagy, V., Balazs, E., Rajnavolgyi, E., . . . Nagy, E. V. (2012). Graves' orbitopathy results in profound changes in tear composition: a study of plasminogen activator inhibitor-1 and seven cytokines. *Thyroid, 22*(4), 407-414. doi:10.1089/thy.2011.0248

Ulrich, J. N., Spannagl, M., Kampik, A., & Gandorfer, A. (2008). Components of the fibrinolytic system in the vitreous body in patients with vitreoretinal disorders. *Clin Exp Ophthalmol, 36*(5), 431-436.

Vadlapatla, R. K., Vadlapudi, A. D., & Mitra, A. K. (2013). Hypoxia-inducible factor-1 (HIF-1): a potential target for intervention in ocular neovascular diseases. *Curr Drug Targets, 14*(8), 919-935. doi:10.2174/13894501113149990015

van 't Veer, P., Strain, J. J., Fernandez-Crehuet, J., Martin, B. C., Thamm, M., Kardinaal, A. F., . . . Kok, F. J. (1996). Tissue antioxidants and postmenopausal breast cancer: the European Community Multicentre Study on Antioxidants, Myocardial Infarction, and Cancer of the Breast (EURAMIC). *Cancer Epidemiol Biomarkers Prev, 5*(6), 441-447.

van Dongen, J., Slagboom, P. E., Draisma, H. H., Martin, N. G., & Boomsma, D. I. (2012). The continuing value of twin studies in the omics era. *Nat Rev Genet, 13*(9), 640-653. doi:10.1038/nrg3243

Vance, J. E. (2015). Phospholipid synthesis and transport in mammalian cells. *Traffic, 16*(1), 1-18. doi:10.1111/tra.12230

Vandekeere, S., Dubois, C., Kalucka, J., Sullivan, M. R., Garcia-Caballero, M., Goveia, J., . . . Carmeliet, P. (2018). Serine Synthesis via PHGDH Is Essential for Heme Production in Endothelial Cells. *Cell Metab, 28*(4), 573-587 e513. doi:10.1016/j.cmet.2018.06.009

VanDerMeid, K. R., Su, S. P., Ward, K. W., & Zhang, J. Z. (2012). Correlation of tear inflammatory cytokines and matrix metalloproteinases with four dry eye diagnostic tests. *Invest Ophthalmol Vis Sci, 53*(3), 1512-1518. doi:10.1167/iovs.11-7627

Vane, J., & Botting, R. (1987). Inflammation and the mechanism of action of anti-inflammatory drugs. *FASEB J, 1*(2), 89-96.

Vannay, A., Dunai, G., Banyasz, I., Szabo, M., Vamos, R., Treszl, A., . . . Vasarhelyi, B. (2005). Association of genetic polymorphisms of vascular endothelial growth factor and risk for proliferative retinopathy of prematurity. *Pediatr Res, 57*(3), 396-398. doi:10.1203/01.PDR.0000153867.80238.E0

Vecino, E., Rodriguez, F. D., Ruzafa, N., Pereiro, X., & Sharma, S. C. (2016). Glia-neuron interactions in the mammalian retina. *Prog Retin Eye Res, 51*, 1-40. doi:10.1016/j.preteyeres.2015.06.003

Versura, P., Bavelloni, A., Grillini, M., Fresina, M., & Campos, E. C. (2013). Diagnostic performance of a tear protein panel in early dry eye. *Mol Vis, 19*, 1247-1257.

Viegas, F. O., & Neuhauss, S. C. F. (2021). A Metabolic Landscape for Maintaining Retina Integrity and Function. *Front Mol Neurosci, 14*, 656000. doi:10.3389/fnmol.2021.656000

Wagner, A. K., Gehrmann, U., Hiltbrunner, S., Carannante, V., Luu, T. T., Naslund, T. I., . . . Gabrielsson, S. (2021). Soluble and Exosome-Bound alpha-Galactosylceramide Mediate Preferential Proliferation of Educated NK Cells with Increased Anti-Tumor Capacity. *Cancers (Basel), 13*(2). doi:10.3390/cancers13020298

Wake, H., Moorhouse, A. J., Jinno, S., Kohsaka, S., & Nabekura, J. (2009). Resting microglia directly monitor the functional state of synapses in vivo and determine the fate of ischemic terminals. *J Neurosci, 29*(13), 3974-3980. doi:10.1523/JNEUROSCI.4363-08.2009

Wanders, R. J., Ruiter, J. P., L, I. J., Waterham, H. R., & Houten, S. M. (2010). The enzymology of mitochondrial fatty acid beta-oxidation and its application to follow-up analysis of positive neonatal screening results. *J Inherit Metab Dis, 33*(5), 479-494. doi:10.1007/s10545-010-9104-8

Wang, B., Wu, L., Chen, J., Dong, L., Chen, C., Wen, Z., . . . Wang, D. W. (2021). Metabolism pathways of arachidonic acids: mechanisms and potential therapeutic targets. *Signal Transduct Target Ther, 6*(1), 94. doi:10.1038/s41392-020-00443-w

Wang, X., Li, K. F., Adams, E., & Van Schepdael, A. (2011). Matrix metalloproteinase inhibitors: a review on bioanalytical methods, pharmacokinetics and metabolism. *Curr Drug Metab, 12*(4), 395-410. doi:10.2174/138920011795202901

Wang, X., Zhao, L., Zhang, J., Fariss, R. N., Ma, W., Kretschmer, F., . . . Wong, W. T. (2016). Requirement for Microglia for the Maintenance of Synaptic Function and Integrity in the Mature Retina. *J Neurosci, 36*(9), 2827-2842. doi:10.1523/JNEUROSCI.3575-15.2016

Wang, X. P., Chen, Y. G., Qin, W. D., Zhang, W., Wei, S. J., Wang, J., . . . Zhang, M. X. (2011). Arginase I attenuates inflammatory cytokine secretion induced by lipopolysaccharide in vascular smooth muscle cells. *Arterioscler Thromb Vasc Biol, 31*(8), 1853-1860. doi:10.1161/ATVBAHA.111.229302

Weiter, J. J., Zuckerman, R., & Schepens, C. L. (1982). A model for the pathogenesis of retrolental fibroplasia based on the metabolic control of blood vessel development. *Ophthalmic Surg, 13*(12), 1013-1017.

Werb, Z. (1997). ECM and cell surface proteolysis: regulating cellular ecology. *Cell, 91*(4), 439-442. doi:10.1016/s0092-8674(00)80429-8

Winkler, B. S., Sauer, M. W., & Starnes, C. A. (2003). Modulation of the Pasteur effect in retinal cells: implications for understanding compensatory metabolic mechanisms. *Exp Eye Res, 76*(6), 715-723. doi:10.1016/s0014-4835(03)00052-6

Wishart, D. S., Feunang, Y. D., Marcu, A., Guo, A. C., Liang, K., Vazquez-Fresno, R., . . . Scalbert, A. (2018). HMDB 4.0: the human metabolome database for 2018. *Nucleic Acids Res, 46*(D1), D608-D617. doi:10.1093/nar/gkx1089

Wright, H. L., Moots, R. J., Bucknall, R. C., & Edwards, S. W. (2010). Neutrophil function in inflammation and inflammatory diseases. *Rheumatology (Oxford), 49*(9), 1618-1631. doi:10.1093/rheumatology/keq045

Wu, C. W., Sauter, J. L., Johnson, P. K., Chen, C. D., & Olsen, T. W. (2004). Identification and localization of major soluble vitreous proteins in human ocular tissue. *Am J Ophthalmol, 137*(4), 655-661. doi:10.1016/j.ajo.2003.11.009

Wynn, T. A. (2008). Cellular and molecular mechanisms of fibrosis. *J Pathol, 214*(2), 199-210. doi:10.1002/path.2277

Xia, J., Wang, Z., & Zhang, F. (2014). Association between Related Purine Metabolites and Diabetic Retinopathy in Type 2 Diabetic Patients. *Int J Endocrinol, 2014*, 651050. doi:10.1155/2014/651050

Xia, J. F., Wang, Z. H., Liang, Q. L., Wang, Y. M., Li, P., & Luo, G. A. (2011). Correlations of six related pyrimidine metabolites and diabetic retinopathy in Chinese type 2 diabetic patients. *Clin Chim Acta, 412*(11-12), 940-945. doi:10.1016/j.cca.2011.01.025

Hajsl, M., Hlavackova, A., Broulikova, K., Sramek, M., Maly, M., Dyr, J. E., & Suttnar, J. (2020). Tryptophan Metabolism, Inflammation, and Oxidative Stress in Patients with Neurovascular Disease. *Metabolites, 10*(5). doi:10.3390/metabo10050208

Xie, N., Zhang, L., Gao, W., Huang, C., Huber, P. E., Zhou, X., . . . Zou, B. (2020). NAD(+) metabolism: pathophysiologic mechanisms and therapeutic potential. *Signal Transduct Target Ther, 5*(1), 227. doi:10.1038/s41392-020-00311-7

Xu, Y., An, X., Guo, X., Habtetsion, T. G., Wang, Y., Xu, X., . . . Huo, Y. (2014). Endothelial PFKFB3 plays a critical role in angiogenesis. *Arterioscler Thromb Vasc Biol, 34*(6), 1231-1239. doi:10.1161/ATVBAHA.113.303041

Barba, I., Garcia-Ramirez, M., Hernandez, C., Alonso, M. A., Masmiquel, L., Garcia-Dorado, D., & Simo, R. (2010). Metabolic fingerprints of proliferative diabetic retinopathy: an 1H-NMR-based metabonomic approach using vitreous humor. *Invest Ophthalmol Vis Sci, 51*(9), 4416-4421. doi:10.1167/iovs.10-5348

Yanamandra, K., Napper, D., Pramanik, A., Bocchini, J. A., Jr., & Dhanireddy, R. (2010). Endothelial nitric oxide synthase genotypes in the etiology of retinopathy of prematurity in premature infants. *Ophthalmic Genet, 31*(4), 173-177. doi:10.3109/13816810.2010.497528

Yang, H., Li, S., Xiao, X., Wang, P., Guo, X., & Zhang, Q. (2012). Identification of FZD4 and LRP5 mutations in 11 of 49 families with familial exudative vitreoretinopathy. *Mol Vis, 18*, 2438-2446.

Yang, X., Dong, X., Jia, C., & Wang, Y. (2013). Profiling of genes associated with the murine model of oxygen-induced retinopathy. *Mol Vis, 19*, 775-788.

Yang, Y., Wu, Z., Li, S., Yang, M., Xiao, X., Lian, C., . . . Zhang, G. (2020). Targeted Blood Metabolomic Study on Retinopathy of Prematurity. *Invest Ophthalmol Vis Sci, 61*(2), 12. doi:10.1167/iovs.61.2.12

Yates, C. M., Calder, P. C., & Ed Rainger, G. (2014). Pharmacology and therapeutics of omega-3 polyunsaturated fatty acids in chronic inflammatory disease. *Pharmacol Ther, 141*(3), 272-282. doi:10.1016/j.pharmthera.2013.10.010

Yavuz, S., Toker, E., Bicakcigil, M., Mumcu, G., & Cakir, S. (2006). Comparative analysis of autoantibodies against a-fodrin in serum, tear fluid, and saliva from patients with Sjogren's syndrome. *J Rheumatol, 33*(7), 1289-1292.

Yazdani, M., Elgstoen, K. B. P., Rootwelt, H., Shahdadfar, A., Utheim, O. A., & Utheim, T. P. (2019). Tear Metabolomics in Dry Eye Disease: A Review. *Int J Mol Sci, 20*(15). doi:10.3390/ijms20153755

Ye, X., Wang, Y., Cahill, H., Yu, M., Badea, T. C., Smallwood, P. M., . . . Nathans, J. (2009). Norrin, frizzled-4, and Lrp5 signaling in endothelial cells controls a genetic program for retinal vascularization. *Cell, 139*(2), 285-298. doi:10.1016/j.cell.2009.07.047

Yeh, W. L., Lin, C. J., & Fu, W. M. (2008). Enhancement of glucose transporter expression of brain endothelial cells by vascular endothelial growth factor derived from glioma exposed to hypoxia. *Mol Pharmacol, 73*(1), 170-177. doi:10.1124/mol.107.038851

Yokota, I., Sasaki, Y., Kashima, L., Idogawa, M., & Tokino, T. (2010). Identification and characterization of early growth response 2, a zinc-finger transcription factor, as a p53-regulated proapoptotic gene. *Int J Oncol, 37*(6), 1407-1416. doi:10.3892/ijo_00000792

Yoon, K. C., Jeong, I. Y., Park, Y. G., & Yang, S. Y. (2007). Interleukin-6 and tumor necrosis factor-alpha levels in tears of patients with dry eye syndrome. *Cornea, 26*(4), 431-437. doi:10.1097/ICO.0b013e31803dcda2

Yoon, K. C., Park, C. S., You, I. C., Choi, H. J., Lee, K. H., Im, S. K., . . . Pflugfelder, S. C. (2010). Expression of CXCL9, -10, -11, and CXCR3 in the tear film and ocular surface of patients with dry eye syndrome. *Invest Ophthalmol Vis Sci, 51*(2), 643-650. doi:10.1167/iovs.09-3425

You, J., Hodge, C., Wen, L., McAvoy, J. W., Madigan, M. C., & Sutton, G. (2013). Tear levels of SFRP1 are significantly reduced in keratoconus patients. *Mol Vis, 19*, 509-xxx.

Yu, M., Wu, Z., Zhang, Z., Huang, X., & Zhang, Q. (2015). Metabolomic Analysis of Human Vitreous in Rhegmatogenous Retinal Detachment Associated With Choroidal Detachment. *Invest Ophthalmol Vis Sci, 56*(9), 5706-5713. doi:10.1167/iovs.14-16338

Zandbelt, M., te Boome, L., Klasen, I., van de Putte, L., & van den Hoogen, F. (2009). Tear fluid measurement of anti-SS-A and anti-SS-B antibody in anti-SS-A and anti-SS-B seronegative Sjogren's syndrome patients. *Clin Exp Rheumatol, 27*(3), 536.

Zasada, M., Madetko-Talowska, A., Revhaug, C., Rognlien, A. G. W., Baumbusch, L. O., Ksiazek, T., . . . Saugstad, O. D. (2020). Short- and long-term impact of hyperoxia on the blood and retinal cells' transcriptome in a mouse model of oxygen-induced retinopathy. *Pediatr Res, 87*(3), 485-493. doi:10.1038/s41390-019-0598-y

Zhang, W., Li, H., Ogando, D. G., Li, S., Feng, M., Price, F. W., Jr., . . . Bonanno, J. A. (2017). Glutaminolysis is Essential for Energy Production and Ion Transport in Human Corneal Endothelium. *EBioMedicine, 16*, 292-301. doi:10.1016/j.ebiom.2017.01.004

Zheng, L., Roeder, R. G., & Luo, Y. (2003). S phase activation of the histone H2B promoter by OCA-S, a coactivator complex that contains GAPDH as a key component. *Cell, 114*(2), 255-266. doi:10.1016/s0092-8674(03)00552-x

Zhou, L., & Beuerman, R. W. (2012). Tear analysis in ocular surface diseases. *Prog Retin Eye Res, 31*(6), 527-550. doi:10.1016/j.preteyeres.2012.06.002

Zhou, L., Beuerman, R. W., Chan, C. M., Zhao, S. Z., Li, X. R., Yang, H., . . . Tan, D. (2009). Identification of tear fluid biomarkers in dry eye syndrome using iTRAQ quantitative proteomics. *J Proteome Res, 8*(11), 4889-4905. doi:10.1021/pr900686s

Zhou, T., Souzeau, E., Sharma, S., Landers, J., Mills, R., Goldberg, I., . . . Craig, J. E. (2017). Whole exome sequencing implicates eye development, the unfolded protein response and plasma membrane homeostasis in primary open-angle glaucoma. *PLoS One, 12*(3), e0172427. doi:10.1371/journal.pone.0172427

Zhou, Y., Tan, W., Zou, J., Cao, J., Huang, Q., Jiang, B., . . . Li, Y. (2021). Metabolomics Analyses of Mouse Retinas in Oxygen-Induced Retinopathy. *Invest Ophthalmol Vis Sci, 62*(10), 9. doi:10.1167/iovs.62.10.9

Zhou, Y., Xu, Y., Zhang, X., Huang, Q., Tan, W., Yang, Y., . . . Li, Y. (2021). Plasma levels of amino acids and derivatives in retinopathy of prematurity. *Int J Med Sci, 18*(15), 3581-3587. doi:10.7150/ijms.63603

Zhou, Y., Xu, Y., Zhang, X., Zhao, P., Gong, X., He, M., . . . Li, Y. (2020). Plasma metabolites in treatment-requiring retinopathy of prematurity: Potential biomarkers identified by metabolomics. *Exp Eye Res, 199*, 108198. doi:10.1016/j.exer.2020.108198

Zhu, L., Zhao, Q., Yang, T., Ding, W., & Zhao, Y. (2015). Cellular metabolism and macrophage functional polarization. *Int Rev Immunol, 34*(1), 82-100. doi:10.3109/08830185.2014.969421

ANNEXURES

10. **Annexure I**

Informed Consent for Collection of Blood / Vitreous Samples for Research on Retinopathy of Prematurity

You are being invited to participate in our ongoing research on genetics of Retinopathy for prematurity. This consent form describes your (you and your family) role in this study. We will explain the whole procedure and the need for your participation in this study. Please read it carefully and do not hesitate to ask if you have any queries at any point of time.

Retinopathy of prematurity (ROP) is a disease that affects premature infants during the neonatal period. In this disease, blood vessels in retina (the posterior part of eye) do not develop properly and can lead to low vision and blindness. This study is being done to understand the role of genetics in the development and progression of ROP in premature infants.

This study aims at better understanding of the disease development so as to devise a simple and inexpensive diagnostic method for routine evaluation and to identify high-risk infants in time. This is an experimental study and we will require blood and vitreous samples of patient with ROP and those with congenital cataract and undergoing surgery for the same for the immunological and genetic analysis. Babies of less than 35 weeks of gestation and/or birth weight ≤1700 grams having advanced stages of ROP and those with congenital cataract and undergoing surgery will be included in the study. Approximately 20 such babies will be included in the study.

If you agree to be in this study, we will ask you to do the following things:

1. Complete family details in the form of questionnaire for studying the hereditary patterns for the disease will be asked.
2. Complete neonatal, systemic and maternal information of infant and mother will be required.
3. Blood sample (i.e. 2 mL/ tablespoon) will be collected intravenously from the infant at the time of regular neonatal screening.
4. Vitreous sample removed as a part of routine surgery for such patients will be stored for immunological tests.

Serum and DNA (the genetic material in the cells) will be extracted form the blood samples and subsequently studied for any change which could have any association to the disease. New born babies having ROP will be taken as cases and those having congenital cataract and undergoing surgery will be taken as normal controls for the purpose of comparison. Your involvement in the study will be only for one time however, your child if having ROP will be examined at 5-6 follow-up visits for assessing the status of ROP as a part of regular medical procedure. A part of your DNA will be stored for any future studies on this disease.

No harm will come to you (your child/ward) by providing the sample. The results of study may or may not be of immediate benefit to the patient. Complete confidentiality will be maintained in the handling and processing of samples and the results of the study. We highly appreciate your cooperation in completing this study. However, if you join this study, you will have liberty to quit at any time during the course of this study without any loss of benefits.

L.V. Prasad Eye Institute has a policy to protect health information that may identify you. By signing this consent form, you agree that health information that identifies you may be used as described in this form for the study purposes only. Information that may be used include your date of birth, birth place and other details about you and your health or medical condition which we get from you or from the questionnaire and experiments described in this consent form

Your information will be used to carry out this study and to evaluate the results of this study. Your identity will not be disclosed at any stage when this information is being shared by other organization for academic purposes. This authorization to use and share health information does not end unless you cancel it.

Geeta Kashyap Vemuganti M.D.
Member Secretary
Ethics Committee
L V Prasad Eye Institute

ACCEPTED

The L.V. Prasad Eye Institute IRB is made up of scientists, non-scientists, doctors, and legal personnel. The IRB's purpose is to review human research studies and to protect the rights and welfare of the people participating in those studies. You may contact the IRB if you have questions about your rights as a participant or if you think you have not been treated fairly. The IRB office number is **040-30612505.** If you have questions about the study, then you may call the principal investigator, **Dr. Inderjeet Kaur** at phone no **040-30612508**.

L.V. Prasad Eye Institute is dedicated to finding the causes and cures of ocular diseases. The data, blood/tissue samples from your body collected during this study are important to this study and to future research. If you join this study, L.V. Prasad Eye Institute will own this data, tissue and blood samples. This material will be studied, tested and used by medical scientists.

By signing this consent form, you are not giving up any legal rights. Your signature means that you understand the information given to you in this form, you accept the provisions in the form, and you agree to join the study.

The above statement has been read out or explained to me, and having understood the same, I voluntarily put my signature or thumb impression.

Patient's Name: Mr. No.:

Signature/left hand thumb impression of patient /guardian

Name (capitals):

Relationship (if guardian):

Witness 1: Signature:

Name (capitals):

Designation: Date:

ACCEPTED

Geeta Kashyap Vemuganti M.D.
Member Secretary
Ethics Committee
L V Prasad Eye Institute

GENETICS OF RETINOPATHY OF PREMATURITY
L. V. Prasad Eye Institute

1. **Date** _____

2. **Study Patient no:** _____

Personal Details:

3. **Name:** _____

4. **ID no.:** _____

5. **Mother' name :** _____

6. **Father's name:** _____

7. **Address:** _____

8. **Phone no.:** _____

9. **Email ID:** _____

Infant's Details:

10. **Neonatal Care:** _____

11. **Date Of Birth:** _____

12. Age: ____

13. Gender: Male \ Female

14. Ethnic Background

	Country	State	City
Self			
Mother's			
Father's			

15. Religion - Hindu \ Muslim \ Jews

16. Gestational Age ____

17. Birth Weight: ____
(grams)

18. APGAR: 1min. 5min. 10min.

19. Appropriate for Gestational Age (AGA): Yes/No

20. Small for gestational Age (SGA): Yes/No

21. Oxygen Yes NO Unknown

22. Surfactant Yes No Unknown
(If Yes) which day of Life:

23. Ventilation Support Yes No Unknown
(If yes) No of Days:

24. Blood Transfusion Yes No Unknown
(If yes) No of units:

25. Respiratory Distress Syndrome Yes No Unknown

26. Pneumothorax Yes No Unknown

27. Meconium Aspiration Syndrome Yes No Unknown

28. Fetal Distress Yes No Unknown

29. Apnoeie Spell Yes No Unknown

30. Brady Spell Yes No Unknown

31. Hyper bilurubenaemia Yes No Unknown

32. Phototherapy Yes No Unknown
(If yes—No of days)

33. Malformation Yes No Unknown
If Yes, Birth defect: 1.
2.
3.

34. Hyaline Membrane Disease

35. Sepsis Yes No Unknown

If yes, Organism: GBS ☐ E coli ☐ Coag-ve Staph. ☐

Fungal ☐ others ☐

36. Congenital viral Infection Yes No Unknown

37. Patent Ductus Yes No Unknown
a. Indomethacin Yes No Unknown
b. PDA Ligation Yes No Unknown

38. Necrotizing Enterocolitis Yes No Unknown

39. Focal GI Perforation Yes No Unknown

40. Intra Cranial Hemorrhage Yes No Unknown

41. Seizures Yes No Unknown

42. Ischemic Encephalopathy Yes No Unknown

43. Surgery:

a. Abdominal Surgery

b. **Cardiac**
c. **Neuroglial**
d. **Thoracic/Non-Cardiac**
e. **Others**

Associated Findings or Disease:

Maternal History:

44. Age:

45. Educational Background: **Literate \ Illiterate**

Highest level of Education Primary school \ Higher secondary \ Graduation \ Post graduation \ Professional

46. Professional Background:

Profession Outdoor \ Indoor

47. Socioeconomic Background:

48. Dietary habits:

Staple diet:- Wheat \ Rice \ Maize \ Any other

Green tea/ Black tea / wine/ Chawanprash / any other source of antioxidants

Smoker \ Nonsmoker
No. of cigarettes/ bidis in a day

Pan / Tobacco

Alcoholic \ Non-alcoholic

Vegetarian/Non-vegetarian Beef/ Pork/ Chicken/ Fish/Mutton

Medical History of Mother

50. Height [ ]

51. Weight [ ]

52. Blood Pressure [ ]

53. Diabetes mellitus Yes\No Duration [ ]

Medication - Insulin / Oral hypoglycemics / Exercise

Control - well controlled /Fluctuating / Poor control

54. Hypertension Yes\No Duration [ ]

Medication [ ]

Control well controlled /Fluctuating / Poor control

55. Allergic disorders Yes\No Duration [ ]

56. Long term chronic illness Yes\No Duration [ ]

57. Congenital disease if any [ ]

58. Inflammatory disease if any [ ]

59. Any systemic medications (If yes details) [ ]

Pregnancy details

Prenatal care	**Yes**	**No**	**Unknown**
Antenatal Steroids	**Yes**	**No**	**Unknown**
Mode of delivery	**Vaginal / Cessarian / Forceps /unknown**		
Multiple birth	**Yes**	**No**	**Unknown**

Genetic history

Family History **Familial \ Sporadic**

Pedigree chart related to refractive error - Attached \ Not attached

Pedigree details:

Father	Age	Affected: Yes/NO
Mother	Age	Affected: Yes/NO

Whether the marriage of parents was within the relation: YES/NO

No of Brothers	Age	Affected: Yes/NO
	Age	Affected: Yes/NO
No of sisters	Age	Affected: Yes/NO
	Age	Affected: Yes/NO
Grandfather (paternal)	Age	Affected: Yes/NO
Grandmother (paternal)	Age	Affected: Yes/NO

Whether the marriage of grandparents was within the relation: YES/NO

Grandfather (maternal)	Age	Affected: Yes/NO
Grandmother (maternal)	Age	Affected: Yes/NO

Whether the marriage of grandparents was within the relation: YES/NO

Any other affected members, please specify with age.

Any history of premature birth in Family:

Any other member having any defect / disease since birth?

60. History of consanguinity Yes \ No

61. Comments by Ophthalmologist:

ROP: Yes ☐ **No** ☐

Regress spontaneously: Yes ☐ **No** ☐

S/p Laser Regress: Yes ☐ **No** ☐

Remarks (if any):

Surgery: Yes ☐ **No** ☐

Remarks (if any):

62. Informed Consent: Yes \ No

63. Permission to contact Family members: Yes \ No

64. Blood sample: Taken \ Not taken

65. DNA Isolation: Yes/No

66. Done by:

67. Signature ☐ **Date** ☐

ANNEXURE II

Supplementary Table 1. Components for gelatin zymography gel

Components	Resolving gel	Stacking gel
H2O	2mL	3.08mL
30% Acrylamide-Bis acrylamide mix	2mL	0.8mL
1.5 M Tris pH 8.8	2mL	-
1 M Tris pH 8.8	-	0.63mL
4 mg/mL gelatin	2mL	-
10% SDS	80µL	50µL
10% APS	80µL	50µL
TEMED	10µL	10µL

Supplementary Table 2. Composition for 12% SDS-PAGE gel

Reagents	Resolving gel (10mL)	Stacking gel (2mL)
dd. H_2O	4	2.1
30% Acrylamide-Bis acrylamide	3.3	0.5
1.5M Tris HCl (pH=8.8)	2.5	-
1M Tris HCl (pH=6.8)	-	0.38
10% SDS (w/v)	0.1	0.03
10% APS (w/v)	0.1	0.03
TEMED	0.004	0.003

1. **Reagents used for agarose gel electrophoresis**

   a) **50X TAE [(Tris- acetate EDTA (ethylenediaminetetraacetic acid)]**

   242 g of Tris-base and 100 ml of 0.5M EDTA were added to 800 ml of autoclaved deionized water and allowed to dissolve on a magnetic stirrer. To this, 57.1 ml of glacial acetic acid was added and the volume was made up to 1 litre with double distilled water. The contents were mixed until a clear solution was obtained and stored at room temperature.

   b) **EtBr (Ethidium Bromide)**

   For EtBr with 10 mg/mL concentration, 1g of Ethidium Bromide was added in 100 mL of autoclaved deionized water and stirred with a magnetic stirrer to dissolve it completely. The solution was stored in a dark bottle, wrapped with aluminium foil and stored at room temperature.

   c) **6X loading dye**

   To make 100 ml of the dye, 40 g of sucrose, 0.025 g of Xylene cyanol and 0.025 g of bromophenol blue were added to obtain a final volume of 100 ml with autoclaved deionized water.

2. **Reagents used for PAGE and Zymography**

   a) **30% acrylamide (acrylamide: bisacrylamide, 29:1)**

   29 g of acrylamide and 1g of N, N'-Methylenebisacrylamide was added to autoclaved deionized water to make a stock solution of 100 ml. The solution was made homogenous by mixing on a magnetic stirrer.

   b) **10X TBE (Tris-Borate EDTA)**

   54 g of Tris-base, 27.5 g of boric acid and 20 ml of 0.5 M EDTA (pH 8) were added to 900 ml of autoclaved deionized water and allowed to dissolve on a magnetic stirrer to give a final volume of 1 liter.

   c) **0.5 M EDTA**

   186.1 g of disodium EDTA.$2H_2O$ was added to 800 ml of autoclaved deionized water and stirred on a magnetic stirrer. The pH was adjusted to 8.0 with NaOH pellets (approximately 20 g of pellets). The solution was sterilized by autoclaving.

   d) **10% APS (Ammonium per sulphate)**

   0.1 g of APS was added to 1 ml of autoclaved deionized water in a 1.5 ml eppendorrf tube and mixed thoroughly by inverting the tube. The tube was wrapped with aluminium foil at stored at 4°C.

   e) **Tris-HCl (1.5M –pH 8.8)**

   For 200 ml of the solution, 36.3 g of Tris base was added to 150 ml of deionized water in a beaker and dissolved on a magnetic stirrer. The pH of the solution was adjusted to8.8 with HCl and the volume was adjusted with water and autoclaved.

   f) **Tris-HCL (1M-pH 6.8)**

   For 100 ml of the solution, 12.21 g of Tris base was added to 50 ml of deionized water in a beaker and dissolved on a magnetic stirrer. The pH of the solution was adjusted to 6.8 with HCl and the volume was adjusted with water and autoclaved.

   g) **10% SDS**

   For 50 ml of the solution, 5 g of SDS was added to 40 ml of autoclaved deionized water in a beaker and dissolved by heating in a water bath. The final volume was adjusted to 50mL with autoclaved deionized water.

h) 5X running buffer

15.1g of Tris base, 5g of SDS and 94g of Glycine were added to 800 mL of autoclaved deionized water. The pH of the solution was adjusted to 8.3 and the final volume of the solution was made to 1000 ml with autoclaved deionized water. The final concentration of the solution was 5X. The working solution of 1X was prepared by diluting the stock solution with autoclaved deionized water.

i) 1% w/v gelatine

1% Gelatin was freshly prepared by dissolved 50mg of gelatine in 5 mL of dH_2O and the solution was heated at 60°C in a water bath (for at least 20 min) until it was dissolved properly. Then the gelatin solution was allowed to cool down at room temperature before use.

j) Renaturing solution stock (10X)

25% v/v Triton X-100 was added in 200 mL of in dH_2O.

k) Developing buffer stock (10X)

1 L of developing buffer stock was prepared by adding 500 mM Tris-HCl (pH 7.8), 2 M NaCl, 50 mM CaCl2, and 0.2% v/v Brij 35.

l) Staining solution

1 L of staining solution was prepared by adding 0.5% w/v Coomassie blue R-250, 5% v/v methanol, and 10% v/v acetic acid in dH_2O. Store it at room temperature.

m) Destaining solution

Prepare 1 L of 10% v/v methanol, 5% v/v acetic acid in dH_2O.

3. Reagents for western blotting

a) Phosphate buffer saline (PBS)

10X PBS was prepared by adding 8 g of NaCl, 0.2 g of KCl and 1.44 g of Na2HPO4 to 800 mL of autoclaved deionized water. The pH of the solution was adjusted to 7.4 with 1M HCl and final volume was made up to 1 L. The working solution of 1X was prepared by diluting the stock solution with autoclaved deionized water.

b) 1X PBS

8 grams of sodium chloride (NaCl), 0.2 grams of potassium chloride (KCl) and 1.44 grams of sodium biphosphate (Na2HPO4) were added to 800 milliliters (ml) of autoclaved deionized water. The pH of the solution was adjusted to 7.4 with 1M hydrochloric acid. The final volume of the solution was made to 1000 ml with autoclaved deionized water. The final concentration of the solution was 10X. The working solution of 1X was prepared by diluting the stock solution with autoclaved deionized water.

c) Transfer buffer

Transfer buffer was prepared by adding 20 mL of methanol to 80 mL of 1X running buffer.

ANNEXURE II

Supplementary Table 1 Data quality parameters observed in WES

Twin Pair (study number)	Loading (%)	Enrichment (%)	Polyclonality (%)	Final Library (%)	Mean Reads (bp)	Total Reads	Aligned Reads (%)	Mean Raw Accuracy (%)	Alignment Quality (AQ20) (GB)
T5, T6	17.4 GB	100	32	96	190	90330688	89880218	99.1	14.4
	94%						99.50%		
T133, T134	13.98 GB	100	31	87	189	72372089	71982830	99.1	11.4
	83%						99.50%		
T150, T151	15.3 GB	100	26	85	189	77742786	77462583	99.1	12.5
	85%						99.60%		
T83, T84	11.8 GB	100	31	80	184	63202158	62955750	99.1	9.8
	78%						99.60%		
T156, T157	18.01 GB	100	28	95	186	94964361	94340854	99	14.2
	95%						99.30%		
T146, T47	14.4 GB	100	32	89	190	74648463	74215056	99.1	11.8
	85%						99.40%		
T9, T52	14 GB	99	32	91	169	81706808	80963028	98.9	11.03
	93%						99.10%		
T20, T21	8 GB	99	24	69	162	48773770	48072156	98.8	6.11
	64%						98.60%		
T152, T153	12.1 GB	100	32	85	189	63323267	62975602	99.1	10.1
	75%						99.50%		
T148, T149	15.2 GB	100	34	94	177	84894626	84089927	98.7	11.2
	84%						99.10%		

Twin Pair (study number)	Loading (%)	Enrichment (%)	Polyclonality (%)	Final Library (%)	Mean Reads (bp)	Total Reads	Aligned Reads (%)	Mean Raw Accuracy (%)	Alignment Quality (AQ20) (GB)
T2, T51	11.5 GB	100	34	83	175	64318168	63921296	98.8	8.73
	81%						99.40%		
T54, T1	18.7 GB	100	25	96	189	96380570	95809747	98.9	14.6
	93%						99.40%		
T3, T4	15.7 GB	100	29	90	184	81816643	81210609	99	12.3
	90%						99.30%		
T22, T23	17.2 GB	100	30	95	187	88508819	87802483	99	13.7
	94%						99.20%		
T19, T47	17 GB	100	26	91	187	87385101	87014070	98.6	12.7
	91%						99.60%		

ANNEXURE IV

Supplementary Table 1 Parameters applied for ionisation

Ion Source Parameters:	
Nitrogen Gas Temp	250^0C
Flow of Drying Gas	8 L/min
Nebulizer pressure	40 psig
Voltage at capillary	3500V
Fragmentor Volt	150V
Skimmer	65V

Supplementary Table 2. Details of gradient applied for separation of ions in a mass spectrophotometer.

Positive mode:	**A: Water +0.1% FA**	
	B: 90% Acetonitrile + 0.1% FA	
Time	A	B
0	92	8
1.5	92	8
25	2	98
35	2	98
35.5	92	8
45	92	8

Note- FA denotes formic acid

11. Awards and Honors

International

1. **DBT and CSIR Travel Grant 2019 to attend the ARVO meeting, 2019 in Vancouver, Canada**

National

1. **Best oral presentation in India Eye Research Group ARVO India Chapter (IERG-ARVO-IC) 2018**

2. Received **Prerna award** for the recognition of service beyond the call of duty, L V Prasad Eye Institute on 31 March 2017

12. List of Presentations

International

2. **Poster presentation** on "Matrix metalloproteases (MMPs) regulate Opticin expression in the Microglia Under Hypoxic Stress" in ARVO, 2019, Vancouver, Canada

National

2. **Oral presentation** on "MMPs regulates opticin degradation in microglia under hypoxia" was given at IERG-ARVO indian chapter meeting, 2018, Hyderabad, India

3. **Poster presentation** on "Differential Gene Expression Profiling among Different Stages of Retinopathy of Prematurity" ARVO-India (International chapter affiliation), 2017 annual meeting held on July 25th-26th at Aravind Eye Hospital, Madurai India

4. **Poster presentation** on "Assessment of the Biomarker in Retinopathy of Prematurity Patients" in Indian Eye Research Group, 2016 annual meeting on July 30th-31st at LV Prasad Eye Institute, Hyderabad, India

5. **Poster presentation** on "Assessment of the Role of Opticin in Retinopathy of Prematurity Patients" in Indian Eye Research Group, 2015 annual meeting held on July 25th-26th at LV Prasad Eye Institute, Hyderabad, India

13. List of Publications

Original research articles

- **Patnaik S**, Rai M, Jalali S, Agarwal K, Badakere A, Puppala L, Vishwakarma S, Balakrishnan D, Rani PK, Kekunnaya R, Chhablani PP, Chakrabarti S, Kaur I. An interplay of microglia and matrix metalloproteinase MMP9 under hypoxic stress regulates the opticin expression in retina. Sci Rep. 2021 Apr 2;11(1):7444. doi: 10.1038/s41598-021-86302-2. PMID: 33811221; PMCID: PMC8018966.

- Ali MJ, **Patnaik S**, Kelkar N, Ali MH, Kaur I. Alteration of Tear Cytokine Expressions in Primary Acquired Nasolacrimal Duct Obstruction - Potential Insights into the Etiopathogenesis. Curr Eye Res. 2020 Apr;45(4):435-439. doi: 10.1080/02713683.2019.1665186. Epub 2019 Oct 4. PMID: 31490706.

- **Patnaik S**, Jalali S, Joshi MB, Satyamoorthy K, Kaur I. Metabolomics Applicable to Retinal Vascular Diseases. Methods Mol Biol. 2019;1996:325-331. doi: 10.1007/978- 1-4939-9488-5_24. PMID: 31127565 (**Springer Nature: Manual**).

- Rathi S, Jalali S, Musada GR, **Patnaik S**, Balakrishnan D, Hussain A, Kaur I. Mutation spectrum of *NDP*, *FZD4* and *TSPAN12* genes in Indian patients with retinopathy of prematurity. Br J Ophthalmol. 2018 Feb;102(2):276-281. doi: 10.1136/bjophthalmol-2017-310958. Epub 2017 Oct 5. PMID: 28982955.

- Rathi S, Jalali S, **Patnaik S**, Shahulhameed S, Musada GR, Balakrishnan D, Rani PK, Kekunnaya R, Chhablani PP, Swain S, Giri L, Chakrabarti S, Kaur I. Abnormal Complement Activation and Inflammation in the Pathogenesis of Retinopathy of Prematurity. Front Immunol. 2017 Dec 22;8:1868. doi: 10.3389/fimmu.2017.01868. PMID: 29312345; PMCID: PMC5743907

Book chapter

- Kaur T, **Patnaik S**, Saurabh Kumar, Kaur I. Molecular mechanisms in the pathophysiology of Retinopathy of prematurity (**Springer Nature: Accepted**)

scientific reports

Check for updates

OPEN

An interplay of microglia and matrix metalloproteinase MMP9 under hypoxic stress regulates the opticin expression in retina

Satish Patnaik[1,2,6], Meenakshi Rai[1,6], Subhadra Jalali[3], Komal Agarwal[3], Akshay Badakere[4], Lavanya Puppala[1], Sushma Vishwakarma[1], Divya Balakrishnan[3], Padmaja K. Rani[3], Ramesh Kekunnaya[4], Preeti Patil Chhablani[4,5], Subhabrata Chakrabarti[1] & Inderjeet Kaur[1]✉

Inflammation plays a key role in the pathogenesis of retinal vascular diseases. We have shown earlier an increase in the activity of matrix metalloproteinases in the vitreous and tears of preterm born babies with retinopathy of prematurity (ROP) compared to those with no-ROP leading to a shift in the balance of angiogenic (vascular endothelial growth factor [VEGF], matrix metalloproteinase [MMPs], complement component [C3]) and anti-angiogenic (opticin, thrombospondin) in ROP eyes. We now confirmed that tear MMP levels in premature infants perfectly correlates with disease severity. Next, we demonstrated that a reduced opticin levels in ROP vitreous are regulated by MMPs secreted by activated microglia. Upon exposing the human microglia cell line (CHME3) to hypoxia, an increased expression of inflammatory proteins (MMP9, VEGF) was noticed while opticin reduced significantly ($p = 0.005$). Further, the reduced opticin's expression by microglial cells under hypoxia could be rescued by inhibiting the MMP activity using doxycycline and EDTA. The inhibition of MMP activity altered the expression of other key signaling molecules under hypoxia. Our study clearly explains that increased activity of MMPs under hypoxia regulates the expression of opticin as seen in the vitreous humor of ROP and could serve as a potential target for ROP management.

Abbreviations

ROP	Retinopathy of prematurity
MMP9	Matrix metalloproteinase 9
MMP2	Matrix metalloproteinase 2
OPTC	Opticin
VEGF	Vascular endothelial growth factor
BRB	Blood-retinal barrier
ECM	Extracellular matrix
TIMP1	Tissue inhibitory metalloproteases 1
TIMP2	Tissue inhibitory metalloproteases 2
C3	Complement component 3
SLRPs	Small leucine rich proteins
EDTA	Ethylene diamine tetraacetic acid
dNTPs	Deoxy nucleotide triphosphates
bp	Base pair
IgG	Immunoglobulin G

[1]Prof. Brien Holden Eye Research Centre, LV Prasad Eye Institute, Hyderabad, India. [2]Department of Animal Biology, School of Life Sciences, University of Hyderabad, Hyderabad, Telangana, India. [3]Smt. Kannuri Santhamma Centre for Vitreo Retinal Diseases, Hyderabad, India. [4]Jasti V Ramanamma Children's Eye Care Centre, LV Prasad Eye Institute, Hyderabad, India. [5]University of Pittsburgh Medical Center, Pittsburgh, USA. [6]These authors contributed equally: Satish Patnaik and Meenakshi Rai. ✉email: inderjeet@lvpei.org

IHC	Immunohistochemistry
IF	Immunofluorescence
FnII	Fibronectin type II
PDB	Protein data bank
$CoCl_2$	Cobalt chloride
ERK1	Extracellular signal-regulated kinases 1
ERK2	Extracellular signal-regulated kinases 2
DKK1	Dickkopf WNT signaling pathway inhibitor 1
NOTCH1	Notch receptor 1
CHME3	Microglia cell line
RPE	Retinal pigment epithelium
EC	Endothelial cells
ml	Millilitre
M	Molar
µl	Microliter
mM	Millimolar
ng	Nanogram
µg	Microgram
µM	Micromolar
GA	Gestational age
BW	Birth weight
OIR	Oxygen induced retinopathy
PAGE	Polyacrylamide gel electrophoresis
NPE	Non-pigmented epithelial
RGH	Retinal growth hormone
OS	Outer segment
IL	Inner nuclear layer
IPL	Inner plexiform layer
NFL	Nerve fiber layer
TNF	Tumor necrosis factor
TGF beta1	Transforming growth factor beta 1
ROS	Reactive oxygen species
NO	Nitric oxide

Retinopathy of prematurity (ROP) is one of the most common causes of childhood blindness[1]. It is a vaso-proliferative eye disease in premature babies characterized by abnormal blood vessel growth in the retina that can cause retinal detachment and eventually lead to blindness[2]. Annually in India, nearly 1.2 million babies are prone to develop ROP[3]. The reported risk factors for ROP include low birth weight, low gestational age, gender, ethnicity, light exposure, blood transfusion and other maternal risk factors. However, gestational age, birth-weight and oxygen supplementation (to some extent) have been found to be the key defining factors across multiple studies worldwide[4]. ROP is an exceedingly complex disease, as in some set of premature infants, it regresses spontaneously while in others, it progresses from mild form (ROP-stage I, II) to severe form (ROP-stage III, IV,V) eventually leading to total vision loss if not treated timely. While ROP is considered to be a hypoxia driven neovascular condition, till date the underlying molecular mechanisms contributing to pathogenesis of ROP remain unclear. Probably, various pathological disease-causing risk factors together lead to the progression of ROP. Most commonly proposed mechanism for the pathogenesis of ROP are hypoxia induced vaso-attenuation and vaso-proliferation leading to oxidative stress[5] that further induces the release of pro-inflammatory and pro-angiogenic molecules in ROP patients[6]. All these factors together play a crucial role in the progression of the disease.

ROP being a vitreoretinal condition, alters the homeostatic balance of anti- and angiogenic proteins in the vitreous[6]. Vitreous gel is optically transparent and is composed of diverse proteins (collagens, albumin, IgG, oxidative stress enzymes and cytokines), proteoglycans (hyaluronan and chondroitin sulfate proteoglycans) and small molecules[7]. Due to proximity of vitreous with retina, especially when the blood-retinal barrier (BRB) is damaged, the secretory product of retina gets accumulated in the vitreous[8]. Moreover, in vitreoretinal diseases, the vitreous composition also changes due to differential expression of proteins under various disease conditions[7]. Therefore, studying differential protein profiling in the vitreous gel may help in understanding the underlying mechanisms of ROP.

Immunohistochemistry of the ridge membrane formed at stage II showed by the presence of endothelial cells, macroglial cells, microglia and few proliferating cells[9]. However, the exact role of microglia in ROP pathogenesis is not completely understood. Findings from our recent study on ROP suggested that activated microglia secretes elevated levels of matrix metalloproteinase (MMPs) and pro-inflammatory molecules into the vitreous and the retina[10]. The elevated levels of activated MMPs might cause extracellular matrix (ECM) degradation, in turn, promoting angiogenesis. The significant increase in MMP9, tissue inhibitory metalloproteases (TIMP1), and α2 macroglobulin in the ROP vitreous further confirmed it. Dysregulation of MMP2, and MMP9 were also detected reproducibly in stage dependent manner in ROP tear samples[10].

A pilot vitreous proteome profiling study (unpublished data) by our group revealed a lower expression of opticin, an anti-angiogenic protein in ROP patients. Opticin is present abundantly in human vitreous, and secreted into the vitreous cavity by non-pigmented epithelial cells constantly to maintain its balanced levels[11]. Opticin is an extra cellular matrix (ECM) glycoprotein associated with the collagen fibrils and the retinal growth

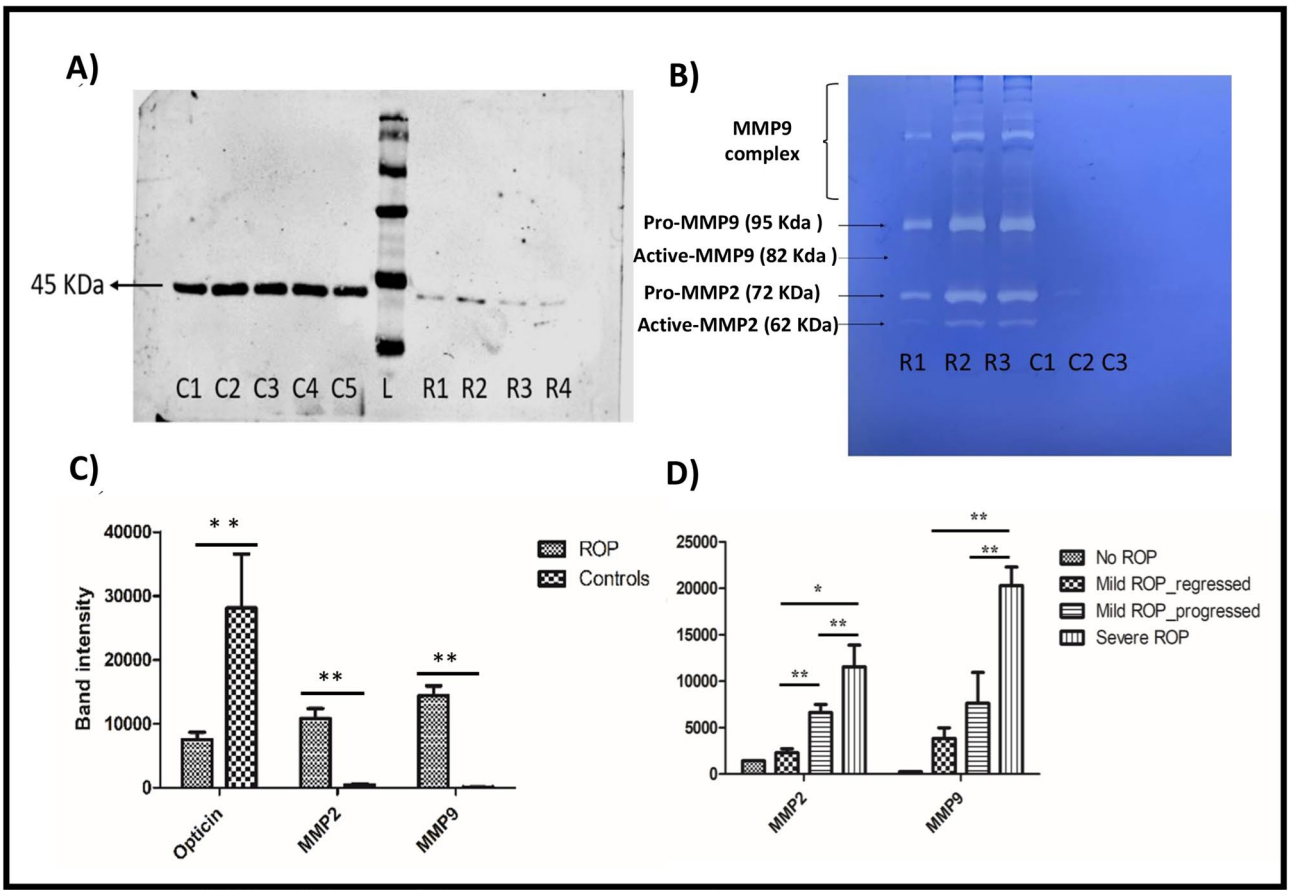

Figure 1. Representative image of (**A**) western blot of opticin levels in ROP patients and controls (**B**) representative gelatin zymography of vitreous from ROP and congenital cataract (controls) (**C**) quantification of opticin (45 K Da) levels in vitreous samples of ROP (n = 30) and control (n = 30) and MMPs in ROP (n = 11) and control (n = 11) (**D**) MMPs levels estimated in ROP tears samples by zymography in extended cohort, quantification of MMP9 and MMP2 estimated for severe ROP (n = 16), mild progressed to progressed ROP (n = 12), mild ROP to regressed ROP (n = 12), and no ROP premature controls (n = 18), $^{**}p = 0.001$, $^{*}p = 0.05$; data represented as mean ± SEM, C, control vitreous; R, ROP vitreous; L, protein ladder.

hormone[12] in the vitreous cavity. It is also identified in the other tissues like cartilage, brain and heart[11,13]. The 332 amino acid protein has a sequence that is homologous to class III small leucine rich proteins (SLRPs), epiphycan and osteoglycan, with a consensus sequence of LXXLXLXXNXL. These SLRP's confined by conserved cysteine residues interact with ECM. The role of opticin in angiogenesis has been previously identified in murine oxygen mouse model and cell culture model[14,15]. The opticin knockout model showed increased neovascularization compared to wild type mice[14]. Based on this background, we hypothesized that the abnormal activity of MMPs under hypoxic conditions affects the opticin levels and thereby contributes to increased inflammation in the retina causing ROP progression.

Results

Role of ECM proteins in ROP. The western blotting and zymography for ECM proteins including opticin and MMPs (MMP2, and MMP9) respectively showed a downregulation of opticin (45 k Da) with an increase in MMPs activity in the vitreous samples of ROP patients (Fig. 1A and B; Supplementary Fig. 1). The differential expression of MMP2 (p-value = 0.00001), MMP9 (p-value = 0.000003) and opticin (p-value = 0.0009) was found to be statistically significant thereby indicating an important role of these proteins in ROP pathogenesis (Fig. 1C). Next, we performed validation of MMPs levels in tear samples collected at the time of initial eye screening for preterm born babies. A significantly higher expression of MMP9 was observed in tear samples of the preterm born babies who later progressed to severe ROP as compared to those who developed mild ROP or had regressed disease (Fig. 1D). Since, there was a significant inverse correlation in the opticin levels with MMPs activity (Supplementary Fig. 1), we therefore wanted to assess the type of interactions between the two proteins by in-silico approaches and in-vitro analysis to check if opticin downregulation under hypoxic environment as seen in ROP could be rescued by inhibiting the increased activity of MMPs.

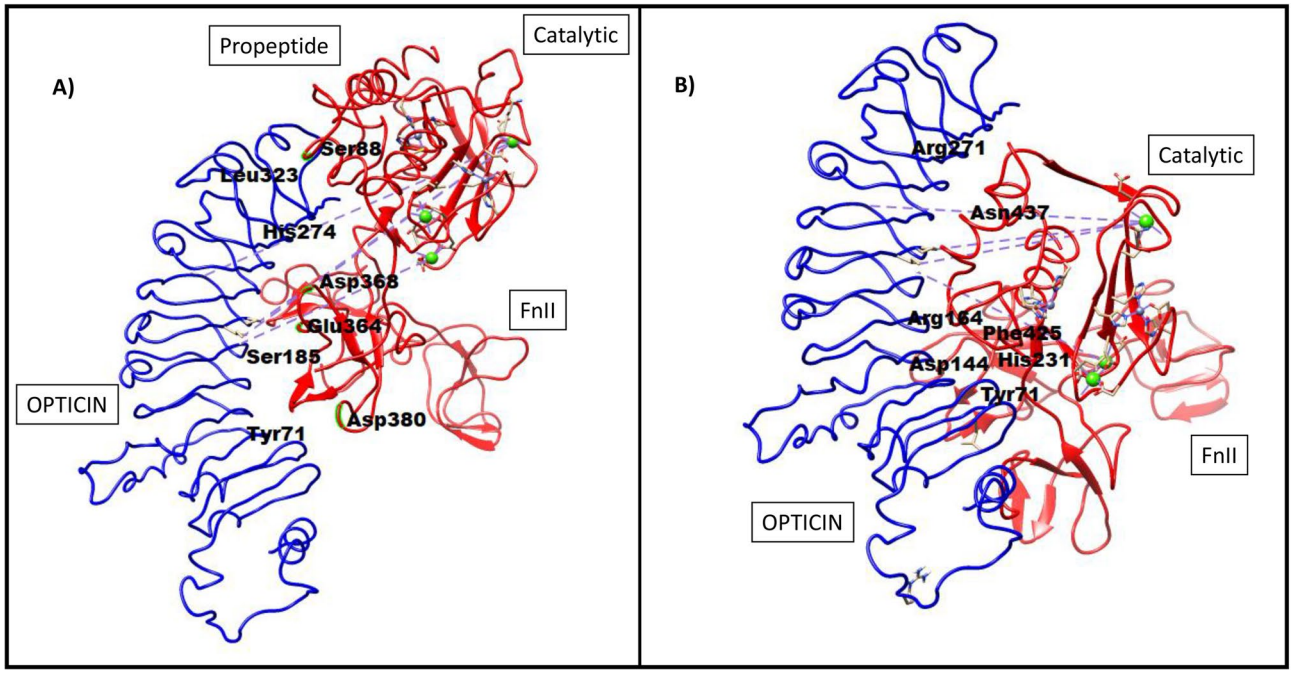

Figure 2. Predicted interactions of opticin with pro-MMP9 (**A**), and active MMP9 (**B**) using PatchDock. The important amino acids involved in these interactions at the predicted sites are shown in bold black colors.

In-silico analysis. The predicted structure for opticin, and PDB derived structures for pro-MMP (with truncated C-terminal) and active MMP, doxycycline and EDTA are shown in Supplementary Fig. 2. In-silico analysis was done in 2 sets and 4 subsets. First set included protein–protein interaction that included the interactions of pro-MMP9 and active MMP9 separately with opticin respectively (Supplementary Tables S5 and S6). In the second set, to assess if blocking MMPs activity could affect its interaction with opticin, protein–ligand interactions i.e., pro-MMP9 and active MMP9 separately with doxycycline and EDTA were studied.

Prediction of protein–protein (MMP9 and opticin) interactions. *Pro MMP9 interacts with opticin.* The pro peptide chain of MMP9 interacts with the C terminal domain of opticin. These results also predicted that only FnII domain of pro-MMP9 interacts with opticin. No interactions were seen between pro-MMP9 and the SLRP domain of opticin (Fig. 2A). Predicted interactions among the two proteins included: the interactions of amino acid residue (Asp380, Glu364, Asp368) of FnII domain and amino acid residue (Ser88) of propeptide chain of MMP9 with amino acid (Tyr77, Ser185, His274, Leu323) residues of opticin (Supplementary Table S5).

Active MMP9 docked with opticin. On the other hand, for active MMP9, both FnII and catalytic domain (generated after cleaving off the propeptide sequence) interacted with opticin. The catalytic domain of active MMP9 was predicted to interact more strongly with the N-terminal and with amino acids of SLRP domains of opticin protein (Fig. 2B). The predicted interaction between the two proteins included: interactions of amino acid residue (His231, Asn437, His231) of catalytic domain and amino acid residue of FnII domain of active MMP9 with amino acid (Arg164, Arg27, Asp144, Tyr71) residue of opticin (Supplementary Table S6).

Prediction of protein–ligand (MMP9 and doxycycline) interactions. *Pro-MMP9: doxycycline interaction.* Several different possible interactions were observed between pro-MMP9 and the MMP inhibitor-1 (doxycycline) by PatchDock. (The top 5 results are shown in the Supplementary Table S7). The doxycycline interacts with pro-MMP9 at FnII domain which is required for later's interaction with opticin (Fig. 3A), a hydrogen bond observed between doxycycline and Glu130 of MMP9 with bond length of 3.569 Å. The other interacting amino acid residues are Thr331, Arg279, and Thr331 (Supplementary Table S7).

Active MMP9: doxycycline interaction. Doxycycline interacts with active MMP9 (Fig. 3B) involving its catalytic domain largely by forming hydrogen bonds with amino acid residue (Glu402, Glu416, Leu418) of active MMP9. Besides some other interactions (Arg424, Tyr423, Met422, His401, Pro421) of active MMP9 were also observed. Since, the His401 is already known to interact with zinc ion, the interaction of doxycycline with the catalytic domain (active MMP9) seems to be involved in inhibiting the MMP9 activity (Supplementary Table S8).

Pro MMP9: EDTA interaction. Several different possible interactions were observed between pro-MMP9 and MMP inhibitor-2 (EDTA) by PatchDock. (The top 5 results are shown in the Supplementary Table S9). The

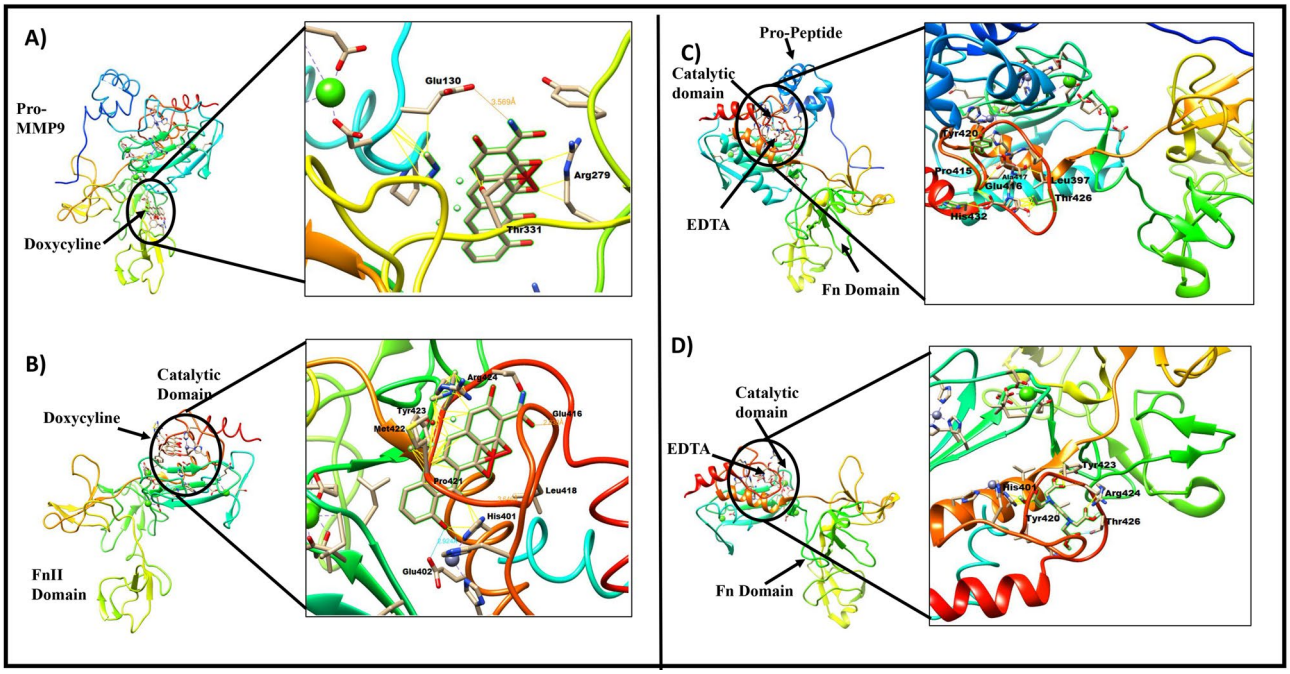

Figure 3. Predicted interactions of doxycycline with pro-MMP9 (**A**), and active MMP9 (**B**). Predicted interactions of EDTA with pro-MMP9 (**C**), and active MMP9 (**D**). The important amino acids involved in these interactions at the predicted sites are shown in bold black colors.

pro-MMP9 interacts with EDTA at catalytic domain (Fig. 3C), a hydrogen bond observed with amino acid residue (Pro415) and other interactions were observed with amino acid residues (Glu416, Thr426, Ala417, Tyr420, His432) (Supplementary Table S9).

Catalytic MMP9: EDTA interaction. EDTA interacts with the catalytic domain of active MMP9 (Fig. 3D) by forming hydrogen bonds with amino acid residue (Arg424, Thr426) of active MMP9 and observed other interactions (Tyr420, Tyr423, His401, Arg424,) with active MMP9 (Supplementary Table S10).

Regulation of opticin expression by MMP9 under hypoxic conditions. Our in-silico analysis predicted that opticin is acted upon by both pro and active form of MMP9. Next, we assessed the same using cellular assay, if the lower expression of opticin in vitreous of ROP is regulated by increased activity of MMPs in the retina and vitreous. We performed an in-vitro assay in human microglial cells (CHME3 cell line) which revealed a normal expression of the opticin and MMPs in no stress condition. The cells were induced with hypoxic stress by giving a titrated dose of 150 µM cobalt chloride that showed 70% cell survival on alamar blue assay (Supplementary Fig. 3). The hypoxia exposed cells showed higher expression of MMP9 and simultaneous reduced expression of opticin (indicating its degradation). Upon inhibition of MMP9 activity by doxycycline and EDTA the human CHME3 line under hypoxic stress resumed the normal opticin expression while TIMP2 and vascular endothelial growth factor (VEGF) expression remained more or less same (Fig. 4).

Relative expression of MMP9, OPTC and other genes in human CHME3 cell line under hypoxic stress with and without the treatment of specific MMP inhibitors. Quantitative real-time PCR based assay for the human microglial cells (CHME3) with and without hypoxic stress also revealed that upon the induction of hypoxia, the microglial cells showed significantly elevated levels of *MMP9* (fold change = 3.52, p-value = 0.008**) and a decrease in *OPTC* expression (fold change = 0.32, p-value = 0.01*). Further, inhibition of the MMPs activity by doxycycline and EDTA showed significant downregulation of MMPs expression (both doxy; fold change = 0.24, p-value = 0.006**, and EDTA; fold change = 0.25, p-value = 0.006**) and concurrent upregulation of *OPTC* (both doxy; fold change = 5.2; p-value = 0.03* and EDTA; fold change = 3.09; p-value = 0.03*) levels. However, not much changes in the expression of *TIMP2* (both doxy; fold change = 0.77; p-value = 0.2, EDTA; fold change = 0.81; p-value = 0.2) and *VEGF* (doxy; fold change = 0.79; p-value = 0.2 and EDTA; fold change = 1.5; p-value = 0.4) was seen upon inhibition of MMPs activity under hypoxic condition (Fig. 5A).

Exploration of different potential signalling pathways. Induction of hypoxia significantly leads to downregulation of *ERK2* (fold change = 0.16; p-value = 0.04*), *DKK1* (fold change = 0.15; p-value = 0.03*) and *NOTCH1* (fold change = 0.20; p-value = 0.04*), signalling genes but not *ERK1* (fold change = 0.23; p-value = 0.08), as compared to controls. Upon inhibition of MMPs activity by doxycycline, all the targeted pathway genes *ERK2* (fold change = 1.71, p-value = 0.006**), *DKK1* (fold change = 3.23; p-value = 0.02*), and *NOTCH1* (fold change = 2.07;

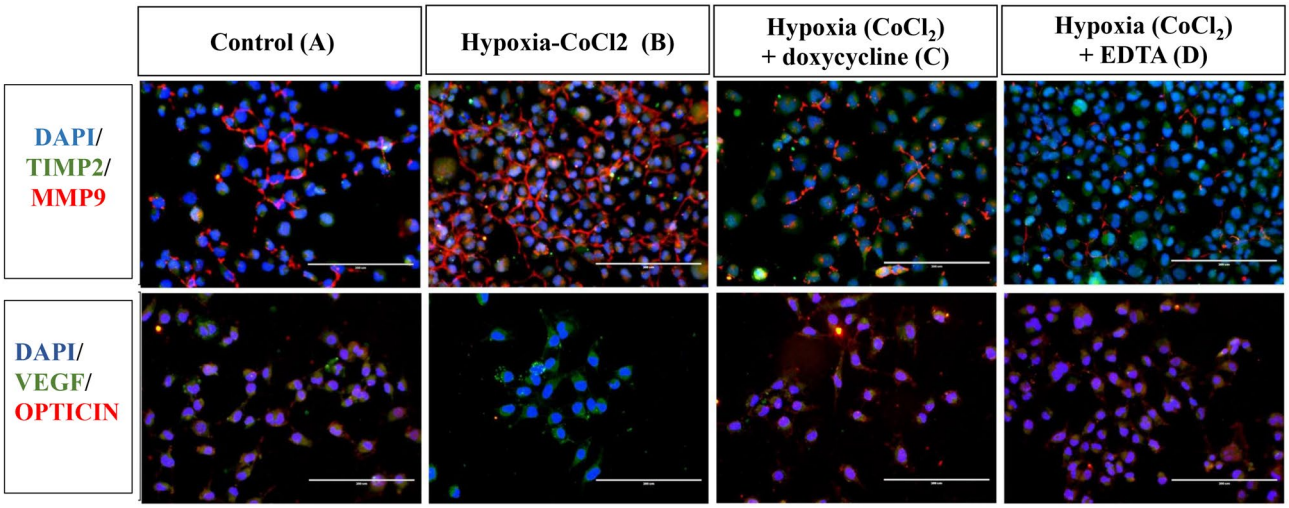

Figure 4. Representative images of immunofluorescence in microglial cells (n = 3, 20× magnified, scale bar 200 µm) showing the expression of MMP9/TIMP2 and VEGF/OPTICIN in control (**A**), hypoxia ($CoCl_2$) (**B**), hypoxia ($CoCl_2$) + doxycycline (**C**), and hypoxia ($CoCl_2$) + EDTA (**D**).

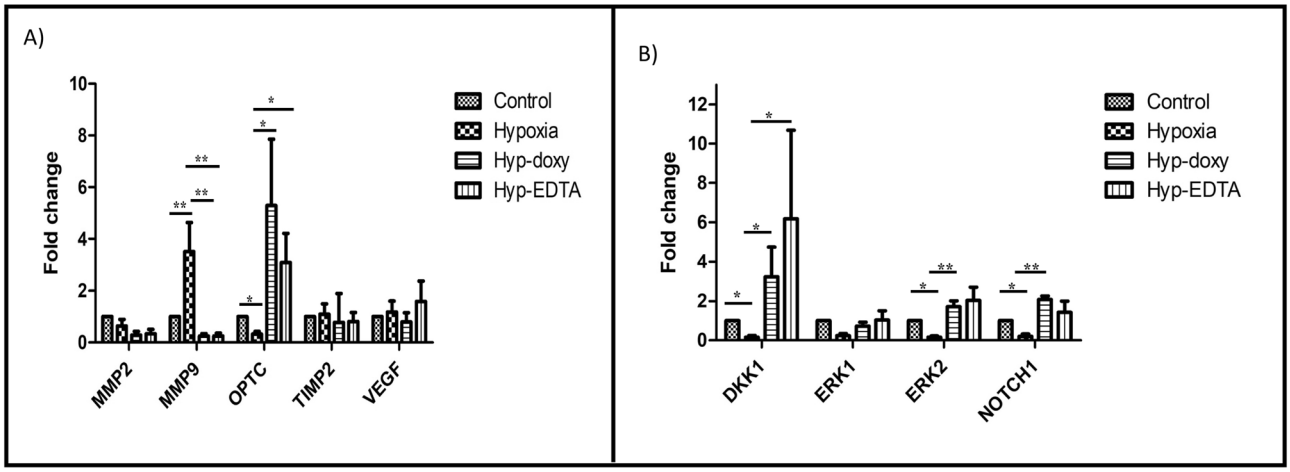

Figure 5. Differential gene expression of *MMP2*, *MMP9*, *OPTC*, *VEGF* and *TIMP2* (**A**), and potential signalling pathway genes (*DKK1*, *ERK1*, *ERK2*, and *NOTCH1*) (**B**) in control, hypoxia ($CoCl_2$), hypoxia ($CoCl_2$) + doxycycline, and hypoxia ($CoCl_2$) + EDTA in microglial cells (n = 3), $^{**}p = 0.001$, $^{*}p = 0.05$; data represented as mean ± SEM.

p-value = 0.02*) showed some rescue in expression levels while *ERK1* levels (fold change = 0.71; *p*-value = 0.14) remained low as of hypoxia treated cells. In the presence of MMP inhibitor 2 (EDTA), the hypoxia treated cells exhibited increased levels of *ERK2* (fold change = 2.02; *p*-value = 0.07) and *DKK1* (fold change = 6.17; *p*-value = 0.04*) expression but *NOTCH1* (fold change = 1.42; *p*-value = 0.4), and *ERK1* (fold change = 1.03; *p*-value = 0.6), levels approximately remained the same as of control (Fig. 5B).

Validation of microglial mediated MMP9 activity in human tissues by the immuno-histochemical examination in fibrovascular membranes of ROP patients. In normal retina, microglia (CD11b), TIMP2 and opticin expressions were found in the outer segment (OS), inner nuclear layer (IL), inner plexiform layer (IPL) and in nerve fiber layer (NFL). While MMP9 and opticin was found to be expressed in all retinal layers except photoreceptor layers (Fig. 6. I), in case of ROP fibrovascular membrane, we found higher expression of MMP9 in microglial cells but no TIMP2 and opticin (Fig. 6. II).

Discussion

ROP is a multifactorial disease leading to childhood blindness worldwide. The disease pathogenesis is poorly understood owing to its complex etiology and access to biological material for research purposes. Activated microglia in the vitreous of ROP patients have been shown to release increased levels of C3 and MMPs in the vitreous[10]. Correspondingly, vitreous mass spectrophotometry results showed that a greater number of opticin

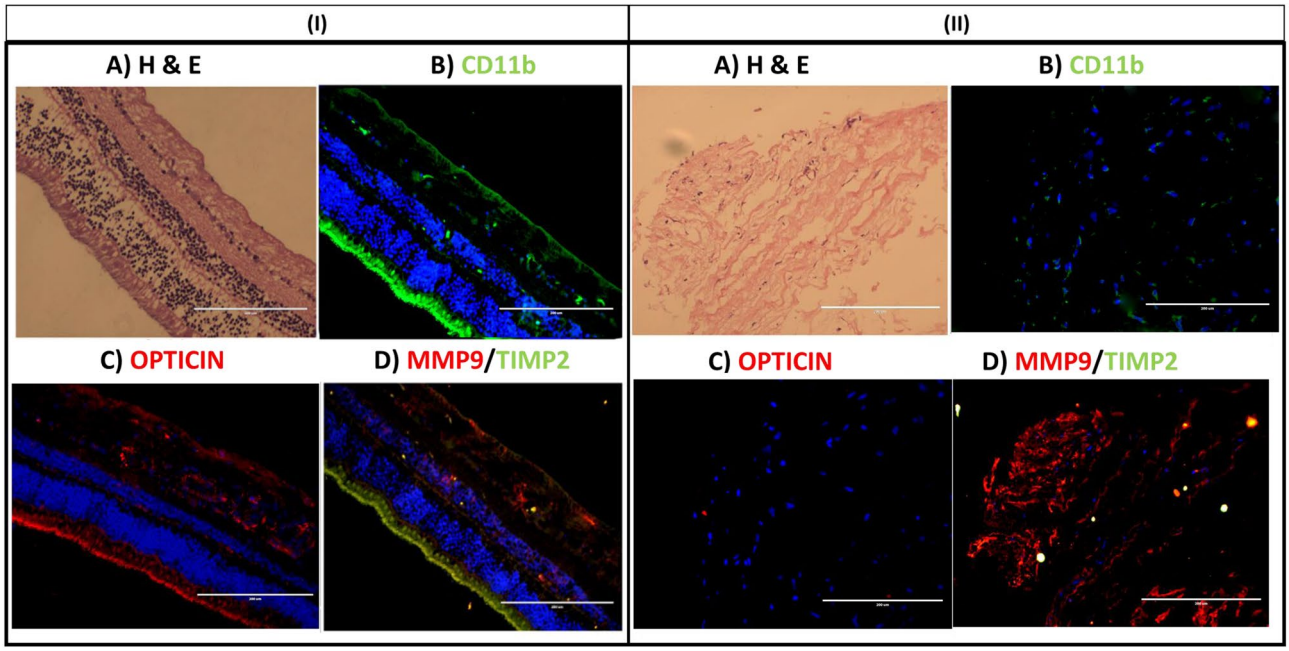

Figure 6. Representative image of H&E (**A**), immunofluorescence of CD11b (**B**), opticin (**C**), MMP9 and TIMP2 (**D**) in normal retinal tissue (I) and fibrovascular membrane (II, n = 3) collected from stage V ROP, (n = 3, 20× magnified, scale bar 200 µm).

peptides are present in the control groups when compared to the ROP probands, indicating opticin levels are dysregulated in ROP disease condition (Our unpublished data). Opticin is an ECM protein with anti-angiogenic properties. Le Goff *et al.* (2012) reported that opticin inhibits the angiogenesis via causing weak adhesions of endothelial cells to collagen mediated by its binding to collagen 1 and 2 and inhibiting collagen's binding to integrins[15]. The same group further showed that opticin inhibits preretinal neovascularization in OIR model[16]. Ma *et al.* (2012) showed that opticin levels are downregulated under hypoxia via MMP2 in retinal pigment epithelium (RPE) cells[17]. While there are reports on opticin's role in inhibiting angiogenesis in cellular and animal studies, till date there are no reports available assessing the role of opticin in human ROP cases. In this article, for the first time we focused on MMP9 mediated opticin degradation in the microglia cells. Our results validated reduced opticin levels in the vitreous of ROP patients. Interestingly, there was a strong inverse correlation between the levels of MMP9 and opticin protein in the vitreous humor samples of ROP patients (Supplementary Fig. 1). A study by Tio *et al.* (2014) that found opticin act as substrate for several MMPs resulting in its proteolytic degradation[18]. Thus, we hypothesized that elevated levels of MMPs might degrade the opticin and disturb the homeostatic balance of anti-angiogenic vs angiogenic factors in the retina and vitreous which has been shown to promote preretinal vascularization in oxygen induced retinopathy (OIR) model[16].

We performed an in-silico analysis that was primarily focused on studying the interactions between MMP9 and opticin to further understand the plausible ways by which MMP inhibition could rescue opticin degradation. Our in-silico analysis also confirmed the possible interaction between MMP9 and opticin and how this could be potentially affected by inhibiting the activity of MMP9. Elkins *et al.* (2002) described the structure of C-terminally truncated MMP9 that has its propeptide attached to the catalytic domain[19]. Since the full-length structure of pro-MMP9 is not available so far, we have used the same structure in the present study to check its interaction with other proteins/ligands[20]. MMP9 is activated by proteolytic cleavage of propeptide leaving catalytic domain available for possible interactions with other proteins. The docking results for doxycycline interactions with pro-MMP9 predicted that doxycycline interact with FnII domain of pro-MMP9 and not with propeptide which predicts that doxycycline does not hinders the conversion of pro-MMP9 to active MMP9, however, this needs to be confirmed by specific protein assays. Further, docking of doxycycline with active MMP9, (where the propeptide sequence have been removed) showed the doxycycline's interactions with His401 which is located in the conserved consensus sequence HExxHxxGxxH of MMP9[19]. His401 interacts with Zn ion[19], therefore, doxycycline's interaction with His401, would affect the MMP activity by blocking the Zn ion. Further, the In-silico analysis clearly demonstrated that the catalytic domain of active MMP9 interacts with opticin causing its possible proteolytic degradation. Thus, inhibition of MMPs activity by doxycycline could serve as an effective potential therapy for ROP that needs further detailed investigations in appropriate cells/animal models.

While an earlier study focused on studying the expression of opticin in RPE cell, in-vitro, we selected the human microglia cell line for studying the microglial cell mediated MMPs activity/inhibition on opticin. Our study for the first time confirmed opticin expression by microglial cells. This was further confirmed on immunohistochemistry of normal retina, showing simultaneous presence of activated microglia (CD11b), TIMP2 and opticin in the outer segment, inner nuclear layer, inner plexiform layer and in nerve fiber layers with MMP9 being expressed in all over the retinal layers. Again, in fibrovascular membrane those are surgically removed from the eyes of severe ROP to prevent retinal detachment, there was a higher expression of MMP9 in microglial

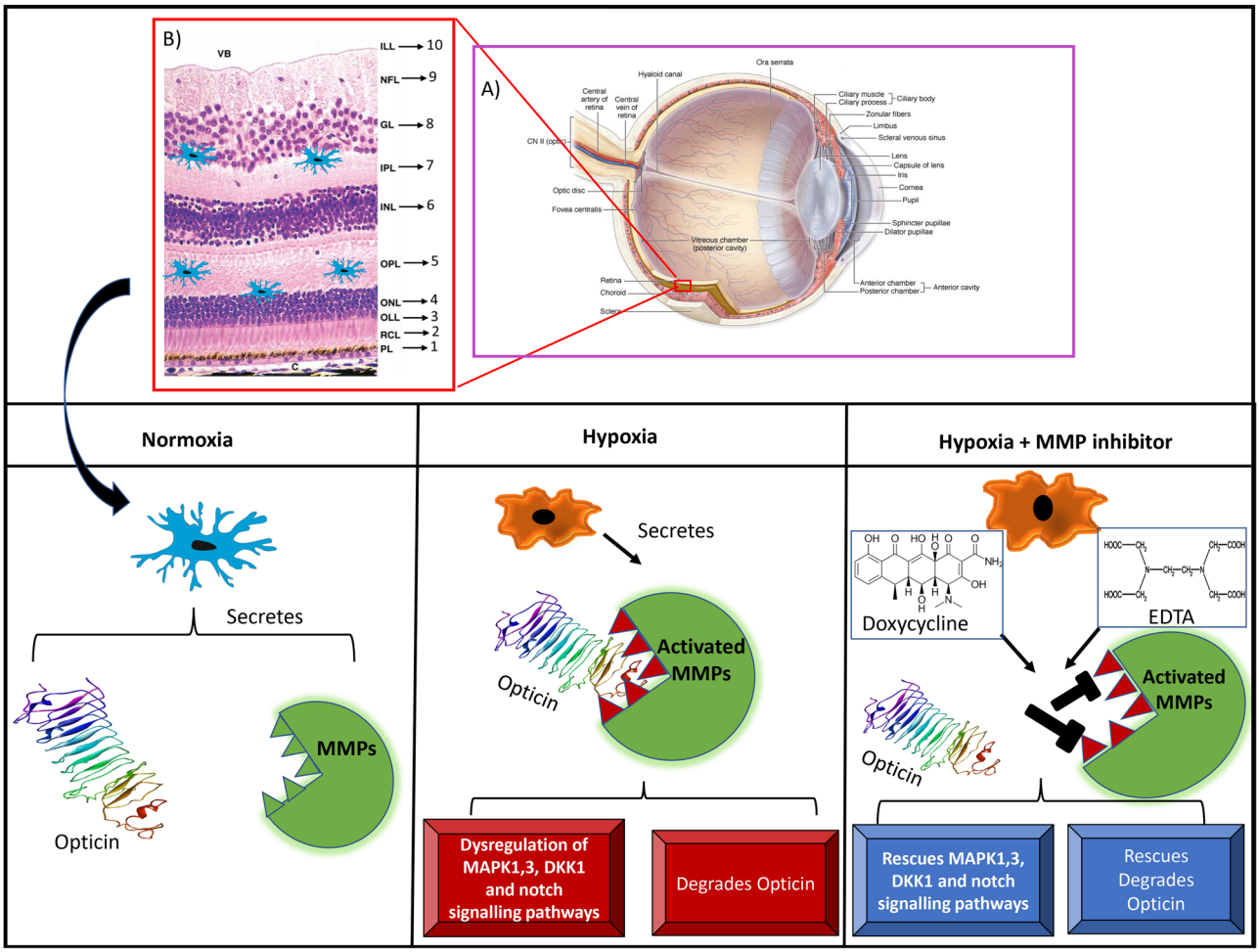

Figure 7. A schematic summary of the role of MMP mediated opticin degradation in microglia under hypoxic stress and in retinopathy of prematurity. Modified and adapted from A: https://quizlet.com/232012123/anatomy-of-the-internal-eye-diagram[39] B: Jacob Cook (2016)[40]

positive cells but no opticin. This absence of opticin could be attributed to its degradation by the increased activity of MMPs (Fig. 7). Since fibrovascular membranes are formed under high inflammatory conditions, a further confirmation of this could be attempted in animal models of ROP/OIR.

Under normal conditions, the human microglial cells showed a good expression of opticin, VEGF, TIMP2 and MMP. However hypoxia caused an abnormally high expression of MMP9 and a parallel reduction of opticin levels. This increase in MMP9 activity could be successfully inhibited by EDTA and doxycycline leading to a rescue of opticin reduction caused by its proteolytic degradation by MMPs in microglia. Thus, it clearly demonstrates that not only MMPs are the key regulators of opticin expression in retina but also that MMP inhibition could serve as a possible treatment for checking ROP progression in highly inflamed eyes of preterm babies as confirmed by the tear levels. Doxycycline is an FDA approved drug for the treatment of inflammatory disorder that acts by inhibiting MMP activity. MMPs participate in multiple biological processes via Zinc-dependent multidomain endopeptidases. One of the ways that doxycycline displays its anti-inflammatory properties is by down regulating the transcription/synthesis of MMP9 (stromelysin)[21] and by selectively chelating the divalent or trivalent metal ion such as Calcium/Magnesium/Zinc. It also inhibits activity of other MMPs and thereby cell division. Hence, further studies on ROP treatment can assess it as a preventive drug to check inflammation in the early stages of the disease after doing clinical trials on suitable animal models of ROP.

Normal expression of MAPK (ERK1/ERK2) is essential for the cell metabolism, differentiation, and proliferation[22]. Flavian *et al*. (2016), showed that doxycycline can inhibit the microglial activation by inhibiting p38 MAPK pathway in primary microglia cells[23] and thus lowers the proinflammatory cytokines in neurodegenerative conditions. EDTA, the other MMPs inhibitor, is also known to play an important role in most of the receptor mediated signaling mechanisms[24,25]. MMP9 expression can also be induced by the TNF, TGF-β and MAPK/ERK pathways[26–28]. The induction of hypoxia caused a significant increase in the *MMP9* activity in microglial cells and down regulation of *ERK2, DKK1* and *NOTCH1* signaling genes. However, the inhibition of the MMPs activity by doxycycline and EDTA, seemed to rescue the reduction in the major signaling pathway genes that contribute to lower inflammation and cell death. While treatment with doxycycline was able to rescue the expression of targeted pathway genes of *ERK2*, *DKK1* and *NOTCH1* under hypoxia, EDTA could only affect the

ERK2 and *DKK1* expression but not *NOTCH1* and *ERK1*. Additionally, MMPs inhibitors are known to inhibit the NO, ROS and TNF signaling which are essential for the Notch pathway[29–33]. MMPs and DKK (wnt signalling inhibitor) cross talk is required for wnt activation[34]. The results of this study suggest that the inhibition of MMPs by doxycycline and EDTA besides inhibiting MMPs activity that prevents opticin degradation, may also prevent downregulation of *ERK2*, *NOTCH1* and *DKK1* levels under hypoxia. Thus collectively, doxycycline treatment could prevent abnormal proliferation of endothelial cells leading to abnormal angiogenesis in the retina, however, this would need further validation by performing appropriate cellular assays in animal models of ROP.

This study thus, demonstrated that MMPs and other signaling mechanisms are dysregulated under hypoxic stress, which play an important role in ROP pathogenesis and MMP inhibition may be useful for rescuing the expression of opticin and other major signaling genes for the best visual outcome in severe stages of ROP. However the results of this study would require detailed investigation in suitable animal models before this could be use a potential therapy to check progression of ROP.

Methodology

This study was approved by the Institutional Review Board (IRB) of L.V. Prasad Eye Institute, Hyderabad, India, (LEC02-14-029) and adhered to the tenets of the Declaration of Helsinki. A prior-informed written consent was obtained from the parents/guardians of the study subjects (preterm infants).

Sample collection and preparation. Tear samples were collected from preterm born babies at the time of their first ocular examination within first month of their birth and then these babies are followed for retinal findings in the subsequent visits. The vitreous humor (50–100 µl) was collected from stage IV and V ROP infants and controls (infants under the age of 1 year with congenital cataract) at the time of pars plana vitrectomy done as part of the routine management of the condition. Both ROP (n = 30) and controls (n = 30) vitreous samples were subjected to RIPA buffer-based lysis followed by acetone precipitation to remove the salt traces and other impurities. The precipitated vitreous proteins were pelleted down at maximum speed for 30 min and dissolved in phosphate buffered saline (PBS). The obtained protein was quantified by using BCA method and normalized to 15 µg.

Analysis of MMP activity by gelatin zymography. A further validation of increased MMP levels in ROP vitreous sample as seen in our earlier study was performed in the extended cohort. The protein samples were separated in an 8% polyacrylamide gel containing a specific gelatin substrate (4 mg/ml), that is co-polymerized with the acrylamide under non-reducing conditions. After electrophoresis, the gel is washed with triton® X-100 to remove SDS and subsequently incubated at 37 °C for 16 h in a calcium-containing buffer (activation buffer-0.05 M Tris HCl, pH-7.8, 0.2 M NaCl, 5 mM $CaCl_2$, 0.02% Brij 35) followed by staining with coomassie brilliant blue solution. The partially renatured enzymes degrade the gelatin leaving a cleared zone that remains unstained appearing as white band under UV light examination. Demographic details of study subjects used for tear samples for zymography showed in the Supplementary Table S2.

Western blotting. The vitreous samples (10 µg) were also subjected for western blotting for the detection of opticin levels in ROP and no ROP babies. 10% SDS PAGE gel was prepared for the separation of proteins. Pre-stained protein ladder (Cat no# LI-COR, P/N 928-40000) was used for protein sizing. Separated proteins were transferred to a prewet (methanol) PVDF membrane (Cat no# LI-COR, P/N 926-31098). Ponceau staining was done for blots to confirm equal loading and complete transfer of proteins from gel to membrane in each lane before performing blocking for an hour with Odyssey blocking buffer (Cat no# LI-COR, P/N 927-40000). The blot was incubated with rabbit polyclonal opticin antibody (ab170886, abcam) (1:500) overnight. The blot was washed with PBST thrice and stained with anti-rabbit fluorescence labeled secondary antibody (LI-COR, Cat no LI-COR, P/N 928-40006). The blot was washed thrice with PBST followed by 1 × PBS to remove any unbound secondary antibody. The signals were detected by Infra-red (IR) based imager (Odyssey, LI-COR, USA). MMP2, MMP9 (zymography) and opticin (western blotting) band intensities were measured by using Image J, A correlation analysis for total MMPs-opticin and MMP9-opticin levels was performed in a subset of cases and controls (Supplementary Fig. 1). Demographic details of study subjects used for vitreous western blotting analysis showed in the Supplementary Table S1.

In-silico analysis for protein–protein and protein: ligand interactions. Protein–protein (MMP9-opticin) interaction and protein–ligand (MMP9-doxycycline and MMP9-EDTA) interactions were studied by in-silico analysis to understand how MMPs degrades opticin in the eye and further how inhibiting the MMP activity using specific MMP inhibitors rescues the opticin levels. Since it was not very clear from the existing literature that whether doxycycline chelates MMP9 in its pro or active form and its interaction with opticin, we performed both protein–protein (MMP9-opticin) and protein–ligand (MMP9-doxycycline) docking.

The protein structure of pro-MMP9 protein (Protein Data Bank PDB id: 1L6J) and the ligand doxycycline (DB00254) and EDTA (DB00974) were retrieved from protein data-bank and drug bank respectively (Supplementary Fig. 2). Active MMP9 was obtained from pro-MMP9 by deleting out the propeptide sequence. Since opticin structure was not available, therefore its structure prediction was done by the threading method after submitting the protein FASTA sequence to I-TASSER (https://zhanglab.ccmb.med.umich.edu/I-TASSER/). The best predicted structures were then selected based on C scores, RMSD score and TM score[35,36].

The protein PDB and ligand PDB structures were uploaded to PatchDock server[37,38] for protein–protein and protein–ligand docking respectively (https://bioinfo3d.cs.tau.ac.il/PatchDock/) with the clustering RMSD of 4 A and complex type as default value was provided to the server.

Human microglial cell culture for studying the activity of MMPs under hypoxic condition. The human microglial cell line (CHME3, n = 3) was cultured in DMEM medium containing 10% FBS along with 1% antibiotics (penicillin and streptomycin) and then exposed to different conditions to check the activity of MMPs on different proteins. For these experiments, approximately 10,000 cells per well were used. Alamar blue assay was done to observe the cytotoxic effect (Supplementary Fig. 3) and determining the optimum concentration of $CoCl_2$, EDTA and doxycycline for the subsequent experiments (Life technologies, Cat.no DAL1025). Serum depleted for 6 h followed by exposure to hypoxia by treating with cobalt chloride (150 µM) and with MMP inhibitors (EDTA-10 µg, doxycycline-20 µg) for 24 h, untreated cells were used as control.

Immunofluorescence. After 24 h treatment, microglia cells (n = 3) were washed with 1 × PBS and fixed with 4% formaldehyde for 10 min at room temperature followed by 3 washes with 1 × PBS. The cells were subjected to 0.3% of triton X 100 treatment at RT for 10 min for permeabilization followed by blocking using 2% BSA (HIGH MEDIA, Cat.no TC194) for 1-h. Cells were incubated overnight at 4 °C in appropriate dilution of primary antibody (MMP9, opticin, VEGF, and TIMP2). The antibody details for the proteins analyzed are provided in Supplementary Table S3. To remove unbound primary antibody, the cells were washed thrice with 1 × PBS. Fluorescent labeled secondary antibodies were used for the detection and then mounted with slow fade gold antifade containing DAPI (Life technologies, ref. S36939). Expression of targeted proteins in microglial cells under different conditions was studied under EVOS fluorescent microscope. A comparative quantitative analysis (Image J analysis) of signal intensities for MMPs and opticin expression in the microglia cells was performed in different categories (Supplementary Fig. 4).

Relative gene expression quantification. RNA was extracted from the same set of the human microglial cells (n = 3) by Trizol method. Quality and quantity of extracted RNA was measured by nanodrop and gel electrophoresis. 500 ng of final concentration of RNA was used for the cDNA conversion using thermostatic verso cDNA synthesis kit (AB1453B). Expressions of *MMP9, OPTC, VEGF* and *TIMP2* were assessed by qPCR using SYBR green chemistry (Biorad cat.no 38220090).

Various potential signaling pathways involved in angiogenesis and ECM reorganization (*ERK1, ERK2, NOTCH1, and DKK1)* that might have been affected by alterations in *MMP*s and *OPTC* levels, were assessed under normal and hypoxic conditions, with and without the treatment of MMP inhibitors (doxycycline and EDTA) treatments. Expressions of *ERK1, ERK2, NOTCH1, and DKK1* were assessed by qPCR. The primer details for the genes analyzed are provided in Supplementary Table S4.

Immunohistochemistry. The changes in MMPs and opticin levels under normal and hypoxic stress in the human microglial cells were further correlated in diseases tissue by performing IHC on fibrovascular membrane obtained from ROP patients (n = 3) along with normal cadaveric retina (n = 1) as a positive control. The fibrovascular membranes formed at vitreo-retinal junctions are removed as a part of routine surgery (membrane peeling) and immediately frozen the tissue in OCT tissue freezing medium in the tissue mold. 5 µm thick sections were taken on charged slides. To check the orientation and quality of tissue hematoxylin and eosin staining was performed. The slides were washed 3 times with 1 × PBS. To permeabilize, 0.3% of triton X 100 treatment was given for 10 min followed by blocking with 2% BSA for 1-h. Incubated the fibrovascular membrane overnight at 4 °C in appropriate antibody (MMP9, opticin, VEGF, and TIMP2) diluted in the 1% BSA (Supplementary Table S3). Fluorescent labeled secondary antibodies were used for the detection. Expression of targeted protein in fibrovascular membrane was identified by EVOS fluorescent microscope.

Data availability

The authors declare that [the/all other] data supporting the findings of this study are available within the paper [and its Supplementary information files].

Received: 30 May 2020; Accepted: 12 March 2021
Published online: 02 April 2021

References

1. Blencowe, H. *et al.* Preterm-associated visual impairment and estimates of retinopathy of prematurity at regional and global levels for 2010. *Pediatr. Res.* **74**, 35–49 (2013).
2. Campbell, K. *et al.* Intensive oxygen therapy as a possible cause of retrolental fibroplasia; a clinical approach. *Med. J. Aust.* **2**, 48–50 (1951).
3. Balakrishnan, U. *et al.* Screening based on incidence of severe retinopathy of prematurity in a tertiary care center in India: are Indian infants different?. *Int. J. Contemp. Pediatr.* **3**, 847–853 (2016).
4. Kumar, P. *et al.* Risk factors for severe retinopathy of prematurity in preterm low birth weight neonates. *Indian J. Pediatr.* **78**, 812–816 (2011).
5. Hartnett, M. E. *et al.* Mechanisms and management of retinopathy of prematurity. *N. Engl. J. Med.* **367**, 2515–2526 (2012).
6. Ma, J. *et al.* Influence of subretinal fluid in advanced stage retinopathy of prematurity on proangiogenic response and cell proliferation. *Mol. Vis.* **20**, 881–893 (2014).
7. Bishop, P. *et al.* The biochemical structure of mammalian vitreous. *Eye* **10**, 664–670 (1996).
8. Crane, I. J. *et al.* Mechanisms of leukocyte migration across the blood-retina barrier. *Semin. Immunopathol.* **30**, 165–177 (2008).
9. Sun, Y. *et al.* Cellular composition of the ridge in retinopathy of prematurity. *Arch. Ophthalmol.* **128**, 638 (2010).
10. Rathi, S. *et al.* Abnormal complement activation and inflammation in the pathogenesis of retinopathy of prematurity. *Front. Immunol.* **8**, 1868 (2017).
11. Takanosu, M. *et al.* Structure, chromosomal location, and tissue-specific expression of the mouse opticin gene. *Invest. Ophthalmol. Vis. Sci.* **42**, 2202–2210 (2001).

12. Sanders, E. J. *et al.* Opticin binds retinal growth hormone in the embryonic vitreous. *Invest. Ophthalmol. Vis. Sci.* **44**, 5404–5409 (2003).
13. Monfort, J. *et al.* Identification of opticin, a member of the small leucine-rich repeat proteoglycan family, in human articular tissues: a novel target for MMP-13 in osteoarthritis. *Osteoarthr. Cartil.* **16**, 749–755 (2008).
14. Le Goff, M. M. *et al.* The vitreous glycoprotein opticin inhibits preretinal neovascularization. *Investig. Opthalmology Vis. Sci.* **53**, 228 (2012).
15. Le Goff, M. M. *et al.* Opticin exerts its anti-angiogenic activity by regulating extracellular matrix adhesiveness. *J. Biol. Chem.* **287**, 28027–28036 (2012).
16. Le Goff, M. M. *et al.* The vitreous glycoprotein opticin inhibits preretinal neovascularization. *Invest. Ophthalmol. Vis. Sci.* **53**, 228–234 (2012).
17. Ma, J. *et al.* Opticin production is reduced by hypoxia and VEGF in human retinal pigment epithelium via MMP-2 activation. *Cytokine* **59**, 100–107 (2012).
18. Tío, L. *et al.* Characterization of opticin digestion by proteases involved in osteoarthritis development. *Joint Bone Spine* **81**(2), 137–141 (2014).
19. Elkin, P. A. *et al.* Structure of the C-terminally truncated human ProMMP9, a gelatin-binding matrix metalloproteinase. *Acta Crystallogr. D Biol. Crystallogr.* **58**, 1182–1192 (2002).
20. Pandey, A. K. *et al.* Resveratrol inhibits matrix metalloproteinases to attenuate neuronal damage in cerebral ischemia: a molecular docking study exploring possible neuroprotection. *Neural Regen Res.* **10**(4), 568–575 (2015) (**Erratum in: Neural Regen Res. 2020;15(9):1708**).
21. Jonat, C. *et al.* Transcriptional downregulation of stromelysin by tetracycline. *J. Cell. Biochem.* **60**(3), 341–347 (1996).
22. Pagès, G. *et al.* Mitogen-activated protein kinases p42mapk and p44mapk are required for fibroblast cell proliferation. *Proc. Natl. Acad. Sci. U.S.A.* **90**, 8319–8323 (1993).
23. Santa-Cecilia, F. V. *et al.* Doxycycline suppresses microglial activation by inhibiting the p38 MAPK and NF-kB signaling pathways. *Neurotox. Res.* **29**(4), 447–459 (2016).
24. Rand, M. D. *et al.* Calcium depletion dissociates and activates heterodimeric notch receptors. *Mol. Cell. Biol.* **20**(5), 1825–1835 (2000).
25. Tiyanont, K. *et al.* Evidence for increased exposure of the Notch1 metalloprotease cleavage site upon conversion to an activated conformation. *Structure* **19**(4), 546–554 (2011).
26. Zhou, L. *et al.* Tumor necrosis factor-alpha induced expression of matrix metalloproteinase-9 through p21-activated kinase-1. *BMC Immunol.* **10**, 15 (2009).
27. Gordon, G. M. *et al.* Cytokines and signaling pathways regulating matrix metalloproteinase-9 (MMP-9) expression in corneal epithelial cells. *J. Cell. Physiol.* **221**(2), 402–411 (2009).
28. Hsieh, H. L. *et al.* Transforming growth factor-beta1 induces matrix metalloproteinase-9 and cell migration in astrocytes: roles of ROS-dependent ERK- and JNK-NF-kappaB pathways. *J. Neuroinflamm.* **7**, 88 (2010).
29. Di Caprio Roberta, *et al*. Anti-inflammatory properties of low and high doxycycline doses: an in vitro study. Med. Inflamm. https://doi.org/10.1155/2015/3294/18 **2015**:10 (2015).
30. Clemens, D. L. *et al.* Novel antioxidant properties of doxycycline. *Int. J. Mol. Sci.* **19**(12), 4078 (2018).
31. Zhu, J. H. *et al.* Cyclic stretch stimulates vascular smooth muscle cell alignment by redox-dependent activation of Notch3. *Am. J. Physiol. Heart Circ. Physiol.* **300**(5), H1770–H1780 (2011).
32. Ando, K. *et al.* Induction of Notch signaling by tumor necrosis factor in rheumatoid synovial fibroblasts. *Oncogene* **22**(49), 7796–7803 (2003).
33. Charles, N. *et al.* Perivascular nitric oxide activates notch signaling and promotes stem-like character in PDGF-induced glioma cells. *Cell Stem Cell* **6**(2), 141–152 (2010).
34. Barbolina, M. V. *et al.* Matrix rigidity activates Wnt signaling through down-regulation of Dickkopf-1 protein. *J. Biol. Chem.* **288**(1), 141–151 (2013).
35. Yang, J. *et al.* The I-TASSER Suite: protein structure and function prediction. *Nat. Methods* **12**, 7–8 (2015).
36. Zhang, Y. I-TASSER server for protein 3D structure prediction. *BMC Bioinform.* **9**, 40 (2008).
37. Duhovny, D. *et al*. Efficient unbound docking of Rigid molecules. In: Gusfield et al. (ed), Proceedings of the 2nd Workshop on Algorithms in Bioinformatics(WABI) Rome, Italy, Lecture Notes in Computer Science 2452, 185–200, Springer Verlag, (2002).
38. Schneidman-Duhovny, D. *et al.* PatchDock and SymmDock: servers for rigid and symmetric docking. *Nucl. Acids. Res.* **33**, W363-367 (2005).
39. Anatomy of the Internal Eye Diagram | Quizlet. https://quizlet.com/232012123/anatomy-of-the-internal-eyediagram/. (Accessed 17 March 2021).
40. Jacob, C. The embryology of the eye. Eye new. https://www.eyenews.uk.com/education/trainees/post/the-embryology-of-the-eye. 22(4) (2016) (Accessed 17 March 2021).

Acknowledgements

We thank the patients and their families for their contribution. This work was supported by Department of Biotechnology (BT/01/COE/06/02/10 and BT/PR3992/MED/97/31/2011) Govt. of India; Champaulimaud Foundation, Portugal, and Hyderabad Eye Research Foundation. SP was supported through fellowships of the University Grants Commission (UGC) of the Government of India. SV was supported through fellowship of the DST-SERB, Ministry of science and technology (EMR/2016/007068) and Indian Council for Medical Research (ICMR) Government of India. The authors thank Mr Sridhar Boyepally, technician at the Ophthalmic Pathology LVPEI, Hyderabad for providing cryosections of retina.

Author contributions

Conceived the idea: I.K.; Designed the study: I.K., S.P.B.; Patient recruitment S.J., K.A., D.B., P.K.R., A.B., R.K., P.P.C.; Sample collection: S.P.B., L.P.; Performed the laboratory work: S.P.B.; Analysis of the data: S.P.B., S.V., I.K.; In-Silico work: M.R., S.P.B.; Wrote the initial draft of the paper: S.P.B., M.R., I.K., S.C.; Supervised the entire work: I.K.All authors viewed and contributed to the final paper.

Competing interests

The authors declare no competing interests.

Additional information

Supplementary Information The online version contains supplementary material available at https://doi.org/10.1038/s41598-021-86302-2.

Correspondence and requests for materials should be addressed to I.K.

Current Eye Research

ISSN: 0271-3683 (Print) 1460-2202 (Online) Journal homepage: https://www.tandfonline.com/loi/icey20

Alteration of Tear Cytokine Expressions in Primary Acquired Nasolacrimal Duct Obstruction – Potential Insights into the Etiopathogenesis.

Mohammad Javed Ali, Satish Patnaik, Natasha Kelkar, Mohammad Hasnat Ali & Inderjeet Kaur

To cite this article: Mohammad Javed Ali, Satish Patnaik, Natasha Kelkar, Mohammad Hasnat Ali & Inderjeet Kaur (2019): Alteration of Tear Cytokine Expressions in Primary Acquired Nasolacrimal Duct Obstruction – Potential Insights into the Etiopathogenesis., Current Eye Research, DOI: 10.1080/02713683.2019.1665186

To link to this article: https://doi.org/10.1080/02713683.2019.1665186

Accepted author version posted online: 06 Sep 2019.

Publisher: Taylor & Francis

Journal: *Current Eye Research*

DOI: 10.1080/02713683.2019.1665186

Alteration of Tear Cytokine Expressions in Primary Acquired Nasolacrimal Duct Obstruction – Potential Insights into the Etiopathogenesis.

First Author: Mohammad Javed Ali, FRCS, Ph.D.[1]

Second Author: Satish Patnaik, Ph.D[2]

Third Author: Natasha Kelkar, Ph.D[2]

Fourth Author: Mohammad Hasnat Ali, MBA[2]

Fifth Author: Inderjeet Kaur, Ph.D[2]

Affiliations: [1]Govindram Seksaria Institute of Dacryology, L.V. Prasad Eye Institute, Hyderabad, India.

[2] Prof. Brien Holden Eye Research Center, L.V. Prasad Eye Institute, Hyderabad, India.

Corresponding Author: Corresponding authorship is shared between Mohammad Javed Ali and Inderjeet Kaur.

Contact author for correspondence: Mohammad Javed Ali

Email of communicating author: drjaved007@gmail.com

Address: LV Prasad Eye Institute, Road no 2, Banjara Hills, Hyderabad-34, India.

Financial Disclosure: Mohammad Javed Ali receives royalties from Springer for the 2nd edition of the textbook “Principles and Practice of Lacrimal Surgery’ and treatise ‘Atlas of Lacrimal Drainage Disorders’.

Declaration of Interests: The authors report no conflict of interests.

ABSTRACT

Purpose: To investigate the presence and level of 35 distinct cytokines in the tear fluid obtained from patients with primary acquired nasolacrimal duct obstruction (PANDO) and compare it with controls in an effort to understand the disease etiopathogenesis.

Methods: Standard protocols were used for collecting tears from 60 eyes (20 diseased eyes and 20 healthy fellow eyes of unilateral PANDO, 20 control eyes of healthy subjects). A total of 35 analytes involved in inflammation, angiogenesis and wound healing were assessed by multiplex ELISA. Alterations in the tear levels of cytokines in PANDO and their comparison with the levels in the non-diseased fellow eye and healthy volunteers were noted. STRING analysis was used to assess the involved biological pathways of the altered cytokines. Linear mixed effect model was used for statistical analysis. A P value of <0.05 was considered significant.

Results: There was significant upregulation of 10 pro-inflammatory cytokines in tears from diseased eyes of PANDO patients in comparison with the non-diseased controls and include matrix metalloproteinase 9 (MMP 9), serpin E1, Interleukin-6 (IL-6), hepatocyte growth factor (HGF), vascular endothelial growth factor-A and R2 (VEGF-A, VEGF R2), platelet-endothelial cell adhesion molecule (PECAM-1), c-reactive protein (CRP), chemokine ligand 2 (CCL2) and platelet-derived growth factor- AA (PDGF-AA). Amongst the anti-inflammatory cytokines, 3 were significantly upregulated in diseased eyes of PANDO patients in comparison with the non-diseased controls and include granulocyte-colony stimulating factor (G-CSF), retinol binding protein 4 (RBP4) and tissue inhibitor of metalloproteinases -1 (TIMP-1). There were no significant differences between the control eyes of the diseased patient and control eyes of healthy subjects. Based on the significantly altered

cytokines, string analysis revealed that the biological pathways involved in the etiopathogenesis of PANDO include inflammation, angiogenesis, negative regulation of apoptosis, cellular proliferation and hormonal regulation.

Conclusions: In cases of PANDO, dysregulation of certain cytokines was disease specific. Biological pathways reflect a possible link and interaction between the inflammatory cytokines with vasculature and hormonal microenvironments of the lacrimal drainage system, which in a way is bringing three promising candidates in the PANDO etiopathogenesis on a common ground.

Key words: PANDO; tear; cytokine; lacrimal; nasolacrimal duct; lacrimal sac.

INTRODUCTION

Primary acquired nasolacrimal duct obstruction is a common lacrimal drainage disorder and a clinical syndrome with a female preponderance, usually characterized

by onset of epiphora after the age of 40 years followed by symptoms and signs of acute or chronic dacryocystitis.[1,2] Numerous factors are considered to play a role in its etiopathogenesis and tear proteomics is a promising candidate for further research in this regard.[3] Few studies assessed quantitative and qualitative changes in the tear composition in cases with PANDO and reported variable findings with regards to tear meniscus height, volumetric, and osmolarity.[4-7] A single study, so far, has reported 7 cytokine levels in tear fluids before and after an endoscopic dacryocystorhinostomy (DCR).[8] Inflammation and the resultant fibrosis have long been considered as common processes in the etiopathogenesis of PANDO.[3] Since tears constantly flow through the lacrimal drainage system, it would be prudent to assess the pro-inflammatory and anti-inflammatory cytokine levels in recent onset cases of PANDO. The current study performed a detailed assessment of 35 cytokines and proteins involved in inflammation, angiogenesis and wound healing in diseased eyes of unilateral PANDO, control eyes of PANDO and normal eyes of healthy subjects.

METHODS

Tear sample collection and processing

This study was approved by the institutional review board of L.V. Prasad Eye Institute and the study protocol adhered to the tenets of declaration of Helsinki. Clinically diagnosed unilateral PANDO patients (n=20, M=6, F=14) and 10 healthy control subjects (n=10, M=4, F=6) were recruited in the study. Unilateral PANDO were recruited to study any differences, if any, between the diseased and the non-diseased eye of the same patient. PANDO with an onset less than 6 months were considered for tear analysis to more accurately assess changes during the initial stages of disease pathogenesis. The diagnosis of PANDO was clinical, based on

symptomatology and findings of lacrimal irrigation. All patients presented with epiphora. None of the patients had any evidence of active sinusitis. Patients with acute dacryocystitis or discharge or any other ocular or systemic abnormality were excluded from the study. Informed consent was obtained prior to tear sample collection. None of the patients were using any topical or systemic medications. The healthy volunteers had patent lacrimal systems without any symptoms that could be ascribed to lacrimal drainage system. 10µl of basal tears from PANDO patients of both affected (n=20 eyes) and unaffected eyes (n=20 eyes) and both eyes of normal and healthy subjects (controls) (n= 20 eyes) were collected without touching conjunctiva. Hence, a total of 60 eyes were studied (20 diseased PANDO eyes (D); 20 control eyes of the diseased PANDO patients (DC) and 20 control eyes of healthy subjects (C). Tear samples were collected using a glass capillary tube and transferred immediately into sterile 0.5 ml centrifuge tubes. The samples were immediately centrifuged for 10,000 rpm for 5 min to remove the debris and transferred into fresh sterile cryovials and then stored in -80^0 C until further use.

Assessment of the cytokines by Multiplex Luminex Assay

35 targeted analytes (Merck Millipore, Massachusetts, USA) involved in the inflammation (Cat. No. HCYTMAG-60K-PX30), angiogenesis (Cat. No. HAGP1MAG-12K), (Cat. No. HANG2MAG-12K), ECM remodelling (Cat. No. HMMP2MAG-55K), (Cat. No. HTMP1MAG-54K), cardiovascular disease (Cat. No. HCVD2MAG-67K, Cat. No. HKI6MAG-99K) and human neurogenerative disease panels (Cat. No.

HNDG3MAG-36K) were selected for quantitative profiling of the 60 tear samples (**Table 1**). All tear samples were diluted in assay buffer (1:12.5 dilution). Standards and quality controls for each panel was replicated.

The experiment was performed following the manufacturer's standard protocols. Prior to the experiment, all the reagents were brought to room temperature (RT). The assay 96 well plate was washed initially with 200µl of 1X assay buffer at RT. After the washing of plate, 25 µl of standards and controls were added in appropriate wells. Finally, a 25 µl of diluted tear sample and 25 µl of targeted antibodies containing beads were added in all the wells and kept for incubation overnight at $4^{O}C$. After overnight incubation, the assay plate was washed 3 times with 1X wash buffer followed by addition of 25 µl of detection antibodies per well and incubated for 1 hour at RT. After 1 hour of incubation, 25 µl of Streptavidin Phycoerythrin was added in all the wells and incubated for 30 min at RT. At the end, the content in the assay plate was decanted and washed 3 times with 1X wash buffer. Finally, 150 µl of sheath fluid was added in each of the wells in the assay plate and then scanned on a Luminex 100 reader with XPONENT 3.1 software using standard default parameters and the results were exported in terms of Median Fluorescent intensity (MFI) that were further used for calculating analyte concentrations in samples using a spline curve-fitting method. STRING (Search Tool for Retrieval of Interacting Genes / Proteins) biological database (version 11) was utilized to ascertain the protein-protein interaction networks among the significantly dysregulated cytokines to better understand the cellular processes occurring in patients with PANDO. The prediction methods used include databases, experimental evidence, co-expression and neighbourhood. Confidence scores were kept high at >0.7.

Statistical analysis

Statistical analyses were performed using R (version 3.3.2, "multcomp" package).

The expression of cytokines between the three groups were compared by multiple comparison of means with Tukey Contrasts using linear mixed effect model. A 95% confidence interval with Bonferroni adjusted P values were also reported for the model estimation. To account possible correlation between both eyes of the same patient, we used a linear mixed effect model. A p-value of <0.05 was considered statistically significant.

RESULTS

There was significant upregulation of 10 pro-inflammatory cytokines in tears from diseased eyes of PANDO patients in comparison with the non-diseased controls and include matrix metalloproteinase 9 (MMP 9), serpin E1, Interleukin-6 (IL-6), hepatocyte growth factor (HGF), vascular endothelial growth factor-A and R2 (VEGF-A, VEGF R2), platelet-endothelial cell adhesion molecule (PECAM-1), c-reactive protein (CRP), chemokine ligand 2 (CCL2) and platelet-derived growth factor- AA (PDGF-AA) (**Table 2 and supplementary table**). Most of these cytokines showed > 5-fold change as compared to the healthy controls. Amongst the anti-inflammatory cytokines, 3 were significantly upregulated in diseased eyes of PANDO patients in comparison with the non-diseased controls and include retinol binding protein 4 (RBP4), granulocyte-colony stimulating factor (G-CSF), and tissue inhibitor of metalloproteinases -1 (TIMP-1) (**Table-2 and supplementary table**). Of these, RBP4 showed a nearly 40-fold change as compared to the healthy controls. There were no significant differences between the control eyes of the diseased patient and control eyes of healthy subjects (**Table 2 and supplementary table**).

STRING analysis showed significant interactions between the elevated cytokines like MMP9, IL-6, Serpin E1, VEGFR2 and TIMP1 (**Table 3**). Biological pathways involved in the etiopathogenesis of PANDO include inflammation, angiogenesis, negative regulation of apoptosis, cellular proliferation and hormonal regulation (**Figure 1**).

DISCUSSION

This study has provided a proof of principle of the altered expression of multiple proteins in the tear fluids obtained from the diseased eyes of patients with PANDO. The possible explanation for the alterations and their potential links in the etiopathogenesis of PANDO have been proposed, which needs to be further validated in detail.

Primary acquired nasolacrimal duct obstruction is a multifactorial disorder with numerous factors being implicated in its etiopathogenesis.[3] Vascular malfunctions, hormonal dysregulation, and tear proteomic alterations are proposed to play crucial roles.[8-10] The common cellular and molecular link and interaction between these factors needs to be ascertained to unravel the basic etiopathogenesis.

Few of the studies assessed the tear osmolarity changes before and after lacrimal surgeries, however only one studied tear levels of 7 cytokines. Lee et al[8] determined the tear levels of IL-1β, IL-2, IL-6, IL-10, transforming growth factor (TGF- β2), fibroblast growth factor (FGF-2) and vascular endothelial growth factor (VEGF). Tear levels were studied before endoscopic dacryocystorhinostomy and at 1, 2, 3, and 4 months post-operatively after the surgery. There were 18 patients, who underwent DCR, of which 7 were bilateral and only 11 contralateral eyes were taken as controls. They found that inflammatory cytokines, IL-2, IL-6, IL-10, VEGF, and FGF-2 were elevated in diseased states as well following DCR as compared to the contralateral eyes. The levels of these returned back to normal after silicone tube extubation. They

also reported higher levels of TGF- β2 and FGF-2 (P<0.005) in cases which recurred as compared to those with surgical success. In comparison, the current study, adhered to strict assessment of the disease status in patients with recent onset unilateral PANDO with the contralateral unaffected eye serving as one of the control group and healthy volunteers serving as another control group. The evaluation was not based on any surgical intervention, since it could have influenced the cytokine productions and functions. In addition, rather than studying only 7 cytokines, the current study evaluated 35 analytes which encompassed groups belonging to inflammatory, angiogenesis and healing responses and assessed both pro and anti-inflammatory agents.

Prolactin (PRL) and prolactin-inducible protein (PIP) are being increasingly recognized in the possible pathogenesis of lacrimal drainage disorders, more so in PANDO.[10-13] PRL receptors (PRLR) have been identified in the epithelia of the lacrimal sac and nasolacrimal duct while PIP has been isolated from the lacrimal sac extracts.[10,11] PRL is known to behave like a cytokine and have significant immunomodulatory effects and its receptors are known to express on lymphocytes, macrophages and fibroblast, all of which are likely to play a role in the etiopathogenesis of PANDO. The highly altered cytokines in the current study like IL-6 and MMP9 are also produced by the macrophages.[14] It would hence be pertinent to study in detail the macrophages infiltrating the nasolacrimal ducts (NLD) during the evolving stages of PANDO. Although, the expressions of PRL receptors are known to be lost in chronic cases of PANDO, it would be interesting to study PRLR and PIP in the NLD of recent onset PANDO. Interestingly in the present study, two cytokines were identified by STRING analysis to be involved in hormonal regulation; IL-6 and RBP4, both of which were significantly altered in patients with PANDO. IL-6 is also a hormonally regulated cytokine and in turn is a lead cytokine that activates the

hypothalamic-pituitary-adrenal axis during inflammatory stress.[15] RBP4 induces certain cytokines, including IL-6 from macrophages and endothelial cells and has been implicated in vasculitis and chronic inflammation.[16-17] Also of interest is the fact that hyperprolactinemia is associated with high levels of inflammatory cytokines which also includes IL-6.[18] Vasodilatation and loss of cavernous sinus functions have also been proposed as one of the mechanisms in PANDO.[3,19] The elevated levels of certain cytokines demonstrated in the current study are known to influence the production of nitric oxide, prostacyclin and endothelial derived hyperpolarizing factor, all of which are potent vasodilators.[20] All these reflect a possible link and interaction between the inflammatory cytokines with vasculature and hormonal microenvironments of the lacrimal drainage system, which in a way is bringing three promising candidates in the PANDO etiopathogenesis on a common ground. Further investigations in this direction has the potential to unravel the mysterious multifactorial etiopathogenesis of PANDO.

The limitations of the current study include the need for further validation of significantly dysregulated cytokines in an extended cohort of patients. Also, a certain cytokine, depending on multiple factors may have a pro or an anti-inflammatory action. However, the strengths of the study include uniform analysis and comparisons of a large number of cytokines in different clinical groups.

In conclusion, biological pathways involved in the etiopathogenesis of PANDO include inflammation, angiogenesis, negative regulation of apoptosis and cellular proliferation. Alterations of certain pro-inflammatory and anti-inflammatory cytokines are disease specific and show significant differences when compared with the controls. it is important to understand that the proposed roles of cytokine alterations are one amongst the many factors that may influence the disease etiopathogenesis in PANDO.

REFERENCES

1. Das AV, Rath S, Naik MN, Ali MJ. The incidence of lacrimal drainage disorders across a tertiary eye care network: customization of an indigenously developed electronic medical record system – eyeSmart. Ophthalmic Plast Reconstr Surg 2018 (Epub).
2. Kamal S, Ali MJ. Primary acquired nasolacrimal duct obstruction (PANDO) and secondary acquired lacrimal duct obstruction (SALDO). In: Ali MJ (ed), 'Principles and Practice of Lacrimal Surgery', 2nd edition. Singapore: Springer, 2018:163-171.
3. Ali MJ, Paulsen F. Etiopathogenesis of primary acquired nasolacrimal duct obstruction: what we know and what we need to know. Ophthalmic Plast Reconstr Surg 2019 (Epub).
4. Lee SM, Chung SJ, Lew H. Evaluation of tear film lipid layer thickness measurements obtained using an ocular surface interferometer in nasolacrimal duct obstruction patients. Korean J Ophthalmol 2018;32:445-450.
5. Yazici A, Bulbul E, Yazici H, Sari E, Tiskaoglu N, Yanik B, Ermis S. Lacrimal gland volume changes in unilateral primary acquired nasolacrimal obstruction. Invest Ophthalmol Vis Sci 2015;56:4425-4429.
6. Ohtomo K, Ueta T, Fukuda R, Usui T, Miyai T, Shirakawa R, Amano S, Nagahara M. Tear meniscus volume changes in dacryocystorhinostomy evaluated with quantitative measurement using anterior segment optical coherence tomography. Invest Ophthalmol Vis Sci 2014;55:2057-2061.
7. Yuksel N, Akcay E, Ayan B, Duru N. Tear-film osmolarity changes following dacryocystorhinostomy in primary acquired nasolacrimal duct obstruction. Curr Eye Res 2017;42:348-350.

8. Lee JK, Kim TH. Changes in cytokines in tears after endoscopic endonasal dacryocystorhinostomy for primary acquired nasolacrimal duct obstruction. Eye 2014;28:600-607.
9. Paulsen FP, Thale AB, Maune S, Tillmann BN. New insights into the pathophysiology of primary acquired dacryostenosis. Ophthalmology 2001;108:2329-2336.
10. Ali MJ, Shicht M, Paulsen F. Qualitative hormonal profiling of the lacrimal drainage system: potential insights into the etiopathogenesis of primary acquired nasolacrimal duct obstruction. Ophthalmic Plast Reconstr Surg 2017;33:381-388.
11. Ali MJ, Venugopal A, Ranganath KS, Jagannadham MV, Nadimpalli SK. Soluble glycoproteins of the lacrimal sac: role in defense with special reference to prolactin-inducible protein. Orbit 2018 (Epub).
12. Ali MJ, Heichel J, Paulsen F. Immunohistochemical analysis of lacrimal sac mucopeptide concretions. Ophthalmic Plast Reconstr Surg 2019 (Epub).
13. Ali MJ, Paulsen F. Prolactin and prolactin-inducible protein (PIP) in the pathogenesis of primary acquired nasolacrimal duct obstruction (PANDO). Med Hypothesis 2019;125:137-138.
14. Rathi S, Jalali S, Patnaik S, Shahulhameed S, Musada GR, Balakrishnan D, Rani PK, Kekunnaya R, Chhablani PP, Swain S, et al. Abnormal complement activation and inflammation in the pathogenesis of retinopathy of prematurity. Front Immunol 2017;8:1868.
15. Mastorakos G, Chrousos GP, Weber JS. Recombinant interleukin-6 activates the hypothalamic-pituitary-adrenal axis in humans. J Clin Endocrinol Metab 1993;1690-1694.
16. Farjo KM, Farjo RA, Halsey S, Moiseyev G, Ma JX. Retinol-binding protein 4 induces inflammation in human endothelial cells by NADPH-oxidase and nuclear

factor kappa B-dependent and retinol independent mechanisms. Mol Cell Biol 2012;32:5103-5115.

17. Norseen J, Hosooka T, Hammarstedt A, Yore MM, Kant S, Aryal P, Kiernan UA, Phillips DA, Maruyama H, Kraus BJ, et al. Retinol-binding protein 4 inhibits insulin signaling in adipocytes by inducing proinflammatory cytokines in macrophages through a c-Jun N-terminal kinase- and toll-like receptor 4-dependent and retinol-independent mechanism. Mol Cell Biol 2012;32:2010-9.
18. Liu Y, Zhang Z, Jin Q, Liu Y, Kang Z, Huo Y, He Z, Feng X, Yin J, Wu X, et al. Hyperprolactinemia is associated with a high prevalence of serum autoantibodies, high levels of inflammatory cytokines and an abnormal distribution of peripheral B-cell subsets. Endocrine. 2019;64:648-656.
19. Paulsen FP, Thale AB, Maune S, Tillmann BN. New insights into the pathophysiology of primary acquired dacryostenosis. Ophthalmology 2001;108:2329-2336.
20. Sprague AH, Khalil RA. Inflammatory cytokines in vascular dysfunction and vascular disease. Biochem Pharmacol. 2009;78:539-552.

LEGENDS

Table 1: Lists of analytes tested in the study subjects along with their estimated molecular weight and functions.

Table 2: Summary of significantly ($p < 0.05$) dysregulated cytokines (inflammatory and anti-inflammatory) in the diseased eye as compared to healthy controls. D-Diseased eye, DC - unaffected eye of the patients with unilateral PANDO and C

indicates healthy subjects with normal eyes. ↑ denotes <2-fold change, ↑↑ denotes more than 2-fold change, ↑↑↑ denotes more than five-fold change.

Table 3: Involved biological pathways of the significantly altered cytokines from patients of PANDO.

Figure 1: String analysis showing interactions among the significantly upregulated cytokines based on experimental evidence, co-localization and neighbourhood.

Supplementary Table: Summary of dysregulated cytokines (inflammatory and protective) in the diseased eye as compared to healthy controls. D- Diseased eye, DC - unaffected eye of the patients with unilateral PANDO and C indicates healthy subjects with normal eyes.

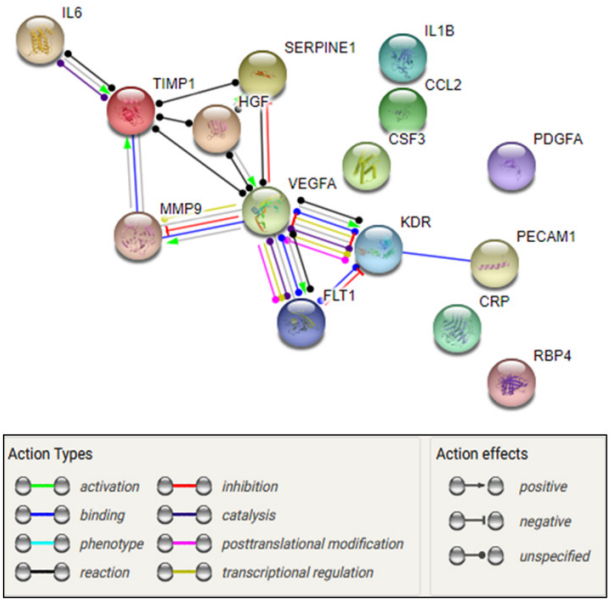

S.No	Name of the Analyte	Molecular weight	Rol
1	Chemokine (C-C motif) ligand 2/monocyte chemoattractant protein 1 [CCL2/MCP-1]	13 KD	Stimulated by interleukin -1β and activates the m inflammation
2	Chemokine (C-C motif) ligand 2/Macrophage inflammatory protein-1β [CCL4/MIP-1β]	7.8 KD	Inflammatory cytokine
3	Granulocyte-macrophage colony-stimulating factor (GM-CSF)	14 KD	Plays an important role in the maturation and act inflammation.
4	Interleukin 1 alpha [IL-1 α]	17 KD	Secreted by activated macrophages, plays a cruc differentiation, which mediates tissue destruction
5	Interleukin 1 beta [IL-1 β]	17.5 KD	Inflammatory cytokine and mainly expressed by
6	Interleukin 10 [IL-10]	21 KD	Anti-inflammatory cytokine which can inhibits m GM-CSF,IL-2, and IL-3)
7	Interleukin alpha 13 [IL-13]	31 KD	Anti-inflammatory cytokine regulates the 1L31R
8	Interleukin 17A [IL-17A]	35 KD	Inflammatory cytokine, secreted by Th17 cells, N important role in inflammation process
9	Interleukin 1 ra [IL-1ra]	17 KD	Important cytokine which induce immune respon conditions.
10	Interleukin 6 [IL-6]	21 KD	IL-6 is monocytes or macrophages derived cytok response
11	Platelet-derived growth factor AA [PDGF-AA]	28.5 KD	Neuroprotective
12	Platelet-derived growth factor BB [PDGF-BB]	24.3 KD	Plays an important role in the embryonic develop survival and chemotaxis
13	Tumor Necrosis Factor Alpha [TNF-α]	25 KD	Potent proinflammatory cytokine secreted by ma
14	Angiopoietin -1	25 KD	Plays a crucial role in the regulation of angiogen
15	Endothelin- 1	24 KD	Plays important role in endothelial-to-mesenchy
16	Granulocyte-colony stimulating factor [G-CSF]	19 KD	Pro-inflammatory cytokine
17	Hepatocyte growth factor [HGF]	34 KD	Regulates the cell growth, and cell motility.
18	Vascular endothelial growth factor A [VEGF-A]	27 KD	Important trigger in angiogenesis, it can induce c
19	Platelet/endothelial cell adhesion molecule-1 [CD31/PECAM-1]	130 KD	A cell adhesion molecule, it is required for trans- inflammation conditions
20	Tyrosine Kinase with Immunoglobulin-like and EGF-like domains 2 [TIE-2]	126 KD	Regulates angiogenesis
21	KDR - Vascular endothelial growth factor receptor R2 [VEGF R2/KDR]	27 KD	Mediator in angiogenesis and inflammation
22	Vascular endothelial growth factor receptor 1 [VEGF R1/FLT-1]	151 KD	Mediator in angiogenesis and inflammation
23	Thrombospondin-2	129 KD	Anti-angiogenic
24	Matrix metalloproteinase-2 [MMP-2]	72 KD	Plays an important role in the tissue remodelling
25	Matrix metalloproteinase-9 [MMP-9]	92 KD	Plays an important role in the tissue remodelling
26	Intercellular Adhesion Molecule 1 [ICAM-1]	75 KD	Cell adhesion molecule, involved in the cell prol
27	Vascular cell adhesion protein 1 [VCAM-1]	81 KD	Important in cell communication and inflammati
28	β 2-Microglobulin [β2M]	11 KD	Proinflammatory cytokine, present abundantly o
29	Retinol binding protein 4 [RBP4]	23 KD	Mediates retinol transport in blood and across th
30	C-Reactive Protein [CRP]	25.1 KD	This cytokine levels elevated under different infl
31	von Willebrand factor [vWF-A2]	20 KD	This is a glycoprotein, plays an important role in
32	Plasminogen activator inhibitor-1 [Serpin E1/PAI-1]	44 KD	Regulator of cell migration, and also act as prote
33	S100 calcium-binding protein B [S100B]	20 KD	Regulates the proliferation, apoptosis and inflam
34	Tissue inhibitor of metalloproteinases [TIMP-1]	23 KD	Regulates the matrix metalloproteinases

35	Pigment epithelium-derived factor [Serpin F1/PEDF]	50 KD	Potent inhibitor for angiogenesis

Table1: Lists of analytes tested in the study subjects along with their estimated molecular weight and functions. KD - Kilodalton.

Description of analytes	F. change
Pro-Inflammatory cytokines	**D-C**
HGF	↑↑↑
VEGF-A	↑↑↑
CD31/PECAM-1	↑↑
VEGF R2/KDR	↑↑
MMP9	↑↑↑
CRP	↑↑↑
Serpin E1/PAI-1	↑↑↑
CCL2/MCP-1	↑↑↑
IL-6	↑↑
PDGF-AA	↑
Anti-inflammatory cytokines	**D-C**
RBP4	↑↑↑
G-CSF	↑↑
TIMP-1	↑

Table 2: Summary of significantly dysregulated cytokines (pro-inflammatory and anti-inflammatory) in the diseased eye as compared to healthy controls. F.change – fold change, D- Diseased eye, DC - unaffected eye of the patients with unilateral PANDO and C indicates healthy subjects with normal eyes. ↑ - <2-fold change, ↑↑ denotes more than 2-fold change, ↑↑↑ denotes more than five-fold change.

S.No.	Gene Ontology	Biological pathways	No. of genes involved	p-value
1.	GO:0050900	Leukocyte migration	7	7.73e-08
2.	GO:0006935	Chemotaxis	7	8.92e-07
3..	GO:0006954	Inflammatory response	5	0.00019
4..	GO:0050727	Regulation of inflammatory response	4	0.00068
5.	GO:0010817	Regulation of hormone levels	3	0.0197
6.	GO:2001234	Negative regulation of apoptotic signaling pathway	4	0.00017
7.	GO:0042127	Regulation of cell population proliferation	12	5.70e-09
8.	GO:0045765	Regulation of angiogenesis	7	5.56e-08
9..	GO:0001570	Vasculogenesis	2	0.0047

Table 3: Involved Biological pathways of the significantly altered cytokines from patients of PANDO.

SUPPLEMENTARY TABLE: The average mean values of tear cytokines and protiens in diseased and control eyes

Pro-inflammatory Cytokines						
Name of the analyte	Average mean				Fold change (FC)	LOG2.FC
	D	C	DC			
HGF (pg/ml)	1664.36868	301.9174066	1155.45024	D - C == 0	**5.51266222**	**2.46274921**
				D - DC == 0	**1.44045033**	**0.52651991**
				DC - C == 0	3.82704082	1.93622929
VEGF.A (pg/ml)	4293.83568	631.3669586	3539.22956	D - C == 0	**6.80085587**	**2.76571632**
				D - DC == 0	1.21321197	0.27883164
				DC - C == 0	5.60566168	2.48688467
sPECAM1 (pg/ml)	1182.58526	510.7203797	572.892213	D - C == 0	**2.31552393**	**1.21133866**
				D - DC == 0	**2.06423692**	**1.04560857**
				DC - C == 0	1.12173361	0.1657301
VEGFR2 (pg/ml)	6567.64921	3068.616005	3156.51347	D - C == 0	**2.14026427**	**1.09778895**
				D - DC == 0	**2.08066567**	**1.05704516**
				DC - C == 0	1.02864401	0.04074378
sVEGFR1 (pg/ml)	5206.43714	3297.700331	3814.209	D - C == 0	1.57880845	0.65883614
				D - DC == 0	1.36501097	0.44891255
				DC - C == 0	1.15662693	0.20992359
MMP2 (pg/ml)	2070.66567	2641.940175	2557.27991	D - C == 0	0.78376706	-0.3515032
				D - DC == 0	0.80971413	-0.3045154
				DC - C == 0	0.96795527	-0.0469877
MMP9 (pg/ml)	161617.49	516.4189057	8573.16121	D - C == 0	**312.95812**	**8.2898258**
				D - DC == 0	**18.8515632**	**4.23661225**
				DC - C == 0	16.6011761	4.05321355
CRP (ng/ml)	11.4207719	1.7583191	6.8428196	**D - C == 0**	**6.49527832**	**2.69939135**
				D - DC == 0	1.66901549	0.73899735
				DC - C == 0	3.89168246	1.960394
PAI (pg/ml)	386.934645	58.75793038	200.284465	**D - C == 0**	**6.58523271**	**2.71923442**
				D - DC == 0	1.9319254	0.95003938
				DC - C == 0	3.40863717	1.76919504
MCP.1 (pg/ml)	516.142996	86.41222141	342.636603	**D - C == 0**	**5.97303238**	**2.57846354**
				D - DC == 0	1.50638604	0.59109154
				DC - C == 0	3.96514054	1.987372
MIP.1b (pg/ml)	85.7363768	68.79967554	70.6689174	D - C == 0	1.24617415	0.31750569
				D - DC == 0	1.21321197	0.27883164
				DC - C == 0	1.02716934	0.03867405
GM.CSF (pg/ml)	11.2648055	11.4236994	10.0973516	D - C == 0	0.98609085	-0.0202075
				D - DC == 0	1.11561981	0.15784546
				DC - C == 0	0.88389507	-0.178053
IL.1a (pg/ml)	30.8053851	16.19519775	28.3137734	D - C == 0	1.90213084	0.92761648
				D - DC == 0	1.08799999	0.12167854
				DC - C == 0	1.74828204	0.80593795
IL.1b (pg/ml)	10.9312613	8.686853367	7.82567659	D - C == 0	1.25836834	0.33155428
				D - DC == 0	1.39684552	0.48217248

				DC - C == 0	0.90086436	-0.1506182
IL.17A (pg/ml)	14.6983634	13.38961804	10.6880474	D - C == 0	1.0977433	0.13454072
				D - DC == 0	1.37521503	0.45965722
				DC - C == 0	0.79823393	-0.3251165

IL.6 (pg/ml)	108.418828	29.79123273	73.9498398	D - C == 0	**3.63928638**	**1.86365558**
				D - DC == 0	**1.46611308**	**0.55199639**
				DC - C == 0	2.48226854	1.3116592
PDGF.AA (pg/ml)	401.369854	203.469823	322.720196	D - C == 0	**1.97262595**	**0.98011742**
				D - DC == 0	1.24370851	0.31464839
				DC - C == 0	1.58608383	0.66546903
PDGF.AB.BB (pg/ml)	183.455837	153.4765106	149.031155	D - C == 0	1.19533495	0.25741494
				D - DC == 0	1.23098984	0.29981885
				DC - C == 0	0.9710356	-0.0424039
TNFa (pg/ml)	20.9022994	22.35095382	21.7349168	D - C == 0	0.93518601	-0.0966747
				D - DC == 0	0.96169217	-0.0563529
				DC - C == 0	0.972438	-0.0403218
angiopoietin.2 (pg/ml)	839.482855	2877.819504	996.946411	D - C == 0	0.29170796	-1.7774033
				D - DC == 0	0.84205414	-0.2480151
				DC - C == 0	0.34642423	-1.5293882
Endothelin (pg/ml)	108.144541	101.1491633	108.862295	D - C == 0	1.06915903	0.09647645
				D - DC == 0	0.99340677	-0.0095435
				DC - C == 0	1.07625502	0.10601997
Anti-inflammatory Cytokines						
IL.10 (pg/ml)	24.8695071	29.57578333	31.1750579	D - C == 0	0.840874	-0.2500385
				D - DC == 0	0.79773732	-0.3260143
				DC - C == 0	1.05407379	0.07597586
IL.13 (pg/ml)	33.9278928	31.78748251	28.6463727	D - C == 0	1.067335	0.09401307
				D - DC == 0	1.1843696	0.24411936
				DC - C == 0	0.90118406	-0.1501063
RBP4 (ng/ml)	59.2045123	1.469917618	7.07646629	D - C == 0	**40.2774357**	**5.33189993**
				D - DC == 0	8.36639502	3.06460612
				DC - C == 0	4.81419245	2.26729381
IL.1RA (pg/ml)	1373.8403	1495.574409	1301.59241	D - C == 0	0.91860378	-0.1224854
				D - DC == 0	1.05550731	0.07793657
				DC - C == 0	0.87029599	-0.2004219
vWF(ng/ml)	15.7279571	15.16125191	12.9103362	D - C == 0	1.03737852	0.0529424
				D - DC == 0	1.21824535	0.28480472
				DC - C == 0	0.85153497	-0.2318623
sTie2 (pg/ml)	6031.23924	5275.567221	5007.13685	D - C == 0	1.14323996	0.19312824
				D - DC == 0	1.20452854	0.26846858
				DC - C == 0	0.9491182	-0.0753403
TSP2 (pg/ml)	23470.6303	12651.43556	16798.391	D - C == 0	1.85517526	0.89155549
				D - DC == 0	1.39719514	0.48253353
				DC - C == 0	1.32778537	0.40902196
G.CSF (pg/ml)	1709.78509	965.4406969	604.387729	D - C == 0	**2.82895402**	**1.50026873**
				D - DC == 0	1.77098925	0.82455545
				DC - C == 0	0.62602264	-0.6757133
TIMP1 (pg/ml)	14187.5378	12442.03577	8697.50587	D - C == 0	**1.14029071**	**0.18940168**
				D - DC == 0	1.63121911	0.70595058

				DC - C == 0	0.69904202	-0.5165489
sVCAM1 (ng/ml)	1.27714195	0.633236867	1.27777384	D - C == 0	2.01684712	1.01210173
				D - DC == 0	0.99950548	-0.0007136
				DC - C == 0	2.01784499	1.01281535

p-value
0.000723
0.001259
1.00
0.0119
0.39270
0.1892
0.0221
0.0399
1.00
0.0143
0.0056
1.0000
0.0883
0.0411
1.0000
1.0000
0.8290
1.0000
0.00001
0.000002
1.0000
0.0083
0.0739
1.0000
0.0103
0.2419
0.6645
0.0560
0.0786
1.0000
0.7150
0.4350
1.0000
1.0000
1.0000
1.0000
0.9220
1.0000
1.0000
0.0842
0.0036

1.0000
1.0000
1.0000
1.0000

0.0001
0.0155
0.4097
0.0036
0.0679
0.6633
0.8540
0.2690
1.0000
1.0000
0.7050
1.0000
0.9100
1.0000
0.2010
1.0000
1.0000
1.0000

1.0000
1.0000
1.0000
1.0000
0.2260
1.0000
0.0022
0.0033
1.0000
0.2980
0.1450
1.0000
1.0000
1.0000
0.8370
0.8160
0.3430
1.0000
0.1510
0.8550
1.0000
0.0000001
0.000003
1.0000
0.0006
0.0548

0.3381
0.5810
1.0000
0.7720

Chapter 24

Metabolomics Applicable to Retinal Vascular Diseases

Satish Patnaik, Subhadra Jalali, Manjunath B. Joshi, Kapaettu Satyamoorthy, and Inderjeet Kaur

Abstract

Metabolomics refers to the systematic identification and quantification of the small molecule metabolites (the metabolome) of a biological system in a given space (cell, tissue, organ, biological fluid, or organism) and time. Global metabolic profiling provides broad range of coverage for most of the analytes present in any tissue. Human retina is metabolically highly active, and retinal vascular diseases such as age-related macular degeneration (AMD), diabetic retinopathy (DR), retinal vein occlusion (RVO), central retinal artery occlusion, and retinopathy of prematurity (ROP) are often associated with the disruptions in metabolic activities. A systematic study of total retinal metabolites from human diseased retina is a major challenge owing to the nonavailability of tissue specimens. Therefore, vitreous humor being very proximal to retina could be used as surrogate for retinal metabolomic analysis. As the extraction method adopted for such analysis determines the type of metabolites, two different types of solvent (methanol and chloroform)-based extraction methods could be used for retinal vascular patient samples (vitreous humor). Metabolites obtained from both the extraction methods are then subjected to LC-MS/MS for detection and identification.

Key words Retinal vascular disease, Vitreous humor, LC-MS, Metabolite profiling, Phenotype

1 Introduction

Retinal vascular diseases are a leading cause of blindness worldwide [1]. Some of the diseases such as age-related macular degeneration (AMD), diabetic retinopathy (DR), retinal vein occlusion (RVO), central retinal artery occlusion, and retinopathy of prematurity (ROP) [2, 3] are associated with many risk factors. Most of these diseases are being treated by targeting neo-vessel growth using LASER or anti-VEGF; however, the outcome is highly variable and unpredictable. Thus, for achieving better outcome, there is a need for the development of newer and sensitive tests for diagnosing these conditions at an earlier stage and careful monitoring of the progression and response to therapy. Being in close proximity with the retina, vitreous humor has been known to serve as an ideal reservoir that accumulates the secretory products (metabolites,

Sanjoy K. Bhattacharya (ed.), *Metabolomics: Methods and Protocols*, Methods in Molecular Biology, vol. 1996, https://doi.org/10.1007/978-1-4939-9488-5_24,

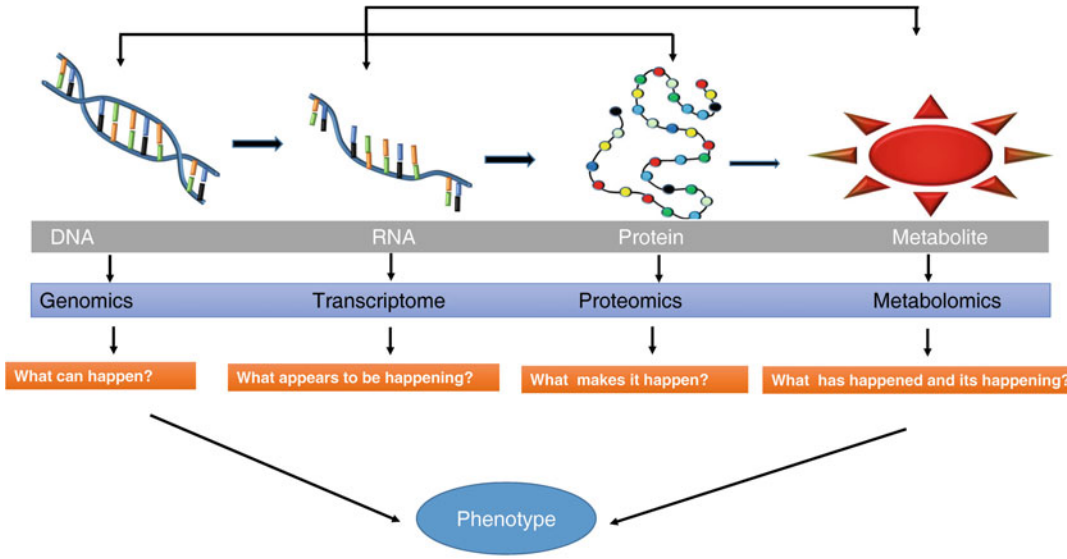

Fig. 1 Omics: from DNA to metabolites (modified and adapted from Dettmer et al. [8])

proteins, immune cells, etc.) of retina and thus can be used to search for the novel molecules for identifying the underlying pathogenic mechanisms and biomarker for these conditions [4].

While genomic and proteomic studies can provide extensive information to understand the basic pathology of the disease, these studies may provide only limited correlation with the phenotype. The closest representation of the phenotype would be to study the metabolites that are low molecular weight compounds and are mostly intermediate products of metabolism (Fig. 1). Based on the origin of metabolites, these can be classified into the endogenous and exogenous metabolites. Endogenous metabolites are subcategorized into the primary and secondary metabolites. Majority of the endogenous metabolites are directly involved in the development, growth, and senescence. Metabolites are very sensitive and can get dysregulated under various pathogenic and stress conditions. Metabolomic analysis is an unbiased survey of all metabolites within and between patient and control samples to reveal biologically relevant changes within a system at specific time.

1.1 Techniques for Measuring the Metabolites

Screening all metabolites (normal and dysregulated) with single technique is very difficult because of complex nature of metabolites, though a target-based screening of metabolite is much more feasible. They are mainly two platforms available for finding relevant structural information about metabolites:

(a) Nuclear magnetic resonance (NMR).

(b) Mass spectrometry (MS).

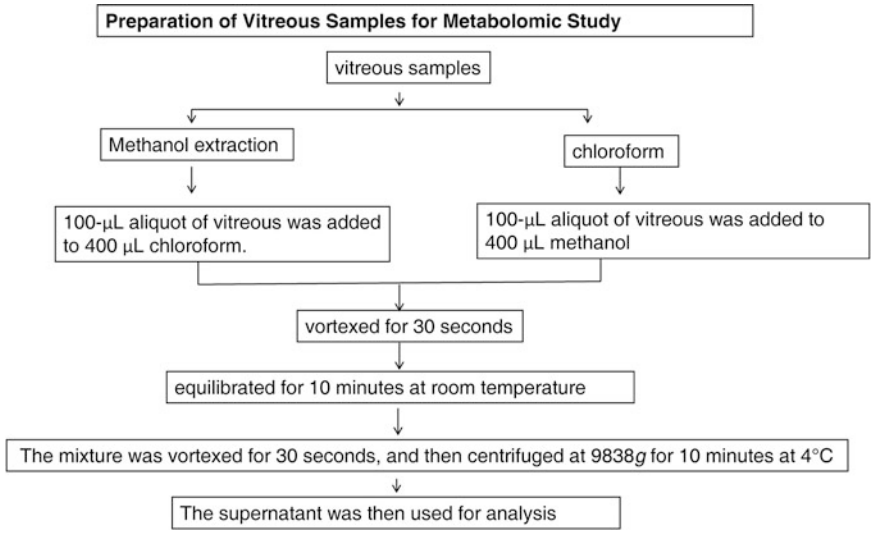

Fig. 2 Metabolite extraction workflow

MS is a very powerful and sensitive method for identification of unknown compounds and quantification of known metabolites within a biological sample as compared to NMR. However, MS-based method also has its own limitations to distinguish all classes of metabolites. Therefore, an untargeted metabolomics-based approach should be able to detect the maximum possible metabolites in a sample. The basic application of LC-MS/MS lies in the identification of features that are differently expressed in patients vs. control experiments for an ultimate identification of key metabolites that can play a major role in understanding disease pathogenesis and biomarker development.

Since metabolites exhibit a high chemical diversity, ranging from sugars to lipids, it is impossible to screen all metabolites in biological media with a single and universal technique; therefore two different extraction methods (methanol and chloroform) can be adopted to extract and screen all possible metabolites. A detailed protocol of metabolomic study is described below (Fig. 2).

2 Materials

1. Vitreous samples.
2. LC-MS system.

   Liquid chromatography coupled to mass spectrometry (LC-MS) analysis is performed with Agilent LC/Q-TOF system (Agilent Technologies, USA) consisting of an Agilent 1200 liquid chromatography system coupled with Agilent

6520 time-of-flight mass spectrometer operated in ESI positive mode.

3. C-18 column (250 mm × 4.6 mm, 5 μm).
4. Methanol (HPLC grade) (*see* **Note 1**).
5. Chloroform (HPLC grade) (*see* **Note 1**).
6. Acetonitrile with 0.1% formic (*see* **Note 1**).
7. Vortex mixer.
8. Centrifuge.
9. Centrifuge tubes.
10. Lyophilizer.

3 Methods

3.1 Subject Recruitment and Sample Collection

1. Ethical clearance should be obtained from the institutional review committee prior to the start of sample collection. The protocol adheres to tenets of declaration of Helsinki. An informed written consent should be obtained from all the participants, those who are undergoing pars plana vitrectomy as part of routine management prior to sample collection.
2. Sample collection and processing (*see* **Notes 2** and **3**).

   Undiluted vitreous humor samples should be collected from patients (retinal vascular disease) and control at the time of vitrectomy before the opening of infusion line and then should be transferred to cryovials to the disease. The tubes should be tightly closed after sample collection and stored over the ice and transported to the laboratory.
3. Centrifuge the samples immediately at 14,000 × *g* for 5 min at 4 °C to remove any cellular debris, and then transfer the supernatant to a fresh cryovial, and store at −80 °C until further use (*see* **Note 4**).
4. The frozen vitreous samples should be completely thawed before performing metabolic extraction. Two methods are generally performed including the methanol extraction (water) and chloroform (hydrophobic) extraction methods [5] so that both non-hydrophobic and hydrophobic metabolites are covered.

3.2 Metabolite Extraction Methods

3.2.1 Methanol (Water) Method

1. Add 200 μl of methanol to 50 μl of vitreous samples, mix well immediately by vortexing, and then incubate for 10 min at 4 °C (*see* **Notes 6** and 7).
2. Centrifuge the vitreous containing methanol at 9,838 × *g* for 10 min at 4 °C.
3. Collect the sublayer (supernatant) into the fresh tube.

4. Collect the supernatant and subject for lyophilization to concentrate the metabolites for approximately 30 min (*see* **Note 8**).
5. After completion of the lyophilization, 15 μl of mixture of acetonitrile with 0.1% formic acid is added to solubilize the lyophilized product.
6. Acetonitrile with 0.1% formic acid should be processed the same way as a blank control.

3.2.2 Chloroform (Hydrophobic) Method

1. Add 200 μl of chloroform to 50 μl of vitreous sample, vortex well, and then incubate for 10 min at 4 °C (*see* **Notes 6** and **7**).
2. After 10 min of incubation, two clear layers separated.
3. Sublayer (supernatant) is collected without disturbing the other layers (*see* **Note 4**).
4. Subject the supernatant to lyophilization to concentrate the metabolites approximately for 30 min.
5. After completion of the lyophilization, 15 μl of mixture of acetonitrile with 0.1% formic acid is added to solubilize the lyophilized product (*see* **Note 8**).

Acetonitrile with 0.1% formic acid should be processed the same way as a blank control.

3.3 Metabolite Separation and Identification

1. Inject 8 μl sample into 5 μm Zorbax C18 column using LC1200 system coupled to quadrupole time-of-flight (Q-TOF) mass spectrophotometer (Agilent Technologies).
2. The column oven should be maintained at 45 °C with a flow rate of 0.3 ml/min.
3. Ultrapure water with acetonitrile 0.1% formic acid should be used as mobile phase (*see* **Note 5**).
4. The spectrometer is operated in both positive and negative ion modes.
5. In positive mode use following gradient at 400 μl/min using mobile phase A (0.1% formic acid in water) and mobile phase B (0.1% formic acid in 90% acetonitrile) (2–98% B in 25 min, 98% B for 10 min, and equilibrated to 2% B for 10 min).
6. In negative mode, neutral and acidic metabolites were separated using mobile phase A (6.5 mM ammonium bicarbonate) and mobile phase B (90% acetonitrile) (2–98% B in 25 min, 98% B for further 10 min, and brought down to 2% by 45 min).
7. The parameters to be applied for mass detection are as follows:
   (a) Nitrogen gas flow rate—8 l/min.
   (b) Gas temperature—330 °C.
   (c) Nebulizer gas pressure—35 psi.
   (d) Vcap—3700 V.

(e) Fragmentor—160 V.
(f) Skimmer—65 V.
(g) Mass scan range—m/z 50–1000.

3.4 Data Analysis

Metabolome data is very complex. There are several ways to analyze the data, and that includes:

3.4.1 Manual Analysis

1. One of the accepted one is to export the data initially into the excel based on the mass-to-charge (m/z) ratio.
2. Subject the m/z ratio of the metabolites into the Human Metabolome Database (HMDB) by using ionization for both positive and negative along with molecular weight tolerance at 15 ppm.
3. Eliminate plant and other drug metabolites.
4. Sort human-related metabolites in other both test and control samples, and further, the short-listed metabolites can be used to assess the significance and relevance in the context of disease.

3.4.2 Using XCMS Software

XCMS is an online freely available software (https://xcmsonline.scripps.edu) [6, 7] to analyze the metabolites by simple steps including:

1. First, export LC-MS data as a net CDF or mz XML or mzData format.
2. Register in the XCMS server using your mail ID.
3. Once registered, upload the data as separate groups, for example, patients and controls.
4. Select the parameters based on target of interest.
5. The raw data files in mzXML format are submitted to XCMS server through a specific Java applet.
6. Once run is complete, a notification will be generated. The analysis here mainly includes retention time, heat map, and pathway enrichment.

4 Notes

1. All organic solvents should be HPLC grade.
2. Prefer to use fresh vitreous samples.
3. Use powder-free gloves and sterile tubes.
4. Separate the aqueous layers without disturbing the other layers.
5. 18 MΩ water should be used for any steps when required.
6. Methanol and chloroform extracts should be prepared freshly.

7. Vitreous samples with solvents should be mixed vigorously to get a homogenous mixture, and short spin should be done to avoid sample loss.
8. Sublayer of the biological samples should be lyophilized immediately.

References

1. Lee P, Wang CC, Adamis AP (1998) Ocular neovascularization: an epidemiologic review. Surv Ophthalmol 43:245–269
2. Bunce C, Xing W, Wormald R (2010) Causes of blind and partial sight certifications in England and Wales: April 2007–March 2008. Eye (Lond) 24:1692–1699
3. Smith LEH (2002) Pathogenesis of retinopathy of prematurity. Acta Paediatr Suppl 91:26–28
4. Stefánsson E (2009) Physiology of vitreous surgery. Graefes Arch Clin Exp Ophthalmol 247:147–163
5. Yu M, Wu Z, Zhang Z, Huang X, Zhang Q (2015) Metabolomic analysis of human vitreous in rhegmatogenous retinal detachment associated with choroidal detachment. Invest Ophthalmol Vis Sci 56:5706–5713
6. Tautenhahn R, Patti GJ, Rinehart D, Siuzdak G, XCMS Online (2012) A web-based platform to process untargeted metabolomic data. Anal Chem 84(11):5035–5039. https://doi.org/10.1021/ac300698c
7. Smith CA, Want EJ, O'Maille G, Abagyan R, Siuzdak G, XCMS (2006) Processing mass spectrometry data for metabolite profiling using nonlinear peak alignment, matching, and identification. Anal Chem 78(3):779–787. https://doi.org/10.1021/ac051437y
8. Dettmer K, Aronov PA, Hammock BD (2007) Mass spectrometry-based metabolomics. Mass Spectrom Rev 26(1):51–78

BJO Online First, published on October 5, 2017 as 10.1136/bjophthalmol-2017-310958

Mutation spectrum of *NDP*, *FZD4* and *TSPAN12* genes in Indian patients with retinopathy of prematurity

Sonika Rathi,[1] Subhadra Jalali,[2] Ganeswara Rao Musada,[1] Satish Patnaik,[1] Divya Balakrishnan,[2] Anjli Hussain,[2] Inderjeet Kaur[1]

[1]Kallam Anji Reddy Molecular Genetics Laboratory, Brien Holden Eye Research Centre, L V Prasad Eye Institute, Hyderabad, India
[2]Smt Kanuri Santhamma Centre for Vitreo Retinal Diseases, L V Prasad Eye Institute, Hyderabad, India

Correspondence to
Dr Inderjeet Kaur, Kallam Anji Reddy Molecular Genetics Laboratory, Prof Brien Holden Eye Research Centre, L V Prasad Eye Institute, Hyderabad 500034, India; inderjeet@lvpei.org

Received 30 June 2017
Revised 18 August 2017
Accepted 9 September 2017

ABSTRACT

Aim Retinopathy of prematurity (ROP) is a vasoproliferative eye disease in preterm infants. Based on its phenotypic similarities with familial exudative vitreo retinopathy (FEVR), the present study was conducted to screen the Norrin signalling pathway genes (already been implicated in FEVR) for understanding their involvement among Indian patients with ROP.

Methods The study cohort consisted of patients with ROP (n=246) and controls (n=300) that included full term (n=110) and preterm babies devoid of ROP (n=190). Screening of the *NDP, FZD4, TSPAN12* genes were accomplished by resequencing the entire coding and untranslated regions (UTR). The genotype data of the patients with ROP were analysed in the background of their clinical manifestations and further analysed in conjunction with other available data on these genes worldwide.

Results Two novel variants in intron 1 (IVS1 +16A>G) and 3′UTR (c.5 22T>C) along with a previously reported change in the 5′UTR (c.395_409del14bp) were observed in the *NDP* gene in three patients with ROP. Screening of the *FZD4* revealed four heterozygous variants, p.(Pro33Ser), p.(Pro168Ser), p.(Ile192Ile) and p.(Ile360Val), a compound heterozygous (p.(Pro33Ser)/p.(Pro168Ser)) and a 3′UTR (c*G>T) variants in the study cohort. Variants p.(Pro33Ser) and p.(Pro168Ser) were found to be significantly associated with ROP. A heterozygous variant p.(Leu119Arg) in *TSPAN12* gene was observed in a patient with threshold ROP. However, a formal genotype–phenotype correlation could not be established due to the low frequencies of the variant alleles in these genes.

Conclusions This is a first study that revealed association of few variants in Norrin signalling genes among Indian patients with ROP that warrants further detailed investigation worldwide.

INTRODUCTION

Retinopathy of prematurity (ROP) is a proliferative retinal vascular disorder, characterised by abnormal retinal vascularisation in the presence of an incomplete retinal vascular development due to premature birth. It is a multifactorial disease contributed by various risk factors (gestational age (GA), birth weight (BW), early oxygen exposure and so on).[1 2] ROP is a self-limiting disease, and only 15% of the preterm babies who develop ROP require treatment,[3] while in others the disease regresses spontaneously. Severe ROP is mainly characterised by an abnormal blood vessel growth in the vitreous leading to vitreoretinal traction, retinal detachment and eventually blindness. Overall, the incidence of ROP in India varies from 30% to 48%.[3 4] Hence, ROP remains a potential cause of avoidable childhood blindness in India.

Norrin β-catenin signalling plays an important role during the development of the fetal vasculature of the inner ear and retina.[5] The genetic disruption of Norrin β-catenin signalling genes *(NDP*, *FZD4*, *LRP5* and *TSPAN12*) has been implicated in many retinal vascular diseases like Coat's disease, Norrie disease and familial exudative vitreoretinopathy (FEVR).[5–9] The resemblance of clinical manifestations of ROP with FEVR further raised the possibility of involvement of Norrin β-catenin signalling genes in ROP pathogenesis. Few studies have looked for mutations in Norrin β-catenin signalling genes in ROP in different population worldwide.[10–14] However, most of these studies targeted only one or two genes from the Norrin β-catenin signalling pathway and had quite conflicting results on the involvement of these genes in ROP pathogenesis.[10 15] This warrant further investigations on the association of Norrin β-catenin signalling genes in ROP. Thus, the present study was conducted to screen *NDP*, *FZD4* and *TSPAN12* genes in patients with ROP from India in order to understand their relative contribution in ROP pathogenesis. We further tried to assess the genotype–phenotype correlation for the observed variants in order to understand their role in predicting the severity and visual outcomes of the disease.

MATERIALS AND METHODS

Enrolment of the study subjects

We adopted a case–control study design recruiting the preterm babies screened at a neonatal intensive care units and a tertiary eye care hospital in Hyderabad from the year 2008 to 2012. The study cohort included preterm babies with GA ≤35 weeks and/or BW ≤1700 g with ROP of any stage as cases and those with no ROP as controls. Additionally, ethnically matched full-term-born babies from the same geographical region with no history of any retinal disease were also recruited to serve as control. The medical and systemic history including race, GA, BW, early oxygen exposure, maternal health, other major complications, stage and zone of ROP, treatment details and pedigrees of the subjects recruited in the study were recorded on a predesigned proforma. Subjects with comorbid eye disease (secondary glaucoma, congenital cataract and so on) were excluded from the study. A prior informed consent was obtained from the parents of all the

To cite: Rathi S, Jalali S, Musada GR, *et al*. *Br J Ophthalmol* Published Online First: [*please include* Day Month Year]. doi:10.1136/bjophthalmol-2017-310958

babies enrolled in this study. Diagnosis and severity of ROP was based on the amount of retinal vascularisation and the extent of each stage (I–V) of ROP as per the revised International Classification of Retinopathy of Prematurity[16] guidelines using indirect ophthalmoscopy-based retinal drawings, done by fellowship trained ROP surgeons. This study was approved by the institutional review board of L.V. Prasad Eye Institute and adhered to tenets of the Declaration of Helsinki. Blood (0.3–1mL) samples were collected from the subjects in heparinised vacutainers (BD Biosciences, New Jersey, USA) by venipuncture for molecular genetic analysis.

Molecular genetic analysis

Isolation of genomic DNA from 0.3–1mL of peripheral blood of the enrolled subjects was done using MagNA Pure LC DNA isolation kit (Roche Applied Science, Indiana) on a MagNA Pure LC 2.0 System (Roche Applied Science). The DNA isolation from this machine is based on magnetic bead technology. DNA extraction protocol described in MagNA Pure LC DNA isolation kit manual was followed. The quality and quantity of DNA was measured using NanoVue plus (GE Life Sciences, New Jersey, USA). The integrity of DNA was further checked by running the DNA in 1% agarose gel. The primer sets used in this study for screening *NDP*, *FZD4* and *TSPAN12* gene were designed using primer designing tool (http://www.ncbi.nlm.nih.gov/tools/primerblast/), and the primers for 5′ untranslated region (UTR) and the coding regions of *NDP* genes were used as previously described[17] (see online supplementary table 1). The specificity of primers was checked by primer blast. DNA of 50–100 ng was used for amplification of intron–exon boundaries, putative core promoter, 5′UTR region and the coding sequences of *NDP*, *FZD4* and *TSPAN12* genes using specific primers by PCR. The amplified PCR products were screened for detection of mutations/variants by sequencing on automated DNA sequencer (ABI 3130xl, Applied Biosystems (ABI), Foster City, California, USA). The observed variants in these genes were further validated by resequencing and further assessed for their association with disease susceptibility. Bioinformatics software like ClustalW Omega, SIFT,[18] PolyPhen[19] and Mutation Taster[20] were used to predict the deleterious effect of the observed variants in these candidate genes.

Statistical analysis

Allele frequencies of the polymorphisms identified in each of the genes screened were calculated by allele counting method. The risk conferred by the genetic polymorphisms towards ROP was assessed by calculating ORs and p value using χ^2 test. The test of significance was set at $p<0.05$, and the CI was set at 95%. The allele frequencies of the observed variants in the present study were compared with the frequencies provided in Exome Aggregation Consortium (ExAC) database.[21]

RESULTS

Of all the preterm babies screened for ROP (approx. 500 per year) by our team of ophthalmologists and nurses from the year 2008–2012, a total of 436 (including 246 ROP, 190 no ROP) were recruited in the study. Additionally, another 110 full-term normal controls who were recruited for a genetic study on FEVR were also screened for the observed variants.[7] Demographics of the study participants are provided in online supplementary table 2. Babies with ROP had significantly lower mean BW ($p=3.2\times10^{-19}$) and mean GA ($p=2.3\times10^{-19}$) as compared with babies with no ROP. A total of 13 variants were observed in our

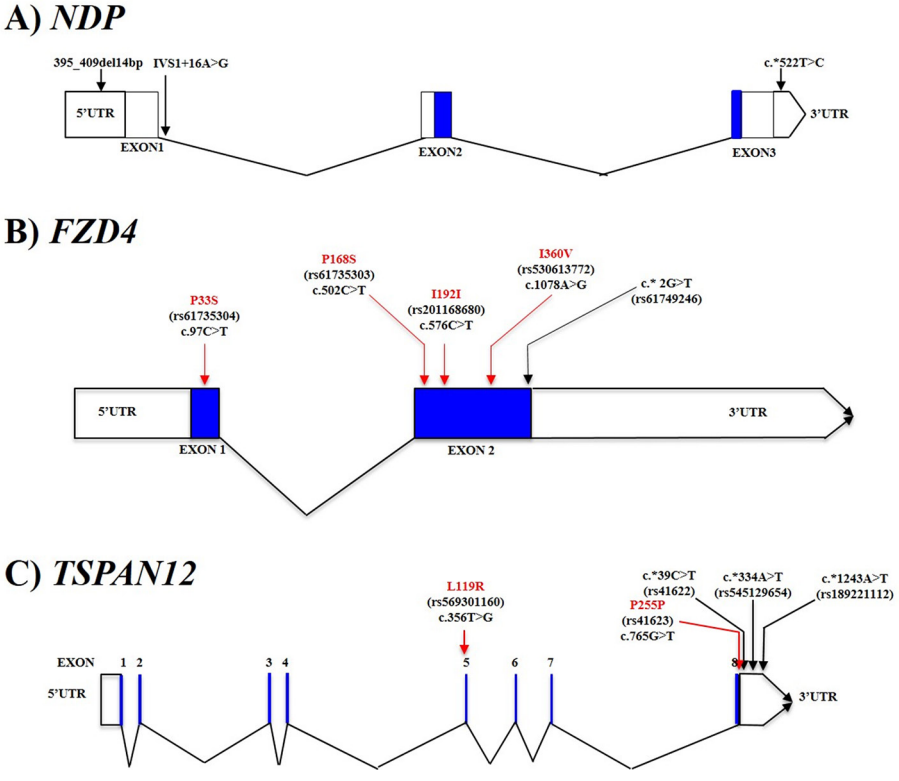

Figure 1 Schematics diagram of (A) *NDP*, (B) *FZD4* and (C) *TSPAN12* showing localisation of observed variants within a gene. Variants identified in the present study in *NDP*, *FZD4* and *TSPAN12* genes are indicated by arrowhead (red arrow indicates position of amino acid change) in coding region and (black arrow indicates change at cDNA position. UTR, untranslated region.

Table 1 Associations of variants/polymorphisms in the *NDP*, *FZD4* and *TSPAN12* gene with ROP

Gene	Location in the gene	cDNA change*	Variation in protein (rs ID)	Minor allele frequency in ROP cases	Minor allele frequency in controls	Minor allele frequency in ExAC database	*p* Value	OR (95% CI)	SIFT (score)	PolyPhen (score)	Mutation Taster (probability value)
NDP	5′UTR	−395_−409del114bp	–	0.0064	0	–	0.1	–	–	–	–
	Intron1	IVS1+16A>G	–	0.0064	0.0026	–	0.5	2.47 (0.15 to 39.7)	–	–	–
	3′UTR	c.*522T>C	(rs778496777)	0.0128	0.005	–	0.349	2.48 (0.35 to 17.76)	–	–	Polymorphism (0.9999)
FZD4	Exon 1	c.97C>T	p.(P33S) (rs61735304)	0.033	0	0.0153	0.029	–	Tolerated (0.09)	0	Polymorphism (0.9999)
	Exon 2	c.502 C>T	p.(P168S) (rs61735303)	0.033	0.0028	0.0166	0.003	12.4 (1.47 to 103.6)	Tolerated (0.06)	Benign (0.146)	Polymorphism (2.95×10^{-9})
	Exon 2	c.576 C>T	p.(I192I) (rs201168680)	0.016	0.0083	0.001	0.38	2.01 (0.4 to 10.09)	Tolerated (0.42)	–	Disease causing (0.9999)
	Exon 2	c.1078 A>G	p.(I360V) (rs530613772)	0.0056	0.0028	0.00007	0.6	2 (0.12 to 32.2)	Tolerated (0.19)	Possibly damaging (0.84)	Disease causing (0.9999)
	3′UTR	c.*2G>T	(rs61749246)	0.011	0.009	0.0212	0.83	1.22 (0.17 to 8.77)	–	–	Polymorphism (1.55×10^{-7})
TSPAN12	Exon5	c.356T>G	p.(L119R) (rs569301160)	0.0025	0	0.00005	0.1	–	Tolerated (0.40)	Benign (0.021)	Polymorphism (0.9714)
	Exon 8	c.765 G>T	p.(P255P) (rs41623)	0.0475	0.068	0.1968	0.27	0.68 (0.33 to 1.37)	1	–	Polymorphism (1.124×10^{-12})
	3′UTR	c.*39C>T	(rs41622)	0.045	0.068	0.1952	0.21	0.64 (0.32 to 1.3)	–	–	Polymorphism (0.9999)
	3′UTR	c.*334A>T	(rs545129654)	0.0125	0.0156	0.0018	0.39	1.62 (0.52 to 5.02)	–	–	Polymorphism (0.9999)
	3′UTR	c.*1243A>T	(rs189221112)	0.055	0.054	0.0094	1	1 (0.56 to 1.79)	–	–	Polymorphism (0.9999)

*NCBI Reference Sequence: *NDP*: NM_000266.3, *FZD4*: NM_012193 and *TSPAN12*: NM_012338.

*, after stop codon; –, not determined; ExAC, Exome Aggregation Consortium; ROP, retinopathy of prematurity; NCBI, National Center for Biotechnology Information; UTR, untranslated region.

ROP cohort after screening of entire coding and flanking region of *NDP*, *FZD4* and *TSPAN12* genes.

The *NDP* gene screening in 78 ROP probands and 82 no ROP preterm controls revealed a 14 bp deletion in 5′UTR, an intronic variant and 3′UTR variant in three sporadic cases of ROP. The schematic locations of these variants are provided in figure 1. The 14 bp deletion (395_409del14bp) was detected in single patient and none of the controls, while the rest of the two variants were observed in both patients and controls (table 1).

Screening of the exons and 3′UTR regions of *FZD4* gene in 90 patients with ROP and 70 no ROP preterm controls revealed three non-synonymous c.97C>T (p.(Pro33Ser)), c.502C>T (p.(Pro168Ser)), c.1078A>G (p.(Ile360Val)) and a synonymous missense c.576 C>T (p.(Ile192Ile)) variants. Of the three observed non-synonymous variants, (p.(Pro33Ser) and p.(Ile360Val)) were detected only in patients while p.(Pro168Ser) was found in both patients and preterm controls (table 1). The schematic locations of these variants are provided in figure 1. The p.(Ile360Val) variant involving a highly conserved residue across the species was predicted to be pathogenic by PolyPhen-2 and Mutation Taster (figure 2). Likewise, both p.(Pro33Ser) ($p=0.029$) and p.(Pro168Ser) ($p=0.003$) were found to be significantly associated with ROP (table 1). While p.(Pro168Ser) was conserved across all the species and p.(Pro33Ser) was conserved in all species except opossum, chick and python (figure 2). The observed synonymous variant p.(Ile192Ile) though predicted to be disease causing by Mutation Taster was not found associated with ROP.

The eight exons of *TSPAN12* gene including intron–exon boundaries and 3′UTR regions were screened in 200 ROP probands and 147 no ROP preterm controls. Two coding region substitutions (p.(Leu119Arg) and p.(Pro255Pro)) and three UTR variants (c.*39C>T, c.*334A>T and c.*1243A>T) were observed in 65 patients with ROP. Schematic locations of these variants are provided in figure 1. On multiple sequence alignment, p.(Leu119Arg) in exon 5 of *TSPAN12* gene was found to be an evolutionarily conserved residue in closely related species like human and macaque but not in mouse, dog, buffalo and so on (figure 2). This variant p.(Leu119Arg) was observed only in a proband and not in controls, while other synonymous variants p.(Pro255Pro) was present in both patients and controls with almost equal allele frequency. A single nucleotide polymorphism (SNP) (c.*39C>T) was observed at the 3′UTR, 39 base pair after the stop codon without any effect on splice site. None of these variants were found to be significantly associated with ROP (table 1).

DISCUSSION

The overall incidence of ROP in southern India alone is almost 30%,[3] which is very high, and this is expected to increase exponentially in the near future. Recently, it was observed that in India and in other middle-income countries,[1 2] even the preterm babies with high BW and GA also tend to develop severe ROP. Varying incidence of ROP across different countries and the presentation of disease even in babies with relatively high GA and BW further

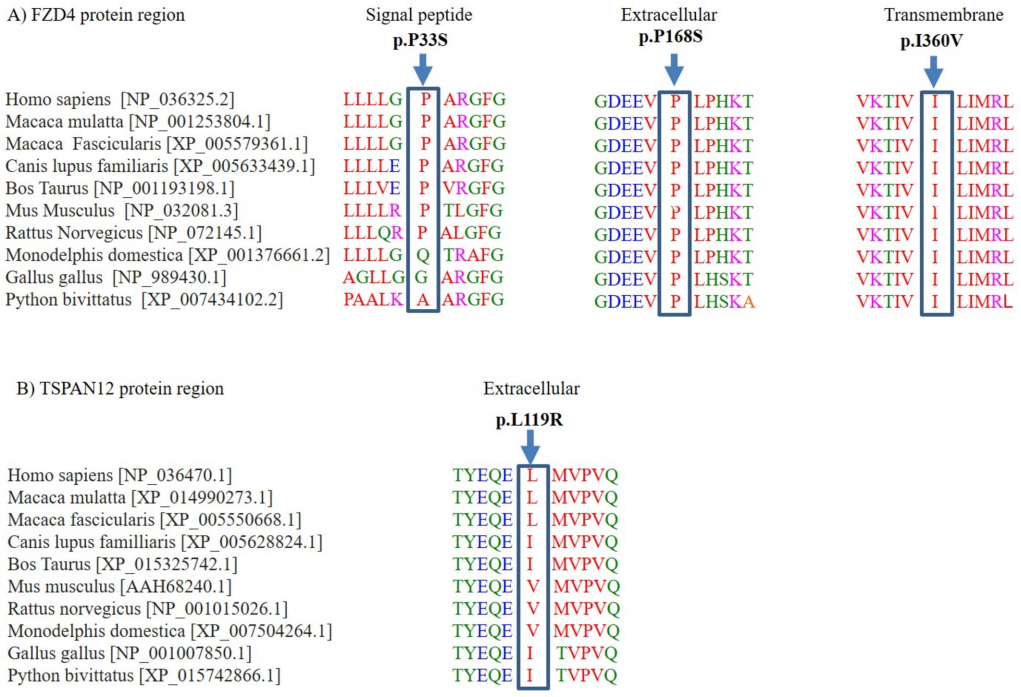

Figure 2 Multiple sequence alignment showing the conservation of wild-type residue with respect to P33S and I360V variants in FZD4 protein and L119R variant in TSPAN12 protein across different species: alignments were generated with the Clustal Omega software. The position of the variants is indicated by an arrow. Accession numbers (NCBI) and name of the species are mentioned at the left side of the picture. NCBI, National Center for Biotechnology Information.

suggested for the role of either genetics or environmental risk factors or their interactions in the disease progression.

Genetic variations in Norrin β-catenin signalling genes in ROP

The screening of candidate genes namely *NDP*, *FZD4* and *TSPAN12* led to the identification of six major coding region variants in 36 ROP probands. Of these, two of them, namely I360V in *FZD4* and L119R in *TSPAN12* gene (as reported in dbSNP databases[22] with a minor allele frequency of 0.00007and 0.00005 in ExAC database[21]), were observed only in two ROP probands in our study cohort; therefore, they seem more likely to be the rare variants. Patients harbouring these variants had clinical features of advanced ROP like leukocoria, retinal haemorrhages and partial or total retinal detachments. Two polymorphisms—p.(Pro33Ser) and p.(Pro168Ser) in *FZD4* gene—were found to be significantly associated with ROP (table 2).

NDP genes variations in ROP

Mutations at the 5′ and 3′UTRs in *NDP* gene in patients with ROP have been suggested to alter the regulation of gene expression and messenger RNA stability thereby resulting in the reduction of Norrin β-catenin signalling and eventually poor vascular development.[23] *NDP* gene mutations mostly have accounted for advanced ROP cases, and their frequencies varied across different population (table 3). In the present study, variants identified at the UTR region of *NDP* gene accounted for 2.7% (4/78) of the patients with ROP, which was comparable with previous studies (table 3).[12 13] Furthermore, it was interesting to note that unlike FEVR, variants in *NDP* gene observed in ROP were exclusively restricted to the UTRs of the gene.[7] In an earlier study, the whole gene screening of *NDP* by a direct sequencing method revealed a higher frequency of 597C>A variant in advanced ROP as compared with regressed ROP and no-ROP preterm controls from Kuwait[14] (table 3). However, we did not observe any such common variant for the advanced ROP cases in our study. Likewise, the 14bp deletion (395_409del14bp) predicted to be disease causing was observed in advanced ROP cases[13]; however, in the present study, the patient harbouring this change along with 3′UTR (c.*522T>C) had regressed ROP. Even in the previous studies on FEVR, similar 3′UTR variant was reported in mild cases[7] thereby suggesting that 3′UTR change might be conferring protection to ROP progression. In a previous report, *NDP* was found to be one of the major genes involved in Indian FEVR cases[7]; however, it seemed to have a relatively minor role in ROP in the present study cohort.

FZD4 gene variations in ROP

Several variations have been reported for severe ROP cases across different populations in *FZD4*, which is one of the key genes of Norrin β-catenin signalling pathway.[10 15 24 25] Four heterozygous coding region variants including p.(Pro33Ser), p.(Pro168Ser), p.(Ile192Ile) and p.(Ile360Val) and a compound heterozygous change (p.(Pro33Ser)/p.(Pro168Ser)) were identified in 17.7% (16/90) of the patients with ROP in the present study. Both p.(Pro33Ser) and p.(Pro168Ser) were found to be significantly associated with ROP. Patients harbouring either of these variants exhibited classical clinical features of ROP and had poor outcome (table 2). Proline is known to exist in the turns of beta pleated sheets and provides rigidity, which is essential for proper conformation of protein. The in silico analysis predicted p.(Pro33Ser) to result in impaired stability of FZD4 protein causing its mistranslocation, which might lead to impaired Norrin β-catenin signalling further resulting in avascular retina.[15] Interestingly, only these two variants from the present study were shared between patients from India and USA, while others were not found to be shared across different populations (table 3).

Table 2 Clinical features of ROP patients at presentation with variants in *NDP, FZD4 and TSPAN12* genes

Study no. of the probands	Variation identified	Age at presentation	Oxygen supplementation at birth	Blood transfusion at birth	Phototherapy	RDS	Stage of the disease	Treatment	Outcomes/ visual acuity	Other complications
110B	−395_−409 del14bp, c.*522T>C	1 month	Yes	Yes	Yes	No	OU: stage 2 zone II ROP	None	OU 20/20	None
145B	c.*522T>C	1 month 8 days	No	No	No	No	OS: stage 2	None	OU 20/20	None
137B	IVS+16A>G	21 days	Yes	No	Yes	No	OD: stage 4B zone, OS: Sstage 5 zone I	Lensectomy and vitrectomy	Poor, no PL OS	Leukocoria in both eyes
R212	p.(P33S)/WT	12 months	Yes	Yes	No	–	OU: stage 5	OD-VR surgery	Poor, no PL	Leukocoria in both eyes
R603	p.(P33S)/WT	72 months	Yes	No	No	No	OD: stage 4B, OS: stage 4A	Prophylactic scleral buckling (OS)	No PL OD; 20/80 OS	High compound myopic astigmatism
R604	p.(P33S)/WT	6 months	Yes	Yes	Yes	No	OD: stage 4B, OS: stage 5	OU-VR surgery	Poor; light perception OD	None
R706	p.(P33S)/WT	1 month	Yes	–	–	–	OU: stage 3 plus	LIO OU	Good, OU 20/30	Low myopic astigmatism OU
315B	p.(P33S)/p.(P168S)	8 months	No	No	No	No	OU: stage 5	None	Poor; no PL; blind	None
R406	p.(P33S)/p.(P168S)	5 months	Yes	No	Yes	–	OD: stage 5; OS: stage 4B	OS-VR surgery	OS-Good	ROP sequels (OU)
199B	I192I	20 days	Yes	Yes	Yes	No	OU: stage 3 zone II plus	LIO	Good; 20/40 OD; 20/60 OS	Anisometropic amblyopia (OS)
242B	I192I	3 month 2 days	Yes	Yes	Yes	No	OD: stage 4A zone II; OS: stage 4B zone II,	OU-VR surgery	Good, 20/130	preretinal haemorrhage & mild disc drag
R503	I192I	7 months	Yes	No	Yes	–	OU: stage 5	None	Poor, no PL; blind	Irreversible blindness
16B	I360V	1 month 17 days	Yes	Yes	Yes	–	OU: stage 2 zone II	None	Good	None
17B	L119V	1 month 10 days	Yes	Yes	No	No	OU: stage 3 zone II, posterior APROP	LIO	Good, 20/80 OU	Preretinal haemorrhage in the left eye

APROP, aggressive posterior retonopathy of prematurity; LIO, laser indirect ophthalmoscopy; OD, right eye; OS, left eye; OU, both eyes; PL, perception in light; RD, respiratory distress; ROP, retinopathy of prematurity; SNP, single nucleotide polymorphism; VR, vitreoretinal; WT, wild type.

Table 3 Frequencies of *NDP*, *FZD4* and *TSPAN12* gene variants in patients with retinopathy of prematurity (ROP) in different ethnic groups

Genes	Country (cases/controls)	Phenotype	Mutations/polymorphisms	Cases with variants, % (n)	References
NDP	USA (100/130)	Advanced ROP	12 bp CT repeat insertion and 14 bp deletion in 5′UTR of exon1	3 (2)	Hiraoka *et al*[13]
	Kuwait (95/115)	Severe ROP	c.597C>A	83.3 (79)	Haider *et al*[14]
	Australia (31/90)	Regressed ROP	14 bp deletion located in 5′UTR	9.6 (3)	Dickinson *et al*[12]
	Japan (17/51)	Severe ROP	237A>G in the 5′UTR of exon 1	5.9 (1)	Hiraoka *et al*[13]
	India (78/82)	All stages of ROP	14 bp deletion in 5′UTR, IVS1+16A>G, c.*522T>C in 3′UTR	3.84 (3)	Present study
FZD4	USA (20/200)	Advanced ROP	p.(I256V)	5 (1)	MacDonald *et al*[24]
	USA (60/42)	All stages ROP	p.(P33S)/p.(P168S)	6.7 (4)	Drenser *et al*[15]
	Japan (17/51)	Advanced ROP	No variation	0 (0)	Hiraoka *et al*[13]
	Canada (71/33)	Advanced ROP	p.(A370G), p.(K203N)	3 (2)	Ells *et al*[11]
	Japan (53/346)	Advanced ROP	p.(H69Y), p.(R127H), p.(Y211H)	7.5 (4)	Kondo *et al*[10]
	USA (93/98)	All stages of ROP	p.(G424E), p.(P33S)/p.(P168S), p.(P33S), p.(P168S)	11.8 (11)	Dailey *et al*[25]
	India (90/150)	All stages ROP	p.(I360V), p.(P168S), p.(P33S), p.(P33S)/p.(P168S)	12.2 (11)	Present study
TSPAN12	Japan (53/346)	Advanced ROP	No variation	0 (0)	Kondo *et al*[10]
	India (200/145)	Threshold ROP	p.(L119R)	0.5 (1)	Present study

TSPAN12 gene variations in ROP

Several reports have demonstrated the important role of *TSPAN12* gene mutations in FEVR pathogenesis. In the present study, we have identified p.(Leu119Arg) variants in only patients with ROP, while the other four reported SNPs c.*334A>T, c.765G>T, c.*39C>T and c.*1243A>T were observed in both patients with ROP and controls. None of the variants in *TSPAN12* gene were pathogenic, and no significant differences in the frequency of these SNPs were observed among ROP patients and controls. Thus, the role of *TSPAN12* gene in ROP needs to be investigated further across different study cohorts to establish its potential role in ROP.

Majority of the variations associated with severe ROP in *NDP*, *FZD4* and *TSPAN12* genes from the previous and present studies were either reported SNPs or non-pathogenic variations.[10 15 24] Across all the studies published on Norrin β-catenin signalling genes in ROP, only very few pathogenic variants have been observed. Moreover, none of the pathogenic variants found in *NDP*, *FZD4* and *TSPAN12* genes for FEVR cases[7 8] were detected in the patients with ROP, providing further evidence of locus heterogeneity across these two different phenotypes. Thus, we conclude that while patients with FEVR are born with specific genetic defects, ROP is much more a complex condition, where rare variants and SNPs might play an important role along with other prenatal and postnatal risk factors.

In conclusion, this study assessed the involvement of variants in *NDP*, *TSPAN12* and *FZD4* gene in the pathogenesis of ROP in Indian cohort. However, due to limited quantity of DNA concentration available for the experiments from a very low volume of blood from the preterm infants, different number of cases were screened for different genes. Additionally, for the above-mentioned reasons, some additional cases with genetic changes in the studied genes and other potential gene such as *LRP5* might have been missed in our cohort. Despite of the challenges observed mainly in getting sufficient samples from preterm tiny infants, the results obtained in this study suggested that unlike FEVR, a Mendelian disorder, ROP seems to be a complex disease that is genetically more heterogeneous with multiple alleles of varying magnitudes of effect. Furthermore, screening of the rest of the Norrin β-catenin signalling pathway genes might expand the information on the involvement of this pathway in ROP pathogenesis. ROP, being a multifactorial disease, involvement of some putative genes apart from Norrin β-catenin signalling genes could not be ruled out. Exome sequencing or whole-genome sequencing could aid in identifying such novel genes in ROP.

Acknowledgements The authors would like to thank Dr Subhabrata Chakrabarti for his kind help in data analysis and other valuable suggestions for the study.

Contributors Inderjeet Kaur and Subhadra Jalali conceived the idea and wrote the protocol; Inderjeet Kaur served as principal investigator; Subhadra Jalali, Divya Balakrishnan and Anjli Hussain were coinvestigators, performed clinical examinations and graded the fundus images and surgeries for the preterm; Sonika Rathi, Satish Patnaik and Ganeswara Rao Musada collected blood samples and family history of the probands; Sonika Rathi performed most of the molecular biology-based analysis of blood; Satish Patnaik and Ganeswara Rao Musada performed a part of molecular screening; Sonika Rathi and Inderjeet Kaur analysed the data and wrote the manuscript; and all authors revised the paper and approved the submitted version.

Funding This work was supported in parts by a grant from the Program Support grant by Department of Biotechnology (BT/01/COE/06/02/10 and BT/PR3992/MED/97/31/2011) and Champaulimaud Foundation grant Portugal to Inderjeet Kaur and Indian Council of Medical Research fellowship to Sonika Rathi.

Competing interests None declared.

Patient consent Obtained.

Ethics approval The study protocol was approved by the Institutional Review Board (LEC029149029) of the L.V. Prasad Eye Institute (LVPEI).

Provenance and peer review Not commissioned; externally peer reviewed.

Data sharing statement Study data is available for research use from the corresponding author and principal investigator of the study upon request.

REFERENCES

1 Jalali S, Matalia J, Hussain A, *et al*. Modification of screening criteria for retinopathy of prematurity in India and other middle-income countries. *Am J Ophthalmol* 2006;141:966–8.
2 Gilbert C, Fielder A, Gordillo L, *et al*. Characteristics of infants with severe retinopathy of prematurity in countries with low, moderate, and high levels of development: implications for screening programs. *Pediatrics* 2005;115:e518–e525.
3 Vijayalakshmi P, Kara T, Gilbert C. Ocular morbidity associated with retinopathy of prematurity in treated and untreated eyes: a review of the literature and data from a tertiary eye-care center in Southern India. *Indian Pediatr* 2016;53:S137–S42.
4 Charan R, Dogra MR, Gupta A, *et al*. The incidence of retinopathy of prematurity in a neonatal care unit. *Indian J Ophthalmol* 1995;43:123–6.
5 Xu Q, Wang Y, Dabdoub A, *et al*. Vascular development in the retina and inner ear: control by Norrin and Frizzled-4, a high-affinity ligand-receptor pair. *Cell* 2004;116:883–95.
6 Black GC, Perveen R, Bonshek R, *et al*. Coats' disease of the retina (unilateral retinal telangiectasis) caused by somatic mutation in the NDP gene: a role for norrin in retinal angiogenesis. *Hum Mol Genet* 1999;8:2031–5.
7 Musada GR, Jalali S, Hussain A, *et al*. Mutation spectrum of the Norrie disease pseudoglioma (NDP) gene in Indian patients with FEVR. *Mol Vis* 2016;22:491–502.
8 Musada GR, Syed H, Jalali S, *et al*. Mutation spectrum of the FZD-4, TSPAN12 AND ZNF408 genes in Indian FEVR patients. *BMC Ophthalmol* 2016;16:90.
9 Seo SH, Yu YS, Park SW, *et al*. Molecular characterization of FZD4, LRP5, and TSPAN12 in familial exudative vitreoretinopathy. *Invest Ophthalmol Vis Sci* 2015;56:5143–51.
10 Kondo H, Kusaka S, Yoshinaga A, *et al*. Genetic variants of FZD4 and LRP5 genes in patients with advanced retinopathy of prematurity. *Mol Vis* 2013;19:476–85.
11 Ells A, Guernsey DL, Wallace K, *et al*. Severe retinopathy of prematurity associated with FZD4 mutations. *Ophthalmic Genet* 2010;31:37–43.
12 Dickinson JL, Sale MM, Passmore A, *et al*. Mutations in the NDP gene: contribution to Norrie disease, familial exudative vitreoretinopathy and retinopathy of prematurity. *Clin Exp Ophthalmol* 2006;34:682–8.
13 Hiraoka M, Berinstein DM, Trese MT, *et al*. Insertion and deletion mutations in the dinucleotide repeat region of the Norrie disease gene in patients with advanced retinopathy of prematurity. *J Hum Genet* 2001;46:178–81.
14 Haider MZ, Devarajan LV, Al-Essa M, *et al*. A C597-->A polymorphism in the Norrie disease gene is associated with advanced retinopathy of prematurity in premature Kuwaiti infants. *J Biomed Sci* 2002;9:365–70.
15 Drenser KA, Dailey W, Vinekar A, *et al*. Clinical presentation and genetic correlation of patients with mutations affecting the FZD4 gene. *Arch Ophthalmol* 2009;127:1649–54.
16 International Committee for the Classification of Retinopathy of Prematurity. The international classification of retinopathy of prematurity revisited. *Arch Ophthalmol* 2005;123:991–9.
17 Meindl A, Berger W, Meitinger T, *et al*. Norrie disease is caused by mutations in an extracellular protein resembling C-terminal globular domain of mucins. *Nat Genet* 1992;2:139–43.
18 Kumar P, Henikoff S, Ng PC. Predicting the effects of coding non-synonymous variants on protein function using the SIFT algorithm. *Nat Protoc* 2009;4:1073–81.
19 Adzhubei I, Jordan DM, Sunyaev SR. Predicting functional effect of human missense mutations using PolyPhen-2. *Curr Protoc Hum Genet* 2013;Chapter 7:720.
20 Schwarz JM, Rödelsperger C, Schuelke M, *et al*. MutationTaster evaluates disease-causing potential of sequence alterations. *Nat Methods* 2010;7:575–6.
21 Lek M, Karczewski KJ, Minikel EV, *et al*. Analysis of protein-coding genetic variation in 60,706 humans. *Nature* 2016;536:285–91.
22 Sherry ST, Ward MH, Kholodov M, *et al*. dbSNP: the NCBI database of genetic variation. *Nucleic Acids Res* 2001;29:308–11.
23 Kenyon JR, Craig IW. Analysis of the 5' regulatory region of the human Norrie's disease gene: evidence that a non-translated CT dinucleotide repeat in exon one has a role in controlling expression. *Gene* 1999;227:181–8.
24 MacDonald ML, Goldberg YP, Macfarlane J, *et al*. Genetic variants of frizzled-4 gene in familial exudative vitreoretinopathy and advanced retinopathy of prematurity. *Clin Genet* 2005;67:363–6.
25 Dailey WA, Gryc W, Garg PG, *et al*. Frizzled-4 variations associated with retinopathy and intrauterine growth retardation: a potential marker for prematurity and retinopathy. *Ophthalmology* 2015;122:1917–23.

Mutation spectrum of *NDP*, *FZD4* and *TSPAN12* genes in Indian patients with retinopathy of prematurity

Sonika Rathi, Subhadra Jalali, Ganeswara Rao Musada, Satish Patnaik, Divya Balakrishnan, Anjli Hussain and Inderjeet Kaur

Br J Ophthalmol published online October 5, 2017

Notes

frontiers in Immunology

ORIGINAL RESEARCH
published: 22 December 2017
doi: 10.3389/fimmu.2017.01868

Abnormal Complement Activation and Inflammation in the Pathogenesis of Retinopathy of Prematurity

*Sonika Rathi[1], Subhadra Jalali[2], Satish Patnaik[1], Shahna Shahulhameed[1], Ganeswara R. Musada[1], Divya Balakrishnan[2], Padmaja K. Rani[2], Ramesh Kekunnaya[3], Preeti Patil Chhablani[3], Sarpras Swain[4], Lopamudra Giri[4], Subhabrata Chakrabarti[1] and Inderjeet Kaur[1]**

[1] Prof Brien Holden Eye Research Centre, Hyderabad, India, [2] Smt. Kanuri Santhamma Centre for Vitreo Retinal Diseases, Hyderabad, India, [3] Jasti V Ramanamma Children's Eye Care Centre, L V Prasad Eye Institute, Hyderabad, India, [4] Indian Institute of Technology, Hyderabad, India

OPEN ACCESS

Edited by:
Uday Kishore, Brunel University London, United Kingdom

Reviewed by:
Taruna Madan, National Institute for Research in Reproductive Health (ICMR), India
Lubka T. Roumenina, INSERM UMRS1138 Centre de Recherche des Cordeliers, France

***Correspondence:**
Inderjeet Kaur
inderjeet@lvpei.org, ikaurs@gmail.com

Specialty section:
This article was submitted to Molecular Innate Immunity, a section of the journal Frontiers in Immunology

Received: *02 October 2017*
Accepted: *08 December 2017*
Published: *22 December 2017*

Citation:
Rathi S, Jalali S, Patnaik S, Shahulhameed S, Musada GR, Balakrishnan D, Rani PK, Kekunnaya R, Chhablani PP, Swain S, Giri L, Chakrabarti S and Kaur I (2017) Abnormal Complement Activation and Inflammation in the Pathogenesis of Retinopathy of Prematurity. Front. Immunol. 8:1868. doi: 10.3389/fimmu.2017.01868

Retinopathy of prematurity (ROP) is a neurovascular complication in preterm babies, leading to severe visual impairment, but the underlying mechanisms are yet unclear. The present study aimed at unraveling the molecular mechanisms underlying the pathogenesis of ROP. A comprehensive screening of candidate genes in preterms with ROP ($n = 189$) and no-ROP ($n = 167$) was undertaken to identify variants conferring disease susceptibility. Allele and genotype frequencies, linkage disequilibrium and haplotypes were analyzed to identify the ROP-associated variants. Variants in *CFH* ($p = 2.94 \times 10^{-7}$), *CFB* ($p = 1.71 \times 10^{-5}$), *FBLN5* ($p = 9.2 \times 10^{-4}$), *CETP* ($p = 2.99 \times 10^{-5}$), and *CXCR4* ($p = 1.32 \times 10^{-8}$) genes exhibited significant associations with ROP. Further, a quantitative assessment of 27 candidate proteins and cytokines in the vitreous and tear samples of babies with severe ROP ($n = 30$) and congenital cataract ($n = 30$) was undertaken by multiplex bead arrays and further validated by western blotting and zymography. Significant elevation and activation of MMP9 ($p = 0.038$), CFH ($p = 2.24 \times 10^{-5}$), C3 ($p = 0.05$), C4 ($p = 0.001$), IL-1ra ($p = 0.0019$), vascular endothelial growth factor (VEGF) ($p = 0.0027$), and G-CSF ($p = 0.0099$) proteins were observed in the vitreous of ROP babies suggesting an increased inflammation under hypoxic condition. Along with inflammatory markers, activated macrophage/microglia were also detected in the vitreous of ROP babies that secreted complement component C3, VEGF, IL-1ra, and MMP-9 under hypoxic stress in a cell culture model. Increased expression of the inflammatory markers like the IL-1ra ($p = 0.014$), MMP2 ($p = 0.0085$), and MMP-9 ($p = 0.03$) in the tears of babies at different stages of ROP further demonstrated their potential role in disease progression. Based on these findings, we conclude that increased complement activation in the retina/vitreous in turn activated microglia leading to increased inflammation. A quantitative assessment of inflammatory markers in tears could help in early prediction of ROP progression and facilitate effective management of the disease, thereby preventing visual impairment.

Keywords: retina, premature birth, inflammation, genetics, cytokines, abnormal angiogenesis, microglia/macrophage, alternative complement pathway

INTRODUCTION

Retinopathy of prematurity (ROP) is a complex disease of the retina with a multi-factorial etiology and an early intervention has been observed to prevent irreversible vision loss in some of these prematurely born infants (1). Its incidence in developed countries with adequate neonatological facilities (like United States) is 19.88% (2) while it is slightly higher (~30%) for middle-income developing countries (3, 4). In India, approx. two million babies are at risk of developing ROP annually (4) with an overall incidence estimated to be around 45% (5, 6). Hence, ROP is one of the major causes of visual impairment in India. Lower gestational age (GA), lower birth weight (BW), and oxygen supplementation are the primary risk factors associated with ROP (7). It is a self-limiting disease with initial symptoms of avascular retina that progresses to abnormal growth of retinal vessels causing retinal detachment (8). Hypoxia in the avascular retina is considered to be the primary cause for neovascularization in ROP that further activates various cellular pathways such as HIF1α, eNOS/iNOS, and vascular endothelial growth factor (VEGF) signaling leading to abnormal neovascularization (9, 10). However, the detailed molecular mechanisms underlying neovascularization in ROP have not been elucidated yet. So far, few functionally relevant genes (*NDP, FZD4, LRP5, CFH, VEGF, ANGPT2, EPO, BDNF,* and *CETP*) have been associated with ROP in a small fraction of cases. But, many of these variants could not be replicated across different ethnicities (11–13). Further, their roles in risk predictions and disease management are yet to be determined.

The protein profiles in the vitreous have been utilized for studying the underlying pathology of the retina due to its proximity. This has largely been accomplished by analyzing the levels of erythropoietin, VEGF, and cytokines like interleukins (IL-6, IL-7, IL-10, and IL-15), Eotaxin, FGF basic, G-CSF, GM-CSF, IP-10, and RANTES in the vitreous to identify their potential as biomarkers for ROP progression (14–16). Interestingly, interleukin-7 (IL-7), monocyte chemotactic protein-1, and macrophage inflammatory protein 1 (MIP-1α and MIP-1β) levels were also found to be significantly elevated in the cord blood serum of ROP (17). Earlier, low serum levels of IGF-1 and VEGF were reported in preterm babies with severe ROP and low GA (18, 19). Thus, the studies on protein profiling and genetic associations of ROP could explain the susceptibility of some preterm babies progressing to severe ROP.

Our study is an attempt to comprehensively elucidate the genomic basis of ROP and identify the potential biomarkers for progression to severe stages. Since, no mutations were observed in the Norrin signaling genes in ROP in our earlier study (20), we explored genes involved in angiogenesis, growth, and development of the fetal retina, trans-endothelial migration, oxidative stress, inflammation, and neurodegenerative processes, in order to understand their role in ROP pathogenesis. We observed strong associations of ROP with the variants in *CFH*, *CFB, CXCR4, FBLN5,* and *CETP* genes along with increased levels of proteins in the extracellular matrix (ECM) and complement pathways in the vitreous of these babies. We observed the presence of the activated microglia/macrophages in the retina and vitreous. We further demonstrated the activated microglial cells under hypoxia expressed complement C3, VEGF, and IL-1β, thereby resulting in abnormal blood vessel proliferation in the ROP-affected eyes. We also evaluated the inflammatory proteins as potential biomarkers for ROP based on their expressions in the tear samples of the ROP patients.

MATERIALS AND METHODS

Study Subjects

The study protocol adhered to the tenets of declaration of Helsinki and was approved by the Institutional Review Board (LEC02-14-029) of the L V Prasad Eye Institute (LVPEI). Preterm babies referred for further management from the neonatal intensive care units of different hospitals in Hyderabad to the LVPEI between January 2007 and December 2010 were enrolled. Overall, the study cohort comprised 372 preterm babies of GA $\leq$ 35 weeks and/or BW $\leq$ 1,700 g with ROP ($n = 189$) and no-ROP ($n = 167$). A detailed demographic and clinical history (Table S1 in Supplementary Material) of all the preterm babies enrolled were documented and a written informed consent was obtained from their parents. The diagnosis and categorization of ROP cases from mild to severe form was based on severity (stages 1–5), location (zones I, II, III), amount of disease (clock hours), and presence or absence of "plus" disease following ICROP guidelines (20, 21) (Figure S2 in Supplementary Material). Severe ROP includes progressive disease, which requires prompt treatment. It includes any stage (1–5) Zone I with plus and stages 2–3 Zone II with plus. Mild ROP cases include less severe disease, which does not require any treatment. Although until the regression of the disease completely, babies are under regular follow-up for ROP screening.

Sample Collection

Venous blood (0.5–1 mL) was collected from the ROP and no-ROP preterm babies by venipuncture. DNA was extracted from the blood samples using an automated DNA extraction platform (MagNa Pure LC 20, Roche) following the manufacturers guidelines. Likewise, for proteomic studies, the vitreous humor samples (100–500 μL) were collected from preterm babies with stage IV and V ROP ($n = 30$) who had undergone vitrectomy as a part of their routine clinical management. The controls for the proteomic studies included babies with congenital cataract (<6 months of age) who underwent partial vitrectomy as part of the surgical management ($n = 30$). The vitreous samples were immediately centrifuged at relative centrifugal force (rcf) of 10,621 g and the supernatant was stored at −80°C deep freezer until further use.

Additionally, crude tears were collected before instilling any drops or drug for pupil dilation in the eyes of preterm babies with ROP (Stage II–V) ($n = 27$) and no-ROP ($n = 13$) using a capillary tube and without touching the conjunctiva. The tear samples for ROP subjects were collected during the active disease condition either before or after 3 months following medical intervention.

Customized Genotyping of Candidate Variants

A customized panel containing 384 single-nucleotide polymorphisms (SNPs) from 26 chosen genes (Table S2 in Supplementary

Material) involved in growth and development of the fetal retina, angiogenesis, inflammation, neurodegeneration, and oxidative stress processes were genotyped using a microarray platform (Illumina Inc., golden gate assay). Following hybridization, the fluorescent signals were scanned by a bead array reader and the raw signal intensities were imported to the Genome Studio software (version 1.9) for assessing quality scores. The assay and sample reliability were measured by means of the gen call score and the genotypes were called following clustering. The genotypes of a subset of samples for all the genes were validated by resequencing on an automated DNA sequencer (ABI 3130 XL) using the BigDye chemistry.

Quantitative Assessment of Cytokines and Other Proteins in the Vitreous and Tear Samples

The concentrations of 27 cytokines (Bio-Plex Human cytokine 27-Plex, Bio-Rad, Hercules, CA, USA) and 28 different proteins (HMMP1-55K, HMMP2-55K, HNDG1-36K, HNDG2-36K, HTIMP2-54K, TGFB-64K-03, HYCYTOMAG-60K, Merck Millipore, Billerica, MA, USA) involved in ECM remodeling, angiogenesis and inflammatory pathways were screened by multiplex bead immunoassays using the Luminex xMAP technology in vitreous samples that were pre-diluted to concentration 1:3. Similar assay was used for estimating the concentrations of MMPs and cytokines in the tears samples and were quantitated by comparing them with their respective standard curve. All standards and some of the samples (due to less volume of samples) were measured in duplicates.

Validation of the Differentially Regulated Proteins by Western Blotting and Zymography

A part of vitreous sample (50–100 μL) was lysed using a buffer containing 50 mM Tris-HCl (pH = 8), 120 mM NaCl, 0.5% NP40, protease inhibitor cocktail, and precipitated with acetone. The protein pellet was eluted in 50 μL of 1× phosphate buffered saline (PBS) containing the protease inhibitor cocktail and quantified by bicinchoninic acid assay. The normalized vitreous proteins (10 μg) were then subjected to western blotting. Western blotting was done using mouse anti-human C3 antibody (sc-28294, Santa Cruz) and mouse anti-human C5 (MAB2037, R&D Systems) followed by incubation with IRDye® 680RD secondary antibody. The entire procedure was done according to the manufacturer's recommended application protocol (https://www.licor.com).

MMP gelatinase activity was measured in the vitreous and tear of ROP babies and controls by zymography as described earlier (22). An equal volume of crude vitreous and tear samples were electrophoresed under non-reducing conditions in 10% SDS-PAGE gels polymerized with 1 mg/mL gelatin. The gel was washed with 2.5% Triton X-100 for 30 minutes at room temperature with gentle agitation, followed by rinsing with distilled water. The gel was then incubated for 30 min in developing buffer containing 50 mM Tris-HCl, pH 7.8, 5 mM $CaCl_2$, 0.2 M NaCl, 0.02% Brij 35. The gel was incubated with fresh developing buffer at 37°C for 16 h and stained with Coomassie blue (Bio-Rad). This was followed by destaining with 10% v/v methanol, 5% v/v acetic acid in dH_2O. Active MMP (MMP2/MMP9) band was detected in the zymogram in the discovery cohort. The observations of discovery cohort were further validated in tears in an extended cohort of patients at different stages of ROP: no-ROP ($n = 9$), mild ROP regressed ($n = 6$), mild ROP_progressed ($n = 7$), and severe ROP ($n = 12$) by zymography in order to confirm their role as biomarker in ROP pathogenesis. Zymogram band intensities were calculated with ImageJ software.

Immunohistochemistry and Hematoxylin and Eosin (H&E) Staining for Macrophage/Microglia in the Vitreous

Vitreous were subjected to cytospin to separate the cells that were embedded in the parafilm block. Sections were cut, air dried, and stained with H&E (23) for understanding their morphology. Tissue sections were then deparaffinized using xylene and gradually rehydrated with ethanol. Antigen retrieval was done by microwaving the sections at full power for 4–5 min in Tris EDTA buffer (10 mM Tris, 1 mM EDTA, 0.5% tween 20, pH 9.0). Blocking was carried out with 2.5% (w/v) BSA in PBS (10 mmol/L sodium phosphate, pH 7.5, 120 mmol/L sodium chloride) for 30 min at room temperature. Thereafter, the slides were incubated for 60 min with the primary antibody (CD 68 for human 1:100) diluted in 1× PBS, followed by three washings with PBS. Further incubation was carried out with biotinylated anti-mouse immunoglobulin. Sections were then washed in PBS and incubated with avidin DH/biotinylated horseradish peroxidase reagent in PBS for 30 min before final washing. The antigen was localized using 1 mg/mL diaminobenzidene tetrahydrochloride (DAB; Sigma), 0.2% H_2O_2 in 50 mmol/L Tris–HCl, pH 7.6, which appeared as a brown end product. Sections were then counter-stained with DAPI for nuclei staining.

Response to Hypoxia by the Cultured Microglia Cells

The human microglial cell line (CHME3) was cultured in DMEM containing 10% FBS along with antibiotics penicillin and streptomycin. The confluent cells were trypsinized using 0.25% trypsin-EDTA. Hypoxic stress was introduced in the microglia cells by treating them with Cobalt chloride ($CoCl_2$) at various concentrations from 100 to 250 μm. Briefly, around 15,000 cells were seeded on a six well plate and then serum deprived for 6 h, followed by treatment with $CoCl_2$ for 24 h on attaining 70–80% confluency. The serum deprived cells in the same duration that were not treated for hypoxia were used as controls.

Ca^{2+} Staining and Live Cell Imaging

The cells were washed in HBSS (Thermoscientific, Waltham, MA, USA) and then incubated with the calcium binding dye Flu-4 (diluted with HBSS 1:750) for 30 min. After washing the cells with HBSS three times, live cell imaging was performed for 10 min using an EVOS fluorescent microscope (Thermo Fischer

Scientific, Waltham, MA, USA) under 20× magnification. The cytosolic calcium flux was measured using the change in Fluo-4 intensity over time for individual cells (Excitation: 494 nm Emission: 506 nm) (24).

Semi-Quantitative PCR

The RNA from untreated and treated cells was extracted by Trizol method (25). The cDNA was prepared using iScript cDNA synthesis kit (Bio-Rad, CA, USA). Semi quantitative PCR was carried out using the specific primers (Table S3 in Supplementary Material) for *VEGF165*, *C3*, *HIF1*α, *BAX*, and *IL-1*β while β-*actin* was used as an endogenous control.

Statistical and Bioinformatic Analysis

Allele frequencies of all the 384 variants were calculated by gene counting method along with odds ratio and 95% CI. A p value < 0.05 was considered to be significant. The associated allele and haplotype frequencies were further analyzed for statistical correction using Bonferroni and permutations tests ($n = 10{,}000$ permutations). Estimates of Hardy–Weinberg equilibrium ($p > 0.001$), linkage disequilibrium (LD), and haplotype frequencies were calculated using the Haploview software (version 4.2) (26).

Protein and cytokine levels in ROP and control samples were represented as bar plot (the mean ± SE) and box plot (median, interquartile range, and whiskers). Comparison of proteins and cytokines levels between ROP and controls vitreous/tears were calculated using the unpaired Student's t-test. A p-value < 0.05 was considered to be statistically significant. Since the cytosolic calcium level does not follow a normal distribution, we performed the testing of equality in medians for control and hypoxic condition using Wilcoxon rank-sum test.

RESULTS

Involvement of Genes in ROP

Of the 384 variants screened (Table S2 in Supplementary Material), 73 were removed from further analysis as they were either not in Hardy-Weinberg equilibrium in the controls ($n = 16$), were monomorphic ($n = 44$), or had a call rate < 97% ($n = 13$). Thus, 311 SNPs from 26 genes were finally analyzed for association with ROP. Among these 37 SNPs in 14 genes (*AGTR1, ANGPT2, C3, CFH, CFB, CXCR4, FBLN5, H2AFX, IHH, MMP2, TGF*β*1, CETP, VEGF*, and *TSPAN12*) exhibited significant association ($p < 0.05$) with ROP (**Table 1**). Additionally, 5/37 associated SNPs in *CFH, CFB, CXCR4, FBLN5,* and *CETP* genes withstood Bonferroni correction. Intriguingly, only the *CETP* variant (rs891141) conferred significant risk of ROP, while the variants across the other genes were protective (**Table 1**). Strong LD was observed across all the variants (except rs1831821) in *CFH* and rs891141 and rs289716 in *CETP* gene, while moderate LD was observed between rs891141 and rs289713 in *CETP* and rs2268002 and rs2284340 in *FBLN5* (Figure S1 in Supplementary Material).

Likewise, haplotypes generated with the associated and flanking variants of these five genes revealed that only the haplotype C-A-T in *CETP* conferred significant risk of ROP, while those with *CFH* and *FBLN5* were protective. Haplotypes with the *CXCR4* and *CFB* were not informative (**Table 2**). Thus, the present study highlights the potential involvement of novel genes (*CFH, CFB, CETP, FBLN5,* and *CXCR4*) in ROP based on their allelic and haplotype associations.

Quantitative Assessment of Proteins Involved in Complement Cascade and Neurodegeneration in the Vitreous Samples of ROP Subjects

Based on strong associations in the *CFH* and *CFB* genes, a quantitative assessment of a neurodegenerative panel containing CRP, SAP, MIP-4, Complement C4, apolipoprotein AI, apolipoprotein CIII, apolipoprotein E, Complement Factor H, and Complement C3 proteins was carried out by multiplex immuno-bead assay in the vitreous samples of ROP patients ($n = 30$) and controls ($n = 30$). All the complement components and apolipoproteins were detectable in the vitreous samples. Overall, we observed significantly elevated levels of C3 ($p = 0.05$), C4 ($p = 0.001$), CFH ($p = 2.24 \times 10^{-5}$), VEGF ($p = 0.0027$), apolipoprotein AI ($p = 0.0007$), and apolipoprotein CIII ($p = 0.004$) in the vitreous of ROP compared to the control subjects indicating their possible involvement in the disease pathogenesis (**Figure 1A**).

Activation of Complement Pathway in Vitreous Humor of Proliferative ROP

We validated the differential expression of complement component C3 by western blotting. An intense band of 192 kDa corresponding to C3 molecule was observed in ROP cases compared to controls (**Figure 1B**). Additionally, we observed the activated C3 fragments; C3b (182 kDa), C3c (145 kDa), and iC3bα (63 kDa) in the ROP vitreous under non-reducing conditions as confirmed by mass spectrometry (data not shown here), but not in the controls (**Figure 1B**), suggesting a higher activation of C3 in ROP. Likewise, a higher expression of complement component C5 was observed in ROP vitreous compared to the controls (data not shown) suggesting a further activation of the complement pathway.

Hypoxia-Induced Activated Macrophage Secretes Angiogenic Molecules

We further demonstrated that along with increased expression of angiogenic molecules in the vitreous samples of patients, activated macrophages/microglia in turn would also be secreting proinflammatory cytokines that might exacerbate the inflammation, further playing a role in the ROP pathogenesis. We detected activated macrophages/microglia on H&E, further confirmed by immunostaining with CD68 in ROP vitreous but not in the controls (**Figure 1C**). The results of this experiment supported for shift in the proangiogenic state as demonstrated by a significant increase in the levels of cytokines IL8 ($p = 0.0149$), G-CSF ($p = 0.0099$), IL1ra ($p = 0.0019$),

TABLE 1 | Association of gene variants with retinopathy of prematurity (ROP).

Genes screened	Single-nucleotide polymorphism (SNP) ID	Location	Nucleotide change	Amino acid change	RegulomeDB (binding score) (27)	Minor allele	Minor allele frequencies		*p*-Value	Odds ratio [95% CI]
							ROP	Controls		
CFH	**rs374896**	**Intron**	g.71371T>C	–	Minimum binding evidence (6)	**T**	**0.0426**	**0.159**	**2.94×10^{-7}**	**0.241 [0.135–0.431]**
CFB	**rs1048709**	**Exon**	g.19461A>G	p.R150R	Likely to affect binding of POLR2A and linked expression of the HLAC, HLA-DQA1, HLADQB1, HLADRB1, HLADRB5	**G**	**0.15**	**0.269**	**1.71×10^{-5}**	**0.484 [0.035–0.676]**
C3	rs344550	Intron	g.37710G>C	–	Likely to affect binding of GATA2, MYC, NR2F2, STAT5A, SPI1CCNT2 (1F)	C	0.223	0.29	0.0409	0.703 [0.501–0.986]
	rs2287846	Intron	g.24106G>C	–	Minimal binding evidence (5)	G	0.298	0.237	0.0658	1.370 [0.979–1.915]
CXCR4	**rs2228014**	**Exon**	g.2652C>T	p.I142I	Minimum binding evidence (4)	**G**	**0.422**	**0.637**	**1.32×10^{-8}**	**0.416 [0.307–0.565]**
ANGPT2	rs2922889	Intron	g.119194A>T	–	Minimum binding evidence (6)	T	0.497	0.431	0.0776	1.305 [0.971–1.756]
	rs2515464	Intron	g.35092A>C	–	Minimum binding evidence (5)	T	0.173	0.251	0.0102	0.622 [0.432–0.895]
	rs734701	Intron	g.32684C>T	–	Minimum binding evidence (6)	A	0.452	0.527	0.0465	0.741 [0.551–0.996]
	rs2959812	Intron	g.29629T>C	–	Minimum binding evidence (5)	C	0.471	0.548	0.0391	0.732 [0.544–0.985]
VEGF	rs2010963	5′-UTR	–	–	Minimum binding evidence (4)	C	0.302	0.243	0.0084	1.352 [0.969–1.888]
	rs1413711	Intron	g.2758T>C	–	Minimum binding evidence (4)	T	0.39	0.482	0.014	0.688 [0.51–0.928]
	rs1005230	Intergenic	–	–	Minimum binding evidence (5)	A	0.388	0.482	0.011	0.680 [0.505–0.917]
FBLN5	**rs2268002**	**Intron**	g.17582G>C	–	Minimum binding evidence (5)	**G**	**0.32**	**0.423**	**9.2×10^{-4}**	**0.641 [0.492–0.835]**
MMP2	rs2285052	Intron	g.88546A>C	–	Minimum binding evidence (5)	G	0.092	0.036	0.0025	2.732 [1.39–5.368]
TGFb1	rs11466359	Intron	g.22217C>T	–	Minimum binding evidence (5)	T	0.093	0.0482	0.021	2.027 [1.1–3.734]
	rs4803457	Upstream	g.4544T>C	–	Minimum binding evidence (4)	A	0.465	0.536	0.061	0.754 [0.561–1.013]
CETP	**rs891141**	**Intron**	g.7962G>T	–	Minimum binding evidence (5)	**C**	**0.234**	**0.114**	**2.99×10^{-5}**	**2.378 [1.57–3.598]**
H2AFX	rs640603	Intergenic 3′ of a gene	–	–	Likely to affect binding of PLR2A, CHD1, E2F6, MXI1, E2F4, E2F6, MYC (2b)	T	0.161	0.09	0.0049	1.940 [1.215–3.085]
TSPAN12	rs41624	Intron	g.62819A>G	–	Minimum binding evidence (6)	T	0.176	0.243	0.0279	0.665 [0.462–0.958]
	rs41629	Intron	g.59568T>G	–	Minimum binding evidence (6)	A	0.176	0.243	0.0279	0.665 [0.462–0.958]
	rs3735467	Intron	g.47721G>T	–	Minimum binding evidence (5)	C	0.177	0.246	0.031	0.669 [0.465–0.964]
	rs12669167	Intron	g.38926T>G	–	NA (7)	C	0.173	0.24	0.0279	0.664 [0.46–0.958]
	rs10225453	Intron	g.36511C>A	–	Minimum binding evidence (5)	T	0.17	0.236	0.0287	0.663 [0.458–0.959]
	rs6953454	Intron	g.33908G>A	–	NA (7)	T	0.172	0.237	0.03	0.666 [0.461–0.964]
	rs996903	Intron	g.32898A>G	–	Likely to affect binding and linked expression of the FLJ21986 (1F)	C	0.17	0.237	0.0279	0.662 [0.458–1.044]
	rs6959328	Intron	g.32490T>A	–	NA (7)	A	0.17	0.237	0.0279	0.662 [0.458–1.044]
	rs6466759	Intron	g.28767A>T	–	Minimum binding evidence (5)	T	0.17	0.238	0.0251	0.657 [0.454–0.95]
	rs7805211	Intron	g.25107G>A	–	Minimum binding evidence (6)	A	0.168	0.237	0.0218	0.65 [0.449–0.941]
	rs6466760	Intron	g.24403C>G	–	Minimum binding evidence (6)	C	0.168	0.237	0.0218	0.65 [0.449–0.941]
	rs6466762	Intron	g.16639G>A	–	Minimum binding evidence (5)	A	0.169	0.241	0.0167	0.638 [0.441–0.923]
	rs3823859	Intron	–	–	Minimum binding evidence (5)	G	0.17	0.24	0.0219	0.651 [0.451–0.941]
	rs17142995	Intron	g.11660A>G	–	Minimum binding evidence (6)	C	0.173	0.24	0.0279	0.664 [0.46–0.958]
	rs7781985	Intron	g.6475A>C	–	Likely to affect binding and linked expression of the FLJ21986/ monocytes (1F)	C	0.17	0.24	0.0219	0.651 [0.451–0.941]
	rs3757557	5′UTR	g.91G>A	–	Minimum binding evidence (4)	A	0.117	0.171	0.0411	0.644 [0.421–0.985]
	rs4141309	Intergenic, upstream 5′ of gene	–	–	Minimum binding evidence (4)	A	0.112	0.171	0.0236	0.611 [0.398–0.939]
AGTR1	rs2739504	Intron	g.13100A>G	–	Minimum binding evidence (4)	C	0.446	0.371	0.041	1.362 [1.012–1.833]
IHH	rs394452	Exon	g.5153T>C	p.T376T	Minimum binding evidence (5)	T	0.261	0.168	0.0027	1.75 [1.211–2.528]

SNPs in bold withstood Bonferroni correction.

TABLE 2 | Estimated haplotype frequencies of the significantly associated variants in *CETP, CFH*, and *FBLN5* genes in retinopathy of prematurity (ROP) and premature controls.

Genes (single-nucleotide polymorphisms)	Haplotypes	Overall frequencies	ROP frequencies	Controls frequencies	Chi square	*p*-Value	Odds ratios (95% CI)
CETP (rs891141, rs289713, rs289716)	A-A-T	0.327	0.313	0.343	0.734	0.3916	0.871 (0.637–1.193)
	A-A-A	0.3	0.294	0.308	0.156	0.6931	0.937 (0.68–1.292)
	C-A-T	0.149	0.191	0.101	11.358	0.0008	2.1 (1.354–3.256)
	A-T-A	0.143	0.121	0.169	3.357	0.0669	0.674 (0.442–1.029)
	A-T-T	0.053	0.04	0.067	2.488	0.1147	0.586 (0.3–1.144)
CFH (rs3753395, rs374896, rs393955)	T-C-T	0.563	0.578	0.547	0.693	0.4052	1.134 (0.843–1.526)
	A-C-G	0.188	0.233	0.139	10.066	0.0015	1.874 (1.268–2.769)
	A-C-T	0.151	0.149	0.154	0.032	0.8586	0.962 (0.638–1.451)
	A-T-G	0.096	0.04	0.156	27.61	1.48×10^{-7}	0.226 (0.125–0.41)
FBLN5 (rs2268002, rs2284340)	G-C	0.38	0.413	0.343	3.621	0.0571	1.346 (0.992–1.826)
	G-G	0.37	0.311	0.437	12.093	5×10^{-4}	0.58 (0.427–0.789)
	A-C	0.242	0.271	0.21	3.625	0.0569	1.4 (0.989–1.983)

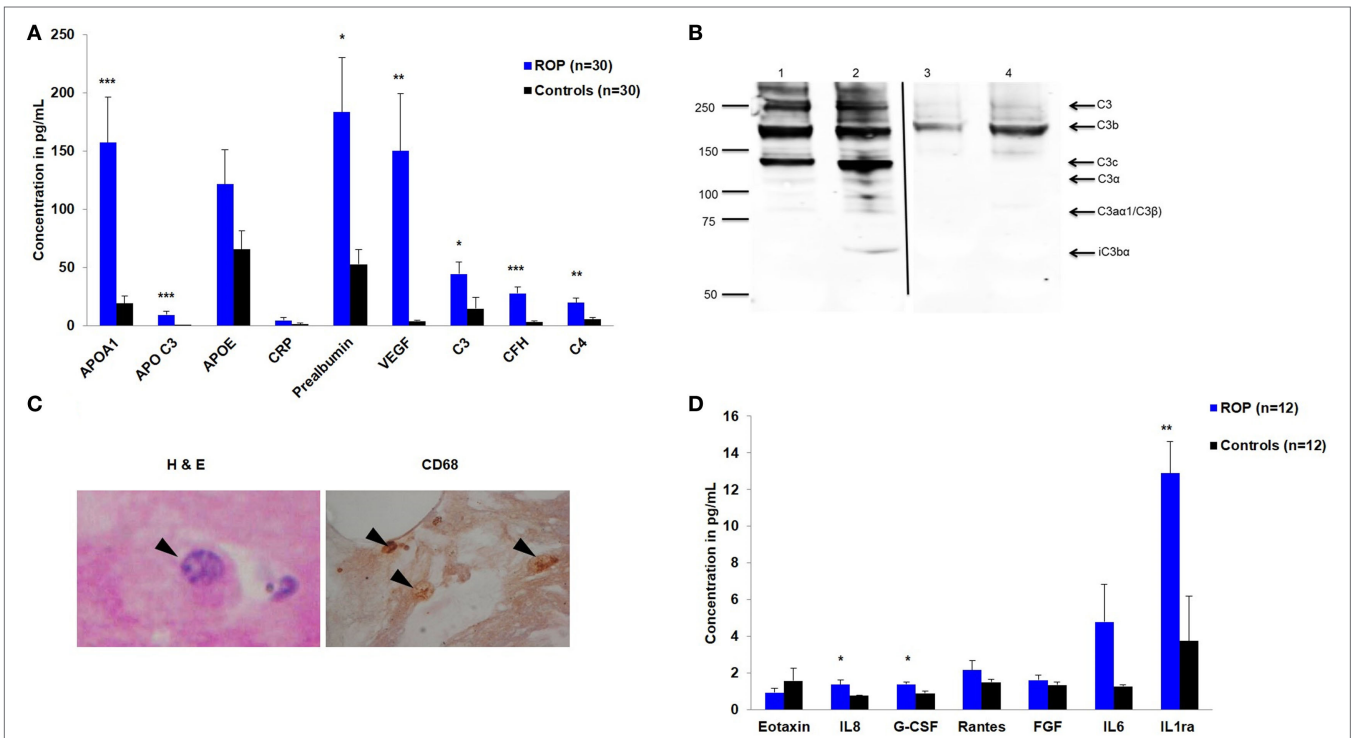

FIGURE 1 | Expression of inflammatory molecules in proliferative retinopathy of prematurity (ROP). **(A)** Differential levels of complement components and apolipoproteins in the vitreous humor of ROP and controls **(B)** Western blotting of C3 done under non-reducing condition, showing its expression in patients (lane 1 and 2) and controls (lane 3 and 4). Arrows indicate the C3 fragments. Thin black line inserted within gel showing that all the lanes were run on the same gel but were not continuous **(C)** Hematoxylin and eosin staining of ROP vitreous. Arrowheads indicate degenerated morphology of macrophages at 40×-magnification (irregular shaped with large vacuole, nucleus with a very prominent nucleolus); Staining of ROP vitreous with CD68 marker. Arrowheads indicate the presence of activated macrophages at 10× magnification. **(D)** Differential levels of inflammatory cytokines in the vitreous humor of ROP and controls. Error bars in **(A)** and **(D)** show SEM, $^{*}p < 0.05$, $^{**}p < 0.005$, $^{***}p < 0.0005$ (ROP vs. controls).

and VEGF ($p = 0.0027$) (**Figures 1A,D**) along with marginal increase of IL6, IL12, IL7, RANTES, and MCP1 in the ROP vitreous (data not shown).

To further confirm these results, we subjected the cultured microglial cells to hypoxic condition and checked for the expression of proinflammatory markers. The effect of hypoxia on the activation of macrophages/microglia was observed with an intense calcium staining in cells exposed to hypoxia compared to the unexposed ones. The result shows that there is increase in cytosolic calcium levels in case of hyperactivated cells subjected to 24 h of hypoxic stress (**Figure 2A**, $n = 50$). Specifically, there is a significant increase ($p < 0.0005$) in cytosolic calcium

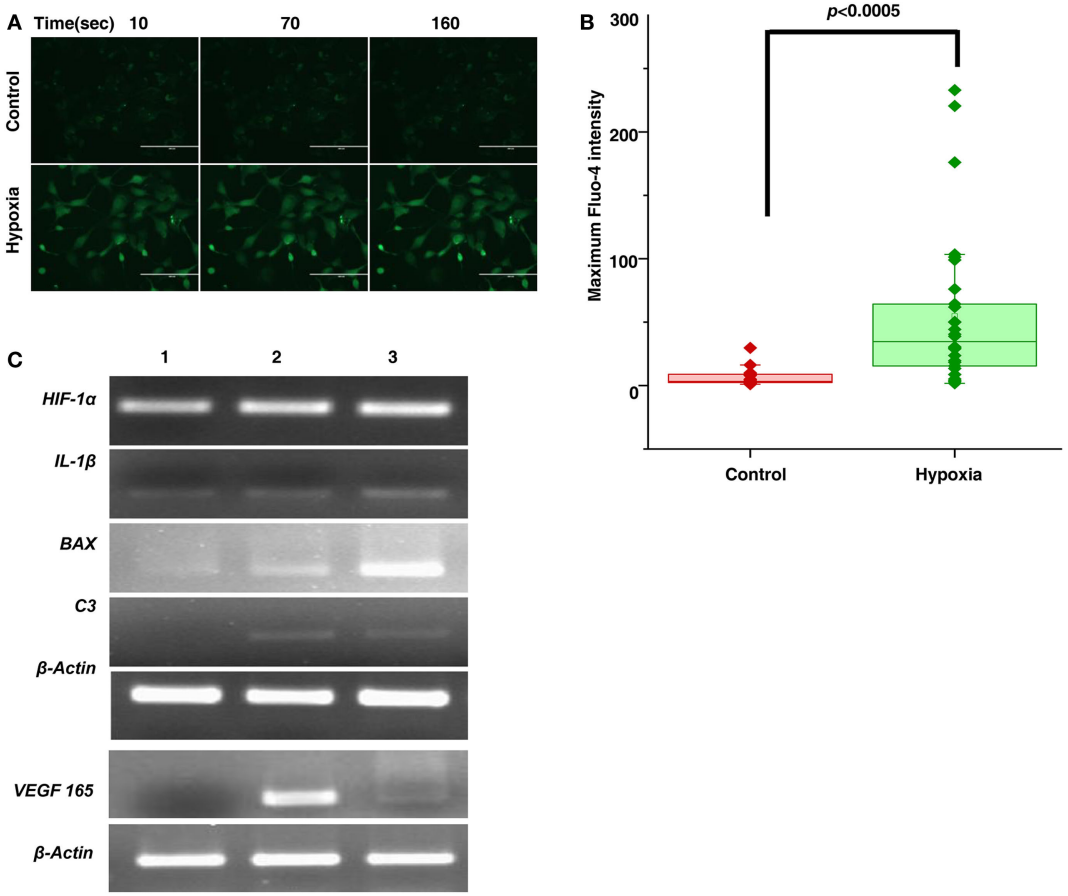

FIGURE 2 | Hypoxia induced microglia secretes inflammatory and angiogenic molecules. **(A)** Time lapse imaging of cytosolic calcium in microglial cells in normal and hypoxic conditions. Scale bar: 200 μm **(B)** Comparison of Ca_{max} (Maximum Fluo-4 intensity) in microglial cells for control and hypoxic condition [Ca^{2+}transients were measured for 50 cells ($n = 50$) for each cases]. Data are presented as box plot and were analyzed using Wilcoxon rank-sum test. **(C)** Semi-quantitative PCR was used to evaluate the expression of secreted product (*HIF-1α, IL-1β, BAX, C3, VEGF*) of hypoxia-induced microglial cells treated with no $CoCl_2$ (lane 1), 100 μM $CoCl_2$ (lane 2), and 150 μM $CoCl_2$ (lane 3) and β-actin as control.

(Ca_{max} = the maximum Fluo-4 intensity) in microglial cells followed by hypoxia exposure (**Figure 2B**). Likewise, a higher expression of complement *C3, VEGF165,* and hypoxia inducing factor-1α (*HIF-1α*) was also observed in exposed cells (**Figure 2C**).

Involvement of Extra-Matrix Metalloproteinases in Pathogenesis of ROP

A strong association of SNPs in *FBLN5* and moderate association of *MMP2, TGF*β gene (**Table 1**) with ROP suggested the role of ECM proteins in ROP pathogenesis. Further, a quantitative assessment of the ECM proteins indicated a significant increase in MMP9 ($p = 0.038$), TIMP1 ($p = 0.004$), and α2 macroglobulin ($p = 0.0018$) in the ROP vitreous (**Figure 3A**). We also assessed the MMP activation in ROP by gelatine zymography. Our results showed higher levels of both pro and activated MMPs (MMP9 and/or MMP2) in the vitreous of patients suggesting its potential role in disease pathogenesis (**Figure 3B**).

Exploring the Potential of Inflammatory Markers in Tear Samples for the Progression of ROP

We explored if increased expression of inflammatory markers (as seen in the vitreous samples of ROP patients) could also be reproducibly detected in tears and further be established as the biomarker for disease progression. A quick multiplex ELISA of tear samples collected from the ROP babies at different stages and no-ROP preterms was performed for some inflammatory markers (interleukins, TNFα, IFNγ, and MMPs). Significantly higher expressions of IL-1ra ($p = 0.014$), MMP2 ($p = 0.0085$), and MMP-9 ($p = 0.03$) were detected in severe ROP cases compared to mild ROP and no-ROP tear samples that was further confirmed by zymography (**Figures 3C–E**). On the zymogram, the tear samples from no-ROP showed very low expression of MMPs as compared to severe ROP (**Figure 3E**). These results were confirmed to be reproducible in the extended cohort of ROP with a significant increased expression of activated MMP2 in severe ROP ($p = 0.0023$) and progressive ROP ($p = 0.007$) as compared

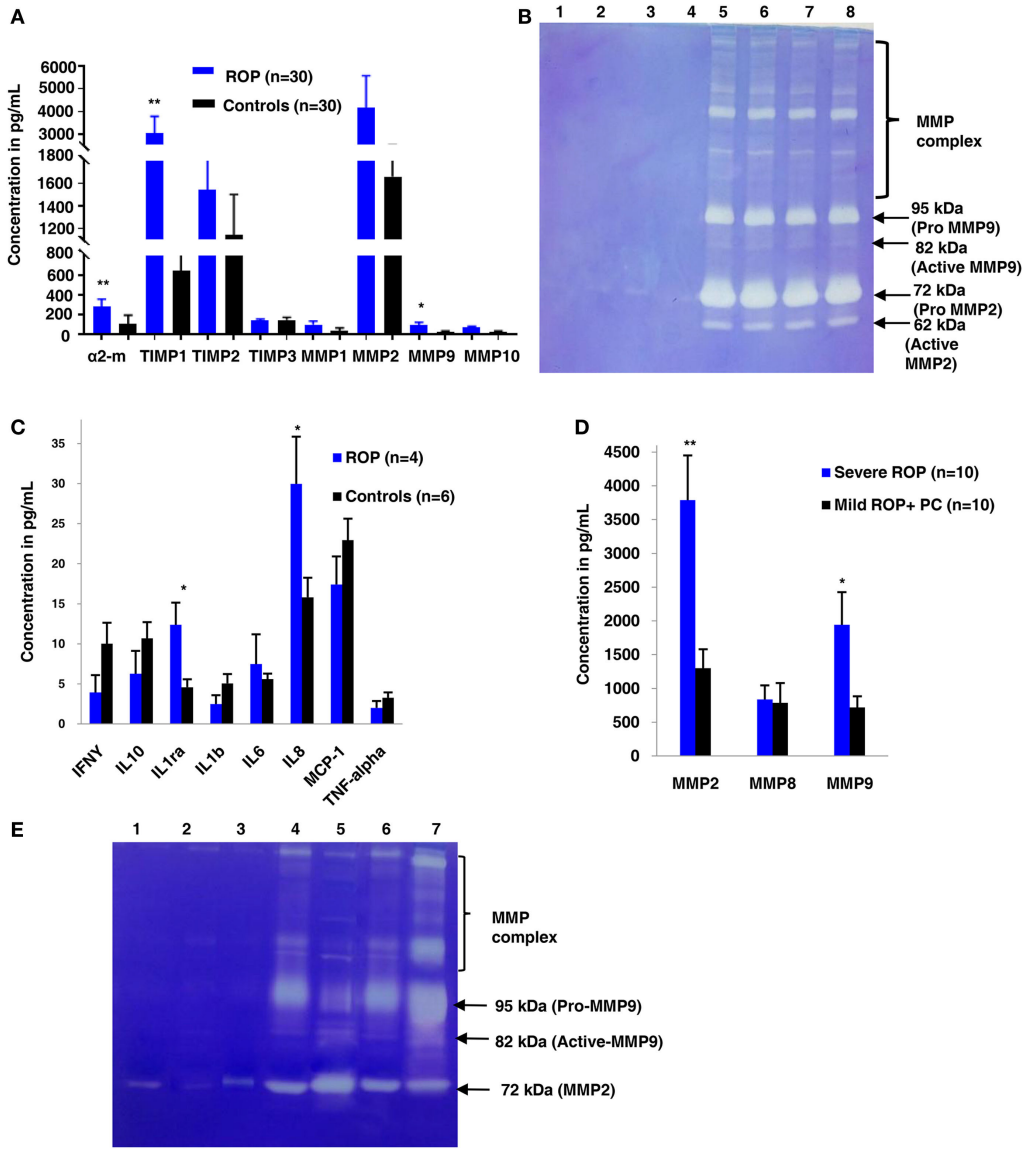

FIGURE 3 | Extracellular matrix (ECM) metalloproteinases and cytokines increases in proliferative retinopathy of prematurity (ROP) in both vitreous and tears samples. **(A)** Differential levels of ECM proteins and its inhibitors in ROP and control vitreous [*$p < 0.05$, **$p < 0.005$, *** $p < 0.0005$ (ROP vs. controls)]. **(B)** Zymogram shows activation of MMPs in ROP vitreous (lanes 5, 6, 7, 8) as compared to controls (1, 2, 3, 4). **(C)** Differential levels of cytokines in ROP (5 μL) and control tears (5 μL). **(D)** Differential levels of MMPs in ROP (5 μL) and control tear (5 μL) [*$p < 0.05$, **$p < 0.005$, ***$p < 0.0005$ (severe ROP vs. mild ROP + premature controls)]. **(E)** Zymography showing more activation of MMPs in severe ROP (lanes 6, 7) as compared to mild ROP (lanes 4,5) and controls (5 μL tears; lanes 1, 2, 3). Error bars show SEM.

to mild ROP ($p = 0.01$) and premature controls. Similar pattern of gradual increase in MMP9 expression was also observed in mild ROP ($p = 0.02$) to progressive ($p = 0.001$) and severe ROP cases ($p = 1.2 \times 10^{-6}$) with respect to premature controls (**Figure 4**).

DISCUSSION

Retinopathy of prematurity is a biphasic disease that includes an initial phase of hyperoxia leading to blood vessel obliteration followed by hypoxia causing vessel proliferation eventually leading to neovascularization and neurodegeneration. It is a complex disease with multifactorial etiologies. An earlier study on monozygotic and dizygotic twin pairs had also noted the genetic involvement in the development of ROP, in absence of other environmental factors (28). While supplemental oxygen is considered as a major risk factor along with lower GA and BW, studies from India and other Asian countries have reported ROP babies with higher GA and BW (29) and oxygen supplementation does not always predict the risk of ROP (6). Therefore, we hypothesized that genetic predisposition along with environmental/maternal or other risk factors may lead to the development of ROP.

A strong association of gene variants involved in the complement pathway (*CFH, CFB, C3*), ECM remodeling (*FBLN5*, *MMP9*), leukocyte transendothelial migration and activation

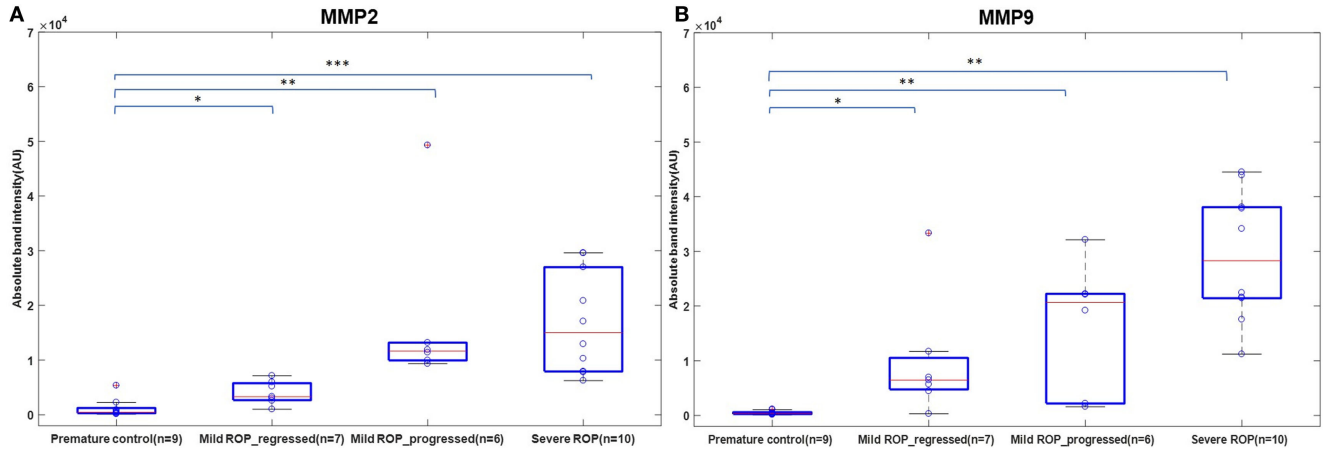

FIGURE 4 | A role of MMPs in tears as biomarker for retinopathy of prematurity (ROP) progression: differential expression of Zymogram band intensities of **(A)** MMP9 and **(B)** MMP2 in extended cohort including severe ROP (n = 10), mild ROP_progressed (n = 6), mild ROP_regressed (n = 7), and no ROP premature controls (n = 9) [*p < 0.05, **p < 0.005, *** p < 0.0005 (ROP vs. controls)], AU, arbitrary unit.

(*CXCR4*), HIF1A signaling and angiogenesis (*ANGPT2, H2AFX,* and *VEGF*), and developmental processes (*TGFb1, IHH*) observed in the present study (**Table 1**), confirms the involvement of genes in ROP pathogenesis. A previous study reported the association of polymorphisms in *IHH, AGTR1, TBX5, CETP, GP1BA, EPAS1, BDNF,* and *CFH* with ROP (11, 13). However, only a few of these associated variants could be replicated in the present cohort, indicating allelic heterogeneity (**Table 3**). Thus, the novel and associated variants identified in the present study (**Tables 1** and **3**) and elsewhere should be screened across multiple populations to understand their implications in ROP.

The strong associations of *CFH*, *CFB*, and *C3* variants in our ROP patients along with elevated levels of C3 and CFH proteins in their vitreous (**Table 1** and **Figure 1A**) indicated a possible involvement of the alternative complement pathway in ROP. CFH and CFB are the regulators of the alternative complement immune pathway (30). Upon activation, CFB is cleaved by complement factor D yielding two subunits, Ba and Bb. The active subunit Bb associates with C3b to form C3 convertase of alternative pathway while CFH regulates the alternative pathway activation by accelerating the decay of C3 convertase (30). It was also noted that there was an increase in the formation of CFB in oxygen induced retinopathy (OIR) mice model (31). Thus, the observed genetic associations of *CFH* and *CFB* complemented with their increased expression of cleaved C3 protein fragments in the vitreous of ROP-affected eyes in our study confirmed their possible involvement in disease pathogenesis (**Figure 5**). Generally, complement factors are known to be downregulated in the normal preterm neonates because of immature development of the immune system (32, 33). On the contrary, we observed an elevation and activation of the complement components and complement factors in the vitreous of ROP patients at infancy (**Figure 1**), suggesting an important role of the complement pathway in ROP pathogenesis.

Interestingly, the genetic variants in *CFH, C3,* and *CFB* genes have also been associated with AMD susceptibility (34, 35).

TABLE 3 | Comparison of commonly associated gene variants in retinopathy of prematurity worldwide.

Associated genes	Associated single-nucleotide polymorphisms (associated allele)	Present study (India), [a]189/167	Study by Mohamed et al. (11) (U.K.), [a]102/228	Study by Hartnett et al. (13) (USA), [a]593/364
CFH	rs529825 (A)	p = 0.7521	p = 0.01	–
	rs800292 (A)	p = 0.3186	p = 0.01	–
	rs379489 (A)	p = 0.4343	–	p = 0.3926
	rs395544 (A)	p = 0.5525	–	p = 0.403
CETP	rs289747 (T)	p = 0.5688	p = 0.004	–
GP1BA	rs2243093 (C)	p = 0.2991	p = 0.005	–
TBX5	rs1895602 (T)	p = 0.352	p = 0.003	–
AGTR1	rs33978228 (G)	p = 0.0196	–	–
	rs427832 (G)	p = 0.2177	p = 0.005	–
IHH	rs3099 (C)	p = 0.1565	p = 0.003	–
EPAS1	rs1867785 (G)	p = 0.958	p = 0.001	–

[a]*Cases/controls.*

A Y402H variant in the *CFH* gene was found to be most strongly associated with AMD patients worldwide. However, the ROP-associated *CFH* variant (rs374896) identified in the present study is located in the intron of the gene (**Table 1**). Further, functional studies on CFH in AMD eyes have shown that chronic low grade intraocular complement activation in patients carrying the risk variants in *CFH* along with exposure to environmental triggers (smoking, oxidative stress, etc.) causes the retinal pigment epithelial damage leading to neurodegeneration and neovascularization and eventually visual loss (36).

Complement components do not mediate neovascularization by itself but *via* the inflammatory cells (37). As was demonstrated in an OIR mouse model, complement factors C3a and C5a activate macrophages by binding to C3aR and C5aR, thereby regulating angiogenesis (38). In the present study, a strong association ($p = 1.32 \times 10^{-8}$) of rs2228014 in *CXCR4* (**Table 1**) along with the presence of activated microglia/macrophages in the vitreous

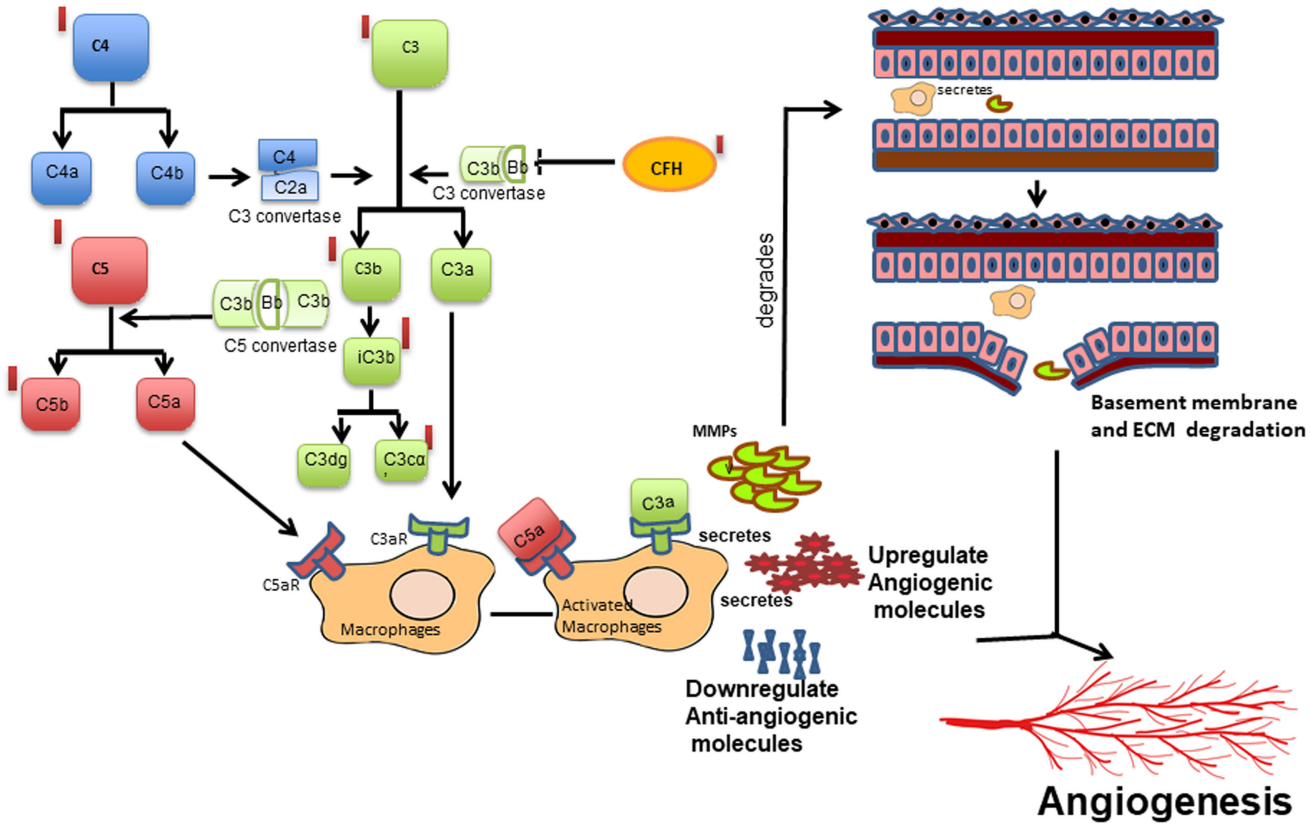

FIGURE 5 | Schematic diagram of the proposed mechanism of complement activation and its potential effect on macrophage-mediated angiogenesis in retinopathy of prematurity. Cleavage of complement components C3 into C3a, C3b and further into iC3b, C3dg and C3cα; C4 into C4a and C4b and C5 into C5a and C5b leading to the activation of complement cascade, which in turn activates macrophage/microglia or *vice versa*. Activated macrophage/microglia secretes MMPs, cytokines, proangiogenic proteins, and reduced angiogenesis inhibitors that may lead to increased vessel proliferation and extracellular matrix (ECM) degradation in turn promoting angiogenesis. Red bars represent upregulation of the complement components observed in the present study.

(**Figure 1C**), implicate their role in ROP angiogenesis via the leukocyte transendothelial migration. CXCR4 is a chemokine receptor for stromal derived factor 1 (CXCL12/SDF-1), which is mainly involved in the extravasation and migration of lymphocytes and monocytes (39). Inhibition of CXCR4 has been shown to result in reduced vascular sprouting following VEGF treatment in retinal explants (40). Our observation of the association of variants in *VEGF, ANGPT2,* and *H2AFX* (**Table 1**) indicate the involvement of HIF1α signaling pathway (hypoxia) in ROP pathogenesis. Furthermore, the secretion of C3 and VEGF by microglial cells under hypoxia (**Figure 2**) validated that hypoxia induced microglia/macrophage along with the complement component, could be contributing to the neovascularization in ROP eyes. The high level of α2-macroglobulin in the ROP vitreous (**Figure 3A**) also indicated the presence of activated macrophages/microglia that further interacts with low-density lipoprotein receptor-related protein 1 (LRP1) which in turn induces MMP9 expression (41, 42).

Based on published studies on macrophages/microglia activation leading to inflammation (37), we proposed that increased expression of the complement components, VEGF, other cytokines, and ECM components (MMPs) in the vitreous of ROP patients are mediated by macrophage/microglia activation by creating an imbalance of angiogenic and anti-angiogenic molecules (**Figure 5**). The proteolytic degradation of ECM is a critical step for the invasion of blood vessels during neovascularization. MMPs are endoproteases that cleaves the protein components of the ECM while TIMPs, α2 macroglobulins, and α1 antitrypsin are the proteinase inhibitors (43). In proliferative diabetic retinopathy, the elevated levels of MMP-2 and MMP-9 were shown to cause ECM remodeling (44, 45) further leading to net collagen IV degradation and vitreous liquefaction (46). The presence of activated MMP-9 in the vitreous along with elevated levels of TIMP1, TIMP2, and α2 macroglobulin in our ROP patients and presence of blood component proteins like apolipoproteins (**Figures 1A** and **3A**) explained its role in the degradation of the basement membrane of blood vessels, seeping out into the vitreous along with the other blood components, thereby causing vitreous hemorrhage and vitreous liquefaction.

Presence of inflammatory markers in the vitreous or other body fluid in young preterm babies might suggest an infectious etiology and inflammatory stimuli contributing to ROP (47). Fetal inflammatory response syndrome (including sepsis, periventricular leukomalacia, intraventricular hemorrhage, necrotizing enterocolitis, and bronchopulmonary dysplasia), chorioamnionitis, and microbial infections are some of the predisposing factors for

inflammation observed in some studies (48). There was no evidence of exposure to infection in our cohort since babies with any microbial infections were excluded. Additionally, we did not find any difference in the complement levels or activation patterns in the serum of these patients and controls unlike in the vitreous samples, further ruling out any systemic infection (data not shown). Based on these evidences, neonatal non-infectious inflammation might be playing a major role in the pathogenesis of ROP.

Based on these findings supplemented with increasing evidences on the role of inflammation in causing neovascularization, we speculated if MMPs could be detected in the tear samples of ROP babies so that it could be used as markers for ROP progression. The tear samples were an obvious choice for this study as it is fairly non-invasive, safe, and convenient, although there were some restrictions of tear volume and sampling in the ROP babies. It was interesting to note that the levels of MMPs in tears were significantly higher in severe ROP compared to no-ROP and mild ROP eyes that underscored its potential use as a biomarker for an early prediction of this condition (**Figures 3E** and **4**). This was further confirmed by zymography, with an increasing trend of the activated MMPs (both 2 and 9) in all the samples of severe stages of ROP along with a case of mild ROP. This mild ROP baby eventually progressed very quickly to a severe stage (plus ROP) in 2 weeks and did not respond to laser therapy (**Figure 3E**). The subsequent validation of these initial findings was done in an extended cohort and the increased levels of MMPs with the increase in severity of disease further established the usefulness of MMPs in tears as potential biomarkers. While our data proved that the levels of MMPs could reliably predict the progression of ROP (**Figure 4**), we could not perform any longitudinal analysis of MMPs levels in the tears due to the difficulties in obtaining samples from preterm babies at regular intervals. Likewise, a direct correlation of genotypes with protein levels or their activities in the corresponding biological material (vitreous/aqueous/tear) and clinical phenotype could not be attempted. Nevertheless, our study provided a proof of concept that tear MMPs levels could be a potential predictor for ROP progression in preterm babies.

In conclusion, the assessment of the activation of alternate complement pathway in ROP based on the novel genetic associations indicated the possible mechanisms of immune activation that could lead to aberrant neovascularization in the retina. However, the detailed underlying mechanisms of immune activation in abnormal blood vessel proliferation and neurodegeneration in the early stages of ROP are yet to be understood. Additionally, our results emphasized the primary role of complement component C3 in abnormal angiogenesis as seen in proliferative ROP. The proteins involved in the alternative complement pathway could be targeted selectively to prevent neovascularization, which might be helpful in preventing vision loss due the progression of ROP. The association of ECM-related genes with ROP along with elevated levels of the corresponding ECM proteins and its activation in the vitreous of ROP patients suggested its possible role in blood-retinal barrier degradation, which could promote neovascularization. Finally, the elevated levels of MMPs in tears of ROP patients established its role as a potential biomarker for the prediction of progression to proliferative stages. However, this needs to be replicated in other extended cohorts worldwide using a longitudinal study design. The present treatment strategies for managing severe ROP are inefficient as they target only the later vasoproliferative phase of ROP. Diagnosing and treating the disease at an earlier stage would definitely help in the timely and efficient management of this disease. The results of this study would aid in finding biomarkers for predictive testing as well as identifying newer drug targets for an efficient management of ROP.

ETHICS STATEMENT

The study protocol adhered to the tenets of declaration of Helsinki and written informed consent was obtained from the parents of all the minor subjects and was approved by the Institutional Review Board (LEC02-14-029) of the L V Prasad Eye Institute (LVPEI).

AUTHOR CONTRIBUTIONS

IK and SJ conceived the idea; IK, SJ, and SC wrote the protocol; IK served as principal investigator; SC, SJ, DB, RK, LG, PR, and PC were co-investigators; SJ, DB, RK, PR, and PC performed clinical examinations, graded the fundus images and did surgeries for the preterm and full term babies; SR, SP, and GM collected blood, vitreous and documented family history in the predesigned questionnaires; SR performed most of the molecular biology based analysis of blood and vitreous; SP performed the tear analysis; SSh performed cell biology work; LG and SS performed analysis for the Ca^{2+} imaging data; SR, IK, and SC analyzed the data and wrote the manuscript; and all authors revised the paper and approved the submitted version.

ACKNOWLEDGMENTS

The authors thank the parents of all the preterm and full term babies for their voluntary participation. The authors also thank Dr. Kumar Somasundaram (Indian Institute of Science, Bengaluru, India) for providing the human microglial cell line (CHME3) and Drs. Ch. Mohan Rao and T. Ramakrishna (Centre for Cellular and Molecular Biology, Hyderabad, India) for helping with a validation experiment using mass spectrometry.

FUNDING

This work was supported by Department of Biotechnology (BT/01/COE/06/02/10 and BT/PR3992/MED/97/31/2011) Govt. of India; Champaulimaud Foundation, Portugal, and Hyderabad Eye Research Foundation. SR and SP were supported through fellowships of the Indian Council of Medical Research (ICMR) and the University Grants Commission (UGC) of the Government of India, respectively.

SUPPLEMENTARY MATERIAL

The Supplementary Material for this article can be found online at http://www.frontiersin.org/articles/10.3389/fimmu.2017.01868/full#supplementary-material.

REFERENCES

1. Gogate P, Gilbert C, Zin A. Severe visual impairment and blindness in infants: causes and opportunities for control. *Middle East Afr J Ophthalmol* (2011) 18:109–14. doi:10.4103/0974-9233.80698
2. Ludwig CA, Chen TA, Hernandez-Boussard T, Moshfeghi AA, Moshfeghi DM. The epidemiology of retinopathy of prematurity in the United States. *Ophthalmic Surg Lasers Imaging Retina* (2017) 48:553–62. doi:10.3928/23258160-20170630-06
3. Gergely K, Gerinec A. Retinopathy of prematurity – epidemics, incidence, prevalence, blindness. *Bratisl Lek Listy* (2010) 111:514–7.
4. Pejaver RK, Bilagi A, Vinekar A. *National Neonatology Foundation's Evidence Based Clinical Practice Guidelines for Retinopathy of Prematurity*. India: NNF (2010). p. 253–62.
5. Jalali S, Anand R, Kumar H, Dogra MR, Azad R, Gopal L. Programme planning and screening strategy in retinopathy of prematurity. *Indian J Ophthalmol* (2003) 51:89–99.
6. Chattopadhyay MP, Pradhan A, Singh R, Datta S. Incidence and risk factors for retinopathy of prematurity in neonates. *Indian Pediatr* (2015) 52:157–8. doi:10.1007/s13312-015-0594-1
7. Kumar P, Sankar MJ, Deorari A, Azad R, Chandra P, Agarwal R, et al. Risk factors for severe retinopathy of prematurity in preterm low birth weight neonates. *Indian J Pediatr* (2011) 78:812–6. doi:10.1007/s12098-011-0363-7
8. Csak K, Szabo V, Szabo A, Vannay A. Pathogenesis and genetic basis for retinopathy of prematurity. *Front Biosci* (2006) 11:908–20. doi:10.2741/1847
9. Krock BL, Skuli N, Simon MC. Hypoxia-induced angiogenesis: good and evil. *Genes Cancer* (2011) 2:1117–33. doi:10.1177/1947601911423654
10. Wang H, Zhang SX, Hartnett ME. Signaling pathways triggered by oxidative stress that mediate features of severe retinopathy of prematurity. *JAMA Ophthalmol* (2013) 131:80–5. doi:10.1001/jamaophthalmol.2013.986
11. Mohamed S, Schaa K, Cooper ME, Ahrens E, Alvarado A, Colaizy T, et al. Genetic contributions to the development of retinopathy of prematurity. *Pediatr Res* (2009) 65:193–7. doi:10.1203/PDR.0b013e31818d1dbd
12. Kondo H, Kusaka S, Yoshinaga A, Uchio E, Tawara A, Tahira T. Genetic variants of FZD4 and LRP5 genes in patients with advanced retinopathy of prematurity. *Mol Vis* (2013) 19:476–85.
13. Hartnett ME, Morrison MA, Smith S, Yanovitch TL, Young TL, Colaizy T, et al. Genetic variants associated with severe retinopathy of prematurity in extremely low birth weight infants. *Invest Ophthalmol Vis Sci* (2014) 55:6194–203. doi:10.1167/iovs.14-14841
14. Sato T, Kusaka S, Shimojo H, Fujikado T. Simultaneous analyses of vitreous levels of 27 cytokines in eyes with retinopathy of prematurity. *Ophthalmology* (2009) 116:2165–9. doi:10.1016/j.ophtha.2009.04.026
15. Sato T, Kusaka S, Shimojo H, Fujikado T. Vitreous levels of erythropoietin and vascular endothelial growth factor in eyes with retinopathy of prematurity. *Ophthalmology* (2009) 116:1599–603. doi:10.1016/j.ophtha.2008.12.023
16. Velez-Montoya R, Clapp C, Rivera JC, Garcia-Aguirre G, Morales-Canton V, Fromow-Guerra J, et al. Intraocular and systemic levels of vascular endothelial growth factor in advanced cases of retinopathy of prematurity. *Clin Ophthalmol* (2010) 4:947–53. doi:10.2147/OPTH.S11650
17. Yu H, Yuan L, Zou Y, Peng L, Wang Y, Li T, et al. Serum concentrations of cytokines in infants with retinopathy of prematurity. *APMIS* (2014) 122:818–23. doi:10.1111/apm.12223
18. Perez-Munuzuri A, Fernandez-Lorenzo JR, Couce-Pico ML, Blanco-Teijeiro MJ, Fraga-Bermudez JM. Serum levels of IGF1 are a useful predictor of retinopathy of prematurity. *Acta Paediatr* (2010) 99:519–25. doi:10.1111/j.1651-2227.2009.01677.x
19. Yenice O, Cerman E, Ashour A, Firat R, Haklar G, Sirikci O, et al. Serum erythropoietin, insulin-like growth factor 1, and vascular endothelial growth factor in etiopathogenesis of retinopathy of prematurity. *Ophthalmic Surg Lasers Imaging Retina* (2013) 44:549–54. doi:10.3928/23258160-20131105-05
20. Rathi S, Jalali S, Musada GR, Patnaik S, Balakrishnan D, Hussain A, et al. Mutation spectrum of NDP, FZD4 and TSPAN12 genes in Indian patients with retinopathy of prematurity. *Br J Ophthalmol* (2017). doi:10.1136/bjophthalmol-2017-310958
21. International Committee for the Classification of Retinopathy of Prematurity. The international classification of retinopathy of prematurity revisited. *Arch Ophthalmol* (2005) 123:991–9. doi:10.1001/archopht.123.7.991
22. Toth M, Fridman R. Assessment of gelatinases (MMP-2 and MMP-9) by gelatin zymography. *Methods Mol Med* (2001) 57:163–74. doi:10.1385/1-59259-136-1:163
23. Fischer AH, Jacobson KA, Rose J, Zeller R. Hematoxylin and eosin staining of tissue and cell sections. *CSH Protoc* (2008) 3:1–2. doi:10.1101/pdb.prot4986
24. Gupta RK, Swain S, Kankanamge D, Priyanka PD, Singh R, Mitra K, et al. Comparison of calcium dynamics and specific features for G protein-coupled receptor-targeting drugs using live cell imaging and automated analysis. *SLAS Discov* (2017) 22:848–58. doi:10.1177/2472555217693378
25. Rio DC, Ares M Jr, Hannon GJ, Nilsen TW. Purification of RNA using TRIzol (TRI reagent). *Cold Spring Harb Protoc* (2010) 2010:1–3. doi:10.1101/pdb.prot5439
26. Barrett JC, Fry B, Maller J, Daly MJ. Haploview: analysis and visualization of LD and haplotype maps. *Bioinformatics* (2005) 21:263–5. doi:10.1093/bioinformatics/bth457
27. Boyle AP, Hong EL, Hariharan M, Cheng Y, Schaub MA, Kasowski M, et al. Annotation of functional variation in personal genomes using RegulomeDB. *Genome Res* (2012) 22(9):1790–7. doi:10.1101/gr.137323.112
28. Bizzarro MJ, Hussain N, Jonsson B, Feng R, Ment LR, Gruen JR, et al. Genetic susceptibility to retinopathy of prematurity. *Pediatrics* (2006) 118:1858–63. doi:10.1542/peds.2006-1088
29. Jalali S, Matalia J, Hussain A, Anand R. Modification of screening criteria for retinopathy of prematurity in India and other middle-income countries. *Am J Ophthalmol* (2006) 141:966–8. doi:10.1016/j.ajo.2005.12.016
30. Noris M, Remuzzi G. Overview of complement activation and regulation. *Semin Nephrol* (2013) 33:479–92. doi:10.1016/j.semnephrol.2013.08.001
31. Sweigard JH, Yanai R, Gaissert P, Saint-Geniez M, Kataoka K, Thanos A, et al. The alternative complement pathway regulates pathological angiogenesis in the retina. *FASEB J* (2014) 28:3171–82. doi:10.1096/fj.14-251041
32. Wolach B, Dolfin T, Regev R, Gilboa S, Schlesinger M. The development of the complement system after 28 weeks' gestation. *Acta Paediatr* (1997) 86:523–7. doi:10.1111/j.1651-2227.1997.tb08924.x
33. Grumach AS, Ceccon ME, Rutz R, Fertig A, Kirschfink M. Complement profile in neonates of different gestational ages. *Scand J Immunol* (2014) 79:276–81. doi:10.1111/sji.12154
34. Klein RJ, Zeiss C, Chew EY, Tsai JY, Sackler RS, Haynes C, et al. Complement factor H polymorphism in age-related macular degeneration. *Science* (2005) 308:385–9. doi:10.1126/science.1109557
35. Francis PJ, Hamon SC, Ott J, Weleber RG, Klein ML. Polymorphisms in C2, CFB and C3 are associated with progression to advanced age related macular degeneration associated with visual loss. *J Med Genet* (2009) 46:300–7. doi:10.1136/jmg.2008.062737
36. Xu H, Chen M. Targeting the complement system for the management of retinal inflammatory and degenerative diseases. *Eur J Pharmacol* (2016) 787:94–104. doi:10.1016/j.ejphar.2016.03.001
37. Rutar M, Valter K, Natoli R, Provis JM. Synthesis and propagation of complement C3 by microglia/monocytes in the aging retina. *PLoS One* (2014) 9:e93343. doi:10.1371/journal.pone.0093343
38. Langer HF, Chung KJ, Orlova VV, Choi EY, Kaul S, Kruhlak MJ, et al. Complement-mediated inhibition of neovascularization reveals a point of convergence between innate immunity and angiogenesis. *Blood* (2010) 116:4395–403. doi:10.1182/blood-2010-01-261503
39. Bleul CC, Farzan M, Choe H, Parolin C, Clark-Lewis I, Sodroski J, et al. The lymphocyte chemoattractant SDF-1 is a ligand for LESTR/fusin and blocks HIV-1 entry. *Nature* (1996) 382:829–33. doi:10.1038/382829a0
40. Unoki N, Murakami T, Nishijima K, Ogino K, Van Rooijen N, Yoshimura N. SDF-1/CXCR4 contributes to the activation of tip cells and microglia in retinal angiogenesis. *Invest Ophthalmol Vis Sci* (2010) 51:3362–71. doi:10.1167/iovs.09-4978
41. Sanchez MC, Barcelona PF, Luna JD, Ortiz SG, Juarez PC, Riera CM, et al. Low-density lipoprotein receptor-related protein-1 (LRP-1) expression in a rat model of oxygen-induced retinal neovascularization. *Exp Eye Res* (2006) 83:1378–85. doi:10.1016/j.exer.2006.07.016
42. Caceres LC, Bonacci GR, Sanchez MC, Chiabrando GA. Activated alpha(2) macroglobulin induces matrix metalloproteinase 9 expression by low-density lipoprotein receptor-related protein 1 through MAPK-ERK1/2 and NF-kappaB activation in macrophage-derived cell lines. *J Cell Biochem* (2010) 111:607–17. doi:10.1002/jcb.22737

43. Visse R, Nagase H. Matrix metalloproteinases and tissue inhibitors of metalloproteinases: structure, function, and biochemistry. *Circ Res* (2003) 92:827–39. doi:10.1161/01.RES.0000070112.80711.3D
44. Noda K, Ishida S, Inoue M, Obata K, Oguchi Y, Okada Y, et al. Production and activation of matrix metalloproteinase-2 in proliferative diabetic retinopathy. *Invest Ophthalmol Vis Sci* (2003) 44:2163–70. doi:10.1167/iovs.02-0662
45. Descamps FJ, Martens E, Kangave D, Struyf S, Geboes K, Van Damme J, et al. The activated form of gelatinase B/matrix metalloproteinase-9 is associated with diabetic vitreous hemorrhage. *Exp Eye Res* (2006) 83:401–7. doi:10.1016/j.exer.2006.01.017
46. Coral K, Angayarkanni N, Madhavan J, Bharathselvi M, Ramakrishnan S, Nandi K, et al. Lysyl oxidase activity in the ocular tissues and the role of LOX in proliferative diabetic retinopathy and rhegmatogenous retinal detachment. *Invest Ophthalmol Vis Sci* (2008) 49:4746–52. doi:10.1167/iovs.07-1550
47. Dammann O. Inflammation and retinopathy of prematurity. *Acta Paediatr* (2010) 99:975–7. doi:10.1111/j.1651-2227.2010.01836.x
48. Sood BG, Madan A, Saha S, Schendel D, Thorsen P, Skogstrand K, et al. Perinatal systemic inflammatory response syndrome and retinopathy of prematurity. *Pediatr Res* (2010) 67:394–400. doi:10.1203/PDR.0b013e3181d01a36

Conflict of Interest Statement: The authors declare that the research was conducted in the absence of any commercial or financial relationships that could be construed as a potential conflict of interest.

Query Details

Back to Main Page

1. We have relabeled the Fig. 9.1. Kindly check and provide better quality figures if any

2. We have redrawn the Fig. 9.2. This is for your information.

Molecular Mechanisms in the Pathogenesis of Retinopathy of Prematurity (ROP)

Tarandeep Kaur
Email : tarandeepkaur03@yahoo.com
Email : tarandeepkaur@lvpei.org
Affiliationids : Aff1

Satish Patnaik
Email : satishbiochem1@gmail.com
Affiliationids : Aff1

Saurabh Kumar
Email : saurabhkumar@lvpei.org
Email : saurabhuoh@gmail.com
Affiliationids : Aff1

Inderjeet Kaur
Email : inderjeet@lvpei.org
Affiliationids : Aff1, Correspondingaffiliationid : Aff1

Aff1 Prof. Brien Holden Eye Research Centre, KAR Campus, L V Prasad Eye Institute, Hyderabad, India

Abstract

The abstract is published online only. If you did not include a short abstract for the online version when you submitted the manuscript, the first paragraph or the first 10 lines of the chapter will be displayed here. If possible, please provide us with an informative abstract.

Retinopathy of prematurity (ROP) is a leading cause of childhood blindness worldwide. Neovascularization of retina in ROP eyes is a result of complex mechanisms that involve plethora of risk factors; however, the exact pathophysiology is still not clear. Even in the absence of risk factors, the disease progress to severe conditions. Thus, understanding the role of cellular molecules/events involved in ROP pathogenesis is very important to check the disease progression. Many studies have focused on investigating the role of cellular macromolecules and oxidative stress in ROP and their functional validations. The aim of this chapter is to discuss the role of various genes, RNA, proteins, lipids, and oxidative stress in physiological mechanism of normal retinal vascularization and various pathological changes that can lead to neovascularization of retina. The identification of such molecular mechanisms involved in neovascularization can help to find out novel therapeutic targets for an effective disease management.

Keywords

Retina
ROP
Genetics
Abnormal angiogenesis
Candidate genes
miRNA
Oxidative stress
Growth factors

Abbreviations

AGTR1: Angiotensin II receptor type 1
Ang2: Angiopoietin-2
ANGPT2: Angiopoietin 2 gene

BH4: Tetrahydrobiopterin
BRB: Blood–retinal barrier
BW: Birth weight
C3: Complement C3
CETP: Cholesteryl Ester Transfer Protein
CFB: Complement Factor B
CFH: Complement Factor H
CXCR4: C-X-C Motif Chemokine Receptor 4
CYP: Cytochrome P450
DNA: Deoxyribonucleic acid
EEQs: Epoxyeicostetraenoic acid
EPA: Eicosapentaenoic acid
EPAS1: Endothelial PAS domain-containing protein 1
EPO: Erythropoietin
EPOR: Erythropoietin receptor
FBLN5: Fibulin 5
FEVR: Familial exudative vitreoretinopathy
FLT1: fms-related tyrosine kinase-1
FZD: Frizzled
FZD4: Frizzled 4
GA: Gestational age
GP1BA: Glycoprotein Ib-alpha
GPX: Glutathione peroxidase
H2AFX: H2A histone family member X
HIF-1: Hypoxia-induced growth factor-1
IFN: Interferons
IGF-1: Insulin-like growth factors
IHH: Indian Hedgehog Signaling Molecule
IL-1ra: Interleukin-1 receptor antagonist
IL6: Interleukin 6
IL8: Interleukin 8
JAK: Janus kinases
KDR: Kinase insert domain receptor
Keap1: Kelch-like ECH-associated protein 1
LRP5: Low-density lipoprotein receptor-related protein 5
MAPK: Mitogen-activated protein kinase
MCP: Monocyte chemoattractant protein
MCP-1: Monocyte chemotactic protein 1
MIP-1a: Macrophage Inflammatory Proteins
miRNA: Micro RNA
MMP2: Matrix metallopeptidase 2
MMP9: Matrix metallopeptidase 9
MMTV: Mouse mammary tumor virus
mRNA: Messenger RNAs
NADPH: Nicotinamide adenine dinucleotide phosphate
NDP: Norrie Disease Protein
NOS: Nitric oxide synthase
Nrf2: Nuclear factor erythroid 2-like 2
OIR: Oxidative stress-induced retinopathy
p62: p62/SQSTM1
PDGF: Platelet-derived growth factor
PI3K: Phosphoinisitol-3-kinase
PlGF: Placental growth factor
PMN: Polymorphonuclear neutrophils
Prx: Peroxiredoxins
PUFAs: Polyunsaturated fatty acids
RANTES: Regulated upon Activation, Normal T Cell Expressed and Presumably secreted
RNA: Ribonucleic Acid
ROI: Reactive Oxygen Intermediates
ROP: Retinopathy of prematurity
ROS: Reactive oxygen species
SDF-1: Stromal cell-derived factor-1

SNP: Single nucleotide polymorphism
STAT: Signal transducer and activator of transcription proteins
TBX5: *T-Box Transcription Factor 5*
TGFβ1: Transforming growth factor beta-1
TNFα: Tumor necrosis factor alpha
TSPAN12: Tetraspanin-12
UTR: Untranslated Region
VEGF: Vascular endothelial growth factor
VEGFR1: Vascular endothelial growth factor receptor 1
VEGFR2: Vascular endothelial growth factor receptor 2
VHL: Von Hippel—Lindau protein

9.1. Introduction

Advancements in neonatal care modalities have led to increased preterm births worldwide. However, babies born prematurely with low gestational age (GA) and birth weight (BW) are increasingly susceptible to the risk of several prematurity-related complications and other diseases. In India, incidence of ROP is approximately 18.4% while the incidence of severe ROP is 6.4% in infants with GA <34 weeks and/or BW <1750 g [1]. Retinopathy of prematurity is one such vision-threatening disease associated with neovascularization in immature retinas of premature infants. The incidence of ROP in India is approximately 18.4% and severe ROP 6.4% in preterm infants with GA <34 weeks and/or BW <1750 g [1]. In phase-I of the disease, retinal vascularization slow or ceases after preterm birth due to hyperoxia. Subsequently in phase-II retina becomes hypoxic due to increased metabolic demand and poor vascularization which further stimulates vasoproliferation resulting in fibrovascular retinal detachment [2]. The transition from phase-I to phase-II of the disease is very complex and involves a lot of molecules and their interactions, e.g., genes, RNA, proteins, and lipids. A large number of factors including maternal and infant factors, prenatal and perinatal factors, comorbidities of prematurity, their treatment and genetic may contribute to the development and progression of ROP [3] by modifying signal transduction pathways. These modifications can result in transition from normal physiological pathways to pathological conditions. Even in the absence of risk factors, some infants tend to develop severe ROP. Since, preterm infants have variable ROP susceptibility, progression, and response to treatment, studies focusing on understanding the causative factors and their interactions that can result in pathophysiological mechanisms leading to ROP are highly warranted. The goal of this book chapter is to provide a brief overview about involvement of various molecules and mechanisms in the pathophysiology of ROP. The individual molecules and mechanisms beginning from genetics to miRNA, oxidative stress, lipids, and proteins will be discussed in the consecutive sections.

9.2. Role of Genetics in Pathophysiology of ROP

ROP is a complex self-restricting condition that progresses to severe stages in only a subset of premature infants who require timely intervention and treatment while in other diseases regress spontaneously without any treatment. Severe ROP is characterized by the formation of abnormal blood vessels in vitreous causing vitreoretinal traction/pull and retinal detachment eventually leading to irreversible blindness.

Several studies have been performed on the oxygen stress-induced retinopathy (OIR) mouse model and ROP patients to understand its pathogenesis and management, however, it still remains unclear. Besides known clinical and demographical risk factors, there are substantial evidence that support a genetic basis of ROP [3, 4]. The genetic factors associated with the disease could explain why only a set of premature infant's progress to severe stages of ROP despite timely intervention while in others it regresses. In past, several studies have reported the varied incidence rate [5] and frequency of ROP across different countries and among different ethnic groups [6, 7, 8, 9]. Even the male infants are shown to be at increased risk of ROP as compared to female infants [10]. The studies pertaining to heritability and concordance estimates among monozygotic and dizygotic twin pair studies have also suggested for the role of genes/genetic pathways in the ROP development [11]. All these studies suggest for the role of several internal disease progressing factors, mainly genetic variants including polymorphisms and mutations in the development of ROP [12]. This raises a need for screening the genetic variants/genes involved in the retinal vascular formation and abnormal angiogenesis in the pathophysiology of ROP. Only a few studies have found genes/variants associated with different stages of ROP, however, their exact role in disease pathogenesis needs to be elucidated [12, 13].

The clinical manifestations and phenotypic changes of ROP strongly correlate with familial exudative vitreoretinopathy (FEVR) hinting for a shared involvement of common genetic factors among them. FEVR is a congenital vitreoretinal disorder with three different modes of inheritance patterns; autosomal dominant [14], autosomal recessive [15], and X-linked recessive [16]. Four candidate genes involved in the Wntβ-catenin signalling pathways (Fig. 9.1) have been identified for FEVR, including *FZD4*, *LRP5*, *NDP*, and *TSPAN12*. These genes play a crucial role in the fetal vasculature development and retinal maturation. Interestingly, these genes are candidates for other retinal vascular diseases also, like Norrie and Coat's disease. In the proceeding paragraphs, we will discuss about these candidate genes and other genes in association with ROP pathogenesis.

Fig. 9.1

Wnt AQ1 signalling in retinal development and maturation (Adapted and modified from [11, 51]). Ligands of norrin and Wnt binds to FZD4 receptor and LRP5 co-receptor. Once bound, Wnt ligand beta-catenin gets deposited in the cytoplasm and then translocate to nucleus. There it activates the transcription of Wnt target genes by interacting with a member of Tcf/Lef family. A norrin-LRP5-FZD4 complex is formed by their binding to norrin that further regulates the downstream effects on norrin-beta-catenin signalling. Any gene abnormalities/defects in Wnt and norrin targeting genes could lead to abnormal vascularization in developmental stages of ROP

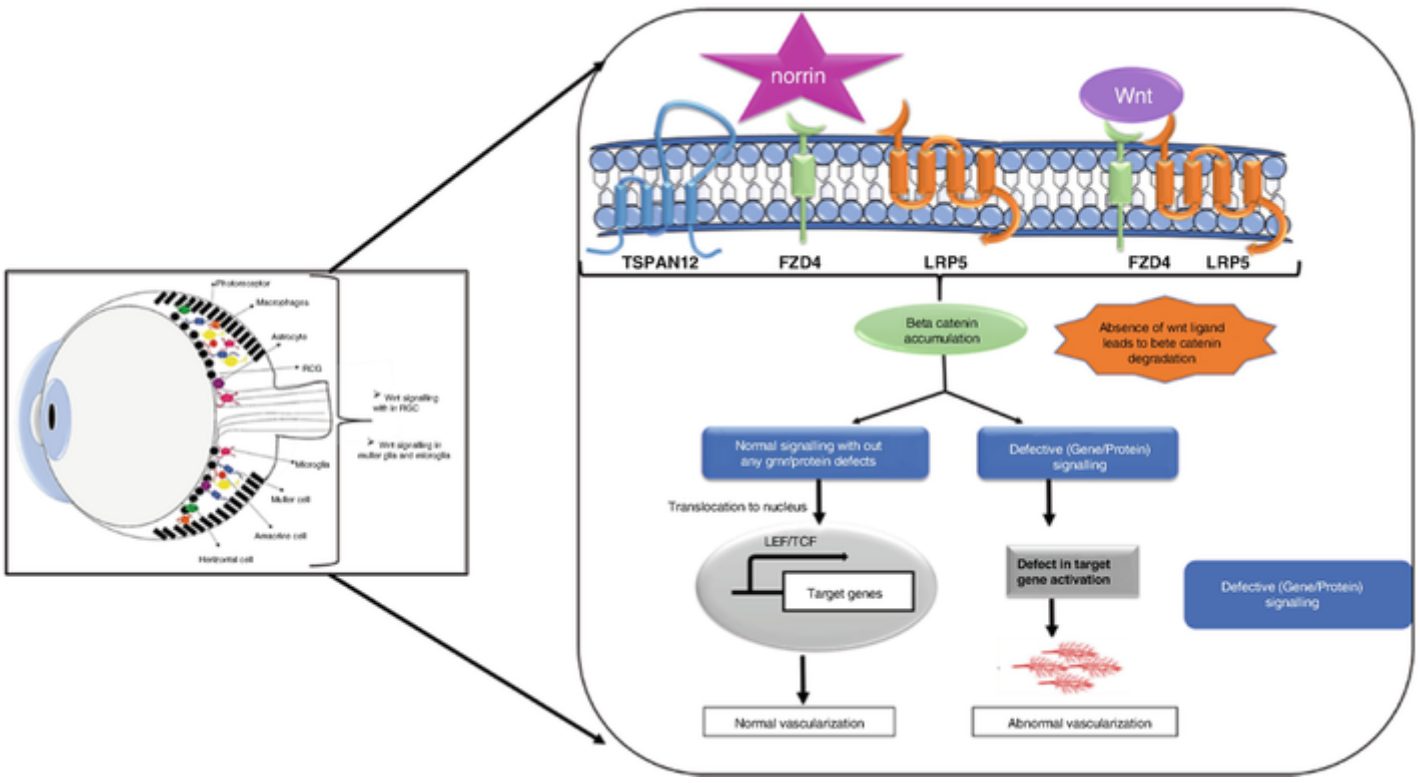

Frizzled 4 (FZD4) Gene Human Frizzled-4 gene is a member of the frizzled gene family, that codes for seven transmembrane domain proteins that act as receptors for the Wnt family of signalling proteins. The Wnt signalling is very important for cell fate determination and polarity, etc. [17]. Wnt ligand binding and activation are facilitated by G-protein-coupled frizzled receptor. So far, ten FZD receptors and 20 Wnt ligand isoforms have been identified in Homo sapiens [18]. FZD4 expression was detected in retina, being required for its proper development and function via canonical Wnt/b-catenin pathway. It plays an important role in vascularization of retina by regulating the expression of its downstream target genes [19, 20]. The muller glial cells in retina produce the non-Wnt ligand that binds to vascular endothelial cells by FZD receptor. The FZD signalling was lost in endothelial cells of knockout mice causing abnormal vascular growth that leads to retinal neuron loss and interrupts the integrity of blood–retinal barrier (BRB) [21].

Mutations in *FZD4* gene have been studied in different populations for its association with ROP. Only a few variations have been reported till date that are associated with advanced stages of ROP. The variants P.(I256V), P.(A370G), P.(K203N), P.(H69Y), P.(R127H), and P.(Y211H) are found to be associated with advanced stages of ROP [22, 23, 24]. Another three heterozygous variants [p.(G424E), p.(P33S) and p.(P168S)] and a compound heterozygous variant p.(P33S)/p.(P168S) have been shown to be associated with all stages of ROP [25, 26]. Our *in-house* Indian study validated and confirmed similar results where these known variants [p.(P33S), p.(P168S), p.(P33S)/p.(P168S) along with another novel heterozygous variant (I360V) were found to be associated with all stages of ROP [27].

NDP Gene *NDP* gene encodes for 133 amino acids containing norrin protein that plays role in chemical signalling pathways and affects the way cells and tissue develop. Defects in the gene lead to Norrie disease. Norrie disease is a state of rare congenital blindness following X-linked recessive pattern. It is also known as retinal dysplasia. Norrie is a specific ligand for the FZD4 receptor, it directly activates the Wnt/b-catenin pathway. In retina, norrin is expressed in muller glial cells [21] and retinal neurons during development stages [28]. This signalling pathway plays a pivotal role in the vascularization of retina in its developmental process. Few studies done on ROP found genetic variations in 5′ and 3′ UTRs of *NDP* exon1. In Norrie disease, variations in the gene lead to deafness and mental retardation along with bilateral retinal malformation, but in case of ROP, it shows only abnormal vascular development and retinal detachment.

To date, only two variations in exon region of *NDP* gene (R121W and L108P) have been reported for their association with ROP [29]. By a direct sequencing method, C597A variation was detected in prematurely born Kuwaiti infants with severe ROP [30]. While in patients who had regressed ROP, a 14-bp deletion was found in the 5′ UTR of *NDP* gene. The heterozygous 14 bp deletion was also found in the unaffected premature control infants [31] suggesting for a protective role for this variant.

Several studies worldwide have shown that mutations/polymorphisms in *NDP* gene are associated with the different stages of ROP disease. In a study performed on 100 ROP patients from different ethnic groups, only two patients with advanced stage of disease showed mutations in the NDP gene. In a patient, a 12-bp CT repeat insertion was found in exon 1 while in another a 14-bp deletion in 5′UTR of same exon was found [32]. The same 14-bp deletion in 5′UTR was also present in 9.6% of regressed ROP patients [31]. In an Indian report along with similar 14 bp deletion, 2 more novel variants (IVS1 + 16A > G, C.522 T > C in 3′ UTR) have been reported in

3.84% of ROP patients [27]. Another two variants in 5′UTR of exon 1 of the gene, i.e., c.597 C > A was found to be present in 83% and 237A > G was found to be present in 5.9% of severe ROP patients [30].

LRP5 Gene *LRP5* is a FZD4 co-receptor, the gene belongs to the low-density lipoprotein family and composed of 1615 amino acids with 23 exons. It consists of four domains, six YWTD repeats that form a beta-propeller structure and an epidermal growth factor-like repeat. Loss-of-function mutations in the *LRP5* gene have been reported in several diseases like FEVR, Osteoporosis-Pseudoglioma Syndrome. The expression of *LRP5* gene has been shown in the retina, pancreas, bone, and heart [33, 34].

However, there are only few studies concerning *LRP5* screening in ROP patients. In a Japanese ROP cohort, a 3-bp (CTG) heterozygous insertion within the coding sequence of gene was found. The insertion of three bases leads to elongation of the leucine repeat in the signal sequence that eventually accounts for the pathogenic features associated with the disease. The study proposed that this variation could cause defects in translation process during protein processing thereby affecting retinal vascularization [35].

TSPAN12 *TSPAN12* gene belongs to the tetraspanin superfamily, encodes for 305 amino acid proteins involved in the norrin signalling and retinal neovascularization. This gene is positioned on chromosome 7q31.31 and contains eight exons and encodes a protein consisting of four transmembrane domains and two extracellular loops [36]. Its gene expression was seen in the endothelial cells of retinal blood vessels. It plays an important role in norrin-beta catenin signalling pathways [37]. Mutations in this gene are responsible for 3–10% of FEVR cases [38].

Very few studies have focused on the association of *TSPAN12* gene with ROP. Our in-house study found an association of p. (L119R) variation in this gene with risk of threshold ROP [27]. In another study, c.954G > A mutation was reported in the *TSPAN12* gene and predicted to cause alterations in protein structure and stability which can further contribute to the pathogenesis of ROP [39]. In a recent study on Malaysian premature infants, two more variants in *TSPAN12* gene viz. c.765G > T (p.P255P) and c.*39C > T (3′UTR) were found but their association with ROP needs to be studied. These were suggested to be common polymorphisms of the Malaysian population [40]. Genetic modifications in *TSPAN12* gene could lead to interference in molecular mechanisms of membrane association activities like cell proliferation and other signalling mechanisms [41] that can alter signal transduction pathways leading to ROP.

Besides the above four FEVR candidate genes, the contribution of other genes was also investigated that can influence the susceptibility to ROP.

Other Candidate Genes Associated with ROP Genetics and hereditary factors control various signalling molecules and pathways that are implicated in the pathogenesis of ROP through known biochemical, molecular, and genetic associations. Vascular endothelial growth factor (VEGF), Insulin-like growth factors (IGF-1), and inflammatory mediators are some of these molecules. Any change in the genes coding these biochemicals involved in different physiological pathways can alter the normal mechanisms hence can lead to diseases state.

VEGF is the most important triggering factor for angiogenesis in the retina. It plays a very critical role in the development of ROP besides being a neuronal survival factor. The intravitreal treatment against VEGF, can revert severe ROP progress [42]. Previous studies have found several SNPs in human *VEGF* gene including rs2010963 (−634G > C and + 405 G > C) which is most commonly associated with ROP [43, 44, 45, 46, 47, 48]. In a British study done on preterm babies, the G allele at rs2010963 was found increasingly common among babies with ROP [43]. The same was validated in an Egyptian ROP cohort too [44].

In addition to VEGF, another growth factor, i.e., hypoxia-induced growth factor-1 (*HIF-1*) regulates the cell's response to diminished oxygen levels as sufficient and uniform oxygen supply is required for appropriate tissue maintenance and homeostasis [49]. Owing to its functional profile, HIF-1 alpha could be an important gene that might be involved in ROP pathogenesis. Under hypoxic stress conditions, *HIF-1* is known to get activated further regulating several genes that play a crucial role in retinal angiogenesis, like *VEGF*, *VEGFR1*, *PDGF*, *SDF-1*, and *ANG2* [50].

Besides the genes controlling various growth factors, changes in the gene involved in other cellular pathways including inflammation and complement system can also modify an individual's susceptibility to ROP.

Association of Inflammatory and Complement System Genes with ROP Two independent studies have shown an association of ROP with alternative complement system pathways genes and association of several other genetic variations in *IHH, AGTR1, TBX5, CETP, GP1BA, EPAS1, BDNF*, and *other* genes with ROP [52, 53].

A study done on Indian preterm infants with and without ROP revealed a significant association of genes with ROP including *CFH, CFB, CXCR4, FBLN5, CFH, CFB, FBLN5, CETP*, *CXCR4, AGTR1, ANGPT2, C3, H2AFX, IHH, MMP2, TGFβ1, CETP, VEGF*, and *TSPAN12*. Association of inflammatory markers (IL6, IL8, IL-1ra, MMP2, MMP9, MCP, IFN gamma) in the vitreous and tear samples was also found [54]. Only a few previously known common variations were replicated in this study but the associated SNPs in these studies suggested that inflammation and other associated genetic defects may expand the risk of ROP by directly recruiting proangiogenic factors or by modifying other genes. Novel genetic interactions identified in this study revealed the potential involvement of immune regulation pathways in abnormal neovascularization of the retina. The expression and regulation of all these genes are controlled at various levels

and are under the control of other small molecules in the cell like transcription factors and small non-coding RNAs. One of the important types of small RNAs that control gene expression is microRNAs (miRNA). By targeting and inhibiting specific growth and developmental pathways/processes miRNAs can also influence the process of angiogenesis.

9.3. Role of MicroRNAs in the Pathophysiology of ROP

Besides other cellular components involved in the process of gene regulation, small microRNAs (miRNA) also regulate gene expression through interaction with messenger RNAs (mRNA). miRNAs being small non-coding class of RNAs can regulate the expression of genes that are directly involved in the development of retina and other similar processes hence indirectly affecting the vasculature development in retina of the eye. MiRNA mostly regulates gene expression by its sequence-specific binding to 3′ untranslated region (3′-UTR) of specific mRNA targets. This binding can result in degradation, deadenylation, or reduced translational activity of the target mRNA. Thus, they play an important role in posttranslational gene regulation [55] and in cellular processes like angiogenesis, cell growth, embryonic development, cell proliferation and differentiation, and apoptosis [56, 57]. miRNAs also play a central regulatory role in vascular angiogenesis [58]. By controlling gene expression for cell differentiation, miRNAs perform a vital role in retina throughout the developmental process as well as in disease conditions [59, 60, 61]. There are some common miRNA molecules that help to maintain both structure and function of retina [62]. The miRNA profiling of human endothelial cells revealed many miRNAs that included miR-126, miR-210, miR-221/222, miR-17-92, and miR-23-27-24 clusters. These miRNAs target angiogenesis-related genes and so, are also known as “angiomiRs” [63]. The miRNA-126 inhibits neovascularization in oxygen-induced retinopathy (OIR) by regulating growth factors comprising VEGF, HIF-1α, and IGF-2 [64]. This indicates that miRNAs have an important role in ROP pathogenesis. Any type of reduction, dysfunction, and dysregulation of miRNA can result in altered expression of their target genes that may result in pathophysiological conditions. Plasma miRNA levels were also compared between preterm infants with and without ROP. The results revealed four miRNAs to be significantly dysregulated of which miR-23a and miR-200b-3p were upregulated while miR-27b-3p were downregulated in ROP [62]. These significantly dysregulated miRNAs could either target antiangiogenic or pro-angiogenic genes and thus confirms their role in causing pathological angiogenesis during ROP development.

In preterm infants, retinal vascular development is insufficient that causes hypoxia which in turn precipitates the production of various proteins/growth factors by upregulation/downregulation of multiple pathways resulting in new and abnormal blood vessel growth. Hence, these proteins can also act as the new targets for managing the disease.

9.4. Major Proteins Involved in the Pathophysiology of ROP

In humans and other large mammals, both in diseased and in normal conditions, the vasculature is formed from two main physiological processes namely vasculogenesis and angiogenesis. While the former occurs during embryogenesis and comprises the formation of new blood vessels directly from the hematopoietic precursor cells, the latter refers to the formation of blood vessels from the pre-existing ones and takes place throughout the life of an organism. Both the processes require many growth factors and other molecules that are involved in directing the precursor cells to differentiate and form mature vessels. During the fetal development, levels of these growth factors are maintained at an optimal level by placental supply from the mother. The sudden loss of maternal–fetal interaction in preterm infants with low birth weight, the concentration of these growth factors also decreases leading to retarded/incomplete vascular development in retina at birth making them very sensitive to hyperoxia environment at preterm birth. This can lead to altered regulation of growth factors and hence pathological retinal vasculature development. The major proteins and growth factors involved in the pathogenesis of ROP are HIF-1, VEGF, IGF-1, PIGF, and erythropoietin.

Hypoxia-Inducible Factor-1 (HIF-1) The low oxygen tension (hypoxia) occurs in avascular retina when preterm infants are removed from supplementary oxygen to room air. For cell survival under hypoxic state, a large number of genes involved in angiogenesis, metabolism, and cell proliferation get activated [65]. HIF-1 is one of the most important transcriptional mediators in response to hypoxic conditions and master regulator of physiological and pathological angiogenesis. The binding of HIF-1 to DNA at hypoxia-responsive element enables the transcription of angiogenic genes including growth factor like VEGF [66]. In normal conditions, HIF-1 is hydroxylated by enzyme prolyl hydroxylases which facilitates its binding to the von Hippel—Lindau protein (VHL) further resulting in its eventual degradation by ubiquitination. Under hypoxic conditions, the hydroxylases become less efficient leading to accumulation of HIF-1 and thereby increased VEGF expression [67].

Vascular Endothelial Growth Factor Another protein family known to play a key role in angiogenesis is vascular growth factors. The family includes placental growth factor (PlGF) and other vascular endothelial growth factors (VEGF) [68]. The three common human isoforms of VEGF (VEGF121, VEGF165, and VEGF189) are generated by various combinations of eight exons in this gene. It has two receptors, i.e., fms-related tyrosine kinase-1 (FLT-1 or VEGFR-1) and the kinase insert domain-containing receptors (KDR or FLK-1 or VEGFR-2) that are specific for each isoform [69]. Both the receptors are present in all embryonic tissues, however, with variable expression levels at different gestational ages [70]. HIF-1α binds to the promoter region of flt-1 gene and hence regulates gene expression in hypoxia conditions while the *KDR* gene is not regulated by HIF-1α. During early gestational age, both the genes are highly expressed while the expression reduces significantly with advanced gestational age. The KDR is required for vasculogenesis and hematopoiesis and therefore its loss of function during embryogenesis can be lethal [71]. This receptor is involved in the induction of proliferation, migration, differentiation, and maturation of vascular endothelial cells [72, 73]. VEGF is very important during the

development phase-I of ROP, its expression being downregulated by hyperoxia whereas the expression is again increased in phase-II under hypoxia which further induces VGEF mRNA and protein expression resulting into neovascularization [74].

9.5. Insulin-Like Growth Factor-1

A potent growth factor that is maternally derived and mediates many other signalling pathways is required for normal retinal development and also been implicated in the ROP pathogenesis [75]. Patients with genetic defects in Insulin-like growth factor-1 (IGF-1) production show a reduced retinal vascularization that could not be restored even after the supplementation of VEGF [76]. The levels of IGF-1 at birth are very low but show a rapid increase in preterm infants who do not develop ROP. The low levels of IGF-1 arrest vasculogenesis resulting in avascular retina that eventually creates hypoxia and accumulation of VEGF in the vitreous. The normal levels of IGF-1 and higher expression of VEGF results into neovascularization in the retina [75]. Increased expression of IGF-1 observed during phase-II of ROP activates Akt signaling pathway along with VEGF and blocks the apoptosis of epithelial cells hence promoting neogenesis. HIF-1 expression that acts through P13k/Akt and MAPK pathways is induced by IGF-1 thereby contributing to neovascularization [77].

9.6. Placental Growth Factor

Placental growth factor (PlGF) also belongs to vascular growth factor family and it plays vital roles in cellular developmental processes along with proliferation and migration of endothelial cells [78]. It increases the activity and expression of VEGF by acting as cofactor. A heterodimer formed from between VEGF and PlGF causes angiogenesis by FLT-1 receptor activation [79, 80], though, the exact involvement of PlGF in this process is still not clear. Some studies showed that PlGF binding to FLT-1 receptor increases the levels of circulating VEGF thereby activating a variety of small less characterized signaling molecules leading to angiogenesis. A reduced PlGF level was observed during hypoxia while it increased during hyperoxia [81]. The dysregulation of PlGF in retina during ROP suggests its contribution to VEGF induced angiogenesis [82].

9.7. Erythropoietin

Erythropoietin (EPO) is hypoxia-induced angiogenic factor that performs the neuroprotective functions in neonates. EPO inhibits apoptosis in endothelial cells and neurons and its receptors are shown to present in the developing retina [83]. EPO is overexpressed in retina under hypoxia [84]. The binding of EPO on erythropoietin receptor (EPOR) activates JAK/STAT pathway. The activated receptor can further form “tissue protective factor” by binding with common beta receptors which are known to have protective effect in stroke and inflammation models [85]. The levels of EPO and VEGF were significantly higher in the vitreous of infants with ROP as compared to those without ROP [86]. The anti-apoptotic and angiogenic action of EPO is important in phase-I ROP while it can worsen the ROP condition in phase-II by overactivating STAT3 in endothelial cells by interaction of activated EPOR and VEGFR2 stimulating abnormal angiogenesis [85].

Our understanding about the involvement of proteins like HIF-1, VEGF, IGF-1, and EPO in pathogenesis of ROP can help to find out new treatment modalities for the disease. The structure and functioning of these proteins/growth factors can be altered further by changing the microenvironment of the cell. Redox imbalance/oxidative stress is also one such alteration caused by increased reactive oxygen and nitrogen species. Increased reactive species can damage the structure of macromolecules of the cell including proteins. The modified proteins can have a detrimental effect on growth and development of preterm infants.

9.8. Role of Oxidative Stress in ROP Pathophysiology

Besides several other intrinsic and extrinsic risk factors, oxidative stress imbalance too plays an important role to initiate the pathological events leading to cardiovascular, renovascular, and neurovascular complications including ROP. Under balanced oxidative potential conditions, reactive oxygen species (ROS) are involved in normal physiological functions including inflammation and autophagy. However, any deviation from the normal function can result in pathological inflammation and autophagy which can further cause damage to retina (Fig. 9.2).

Fig. 9.2

Representative AQ2 image showing pathways involved in ROP progression

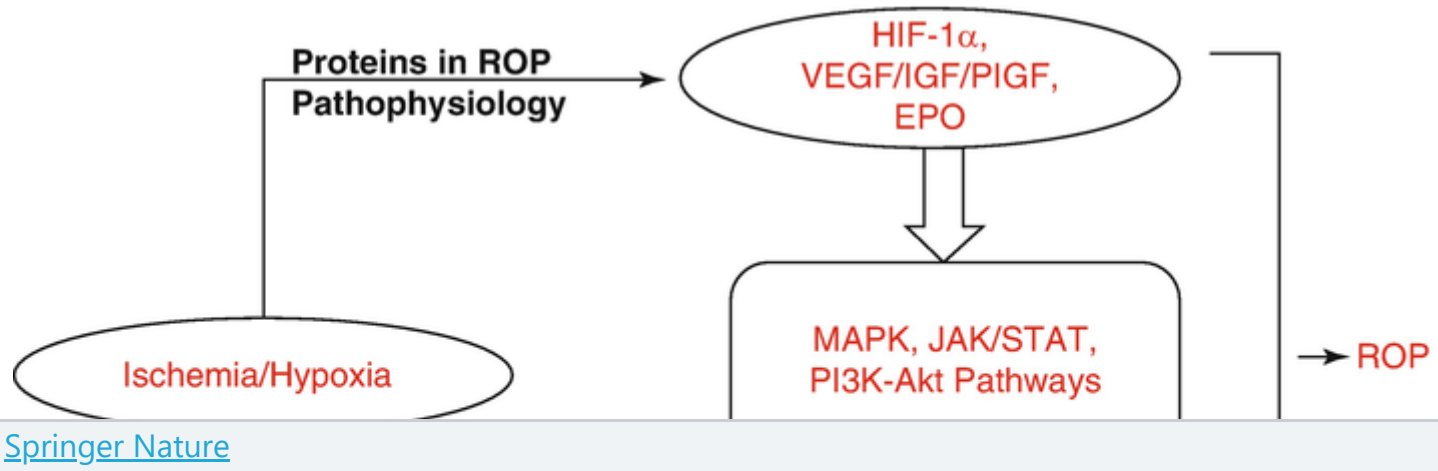

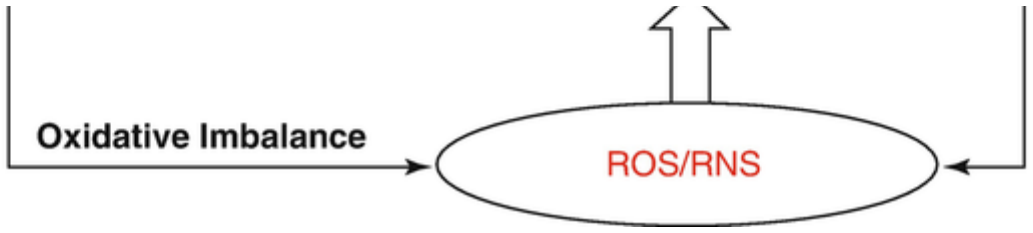

Oxidative stress is a result of an imbalance in generation and degeneration of ROS. ROS also known as reactive oxygen intermediates (ROI) are generated as by-products of physiological metabolic activity of the cells. ROS are also formed in response to endogenous sources like mitochondrial chain reaction, respiratory burst, inflammatory disorders, oxygenases, chronic infections, ischemia-reperfusion injury, and exogenous factors like pollutants, ultraviolet radiation, alcohol, and cigarette smoking. Several enzymes such as superoxide dismutase, glutathione peroxidase, and catalase actively protect the cells from the pathogenic effects of ROS. ROS have beneficial/supportive effects on different biological processes including clearance of invading pathogens, wound healing, and tissue repair processes. Imbalance in the generation of ROS can disrupt the retinal homeostasis and thereby leading to cell death.

The key ROS molecules that contribute to oxidative stress are hydrogen peroxide (H_2O_2), hydroxyl radicals (OH), hydroxyl anions (OH^-), hypochlorous acid (HOCl), and superoxide (O^{2-}). Enzymes such as NADPH oxidase/Xanthine oxidase, endothelial nitric acid synthase, or the enzymes of the electron transport chain reduce the molecular oxygen to yield superoxide molecules. Superoxide dismutase (SOD) enzyme rapidly converts superoxide molecules into hydrogen peroxides. It also forms the highly reactive intermediate peroxynitrite ($ONOO^-$) by reacting with nitric oxide (NO), which can be protonated to peroxynitrous acid to generate the hydroxyl radical (OH.). At the site of inflammation, the enzyme myeloperoxidase (MPO), expressed by phagocytic neutrophils leads to the formation of highly reactive hypochlorous acid from H_2O_2. H_2O_2 is then disintegrated into toxic hydroxyl anions (OH^-) or scavenged to water and molecular oxygen by antioxidant enzymes such as catalase, glutathione peroxidase (GPX), or peroxiredoxins (Prx).

The retina of the eye is extremely vulnerable to oxidative insults by the ROS molecules. Retina is highly susceptible to photooxidation being constantly exposed to incoming light and high on oxygen consumption [87] and likely to further generate ROS molecules. Also, the high lipid constituent in the retina due to abundant PUFAs in the photoreceptors layer of retina makes it prone to lipid peroxidation. During pathological disorders such as retinopathy of prematurity, the balance between the generation of ROS and the capability of cells to scavenge these ROS by endogenous antioxidant is disrupted that activates several signalling pathways affecting lipids, proteins, and DNA present inside the cell and consequently causes cell death.

9.9. Retinopathy of Prematurity and ROS

Retinal ischemia or hypoxia is a characteristic feature of ROP. ROP being a biphasic ocular disease is characterized by vascular deformities induced by two alternate phases (hyperoxia followed by hypoxia). The first phase is characterized by state of hyperoxia that subsequently leads to the obliteration of developing retinal vessels. In the second phase, high metabolic demand of the relatively avascular retina inflicts a hypoxic injury to the retinal tissues. This relative hypoxic condition of the retina produces the abnormal proliferation of blood vessels and thereby neovascularization [88]. In both perinatal and neonatal periods, new born infants are exposed to oxidative stress due to low efficacy of enzymatic and nonenzymatic antioxidants like catalase, glutathione peroxidases, superoxide dismutase, and vitamin E (responsible for maintaining ROS level). These two phases of ROP pathogenesis result in overproduction of ROS that activates the enzyme NADPH oxidase. NADPH oxidases can present in seven different homologs (NOX1–NOX5 and Duox1–2), which have variable expression as well as activation mechanisms. Major homologs of NADPH oxidase like NOX1, NOX2, and NOX4 are strongly associated with inflammation-activated blood vessel damage. Enhanced NOX2 expression can lead to increase in VEGF expression, retinal ROS generation, and vascular permeability. The increased NADPH oxidase also activates the JAK/STAT signalling pathway which eventually leads to intravitreal neovascularization [89]. Inhibition of JAK/STAT signalling pathway and NADPH oxidase reduces the level of caspase-3, which checks the neovascularization and apoptosis in ROP pathogenesis. Independent studies have shown that NADPH oxidase-derived ROS are important for ischemia-induced neovascularization as it increases VEGF and retinal neovascularization.

Oxides of nitrogen also referred to as reactive oxygen species (RNS) such as NO-, NO, ONO, and NO_2 are also a major contributor to the ROP progression. Increased concentration of nitric oxide synthase (NOS) significantly contributes to the increase in NO production under the hypoxic environment [90]. NOS is a group of enzymes that acts on L-arginine to produce NO. NOS in mammals have three different isoforms, namely neuronal NOS (nNOS), endothelial NOS (eNOS), and inducible NOS (iNOS). Among these isoforms, eNOS is the major source of NO in the endothelial cells responsible for the maintenance of blood vessels and angiogenesis. Deficiency of tetrahydrobiopterin (BH4) that plays important role in maintaining integrity of eNOS can lead to uncoupling of eNOS and finally resulting in enhanced superoxide radicals. Increased apoptosis of retinal endothelial cells and synthesis of nitric oxides are known to contribute to the increase in cleaved caspase-3 and tyrosine nitration of phosphoinisitol-3-kinase (PI3K). Increased NOs production further causes the activation of MAPK signalling pathway and decrease in Akt Phosphorylation. The use of inhibitors like N-acetyl cysteine and epicatechin are shown to block tyrosine nitration and decrease the ROP severity induced by oxides of nitrogen. Deletion of NOS genes or application of NOS inhibitors (NG-nitro-l-arginine) has also been shown to decrease the progression of ROP in mice models, depicting their crucial role in ROP pathogenesis [91].

9.10. ROS, Inflammation, and ROP

Besides activation of various signalling pathways in ROP, ROS generation is also a key characteristic for the progression of many inflammatory diseases. Inflammation is a major feature of the immune system for the repair of damaged tissue of the body. Role of inflammation is poorly investigated in the case of ROP progression though it plays an important role in blood vessel proliferation under both normal and diseased conditions [86]. Moreover, a series of epidemiological studies since last one decade have supported the hypothesis that inflammation in the eyes of premature infants is a key modulator in the progression and development of ROP [92]. Studies suggested that a gradual increase in ROP progression might be due to prenatal and postnatal inflammation [93]. Small inflammatory protein molecules such as cytokines and chemokines released by immune system plays important role in ROP progression. Moreover, ROS generated by the polymorphonuclear neutrophils (PMNs) causes tissue injury and endothelial dysfunction at the site of inflammation. The vascular endothelial layer plays a significant role in transporting the inflammatory proteins from blood to tissue. Oxidative stress under inflammatory conditions promotes the opening of gap junctions present in the endothelial cell and transport of inflammatory proteins across the barrier.

Cytokines such as TNFα, IL-1β, and IL-6 are key inflammatory markers that contribute to tissue damage or infection [94]. Retinal microglial cells secrete IL-1β and TNFα when conditioned to relative hypoxia. Moreover, IL-1β is linked to retinal microvascular degeneration [95]. While cytokines IL-4 and IL-10 being anti-inflammatory, protects the developing retinal and brain cells from inflammation [96]. Certain experimental studies in oxygen-induced retinopathy mice models suggested that IL-10 is involved in promoting pathological angiogenesis, leading to inhibition of TNFα and MIP-1a in microglial cells [97]. New born infants with high expression levels of IL-10 genes tend to have less chances of severe ROP [98].

Chemokines are primarily involved in regulation of movements of microglial cells to the site of inflammation. Chemokines such as monocyte chemotactic protein 1 (MCP-1), IL-8, and RANTES are shown to be involved in ROP physiology. Inflammation and neovascularization in the eye are regulated by IL-8 in case of tissue damage [99]. An enhanced level of IL-8 homologue is observed during neovascularization in rat model of ROP [100]. The role of RANTES, a chemotactic chemokine, in ROP progression is not clear but a low concentration of RANTES was observed in serum as well as in vitreous humor of patients with vasoproliferative severe ROP [101]. MCP-1 is majorly expressed in the microglia, astrocytes and neurons, and neuro–retinal junction. MCP-1 causes disruption in blood–brain barrier and many other neurodegenerative diseases. The concentration of MCP-1 is seen to be higher in case of ROP infants when compared to the premature born normal infants [102]. It is also observed that premature infants who receive higher doses of oxygen, tend to have high level of MCP-1 concentration in the serum [103].

ROS is required at nominal concentration for maintaining the homeostasis of cellular components while the higher ROS levels are significantly involved in pathological changes. If these ROS concentrations are not checked by the antioxidants, it will eventually lead to inflammation related to tissue damage and injury. ROS being the important contributor of inflammation, much more have to be explored about how these ROS functions physiologically under ROP pathogenesis and contribute to inflammation and tissue injury.

9.11. ROS, Autophagy, and ROP

Apart from the inflammation, increased oxidative stress also plays an important role in autophagy. Autophagy is removal and recycling of damaged cellular components in response to their exposure to conditions like oxidative and nutritional stress as well as pathogenic infections. The major pathway involved in the regulation of oxidative stress and autophagy is through p62/Nrf2/Keap1 pathway [104] (Fig. 9.3). Mitochondria act as the main cellular component which regulates autophagy under the oxidative and nitrosative stress. Although the role of autophagy is not well understood in ROP progression but certain lipid and protein molecules involved in astrocyte survival are also linked to autophagy. Soluble epoxide hydrolase (sEH) promotes astrocyte survival in ROP [105] and are also involved in the regulation of inflammation and autophagy [106]. Nutritional supplements such as long-chain polyunsaturated fatty acids (PUFAs) are structural components of retina and endothelial layer. Soluble epoxide hydrolase is involved in the conversion of these PUFAs into hydroxyl alcohols which regulate angiogenesis and neovascularization. The link between PUFAs (particularly docosahexaenoic acid, DHA) and ROP is important as the sEH in retinal layer can metabolize PUFAs into fatty acid mediators, affecting the cellular viability and angiogenesis. Soluble epoxide hydrolase is required for the maintenance of mitochondrial integrity by preventing mitochondrial pathway-dependent apoptosis and retinal astrocyte survival in ROP [106]. The role of autophagy under two different phases of ROP development will give clear understanding between different pathways involved in the angiogenesis, autophagy, and apoptosis. While the total metabolome profile of ROP retina and vitreous has not been explored, certain PUFAs are found to play important role in microglial cells survival under autophagy and oxidative stress.

Fig. 9.3

Representative image showing ROS generation in mitochondria leading to imbalance in lipid metabolism, angiogenesis, inflammation, and autophagy by p62/Nrf2/Keap1 Pathway [1]. p62, a protein that is bound to ubiquitylated protein aggregates undergoes phosphorylation, thereby requisitioning Keap1 and leading to its detachment from Nrf2. While Nrf2 is not involved in ubiquitin-mediated proteasome degradation system, it is translocated to the nucleus, where it binds to antioxidant-responsive elements (AREs) located in the promoter regions of antioxidant genes and activates their transcription leading to autophagy

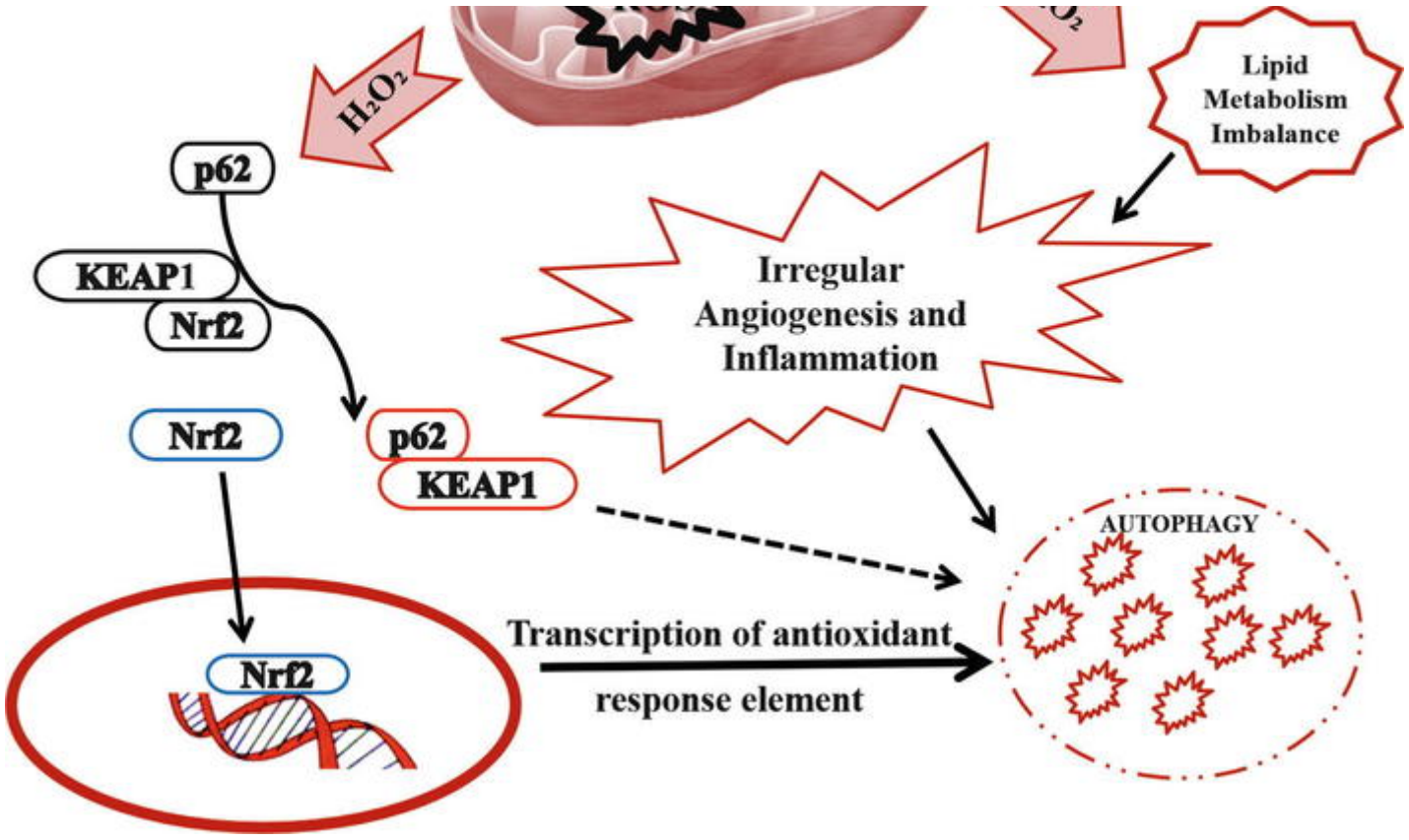

9.12. Conclusion

ROP is a developmental disease modulated by several intrinsic and extrinsic factors. All extrinsic risk factors could act as stimuli or trigger for various developmental pathways. The activation and deactivation of those pathways further depend on the expression of genes that regulate them. The gene expression in turn depends upon micro/macromolecules of the cell like free radicals, RNA, proteins, lipids, and other molecules involved in various physiological pathways. The altered expression of genes further modifies the expression of its downstream target genes and molecules in the cell leading to diseases like ROP. The identification and association of genetic variants and other cellular molecules with ROP may be useful to predict the risk of ROP progression among premature infants and hence, can be helpful in providing genetic counselling to the parents and for the development of new therapies. Several omics studies performed using genomic-, transcriptomic-, and proteomic-based approaches have provided evidence for genetic and molecular defects in ROP progression. However, still there is a huge knowledge gap in the understanding of molecular mechanism that leads to neovascularization in retina of eye leading to ROP. The screening of such hidden genetic and molecular markers could make the disease pathogenesis more comprehensible and therefore enhanced understanding of the pathophysiology of ROP could lead to better understanding of therapeutic options for the affected infants.

Financial Interest None.

References

1. Balakrishnan U, Shaik S, Manian N, Muthukumar M, Thomas M, Amboiram P, et al. Screening based on incidence of severe retinopathy of prematurity in a tertiary care center in India: are Indian infants different? Int J Contemp Pediatr. 2016;3(3):847–53. https://doi.org/10.18203/2349-3291.ijcp20162263.

2. Hartnett ME. Pathophysiology and mechanisms of severe retinopathy of prematurity. Opthalmology. 2015;122:200–10. https://doi.org/10.1016/j.ophtha.2014.07.050.

3. Kim SJ, Port AD, Swan R, Campbell JP, Chan RVP, Chiang MF. Retinopathy of prematurity: a review of risk factors and their clinical significance. Surv Opthalmol. 2018;63:618–37. https://doi.org/10.1016/j.survophthal.2018.04.002.

4. Swan R, Kim SJ, Campbell JP, Chan RVP, Sonmez K, Taylor KD, et al. The genetics of retinopathy of prematurity: a model for neovascular retinal disease. Ophthalmol Retina. 2018;2:949–62. https://doi.org/10.1016/j.oret.2018.01.016.

5. Saunders RA, Donahue ML, Christmann LM, Pakalnis AV, Tung B, Hardy RJ, et al. Racial variation in retinopathy of prematurity. The Cryotherapy for Retinopathy of Prematurity Cooperative Group. Arch Ophthalmol. 1997;115:604–8. https://doi.org/10.1001/archopht.1997.01100150606005.

6. Hussain N, Clive J, Bhandari V. Current incidence of retinopathy of prematurity, 1989–1997. Pediatrics. 1999;104:e26. https://doi.org/10.1542/peds.104.3.e26.

7. Tommiska V, Heinonen K, Ikonen S, Kero P, Pokela ML, Renlund M, et al. A national short-term follow-Up study of extremely low birth weight infants born in Finland in 1996-1997. Pediatrics. 2001;107:E2. https://doi.org/10.1542/peds.107.1.e2.

8. Larsson E, Carle-Petrelius B, Cernerud G, Wallin A, Holmström G. Incidence of ROP in two consecutive Swedish population based studies. Br J Ophthalmol. 2002;86:1122–6. https://doi.org/10.1136/bjo.86.10.1122.

9. Bowe T, Nyamai L, Ademola-Popoola D, Amphornphruet A, Anzures R, Cernichiaro-Espinosa LA, et al. The current state of retinopathy of prematurity in India, Kenya, Mexico, Nigeria, Philippines, Romania, Thailand, and Venezuela. Digit J Ophthalmol. 2019;25(4):49–58. https://doi.org/10.5693/djo.01.2019.08.002.

10. Darlow BA, Hutchinson JL, Henderson-Smart DJ, Donoghue DA, Simpson JM, Evans NJ. Prenatal risk factors for severe retinopathy of prematurity among very preterm infants of the Australian and New Zealand neonatal network. Pediatrics. 2005;115:990–6. https://doi.org/10.1542/peds.2004-1309.

11. Shastry BS. Genetic susceptibility to advanced retinopathy of prematurity (ROP). J Biomed Sci. 2010;17(1):69. https://doi.org/10.1186/1423-0127-17-69.

12. Holmstrom G, Wijngaarden PV, Coster DJ, Williams KA. Genetic susceptibility to retinopathy of prematurity: the evidence from clinical and experimental animal studies. Br J Ophthalmol. 2007;91(12):1704–8. https://doi.org/10.1136/bjo.2007.117283.

13. Bizzarro MJ, Hussain N, Jonsson B, Feng R, Ment LR, Gruenet JR, et al. Genetic susceptibility to retinopathy of prematurity. Pediatrics. 2006;118(5):1858–63. https://doi.org/10.1542/peds.2006-1088.

14. Gow J, Oliver GL. Familial exudative vitreoretinopathy. An expanded view. Arch Ophthalmol. 1971;86(2):150–5. https://doi.org/10.1001/archopht.1971.01000010152007.

15. Shastry BS, Trese MT. Familial exudative vitreoretinopathy: further evidence for genetic heterogeneity. Am J Med Genet. 1997;69(2):217–8. https://doi.org/10.1002/(sici)1096-8628(19970317)69:2<217::aid-ajmg19>3.0.co;2-o.

16. Plager DA, Orgel IK, Ellis FD, Hartzer M, Trese MT, Shastry BS. X-linked recessive familial exudative vitreoretinopathy. Am J Ophthalmol. 1992;114(2):145–8. https://doi.org/10.1016/s0002-9394(14)73977-7.

17. Cadigan KM, Nusse R. Wnt signaling: a common theme in animal development. Genes Dev. 1997;11(24):3286–305. https://doi.org/10.1101/gad.11.24.3286.

18. Kirikoshi H, Sagara N, Koike J, Tanaka K, Sekihara H, Hirai M, et al. Molecular cloning and characterization of human Frizzled-4 on chromosome 11q14-q21. Biochem Biophys Res Commun. 1999;264(3):955–61. https://doi.org/10.1006/bbrc.1999.1612.

19. Robitaille J, MacDonald ML, Kaykas A, Sheldahl LC, Zeisler J, Dubé MP, et al. Mutant frizzled-4 disrupts retinal angiogenesis in familial exudative vitreoretinopathy. Nat Genet. 2002;32(2):326–30. https://doi.org/10.1038/ng957.

20. Xu Q, Wang Y, Dabdoub A, Smallwood PM, Williams J, Woods C, et al. Vascular development in the retina and inner ear: control by Norrin and Frizzled-4, a high-affinity ligand-receptor pair. Cell. 2004;116(6):883–95. https://doi.org/10.1016/s0092-8674(04)00216-8.

21. Ye X, Wang Y, Cahill H, Yu M, Badea TC, Smallwood PM, et al. Norrin, frizzled-4, and Lrp5 signaling in endothelial cells controls a genetic program for retinal vascularization [published correction appears in Cell. 2010 Apr 2;141(1):191]. Cell. 2009;139(2):285–98. https://doi.org/10.1016/j.cell.2009.07.047.

22. MacDonald ML, Goldberg YP, Macfarlane J, Samuels ME, Trese MT, Shastry BS. Genetic variants of frizzled-4 gene in familial exudative vitreoretinopathy and advanced retinopathy of prematurity. Clin Genet. 2005;67(4):363–6. https://doi.org/10.1111/j.1399-0004.2005.00408.x.

23. Ells A, Guernsey DL, Wallace K, Zheng B, Vincer M, Allen A, et al. Severe retinopathy of prematurity associated with FZD4 mutations. Ophthalmic Genet. 2010;31(1):37–43. https://doi.org/10.3109/13816810903479834.

24. Kondo H, Kusaka S, Yoshinaga A, Uchio E, Tawara A, Tahira T. Genetic variants of FZD4 and LRP5 genes in patients with advanced retinopathy of prematurity. Mol Vis. 2013;19:476–85.

25. Drenser KA, Dailey W, Vinekar A, Dalal K, Capone A Jr, Trese MT. Clinical presentation and genetic correlation of patients with mutations affecting the FZD4 gene. Arch Ophthalmol. 2009;127(12):1649–54. https://doi.org/10.1001/archophthalmol.2009.322.

26. Dailey WA, Gryc W, Garg PG, Drenser KA. Frizzled-4 variations associated with retinopathy and intrauterine growth retardation: a potential marker for prematurity and retinopathy. Ophthalmology. 2015;122(9):1917–23. https://doi.org/10.1016/j.ophtha.2015.05.036.

27. Rathi S, Jalali S, Musada GR, Patnaik S, Balakrishnan D, Hussain A, et al. Mutation spectrum of NDP, FZD4 and TSPAN12 genes in Indian patients with retinopathy of prematurity. Br J Ophthalmol. 2018;102(2):276–81. https://doi.org/10.1136/bjophthalmol-2017-310958.

28. Berger W, van de Pol D, Bächner D, Oerlemans F, Winkens H, Hameister H, et al. An animal model for Norrie disease (ND): gene targeting of the mouse ND gene. Hum Mol Genet. 1996;5(1):51–9. https://doi.org/10.1093/hmg/5.1.51.

29. Shastry BS, Pendergast SD, Hartzer MK, Liu X, Trese MT. Identification of missense mutations in the Norrie disease gene associated with advanced retinopathy of prematurity. Arch Ophthalmol. 1997;115(5):651–5. https://doi.org/10.1001/archopht.1997.01100150653015.

30. Haider MZ, Devarajan LV, Al-Essa M, Kumar H. A C597-- > A polymorphism in the Norrie disease gene is associated with advanced retinopathy of prematurity in premature Kuwaiti infants. J Biomed Sci. 2002;9(4):365–70. https://doi.org/10.1007/BF02256593.

31. Dickinson JL, Sale MM, Passmore A, Wheatley CM, Burdon KP, Craig JE, et al. Mutations in the NDP gene: contribution to Norrie disease, familial exudative vitreoretinopathy and retinopathy of prematurity. Clin Exp Ophthalmol. 2006;34(7):682–8. https://doi.org/10.1111/j.1442-9071.2006.01314.x.

32. Hiraoka M, Berinstein DM, Trese MT, Shastry BS. Insertion and deletion mutations in the dinucleotide repeat region of the Norrie disease gene in patients with advanced retinopathy of prematurity. J Hum Genet. 2001;46(4):178–81. https://doi.org/10.1007/s100380170085.

33. Kim DH, Inagaki Y, Suzuki T, Ioka RX, Yoshioka SZ, Magoori K, et al. A new low density lipoprotein receptor related protein, LRP5, is expressed in hepatocytes and adrenal cortex, and recognizes apolipoprotein E. J Biochem. 1998;124(6):1072–6. https://doi.org/10.1093/oxfordjournals.jbchem.a022223.

34. Gong Y, Slee RB, Fukai N, Rawadi G, Roman-Roman S, Reginato AM, et al. LDL receptor-related protein 5 (LRP5) affects bone accrual and eye development. Cell. 2001;107(4):513–23. https://doi.org/10.1016/s0092-8674(01)00571-2.

35. Hiraoka M, Takahashi H, Orimo H, Hiraoka M, Ogata T, Azuma N, et al. Genetic screening of Wnt signaling factors in advanced retinopathy of prematurity. Mol Vis. 2010;16:2572–7.

36. Nikopoulos K, Gilissen C, Hoischen A, Nouhuys CE, Boonstra FN, Blokland EAW, et al. Next-generation sequencing of a 40 Mb linkage interval reveals TSPAN12 mutations in patients with familial exudative vitreoretinopathy. Am J Hum Genet. 2010;86(2):240–7. https://doi.org/10.1016/j.ajhg.2009.12.016.

37. Junge HJ, Yang S, Burton JB, Paes K, Shu X, French DM, et al. TSPAN12 regulates retinal vascular development by promoting Norrin- but not Wnt-induced FZD4/beta-catenin signaling. Cell. 2009;139(2):299–311. https://doi.org/10.1016/j.cell.2009.07.048.

38. Hemler ME. Tetraspanin functions and associated microdomains. Nat Rev Mol Cell Biol. 2005;6(10):801–11. https://doi.org/10.1038/nrm1736.

39. Zhang T, Sun X, Han J, Han M. Genetic variants of TSPAN12 gene in patients with retinopathy of prematurity. J Cell Biochem. 2019;120(9):14544–51. https://doi.org/10.1002/jcb.28715.

40. Mohd Khair SZN, Ismail AS, Embong Z, Mohamed Yusoff AA. Detection of *FZD4*, *LRP5* and *TSPAN12* genes variants in malay premature babies with retinopathy of prematurity. J Ophthalmic Vision Res. 2019;14(2):171–8. https://doi.org/10.4103/jovr.jovr_210_17.

41. Garcia-España A, Chung PJ, Sarkar IN, Stiner E, Sun TT, Desalle R. Appearance of new tetraspanin genes during vertebrate evolution. Genomics. 2008;91(4):326–34. https://doi.org/10.1016/j.ygeno.2007.12.005.

42. Mintz-Hittner HA, Kennedy KA, Chuang AZ, BEAT-ROP Cooperative Group. Efficacy of intravitreal bevacizumab for stage 3+ retinopathy of prematurity. N Engl J Med. 2011;364(7):603–15. https://doi.org/10.1056/NEJMoa1007374.

43. Cooke RW, Drury JA, Mountford R, Clark D. Genetic polymorphisms and retinopathy of prematurity. Investig Ophthalmol Vis Sci. 2004;45(6):1712–5. https://doi.org/10.1167/iovs.03-1303.

44. Ali AA, Hussien NF, Samy RM, Husseiny KA. Polymorphisms of Vascular Endothelial Growth Factor and Retinopathy of Prematurity. J Pediatr Ophthalmol Strabismus. 2015;52(4):245–53. https://doi.org/10.3928/01913913-20150506-02.

45. Vannay A, Dunai G, Bányász I, Szabó M, Vámos R, Treszl A, et al. Association of genetic polymorphisms of vascular endothelial growth factor and risk for proliferative retinopathy of prematurity. Pediatr Res. 2005;57(3):396–8. https://doi.org/10.1203/01.PDR.0000153867.80238.E0.

46. Kaya M, Çokakli M, Berk AT, Yaman A, Yesilirmak D, Kumral A, et al. Associations of VEGF/VEGF-receptor and HGF/c-Met promoter polymorphisms with progression/regression of retinopathy of prematurity. Curr Eye Res. 2013;38(1):137–42. https://doi.org/10.3109/02713683.2012.731550.

47. Shastry BS, Qu X. Lack of association of the VEGF gene promoter (−634 G-- > C and − 460 C-- > T) polymorphism and the risk of advanced retinopathy of prematurity. Graefes Arch Clin Exp Ophthalmol. 2007;245(5):741–3. https://doi.org/10.1007/s00417-006-0480-6.

48. Kusuda T, Hikino S, Ohga S, Kinjo T, Ochiai M, Takahata Y, et al. Genetic variation of vascular endothelial growth factor pathway does not correlate with the severity of retinopathy of prematurity. J Perinatol. 2011;31(4):246–50. https://doi.org/10.1038/jp.2010.111.

49. Semenza GL. Oxygen sensing, homeostasis, and disease [published correction appears in N Engl J Med. 2011 Sep 8;365(10):968]. N Engl J Med. 2011;365(6):537–47. https://doi.org/10.1056/NEJMra1011165.

50. Campochiaro PA. Molecular pathogenesis of retinal and choroidal vascular diseases. Prog Retin Eye Res. 2015;49:67–81. https://doi.org/10.1016/j.preteyeres.2015.06.002.

51. Garcia AL, Udeh A, Kalahasty K, Hackam AS. A growing field: the regulation of axonal regeneration by Wnt signaling. Neural Regen Res. 2018;13(1):43–52. https://doi.org/10.4103/1673-5374.224359.

52. Mohamed S, Schaa K, Cooper ME, Ahrens E, Alvarado A, Colaizy T, et al. Genetic contributions to the development of retinopathy of prematurity. Pediatr Res. 2009;65(2):193–7. https://doi.org/10.1203/PDR.0b013e31818d1dbd.

53. Hartnett ME, Morrison MA, Smith S, Yanovitch TL, Young TL, Colaizy T, et al. Genetic variants associated with severe retinopathy of prematurity in extremely low birth weight infants. Investig Ophthalmol Vis SciI. 2014;55(10):6194–203. https://doi.org/10.1167/iovs.14-14841.

54. Rathi S, Jalali S, Patnaik S, Shahulhameed S, Musada GR, Balakrishnan D, et al. Abnormal complement activation and inflammation in the pathogenesis of retinopathy of prematurity. Front Immunol. 2017;8:1868. https://doi.org/10.3389/fimmu.2017.01868.

55. He L, Hannon GJ. MicroRNAs: small RNAs with a big role in gene regulation [published correction appears in Nat Rev. Genet. 2004 Aug;5(8):631]. Nat Rev Genet. 2004;5(7):522–31. https://doi.org/10.1038/nrg1379.

56. Chen X, Ba Y, Ma L, Cai X, Yin Y, Wang K, et al. Characterization of microRNAs in serum: a novel class of biomarkers for diagnosis of cancer and other diseases. Cell Res. 2008;18:997–1006. https://doi.org/10.1038/cr.2008.282.

57. Kuehbacher A, Urbich C, Zeiher AM, Dimmeler S. Role of Dicer and Drosha for endothelial microRNA expression and angiogenesis. Circ Res. 2007;101(1):59–68. https://doi.org/10.1161/CIRCRESAHA.107.153916.

58. Shen WF, Hu YL, Uttarwar L, Passegue E, Largman C. MicroRNA-126 regulates HOXA9 by binding to the homeobox. Mol Cell Biol. 2008;28(14):4609–19. https://doi.org/10.1128/MCB.01652-07.

59. Reh TA, Hindges R. MicroRNAs in retinal development. Ann Rev Vision Sci. 2018;4:25–44. https://doi.org/10.1146/annurev-vision-091517-034357.

60. Karali M, Banfi S. Non-coding RNAs in retinal development and function. Hum Genet. 2019;138:957–71. https://doi.org/10.1007/s00439-018-1931-y.

61. Zuzic M, Rojo Arias JE, Wohl SG, Busskamp V. Retinal miRNA functions in health and disease. Genes. 2019;10:377. https://doi.org/10.3390/genes10050377.

62. Metin T, Dinç E, Görür A, Erdoğan S, Ertekin S, Sarı AA, et al. Evaluation of the plasma microRNA levels in stage 3 premature retinopathy with plus disease: preliminary study. Eye. 2018;32:415–20. https://doi.org/10.1038/eye.2017.193.

63. Wang S, Olson EN. AngiomiRs-Key regulators of angiogenesis. Curr Opinion Genet. 2009;19(3):205–11. https://doi.org/10.1016/j.gde.2009.04.002.

64. Bai Y, Bai X, Wang Z, Zhang X, Ruan C, Miao JC. MicroRNA-126 inhibits ischemia-induced retinal neovascularization via regulating angiogenic growth factors. Exp Mol Pathol. 2011;91(1):471–7. https://doi.org/10.1016/j.yexmp.2011.04.016.

65. Zimna A, Kurpisz M. Hypoxia-inducible factor-1 in physiological and pathophysiological angiogenesis: applications and therapies. Biomed Res Int. 2015;2015:549412. https://doi.org/10.1155/2015/549412.

66. Hartnett ME, Penn JS. Mechanisms and management of retinopathy of prematurity. N Engl J Med. 2012;367(26):2515–26. https://doi.org/10.1056/NEJMra1208129.

67. Ozaki H, Yu AY, Della N, Ozaki K, Luna JD, Yamada H, et al. Hypoxia inducible factor-1alpha is increased in ischemic retina: temporal and spatial correlation with VEGF expression. Investig Ophthalmol Vis Sci. 1999;40(1):182–9.

68. Olofsson B, Korpelainen E, Pepper MS, Mandriota SJ, Aase K, Kumar V, et al. Vascular endothelial growth factor B (VEGF-B) binds to VEGF receptor-1 and regulates plasminogen activator activity in endothelial cells. Proc Natl Acad Sci U S A. 1998;95(20):11709–14. https://doi.org/10.1073/pnas.95.20.11709.

69. Cavallaro G, Filippi L, Bagnoli P, Marca GL, Cristofori G, Raffaeli G, et al. The pathophysiology of retinopathy of prematurity: an update of previous and recent knowledge. Acta Opthalmologica. 2013;91(1):2–20. https://doi.org/10.1111/aos.12049.

70. Peters KG, De Vries C, Williams LT. Vascular endothelial growth factor receptor expression during embryogenesis and tissue repair suggests a role in endothelial differentiation and blood vessel growth. Proc Natl Acad Sci U S A. 1993;90(19):8915–9. https://doi.org/10.1073/pnas.90.19.8915.

71. Shalaby F, Rossant J, Yamaguchi TP, Gertsenstein M, Wu XF, Breitman ML, et al. Failure of blood-island formation and vasculogenesis in Flk-1-deficient mice. Nature. 1995;376(6535):62–6. https://doi.org/10.1038/376062a0.

72. Terman BI, Dougher-Vermazen M, Carrion ME, Dimitrov D, Armellino DC, Gospodarowicz D, et al. Identification of the KDR tyrosine kinase as a receptor for vascular endothelial cell growth factor. Biochem Biophys Res Commun. 1992;187(3):1579–86. https://doi.org/10.1016/0006-291x(92)90483-2.

73. Quinn TP, Peters KG, de Vries C, Ferrare N, Williams LT. Fetal liver kinase 1 is a receptor for vascular endothelial growth factor and is selectively expressed in vascular endothelium. Proc Natl Acad Sci U S A. 1993;90:7533–7.

74. Pierce EA, Avery RL, Foley ED, Aiello LP, Smith LE. Vascular endothelial growth factor/vascular permeability factor expression in a mouse model of retinal neovascularization. Proc Natl Acad Sci U S A. 1995;92(3):905–9. https://doi.org/10.1073/pnas.92.3.905.

75. Hellstrom A, Perruzzi C, Ju M, Engström E, Hard AL, Liu JL, et al. Low IGF-I suppresses VEGF-survival signaling in retinal endothelial cells: direct correlation with clinical retinopathy of prematurity. Proc Natl Acad Sci. 2001;98(10):5804–8. https://doi.org/10.1073/pnas.101113998.

76. Hellström A, Carlsson B, Niklasson A, Segnestam K, Boguszewski M, Lacerda L, et al. IGF-I is critical for normal vascularization of the human retina. J Clin Endocrinol Metab. 2002;87(7):3413–6. https://doi.org/10.1210/jcem.87.7.8629.

77. Fukuda R, Hirota K, Fan F, Jung YD, Ellis LM, Semenza GL. Insulin-like growth factor 1 induces hypoxia-inducible factor 1-mediated vascular endothelial growth factor expression, which is dependent on MAP kinase and phosphatidylinositol 3-kinase signaling in colon cancer cells. J Biol Chem. 2002;277(41):38205–11. https://doi.org/10.1074/jbc.M203781200.

78. Rakic JM, Lambert V, Devy L, Luttun A, Carmeliet P, Claes C, et al. Placental growth factor, a member of the VEGF family, contributes to the development of choroidal neovascularization. Investig Ophthalmol Vis SciI. 2003;44(7):3186–93. https://doi.org/10.1167/iovs.02-1092.

79. Michels S, Schmidt-Erfurth U, Rosenfeld PJ. Promising new treatments for neovascular age-related macular degeneration. Expert Opin Investig Drugs. 2006;15(7):779–93. https://doi.org/10.1517/13543784.15.7.779.

80. Cao Y. Positive and negative modulation of angiogenesis by VEGFR1 ligands. Sci Signal. 2009;2(59):re1. https://doi.org/10.1126/scisignal.259re1.

81. Simpson DAC, Murphy GM, Bhaduri T, Gardiner TA, Archer DB, Stitt AW. Expression of the VEGF gene family during retinal vaso-obliteration and hypoxia. Biochem Biophys Res Commun. 1999;262(2):333–40. https://doi.org/10.1006/bbrc.1999.1201.

82. Carmeliet P, Moons L, Luttun A, Vincenti V, Compernolle V, Mol MD, et al. Synergism between vascular endothelial growth factor and placental growth factor contributes to angiogenesis and plasma extravasation in pathological conditions. Nat Med. 2001;7:575–83. https://doi.org/10.1038/87904.

83. Juul SE, Anderson DK, Li Y, Christensen RD. Erythropoietinand erythropoietin receptor in the developing human centralnervous system. Pediatr Res. 1998;43:40–9.

84. Wang GL, Semenza GL. General involvement of hypoxia-inducible factor 1 in transcriptional response to hypoxia. Proc Natl Acad Sci U S A. 1993;90(9):4304–8. https://doi.org/10.1073/pnas.90.9.4304.

85. Yang Z, Wang H, Jiang Y, Hartnett ME. VEGFA activates erythropoietin receptor and enhances VEGFR2-mediated pathological angiogenesis. Am J Pathol. 2014;184(4):1230–9. https://doi.org/10.1016/j.ajpath.2013.12.023.

86. Sato T, Kusaka S, Shimojo H, Fujikado T. Vitreous levels of erythropoietin and vascular endothelial growth factor in eyes with retinopathy of prematurity. Ophthalmology. 2009;116(9):1599–603. https://doi.org/10.1016/j.ophtha.2008.12.023. Epub 2009 Apr 15.

87. Sickel W. Electrical and metabolic manifestations of receptor and higher-order neuron activity in vertebrate retina. In: Arden GB, editor. The visual system. Advances in experimental medicine and biology, vol. 24. Boston: Springer; 1972. p. 101–8. https://doi.org/10.1007/978-1-4684-8231-7_11.

88. Rivera JC, Sapieha P, Joyal JS, Duhamel F, Shao Z, Sitaras N, et al. Understanding retinopathy of prematurity: update on pathogenesis. Neonatology. 2011;100:343–53. https://doi.org/10.1159/000330174.

89. Hartnett ME. The effects of oxygen stresses on the development of features of severe retinopathy of prematurity: knowledge from the 50/10 OIR model. Documenta ophthalmologica. Adv Ophthalmol. 2010;120(1):25–39. https://doi.org/10.1007/s10633-009-9181-x.

90. Kaur C, Sivakumar V, Foulds WS, Luu CD, Ling E. Cellular and vascular changes in the retina of neonatal rats after an acute exposure to hypoxia. Investig Ophthalmol Vis SciI. 2009;50(11):5364–74. https://doi.org/10.1167/iovs.09-3552.

91. Brooks SE, Gu X, Samuel S, Marcus DM, Bartoli M, Huang PL, et al. Caldwell; reduced severity of oxygen-induced retinopathy in eNOS-deficient mice. Invest Ophthalmol Vis Sci. 2001;42(1):222–8.

92. Holmström G, Broberger U, Thomassen P. Neonatal risk factors for retinopathy of prematurity--a population-based study. Acta Ophthalmol Scand. 1998;76(2):204–7. https://doi.org/10.1034/j.1600-0420.1998.760216.x.

93. Lee J, Dammann O. Perinatal infection, inflammation, and retinopathy of prematurity. Semin Fetal Neonatal Med. 2012;17(1):26–9. https://doi.org/10.1016/j.siny.2011.08.007.

94. Gabay C, Kushner I. Acute-phase proteins and other systemic responses to inflammation. N Engl J Med. 1999;340(6):448–54. https://doi.org/10.1056/NEJM199902113400607.

95. Rivera JC, Sitaras N, Noueihed B, Hamel D, Madaan A, Zhou T, et al. Microglia and interleukin-1beta in ischemic retinopathy elicit microvascular degeneration through neuronal semaphorin-3A. Arterioscler Thromb Vasc Biol. 2013;33:1881–91. https://doi.org/10.1161/ATVBAHA.113.301331.

96. Opal SM, DePalo VA. Anti-inflammatory cytokines. Chest. 2000;117(4):1162–72. https://doi.org/10.1378/chest.117.4.1162.

97. Kremlev SG, Palmer C. Interleukin-10 inhibits endotoxin-induced pro-inflammatory cytokines in microglial cell cultures. J Neuroimmunol. 2005;162:71–80. https://doi.org/10.1016/j.jneuroim.2005.01.010.

98. Dordelmann M, Kerk J, Dressler F, Brinkhaus MJ, Bartels DB, Dammann CE, et al. Interleukin-10 high producer allele and ultrasound defined periventricular white matter abnormalities in preterm infants: a preliminary study. Neuropediatrics. 2006;37:130–6. https://doi.org/10.1203/PDR.0b013e3181b3b0fa.

99. Silveira RC, Filho FJB, Procianoy RS. Assessment of the contribution of cytokine plasma levels to detect retinopathy of prematurity in very low birth weight infants. Investig Ophthalmol Vis Sci. 2011;52:1297–301. https://doi.org/10.1167/iovs.10-6279.

100. Powers MR, Davies MH, Eubanks JP. Increased expression of chemokine KC, an interleukin-8 homologue, in a model of oxygen-induced retinopathy. Curr Eye Res. 2005;30(4):299–307. https://doi.org/10.1080/02713680590923276.

101. Hellgren G, Willett K, Engstrom E, Thorsen P, Hougaard DM, Jacobsson B, et al. Proliferative retinopathy is associated with impaired increase in BDNF and RANTES expression levels after preterm birth. Neonatology. 2010;98:409–18. https://doi.org/10.1159/000317779.

102. Yao Y, Tsirka SE. Monocyte chemoattractant protein-1 and the blood-brain barrier. Cell Mol Life Sci. 2014;71:683–97. https://doi.org/10.1007/s00018-013-1459-1.

103. Natarajan G, Shankaran S, McDonald SA, Das A, Stoll BJ, Higgins RD, et al. Circulating beta chemokine and MMP 9 as markers of oxidative injury in extremely low birth weight infants. Pediatr Res. 2010;67(1):77–82. https://doi.org/10.1203/pdr.0b013e3181c0b16c.

104. Filomeni G, Zio D, Cocconi F. Oxidative stress and autophagy: the clash between damage and metabolic needs. Cell Death Differ. 2015;22(3):377–88. https://doi.org/10.1038/cdd.2014.150.

105. Jiong H, Sofia-Iris B, Janina W, Sven Z, Jihong L, Rüdiger P, et al. Soluble epoxide hydrolase promotes astrocyte survival in retinopathy of prematurity. J Clin Investig. 2019;129(12):5204–18. https://doi.org/10.1172/JCI123835.

106. Cristina L, Jose A, Veronica G, Bruce D, Vicente A, Joan C, et al. Inhibition of soluble epoxide hydrolase modulates inflammation and autophagy in obese adipose tissue and liver: Role for omega-3 epoxides. Proc Natl Acad Sci U S A. 2015;112(2):536–41. https://doi.org/10.1073/pnas.1422590112.

Multi-OMICS Approach Towards Understanding the Pathogenesis of Retinopathy of Prematurity

by B Satish Patnaik

Submission date: 25-Nov-2021 05:40PM (UTC+0530)
Submission ID: 1712606471
File name: B._Satish_Patnaik_15LAPH12.pdf (15.71M)
Word count: 48708
Character count: 261888

Multi-OMICS Approach Towards Understanding the Pathogenesis of Retinopathy of Prematurity

ORIGINALITY REPORT

10%	6%	7%	4%
SIMILARITY INDEX	INTERNET SOURCES	PUBLICATIONS	STUDENT PAPERS

PRIMARY SOURCES

1	Submitted to University of Hyderabad, Hyderabad Student Paper	2%
2	www.ncbi.nlm.nih.gov Internet Source	1%
3	Satish Patnaik, Meenakshi Rai, Subhadra Jalali, Komal Agarwal et al. "An interplay of microglia and matrix metalloproteinase MMP9 under hypoxic stress regulates the opticin expression in retina", Scientific Reports, 2021 Publication	<1%
4	Alejandra I. Romero-Morales, Gabriella L. Robertson, Anuj Rastogi, Megan L. Rasmussen et al. "Human iPSC-derived cerebral organoids model features of Leigh Syndrome and reveal abnormal corticogenesis", Cold Spring Harbor Laboratory, 2021 Publication	<1%
5	backend.orbit.dtu.dk Internet Source	<1%

6	"Encyclopedia of Cancer", Springer Science and Business Media LLC, 2017 Publication	<1 %
7	www.frontiersin.org Internet Source	<1 %
8	Submitted to Heriot-Watt University Student Paper	<1 %
9	assets.thermofisher.com Internet Source	<1 %
10	Aimy Sebastian, Nicholas R. Hum, Deepa K. Murugesh, Sarah Hatsell, Aris N. Economides, Gabriela G. Loots. "Wnt co-receptors Lrp5 and Lrp6 differentially mediate Wnt3a signaling in osteoblasts", PLOS ONE, 2017 Publication	<1 %
11	"Tumor Microenvironment", Springer Science and Business Media LLC, 2020 Publication	<1 %
12	coek.info Internet Source	<1 %
13	"17th International Congress of Immunology, 19–23 October 2019, Beijing, China", European Journal of Immunology, 2019 Publication	<1 %
14	hdl.handle.net Internet Source	<1 %

15	mafiadoc.com Internet Source	<1 %
16	espace.library.uq.edu.au Internet Source	<1 %
17	Sonika Rathi, Subhadra Jalali, Ganeswara Rao Musada, Satish Patnaik, Divya Balakrishnan, Anjli Hussain, Inderjeet Kaur. " Mutation spectrum of , and genes in Indian patients with retinopathy of prematurity ", British Journal of Ophthalmology, 2017 Publication	<1 %
18	www.nature.com Internet Source	<1 %
19	pt.scribd.com Internet Source	<1 %
20	bura.brunel.ac.uk Internet Source	<1 %
21	www.cambridge.org Internet Source	<1 %
22	creativecommons.org Internet Source	<1 %
23	www.mdpi.com Internet Source	<1 %
24	worldwidescience.org Internet Source	<1 %

25	"Encyclopedia of Cancer", Springer Nature, 2011 Publication	<1 %
26	Anand Vinekar, Archana Padmanabhan Nair, Shivani Sinha, Tanuja Vaidya et al. "Tear Fluid Angiogenic Factors: Potential Noninvasive Biomarkers for Retinopathy of Prematurity Screening in Preterm Infants", Investigative Opthalmology & Visual Science, 2021 Publication	<1 %
27	Brieana Fregeau, Bum Jun Kim, Andrés Hernández-García, Valerie K. Jordan et al. "De Novo Mutations of RERE Cause a Genetic Syndrome with Features that Overlap Those Associated with Proximal 1p36 Deletions", The American Journal of Human Genetics, 2016 Publication	<1 %
28	www.genocheck.com Internet Source	<1 %
29	peerj.com Internet Source	<1 %
30	Yinbing Zhang, Sahar Qazi, Khalid Raza. "Differential expression analysis in Ovarian Cancer: A functional genomics and systems biology approach", Saudi Journal of Biological Sciences, 2021 Publication	<1 %

31	onlinelibrary.wiley.com Internet Source	<1%
32	Submitted to National Institute of Technology Warangal Student Paper	<1%
33	Franco M. Recchia, Lili Xu, John S. Penn, Braden Boone, Phillip J. Dexheimer. "Identification of Genes and Pathways Involved in Retinal Neovascularization by Microarray Analysis of Two Animal Models of Retinal Angiogenesis", Investigative Opthalmology & Visual Science, 2010 Publication	<1%
34	Peng Wang, Xiao-Jing Kang, Xiao-Hui Tang, Jian-Yong Liu et al. "Six generations of epidermolytic palmoplantar keratoderma, associated with a KRT9 R163W mutation", Cancer Genetics, 2016 Publication	<1%
35	Submitted to University of Sheffield Student Paper	<1%
36	Submitted to University of Surrey Student Paper	<1%
37	Gurugirijha Rathnasamy, Wallace S. Fould, Eng-Ang Ling, Charanjit Kaur. "Retinal Microglia – a Key Player in Healthy and	<1%

Diseased Retina", Progress in Neurobiology, 2018
Publication

38	Tailoi Chan-Ling, Glen A. Gole, Graham E. Quinn, Samuel J. Adamson, Brian A. Darlow. "Pathophysiology, screening and treatment of ROP: A multi-disciplinary perspective", Progress in Retinal and Eye Research, 2018 Publication	<1 %
39	ses.library.usyd.edu.au Internet Source	<1 %
40	Songqing Lai, Xiumeng Hua, Ran Gao, Liang Zeng, Jiangping Song, Jichun Liu, Jing Zhang. "Combinational Biomarkers for Atrial Fibrillation Derived from Atrial Appendage and Plasma Metabolomics Analysis", Scientific Reports, 2018 Publication	<1 %
41	nutritionandmetabolism.biomedcentral.com Internet Source	<1 %
42	livrepository.liverpool.ac.uk Internet Source	<1 %
43	webtom.cabgrid.res.in Internet Source	<1 %
44	bmcinfectdis.biomedcentral.com Internet Source	<1 %

45	iovs.arvojournals.org Internet Source	<1 %
46	M. Mecha, F.J. Carrillo-Salinas, A. Feliú, L. Mestre, C. Guaza. "Microglia activation states and cannabinoid system: Therapeutic implications", Pharmacology & Therapeutics, 2016 Publication	<1 %
47	downloads.hindawi.com Internet Source	<1 %
48	ia803208.us.archive.org Internet Source	<1 %
49	Submitted to Queen's University of Belfast Student Paper	<1 %
50	Rebecca Green, Jodie Lord, Jin Xu, Jane Maddock et al. "Metabolic correlates of late midlife cognitive function: findings from the 1946 British Birth Cohort", Cold Spring Harbor Laboratory, 2020 Publication	<1 %
51	Yedi Zhou, Yu Xu, Xiang Zhang, Peiquan Zhao, Xiaoyun Gong, Mingfeng He, Jian Cao, Bing Jiang, Shigeo Yoshida, Yun Li. "Plasma metabolites in treatment-requiring retinopathy of prematurity: Potential	<1 %

biomarkers identified by metabolomics", Experimental Eye Research, 2020
Publication

52	qmro.qmul.ac.uk Internet Source	<1%
53	www.anzctr.org.au Internet Source	<1%
54	Aaron R. Prosnitz, Jeffrey R. Gruen, Vineet Bhandari. "The Genetics of Disorders Affecting the Premature Newborn", Elsevier BV, 2022 Publication	<1%
55	Peter Stapor, Xingwu Wang, Jermaine Goveia, Stijn Moens, Peter Carmeliet. "Angiogenesis revisited – role and therapeutic potential of targeting endothelial metabolism", Journal of Cell Science, 2014 Publication	<1%
56	SufenZhang, Lianghui You, Qu Xu, Jiaxin Ou, Di Wu, Xiaojie Yuan, Zhonghui Liu, Qin Hong, Meiling Tong, Lei Yang, Xia Chi. "Distinct long non-coding RNA and mRNA expression profiles in the hippocampus of an attention deficit hyperactivity disorder model in spontaneously hypertensive rats and control wistar Kyoto rats", Brain Research Bulletin, 2020 Publication	<1%

57	discovery.dundee.ac.uk Internet Source	<1 %
58	www.yumpu.com Internet Source	<1 %
59	"Continuing Progress in Vasculitis Research. Abstracts of the 17th International Vasculitis & ANCA WorkshopLondon, April 19-22, 2015: Abstracts", Nephron, 2015 Publication	<1 %
60	Submitted to Jaypee University of Information Technology Student Paper	<1 %
61	Qianqian Zhang, Chunran Cao, Yudong Guo, Yuchi Hu, Jing Lv, Chunyue Zhu, Xiaofei Wu, Min Ye, Hongzhu Guo. "Consistency evaluation of Chaihuang granules based on pharmacokinetics and metabolomics", Journal of Pharmaceutical and Biomedical Analysis, 2021 Publication	<1 %
62	Submitted to University College London Student Paper	<1 %
63	kops.uni-konstanz.de Internet Source	<1 %
64	rupress.org Internet Source	<1 %

65	Philippe Labelle. "The Eye", Elsevier BV, 2017 Publication	<1 %
66	atm.amegroups.com Internet Source	<1 %
67	dokumen.pub Internet Source	<1 %
68	Ji, Bo, Ben Ernest, Jessica R Gooding, Suchita Das, Arnold M Saxton, Jean Simon, Joelle Dupont, Sonia MÃ©tayer-Coustard, Shawn R Campagna, and Brynn H Voy. "Transcriptomic and metabolomic profiling of chicken adipose tissue in response to insulin neutralization and fasting", BMC Genomics, 2012. Publication	<1 %
69	Submitted to Roosevelt High School Student Paper	<1 %
70	Submitted to Universiti Sains Malaysia Student Paper	<1 %
71	Zhou, Ri, Zhi Yuan, Jierong Liu, and Jian Liu. "Calcitonin gene-related peptide promotes the expression of osteoblastic genes and activates the WNT signal transduction pathway in bone marrow stromal stem cells", Molecular Medicine Reports, 2016. Publication	<1 %
72	etheses.whiterose.ac.uk	

	Internet Source	<1%
73	media.proquest.com Internet Source	<1%
74	www.science.gov Internet Source	<1%
75	Submitted to University of Wales, Bangor Student Paper	<1%
76	Wei Li, Ziwei Wang, Yan Sun, Zhuoshi Wang, Jinyue Bai, Bo Xing, Xiao Sun, Lusheng Wang, Jiankang Li, Wei He. " A start codon mutation of the gene in Chinese families causes clinical heterogeneous familial exudative vitreoretinopathy ", Molecular Genetics & Genomic Medicine, 2019 Publication	<1%
77	academic.oup.com Internet Source	<1%
78	ddd.uab.cat Internet Source	<1%
79	pubs.rsc.org Internet Source	<1%
80	www.hindawi.com Internet Source	<1%
81	www.la-press.comwww.la-press.com Internet Source	

<1 %

82 Alessandra Bridi. "Extracellular vesicles secreted by bovine embryos produced >i/i< and >i/i<: miRNAs content and molecular effects in endometrial and luteal tissues", Universidade de Sao Paulo, Agencia USP de Gestao da Informacao Academica (AGUIA), 2021
Publication
<1 %

83 Gonzalez, H.O.. "Physiological changes and differential gene expression in mummichogs (Fundulus heteroclitus) exposed to arsenic", Aquatic Toxicology, 20060420
Publication
<1 %

84 Laura Tío, Johanne Martel-Pelletier, Jean-Pierre Pelletier, Paul N. Bishop et al. "Characterization of opticin digestion by proteases involved in osteoarthritis development", Joint Bone Spine, 2014
Publication
<1 %

85 Lehrner, L.M.. "Analysis of the structural forms of @a-amylase present in chicken (Gallus domesticus) pancreatic duct juice and intestinal lumen", Comparative Biochemistry and Physiology -- Part B: Biochemistry and Molecular Biology, 1976
Publication
<1 %

86	Nack-Shick Choi, Jeung-Ho Hahm, Pil-Jae Maeng, Seung-Ho Kim. "Comparative Study of Enzyme Activity and Stability of Bovine and Human Plasmins in Electrophoretic Reagents, β-mercaptoethanol, DTT, SDS, Triton X-100, and Urea", BMB Reports, 2005 Publication	<1 %
87	Submitted to San Sisto College Student Paper	<1 %
88	epdf.pub Internet Source	<1 %
89	medcraveonline.com Internet Source	<1 %
90	Goel, M.. "Intermediary metabolism in sea urchin: The first inferences from the genome sequence", Developmental Biology, 20061201 Publication	<1 %
91	Kun Liu, Junwei Fang, Jing Jin, Shaopin Zhu, Xiaoyin Xu, Yupeng Xu, Bin Ye, Shu-Hai Lin, Xun Xu. "Serum Metabolomics Reveals Personalized Metabolic Patterns for Macular Neovascular Disease Patient Stratification", Journal of Proteome Research, 2019 Publication	<1 %
92	Submitted to National University of Singapore Student Paper	<1 %

93	Submitted to Queensland University of Technology Student Paper	<1%
94	Submitted to University of KwaZulu-Natal Student Paper	<1%
95	nexusacademicpublishers.com Internet Source	<1%
96	www.freepatentsonline.com Internet Source	<1%
97	D.M. Pattwell, C.M. Sheridan, M. Le Goff, P.N. Bishop, P. Hiscott. "Localisation of opticin in human proliferative retinal disease", Experimental Eye Research, 2010 Publication	<1%
98	Submitted to Universiti Putra Malaysia Student Paper	<1%
99	Submitted to University of Hong Kong Student Paper	<1%
100	Submitted to University of Wales Institute, Cardiff Student Paper	<1%
101	journals.plos.org Internet Source	<1%
102	pubmed.ncbi.nlm.nih.gov Internet Source	<1%

103	www.biorxiv.org Internet Source	<1%
104	www.physiology.org Internet Source	<1%

Exclude quotes	On	Exclude matches	< 14 words
Exclude bibliography	On		